frontiers | Research Topics

Crosstalk between cell death, oxidative stress, and immune regulation

Edited by
Chao Yang, Chung Nga Ko, Chao Mao and Shicheng Guo

Published in
Frontiers in Immunology

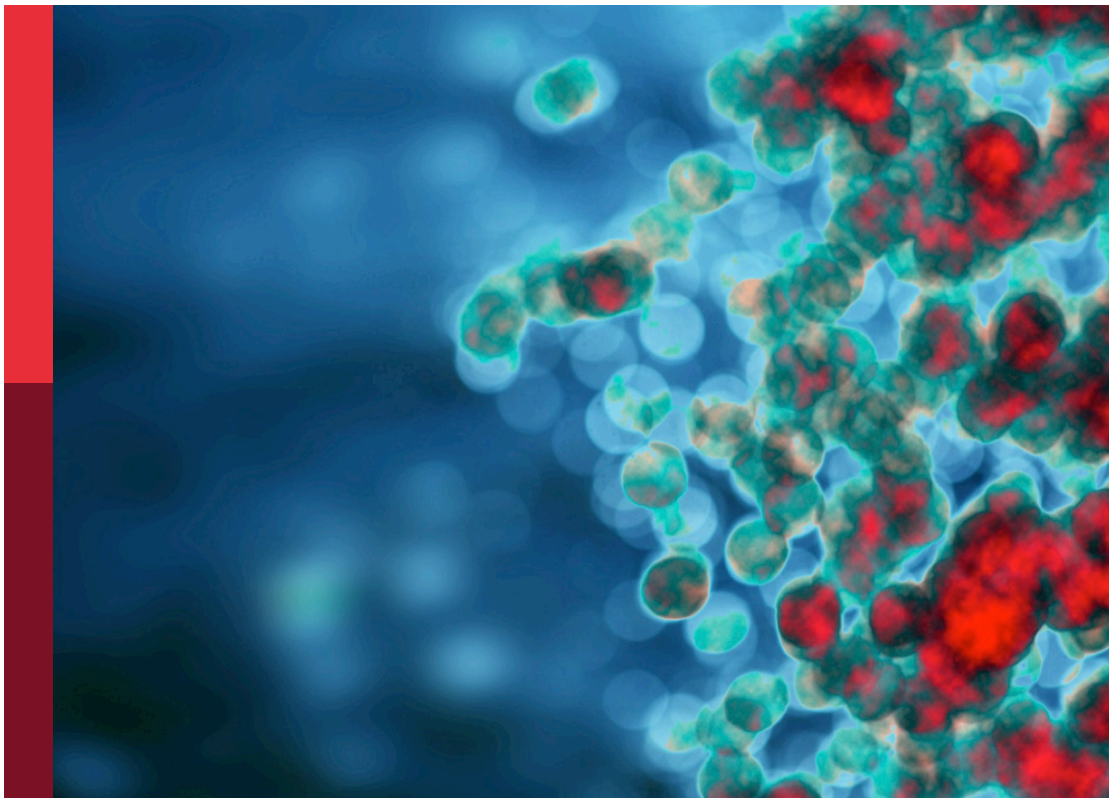

ISSN 1664-8714
ISBN 978-2-8325-5664-1
DOI 10.3389/978-2-8325-5664-1

About Frontiers

Frontiers is more than just an open access publisher of scholarly articles: it is a pioneering approach to the world of academia, radically improving the way scholarly research is managed. The grand vision of Frontiers is a world where all people have an equal opportunity to seek, share and generate knowledge. Frontiers provides immediate and permanent online open access to all its publications, but this alone is not enough to realize our grand goals.

Frontiers journal series

The Frontiers journal series is a multi-tier and interdisciplinary set of open-access, online journals, promising a paradigm shift from the current review, selection and dissemination processes in academic publishing. All Frontiers journals are driven by researchers for researchers; therefore, they constitute a service to the scholarly community. At the same time, the *Frontiers journal series* operates on a revolutionary invention, the tiered publishing system, initially addressing specific communities of scholars, and gradually climbing up to broader public understanding, thus serving the interests of the lay society, too.

Dedication to quality

Each Frontiers article is a landmark of the highest quality, thanks to genuinely collaborative interactions between authors and review editors, who include some of the world's best academicians. Research must be certified by peers before entering a stream of knowledge that may eventually reach the public - and shape society; therefore, Frontiers only applies the most rigorous and unbiased reviews. Frontiers revolutionizes research publishing by freely delivering the most outstanding research, evaluated with no bias from both the academic and social point of view. By applying the most advanced information technologies, Frontiers is catapulting scholarly publishing into a new generation.

What are Frontiers Research Topics?

Frontiers Research Topics are very popular trademarks of the *Frontiers journals series*: they are collections of at least ten articles, all centered on a particular subject. With their unique mix of varied contributions from Original Research to Review Articles, Frontiers Research Topics unify the most influential researchers, the latest key findings and historical advances in a hot research area.

Find out more on how to host your own Frontiers Research Topic or contribute to one as an author by contacting the Frontiers editorial office: frontiersin.org/about/contact

Crosstalk between cell death, oxidative stress, and immune regulation

Topic editors

Chao Yang — Zhejiang Ocean University, China

Chung Nga Ko — Hong Kong Baptist University, Hong Kong, SAR China

Chao Mao — University of Texas MD Anderson Cancer Center, United States

Shicheng Guo — Arrowhead Pharmaceuticals, United States

Citation

Yang, C., Ko, C. N., Mao, C., Guo, S., eds. (2024). *Crosstalk between cell death, oxidative stress, and immune regulation*. Lausanne: Frontiers Media SA.

doi: 10.3389/978-2-8325-5664-1

Table of contents

frontiers | Frontiers in Immunology

TYPE Editorial
PUBLISHED 29 October 2024
DOI 10.3389/fimmu.2024.1503252

OPEN ACCESS

EDITED AND REVIEWED BY
Francesca Granucci,
University of Milano-Bicocca, Italy

*CORRESPONDENCE
Chung-Nga Ko
andreako@hkbu.edu.hk
Chao Yang
yc52028@hotmail.com

RECEIVED 28 September 2024
ACCEPTED 07 October 2024
PUBLISHED 29 October 2024

CITATION
Ko C-N and Yang C (2024) Editorial: Crosstalk between cell death, oxidative stress, and immune regulation.
Front. Immunol. 15:1503252.
doi: 10.3389/fimmu.2024.1503252

Editorial: Crosstalk between cell death, oxidative stress, and immune regulation

Chung-Nga Ko[1]* and Chao Yang[2]*

[1]Department of Chemistry, Hong Kong Baptist University, Hong Kong, Hong Kong SAR, China, [2]National Engineering Research Center for Marine Aquaculture, Institute of Innovation & Application, Zhejiang Ocean University, Zhoushan, China

KEYWORDS

cell death, oxidative stress, immune regulation, immune-mediated diseases, apoptosis

Editorial on the Research Topic
Crosstalk between cell death, oxidative stress, and immune regulation

Cell death, a basic physiological process of all organisms, involves a series of core players capable of destroying the homeostasis of cellular environment. With more thorough research in recent years, different types of cell death such as apoptosis, autophagy, necroptosis and ferroptosis have been clarified (1–3). This Research Topic compiles a range of contributions exploring the intricate relationships among cell death, oxidative stress, and immune regulation, as well as their pathobiology and therapeutic implications in immune-mediated diseases.

The review from Liu et al. summarized the pre-clinical and clinical studies of the pathogenesis of transfusion-related acute lung injury (TRALI). In the presence of stimuli, neutrophil extracellular traps (NETs) are formed by activated neutrophils and are established as effector molecules, contributing to the release of ROS that destroys pulmonary vascular endothelial cells. The authors discussed the mechanism through which NETs induce TRALI, and highlighted the possible therapeutic targets based on the modulation of NETosis/NETs, for example, through activation of the glycolytic pathway, targeting inflammasome, chemokines/cytokines and neutrophil receptors. Another review from Zhang et al. described the role of cGAS-STING pathway in viral infection. Apart from its most common function in regulating IFN-α and inflammation, cGAS-STING also has major impacts on a series of cellular responses, such as endoplasmic reticulum stress, autophagy and oxidative stress. However, overactivation and inactivation of the cGAS-STING pathway are both detrimental to the clearance of pathogens. Further studies on how to modulate the activity of cGAS-STING and promote elimination of virus by host cells are still required.

This Research Topic also focuses on the therapeutic strategies targeting the "cell death-oxidative stress-immune regulation" signaling axis. For example, the research article from Dos Santos et al. reported a repurposed drug deucravacitinib, which is a tyrosine kinase 2 (TYK2) inhibitor, for the prevention and treatment of type 1 diabetes. The result shows that deucravacitinib could prevent the effects of IFN-α in a dose-dependent manner while not affecting the function and survival of β-cells. In cells pre-treated with proinflammatory cytokines, deucravacitinib could partially reduce inflammation and apoptosis. This pre-clinical data suggests that TYK2 inhibition may be an effective strategy for treating type 1

diabetes. Another review article from Zhang et al. reported the research progress of mesenchymal stem cells-derived extracellular vesicles (MSC-EVs) and exosomes (MSC-Exos), which carry bioactive molecules e.g. regulatory proteins and miRNA, in the treatment of oxidative stress-related diseases. The regulatory activities of MSC-EVs and MSC-Exos, including apoptosis, necrosis and oxidative stress, on many systemic diseases have been widely validated by cellular and animal models. However, the same bioactive molecules in MSC-EVs and MSC-Exos seem to have different effects in different studies. It is therefore necessary to formulate a protocol to better control the isolation steps of MSC-EVs and MSC-Exos, as well as to select study models closer to human pathology for better clinical usage. The review from Mackiewicz et al. discussed the role of nuclear factor of activated T-cells (NFAT), which is a family of main transcription factors responsible for regulating the expression of genes important for inflammatory and immune responses, in Alzheimer's diseases. The inflammatory mediators produced by NFAT-dependent pathway is controlled by Ca^{2+}-dependent protein phosphatase calcineurin (CaN) and aberrant NFAT-CaN signaling may play a deleterious role in the pathologies of Alzheimer's diseases, including neuronal apoptosis. Although targeted inhibition of CaN/NFAT may offer a promising strategy in the treatment of Alzheimer's diseases, the severe adverse effects of many CaN inhibitors and scarce research on NFAT inhibitors have markedly limited their translational potential. Another review from Maiese discussed three pathways of programmed cell death, including SIRT1, AMPK and WISP1, and suggested that these pathways are potentially important in maintaining nervous system function and metabolic homeostasis, which warrant more thoughtful research.

The study of gene regulatory networks is useful to understand transcriptional dynamics in biological systems. Computational recognition of regulator genes has been successfully applied to study the relationship between programmed cell death/oxidative stress and different diseases. The research article from Xu et al. explored the patho-physiobiological mechanisms underlying atopic dermatitis (AD). The authors identified 278 differentially expressed genes (DEGs) and seven ferroptosis signature genes in four AD-related cohorts from the GEO database (samples from patients with AD and healthy controls). Four ferroptosis genes (*EGR1, MAP3K1, FABP4, ALOXE3*) were selected to construct a FerrSig predictive model and was shown to be able to accurately identify patients at higher risks of AD. Another research conducted by Li et al. integrated single-cell RNA sequencing and bulk transcriptomic datasets to elucidate the mechanisms underlying renal ischemia-reperfusion injury (RIRI). The authors identified five necroptosis-related DEGs from the pre- and post-reperfusion renal biopsies using gene expression data, constructed a predictive model for delayed graft function (DGF) and divided patients into different risk groups. The model revealed reliable performance in identifying patients with higher risks of developing DGF. The result was further validated by mouse models that exhibited up-regulated necroptosis-related DEGs after ischemia-reperfusion. The same research group (Zhang et al.) conducted another study identifying three endoplasmic reticulum stress-related genes (*ATF3, JUN* and *PPP1R15A*) which were found to be associated with different kidney injury-related pathways, including apoptosis, pyroptosis, oxidative stress and inflammatory response. Intriguingly, compared with the sham group, the expression of the three genes were significantly higher after RIRI, and were decreased after treatment with a potential drug for RIRI. Furthermore, a research article from Yang et al. established three transcriptional co-expression networks (clusters C1, C2 and C3) with distinct antioxidative potential in glioblastoma cancer cells. C2, which was identified as a cluster with a moderate level of ROS, was found to exhibit a strong correlation with the highly aggressive mesenchymal subtype of glioblastoma. Among the transcriptional factors in C2, *FOSL1* demonstrates a prognostic value in both overall survival and overall-free interval.

In summary, therapeutic strategies targeting the pathways of cell death offer exciting prospects for maintaining homeostasis of cellular environment that can be compromised in immune-mediated diseases. Integrating predictive models with other clinical indicators may also provide a comprehensive assessment to identify patients with higher risks of disease development/recurrence and can potentially offer a promising prognostic application to alleviate disease burden. We hope that this Research Topic will enrich our understanding of the crosstalk between cell death, oxidative stress, and immune regulation, and will open up new avenues for the diagnosis and treatment of immune-mediated diseases.

Author contributions

CK: Writing – original draft, Writing – review & editing. CY: Writing – original draft, Writing – review & editing.

Conflict of interest

The authors declare that the research was conducted in the absence of any commercial or financial relationships that could be construed as a potential conflict of interest.

Publisher's note

References

1. Shen S, Shao Y, Li C. Different types of cell death and their shift in shaping disease. *Cell Death Discovery*. (2023) 9:284. doi: 10.1038/s41420-023-01581-0

2. Hotchkiss RS, Strasser A, McDunn JE, Swanson PE. Cell death. *New Engl J Med*. (2009) 361:1570–83. doi: 10.1056/NEJMra0901217

3. Berghe TV, Vanlangenakker N, Parthoens E, Deckers W, Devos M, Festjens N, et al. Necroptosis, necrosis and secondary necrosis converge on similar cellular disintegration features. *Cell Death Differentiation*. (2010) 17:922–30. doi: 10.1038/cdd.2009.184

frontiers | Frontiers in Immunology

TYPE Review
PUBLISHED 14 August 2023
DOI 10.3389/fimmu.2023.1238789

OPEN ACCESS

EDITED BY
Chao Yang,
Zhejiang Ocean University, China

REVIEWED BY
Yimei Feng,
Xinqiao Hospital, China
Yan Wang,
Guangdong Pharmaceutical University, China
Yujie Shi,
Peking University, China

*CORRESPONDENCE
Yanfang Zhou
yfzhou@gdmu.edu.cn
Xinsheng Peng
xshpeng@gdmu.edu.cn

RECEIVED 12 June 2023
ACCEPTED 24 July 2023
PUBLISHED 14 August 2023

CITATION
Zhang W, Wang T, Xue Y, Zhan B, Lai Z, Huang W, Peng X and Zhou Y (2023) Research progress of extracellular vesicles and exosomes derived from mesenchymal stem cells in the treatment of oxidative stress-related diseases.
Front. Immunol. 14:1238789.
doi: 10.3389/fimmu.2023.1238789

Research progress of extracellular vesicles and exosomes derived from mesenchymal stem cells in the treatment of oxidative stress-related diseases

Wenwen Zhang[1,2], Tingyu Wang[1,2], Yuanye Xue[1,2], Bingbing Zhan[3], Zengjie Lai[4], Wenjie Huang[5], Xinsheng Peng[6,7]* and Yanfang Zhou[1,2]*

[1]The First Dongguan Affiliated Hospital of Guangdong Medical University, Dongguan, Guangdong, China, [2]Department of Pathophysiology, Guangdong Medical University, Dongguan, Guangdong, China, [3]School of Pharmaceutical Sciences, Guangdong Medical University, Dongguan, China, [4]The Second Clinical Medical College of Guangdong Medical University, Dongguan, China, [5]School of Medical Technology, Guangdong Medical University, Dongguan, China, [6]Biomedical Innovation Center, Guangdong Medical University, Dongguan, China, [7]Institute of Marine Medicine, Guangdong Medical University, Zhanjiang, China

There is growing evidence that mesenchymal stem cell-derived extracellular vesicles and exosomes can significantly improve the curative effect of oxidative stress-related diseases. Mesenchymal stem cell extracellular vesicles and exosomes (MSC-EVs and MSC-Exos) are rich in bioactive molecules and have many biological regulatory functions. In this review, we describe how MSC-EVs and MSC-Exos reduce the related markers of oxidative stress and inflammation in various systemic diseases, and the molecular mechanism of MSC-EVs and MSC-Exos in treating apoptosis and vascular injury induced by oxidative stress. The results of a large number of experimental studies have shown that both local and systemic administration can effectively inhibit the oxidative stress response in diseases and promote the survival and regeneration of damaged parenchymal cells. The mRNA and miRNAs in MSC-EVs and MSC-Exos are the most important bioactive molecules in disease treatment, which can inhibit the apoptosis, necrosis and oxidative stress of lung, heart, kidney, liver, bone, skin and other cells, and promote their survive and regenerate.

KEYWORDS

mesenchymal stem cells, extracellular vesicles, exosomes, oxidative stress, inflammation, cell proliferation

1 Introduction

Mesenchymal stem cells belong to a heterogeneous cell population of stromal cells. They proliferate and differentiate *in vitro* in the form of plastic adherent cells. They can be isolated from many human tissues and differentiate into mesoderm and endoderm (1), neuroectodermal cells (2) and other embryonic lineage cells (3). Mesenchymal stem cells have been proven to have a variety of biological functions. They can interact with cells in the immune system for immune regulation, inhibit tumor necrosis factor (TNF), upregulate IL-10 (4), reduce inflammation, inhibit respiratory burst and Activate the spontaneous apoptosis of neutrophils, etc. (5). Although mesenchymal stem cells have many applications in the field of life sciences, their effectiveness is restricted by many factors. For example, the phenomenon of immune rejection of allogeneic mesenchymal stem cells (6), low persistence of curative effect of limited infusion of mesenchymal stem cells, deprivation of nutrients and growth factors and limitation of oxygen transport during mesenchymal stem cell transplantation (7), Passaged late mesenchymal stem cells trigger immediate menstrual blood-mediated inflammatory response (IBMIR) and form blood activation markers, etc. (8). In recent years, due to the vigorous development of research on exosomes derived from mesenchymal stem cells (MSC-Exos), it has been found that exosomes can avoid some of the shortcomings of mesenchymal stem cells in the treatment of various diseases.

Exosomes are spherical particles with a diameter of about 40 ~ 150 nm, which are released after the fusion of vesicles and cell membrane (9). It has lipid bilayer membrane structure, which is produced in cell culture or body fluid supernatant, such as blood, saliva, urine, breast milk, cerebrospinal fluid, bile and lymph, and can secrete exosomes (10–12). Compared with plasma membrane, exosomal membrane is harder and more stable in external environment. Exosomes carry a lot of genetic material similar to stem cells, including microRNAs (miRNAs) and mRNAs (13). In addition, exosomes contain a specific family of proteins such as heat shock protein integrins and tetrathione involved in membrane transport and fusion (14–16). It is worth noting that exosomes-based cell origin exosomes also play a unique role in cell communication (17). MSC-Exos has become the preferred treatment for many diseases and is a safe and effective stem cell-free replacement therapy (18). Exosomes are more stable and modifiable than mesenchymal stem cells and have no risk of tumor formation Due to the nanometer size and lipid bilayer structure of exosomes, exosomes can easily cross the biological barrier and enter the target organs (19). The therapeutic effect of MSC-Exos has been confirmed in a variety of diseases, including lung injury, myocardial injury, kidney injury, nerve injury, skin injury and aging (20).

When a living cell is damaged by free radicals or non-free radicals, it will obtain electrons from its molecules, which will produce a chain reaction and eventually lead to the damage of cell structure. Among these molecules, molecules from ROS (reactive oxygen species) have major biological effects, and the concept of oxidative stress is derived from this (21). Oxidative stress injury refers to the condition that oxygen and oxygen-derived free radicals exceed the natural antioxidant defense capacity of cells (22). The aggravation and prolongation of symptoms caused by oxidative stress is always a major problem in various common clinical diseases. The antioxidant activity of MSC-Exos and MSC-EVs has its unique advantages in inhibiting oxidative damage and alleviating inflammatory reaction MSC-Exos and MSC-EVs can increase calcium inflow, reduce the concentration of pro-inflammatory factors and reduce the production of ROS (23). Exosomal therapy has a looser regulatory approach than cell therapy and is considered as a "biological drug" with broad development prospects (24). In recent years, the research on exosomes is very active, and the articles on exosomes in the treatment of oxidative stress have accumulated a certain amount. This paper mainly reviews the mechanism, advantages, disadvantages and prospects of MSC-Exos and MSC-EVs derived from mesenchymal stem cells in the treatment of oxidative stress-related diseases in various systems. Based on previous studies, it details the related mechanisms, looks for the intersection of research directions, and deeply discusses the future research directions in this field (Figure 1).

2 Respiratory diseases

Therapies based on MSC-EVs or MSC-Exos have great application prospect in the treatment of oxidative stress-related lung injury. For example, acute lung injury (ALI), neonatal hypoxia-ischemia-reperfusion COVID-19 radiation lung injury, etc.

The main characteristic of ALI progression is oxidative stress response (25). The accumulation of excess pro-inflammatory factors can lead to the occurrence of oxidative stress in lung tissue, which then leads to the occurrence of ALI. At present, many drugs in the market cannot pass through the lung blood-air barrier, which leads to low curative effect, which is the main problem in treating ALI. Studies have shown that MSC-EVs can cross the blood-air barrier and other biological barriers in the lungs to enhance the therapeutic effect (26). Hyperoxia-induced lung injury can lead to the imbalance of oxidative-antioxidant system *in vivo* and lead to oxidative stress injury. The negative effects of ischemia-reperfusion are caused by the induction of inflammation and oxidative stress and the damage of cell energy metabolism, which leads to a series of harmful biological events from ion homeostasis failure to cell death (27). In severe acute respiratory syndrome (SARS) caused by SARS-associated coronavirus (SARS-CoV), the immune response to virus infection and cytokine storm play a key role in the severity of the disease (28). Cytokine storm will lead to the development of oxidative stress due to ROS produced by immune cells (29). Complex pathophysiological mechanisms indicate that severe COVID-19 is more suitable for multi-effect drug therapy than single target drug (30). Therefore, it is an innovative method to use MSC-EVs or MSC-Exos combined with COVID-19 clinical drugs.

Determining the effective therapeutic components carried by exosomes is the basis for explaining the therapeutic mechanism, including effective secretory proteins and microRNA (miRNA), etc. (31) At the same time, it is also important to further understand the

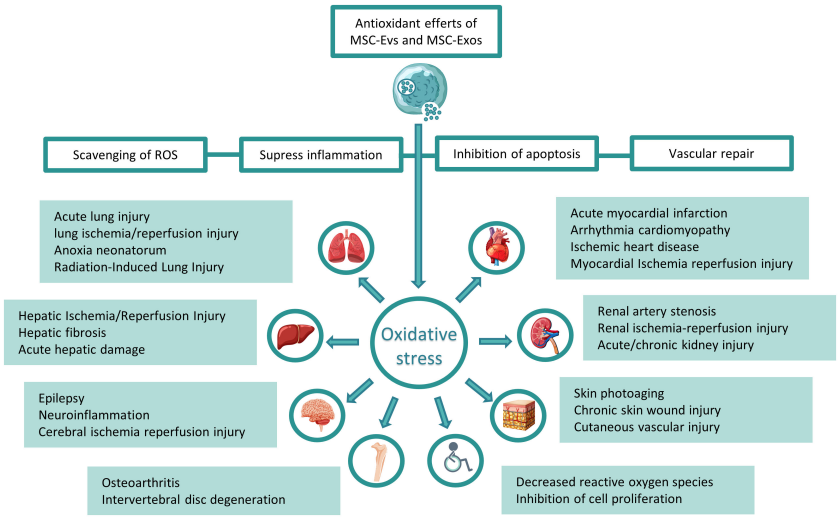

FIGURE 1
Treatment of related systemic diseases caused by oxidative stress with mesenchymal stem cell exosomes and vesicles: Mesenchymal stem cell-derived exosomes and exosomes can decrease ROS, inhibit inflammation, reduce cell apoptosis, and enhance angiogenesis, thereby treating respiratory, circulatory, and digestive systems, nervous system, motor system and other system diseases caused by oxidative stress.

therapeutic mechanism of exosomes in the lung, including antioxidant and anti-inflammatory treatment of target cells or injured tissues. miRNA is a small non-coding RNA molecule with 19-25 nucleotides that play various roles in physiology and disease progression (32). MSC-EVs have been shown to promote the repair of lung injury by delivering miR125amiR-181b and miR-126 in the field of ALI (25). Both inhalation and tail vein injection of MSC-EVs decreased the levels of pro-inflammatory cytokines IL-1 β MCP-1IL-1 α TNF α and IL-12 and increased the levels of anti-inflammatory cytokines IL-10. HE staining showed that MSC-EVs could improve pulmonary morphological changes such as alveolar wall thickening, alveolar septum congestion and inflammatory infiltration after lipopolysaccharide (LPS) stimulation (33). In addition, NF-kB is a key transcription factor, which has been proved to be a key signal factor for regulating pro-inflammatory cytokines in sepsis-induced ALI (25). The increase of pathological score showed that MSC-EVs treatment reversed the changes related to inflammatory infiltration. These studies suggest that MSC-EVs and MSC-Exos can improve the damage and pathological changes of oxidative stress-related lung diseases in the early stage and are excellent new therapeutic drugs.

2.1 MSC-EVs and MSC-Exos improve the related indexes of pulmonary oxidative stress

The antioxidant effects of MSC-EVs and MSC-Exos are closely related to their secreted proteins and microRNA. In exosomes-treated rat alveolar macrophages (NR8383 cells), the activity of SOD and GSH increased and the content of MDA decreased, and the effect was more obvious when the exosomes overexpressed miR-22-3p However, inhibiting FZD6 in exosomes inhibited SOD and GSH activities and increased MDA content, which indicated that miR-22-3p improved the antioxidant activity of cells through FZD6 (32). After adding MSC-EVs to raw 264.7 cells, the expression of Nrf2HO-1HMGB1 and other oxidative regulators decreased, and the number of 8-OHdG positive cells decreased. After knocking out Nrf2 in MSC-EVs and adding MSC-EVs again in raw 264.7 cells stimulated by LPS, the expression of HO-1IL-6 was up-regulated, and the expression of Nrf2Keap-1TNF-α did not change. These results indicate that knockout of Nrf2 in MSC-EVs can weaken the anti-inflammatory and antioxidant activities of EVs (33)

Transcriptome sequencing of mouse ALI model treated with MSC-EVs for 4 days showed that many genes related to immune regulation and oxidative stress were less different than those of ALI mice (34). In addition, a series of genes such as TLR4,Arg-1 and HMOX1 have been shown to be involved in immune regulation and antioxidant activity HO-1 is an antioxidant enzyme that can inhibit apoptosis, inflammation and cell proliferation to reduce cell death in ALI animal models by inducing several detoxification enzymes and antioxidant proteins (25). In summary, MSC-EVs plays an important therapeutic role in immune regulation and reduction of oxidative stress in ALI mouse model (33).

2.2 MSC-EVs and MSC-Exos in the treatment of lung cell injury and apoptosis induced by oxidative stress

MSC-EVs and MSC-Exos have been proved by many studies to alleviate lung pathological injury and apoptosis.

In vitro, the cell viability of NR8383 cells decreased and apoptosis was promoted after LPS treatment, while miR-22-3p

up-regulated MSC-EVs increased cell viability and inhibited cell apoptosis FZD6 belongs to the "curl" gene family and is highly expressed in both adult and fetal lung tissues (35). Up-regulation of miR-22-3p or down-regulation of FZD6 in MSC-Exos can improve cell viability and inhibit apoptosis (32). In addition, up-regulation of miR-30b-3p of MSC-Exos in LPS-treated mouse lung epithelial cells (MLE-12 cells) also showed increased cell proliferation and inhibition of apoptosis (36).

In vivo experiment, the acute lung injury induced by sepsis in mice was basically normal after MSCs-EVs treatment, and the blood barrier of type I alveolar cells and endothelial cells were only slightly swollen. After exosomes treatment, the edema and bleeding of mice were alleviated (25). In the survival analysis, Kaplan-Meier survival curve showed that the survival rate of mice with cecal ligation and puncture (CLP) treated with MSCs-EVs was significantly higher (25). MiR-21-5p carried by MSC-Exos is a kind of cancer-promoting miRNA, which can effectively resist apoptosis. Ji Wei Li et al. treated mouse bone marrow-derived MSCs with hypoxia or miR-21-5p antagomir respectively to increase or decrease miR-21-5p concentration in MSC-Exos. It was found that MSC-Exos treatment weakened mouse lung ischemia-reperfusion injury in a miR-21-5p-dependent manner, effectively reduced oxidative stress-induced apoptosis and partially reduced hypoxia/reoxygenation-induced pro-inflammatory "M1" polarization of alveolar macrophages (37).

EVs can release glycosaminoglycan serum hyaluronic acid (HA) and improve energy metabolism of lung cells exposed to ischemia-reperfusion. This is particularly important in protecting against ischemic injury because HA is essential for maintaining the integrity of lung epithelial cells and inducing tissue healing and regeneration HA released by mesenchymal stem cells can trap immune cells in extracellular matrix (38–40) and prevent leukocytes from adhering to activated endothelial cells (40, 41). The impaired energy metabolism after ischemia-reperfusion injury is the main reason for the failure of ion homeostasis, which leads to cell swelling and apoptosis/autophagy activation. The treatment of MSC-EVs can restore ATP to baseline level and promote leukocyte homing in perfusion lung injury (27). These results suggest that MSC-EVs and MSC-Exos can enhance the inhibition of cell regeneration and apoptosis in oxidative stress-induced lung injury, especially miRNA in exosomes.

2.3 MSC-EVs and MSC-Exos in the treatment of lung inflammatory injury induced by oxidative stress

MSC-EVs and MSC-Exos play a significant biological role in anti-inflammation. ROS signal plays an important role in the occurrence and development of inflammatory injury. Excessive ROS promotes cell injury and death when the production and elimination of ROS are unbalanced (42). MSC-EVs and MSC-Exos can regulate and attenuate the inflammatory injury induced by oxidative stress in the lungs.

The expression of CD86 in mouse mononuclear macrophages was increased by LPS stimulation *in vitro*. After administration of MSC-EVs, the expression of CD86 decreased significantly, and the expression of Arg-1 increased, which indicated that macrophages polarized towards M2 anti-inflammatory direction (33).

In vivo MSC-EVs significantly reduced the levels of pro-inflammatory cytokines including TNF-alpha IL-1bIL-6MPO and significantly increased IL-10 levels and resulted in neutropenia in alveolar lavage fluid in a sepsis-induced acute lung injury model in mice. The phosphorylation activation of MAPK pathway is thought to play an important role in the pathogenesis of ALI and administration of MSC-EVs significantly inhibits their phosphorylation. Treatment with MSC-EVs decreased the phosphorylation level of NF-kB p65 and inhibited the increase of NF-kB p65 degradation. In addition, TLR4 also plays an important role in the regulation of inflammation and signal transduction. The decreased expression of TLR4 and its downstream signals (IL-1 β IL-6 and NF-kabb-p65) after MSC-EVs treatment also indicates that MSC-EVs can alleviate inflammation stimulated by LPS (33). These phenomena suggest that MSC-EVs play an important role in inhibiting inflammatory markers related to oxidative stress in the lungs.

2.4 MSC-EVs and MSC-Exos in the treatment of pulmonary vascular injury induced by oxidative stress

Vascular endothelial growth factor (VEGF) plays an important role in promoting angiogenesis and enhancing vascular permeability. Tracheal transplantation of MSC-EVs in rat lung tissue can significantly improve hyperoxia-induced angiogenesis damage and reduce the number of apoptotic cells in lung tissue (43).

Pericytes are cells that surround capillaries and veins throughout the body. Franco et al. (44) reported that pericytes can protect vascular endothelial cells from cytotoxicity. Covering vascular endothelial cells with pericyte prevents EVs from being phagocysed by vascular endothelial cells. Pericyte-dependent survival signals are forced by paracrine and autocrine circulation involving VEGF-A expression. In addition, some studies have shown that the expression of VEGF in differentiated pericyte enhances the survival of endothelial cells and the stability of microvessels (45). In general, these findings suggest that the improvement of angiogenesis of MSC-EVs is not mediated directly by phagocytosis of vascular endothelial cells, but indirectly induced by phagocytosis of pericyte by EVs. These results indicate that VEGF protein and mRNA carried by EVS are very important for angiogenesis, and the specific mechanism needs further study (43).

In conclusion, MSC-EVs or MSC-Exos play a positive role in various diseases of respiratory system. Firstly, exosomal proteins and miRNA have powerful functions, which can reach lung injury tissues through their targeting and homing properties to treat oxidative stress, inflammation and vascular injury (46). Secondly, exosomes can be used as carriers to encapsulate drugs across the air-blood barrier and alveolar epithelial-endothelial barrier to reach some places that drugs cannot reach. Finally, exosomes also show potential in disease diagnosis. Exosomes released by infected cells

carry many pathogen-derived molecules and can be used as biomarkers of specific infectious factors. In addition to the frontier research directions such as exosomes and miRNAs, exosomes and autophagy, we believe that the combination of exosomes of infected cells and omics techniques to find biomarkers of various lung diseases may be the future research direction (47).

3 Diseases of circulatory system

It is well known that cytokines secreted by MSCs can enhance cardiomyocyte proliferation, reduce cardiomyocyte apoptosis, improve the microenvironment of damaged sites and repair damaged tissues (48).

3.1 MSC-EVs and MSC-Exos improve the related indexes of oxidative stress in circulatory system

Exosomes extracted from mesenchymal stem cells can improve myocardial dysfunction after hypoxia and myocardial infarction. Studies have shown that miR-182-5p carried by MSC-exos can treat myocardial ischemia-reperfusion (I/R) injury. MiR-199a-3p and miR-214 are similar to miR-182-5p in the response to I/R in rat myocardial cells, and both of them can improve the survival rate of myocardial cells and thus treat myocardial ischemia-reperfusion injury (49). At the same time, after hypoxia-induced injury, a low expression level of miR-182-5p was also observed in rat cardiomyocytes. Exosomal miR-182-5p engrafted NLRP3 inflammasome activation and cellular oxidative stress, thereby alleviating myocardial ischemia-reperfusion injury NLRP3 plays a key role in many diseases and can be activated by many types of agonists or risks. miRNA (miR-223) can bind to the 3 'UTR of NLRP3 to inhibit the inflammatory response caused by NLRP3 (50). On the other hand, overexpression of miR-182-5p downregulates Toll-like receptor 4 (TLR4), inactivates proinflammatory cytokines, TNF-α, and IL-6, thereby ameliorating liver I/R injury. In addition, miR-182-5p can also down-regulate TLR4 and inhibit ROS production to treat oxidative stress injury and apoptosis induced by atherosclerosis (51).

O'Brien CG et al. participated in the Seneca trial sponsored by the National Institutes of Health/National Heart Lung and Blood Institute. Peripheral blood mononuclear cells were successfully induced into induced pluripotent stem cells (IPSCs) and then differentiated into cardiomyocytes (ICMs). Using these AIC patient-specific MSCs, it was demonstrated that specific MSCs successfully reactivated iCMs after doxorubicin (DOX) injury. This effect is due to the active mitochondria carried by MSC-EVs (51).

Previous studies have shown that the re-expression of lncRNA alpha-2-macroglobulin antisense RNA 1 (Lnc RNA A2M-AS1) and Lnc RNA A2M-AS1 in myocardial infarction can significantly attenuate the hypoxia/resuscitation effect through the expression of inflammatory factor receptor IL1R2 (52). Oxygen (H/R)-induced cardiomyocyte apoptosis suggested that Lnc RNA A2M-AS1 may be involved in myocardial I/R injury.

AC16 cells were pretreated with exosomes and treated with ischemia-reperfusion. Cell proliferation was detected by CCK-8 assay, which showed that hMSCs-Exos treatment could reverse the decline in cell viability caused by ischemia reperfusion (53). Furthermore, H/R resulted in the apoptotic rate of AC16 cells, accompanied by downregulation of Bcl-2 protein levels and upregulation of Bax and Caspase-3 protein levels, which was attenuated in hMSCs-Exos treatment. hMSCs-Exos treated the content of LDH and MDA in H/R AC16 cells, but increased the content of SOD, thereby inhibiting oxidative stress. These results suggest that exosomes isolated from hMSCs can protect cardiomyocytes from H/R injury (54). It was further found that the level of Lnc RNA A2M-AS1-Exos was upregulated in AC16 cells cultured with hMSCs-Exos, alleviating H/R-induced apoptosis and oxidative stress in cardiomyocytes (54). Sánchez-Sánchez R et al. found that miR-4732-3p can induce apoptosis, ROS level and LDH activity in neonatal rat cardiomyocytes after OGD (glucose and oxygen deprivation model), prevent fibroblast migration and myofibroblast differentiation, induce *in vitro* and *in vivo* Angiogenesis. Intramyocardial injection of miR-4732-3p in exosomes in infarcted nude rats confers cardioprotection through functional and morphometric studies (55).

3.2 MSC-EVs and MSC-Exos in the treatment of circulatory vascular injury induced by oxidative stress

In recent years, a large number of evidences have shown that exosomes have protective effect in ischemic heart, which can alleviate myocardial I/R injury, promote cardiac regeneration and angiogenesis and inhibit fibrosis (56, 57). It has been proved that MSC-Exos overexpressing miR-486-5p can restore cardiac function after myocardial infarction in mice and non-human primates (58). Delivery of MSC-EVs containing miR-1505p in I/R rat model also alleviates poor myocardial remodeling (59). MSC-EVs-derived miR-21a5p induces cardiac protection in mice after I/R injury (60). adenovirus-transmitted miR-148a prevents ventricular remodeling in pressure overloaded mice (61). In mechanism, miR-210 was found to enhance myocardial vascularization in AMI rat model after myocardial transduction by up-regulating the expression of hepatocyte growth factor (62). Nevertheless, some miRNA in MSC-EVs may still be harmful to heart function, and the strategy of eliminating specific packaged miRNA molecules has been proved to improve the anti-apoptosis and angiogenesis of EVs (63).

Overexpression of Notch1 intracellular domain (N1ICD) in MSC-EVs can prevent apoptosis of CMS (cardiomyocytes) and promote cardiac angiogenesis under oxidative stress and ischemia injury. Notch plays an important role in cardiac repair after myocardial injury, Overexpressed MSC-EVs of N1ICD have good curative effect on angiogenesis of ischemic myocardium, proliferation of CMS (myocardial cells), improvement of cardiac function and fibrosis, Notch1 is strong for heart (64).

3.3 MSC-EVs and MSC-Exos in the treatment of cardiomyocyte apoptosis induced by oxidative stress

Mesenchymal stem cells can secrete a large number of soluble factors to promote myocardial cell proliferation, reduce apoptosis, improve ischemic microenvironment and mobilize endogenous cardiac stem cells by paracrine. However, studies have shown that although exogenous mesenchymal stem cells prefer to homing to myocardial ischemia sites, their survival rate in infarct areas is low (65). MSCs-Exos mediates cell-to-cell communication through horizontal transfer of bioactive RNA molecules and proteins (66). It is important that exosomes have good stability without the risk of chromosome loss and poor immune responses are rare (48). Therefore, MSCs-Exos is considered as an ideal drug delivery carrier and has great prospects in the treatment of oxidative stress-induced cardiomyocyte apoptosis.

3.4 MSC-EVs, MSC-Exos and autophagy of myocardial cells

Autophagy is involved in regulating the metabolic balance between synthesis, degradation and reuse of cellular substances. Both autophagy defect and overactivation will cause damage to homeostasis to some extent (67). Bafecycin A1 (Baf-A1) inhibited autophagy, and observed the effect of exosomes on autophagy. Compared with pure H_2O_2-induced autophagy, the expression of Beclin-1 and LC3B-II in exosomes + H_2O_2-treated cells increased and the expression of P62 decreased, while the protein levels of LC3B-IIBeclin-1 and P62 in H_2O_2 + exosomes + Baf-A1-treated cells were higher than those in H_2O_2 + exosomes and H_2O_2-treated cells. Therefore, autophagy induced by MSCs-Exos may be an important mechanism of cell protection after H_2O_2 (48). Autophagy is known to be associated with many pathways involving MAPK/mTOR and Akt/mTOR. Enhanced autophagy after hypoxia or ischemia injury has myocardial protection. Excessive ROS production in post-ischemia reperfusion stage can lead to autophagy. Matsui et al. reported that activation of MAPK pathway can induce autophagy, but activation of Beclin-1 pathway can induce autophagy, which may lead to cell death during reperfusion after ischemia (30). Therefore, ROS-induced autophagy is multifaceted (68).

At present, the research on the application of MSC-EVs and MSC-Exos in circulatory system diseases mainly focuses on microRNA. Numerous studies have found which microRNA in exosomes has a therapeutic effect on circulatory system diseases through sequencing technology. For example, miR-182-5p of MSC-Exos can improve myocardial I/R injury through the expression of GSDMD (51), miR-21a5p derived from MSC-EVs induced cardioprotection in mice after I/R injury (60), etc. Exosomes are natural carriers of bioactive molecules, and using them as carriers of drugs or siRNA to control gene expression and accelerate disease recovery may be a research hotspot in the future of exosomes in the circulatory system (69).

4 Diseases of digestive system

Oxidative stress is the main pathogenic phenomenon peculiar to liver diseases, which may lead to common liver diseases (70). Under normal circumstances, hepatocytes can balance the advantages and disadvantages of oxidative stress, control the level of oxidative stress within a reasonable range, and have the ability to regulate the balance of oxidants and antioxidants. However, due to the damage caused by toxins, there will be an imbalance between these particles. Oxidative stress is caused by mitochondrial dysfunction of hepatocytes, which leads to ROS production. This will not only induce irreversible changes in lipid protein and DNA content, but also regulate the pathway of controlling normal biological function (71). Studies have shown that MSCs-Exo can produce beneficial effects in animal models of various liver diseases, including liver injury, liver fibrosis, ischemia-reperfusion and so on.

4.1 MSC-EVs and MSC-Exos improve the related indexes of oxidative stress in liver injury

MSC-Exos can be used as an antioxidant to oxidative stress in mice with liver injury. *In vitro*, Hiroaki Haga et al. evaluated the effects of MSC-EVs on ROS production and NF-kB activity in normal mouse stem cells induced by H_2O_2 ROS activity was observed after 1 hour of H_2O_2. This activity was significant after 24 hours pre-incubation with MSC-EVs. The same NF-kB activity was also detected by MSC-EVs. Therefore, the results show that MSC-EVs can regulate the response to oxidative stress in liver IRI (72). GPX1 is an antioxidant that can induce oxidative stress injury induced by H_2O_2 to promote cell survival. When GPX1 in hucMSC-Exos is knocked out, the antioxidant activity of exosomes indicates that GPX1 is an important factor in hucMSC-Exos-mediated antioxidant activity and liver protection. Inducing increased GPX1 activity can induce liver injury and activate mitochondrial apoptosis pathway in hepatocytes (70). *In vivo*, hucMSC-Exos significantly inhibited the activation of oxidative stress products 8-OHdG and SOX9 in CCl4-induced liver tumor model. In CCl4-induced acute liver injury model, 8-OHdG also had more obvious antioxidant and liver protection effects than biphenyl ester (DDB) treatment, and hucMSC-Exos was a more effective antioxidant than DDB (73).

4.2 MSC-EVs and MSC-Exos in the treatment of liver inflammatory injury induced by oxidative stress

Macrophages and Kupffer cells are involved in regulating liver inflammation and hepatocyte death in liver. Studies have shown that exosomes can promote disease recovery by expressing inflammatory factors (72). MSC-EVs can reduce ROS production and overexpression of inflammatory cytokines such as IL-6 and IL-1B due to activation of the NF-kB signaling pathway. In addition,

MSC-EVs can inhibit inflammation in liver through NLRP12, which is a negative regulator of inflammatory activity *in vitro* immune system and others, and plays a role through attenuated NF-kB (72).

4.3 MSC-EVs and MSC-Exos in the treatment of hepatocyte apoptosis induced by oxidative stress

The results of clinical studies show that HUCMSCs transplantation can improve the blood supply of hepatocyte extensive necrosis and other clinical symptoms in decompensated cirrhosis (70). The levels of ALT and AST, the markers of hepatocyte injury, and the levels of Caspase-3 and Bcl-2, the activity of Bax and the anti-apoptosis protein increased after treatment with hucMSC-Exos. These results suggest that hucMSC-Exos treatment can improve liver I/R injury (74). In acetaminophen (APAP) and hydrogen peroxide (HP) induced hepatocyte injury models treated with hucMSC-Exos, cell activity increased, necrosis and apoptosis decreased, LDH activity decreased and ROS decreased. In CCl4-induced acute liver injury cells treated with hucMSC-Exos, Bax and activated caspase 3 expressed TUNEL positive cells can inhibit hepatocyte degeneration and hepatic lobules at the same time, and even partially save the life of mice in acute liver injury model. It is confirmed that hucMSC-Exos can induce acute extensive liver injury induced by CCl4 (73). ERK1/2 phosphorylation and Bcl-2 expression induced by glutathione peroxidase 1 (GPX1) hucMSC-Exos in mice. The phosphorylation of I-Kappa-B Kinase b (IKKb) and NF-kB was inhibited 24 hours after hucMSC-Exos treatment. The expression of Casp-9 and Casp-3 was inhibited HucMSC-Exos inhibited the I-Kappa-B Kinase b (IKKb) NF-kBcaspase 3 pathway and pNF-kB nuclear translocation in CCl4-injured hepatocytes in a dose-dependent manner and induced Bcl-2 expression and ERK1/2 phosphorylation to reverse oxidative stress-induced apoptosis (70).

4.4 MSC-EVs and MSC-Exos regulate iron death in the treatment of liver injury

Iron death is a regulatory cell death caused by lipid peroxidation. Iron death is very important for preventing various liver diseases, including liver fibrosis. HSCs iron prolapse has become the target of inhibiting liver fibrosis (75). Benzyl chloride 1 (BECN1) is the key regulator of iron sag (76). It was found that BECN1 enriched down-regulated GPX4 in both MSCs-EVs and MSC-Exos, which contributed to iron sagging, which was necessary to activate HSCs (77). An increase in BECN1 was detected after MSC-Exos treatment, and a decrease in GPX4 and alpha-SMA (HSCs-activated markers) was also found in fibrotic mouse livers and collagen deposition. Therefore, MSC-Exos containing BECN1 can induce BECN1/GPX4-mediated iron prolapse and activation of HSCs in mouse fibrotic liver. When BECN1 was knocked out, ROS expressed by GPX4 produced mitochondrial membrane potential. Therefore, BECN1 can induce iron poisoning by down-regulating GPX4. BECN1 overexpression can produce ROS and decrease mitochondrial membrane potential *in vivo* experiments also showed the same results (77).

In the current report, MSCs-EVs and MSC-Exos were not only able to down-regulate inflammatory factors and oxidative stress indicators in diseases of digestive system, but exosomes were also found to regulate iron death in liver fibrosis. Iron death, a novel type of programmed cell death, occurs in a wide range of injured cells, and there are numerous research points that can be explored, which deserve to be deeply investigated.

5 Urinary system disease

Combination of MSC-EVs and MSC-Exos transport with renal artery revascularization can improve renal function and structure and narrow oxidative stress, apoptosis, fibrosis and microvascular remodeling (78, 79). Renal artery stenosis (RAS) is very common in patients with chronic kidney disease. RAS patients are prone to renovascular hypertension and progress to end-stage renal disease (80). MSC-EVs have been shown to alleviate renal inflammation and microvascular damage and improve hemodynamics and function beyond stenosis in porcine RAS (81, 82). This suggests that MSC-EVs are effective in preserving stenosis.

5.1 MSC-EVs and MSC-Exos regulate renal oxidative stress-related diseases through mitochondria

Mitochondria regulate many functions of renal cells, including redox state, survival, proliferation and death. The damage of mitochondrial structure and function is often accompanied by oxidative stress, which is mainly due to the production of superoxide (83) and H_20_2 by complex I and III, which damages several components of mitochondria and forms a vicious circle of mitochondrial damage and oxidative stress. Mitosis can improve the revascularization results of experimental (84) and clinical RAS and protect renal function. Studies have shown that MSC-EVs and MSC-Exos play an important filamentous protective role in stenotic kidney, which improves mitochondrial density and mitochondrial swelling (85).

The important role of mitochondria in mammalian cells is to produce ATP through OXPHOS (86). Loss of a nuclear-encoded mitochondrial protein, TFAM, causes mtDNA depletion and OXPHOS (87, 88). After treatment of HK-2 with H_20_2, the basal respiration rate, the maximum respiration rate, the ATP production respiration rate and the standby respiration capacity level all made MSC-EVs reverse these phenomena. Therefore, MSC-EVs can function as mitochondria (89).

Faisal A Alzahrani and others found that MSC-Exos significantly decreased the levels of MDA,HIF-1 α, mRNA and NADPH oxidase 2 (NOX2) protein and increased the levels of three antioxidant enzymes and HO-1 mRNA. The changes of oxidative stress or antioxidant related parameters were more prominent after ischemia. This indicates that MSC-Exos can play a role by inducing

antioxidant activity and inhibiting oxidative stress in injured kidney tissue (90). Pallavi Bhargava et al. (86) used renal I/R injury model to evaluate the therapeutic effect of MSC-EVs. The results showed that the rate of renal tubular necrosis, the expression of KIM-1 and the number of apoptotic cells in I/R mice, And I/R mice showed higher levels of renal cytokines mRNAs (IL-6,IL-1 β and ICAM1) and serum cytokines (TNF-α and TWEAK) (91, 92). MSC-EVs treatment can reverse the levels of these cytokines.

5.2 MSC-EVs and MSC-Exos regulate related indexes of kidney oxidative stress

It is well known that most of the beneficial effects of MSCs are mediated by their exosomes containing miRNA, mRNA and LncRNA. These exosomal RNA are responsible for intercellular communication through which RNA-based information is transmitted to recipient cells (93). Interestingly, when exosomes were pretreated with RNase, the ameliorative effect of exosomes on renal ischemia-reperfusion injury was eliminated, which means that exosomal RNA has an ameliorative effect on oxidative stress in renal injury (94). In addition, Rafael S Lindoso et al. (95) reported that the ameliorative effect of MSCs-Exos on Renal ischemia-reperfusion injury and metabolic syndrome is related to the expression of some miRNA involved in apoptosis and hypoxia, which means that exosomes can improve their effects by post-transcriptional targeting of some genes in cells by exosomal miRNA Melatonin (Mel) preconditioning may induce MSCs to produce exosomes with higher expression of RNA vectors, which induce renal repair by inhibiting certain molecules involved in oxidative stress cell apoptosis and inflammation (90).

5.3 MSC-EVs and MSC-Exos in the treatment of apoptosis induced by oxidative stress

Renal ischemia-reperfusion injury may accelerate the development of chronic kidney (CKD). Renal ischemia-reperfusion injury releases free radicals and mitochondrial function induces apoptosis and inflammation (96, 97). The degree of renal function was evaluated by detecting BUN in plasma and creatinine in serum BUN and creatinine levels decreased sharply after 4 weeks of renal ischemia-reperfusion injury, but they were still higher than normal renal tissue. These elevated levels improved significantly after MSC-Exos preconditioning and creatinine levels returned to normal at 4 weeks. Therefore, the renal dysfunction after renal ischemia-reperfusion injury is relieved after MSC-Exos treatment, which means that MSC-Exos has broad prospects in the treatment of CKD (90). Exosomes can improve renal ischemia-reperfusion injury by interfering with apoptosis of renal cells. This inhibition of apoptosis can be evaluated by measuring the activity of caspase-3, the final marker of apoptosis. qPCR results showed that apoptosis markers Bax,PARP1 and caspase-3 were up-regulated and anti-apoptosis marker. Bcl2 was down-regulated in renal ischemia-reperfusion injury rats Bax,PARP1 and caspase-3 mRNA levels, and Bcl2 mRNA levels were significantly increased after treatment with MSC-Exos. These results suggest that the ameliorative effect of MSC-Exos on renal ischemia-reperfusion injury is related to the inhibition of apoptosis in damaged kidneys (90). In addition, MSC-Exos had similar anti-apoptosis effects on ischemia-reperfusion injury (98, 99) cisplatin-induced acute kidney injury (100, 101) and glycerol-induced acute kidney injury (102). This anti-apoptosis effect is also related to enhanced proliferation of renal tubular epithelial cells and improved renal function and structure (90).

5.4 MSC-EVs and MSC-Exos in the treatment of vascular injury induced by oxidative stress

Transcription factor Sox9 plays a key role in renal development, and its dysfunction can lead to severe renal dysplasia (103). It is reported that the improvement of AKI by MSC-Exos is mediated by up-regulating the expression of Sox9 in renal tubular cells (104). Injection of MSC-Exos in renal ischemia-reperfusion injury rats induced the expression of various angiogenic factors, resulting in the improvement of renal function (94, 105), suggesting that these angiogenic factors may be involved in exosomal-induced renal repair. Studies reveal the important role of bFGF, HGF and Sox9 in renal tubular regeneration after renal ischemia-reperfusion injury (106). The expression of these regeneration markers was also induced after treatment with MSC-Exos (104).

MSC-EVs and MSC-Exos have a dual role including regeneration and reduction of inflammation and oxidative stress in urinary tract diseases. It is rich in growth factors that can provide nutrients. At the same time, *in vitro*, mesenchymal stem cells can transfer many cytokines with anti-apoptosis, anti-inflammatory angiogenesis and immunomodulation properties into conditioned medium to promote the recovery of model animal diseases effectively. However, the safety and ethics of this therapy should be further explored and corrected in order to try to apply it to clinical practice (107).

6 Diseases of nervous system

Stem cell therapy shows great prospect in nervous system diseases. However, stem cell therapy is limited by its safety ethics or national legislation. Many evidences show that MSC-Exos and MSC-EVs are more effective than their parent cells in the treatment and recovery of nervous system diseases (108). EVs have many biological characteristics, including crossing the blood-brain barrier and the ability to resist freezing and thawing, which is beneficial for EVs to play a therapeutic role in nervous system defects (109). EV carries a variety of complex RNA and protein. EV has a good ability to regulate oxidative stress pathophysiology and immune response in nervous system diseases. Especially, the ability of miRNA transfer to target cells mediated by EVs plays a key role in antioxidant activity (110) and MSCs pretreated with H_2O_2 have better antioxidant activity (111). Studies have shown that EVs contain a series of up-regulated antioxidants miRNA, such as miR-215-5p,

miR-424-5p,miR-31-3p,miR-193b-3p and miR-200b-3p. This indicates that exosomal miRNA plays an important role in antioxidant stress (112).

6.1 MSC-EVs and MSC-Exos improve the indicators related to oxidative stress in the nervous system

Seizures have a disproportionate impact on patients with traumatic brain injury and stroke (113). ROS overproduction caused by oxidative stress is an important pathophysiological mechanism in human epilepsy. Oxidative stress in epilepsy-causing hippocampal neurons can lead to neuronal apoptosis, cell loss and mitochondrial function. Therefore, targeting the changes in the pathophysiology of oxidative stress in the hippocampus has a significant improvement effect on the disease (114). Electrophysiological disturbances are often manifested in neuronal function (115), depolarization responses lead to spontaneous firing and AP numbers, and input resistance can lead to impaired excitability of neuronal cells (116), especially CA1 pyramidal neurons, in Oxidative stress is particularly vulnerable during epilepsy. Improvement of neuronal membrane excitability after EVs treatment, suggesting the ability of MSC-EVs to restore hippocampal electrophysiology in cellular and animal models.

SAMPs are involved in oxidative responses and cellular homeostasis, including iNOS, HMGB1, HO-1, and Nrf2 (117). MSC-EVs treatment resulted in improvement of SAMPs, suggesting that MSC-EVs have excellent therapeutic effect on H_2O_2-induced oxidative neuronal injury. Furthermore, There are two types of glutamate receptors that control oxidative stress levels through mediated signal transduction. Glut 1 is also strongly associated with the proliferation and death of neurons after the cell is stimulated (117). Reversal of the expression of SAMPs, AMPA, and Glut1 after EVs treatment indicated that MSC-EVs attenuated seizure-induced oxidative stress in the mouse hippocampus.

Nrf2 is closely related to antioxidant, and the antioxidant effect of Nrf2 enables it to play a neuroprotective role in epilepsy and other neurological diseases through targeted therapy. The function of NRF2 is closely related to KEAP1, which plays a coordinated role in the expression of several target genes, such as NADPH quinone oxidoreductase 1(NQO1) and heme oxygenase 1(HO-1), which encode antioxidant mediators and have protective effects against hippocampal neuronal damage caused by seizures (118). MSC-EVs are rich in antioxidant miRNAs, and knockdown of Nrf2 abolished the antioxidant capacity of MSC-EVs against epilepsy-induced hippocampal injury, suggesting that the Nrf2 defense system is involved in the antioxidant effect of MSC-EVs in epilepsy (112).

Qiang Luo et al. pretreated hippocampal neurons with 10 μg MSC-EVs, and then with 100 μM H_2O_2, MSC-EVs pretreated the activities of FRAP, CAT, SOD and GSH-PX. Furthermore, ROS production in hippocampal neurons of H_2O_2 was assessed by flow cytometry, and a significant rate of ROS production was detected in the group pretreated with MSC-EVs. Experiments showed that H_2O_2 led to increased expression of 8-OHdG (DNA damage marker), 4-HNE (lipid peroxidation marker) and DT (protein oxidation marker), and EVs treatment significantly enhanced the expression of these markers, and immunofluorescence staining confirmed that MSC-EVs can process and repair DNA damage. These results suggest that MSC-EVs have a strong antioxidant capacity in hippocampal neurons in response to H_2O_2 (112).

Through miRNA sequencing technology, find and identify substances that may have antioxidant potential in MSC-EVs. Comparing the differentially expressed miRNAs between MSC-EVs and H_2O_2-derived MSCs-EVs, many miRNAs were found to be upregulated in H_2O_2-derived MSCs-EVs, such as miR-215-5p, miR-424-5p, miR-31-3p, miR- 193b-3p and miR-200b-3p (119). GO classification showed that exosomal miRNA target genes were closely related to antioxidant active molecules. miRNA transfection revealed that miRNA inhibitors reduced oxidative stress-induced 8-OHdG concentrations in hippocampal neurons. This suggests that these miRNAs in MSC-EVs exert an antioxidant effect on H_2O_2 in hippocampal neurons (112).

Calcium, as an intracellular messenger, is ubiquitous in oxidative stress (120). mitochondria are important organelles in the control of calcium homeostasis (121). MSC-EVs can restore seizure-induced hippocampal neuronal morphological changes and mitochondrial function. The expression of TOM20, FIS1, and COXIV after EVs treatment indicated that MSC-EVs could restore mitochondrial/fusion and respiratory chains, so calcium and mitochondrial changes are critical for maintaining the stability of neuronal function (122). These results indicated that MSC-EVs improved calcium transients and mitochondrial function in primary cultures in H_2O_2.

The MWM test, which measures cognitive ability, found that MSC-EVs-treated seizure mice had shorter escape latencies. These data suggest that MSC-EVs treatment promotes functional reconstitution of hippocampal neurons during epileptic chronic seizures (123). Qiang Luo et al. pretreated hippocampal neurons with MSC-EVs to induce the uptake of nanoparticles, and then used H_2O_2 cells to induce oxidative stress. The results showed that the activities of various antioxidant enzymes decreased and excessive ROS production (124). It is evident that MSC-EVs have a significant antioxidant effect on seizure-induced neuronal damage by reversing H_2O_2-induced oxidative stress (112).

6.2 MSC-EVs and MSC-Exos treat inflammatory injury of nervous system induced by oxidative stress

Astrocytes play an important role in the formation of blood-brain barrier. They can produce and express neurotransmitters and some neurotransmitter receptors In addition, astrocytes can biotransform exogenous compounds and help regulate ionization around neurons. Studies have shown that astrocytes can be activated by inflammation or ROS (125). Sexual astrocyte activation can enable mitochondrial function (126). There is an extensive interaction between Nrf2 and NF-κB, which has been shown to be involved in the regulation of transcriptional, anti-oxidative, and anti-inflammatory pathways, regulation of NRF2 and

NF-κB signaling pathway can reduce some inflammatory factors and improve the function of astrocytes (127).

MSC-Exos has a good therapeutic effect on inflammatory astrocytes and can improve a series of diseases caused by inflammatory astrocytes (128). MSC-Exos can enhance the cytotoxicity of astrocytes induced by LPS; The markers of reactive astrocyte proliferation, such as GFAP,C3,CD81 and Ki67, increased significantly after MSC-Exos treatment of inflammatory astrocytes. TNF α and IL-1 β in culture medium decreased after MSC-Exos treatment of LPS-induced astrocytes. These results indicate that MSC-Exos has a good effect on inhibiting LPS-induced decrease of cytotoxic astrocyte proliferation and inflammatory response (127).

Panpan Xian et al. used calcium imaging to study calcium changes in primary cultures of astrocytes. The data revealed that different groups of astrocytes had different fluorescent properties. MSC-Exos treatment of LPS-induced hippocampal astrocytes significantly enhanced their Ca^{2+} influx, and LPS resulted in faster changes in response rise time and decay time. It is worth noting that MSC-Exos has a significant therapeutic effect on astrocyte Ca^{2+} oscillation rate and mitochondrial dysfunction in patients with LPS (129).

In conclusion, mesenchymal stem cell exosomes can reduce inflammation and oxidative stress in nervous system diseases. Exosomes are closely related to the pathogenesis of central nervous system diseases, so exosomes have the potential to become unique biomarkers of nervous system diseases. In addition, exosomes can cross the blood-brain barrier, making them a new candidate for drug carriers for nervous system diseases.

7 Skin tissue trauma and repair

With the development of regenerative medicine, autologous mesenchymal stem cells can be cultured *in vitro* and then injected into vivo to promote the regeneration and repair of damaged tissues (130). More and more evidences show that exosomes have excellent therapeutic effects in various disease models besides stem cells. Exogenous skin aging is usually caused by various chronic injuries such as drinking, smoking and ultraviolet radiation. Cause skin aging based on the important role of ROS in photoaging. Protect skin from photoaging by producing ROS or inducing antioxidant defense (131, 132). MSC-Exos can inhibit oxidative damage of H_2O_2 keratinocytes, improve antioxidant activity, reduce oxidative reactivity and improve abnormal calcium and mitochondrial changes induced by oxidative stress. Subcutaneous injection of MSC-Exos can alleviate ultraviolet-induced skin tissue damage and inflammatory reaction in mice, inhibit cell proliferation and collagen deposition in skin of mice irradiated by ultraviolet radiation, alleviate oxidative damage of mice irradiated by ultraviolet radiation, improve antioxidant activity and alleviate oxidative reaction in mice. All in all, exosomes can promote wound healing and recovery through oxidative stress in various ways in the treatment of skin injury and photoaging (23, 132).

7.1 MSC-EVs and MSC-Exos in the treatment of photoaging injury induced by oxidative stress

It is well known that DNA damage is a marker of oxidative stress. Skin cells will produce ROS and DNA damage after oxidation (133). The results showed that MSC-Exos treatment could prevent ROS formation and DNA damage induced by oxidative stress in mouse keratinocytes.

R. S. Stern demonstrated that both MSC-EVs and Fb-EVs could proliferate cells and prevent cell cycle arrest induced by UVB and intracellular ROS levels induced by UVB radiation. In addition, the expression of MMP-1, the expression of Col-1, the expression of MSC-EVs and the enhancement of antioxidant activity of Fb-EVs in senescent cells after EVs treatment may be related to the up-regulation of GPX-1 gene expression (134, 135). Oxidative stress can lead to inflammation and inflammation can also induce subsequent oxidative damage (136). S. Candel et al. observed that MSC-Exos injection induced the expression of pro-inflammatory cytokines (TNF α IL-1 β and IL-6) in mouse skin after ultraviolet irradiation, which means that MSC-Exos alleviated inflammatory reaction and oxidative damage in mice exposed to ultraviolet irradiation (137).

MSC-EVs can transfer MSC-EVs through GPX-1 protein to achieve antioxidant effect. Higher levels of GPX-1 can be observed in EVs treated cells (70, 138). To elucidate the mechanism of EVs-dependent ROS, the expression of antioxidant protein GPX-1 after EVs treatment, but the expression of SOD1, SOD2 and catalase was not (139).

Keratinocytes are the main constituent cells of the epidermis and form an important skin barrier to prevent damage caused by ultraviolet radiation, water loss, pathogens, fungi and viruses (140). Studies have shown that Nrf2 is very important in regulating cell homeostasis, including antioxidant proteins, detoxification enzymes, drug transporters and many cytoprotective proteins (141). Regulation of Nrf2 pathway of keratinocytes to external oxidation is a promising treatment strategy for skin photoaging injury. The results of M. Schafer et al. showed that the recovery effect of MSC-Exos after oxidation was related to the down-regulation of Nrf2. By knocking down Nrf2, we can explore the detailed mechanism of MSC-Exos activity on oxidative keratinocyte reactivity (141). The results of Wang T et al. Show that MSC-EXOS can improve oxidative stress in both *in vivo* and *in vitro* experiments. Exosomes can improve oxidative stress injury of H_2O_2 pretreated keratinocytes at cellular level. Exosomes at animal level can improve DNA damage and mitochondrial changes of mouse skin after ultraviolet radiation. Exosomal therapy enhances the antioxidant capacity of skin as shown by iron ion antioxidant capacity and enhances the activity of glutathione POD or superoxide dismutase in cell and skin damage induced by oxidative stress. Therefore, MSC-Exos may be used as a potential skin nano-therapeutic agent to treat skin diseases or disorders caused by oxidative stress (23).

7.2 MSC-EVs and MSC-Exos in the treatment of chronic wound injury induced by oxidative stress

MSC-EVs not only has a broad prospect in the study of skin photoaging, but also has a good therapeutic effect on chronic skin injury. Diabetic ulcer is a chronic trauma characterized by an inflammatory state of hypoxia and undernutrition caused by elevated blood glucose levels followed by an elevated hypoxia of oxidative stress leading to the death of fibroblasts and other skin cell types (142, 143). Parvaiz A Shiekh et al. pretreated HDFs with EVs for 6 hours and then put them in hyperglycemia in order to study the cell survival of HDFs (fibroblasts) under hyperglycemia (143). All EVs were able to protect HDFs from cytotoxic hyperglycemia at least 24 hours after treatment until at least 72 hours after determination. Interestingly, the results are even better than those of the positive control group-complete medium. They found that both AT-MSCs and HF-MSCs can oxidative stress HDFs metabolism and activity under hyperglycemia (144).

7.3 MSC-EVs and MSC-Exos in the treatment of skin vascular injury induced by oxidative stress

The biology of angiogenesis includes the proliferation and migration of endothelial cells and angiogenesis. New blood vessels can supply oxygen and nutrition to the wound site, so the formation of new blood vessels can determine the effect of chronic wound healing (145, 146). Many studies have shown that inflammatory reaction of oxidative stress tissue leads to stagnation of wound healing. In addition, limited vascular function and angiogenesis will cause hypoxia in chronic injuries and lead to prolonged wound healing (147). Xiao X et al. made wound models and performed healing operations on 8-week-old and 64-week-old mice. The results showed that the healing ability of old mice was weaker than that of young mice. Quantitative measurements showed that MSC-EVs had a high level of reepithelization and a low level of scar formation. The quantitative analysis of neovascularization density confirmed the beneficial effect of MSC-EVs on wound vascular reconstruction (148).

MSC-EVs play an important role in regulating functional recovery and treating wound healing. MiR-146a and Src play an important role in promoting angiogenesis and wound healing, thus dephosphorylating Src (148). Next-generation mRNA sequencing and proteomics showed that EVs contain many angiogenic genes and proteins including growth factors, nuclear receptors, adhesion molecules, protease inhibitors, matrix protein transcription factors and other factors involved in angiogenesis, suggesting that MSC-EVs have important angiogenic potential (149).

7.4 MSC-EVs and MSC-Exos for skin aging induced by oxidative stress

The pursuit of eternal youth to resist aging is the lifelong pursuit of human beings. Using MSC-EVs to reduce oxidative stress to achieve anti-aging effects, this research direction has become the focus of many scholars, and many research results have been achieved. H_2O_2 reduced the expression of skin moisture-related mRNAs (aquaporin-1 and aquaporin-3) and hyaluronic acid, while MSC-Exos reversed these effects, and H_2O_2-induced cellular senescence was also reproduced in fibroblasts. Matsuoka T et al. found that over time, the downregulation of SIRT1 leads to the acetylation expression of p53, thereby inducing the expression of p21, a downstream molecule of p53, delaying the cell cycle and leading to cell senescence. MSC-Exos enhanced these transduction systems, effectively blocking the increase in intracellular β-galactosidase activity and the accumulation of ROS (150).

The anti-aging effect of MSC-EVs and its mechanism are still unclear, especially the effect on endothelial cell (EC) senescence. Xiao X et al. investigated the *in vitro* effects of MSC-EVs on oxidative stress-induced aging of human umbilical vein endothelial cells (HUVEC), as well as the *in vivo* effects on natural aging and diabetic mouse wound healing models (151). In addition, they investigated its molecular mechanism using miRNA sequencing and phosphokinase antibody arrays. It is suggested that MSC-EVs can be used as nanotherapeutics through the miR-146/Src pathway. In senescent HUVECs, MSC-EVs treatment prevented senescence-induced functions and promoted angiogenesis, cell migration and proliferation ability, mitochondrial function, and ROS levels (148).

Src kinase family is inextricably linked with aging. Senescence can activate the Src kinase family, which leads to oxidative stress, lipid peroxidation and DNA strand breakage, and finally leads to fatal damage to cells. Studies have shown that Src family inhibitors (PP2) can completely block $H2O_2$-induced EC_S aging. MSC-Exos has the same inhibitory effect as PP2. MSC-Exos can prevent senescence by inhibiting the activation of Src (152).

Studies by Zou et al. have shown that H_2O_2 can induce senescence in HUVEC and human aortic myocytes by up-regulating the alternative splicing body, Oct4A (153). H_2O_2-induced EC senescence induces a DNA damage response that activates p53 and p16, two important cell cycle regulatory pathways (154). High glucose can induce the senescence of HUVECs through the expression level of mitochondrial sirtuin (SIRT3), the expression of SA-gal, and the tube-forming ability of HUVECs (155). Oxidative stress is involved in the pathogenesis of diabetic vascular abnormalities, inducing premature senescence through DNA damage, and streptozotocin (STZ)-induced diabetes can induce senescence in ECs (156).

The miRNAs carried by MSC-EXOS has a significant effect on the treatment of cell senescence and the promotion of angiogenesis. Studies have shown that four miRNAs, miR-146a-5pmiR-34b-3pmiR-28-3p and miR-412-5p, play a promoting role in the treatment of aging ECs (157). High expression of miR-146a in MSC-EVS, when miR-146a inhibitor was used, the effect of MSC-EVS on aging disappeared. In addition, Xiao X et al. found that miR-146a can inhibit Src phosphorylation and its downstream target cavelin-1, thus inhibiting aging (148).

A large body of evidence shows that ROS can induce or accelerate ECs senescence at multiple subcellular levels. In cultured senescent HUVECs, MSC-EVs treatment prevented oxidative stress-induced ROS formation and DNA damage. Mitochondria are not the main

source of ATP in ECs, but as ROS organelles, play an important role in the response of cells to pairs (158) and maintain the homeostasis of ECs (158). Experiments showed that aging-induced mitochondrial function of HUVECs could be improved by MSC-EVs treatment. Taken together, MSC-EVs have a comprehensive rescue effect on aging-induced endothelial cell function.

MSC-EVs and MSC-Exos have excellent therapeutic effects in both acute and chronic skin injuries. Exosomes can improve various functions caused by skin aging by inflammation and oxidative stress in skin injury. In recent reports, some scholars began to explore the effects of MSC-EVs and MSC-Exos on iron death and copper death induced by skin injury, which may be a research hotspot in the treatment of skin injury with exosomes in the future.

8 Diseases of motor system

ROS is involved in regulating many chondrocyte activities such as cell proliferation and matrix remodeling (159). Osteoarthritis (OA) is a joint disease characterized by cartilage degeneration and low-grade synovitis In damaged joints, chondrocyte homeostasis is gradually increased with the gradual increase of oxidative stress (160). MSC-EVs treatment of OA joint cells can down-regulate inflammatory factors and increase the synthesis of extracellular matrix of chondrocytes (160). Low levels of ROS play an indelible role in various physiological processes, but the formation of ROS can lead to tissue damage. The endogenous mechanism of MSC-EVs is activated by oxidative stress and can offset the influence of ROS. Therefore, oxidative stress induces both antioxidant reaction and autophagy, which leads to excessive production of active substances and oxidative damage to macromolecules (21).

Bone marrow mesenchymal stem cells are exposed to radiation, which will affect their survival and differentiation potential and lead to bone loss (161). Radiation can cause DNA damage on bone marrow mesenchymal stem cells, chromosome aberration, reactive oxygen species and cell senescence, which hinder the proliferation ability of bone marrow mesenchymal cells (162). In addition, radiation has a great influence on the differentiation of bone marrow mesenchymal stem cells, which will lead to the first choice of bone marrow mesenchymal stem cells to differentiate into adipocytes instead of osteoblasts, and finally lead to fat accumulation (163). Recently, some scholars have shown that BMSC-Exos can treat the effect of radiation on the differentiation of bone marrow mesenchymal stem cells. Liu et al. (164) transplantation of BMSC-Exos to save osteoporotic phenotype of recipient bone marrow mesenchymal cells improves bone through epigenetic regulation. In addition, Liu et al. (165) found that BMSC-Exos transplantation can prevent femoral head necrosis. The main preventive mechanism is to promote angiogenesis and prevent bone loss (166).

8.1 MSC-EVs and MSC-Exos regulate oxidative stress-related indicators in bone

It is known that 4-hydroxynonenal (HNE), a product of lipid peroxidation, can form a variety of protein complexes, which affect the activity and physiological function of OA chondrocytes. It is found that EVs treatment of OA chondrocytes can significantly form HNE complexes (160). Members of the POD (Prdx) family participate in the fight against ROS-induced cartilage injury. The exact mechanism of antioxidant protection of Prdx6 has not been clarified. Some scholars suggest that it may be directly scavenging low molecular weight peroxides and phospholipid peroxides. The protein expressed the activities of POD phospholipase A2 and lysophosphatidylcholine acyltransferase, which participated in the repair of cell membrane (167).

Mesenchymal stem cell injury is an important pathological mechanism of radiation-induced bone loss. Radiation can cause bone marrow mesenchymal stem cells to produce reactive oxygen species. Excessive ROS can lead to DNA damage (163, 168). Therefore, it is extremely important to treat radiation-induced bone loss and remove reactive oxygen species and DNA damage. Studies have shown that MSCs-Exos has excellent effects on oxidative stress and alleviating DNA damage. After irradiation, the kinds of reactive oxygen species will cause cell damage. DCF fluorescence in BM-MSCs is significant after exosomal treatment. The results of Western Blot also showed the expression of antioxidant proteins after co-incubation with exosomes. These results indicate that exudate can enhance the antioxidant capacity of BM-MSC after irradiation (166).

ATF6 is the target gene of miR-31-5P. When miR-31-5P is elevated, ATF6 does not promote endoplasmic reticulum stress of endothelial progenitor cells, which leads to apoptosis and calcification of endothelial progenitor cells. Recently, it has been reported that oxidative stress induces endoplasmic reticulum stress of endothelial progenitor cells (169). MSC-Exos down-regulates the expression of ATF6,CHOP,XBP1 and GRP78, suggesting that MSC-Exos has protective effect on endothelial endoplasmic reticulum stress induced by oxidative stress (170).

In the H_2O_2-induced NP cell injury model, Western blot showed that the levels of apoptotic proteins such as caspase-9 and caspase-3 were significant after H_2O_2 treatment, however, these were inhibited by exosome pretreatment and positive cells stained by TUNEL Significantly (17). Daisuke Sakai et al. used a microscope to observe the status of NP and annulus fibrosus, and a histological grading system to evaluate disc degeneration (171), and found slight changes in NP organization after exosome treatment. Using both X-ray and MRI examinations, exosome-treated disc height decreased more slowly at 2, 4, and 8 weeks, and IVDD treated with exosomes showed significantly higher intensity, suggesting that exosomes can delay Progression of IVDD (17).

8.2 MSC-EVs and MSC-Exos in the treatment of bone inflammation induced by oxidative stress

A great deal of evidence shows that inflammatory mediators can induce oxidative stress, which leads to the decrease of chondrocyte viability and the change of chondrocyte function (160). Proinflammatory cytokines produced by different joint cells can promote cartilage degradation. IL-1β stimulates OA chondrocytes to

produce inflammatory cytokines. MSCs-EVs, which can exert anti-inflammatory and anti-catabolic effects. IL-6 and different cytokines can induce collagenase to produce cartilage degradation (160) and inhibit the expression of type II collagen (172). EVs can release IL-6. MSCs-EVs also demonstrated the release of MMP-13, a major collagenase that degrades type II collagen and promotes the development of OA chondrocytes into a state of like differentiation (173). Therefore, EVs can not only produce inflammatory mediators, but also control the consequences of mediator activation of cells.

NLRP3/IL-1 β plays a key role in inflammation through TXNIP activation (174). In H_2O_2-treated NP cells, H_2O_2 was significantly associated with inflammatory activation of the genes IL-1 β,TXNIP and NLRP3, which were inhibited by exosomal preconditioning. Western Blot and cellular immunity also showed the same results indicating that exosomes attenuated H_2O_2-induced activation of TXNIP-NLRP3 inflammatory corpuscles (17).

8.3 MSC-EVs and MSC-Exos down-regulate bone oxidative stress injury through mitochondria

Exosomes have obvious protective effect on the deterioration of mitochondria, exosomes can down-regulate ROS level and decrease apoptosis of NP cells, which can be seen from the low expression of caspase-3 and caspase-9. In addition, exosomes successfully expressed NLRP3 and TXNIP, thus inhibiting the decomposition of IL-1 β (17). Although systemic delivery of exosomes is generally considered to be the simplest, biological distribution indicates accumulation in the liver, spleen and lungs (175). Particularly when the avascular nature of IVDD is considered, local delivery of the subplate region is considered to be a good alternative. Previous evidence *in vivo* and *in vitro* indicates that oxidation products are widely present in IVDD (176). Cardiovascular calcification induced by oxidative stress products (177) and apoptosis and calcification of endothelial progenitor cells. These studies suggest that oxidative stress is a common pathological condition for apoptosis and calcification, including endothelial progenitor cells (178).

TEM showed that exosomal treatment alleviated mitochondrial morphological abnormalities and mitochondrial cristae breakage and disappearance induced by H_2O_2. Exosomal pretreatment also inhibited the production of mitochondrial ROS in NP cells induced by H_2O_2 (17). Proteomics MSC-Exos showed that 10.7% of exosomal proteins originated from mitochondria and 14.3% of exosomal proteins participated in ATP binding. In addition, 3.8% of exosomal proteins were involved in metabolism. It is important that MSC-Exos are enriched in different parts of mitochondria, including mitochondrial inner membrane, envelope, matrix, outer membrane and nucleoids. All in all, these data suggest that MSC-Exos may provide NP cells with mitochondrial proteins. Damaged mitochondria can be recovered by this treatment (17).

The progression of degenerative NP cells is accompanied by matrix degeneration caused by inflammation (179, 180). In order to study whether MSC-Exos can enhance mitochondrial biogenesis, Pengfei Chen et al. discovered that 10.3% of exosomes were derived from mitochondria through proteomics. Molecular function showed that 15.4% of exosomal proteins were involved in ATP binding. The enrichment of GO pathway also showed that mitochondrial fragments including mitochondrial inner membrane, envelope, matrix, space outer membrane and nucleoid were enriched in MSC-Exos (181).

Mitochondrial injury induced by mitochondrial electron transport chain complex I inhibitor reveals the chondroprotective mechanism of exosomes and whether it is inhibited by mitochondrial function. The exosomes restored the normal appearance of mitochondria in the chondrocytes (182). Chondrocytes treated with exosomes also showed mitochondrial and mtDNA content. In addition, rotenone treatment significantly inhibited the production of mitochondrial ROS in chondrocytes, which was significantly inhibited by exon treatment. The intracellular ATP level of exosomes-treated chondrocytes was 21% higher than that of rotenone-treated chondrocytes in function. These results indicate that MSC-Exos provide mitochondrial proteins to chondrocytes and thus restore damaged mitochondria (181).

The targeting and homing ability of exosomes is particularly important for their treatment in the locomotor system. Exosome hydrogel scaffolds are able to penetrate deeper into the wound and connect to the injury site when treating injuries in the locomotor system, and exosomes are homed to the peri-wound area for a more effective therapeutic effect. The combination of exosomes and materials and translation to clinical applications may be a hotspot for future research (183).

9 Senescence

Aging has been a topic of great concern to human beings. Aging is accompanied by the accumulation of aging cells, which changes the communication between cells and damages the homeostasis of tissues and the regeneration potential of organs (184). Recently, MSC-EVs have proved to be more effective and challenging than current stem cell-based treatments. Extracellular vesicles contain cell-specific proteins, lipids and nucleic acids, which may be released and absorbed by all types of cells to induce functional changes through horizontal transfer of their cargo. Non-aging mesenchymal stem cells cultured in low physiological oxygen tension (3%) to premature aging mesenchymal stem cells. Extracellular vesicles cultured in high oxygen (the usual oxygen culture condition is 21%) have many beneficial characteristics (185). Free radical theory holds that oxidative stress induced cell damage is one of the main causes of various senile diseases, which changes the biological structure and function (186). In particular, the cells treated with H_2O_2 will produce a large amount of reactive oxygen species (ROS), and the excessive accumulation of ROS will damage the macromolecular function and membrane system of cells, which will irreversibly damage various senile diseases and senescence (187, 188).

9.1 MSC-EVs and MSC-Exos inhibit senescence through ROS

Aging induces many cell disorders. The regeneration of mesenchymal stem cells in old age is a hot spot in regenerative medicine research in recent years. MSC-EVs have become a new tool for stem cell regeneration because of their systemic effect and

safe gene transfer ability (189). In the present study, the role of aging-related ROS in the function and regeneration of mesenchymal stem cells in infant EVs was studied. The data clearly showed that the elderly MSCs showed down-regulation of SOD1 and SOD3, which led to ROS elevation and down-regulation of MEK/ERK pathway, which was related to the impaired ability of MSCs to necrotic area in flap model. In addition, edaravone or co-overexpression of SOD1 and SOD3 can save ROS increase and cell senescence of mesenchymal stem cells in old age, thus improving their function (190). It is worth noting that EVs derived from infant bone marrow mesenchymal stem cells in type 1 and type 2 diabetic mice can revitalize elderly bone marrow mesenchymal stem cells by inhibiting ROS production and accelerating cell aging to promote proliferation and *in vivo* function (191).

EVs are a powerful tool that not only inhibits ROS production, but also restores altered intercellular communication, improves stem cell function and stem cell quality, and thus delays stem cell failure in aging. It has been shown that treatment of senescent MSCs with non-senescent MSC-EVs can induce glycolytic oxidative phosphorylation of SA-β-galactosidase activity and over-expression of pluripotent factors (OCT4, SOX2, KLF4 and cMYC or OSKM). In addition, the cargo of these EVs induces up-regulation of miR-302b and HIF-1 α levels in target cells. It is concluded that miR-302b triggers the up-regulation of HIF-1 α and activates different pathways to delay premature senescence, improve stem and transform energy metabolism into glycolysis (192).

9.2 MSC-EVs and MSC-Exos cell proliferation inhibits senescence

miR-302b can proliferate cells and protect cells from oxidant-induced death of human mesenchymal stem cells (193). Kim, J. Y et al. studied ROS levels and cell death of human dental pulp stem cells (hDPSCs) after EVs treatment. It was found that the cells cultured under physiological hypoxia showed ROS and apoptosis levels compared with those cultured under 21% oxygen. Interestingly, no changes in ROS levels were observed after treatment, and cell cycles parallel to these observations showed no difference in G0/G1 phase, S phase and G2/M phase after EVs treatment. Cells cultured at 3% O_2 showed higher levels in G0/G1 phase, S phase and G2/M phase, which indicated the overall proliferation of cells (191). Studies have shown that EVs can promote the function of aged AT-MSCs by inducing proliferation and up-regulating the expression of damaged cytokines, thus promoting the necrotic area of aged AT-MSCs in type 1 and type 2 diabetic mice. EVs significantly increased the proliferation of AT-MSCs in the elderly and increased the number of β-gal positive AT-MSCs in the elderly. Due to the up-regulation of SOD1 and SOD3 protein expression, the accumulation of ROS in aged AT-MSCs cells was induced by the addition of EVs. In addition, the addition of EVs up-regulated the expression of wound healing related cytokines (SDF-1VEGFAng1 and Flk1) in the elderly AT-MSCs. Transplantation studies show that the ability of aged AT-MSCs to show obvious necrotic area of flap mice after adding EVs is similar to that of infant AT-MSCs (191). Impaired expression of growth factors responsible for homing (SDF1) and angiogenesis (VEGF, Ang1, bFGF) was observed in elderly AT-MSCs. These growth factors are involved in regulating the function of EC and endothelial precursor cells (EPC) (191).

10 Immune

Studies have shown that MSC-EVs and MSC-Exos play both immune activation and immunosuppressive functions in cancer. The immune activation of exosomes mainly depends on the antigen presentation of exosomes, and the immunosuppression of exosomes mainly depends on the ligand protein and miRNA carried by exosomes (194). It has been reported that the existence of exosomes can provide several different mediators for cancer cells to form tumorigenic microorganisms, which belongs to the immunosuppressive effect of exosomes in cancer (195, 196). Many scholars have taken this as the breakthrough point to study cancer treatment. For example, Giovanna Andreola reported that FasL-positive exosomes released by melanoma cells can induce apoptosis of FasL-mediated Jurkat T lymphocytes (197). Phenotypically similar pro-apoptotic exosomes in the plasma of cancer patients indicate that these exosomes have a potential role in regulating host immunity and that they may become prognostic markers (198). Exosomes not only play an immunosuppressive role, but also play an immune activation role through other mechanisms. For example, exosomes released by mycobacterium-infected macrophages contain components that promote activation of adjacent uninfected macrophages (199) and many other exosomes-mediated to promote immune responses during infection with different types of microorganisms (200). In addition, synovial fibroblasts from patients with rheumatoid arthritis have been shown to release exosomes containing membrane-bound TNF-alpha that inhibit activation-induced cell death in CD4 T cells (201). Many of these studies suggest that exosomes may operate simultaneously in congenital and adaptive immune activation (202, 203) (Figure 2).

11 Conclusions and future directions

In conclusion, MSC-EVs and MSC-Exos are closely related to the regulation of oxidative stress injury in many systemic diseases. It has been fully verified in both cell model (Table 1) and animal model (Table 2). Oxidative stress can cause inflammatory factors to damage mitochondrial function, inhibit cell proliferation and enhance cell apoptosis. Inhibition of oxidative stress injury is of great significance to the treatment of various systemic diseases (233).

In the study of the mechanism of stem cell exosomes, iron death, copper death, autophagy and proteomics may be the hot spots in the future. In the application research of stem cell exosomes, hydrogel, collagen and other materials combined with exosomes to form composite scaffolds have been carried out by many scholars in cell experiments and animal experiments, but its clinical transformation has not yet been realized. Verifying its human safety and ethical rationality is the direction that needs to be worked hard now.

Regulatory proteins and miRNA in MSC-EVs and MSC-Exos are the core of treatment. However, the same protein and miRNA seem to show different results in different studies (234). At present, no research has shown the reason for this result. Potential effects of stem

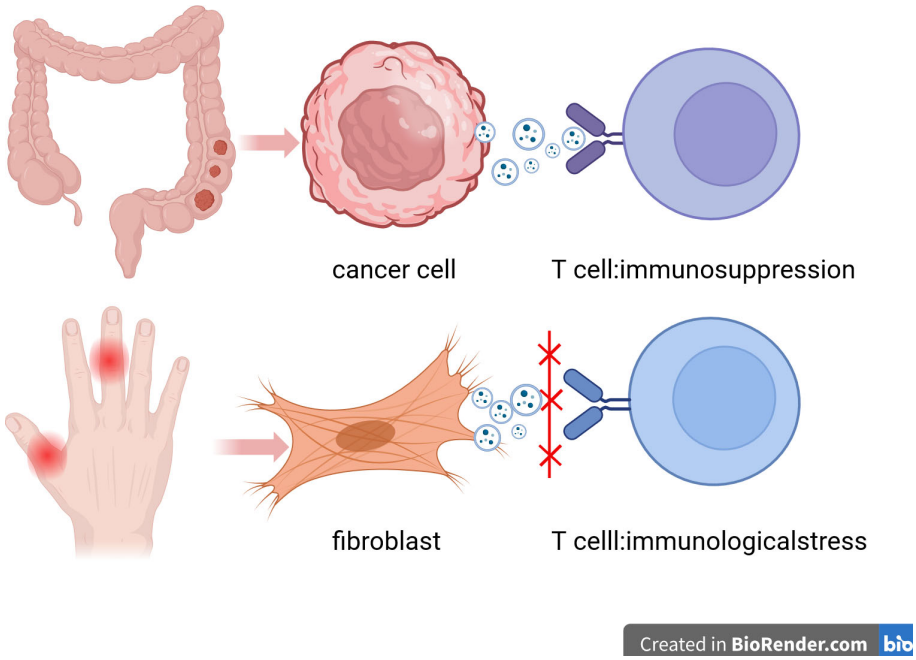

FIGURE 2
Immunosuppression and immune activation of exosomes. This figure describes the immunosuppressive effect of exosomes in cancer and the activation of immune response in synovial fibroblasts of patients with rheumatoid arthritis. Exosomes can help tumor cells escape killing by using human immunosuppressive mechanism. Exosomes can also be used as blockers of immune checkpoints to activate the immune response of T cells to kill tumor cells .

cell origin, such as the age of stem cell donors, may be related to the production of oxidative stress and inflammatory mediators, which may affect their immunomodulatory function (235). It may also be caused by sex, for example, female MSCs cause greater immunomodulatory effect than male MSCs (236). For example, some studies have not clarified the effective proteins in MSC-EVs and MSC-Exos. Although researchers have used proteomic databases to show which antioxidant proteins MSC-EVs and MSC-Exos contain, further work is needed to isolate and accurately identify these proteins (237). In addition, only one dose was used in some studies, and it is necessary to explore the possible dose-dependent protective effects of MSC-EVs and MSC-Exos (17).

At present, many functions of MSC-EVs and MSC-Exos have been discovered one after another, but these studies also have some limitations, MSC-EVs and MSC-Exos may have different inhibitory effects in different cell species and animal species (16). In addition, the differences in the isolation and application steps of EVs in different studies may lead to different effects of the same regulatory protein and miRNA. In order to ensure the repeatability of the effects of MSC-EVs and MSC-Exos, it is necessary to explore and

TABLE 1 Cell model: Summary of the mechanism of MSC-EVs and MSC-Exos in the treatment of oxidative stress-related diseases.

Disease	Disease Model	Source of MSC	Excreta	Target Cell	Oxidative stress mechanism	Therapeutic Effect	Reference
liver injury	APAP and HP injury-induced liver cells	BM(rat)	Exos	HepG2	ROS↓	Necrosis and apoptosis↓ Cell viability↑LDH activity↓	(204)
ALI	Erastin-induced ferroptosis	BM (mice)	Exos	Hepatocyte	Nrf2↑Keap1↓ROS↓ GSH↑MDA↓	GPX4↓SLC7A11↓5-LOX↑Fe^{2+}↓ Cell death↓	(205)
liver fibrosis	CCl4 induced liver fibrosis in mice	HUC (human)	Exos	human HSCs line LX-2	BECN1↑xCT↓,GPX4↓ROS↑ p-MLKL↑LC3B↑	Cell death↑α-SMA↓	(77)
liver injury	$CCl4/H_2O_2$-Induced liver cell	HUC (human)	Exos	L02 Liver cells	ROS↓MDA↓GPX1↑ Mitochondrial membrane potential↓GST↓	Cell viability↑Cell apoptosis↓ p-ERK1/2↑bcl-2↑p-IKKB↓p-NFkB↓ Casp-9↓Casp-3↓	(70)
Ischemic cerebrovascular disease	tMCAO mouse	BM (mice)	Exos	H/R-injured ECs	miR-132-3p↑RASA1↓ RAS↑P-PIK3↑ p-Akt/Akt↓ROS↓ peNOS/eNOS↓	Apoptosis↓ Paracellular permeability↓ ZO-1↑ Claudin-5↑	(206)

(Continued)

TABLE 1 Continued

Disease	Disease Model	Source of MSC	Excreta	Target Cell	Oxidative stress mechanism	Therapeutic Effect	Reference
Myocardial i8509schaemia reperfusion	H_2O_2-induced MIRI	BM(rat)	Exos	H9C2(rat)card-iomyocytes	ROS↓	Cell viability↑apoptosis ↓ Beclin-1↑LC3B-II↑p62↓ Autophagosomes↑ Autolysosomes↑ p-mTOR/mTOR↓p-Akt/Akt↓ p-AMPK/AMPK↑	(48)
COVID-19	LPS-induced A549 cells and PBMC	HPP	Evs	Alveolar basal epithelial cell	/	IL-8↓	(28)
ALI	LPS-induced ALI	UCB (human)	Exos	NR8383 cell	SOD↑GSH↑ MDA↓	miR-22-3p↑FZD6↓TNF-α↓IL-1β↓ IL-6↓Proliferation activity↑ Apoptosis↓	(32)
Neonatal hyperoxic lung injuries	H_2O_2-induced lung injury	UCB (human)	Evs	Rat lung epithelial cell line L2	/	VEGF↑ Cell survival↑	(43)
Radiation-induced lung injury	Radiation-induced injury	HP (human)	Evs	HUVECs	DNA injury↓ γ-H2AX↓	Senescent cells↓ATM↓P53↓P21↓ Inflammation-and fibrosis-related genes↓ Senescent fibroblast cells↓miR-214-3p↑	(207)
ALI	LPS-induced lung injury	UCB (human)	Evs	RAW 264.7	Nrf2↓HO-1↓ HMGB1↓8-OHDG↓	Promoted the polarization of macrophages from the M1 to the M2 phenotype CD86↓Arg1↑TLR4↓TNFα↓IL-1β↓	(208)
OA	IL-1β-induced oxidative stress	AD (human)	Evs	Chondrocytes	Oxidative stress↓ prdx6↑	LC3B↑IL-6↓MMP-13↓atg5↑P62↑ The number of associated autophagosomes↑	(160)
IDD	H_2O_2-induced oxidative stress	VB (human)	Exos	EPCs	/	Runx2↓caspase-3↓caspase-7↓ caspase-9↓miR-31-5p↑ATF6↓ ER-stress-related apoptosis and calcification↓	(170)
IDD	H_2O_2-induced inflammation	C57BL/6 mice	Exos	NP cell	Mitochondrial ROS production↓	caspase-9↓caspase-3↓iNOS↓IL-6↓ MMP3↓MMP13↓SOX9↑Col2a1↑ IL-1β↓TXNIP,NLRP3↓	(17)
Radiation bone loss	Irradiation-induced injury	BM (rat)	Exos	BM-MSC	ROS↓ SOD1↑ SOD2↑CAT↑	γ-H2AX↑Cell proliferation↑ Rb↓p53↓p21↓p16↓PPARγ↓ Ebf1↓ RUNX2↑ OPG↑Calcium deposition↑	(166)
Degeneration of cartilage	IL-1β-stimulated chondrocyte model	BM (rat)	Exos	Chondrocyte	Mitochondrial ROS↓	MMP13↓ADAMTS-5↓ COL2A1↑ATP↑ Restored mitochondria exhibiting a normal appearance Increased mitochondrial mass and mtDNA content	(181)
Epilepsy	H_2O_2-induced injury	UCB (Human)	Evs	Hippocampal neurons	FRAP↑CAT↑SOD↑ GSH-PX↑ROS↓DT↓ 8-OHdG↓4-HNE↓	SAMPs↓iNOS↓HMGB1↓HO-1↓Nrf2↓ Late apoptosis↓Nuclear translocation↓ Amplitude (ΔF/F) ↑MMP↑ TOM20↓FIS1↓COX IV↓	(112)
Neurological diseases	LPS-stimulated hippocampal astrocytes	UCB (Human)	Exos	Hippocampal astrocytes	Nrf2,Keap1,HO-1↓	Cell viability↑GFAP↑C3↓CD81↓ki67↓ TNFα↓IL-1β↓MMP↑p-P65/P-65↓ NF-κB↓GFAP↓ Nuclear translocation of Nrf2 and P-65 ↓	(127)
Diabetic ulcers	HDF/H_2O_2+HDF-induced Glucose (150mM) hyperglycemic	HF (Human)	Evs	HDF	/	The survival rate of AT-MSC and HF-MSC treated HDF cells under high glucose condition was higher than that of the positive control group.	(144)
Oxidative stress	H_2O_2-induced NHDFs	AD (Human)	Exos	NHDFs	Cell viability↑	Aquaporin 1↑Aquaporin 3↑ Hyaluronic acid↑SIRT1↑	(150)
Senescence	H_2O_2/HG-induced HUVECs	HUC, AD,BM (Human)	Evs	HUVECs	Mitochondrial ROS↓	SASP↓IL-1α↓IL-6↓IL-8↓ Aging HUVECs↑ miR-146a↑OCR↑	(148)
Photoaging	UVB radiation-induced dermal fibroblast photoaging	HUC,DF (Human)	Evs	HDFs	ROS↓ GPX-1↑	MMP-1↓,Col-1↑ SA-β-gal-positive cells↓ EVs increased cell proliferation and prevented UVB-induced cell cycle arrest	(139)
Fibrosis of the Kidney	Enicillin+streptomycin/ CO_2-induced Human renal proximal tubule epithelial cells	HP (Human)	Evs	HK-2	OXPHOS↑ ATPB↑SDHB↑COX IV↑ ROS↓	Restored morphological alterations of mitochondrial damage.	(209)
Oxidative stress	H_2O_2-induced keratinocytes	HUC (human)	Exos	Keratinocytes	DCF↓8-OHdG↓ FRAP↑GSH-PX↑SOD↑	GLUT1↓Calcium influx↑MMP↑ NRF2↓KEAP1↓HO-1↓NQO1↓	(23)

(Continued)

TABLE 1 Continued

Disease	Disease Model	Source of MSC	Excreta	Target Cell	Oxidative stress mechanism	Therapeutic Effect	Reference
Chronic granulomatous disease	Chronic granulomatous disease patients' neutrophils of their heparinized blood	AD (human)	Exos, Evs	Neutrophils in heparinized blood	CGD↑ SOD↑	Average number of yeasts that neutrophils ingested↑NBT↓	(210)
Pregnancy inflammation	LPS/AF-MSC-induced inflammatory trophoblast cells	AF (human)	Exos	HTR8/SVneo HTR8/Svneo	Inhibition of miR-548e-5p induced oxidative stress and reduced MMP in HTR8/SVneo cells.	NF-κB↓TRAF6↓IRAK1↓IL1β↓IL6↓IL8↑ miR-146a-5p↑miR-146a-3p↑ miR-146b-5p↑miR-548e-5p↑ AKT↓JNK↓ERK1/2↓P38↓	(211)
AKI	H_2O_2-induced HK-2	BMSC (mice\rat \ human)	Evs	HK-2	/	TFAM/TOM20protein,mtDNA↑Mitochondrial integrity in injured HK-2 cells↑ATP production respiration rate↑	(89)
Ischemia and reperfusion	Primary hippocampal cells and OGD/R	BMSC (rat)	Exos	Hippocampal cells	ROS↓ SOD↓	Nrf2↓GPx↓DJ1↑OP A1↑Mfn1↑Mfn-2↑ LRRK2,PINK↓	(212)
AD	AβOs-reduced rat hippocampal neurons	BMSC (rat)	Evs	Hippocampal neurons	H_2O_2↓O_2↓ROS↓	MSCs blocked the reduction in PSD-95 levels and loss of synapses induced by AβOs	(213)
Injury of isolated hearts after cold storage ex vivo	The H9c2 rat cardiomyoblast cell line subjected to cold storage	BMSC (human), AD (human)	Exos	Cardiomyoblast cell	ROS production↓	Circadian pathways↑Mitochondrial activity↑Per2↑ Left ventricular function↓Apoptosis↓MtMP was preserved.	(214)
AMI	H/R induced human cardiomyocyte AC16 cell line	BM (human)	Exos	Heart muscle cell	LDH,MDA↓ SOD↑	Bcl-2↑ Baxc-caspase 3↓ Lnc A2M-AS1↑	(54)
Acute Myocardial Infarction(AMI)	Oxygen/Glucose Deprivation (OGD) Procedure-subjected NRCM	DP (human)	Evs	NRCM	ROS,LDH↓	Apoptosis↓ α-SMA↓Collagen protein↓	(55)
AIC	DOX/specific-induced pluripotent stem cell–derived iCMs	BM (human)	Evs	iCMs	ROS↓	contractility↑ATP↑Mitochondrial biogenesis↑Cardiomyocyte viability↑iCM viability↑Attenuated apoptosisapoptosis was inhibited by MSC-EV.	(215)
MI	Notch1 gene-deleted/ N1ICD-over expressed C-MSCs	CMSC (mice)	Evs	CMVECs HAECs	/	The apoptosis of endothelial cells↓CM↓	(64)
Aging	Elderly AT-MSCs	AT	Evs	Aging AT-MSCs	ROS↑	ROS↑IL6↑IL8↑CCL5↑CCL3↑ SDF1↓VEGF↓Ang1↓bFGF↓OCT4↓	(191)
Aging	Elderly MSCs	DP	Evs	Aging MSC	OXPHOS↓	SA-β-galactosidase↓ SOX2↓KLF4↓cMYC↓ OSKM↓miR-302b↑HIF-1α↑Glycolysis↑	(192)
Urinary stone	Oxalate and COM crystals-induced HK-2 cells	HUC (human)	Evs	HK-2 cell	LDH↓H2O2↓ MDA↓ROS↓	HK-2 cells viability↑ Cytoplasmic and nuclear N-cadherin↓ ZO-1↑	(216)
SS	Myeloid-derived suppressor cells	OE	Exos	Suppressor cells	ROS↑CD40↓CD80↓ CD86↓MHCII↓	Proliferation of MDSCs↑CD4+T↓ Arginase activity↑NO↑	(217)
Hypoxia-Reperfusion injury	H/R-induced cardiomyoblasts (H9c2)	BM(rat)	Exos	H9c2 cells	miR149-5p↑let-7c-5p↑	β-catenin↑ Faslg↓	(218)
Ischemia/ reperfusion injury	Lung I/R model and *in vitro* H/R	BM (mice)	Exos	Primary Lung Microvascular Endothelial Cells	PTEN↓PDCD4↓	Lung wet/dry weight ratio↓ M1 polarization↓ M2 polarization↑	(37)
Diabetic retinopathy	STZ-established diabetic retinopathy	HUC (human)	Evs	.	ROS↓MDA↑SOD↑ NRF2↓GPX1↑NQO1↑ HO-1↑	/	(219)
Heart Failure	oxygen–glucose deprivation (OGD)-induced damages to HL-1 cells	BM (mice)	MV, EV,CM	HL-1 cells	SOD↑GSH-PX↑Bcl2↑ IκBα↓p65↓LDH↓MDA↓ SOD↑GSH-PX↑Bax↓ Cleaved caspase-3↓Bcl2↑ GSHPX↑	/	(220)
Neutrophil function and apoptosis	human adipose tissue MSCs-isolated Exosomes and CM	AD (human)	Exos and CM	Neutrophil	ROS↑ Apoptosis of neutrophils↓	Phagocytosis percentage↑ Phagocytosis index↑	(221)

(Continued)

TABLE 1 Continued

Disease	Disease Model	Source of MSC	Excreta	Target Cell	Oxidative stress mechanism	Therapeutic Effect	Reference
PD	6-OHDA-induced PD cell	HUC (human)	Evs	Neuroblastoma cell line SH-SY5Y	SOD↑MDA↓ ROS↓miR-181a-2-3p↑	EGR1↓NOX4↑ SH-SY5Y cells↑Apoptosis↓	(222)
SCI	LPS-induced differentiated PC12 cells	BM (rat)	Exos	PC12 cells	EXO-TCTN2↑ SOD↑MDA↓ miR-329-3p↑	IL-6↓TNF-α↓Bax↓Bcl-2↑ MEG3-WT↓WT-IGF1R 3' UTR↓	(223)
Hippocampal damage due to diabetes	STZ-induced Hyperglycemia	BMSC (rat)	Exos	Primary rat astrocytes	TNF-α expression↓ miR-146a↑IRAK1↑ TRAF6↑ NF-κB expression↓	Diabetic wound healing ↑	(224)
MI	Trypsin and collagenase II-induced MI	BM (human)	Exos	NRCMs	MIF↑LVEF↑LVFS↑ The level of ROS↓	Apoptosis of NRCMs ↓ The scar size in MI↓Infarct size↓	(225)

BM (Bone marrow), HUC (human umbilical cord), OE (Olfactory ecto), DP (dental pulp), HPP (Human postpartum placentas), UCB (human umbilical cord blood), AF (amniotic fluid), AD (adipose tissue), VB (vertebral body), HP (Human placenta), DF (dermal fibroblast), HF (hair follicle), Acetaminophen (APAP), hydrogen peroxide (HP), Acute liver injury (ALI), Glutathione-S-transferase(GST), Hypoxia/reoxygenation (H/R), Transient middle cerebral artery occlusion(tMCAO), Myocardial ischemia reperfusion injury (MIRI), Peripheral blood mononuclear cells (PBMC), Line of rat pulmonary macrophages(NR8383)cell, Osteoarthritis (OA), Intervertebral Disc Degeneration(IDD), Endplate chondrocytes (EPCs), Nucleus pulposus (NP), Mitochondrial O2 consumption rate(OCR), Acute Kidney Injury(AKI), Oxygen-glucose deprivation/reperfusion (OGD/R), Alzheimer's disease(AD), Amyloid-β-peptide(AβOs), mitochondrial membrane potential (MtMP), Acute Myocardial Infarction(AMI), Neonatal rat cardiomyocytes(NRCM), Cardiomyopathy(AIC), Cardiomyocytes(iCMs), Myocardial infarction(MI), Human aortic endothelial cells (HAECs), Mouse Aortic Endothelial Cell (CMVECs), Sjogren's syndrome (SS), Streptozotocin(STZ), Parkinson's disease (PD), 6-hydroxydopamine (6-OHDA), Traumatic spinal cord injury (SCI), Neonatal mice cardiomyocytes (NRCMs). ↓, decline; ↑, increase. /, this mechanism is not included.

TABLE 2 Animal model: Summary of the mechanism of MSC-EVs and MSC-Exos in the treatment of oxidative stress-related diseases.

Application	Model	MSC Source	Excreta	Effect of MSC treatment	Antioxidant mechanisms	Reference
PD	6-OHDA-induced PD (mouse)	In mouse brain tissue SN	Evs	miR-181a-2-3p↑EGR1↓ NOX4↓p-p38↓	Contralateral rotation↓α-syn↑4-HNE↓ Dopaminergic neurons↑TH expression levels↑	(222)
SCI	Contusive SCI (rat)	BM(rat)	Exos	TCTN2↑GFAP↓CCL2↓	LPS-stimulated NHAs viability↓	(223)
Hippocampal damage due to diabetes	diabetic STZ-induced hyperglycemia (rat)	Endogenous BM/stromal cells	Exos	Oxidative stress↓ Synaptic density↑ TNF-α expression↓	Synaptic plasticity in the CA1 region↑	(224)
MI	An acute MI model was created by ligation of the LAD coronary artery in adult (rat)	BM(human)	Exos	MSC-exo↑ level of Mfn2↑ level of Fis1↓	Mitochondrial fragmentation↓ ROS generation↓	(225)
DM	STZ-induced DM (rat)	BM(rat)	Evs	Corticosterone↑ TSH↑	Thyroid H2O2 generation↓ NOX2 mRNA levels↓TPO activity↓ The pituitary 5′-deiodinase activity	(226)
AKI	AKI model(rat)	HUC	Evs	SOD↑Nrf2↑ARE↑	Apoptosis were mitigated TUNEL positive cells↓sNGAL levels↑	(227)
Liver injury	Partial hepatectomy and ischemic injury/ Carbon tetrachloride intoxication-induced liver failure(rat)	BM(rat)	Exos	ROS↓	liver regeneration rate ↑AST↓ALT↓bilirubin↓ Albumin↑PCNA↑cell death↓8-Ohdg↓	(204)
ALI	D-GaIN/LPS-induced ALI (mouse)	BM(mouse)	Exos	ROS↓P62↑	AST↓ALT↓TNF-a↓ IL-6↓MCP-1↓MDA↓GSH↑ Liver weight/body weight ratio↓	(205)

(Continued)

TABLE 2 Continued

Application	Model	MSC Source	Excreta	Effect of MSC treatment	Antioxidant mechanisms	Reference
Liver damage and iron death	CCL4-induced liver fibrosis (mouse)	HUC	Exos	BECN1↑xCT↓ GPX4↓ROS↑	α-SMA↓ Collagen deposition↓	(77)
Liver injury	CCL4-induced Acute Liver Injury (mouse)	HUC	Exos	/	Hepatocyte denaturation↓ Hepatic lobule destruction ↓ Survival rate of mice↑	(70)
Cardiac ischemia-reperfusion	I/R model was developed by left anterior descending coronary artery occlusion (mouse)	BM (mouse)	Exos	miR-182-5p↑ GSDMD↓ ROS↓	Alleviated cardiac dysfunction MI size↓IL-1β↓IL-18↓LDH activity↓ ASC↓caspase-1↓cell pyroptosis↑ arrest↑	(49)
I/R	Focal ischemic stroke induced by tMCAO(mouse)	BM(mouse)	Exos	miR-132-3p↑ ROS↓	Apoptosis↓BBB function↑ cMVD and CBF in the peri-infarct area↑	(206)
Lung I/R	180-minutes EVLP (rat)	BM(rat)	Evs	Hspa1a↑ Sod2↑	TPVR↓Pulmonary artery pressure↓ NO total metabolites↑Nos 2↑Edn1↓Ppeak↑ Cellular metabolism↑Glucose concentration↓ Lactate concentrations↓ATP↑HA↑Has1 and 2↑ CXCL2/CINC-3↑Cxcl1↑Cxcl2↑Ccl2↑Icam1↑ Ptgs2↑Il1rn↑Il10↑Irak3↑TTP↑Socs3↑Dusp1↑	(27)
Renal I/R	Bilateral renal arteries clamping induced RIRI(rat)	BM(rat)	Exos	MDA↓HIF1α↓NOX2↓ SOD↑GPX↑CAT↑HO-1↑	Creatinine↓BUN↓Apoptosis↓Caspase-3 activity↓ Bax↓PARP1↓Bcl-2↑MPO/ICAM1/IL1β/NFκB↓ IL10↑bFGF↑HGF↑SOX9↑VEGF↑	(90)
MIR	LAD-induced I/R injury model	BM (rat)	Exos	/	LC3B↑Apoptosis↓IS↓ EF↑LVFS↑	(48)
ALI	LPS-induced acute lung injury	UCB	Exos	/	miR-22-3p↑FZD6↓apoptosis↓p-NF-κB↓	(32)
ALI	Sepsis-induced ALI model(mouse)	UCB	Evs	SOD↑GPx↑CAT↑HO-1↑ Nrf2↑iNOS↓MDA↓	Rate of survival↑Total lung injury scores↓ Wet:dry ratios↓TNFa↓IL-1b↓IL-6↓IL-10↑ MPO↓Neutrophiles in BALF↓p-ERK↓p-JNK↓ p-P38↓p-p65↓IkB-α↓	(25)
Neonatal hyperoxic lung injuries	Exposed to hyperoxia(90%)for 14 days(rat)	UCB	Evs	/	Mean linear index↓Alveolar volume↓vWF↑ Apoptosis↓IL-1α↓IL-1β↓IL-6↓TNF-α↓ ED-1-positive alveolar macrophages↓	(43)
Radiation-induced lung injury	Exposed to thoracic radiation with a total dose of 15 Gy (mouse)	HP	Evs	MDA↓	P53↓P21↓β-galactosidase↓Vascular leakage↓ The number of infiltrated inflammatory cells↓ Inflammation↓TNFα↓IL-1β↓IL-6↓IL-10↑ Tissue fibrosis level↓COL1α1↓TGF-β↓α-SMA↓ MMP-9↓Anti-fibrotic genes↑TIMP-1↑TIMP-2↑ BMP-7↑miR-214-3p↑	(207)
ALI	LPS induced lung injury	UCB	Evs	Nrf2↑HO-1↑Keap1↓ Nrf2↓Keap1↑	IL-1β↓MCP-1↓IL-1α↓TNFα↓IL-12↓IL-10↑ Pathological scores↓iNOS↓Arg1↑CD86↓CD206↑ TLR4↓NF-κB p65↓	(33)
IVDD	IVDD rat model	BM (human)	Exos	/	MRI score↓CEP and NP tissues were better preserved CEP was thicker and that the structure was more intact histological score apoptosis↓calcification↓Runx2↓	(170)
IVDD	IVDD model (rabbit)	BM (mouse)	Exos	/	DHI improved, MMP13↓Col2a1↑ Histological score improved, Proteoglycan content↑	(17)
Epilepsy	Pilocarpine-induced seizures in wild-type and	UCB	Evs	8-OHdG↓4-HNE↓DT↓AMPA↓ Glut1↓iNOS↓HMGB1↓Nrf2↓	TOM20↓FIS1↓COXIV↓ Neuronal membrane properties and excitability were improved	(112)

(Continued)

TABLE 2 Continued

Application	Model	MSC Source	Excreta	Effect of MSC treatment	Antioxidant mechanisms	Reference
	AAV-injected (mouse)			HO-1↓ Nuclear translocation of Nrf2 ↓	Reconstruction of hippocampal neuronal function	
Nerve disease	Pilocarpine-induced SE (mouse)	UCB	Exos	Nrf2↓HO-1↓Keap1↑	Hippocampal reactive astrogliosis↓C3↓CD81↓ki67↓ GFAP↓TNFα↓IL-1α↓IL-1β↓GFAP↓P-65↓ Learning and memory impairment were reduced	(127)
Renal fibrosis	Renal ischemia (mouse)	HP	Evs	Hypo-EVs inhibits tubular atrophy in renal fibrosis Hypo-Evs causes the levels of blood urea nitrogen↓ Hypo-EVs suppressed the protein expression levels of vimentin	Hypo-Evs causes collagen I in the fibrotic kidney tissue ↓α-SMA ↓ Hypo-Evs makes the fibrotic kidney tissue CPT1A↑ Hypo-Evs makes ATP in the fibrotic kidney tissue↑	(209)
Light aging	Knock out NRF2 for modeling (mouse)	HUC	Exos	The epidermal thickness↓ The density of the collagen fibers↑ Inhibits cell proliferation and collagen deposition	TNFα↓IL-1β↓IL-6↓CK14↓Ki67↓P53↓P21↓NRF2↓ Keap1↑HO-1↑NQO1↑MFI positive rate of NRF2↓	(23)
Inflammation of pregnancy	LPS+ICR (mouse)	AF	Exos	/	NFκB↑NFκB↓TRAF6↑TNFα↑IL1β↑IL6↑TRAF6↓ TNFα↓IL1β↓IL6↓	(211)
RAS+MetS	MetS plus surgically induced RAS (MetS+RAS) (pig)	Swine MSC	Evs	Mitochondrial matrix density↓ Total LDL cholesterol↓ Triglyceride levels↓	miR196a↑miR-132↑miR-192↓miR-320↓ATP↑	(228)
AKI	Renal I/R injury (mouse)	BM (mouse) BM (rat) BM (human)	Evs	KIM-1↓Number of apoptotic cells↓	IL-6↓IL-1β↓ICAM1TNF-α↓TFAM↑PGC-1α↑ NDUFS8↑ATP5a1TFAM expression↑ATP↑ mtDNA copy number↑	(89)
Unilateral renal vascular disease with metabolic syndrome	A pig model of unilateral renal vascular disease with metabolic syndrome	Pig autologous fatMSC-Evs	Evs	RBF↑GFR↑Cortical microvascular and peritubular capillary density↑ Apoptosis of renal cells↓ Renal tubule injury and fibrosis↓ Superoxide nion↓Isoprostaglandin↓	VEGF↑Notch-1↑DLL4↑ Oxidative stress↓	(149)
Injury of isolated heart after external refrigeration	Isolated mouse heart (mouse)	BM (human) AD	Exos	/	TNF-α↓IL-1β↓Hspa1a↓caspase-3 levels↓ I-NDUFB8↑II-SDHB↑IV-MTCO1↑ V-ATP5A↑The production of H2O2↓	(214)
AMI	LAD(rat)	DP-derived MSC	Evs	EVs+miR-4732-3p significantly restored the systolic function of AMI reduced the area of fibrous scar tissue	/	(55)
MI	LAD(mouse)	Mouse Cardiac MSC	Evs	Reduced infarct size Promote blood vessel formation Reduce cell apoptosis Stimulate CM proliferation	/	(64)
Liver Injury	Liver tumor (mouse)	HUC	Exos	SOX9↓BAX↓bcl↑	8-OHdG↓aspase 3↓MDA↓TGFβ↓	(73)
Hepatic I/R Injury	Hepatic I/R Injury (mouse)	BM (mouse)	Evs	Caspase 3–positive cells↓ Apoptotic cells↓TNF↓IL1a↓IL1b↓IL6↓IL12↓IFN↓	NF-jB↓ROS↓NLRP12↑CCL7↓NLRP3↑ Mitogen-activated protein kinase 13↑	(72)

(Continued)

TABLE 2 Continued

Application	Model	MSC Source	Excreta	Effect of MSC treatment	Antioxidant mechanisms	Reference
				Chemoattractant protein 1↑ F4/80positive cells↑ALT↑	CXCL1↑IFNb1↓IFNc↓l 1b↓IL33↓kappa B↓ IL6I↓L1b↓PTGS2↑	
DR	Diabetic model (rat)	HUC	Evs	PETN↓AKT↑NRF2↑ Retinal thick-ness↑ Caspase-3 positive cells↓	NEDD4↓PCNA↑Bcl-2↑Bax↓MDA↓SOD↑NRF2↑ GPX1↑NQO1↑HO-1↑GCLC↑GCLM↑	(219)
Cerebral infarction	MCAO for cerebral infarction model (mouse)	HUC	Exos	Recover cell viability↓ Apoptotic cell numbers↓ ROS↓TLR4↓infarcted area↓ Brain water content↓ Neurological grading scores↓ FJC-positive cell numbers↓	Tnf-α and MCP-1 inhibition increased TNFα↓IL 6↓	(229)
Heart failure	Heart failure (mouse)	BM (mouse)	Exos	CD31↑CD206↑CTGF↓Bax↓ Cleaved caspase-3↑Bax↑ BCL↓IκBα↓p65↓caspase-3↓ Activity of MDA and LDH↓	/	(220)
Hepatic I/R injury	hepatic I/R injury (mouse)	human-induced pluripotent stem cell	Exos	TNF-α↓IL-6↓HMGB1↓ Caspase-3↓bax↓ALT↓ AST↓bcl↑Ki67-positive cells ↑	GSH↑GSH- px↑SOD↑MDA↓	(74)
Osteoarthritis	Osteoarthritis (mouse)	BM	Exos	MMP-13↓SOD↑NO↓MDA↓iNOS↓ COX2↓IL-1↓IL-6↓TNF-α↓	SDC1↓CRP↓	(230)
MI	model of myocardial infarction (rat)	HUC	Evs	DEF↑ FS↑ DFS↑ LVIDs↑LVEF↑	/	(231)
ED	model of internal iliac artery injury-induced ED (rat)	BM(rat)	Exos	ICP/MAP↑CD31↑VEGFA↑ iNOS↓SOD↑8-OHdG↓	/	(232)

Parkinson's disease (PD), Substantia nigra (SN), Spinal cord injury (SCI), Myocardial infarction (MI), Type 1 diabetes mellitus(DM), Acute Kidney Injury(AKI), Acute liver injury (ALI), Ischemia reperfusion(I/R), Ex vivo lung perfusion (EVLP), Myocardial ischemia reperfusion(MIR), Intervertebral disc degeneration (IVDD), Renal tubular necrosis rate Renal Damage Molecular 1(KIM-1), Diabetic retinopathy (DR), Erectile dysfunction (ED), Alzheimer's disease (AD). ↓, decline; ↑, increase. /, this mechanism is not included.

formulate a protocol to control all the steps of their isolation and application (160). Therefore, MSC-EVs and MSC-Exos in the treatment of oxidative stress injury of various systems need to use models closer to human pathology for better clinical use (235).

Author contributions

All authors contributed to the conception and design of the review central idea. WZ wrote the first draft of the manuscript; YX and TW prepared the tables and retrieved literature; XP and YZ corrected the drafts of the paper. All authors contributed to the article and approved the submitted version.

Funding

Our work described in the present manuscript is supported by research grants from Guangdong Provincial Natural Science Foundation, Guangdong, China, No.2021A1515012437 and Guangdong Provincial Scientific Research Project, Guangdong Provincial Department of Education, No. 2021KTSCX040, Guangdong, China.

Acknowledgments

We thank all the authors who participated in the research on exosomes in the treatment of oxidative stress-related diseases, and thank the editors and reviewers for their valuable opinions and suggestions to improve the paper.

Conflict of interest

The authors declare that the research was conducted in the absence of any commercial or financial relationships that could be construed as a potential conflict of interest.

Publisher's note

References

1. Petersen BE, Bowen WC, Patrene KD, Mars WM, Sullivan AK, Murase N, et al. Bone marrow as a potential source of hepatic oval cells. *Science* (1999) 284:1168–70. doi: 10.1126/science.284.5417.1168

2. Pittenger MF, Mackay AM, Beck SC, Jaiswal RK, Douglas R, Mosca JD, et al. Multilineage potential of adult human mesenchymal stem cells. *Science* (1999) 284:143–7. doi: 10.1126/science.284.5411.143

3. Kopen GC, Prockop DJ, Phinney DG. Marrow stromal cells migrate throughout forebrain and cerebellum, and they differentiate into astrocytes after injection into neonatal mouse brains. *Proc Natl Acad Sci U.S.A.* (1999) 96:10711–6. doi: 10.1073/pnas.96.19.10711

4. Aggarwal S, Pittenger MF. Human mesenchymal stem cells modulate allogeneic immune cell responses. *Blood* (2005) 105:1815–22. doi: 10.1182/blood-2004-04-1559

5. Raffaghello L, Bianchi G, Bertolotto M, Montecucco F, Busca A, Dallegri F, et al. Human mesenchymal stem cells inhibit neutrophil apoptosis: a model for neutrophil preservation in the bone marrow niche. *Stem Cells* (2008) 26:151–62. doi: 10.1634/stemcells.2007-0416

6. Ankrum J, Karp JM. Mesenchymal stem cell therapy: Two steps forward, one step back. *Trends Mol Med* (2010) 16:203–9. doi: 10.1016/j.molmed.2010.02.005

7. Muschler GF, Nakamoto C, Griffith LG. Engineering principles of clinical cell-based tissue engineering. *J Bone Joint Surg Am* (2004) 86:1541–58. doi: 10.2106/00004623-200407000-00029

8. Moll G, Rasmusson-Duprez I, Von Bahr L, Connolly-Andersen AM, Elgue G, Funke L, et al. Are therapeutic human mesenchymal stromal cells compatible with human blood? *Stem Cells* (2012) 30:1565–74. doi: 10.1002/stem.1111

9. Mathivanan S, Fahner CJ, Reid GE, Simpson RJ. ExoCarta 2012: database of exosomal proteins, RNA and lipids. *Nucleic Acids Res* (2012) 40:D1241–4. doi: 10.1093/nar/gkr828

10. Caplan AI, Correa D. The MSC: an injury drugstore. *Cell Stem Cell* (2011) 9:11–5. doi: 10.1016/j.stem.2011.06.008

11. Morrison TJ, Jackson MV, Cunningham EK, Kissenpfennig A, Mcauley DF, O'kane CM, et al. Mesenchymal stromal cells modulate macrophages in clinically relevant lung injury models by extracellular vesicle mitochondrial transfer. *Am J Respir Crit Care Med* (2017) 196:1275–86. doi: 10.1164/rccm.201701-0170OC

12. Ogisu K, Fujio M, Tsuchiya S, Tsuboi M, Qi C, Toyama N, et al. Conditioned media from mesenchymal stromal cells and periodontal ligament fibroblasts under cyclic stretch stimulation promote bone healing in mouse calvarial defects. *Cytotherapy* (2020) 22:543–51. doi: 10.1016/j.jcyt.2020.05.008

13. Zhang Z, Mi T, Jin L, Li M, Zhanghuang C, Wang J, et al. Comprehensive proteomic analysis of exosome mimetic vesicles and exosomes derived from human umbilical cord mesenchymal stem cells. *Stem Cell Res Ther* (2022) 13:312. doi: 10.1186/s13287-022-03008-6

14. Subra C, Laulagnier K, Perret B, Record M. Exosome lipidomics unravels lipid sorting at the level of multivesicular bodies. *Biochimie* (2007) 89:205–12. doi: 10.1016/j.biochi.2006.10.014

15. Simons M, Raposo G. Exosomes–vesicular carriers for intercellular communication. *Curr Opin Cell Biol* (2009) 21:575–81. doi: 10.1016/j.ceb.2009.03.007

16. Lee Y, El Andaloussi S, Wood MJ. Exosomes and microvesicles: extracellular vesicles for genetic information transfer and gene therapy. *Hum Mol Genet* (2012) 21:R125–34. doi: 10.1093/hmg/dds317

17. Xia C, Zeng Z, Fang B, Tao M, Gu C, Zheng L, et al. Mesenchymal stem cell-derived exosomes ameliorate intervertebral disc degeneration via anti-oxidant and anti-inflammatory effects. *Free Radical Biol Med* (2019) 143:1–15. doi: 10.1016/j.freeradbiomed.2019.07.026

18. Wang ZG, He ZY, Liang S, Yang Q, Cheng P, Chen AM. Comprehensive proteomic analysis of exosomes derived from human bone marrow, adipose tissue, and umbilical cord mesenchymal stem cells. *Stem Cell Res Ther* (2020) 11:511. doi: 10.1186/s13287-020-02032-8

19. Ma M, Li B, Zhang M, Zhou L, Yang F, Ma F, et al. Therapeutic effects of mesenchymal stem cell-derived exosomes on retinal detachment. *Exp Eye Res* (2020) 191:107899. doi: 10.1016/j.exer.2019.107899

20. Ebrahim N, Ahmed IA, Hussien NI, Dessouky AA, Farid AS, Elshazly AM, et al. Mesenchymal Stem Cell-Derived Exosomes Ameliorated Diabetic Nephropathy by Autophagy Induction through the mTOR Signaling Pathway. *Cells* (2018) 7(12):226. doi: 10.20944/preprints201809.0153.v1

21. Filomeni G, De Zio D, Cecconi F. Oxidative stress and autophagy: the clash between damage and metabolic needs. *Cell Death Differ* (2015) 22:377–88. doi: 10.1038/cdd.2014.150

22. Bisht S, Faiq M, Tolahunase M, Dada R. Oxidative stress and male infertility. *Nat Rev Urol* (2017) 14:470–85. doi: 10.1038/nrurol.2017.69

23. Wang T, Jian Z, Baskys A, Yang J, Li J, Guo H, et al. MSC-derived exosomes protect against oxidative stress-induced skin injury via adaptive regulation of the NRF2 defense system. *Biomaterials* (2020) 257:120264. doi: 10.1016/j.biomaterials.2020.120264

24. Silva AKA, Morille M, Piffoux M, Arumugam S, Mauduit P, Larghero J, et al. Development of extracellular vesicle-based medicinal products: A position paper of the group "Extracellular Vesicle translatiOn to clinicaL perspectiVEs - EVOLVE France". *Adv Drug Delivery Rev* (2021) 179:114001. doi: 10.1016/j.addr.2021.114001

25. Chen J, Li C, Liang Z, Li C, Li Y, Zhao Z, et al. Human mesenchymal stromal cells small extracellular vesicles attenuate sepsis-induced acute lung injury in a mouse model: the role of oxidative stress and the mitogen-activated protein kinase/nuclear factor kappa B pathway. *Cytotherapy* (2021) 23:918–30. doi: 10.1016/j.jcyt.2021.05.009

26. Qiao Q, Liu X, Yang T, Cui K, Kong L, Yang C, et al. Nanomedicine for acute respiratory distress syndrome: The latest application, targeting strategy, and rational design. *Acta Pharm Sinica. B* (2021) 11:3060–91. doi: 10.1016/j.apsb.2021.04.023

27. Lonati C, Bassani GA, Brambilla D, Leonardi P, Carlin A, Maggioni M, et al. Mesenchymal stem cell-derived extracellular vesicles improve the molecular phenotype of isolated rat lungs during ischemia/reperfusion injury. *J Heart Lung Transplant* (2019) 38:1306–16. doi: 10.1016/j.healun.2019.08.016

28. Shevtsova Y, Goryunov K, Babenko V, Pevzner I, Vtorushina V, Inviyaeva E, et al. Development of an *in vitro* model of SARS-coV-induced acute lung injury for studying new therapeutic approaches. *Antioxidants (Basel Switzerland)* (2022) 11(10):1910. doi: 10.3390/antiox11101910

29. Vardakas P, Skaperda Z, Tekos F, Kouretas D. ROS and COVID. *Antioxidants (Basel)* (2022) 11(2):339. doi: 10.3390/antiox11020339

30. Sengupta V, Sengupta S, Lazo A, Woods P, Nolan A, Bremer N. Exosomes derived from bone marrow mesenchymal stem cells as treatment for severe COVID-19. *Stem Cells Dev* (2020) 29:747–54. doi: 10.1089/scd.2020.0080

31. Risbud MV, Shapiro IM. Role of cytokines in intervertebral disc degeneration: pain and disc content. *Nat Rev Rheumatol* (2014) 10:44–56. doi: 10.1038/nrrheum.2013.160

32. Zheng Y, Liu J, Chen P, Lin L, Luo Y, Ma X, et al. Exosomal miR-22-3p from human umbilical cord blood-derived mesenchymal stem cells protects against lipopolysaccharid-induced acute lung injury. *Life Sci* (2021) 269:119004. doi: 10.1016/j.lfs.2020.119004

33. Zhao R, Wang L, Wang T, Xian P, Wang H, Long Q. Inhalation of MSC-EVs is a noninvasive strategy for ameliorating acute lung injury. *J Control Release* (2022) 345:214–30. doi: 10.1016/j.jconrel.2022.03.025

34. Sasaki H, Takayama K, Matsushita T, Ishida K, Kubo S, Matsumoto T, et al. Autophagy modulates osteoarthritis-related gene expression in human chondrocytes. *Arthritis Rheum* (2012) 64:1920–8. doi: 10.1002/art.34323

35. Piga R, Van Dartel D, Bunschoten A, Van Der Stelt I, Keijer J. Role of Frizzled6 in the molecular mechanism of beta-carotene action in the lung. *Toxicology* (2014) 320:67–73. doi: 10.1016/j.tox.2014.03.002

36. Yi X, Wei X, Lv H, An Y, Li L, Lu P, et al. Exosomes derived from microRNA-30b-3p-overexpressing mesenchymal stem cells protect against lipopolysaccharide-induced acute lung injury by inhibiting SAA3. *Exp Cell Res* (2019) 383:111454. doi: 10.1016/j.yexcr.2019.05.035

37. Li JW, Wei L, Han Z, Chen Z. Mesenchymal stromal cells-derived exosomes alleviate ischemia/reperfusion injury in mouse lung by transporting anti-apoptotic miR-21-5p. *Eur J Pharmacol* (2019) 852:68–76. doi: 10.1016/j.ejphar.2019.01.022

38. Coulson-Thomas VJ, Gesteira TF, Hascall V, Kao W. Umbilical cord mesenchymal stem cells suppress host rejection: the role of the glycocalyx. *J Biol Chem* (2014) 289:23465–81. doi: 10.1074/jbc.M114.557447

39. Kota DJ, Dicarlo B, Hetz RA, Smith P, Cox CSJr., Olson SD. Differential MSC activation leads to distinct mononuclear leukocyte binding mechanisms. *Sci Rep* (2014) 4:4565. doi: 10.1038/srep04565

40. Kota DJ, Prabhakara KS, Cox CS, Olson SD. MSCs and hyaluronan: sticking together for new therapeutic potential? *Int J Biochem Cell Biol* (2014) 55:1–10. doi: 10.1016/j.biocel.2014.07.022

41. Day AJ, De La Motte CA. Hyaluronan cross-linking: a protective mechanism in inflammation? *Trends Immunol* (2005) 26:637–43. doi: 10.1016/j.it.2005.09.009

42. Kellner M, NooNepalle S, Lu Q, Srivastava A, Zemskov E, Black SM. ROS signaling in the pathogenesis of Acute Lung Injury (ALI) and Acute Respiratory Distress Syndrome (ARDS). *Adv Exp Med Biol* (2017) 967:105–37. doi: 10.1007/978-3-319-63245-2_8

43. Ahn SY, Park WS, Kim YE, Sung DK, Sung SI, Ahn JY, et al. Vascular endothelial growth factor mediates the therapeutic efficacy of mesenchymal stem cell-derived extracellular vesicles against neonatal hyperoxic lung injury. *Exp Mol Med* (2018) 50:1–12. doi: 10.1038/s12276-018-0055-8

44. Franco M, Roswall P, Cortez E, Hanahan D, Pietras K. Pericytes promote endothelial cell survival through induction of autocrine VEGF-A signaling and Bcl-w expression. *Blood* (2011) 118:2906–17. doi: 10.1182/blood-2011-01-331694

45. Geevarghese A, Herman IM. Pericyte-endothelial crosstalk: implications and opportunities for advanced cellular therapies. *Transl Res* (2014) 163:296–306. doi: 10.1016/j.trsl.2014.01.011

46. Tang P, Gu JM, Xie ZA, Gu Y, Jie ZW, Huang KM, et al. Honokiol alleviates the degeneration of intervertebral disc via suppressing the activation of TXNIP-NLRP3 inflammasome signal pathway. *Free Radic Biol Med* (2018) 120:368–79. doi: 10.1016/j.freeradbiomed.2018.04.008

47. Vejpongsa P, Yeh ET. Topoisomerase 2β: a promising molecular target for primary prevention of anthracycline-induced cardiotoxicity. *Clin Pharmacol Ther* (2014) 95:45–52. doi: 10.1038/clpt.2013.201

48. Liu L, Jin X, Hu CF, Li R, Zhou Z, Shen CX. Exosomes derived from mesenchymal stem cells rescue myocardial ischaemia/reperfusion injury by inducing cardiomyocyte autophagy via AMPK and akt pathways. *Cell Physiol Biochem* (2017) 43:52–68. doi: 10.1159/000480317

49. Yue R, Lu S, Luo Y, Zeng J, Liang H, Qin D, et al. Mesenchymal stem cell-derived exosomal microRNA-182-5p alleviates myocardial ischemia/reperfusion injury by targeting GSDMD in mice. *Cell Death Discovery* (2022) 8:202. doi: 10.1038/s41420-022-00909-6

50. Bauernfeind F, Rieger A, Schildberg FA, Knolle PA, Schmid-Burgk JL, Hornung V. NLRP3 inflammasome activity is negatively controlled by miR-223. *J Immunol* (2012) 189:4175–81. doi: 10.4049/jimmunol.1201516

51. Qin SB, Peng DY, Lu JM, Ke ZP. MiR-182-5p inhibited oxidative stress and apoptosis triggered by oxidized low-density lipoprotein via targeting toll-like receptor 4. *J Cell Physiol* (2018) 233:6630–7. doi: 10.1002/jcp.26389

52. Song XL, Zhang FF, Wang WJ, Li XN, Dang Y, Li YX, et al. LncRNA A2M-AS1 lessens the injury of cardiomyocytes caused by hypoxia and reoxygenation via regulating IL1R2. *Genes Genomics* (2020) 42:1431–41. doi: 10.1007/s13258-020-01007-6

53. Zhang B, Xu L, Zhuo N, Shen J. Resveratrol protects against mitochondrial dysfunction through autophagy activation in human nucleus pulposus cells. *Biochem Biophys Res Commun* (2017) 493:373–81. doi: 10.1016/j.bbrc.2017.09.015

54. Yu H, Pan Y, Dai M, Wang X, Chen H. Mesenchymal stem cell-originated exosomal Lnc A2M-AS1 alleviates hypoxia/reperfusion-induced apoptosis and oxidative stress in cardiomyocytes. *Cardiovasc Drugs Ther* (2022). doi: 10.1007/s10557-022-07339-7

55. Sánchez-Sánchez R, Gómez-Ferrer M, Reinal I, Buigues M, Villanueva-bádenas E, Ontoria-oviedo I, et al. miR-4732-3p in extracellular vesicles from mesenchymal stromal cells is cardioprotective during myocardial ischemia. *Front Cell Dev Biol* (2021) 9:734143. doi: 10.3389/fcell.2021.734143

56. Chen GH, Xu J, Yang YJ. Exosomes: promising sacks for treating ischemic heart disease? *Am J Physiol Heart Circ Physiol* (2017) 313:H508–h523. doi: 10.1152/ajpheart.00213.2017

57. Zhou H, Wang B, Yang Y, Jia Q, Qi Z, Zhang A, et al. Exosomes in ischemic heart disease: novel carriers for bioinformation. *BioMed Pharmacother* (2019) 120:109451. doi: 10.1016/j.biopha.2019.109451

58. Li Q, Xu Y, Lv K, Wang Y, Zhong Z, Xiao C, et al. Small extracellular vesicles containing miR-486-5p promote angiogenesis after myocardial infarction in mice and nonhuman primates. *Sci Transl Med* (2021) 13(584):eabb0202. doi: 10.1126/scitranslmed.abb0202

59. Ou H, Teng H, Qin Y, Luo X, Yang P, Zhang W, et al. Extracellular vesicles derived from microRNA-150-5p-overexpressing mesenchymal stem cells protect rat hearts against ischemia/reperfusion. *Aging (Albany NY)* (2020) 12:12669–83. doi: 10.18632/aging.102792

60. Luther KM, Haar L, Mcguinness M, Wang Y, Lynch Iv TL, Phan A, et al. Exosomal miR-21a-5p mediates cardioprotection by mesenchymal stem cells. *J Mol Cell Cardiol* (2018) 119:125–37. doi: 10.1016/j.yjmcc.2018.04.012

61. Raso A, Dirkx E, Philippen LE, Fernandez-Celis A, De Majo F, Sampaio-Pinto V, et al. Therapeutic delivery of miR-148a suppresses ventricular dilation in heart failure. *Mol Ther* (2019) 27:584–99. doi: 10.1016/j.ymthe.2018.11.011

62. Fan ZG, Qu XL, Chu P, Gao YL, Gao XF, Chen SL, et al. MicroRNA-210 promotes angiogenesis in acute myocardial infarction. *Mol Med Rep* (2018) 17:5658–65. doi: 10.3892/mmr.2018.8620

63. Zhang LL, Xiong YY, Yang YJ. The vital roles of mesenchymal stem cells and the derived extracellular vesicles in promoting angiogenesis after acute myocardial infarction. *Stem Cells Dev* (2021) 30:561–77. doi: 10.1089/scd.2021.0006

64. Xuan W, Khan M, Ashraf M. Extracellular vesicles from notch activated cardiac mesenchymal stem cells promote myocyte proliferation and neovasculogenesis. *Front Cell Dev Biol* (2020) 8:11. doi: 10.3389/fcell.2020.00011

65. Martin-Rendon E, Sweeney D, Lu F, Girdlestone J, Navarrete C, Watt SM. 5-Azacytidine-treated human mesenchymal stem/progenitor cells derived from umbilical cord, cord blood and bone marrow do not generate cardiomyocytes in *vitro* at high frequencies. *Vox Sang* (2008) 95:137–48. doi: 10.1111/j.1423-0410.2008.01076.x

66. Lugea A, Waldron RT. Exosome-mediated intercellular communication between stellate cells and cancer cells in pancreatic ductal adenocarcinoma. *Pancreas* (2017) 46:1–4. doi: 10.1097/MPA.0000000000000686

67. Bélanger M, Rodrigues PH, Dunn W. A., JR., Progulske-Fox A. Autophagy: a highway for Porphyromonas gingivalis in endothelial cells. *Autophagy* (2006) 2:165–70. doi: 10.4161/auto.2828

68. Matsui Y, Takagi H, Qu X, Abdellatif M, Sakoda H, Asano T, et al. Distinct roles of autophagy in the heart during ischemia and reperfusion: roles of AMP-activated protein kinase and Beclin 1 in mediating autophagy. *Circ Res* (2007) 100:914–22. doi: 10.1161/01.RES.0000261924.76669.36

69. Lin B, Yang J, Song Y, Dang G, Feng J. Exosomes and atherogenesis. *Front Cardiovasc Med* (2021) 8:738031. doi: 10.3389/fcvm.2021.738031

70. Yan Y, Jiang W, Tan Y, Zou S, Zhang H, Mao F, et al. hucMSC exosome-derived GPX1 is required for the recovery of hepatic oxidant injury. *Mol therapy: J Am Soc Gene Ther* (2017) 25:465–79. doi: 10.1016/j.ymthe.2016.11.019

71. Peralta C, Jiménez-Castro MB, Gracia-Sancho J. Hepatic ischemia and reperfusion injury: effects on the liver sinusoidal milieu. *J Hepatol* (2013) 59:1094–106. doi: 10.1016/j.jhep.2013.06.017

72. Haga H, Yan IK, Borrelli DA, Matsuda A, Parasramka M, Shukla N, et al. Extracellular vesicles from bone marrow-derived mesenchymal stem cells protect against murine hepatic ischemia/reperfusion injury. *Liver Transpl* (2017) 23:791–803. doi: 10.1002/lt.24770

73. Jiang W, Tan Y, Cai M, Zhao T, Mao F, Zhang X, et al. Human umbilical cord MSC-derived exosomes suppress the development of CCl(4)-induced liver injury through antioxidant effect. *Stem Cells Int* (2018) 2018:6079642. doi: 10.1155/2018/6079642

74. Nong K, Wang W, Niu X, Hu B, Ma C, Bai Y, et al. Hepatoprotective effect of exosomes from human-induced pluripotent stem cell-derived mesenchymal stromal cells against hepatic ischemia-reperfusion injury in rats. *Cytotherapy* (2016) 18:1548–59. doi: 10.1016/j.jcyt.2016.08.002

75. Sui M, Jiang X, Chen J, Yang H, Zhu Y. Magnesium isoglycyrrhizinate ameliorates liver fibrosis and hepatic stellate cell activation by regulating ferroptosis signaling pathway. *BioMed Pharmacother* (2018) 106:125–33. doi: 10.1016/j.biopha.2018.06.060

76. Kang R, Zhu S, Zeh HJ, Klionsky DJ, Tang D. BECN1 is a new driver of ferroptosis. *Autophagy* (2018) 14:2173–5. doi: 10.1080/15548627.2018.1513758

77. Tan Y, Huang Y, Mei R, Mao F, Yang D, Liu J, et al. HucMSC-derived exosomes delivered BECN1 induces ferroptosis of hepatic stellate cells via regulating the xCT/GPX4 axis. *Cell Death Dis* (2022) 13:319. doi: 10.1038/s41419-022-04764-2

78. Eirin A, Zhu XY, Krier JD, Tang H, Jordan KL, Grande JP, et al. Adipose tissue-derived mesenchymal stem cells improve revascularization outcomes to restore renal function in swine atherosclerotic renal artery stenosis. *Stem Cells* (2012) 30:1030–41. doi: 10.1002/stem.1047

79. Ebrahimi B, Eirin A, Li Z, Zhu XY, Zhang X, Lerman A, et al. Mesenchymal stem cells improve medullary inflammation and fibrosis after revascularization of swine atherosclerotic renal artery stenosis. *PLoS One* (2013) 8:e67474. doi: 10.1371/journal.pone.0067474

80. Textor SC, Lerman LO. Paradigm shifts in atherosclerotic renovascular disease: where are we now? *J Am Soc Nephrol* (2015) 26:2074–80. doi: 10.1681/ASN.2014121274

81. Eirin A, Zhu XY, Ebrahimi B, Krier JD, Riester SM, Van Wijnen AJ, et al. Intrarenal delivery of mesenchymal stem cells and endothelial progenitor cells attenuates hypertensive cardiomyopathy in experimental renovascular hypertension. *Cell Transplant* (2015) 24:2041–53. doi: 10.3727/096368914X685582

82. Eirin A, Zhu XY, Puranik AS, Tang H, Mcgurren KA, Van Wijnen AJ, et al. Mesenchymal stem cell-derived extracellular vesicles attenuate kidney inflammation. *Kidney Int* (2017) 92:114–24. doi: 10.1016/j.kint.2016.12.023

83. Murphy MP. Mitochondrial dysfunction indirectly elevates ROS production by the endoplasmic reticulum. *Cell Metab* (2013) 18:145–6. doi: 10.1016/j.cmet.2013.07.006

84. Eirin A, Li Z, Zhang X, Krier JD, Woollard JR, Zhu XY, et al. A mitochondrial permeability transition pore inhibitor improves renal outcomes after revascularization in experimental atherosclerotic renal artery stenosis. *Hypertension* (2012) 60:1242–9. doi: 10.1161/HYPERTENSIONAHA.112.199919

85. Kaasik A, Safiulina D, Zharkovsky A, Veksler V. Regulation of mitochondrial matrix volume. *Am J Physiol Cell Physiol* (2007) 292:C157–63. doi: 10.1152/ajpcell.00272.2006

86. Bhargava P, Schnellmann RG. Mitochondrial energetics in the kidney. *Nat Rev Nephrol* (2017) 13:629–46. doi: 10.1038/nrneph.2017.107

87. Kang D, Kim SH, Hamasaki N. Mitochondrial transcription factor A (TFAM): roles in maintenance of mtDNA and cellular functions. *Mitochondrion* (2007) 7:39–44. doi: 10.1016/j.mito.2006.11.017

88. Kunkel GH, Chaturvedi P, Tyagi SC. Mitochondrial pathways to cardiac recovery: TFAM. *Heart Fail Rev* (2016) 21:499–517. doi: 10.1007/s10741-016-9561-8

89. Zhao M, Liu S, Wang C, Wang Y, Wan M, Liu F, et al. Mesenchymal stem cell-derived extracellular vesicles attenuate mitochondrial damage and inflammation by stabilizing mitochondrial DNA. *ACS nano* (2021) 15:1519–38. doi: 10.1021/acsnano.0c08947

90. Alzahrani FA. Melatonin improves therapeutic potential of mesenchymal stem cells-derived exosomes against renal ischemia-reperfusion injury in rats. *Am J Transl Res* (2019) 11:2887–907.

91. Stallons LJ, Whitaker RM, Schnellmann RG. Suppressed mitochondrial biogenesis in folic acid-induced acute kidney injury and early fibrosis. *Toxicol Lett* (2014) 224:326–32. doi: 10.1016/j.toxlet.2013.11.014

92. West AP, Khoury-Hanold W, Staron M, Tal MC, Pineda CM, Lang SM, et al. Mitochondrial DNA stress primes the antiviral innate immune response. *Nature* (2015) 520:553–7. doi: 10.1038/nature14156

93. Quesenberry PJ, Dooner MS, Aliotta JM. Stem cell plasticity revisited: the continuum marrow model and phenotypic changes mediated by microvesicles. *Exp Hematol* (2010) 38:581–92. doi: 10.1016/j.exphem.2010.03.021

94. Zou X, Gu D, Xing X, Cheng Z, Gong D, Zhang G, et al. Human mesenchymal stromal cell-derived extracellular vesicles alleviate renal ischemic reperfusion injury and enhance angiogenesis in rats. *Am J Transl Res* (2016) 8:4289–99.

95. Lindoso RS, Collino F, Bruno S, Araujo DS, Sant'anna JF, Tetta C, et al. Extracellular vesicles released from mesenchymal stromal cells modulate miRNA in renal tubular cells and inhibit ATP depletion injury. *Stem Cells Dev* (2014) 23:1809–19. doi: 10.1089/scd.2013.0618

96. Williams P, Lopez H, Britt D, Chan C, Ezrin A, Hottendorf R. Characterization of renal ischemia-reperfusion injury in rats. *J Pharmacol Toxicol Methods* (1997) 37:1–7. doi: 10.1016/S1056-8719(96)00141-4

97. Zager RA, Johnson AC, Lund S. Uremia impacts renal inflammatory cytokine gene expression in the setting of experimental acute kidney injury. *Am J Physiol Renal Physiol* (2009) 297:F961–70. doi: 10.1152/ajprenal.00381.2009

98. Gatti S, Bruno S, Deregibus MC, Sordi A, Cantaluppi V, Tetta C, et al. Microvesicles derived from human adult mesenchymal stem cells protect against ischaemia-reperfusion-induced acute and chronic kidney injury. *Nephrol Dial Transplant* (2011) 26:1474–83. doi: 10.1093/ndt/gfr015

99. Zou X, Zhang G, Cheng Z, Yin D, Du T, Ju G, et al. Microvesicles derived from human Wharton's Jelly mesenchymal stromal cells ameliorate renal ischemia-reperfusion injury in rats by suppressing CX3CL1. *Stem Cell Res Ther* (2014) 5:40. doi: 10.1186/scrt428

100. Bruno S, Grange C, Collino F, Deregibus MC, Cantaluppi V, Biancone L, et al. Microvesicles derived from mesenchymal stem cells enhance survival in a lethal model of acute kidney injury. *PloS One* (2012) 7:e33115. doi: 10.1371/journal.pone.0033115

101. Zhou Y, Xu H, Xu W, Wang B, Wu H, Tao Y, et al. Exosomes released by human umbilical cord mesenchymal stem cells protect against cisplatin-induced renal oxidative stress and apoptosis in *vivo* and in *vitro*. *Stem Cell Res Ther* (2013) 4:34. doi: 10.1186/scrt194

102. Bruno S, Tapparo M, Collino F, Chiabotto G, Deregibus MC, Soares Lindoso R, et al. Renal regenerative potential of different extracellular vesicle populations derived from bone marrow mesenchymal stromal cells. *Tissue Eng Part A* (2017) 23:1262–73. doi: 10.1089/ten.tea.2017.0069

103. Kumar S, Liu J, Pang P, Krautzberger AM, Reginensi A, Akiyama H, et al. Sox9 activation highlights a cellular pathway of renal repair in the acutely injured MamMalian kidney. *Cell Rep* (2015) 12:1325–38. doi: 10.1016/j.celrep.2015.07.034

104. Zhu F, Chong Lee Shin OLS, Pei G, Hu Z, Yang J, Zhu H, et al. Adipose-derived mesenchymal stem cells employed exosomes to attenuate AKI-CKD transition through tubular epithelial cell dependent Sox9 activation. *Oncotarget* (2017) 8:70707–26. doi: 10.18632/oncotarget.19979

105. Choi HY, Moon SJ, Ratliff BB, Ahn SH, Jung A, Lee M, et al. Microparticles from kidney-derived mesenchymal stem cells act as carriers of proangiogenic signals and contribute to recovery from acute kidney injury. *PloS One* (2014) 9:e87853. doi: 10.1371/journal.pone.0087853

106. Little MH, Kairath P. Does renal repair recapitulate kidney development? *J Am Soc Nephrol* (2017) 28:34–46. doi: 10.1681/ASN.2016070748

107. Hong C, Seo H, Kwak M, Jeon J, Jang J, Jeong EM, et al. Increased TRPC5 glutathionylation contributes to striatal neuron loss in Huntington's disease. *Brain* (2015) 138:3030–47. doi: 10.1093/brain/awv188

108. Zhang ZG, Buller B, Chopp M. Exosomes - beyond stem cells for restorative therapy in stroke and neurological injury. *Nat Rev Neurol* (2019) 15:193–203. doi: 10.1038/s41582-018-0126-4

109. Holm MM, Kaiser J, Schwab ME. Extracellular vesicles: multimodal envoys in neural maintenance and repair. *Trends Neurosci* (2018) 41:360–72. doi: 10.1016/j.tins.2018.03.006

110. Santulli G. Exosomal microRNA: The revolutionary endogenous Innerspace nanotechnology. *Sci Transl Med* (2018) 10(467):eaav9141. doi: 10.1126/scitranslmed.aav9141

111. Garrido-Pascual P, Alonso-Varona A, Castro B, Burón M, Palomares T. H(2)O (2)-preconditioned human adipose-derived stem cells (HC016) increase their resistance to oxidative stress by overexpressing Nrf2 and bioenergetic adaptation. *Stem Cell Res Ther* (2020) 11:335. doi: 10.1186/s13287-020-01851-z

112. Luo Q, Xian P, Wang T, Wu S, Sun T, Wang W, et al. Antioxidant activity of mesenchymal stem cell-derived extracellular vesicles restores hippocampal neurons following seizure damage. *Theranostics* (2021) 11:5986–6005. doi: 10.7150/thno.58632

113. Thijs RD, Surges R, O'brien TJ, Sander JW. Epilepsy in adults. *Lancet* (2019) 393:689–701. doi: 10.1016/S0140-6736(18)32596-0

114. Pauletti A, Terrone G, Shekh-Ahmad T, Salamone A, Ravizza T, Rizzi M, et al. Targeting oxidative stress improves disease outcomes in a rat model of acquired epilepsy. *Brain* (2019) 142:e39. doi: 10.1093/brain/awz130

115. Zhu X, Shen K, Bai Y, Zhang A, Xia Z, Chao J, et al. NADPH oxidase activation is required for pentylenetetrazole kindling-induced hippocampal autophagy. *Free Radic Biol Med* (2016) 94:230–42. doi: 10.1016/j.freeradbiomed.2016.03.004

116. Ordemann GJ, Apgar CJ, Brager DH. D-type potassium channels norMalize action potential firing between dorsal and ventral CA1 neurons of the mouse hippocampus. *J Neurophysiol* (2019) 121:983–95. doi: 10.1152/jn.00737.2018

117. Hirao H, Dery KJ, Kageyama S, Nakamura K, Kupiec-Weglinski JW. Heme Oxygenase-1 in liver transplant ischemia-reperfusion injury: From bench-to-bedside. *Free Radic Biol Med* (2020) 157:75–82. doi: 10.1016/j.freeradbiomed.2020.02.012

118. Devinsky O, Vezzani A, O'brien TJ, Jette N, Scheffer IE, De Curtis M, et al. Epilepsy. *Nat Rev Dis Primers* (2018) 4:18024. doi: 10.1038/nrdp.2018.24

119. Haut SR, Velísková J, Moshé SL. Susceptibility of immature and adult brains to seizure effects. *Lancet Neurol* (2004) 3:608–17. doi: 10.1016/S1474-4422(04)00881-6

120. Berridge MJ, Bootman MD, Roderick HL. Calcium signalling: dynamics, homeostasis and remodelling. *Nat Rev Mol Cell Biol* (2003) 4:517–29. doi: 10.1038/nrm1155

121. Rahman S. Mitochondrial diseases and status epilepticus. *Epilepsia* (2018) 59 Suppl 2:70–7. doi: 10.1111/epi.14485

122. Burté F, Carelli V, Chinnery PF, Yu-Wai-Man P. Disturbed mitochondrial dynamics and neurodegenerative disorders. *Nat Rev Neurol* (2015) 11:11–24. doi: 10.1038/nrneurol.2014.228

123. Hausenloy DJ, Yellon DM. Myocardial ischemia-reperfusion injury: a neglected therapeutic target. *J Clin Invest* (2013) 123:92–100. doi: 10.1172/JCI62874

124. Jiang T, Sun Q, Chen S. Oxidative stress: A major pathogenesis and potential therapeutic target of antioxidative agents in Parkinson's disease and Alzheimer's disease. *Prog Neurobiol* (2016) 147:1–19. doi: 10.1016/j.pneurobio.2016.07.005

125. Verkhratsky A, Steardo L, Parpura V, Montana V. Translational potential of astrocytes in brain disorders. *Prog Neurobiol* (2016) 144:188–205. doi: 10.1016/j.pneurobio.2015.09.003

126. Pekny M, Pekna M, Messing A, Steinhäuser C, Lee JM, Parpura V, et al. Astrocytes: a central element in neurological diseases. *Acta Neuropathol* (2016) 131:323–45. doi: 10.1007/s00401-015-1513-1

127. Xian P, Hei Y, Wang R, Wang T, Yang J, Li J, et al. Mesenchymal stem cell-derived exosomes as a nanotherapeutic agent for amelioration of inflammation-induced astrocyte alterations in mice. *Theranostics* (2019) 9:5956–75. doi: 10.7150/thno.33872

128. Long Q, Upadhya D, Hattiangady B, Kim DK, An SY, Shuai B, et al. Intranasal MSC-derived A1-exosomes ease inflammation, and prevent abnormal neurogenesis and memory dysfunction after status epilepticus. *Proc Natl Acad Sci U.S.A.* (2017) 114:E3536–e3545. doi: 10.1073/pnas.1703920114

129. Levy S. Function of the tetraspanin molecule CD81 in B and T cells. *Immunol Res* (2014) 58:179–85. doi: 10.1007/s12026-014-8490-7

130. Kraitchman DL, Tatsumi M, Gilson WD, Ishimori T, Kedziorek D, Walczak P, et al. Dynamic imaging of allogeneic mesenchymal stem cells trafficking to myocardial infarction. *Circulation* (2005) 112:1451–61. doi: 10.1161/CIRCULATIONAHA.105.537480

131. Kammeyer A, Luiten RM. Oxidation events and skin aging. *Ageing Res Rev* (2015) 21:16–29. doi: 10.1016/j.arr.2015.01.001

132. Poon F, Kang S, Chien AL. Mechanisms and treatments of photoaging. *Photodermatol Photoimmunol Photomed* (2015) 31:65–74. doi: 10.1111/phpp.12145

133. Kuehne A, Emmert H, Soehle J, Winnefeld M, Fischer F, Wenck H, et al. Acute activation of oxidative pentose phosphate pathway as first-line response to oxidative stress in human skin cells. *Mol Cell* (2015) 59:359–71. doi: 10.1016/j.molcel.2015.06.017

134. Abdel-Malek ZA, Kadekaro AL, Swope VB. Stepping up melanocytes to the challenge of UV exposure. *Pigment Cell Melanoma Res* (2010) 23:171–86. doi: 10.1111/j.1755-148X.2010.00679.x

135. Wang SQ, Balagula Y, Osterwalder U. Photoprotection: a review of the current and future technologies. *Dermatol Ther* (2010) 23:31–47. doi: 10.1111/j.1529-8019.2009.01289.x

136. Rodgers K, Jadhav SS. The application of mesenchymal stem cells to treat thermal and radiation burns. *Adv Drug Delivery Rev* (2018) 123:75–81. doi: 10.1016/j.addr.2017.10.003

137. Velarde MC, Demaria M, Melov S, Campisi J. Pleiotropic age-dependent effects of mitochondrial dysfunction on epidermal stem cells. *Proc Natl Acad Sci U.S.A.* (2015) 112:10407–12.

138. Zhang B, Shen L, Shi H, Pan Z, Wu L, Yan Y, et al. Exosomes from human umbilical cord mesenchymal stem cells: identification, purification, and biological characteristics. *Stem Cells Int* (2016) 2016:1929536. doi: 10.1155/2016/1929536

139. Deng M, Yu T, Li D, Wang X, Zhou G, Liu W, et al. Human umbilical cord mesenchymal stem cell-derived and dermal fibroblast-derived extracellular vesicles protect dermal fibroblasts from ultraviolet radiation-induced photoaging in *vitro*. *Photochemical photobiological sciences: Off J Eur Photochem Assoc Eur Soc Photobiol* (2020) 19:406–14. doi: 10.1039/c9pp00421a

140. Zhang Z, Zi Z, Lee EE, Zhao J, Contreras DC, South AP, et al. Differential glucose requirement in skin homeostasis and injury identifies a therapeutic target for psoriasis. *Nat Med* (2018) 24:617–27. doi: 10.1038/s41591-018-0003-0

141. Schäfer M, Farwanah H, Willrodt AH, Huebner AJ, Sandhoff K, Roop D, et al. Nrf2 links epidermal barrier function with antioxidant defense. *EMBO Mol Med* (2012) 4:364–79. doi: 10.1002/emmm.201200219

142. Nunan R, Harding KG, Martin P. Clinical challenges of chronic wounds: searching for an optimal animal model to recapitulate their complexity. *Dis Model Mech* (2014) 7:1205–13. doi: 10.1242/dmm.016782

143. Shiekh PA, Singh A, Kumar A. Exosome laden oxygen releasing antioxidant and antibacterial cryogel wound dressing OxOBand alleviate diabetic and infectious wound healing. *Biomaterials* (2020) 249:120020. doi: 10.1016/j.biomaterials.2020.120020

144. Las Heras K, Royo F, Garcia-Vallicrosa C, Igartua M, Santos-Vizcaino E, Falcon-Perez J, et al. Extracellular vesicles from hair follicle-derived mesenchymal stromal cells: isolation, characterization and therapeutic potential for chronic wound healing. *Stem Cell Res Ther* (2022) 13:147. doi: 10.1186/s13287-022-02824-0

145. Martin P. Wound healing–aiming for perfect skin regeneration. *Science* (1997) 276:75–81. doi: 10.1126/science.276.5309.75

146. Las Heras K, Igartua M, Santos-Vizcaino E, Hernandez RM. Chronic wounds: Current status, available strategies and emerging therapeutic solutions. *J Control Release* (2020) 328:532–50. doi: 10.1016/j.jconrel.2020.09.039

147. Schäfer M, Werner S. Oxidative stress in normal and impaired wound repair. *Pharmacol Res* (2008) 58:165–71. doi: 10.1016/j.phrs.2008.06.004

148. Xiao X, Xu M, Yu H, Wang L, Li X, Rak J, et al. Mesenchymal stem cell-derived small extracellular vesicles mitigate oxidative stress-induced senescence in endothelial cells via regulation of miR-146a/Src. *Signal transduction targeted Ther* (2021) 6:354. doi: 10.1038/s41392-021-00765-3

149. Eirin A, Zhu X, Jonnada S, Lerman A, Van Wijnen A, Lerman L. Mesenchymal stem cell-derived extracellular vesicles improve the renal microvasculature in metabolic renovascular disease in swine. *Cell Transplant* (2018) 27:1080–95. doi: 10.1177/0963689718780942

150. Matsuoka T, Takanashi K, Dan K, Yamamoto K, Tomobe K, Shinozuka T. Effects of mesenchymal stem cell-derived exosomes on oxidative stress responses in skin cells. *Mol Biol Rep* (2021) 48:4527–35. doi: 10.1007/s11033-021-06473-z

151. Fornaro A, Olivotto I, Rigacci L, Ciaccheri M, Tomberli B, Ferrantini C, et al. Comparison of long-term outcome in anthracycline-related versus idiopathic dilated cardiomyopathy: a single centre experience. *Eur J Heart Fail* (2018) 20:898–906. doi: 10.1002/ejhf.1049

152. Haendeler J, Hoffmann J, Diehl JF, Vasa M, Spyridopoulos I, Zeiher AM, et al. Antioxidants inhibit nuclear export of telomerase reverse transcriptase and delay replicative senescence of endothelial cells. *Circ Res* (2004) 94:768–75. doi: 10.1161/01.RES.0000121104.05977.F3

153. Han YM, Bedarida T, Ding Y, Somba BK, Lu Q, Wang Q, et al. β-Hydroxybutyrate Prevents Vascular Senescence through hnRNP A1-Mediated Upregulation of Oct4. *Mol Cell* (2018) 71:1064–1078.e5. doi: 10.1016/j.molcel.2018.07.036

154. Shakeri H, Gevaert AB, Schrijvers DM, De Meyer GRY, De Keulenaer GW, Guns PDF, et al. Neuregulin-1 attenuates stress-induced vascular senescence. *Cardiovasc Res* (2018) 114:1041–51. doi: 10.1093/cvr/cvy059

155. Chen T, Ma C, Fan G, Liu H, Lin X, Li J, et al. SIRT3 protects endothelial cells from high glucose-induced senescence and dysfunction via the p53 pathway. *Life Sci* (2021) 264:118724. doi: 10.1016/j.lfs.2020.118724

156. Rossini AA, Like AA, Chick WL, Appel MC, Cahill GFJr. Studies of streptozotocin-induced insulitis and diabetes. *Proc Natl Acad Sci U.S.A.* (1977) 74:2485–9.

157. Fang SB, Zhang HY, Wang C, He BX, Liu XQ, Meng XC, et al. Small extracellular vesicles derived from human mesenchymal stromal cells prevent group 2 innate lymphoid cell-dominant allergic airway inflammation through delivery of miR-146a-5p. *J Extracell Vesicles* (2020) 9:1723260. doi: 10.1080/20013078.2020.1723260

158. Erusalimsky JD. Vascular endothelial senescence: from mechanisms to pathophysiology. *J Appl Physiol (1985)* (2009) 106:326–32. doi: 10.1152/japplphysiol.91353.2008

159. Ahmad R, Sylvester J, Ahmad M, Zafarullah M. Involvement of H-Ras and reactive oxygen species in proinflammatory cytokine-induced matrix metalloproteinase-13 expression in human articular chondrocytes. *Arch Biochem Biophys* (2011) 507:350–5. doi: 10.1016/j.abb.2010.12.032

160. Guillén M, Tofiño-Vian M, Silvestre A, Castejón M, Alcaraz M. Role of peroxiredoxin 6 in the chondroprotective effects of microvesicles from human adipose tissue-derived mesenchymal stem cells. *J orthopaedic translation* (2021) 30:61–9. doi: 10.1016/j.jot.2021.08.003

161. Lo WJ, Lin CL, Chang YC, Bai LY, Lin CY, Liang JA, et al. Total body irradiation tremendously impair the proliferation, differentiation and chromosomal integrity of bone marrow-derived mesenchymal stromal stem cells. *Ann Hematol* (2018) 97:697–707. doi: 10.1007/s00277-018-3231-y

162. Alessio N, Del Gaudio S, Capasso S, Di Bernardo G, Cappabianca S, Cipollaro M, et al. Low dose radiation induced senescence of human mesenchymal stromal cells and impaired the autophagy process. *Oncotarget* (2015) 6:8155–66. doi: 10.18632/oncotarget.2692

163. Zou Q, Hong W, Zhou Y, Ding Q, Wang J, Jin W, et al. Bone marrow stem cell dysfunction in radiation-induced abscopal bone loss. *J Orthop Surg Res* (2016) 11:3. doi: 10.1186/s13018-015-0339-9

164. Liu S, Liu D, Chen C, Hamamura K, Moshaverinia A, Yang R, et al. MSC transplantation improves osteopenia via epigenetic regulation of notch signaling in lupus. *Cell Metab* (2015) 22:606–18. doi: 10.1016/j.cmet.2015.08.018

165. Liu X, Li Q, Niu X, Hu B, Chen S, Song W, et al. Exosomes secreted from human-induced pluripotent stem cell-derived mesenchymal stem cells prevent osteonecrosis of the femoral head by promoting angiogenesis. *Int J Biol Sci* (2017) 13:232–44. doi: 10.7150/ijbs.16951

166. Zuo R, Liu M, Wang Y, Li J, Wang W, Wu J, et al. BM-MSC-derived exosomes alleviate radiation-induced bone loss by restoring the function of recipient BM-MSCs and activating Wnt/β-catenin signaling. *Stem Cell Res Ther* (2019) 10:30. doi: 10.1186/s13287-018-1121-9

167. Fisher AB. Peroxiredoxin 6 in the repair of peroxidized cell membranes and cell signaling. *Arch Biochem Biophys* (2017) 617:68–83. doi: 10.1016/j.abb.2016.12.003

168. Hou J, Han ZP, Jing YY, Yang X, Zhang SS, Sun K, et al. Autophagy prevents irradiation injury and maintains stemness through decreasing ROS generation in mesenchymal stem cells. *Cell Death Dis* (2013) 4:e844. doi: 10.1038/cddis.2013.338

169. Zhao CQ, Zhang YH, Jiang SD, Jiang LS, Dai LY. Both endoplasmic reticulum and mitochondria are involved in disc cell apoptosis and intervertebral disc degeneration in rats. *Age (Dordr)* (2010) 32:161–77. doi: 10.1007/s11357-009-9121-4

170. Xie L, Chen Z, Liu M, Huang W, Zou F, Ma X, et al. MSC-Derived Exosomes Protect Vertebral Endplate Chondrocytes against Apoptosis and Calcification via the miR-31-5p/ATF6 Axis. *Mol Ther Nucleic Acids* (2020) 22:601–14. doi: 10.1016/j.omtn.2020.09.026

171. Sakai D, Mochida J, Iwashina T, Hiyama A, Omi H, Imai M, et al. Regenerative effects of transplanting mesenchymal stem cells embedded in atelocollagen to the degenerated intervertebral disc. *Biomaterials* (2006) 27:335–45. doi: 10.1016/j.biomaterials.2005.06.038

172. Porée B, Kypriotou M, Chadjichristos C, Beauchef G, Renard E, Legendre F, et al. Interleukin-6 (IL-6) and/or soluble IL-6 receptor down-regulation of human type II collagen gene expression in articular chondrocytes requires a decrease of Sp1.Sp3 ratio and of the binding activity of both factors to the COL2A1 promoter. *J Biol Chem* (2008) 283:4850–65. doi: 10.1074/jbc.M706387200

173. Goldring MB, Otero M, Plumb DA, Dragomir C, Favero M, El Hachem K, et al. Roles of inflammatory and anabolic cytokines in cartilage metabolism: signals and multiple effectors converge upon MMP-13 regulation in osteoarthritis. *Eur Cell Mater* (2011) 21:202–20. doi: 10.22203/eCM.v021a16

174. Han Y, Xu X, Tang C, Gao P, Chen X, Xiong X, et al. Reactive oxygen species promote tubular injury in diabetic nephropathy: The role of the mitochondrial ros-txnip-nlrp3 biological axis. *Redox Biol* (2018) 16:32–46. doi: 10.1016/j.redox.2018.02.013

175. Piazza N, Dehghani M, Gaborski TR, Wuertz-Kozak K. Therapeutic potential of extracellular vesicles in degenerative diseases of the intervertebral disc. *Front Bioeng Biotechnol* (2020) 8:311. doi: 10.3389/fbioe.2020.00311

176. Su T, Xiao Y, Xiao Y, Guo Q, Li C, Huang Y, et al. Bone marrow mesenchymal stem cells-derived exosomal miR-29b-3p regulates aging-associated insulin resistance. *ACS Nano* (2019) 13:2450–62. doi: 10.1021/acsnano.8b09375

177. Aghagolzadeh P, Radpour R, Bachtler M, Van Goor H, Smith ER, Lister A, et al. Hydrogen sulfide attenuates calcification of vascular smooth muscle cells via KEAP1/NRF2/NQO1 activation. *Atherosclerosis* (2017) 265:78–86. doi: 10.1016/j.atherosclerosis.2017.08.012

178. Ageta H, Tsuchida K. Post-translational modification and protein sorting to small extracellular vesicles including exosomes by ubiquitin and UBLs. *Cell Mol Life Sci* (2019) 76:4829–48. doi: 10.1007/s00018-019-03246-7

179. Pockert AJ, Richardson SM, Le Maitre CL, Lyon M, Deakin JA, Buttle DJ, et al. Modified expression of the ADAMTS enzymes and tissue inhibitor of metalloproteinases 3 during human intervertebral disc degeneration. *Arthritis Rheum* (2009) 60:482–91. doi: 10.1002/art.24291

180. Tian Y, Yuan W, Fujita N, Wang J, Wang H, Shapiro IM, et al. Inflammatory cytokines associated with degenerative disc disease control aggrecanase-1 (ADAMTS-4) expression in nucleus pulposus cells through MAPK and NF-κB. *Am J Pathol* (2013) 182:2310–21. doi: 10.1016/j.ajpath.2013.02.037

181. Chen P, Zheng L, Wang Y, Tao M, Xie Z, Xia C, et al. Desktop-stereolithography 3D printing of a radially oriented extracellular matrix/mesenchymal stem cell exosome bioink for osteochondral defect regeneration. *Theranostics* (2019) 9:2439–59. doi: 10.7150/thno.31017

182. Aghajani Nargesi A, Lerman LO, Eirin A. Mesenchymal stem cell-derived extracellular vesicles for kidney repair: current status and looming challenges. *Stem Cell Res Ther* (2017) 8:273. doi: 10.1186/s13287-017-0727-7

183. Bigarella CL, Liang R, Ghaffari S. Stem cells and the impact of ROS signaling. *Development* (2014) 141:4206–18. doi: 10.1242/dev.107086

184. Davalli P, Mitic T, Caporali A, Lauriola A, D'arca D. ROS, cell senescence, and novel molecular mechanisms in aging and age-related diseases. *Oxid Med Cell Longev* (2016) 2016:3565127. doi: 10.1155/2016/3565127

185. Deretic V, Saitoh T, Akira S. Autophagy in infection, inflammation and immunity. *Nat Rev Immunol* (2013) 13:722–37. doi: 10.1038/nri3532

186. Harman D. Free radical theory of aging: an update: increasing the functional life span. *Ann N Y Acad Sci* (2006) 1067:10–21. doi: 10.1196/annals.1354.003

187. Kawanishi S, Hiraku Y, Oikawa S. Mechanism of guanine-specific DNA damage by oxidative stress and its role in carcinogenesis and aging. *Mutat Res* (2001) 488:65–76. doi: 10.1016/S1383-5742(00)00059-4

188. Saxena S, Vekaria H, Sullivan PG, Seifert AW. Connective tissue fibroblasts from highly regenerative mammals are refractory to ROS-induced cellular senescence. *Nat Commun* (2019) 10:4400. doi: 10.1038/s41467-019-12398-w

189. Dixon SJ, Lemberg KM, Lamprecht MR, Skouta R, Zaitsev EM, Gleason CE, et al. Ferroptosis: an iron-dependent form of nonapoptotic cell death. *Cell* (2012) 149:1060–72. doi: 10.1016/j.cell.2012.03.042

190. Feng C, Yang M, Lan M, Liu C, Zhang Y, Huang B, et al. ROS: crucial intermediators in the pathogenesis of intervertebral disc degeneration. *Oxid Med Cell Longev* (2017) 2017:5601593. doi: 10.1155/2017/5601593

191. Khanh VC, Yamashita T, Ohneda K, Tokunaga C, Kato H, Osaka M, et al. Rejuvenation of mesenchymal stem cells by extracellular vesicles inhibits the elevation of reactive oxygen species. *Sci Rep* (2020) 10:17315. doi: 10.1038/s41598-020-74444-8

192. Mas-Bargues C, Sanz-Ros J, Román-Domínguez A, Gimeno-Mallench L, Inglés M, Viña J, et al. Extracellular vesicles from healthy cells improves cell function and

stemness in premature senescent stem cells by miR-302b and HIF-1α Activation. *Biomolecules* (2020) 10(6):957. doi: 10.3390/biom10060957

193. Kim JY, Shin KK, Lee AL, Kim YS, Park HJ, Park YK, et al. MicroRNA-302 induces proliferation and inhibits oxidant-induced cell death in human adipose tissue-derived mesenchymal stem cells. *Cell Death Dis* (2014) 5:e1385. doi: 10.1038/cddis.2014.344

194. Zhang L, Yu D. Exosomes in cancer development, metastasis, and immunity. *Biochim Biophys Acta Rev Cancer* (2019) 1871:455–68. doi: 10.1016/j.bbcan.2019.04.004

195. Wieckowski EU, Visus C, Szajnik M, Szczepanski MJ, Storkus WJ, Whiteside TL. Tumor-derived microvesicles promote regulatory T cell expansion and induce apoptosis in tumor-reactive activated CD8+ T lymphocytes. *J Immunol* (2009) 183:3720–30. doi: 10.4049/jimmunol.0900970

196. Szajnik M, Czystowska M, Szczepanski MJ, Mandapathil M, Whiteside TL. Tumor-derived microvesicles induce, expand and up-regulate biological activities of human regulatory T cells (Treg). *PloS One* (2010) 5:e11469. doi: 10.1371/journal.pone.0011469

197. Andreola G, Rivoltini L, Castelli C, Huber V, Perego P, Deho P, et al. Induction of lymphocyte apoptosis by tumor cell secretion of FasL-bearing microvesicles. *J Exp Med* (2002) 195:1303–16. doi: 10.1084/jem.20011624

198. Huber V, Fais S, Iero M, Lugini L, Canese P, Squarcina P, et al. Human colorectal cancer cells induce T-cell death through release of proapoptotic microvesicles: role in immune escape. *Gastroenterology* (2005) 128:1796–804. doi: 10.1053/j.gastro.2005.03.045

199. Bhatnagar S, Schorey JS. Exosomes released from infected macrophages contain Mycobacterium avium glycopeptidolipids and are proinflammatory. *J Biol Chem* (2007) 282:25779–89. doi: 10.1074/jbc.M702277200

200. Schorey JS, Harding CV. Extracellular vesicles and infectious diseases: new complexity to an old story. *J Clin Invest* (2016) 126:1181–9. doi: 10.1172/JCI81132

201. Zhang HG, Liu C, Su K, Yu S, Zhang L, Zhang S, et al. A membrane form of TNF-alpha presented by exosomes delays T cell activation-induced cell death. *J Immunol* (2006) 176:7385–93. doi: 10.4049/jimmunol.176.12.7385

202. Chaput N, Flament C, Viaud S, Taieb J, Roux S, Spatz A, et al. Dendritic cell derived-exosomes: biology and clinical implementations. *J Leukoc Biol* (2006) 80:471–8. doi: 10.1189/jlb.0206094

203. Barros FM, Carneiro F, MaChado JC, Melo SA. Exosomes and immune response in cancer: friends or foes? *Front Immunol* (2018) 9:730. doi: 10.3389/fimmu.2018.00730

204. Damania A, Jaiman D, Teotia AK, Kumar A. Mesenchymal stromal cell-derived exosome-rich fractionated secretome confers a hepatoprotective effect in liver injury. *Stem Cell Res Ther* (2018) 9:31. doi: 10.1186/s13287-017-0752-6

205. Zhao S, Huang M, Yan L, Zhang H, Shi C, Liu J, et al. Exosomes Derived from Baicalin-Pretreated Mesenchymal Stem Cells Alleviate Hepatocyte Ferroptosis after Acute Liver Injury via the Keap1-NRF2 Pathway. *Oxid Med Cell Longev* (2022) 2022:8287227. doi: 10.1155/2022/8287227

206. Pan Q, Kuang X, Cai S, Wang X, Du D, Wang J, et al. miR-132-3p priming enhances the effects of mesenchymal stromal cell-derived exosomes on ameliorating brain ischemic injury. *Stem Cell Res Ther* (2020) 11:260. doi: 10.1186/s13287-020-01761-0

207. Lei X, He N, Zhu L, Zhou M, Zhang K, Wang C, et al. Mesenchymal Stem Cell-Derived Extracellular Vesicles Attenuate Radiation-Induced Lung Injury via miRNA-214-3p. *Antioxid Redox Signal* (2021) 35:849–62. doi: 10.1089/ars.2019.7965

208. Xu N, Shao Y, Ye K, Qu Y, Memet O, He D, et al. Mesenchymal stem cell-derived exosomes attenuate phosgene-induced acute lung injury in rats. *Inhal Toxicol* (2019) 31:52–60. doi: 10.1080/08958378.2019.1597220

209. Gao Z, Zhang C, Peng F, Chen Q, Zhao Y, Chen L, et al. Hypoxic mesenchymal stem cell-derived extracellular vesicles ameliorate renal fibrosis after ischemia-reperfusion injure by restoring CPT1A mediated fatty acid oxidation. *Stem Cell Res Ther* (2022) 13:191. doi: 10.1186/s13287-022-02861-9

210. Taghavi-Farahabadi M, Mahmoudi M, Mahdaviani SA, Baghaei K, Rayzan E, Hashemi SM, et al. Improving the function of neutrophils from chronic granulomatous disease patients using mesenchymal stem cells' exosomes. *Hum Immunol* (2020) 81:614–24. doi: 10.1016/j.humimm.2020.05.009

211. Yang C, Lim W, Park J, Park S, You S, Song G. Anti-inflammatory effects of mesenchymal stem cell-derived exosomal microRNA-146a-5p and microRNA-548e-5p on human trophoblast cells. *Mol Hum Reprod* (2019) 25:755–71. doi: 10.1093/molehr/gaz054

212. Guo XF, Gu SS, Wang J, Sun H, Zhang YJ, Yu PF, et al. Protective effect of mesenchymal stem cell-derived exosomal treatment of hippocampal neurons against oxygen-glucose deprivation/reperfusion-induced injury. *World J Emerg Med* (2022) 13:46–53. doi: 10.5847/wjem.j.1920-8642.2022.015

213. De Godoy MA, Saraiva LM, De Carvalho LRP, Vasconcelos-Dos-Santos A, Beiral HJV, Ramos AB, et al. Mesenchymal stem cells and cell-derived extracellular vesicles protect hippocampal neurons from oxidative stress and synapse damage induced by amyloid-β oligomers. *J Biol Chem* (2018) 293:1957–75. doi: 10.1074/jbc.M117.807180

214. Scott SR, March KL, Wang IW, Singh K, Liu J, Turrentine M, et al. Bone marrow- or adipose-mesenchymal stromal cell secretome preserves myocardial transcriptome profile and ameliorates cardiac damage following ex vivo cold storage. *J Mol Cell Cardiol* (2022) 164:1–12. doi: 10.1016/j.yjmcc.2021.11.002

215. O'Brien CG, Ozen MO, Ikeda G, Vaskova E, Jung JH, Bayardo N, et al. Mitochondria-rich extracellular vesicles rescue patient-specific cardiomyocytes from doxorubicin injury: insights into the SENECA trial. *JACC CardioOncol* (2021) 3:428–40. doi: 10.1016/j.jaccao.2021.05.006

216. Li D, Zhang D, Tang B, Zhou Y, Guo W, Kang Q, et al. Exosomes from human umbilical cord mesenchymal stem cells reduce damage from oxidative stress and the epithelial-mesenchymal transition in renal epithelial cells exposed to oxalate and calcium oxalate monohydrate. *Stem Cells Int* (2019) 2019:6935806. doi: 10.1155/2019/6935806

217. Rui K, Hong Y, Zhu Q, Shi X, Xiao F, Fu H, et al. Olfactory ecto-mesenchymal stem cell-derived exosomes ameliorate murine Sjögren's syndrome by modulating the function of myeloid-derived suppressor cells. *Cell Mol Immunol* (2021) 18:440–51. doi: 10.1038/s41423-020-00587-3

218. Zou L, Ma X, Wu B, Chen Y, Xie D, Peng C. Protective effect of bone marrow mesenchymal stem cell-derived exosomes on cardiomyoblast hypoxia-reperfusion injury through the miR-149/let-7c/Faslg axis. *Free Radic Res* (2020) 54:722–31. doi: 10.1080/10715762.2020.1837793

219. Sun F, Sun Y, Zhu J, Wang X, Ji C, Zhang J, et al. Mesenchymal stem cells-derived small extracellular vesicles alleviate diabetic retinopathy by delivering NEDD4. *Stem Cell Res Ther* (2022) 13:293. doi: 10.1186/s13287-022-02983-0

220. Yan F, Cui W, Chen Z. Mesenchymal stem cell-derived exosome-loaded microRNA-129-5p inhibits TRAF3 expression to alleviate apoptosis and oxidative stress in heart failure. *Cardiovasc Toxicol* (2022) 22:631–45. doi: 10.1007/s12012-022-09743-9

221. Mahmoudi M, Taghavi-Farahabadi M, Rezaei N, Hashemi SM. Comparison of the effects of adipose tissue mesenchymal stromal cell-derived exosomes with conditioned media on neutrophil function and apoptosis. *Int Immunopharmacol* (2019) 74:105689. doi: 10.1016/j.intimp.2019.105689

222. Ma J, Shi X, Li M, Chen S, Gu Q, Zheng J, et al. MicroRNA-181a-2-3p shuttled by mesenchymal stem cell-secreted extracellular vesicles inhibits oxidative stress in Parkinson's disease by inhibiting EGR1 and NOX4. *Cell Death Discovery* (2022) 8:33. doi: 10.1038/s41420-022-00823-x

223. Liu J, Lin M, Qiao F, Zhang C. Exosomes Derived from lncRNA TCTN2-Modified Mesenchymal Stem Cells Improve Spinal Cord Injury by miR-329-3p/IGF1R Axis. *J Mol Neurosci* (2022) 72:482–95. doi: 10.1007/s12031-021-01914-7

224. Kubota K, Nakano M, Kobayashi E, Mizue Y, Chikenji T, Otani M, et al. An enriched environment prevents diabetes-induced cognitive impairment in rats by enhancing exosomal miR-146a secretion from endogenous bone marrow-derived mesenchymal stem cells. *PloS One* (2018) 13:e0204252. doi: 10.1371/journal.pone.0204252

225. Liu X, Li X, Zhu W, Zhang Y, Hong Y, Liang X, et al. Exosomes from mesenchymal stem cells overexpressing MIF enhance myocardial repair. *J Cell Physiol* (2020) 235:8010–22. doi: 10.1002/jcp.29456

226. Da Silva D, De Freitas ML, Cahil GM, De São José VS, Neto FM, Cardoso RC, et al. Influence of stem cell therapy on thyroid function and reactive oxygen species production in diabetic rats. *Horm Metab Res* (2018) 50:331–9. doi: 10.1055/a-0588-7944

227. Zhang G, Zou X, Huang Y, Wang F, Miao S, Liu G, et al. Mesenchymal stromal cell-derived extracellular vesicles protect against acute kidney injury through anti-oxidation by enhancing Nrf2/ARE activation in rats. *Kidney Blood Press Res* (2016) 41:119–28. doi: 10.1159/000443413

228. Farahani RA, Zhu XY, Tang H, Jordan KL, Lerman A, Lerman LO, et al. Metabolic syndrome alters the cargo of mitochondria-related microRNAs in swine mesenchymal stem cell-derived extracellular vesicles, impairing their capacity to repair the stenotic kidney. *Stem Cells Int* (2020) 2020:8845635. doi: 10.1155/2020/8845635

229. Cai G, Cai G, Zhou H, Zhuang Z, Liu K, Pei S, et al. Mesenchymal stem cell-derived exosome miR-542-3p suppresses inflammation and prevents cerebral infarction. *Stem Cell Res Ther* (2021) 12:2. doi: 10.1186/s13287-020-02030-w

230. Jin Z, Ren J, Qi S. Exosomal miR-9-5p secreted by bone marrow-derived mesenchymal stem cells alleviates osteoarthritis by inhibiting syndecan-1. *Cell Tissue Res* (2020) 381:99–114. doi: 10.1007/s00441-020-03193-x

231. Firoozi S, Pahlavan S, Ghanian MH, Rabbani S, Barekat M, Nazari A, et al. Mesenchymal stem cell-derived extracellular vesicles alone or in conjunction with a SDKP-conjugated self-assembling peptide improve a rat model of myocardial infarction. *Biochem Biophys Res Commun* (2020) 524:903–9. doi: 10.1016/j.bbrc.2020.02.009

232. Liu Y, Zhao S, Luo L, Wang J, Zhu Z, Xiang Q, et al. Mesenchymal stem cell-derived exosomes ameliorate erection by reducing oxidative stress damage of corpus cavernosum in a rat model of artery injury. *J Cell Mol Med* (2019) 23:7462–73. doi: 10.1111/jcmm.14615

233. Lamkanfi M, Dixit VM. Mechanisms and functions of inflammasomes. *Cell* (2014) 157:1013–22. doi: 10.1016/j.cell.2014.04.007

234. Milkovic L, Cipak Gasparovic A, Cindric M, Mouthuy PA, Zarkovic N. Short overview of ROS as cell function regulators and their implications in therapy concepts. *Cells* (2019) 8(8):793. doi: 10.3390/cells8080793

235. Boulestreau J, Maumus M, Rozier P, Jorgensen C, Noël D. Mesenchymal stem cell derived extracellular vesicles in aging. *Front Cell Dev Biol* (2020) 8:107. doi: 10.3389/fcell.2020.00107

236. Mckinnirey F, Herbert B, Vesey G, Mccracken S. Immune modulation via adipose derived Mesenchymal Stem cells is driven by donor sex in *vitro*. *Sci Rep* (2021) 11:12454. doi: 10.1038/s41598-021-91870-4

237. Ran X, Diao JX, Sun XG, Wang M, An H , Huang GQ, et al. Huangzhi oral liquid prevents arrhythmias by upregulating caspase-3 and apoptosis network proteins in myocardial ischemia-reperfusion injury in rats. *Evid Based Complement Alternat Med* (2015) 2015:518926. doi: 10.1155/2015/518926

frontiers | Frontiers in Immunology

TYPE Original Research
PUBLISHED 03 October 2023
DOI 10.3389/fimmu.2023.1263926

OPEN ACCESS

EDITED BY
Chao Yang,
Zhejiang Ocean University, China

REVIEWED BY
Joseph Larkin,
University of Florida, United States
Ceren Ciraci,
Istanbul Technical University, Türkiye
Tina Fløyel,
Steno Diabetes Center Copenhagen (SDCC), Denmark

*CORRESPONDENCE
Reinaldo S. Dos Santos
r.sousa@umh.es
Laura Marroqui
lmarroqui@umh.es

RECEIVED 20 July 2023
ACCEPTED 19 September 2023
PUBLISHED 03 October 2023

CITATION
Dos Santos RS, Guzman-Llorens D, Perez-Serna AA, Nadal A and Marroqui L (2023) Deucravacitinib, a tyrosine kinase 2 pseudokinase inhibitor, protects human EndoC-βH1 β-cells against proinflammatory insults. *Front. Immunol.* 14:1263926. doi: 10.3389/fimmu.2023.1263926

Deucravacitinib, a tyrosine kinase 2 pseudokinase inhibitor, protects human EndoC-βH1 β-cells against proinflammatory insults

Reinaldo S. Dos Santos[1,2*], Daniel Guzman-Llorens[1], Atenea A. Perez-Serna[1,2], Angel Nadal[1,2] and Laura Marroqui[1,2*]

[1]Instituto de Investigación, Desarrollo e Innovación en Biotecnología Sanitaria de Elche (IDiBE), Universidad Miguel Hernández de Elche, Alicante, Spain, [2]CIBER de Diabetes y Enfermedades Metabólicas Asociadas, Instituto de Salud Carlos III, Madrid, Spain

Introduction: Type 1 diabetes is characterized by pancreatic islet inflammation and autoimmune-driven pancreatic β-cell destruction. Interferon-α (IFNα) is a key player in early human type 1 diabetes pathogenesis. IFNα activates the tyrosine kinase 2 (TYK2)-signal transducer and activator of transcription (STAT) pathway, leading to inflammation, HLA class I overexpression, endoplasmic reticulum (ER) stress, and β-cell apoptosis (in synergy with IL-1β). As TYK2 inhibition has raised as a potential therapeutic target for the prevention or treatment of type 1 diabetes, we investigated whether the selective TYK2 inhibitor deucravacitinib could protect β-cells from the effects of IFNα and other proinflammatory cytokines (i.e., IFNγ and IL-1β).

Methods: All experiments were performed in the human EndoC-βH1 β-cell line. HLA class I expression, inflammation, and ER stress were evaluated by real-time PCR, immunoblotting, and/or immunofluorescence. Apoptosis was assessed by the DNA-binding dyes Hoechst 33342 and propidium iodide or caspase 3/7 activity. The promoter activity was assessed by luciferase assay.

Results: Deucravacitinib prevented IFNα effects, such as STAT1 and STAT2 activation and MHC class I hyperexpression, in a dose-dependent manner without affecting β-cell survival and function. A comparison between deucravacitinib and two Janus kinase inhibitors, ruxolitinib and baricitinib, showed that deucravacitinib blocked IFNα- but not IFNγ-induced signaling pathway. Deucravacitinib protected β-cells from the effects of two different combinations of cytokines: IFNα + IL-1β and IFNγ + IL-1β. Moreover, this TYK2 inhibitor could partially reduce apoptosis and inflammation in cells pre-treated with IFNα + IL-1β or IFNγ + IL-1β.

Discussion: Our findings suggest that, by protecting β-cells against the deleterious effects of proinflammatory cytokines without affecting β-cell function and survival, deucravacitinib could be repurposed for the prevention or treatment of early type 1 diabetes.

KEYWORDS

apoptosis, deucravacitinib, inflammation, pancreatic β-cells, TYK2, type 1 diabetes, type I interferons

1 Introduction

Type 1 diabetes is characterized by pancreatic islet inflammation and specific destruction of pancreatic β-cells by an autoimmune assault, which develops in the context of an inadequate "dialogue" between β-cells and the invading immune cells (1, 2).

A growing body of evidence places type I interferons (IFNs) as key players in the early stages of human type 1 diabetes pathogenesis (3). IFNα was found in islets from type 1 diabetes patients (4–6), and laser-captured islets from living donors with recent-onset type 1 diabetes showed increased expression of IFN-stimulated genes (ISGs) (7). In genetically susceptible children, an IFN signature was temporarily amplified preceding the development of autoantibodies and throughout the progress of type 1 diabetes (8, 9). Recently, three type I IFN response markers, namely human MX Dynamin Like GTPase 1 (MX1), double-stranded RNA sensor protein kinase R, and HLA class I, were found to be expressed in a significantly higher percentage of insulin-containing islets from autoantibody-positive and/or recent-onset type 1 diabetes donors (10). In human β-cells, IFNα induced inflammation, endoplasmic reticulum (ER) stress as well as a long-lasting overexpression of HLA class I via activation of the tyrosine kinase 2 (TYK2)-signal transducer and activator of transcription (STAT) pathway. Moreover, IFNα induced apoptosis in the presence of IL-1β (11–14).

Targeting the type I IFN signaling pathway has been proposed as a potential adjuvant therapy to treat at-risk individuals or patients still in the very early stages of the disease (3, 15). Among some of the strategies that have been suggested, inhibitors of Janus kinase (JAK) proteins (JAK1-3 and TYK2) show great promise. Treatment with AZD1480 (a JAK1/JAK2 inhibitor) and ABT 317 (a JAK1-selective inhibitor) protected non-obese diabetic mice against autoimmune diabetes and reversed diabetes in newly diagnosed non-obese diabetic mice (16, 17). In human β-cells, clinically used JAK inhibitors, namely ruxolitinib, cerdulatinib, and baricitinib, prevented MHC class I overexpression, ER stress, chemokine production, and apoptosis (13, 14).

Lately, attention has focused on *TYK2*, a candidate gene for type 1 diabetes whose genetic variants that decrease TYK2 activity are associated with protection against the disease (18–20). TYK2 is crucial for cell development and IFNα-mediated responses in human β-cells (11, 21, 22). Partial TYK2 knockdown protected human β-cells against apoptosis and inflammation induced by polyinosinic-polycitidilic acid, a mimic of double-stranded RNA produced during viral infection (21). In mature stem cell-islets, TYK2 knockout or pharmacologic inhibition decreased T-cell-mediated cytotoxicity by preventing IFNα-induced antigen processing and presentation, including MHC class I expression (22). As these findings place TYK2 as a critical regulator of the type I IFN signaling pathway in β-cells, selective TYK2 inhibition has emerged as a drug target to treat type 1 diabetes. Recently, two novel small molecule inhibitors binding to the TYK2 pseudokinase domain protected human β-cells against the deleterious effects of IFNα without compromising β-cell function and susceptibility to potentially diabetogenic viruses (23).

Deucravacitinib, a small molecule that selectively targets the TYK2 pseudokinase domain, has shown great therapeutic potential for immune-mediated diseases, such as lupus nephritis and systemic lupus erythematosus (24, 25). In fact, deucravacitinib has been recently approved for treatment of plaque psoriasis (26). However, no preclinical studies have deeply explored the possible use of deucravacitinib in the context of type 1 diabetes. Notably, Chandra et al. recently used deucravacitinib to validate their CRISPR-Cas9-generated *TYK2* knockout in human induced pluripotent stem cells, but did not provide further characterisation of its effects on β-cells (22).

In this study, we report the effects of deucravacitinib on the human insulin-producing EndoC-βH1 cells, including its ability to prevent IFNα-triggered signaling pathway and damaging effects on β-cells.

2 Materials and methods

2.1 Culture of EndoC-βH1 cells

The human EndoC-βH1 β-cell line [research resource identifier (RRID): CVCL_L909, Univercell-Biosolutions, France] was cultured in Matrigel/fibronectin-coated plates as previously described (27). Cells were cultured in DMEM containing 5.6 mmol/L glucose, 10 mmol/L nicotinamide, 5.5 µg/mL transferrin, 50 µmol/L 2-mercaptoethanol, 6.7 ng/mL selenite, 2% BSA fatty acid free, 100 U/mL penicillin, and 100 µg/mL streptomycin. We confirmed that cells were mycoplasma-free using the MycoAlert Mycoplasma Detection Kit (Lonza, Basel, Switzerland).

2.2 Cell treatments

Proinflammatory cytokine concentrations were selected according to previously established experiments in human β-cells (11, 28): recombinant human IFNα (PeproTech Inc., Rocky Hill, NJ) at 1000 U/mL; recombinant human IFNγ (PeproTech Inc., Rocky Hill, NJ) at 1000 U/mL; and recombinant human IL-1β (R&D Systems, Abingdon, UK) at 50 U/mL. Ruxolitinib, baricitinib, or deucravacitinib (Selleckchem, Planegg, Germany) were prepared in DMSO (used as vehicle) and cells were treated as indicated in the figures. Ruxolitinib and baricitinib concentrations were selected based on previous dose-response experiments (unpublished data). For treatments involving cytokines, 2% FBS was added to the culture medium.

2.3 Cell viability assessment

The percentage of apoptosis was measured by fluorescence microscopy upon staining with the DNA-binding dyes Hoechst 33342 and propidium iodide (Sigma-Aldrich, Saint Louis, MO, USA) as described (29). At least 600 cells were counted for each experimental condition. Viability was assessed by two independent researchers, one of whom was unaware of sample identity, with >90% agreement between results.

2.4 Caspase 3/7 activity

Caspase 3/7 activity was determined using the Caspase-Glo® 3/7 assay (Promega, Madison, WI, USA) following the manufacturer's instructions. Briefly, upon incubation in 100 µL culture medium, cells were incubated with 100 µL Caspase-Glo® 3/7 reagent at room temperature for 1 h before recording luminescence with a POLASTAR plate reader (BMG Labtech, Ortenberg, Germany).

2.5 C-X-C motif chemokine ligand 10 measurements

The release of C-X-C motif chemokine ligand 10 (CXCL10) to the culture medium was detected using Human ProcartaPlex immunoassays (Invitrogen, Vienna, Austria) following the manufacturer's recommendations. Reactions were read with a MagPix system (Luminex, Austin, TX, USA).

2.6 Luciferase reporter assays

Cells were transfected using Lipofectamine 2000 (Invitrogen) with pRL-CMV encoding *Renilla* luciferase (Promega) and luciferase reporter constructs for either gamma-interferon activation site (GAS) (Panomics, Fremont, CA, USA) or IFN-stimulated regulatory element (ISRE) (kindly provided by Dr Izortze Santin, University of the Basque Country, Spain). After recovery, cells were treated with either IFNα for 2 h or IFNγ for 24 h (30). Luciferase activity was measured in a POLASTAR plate reader (BMG Labtech) using the Dual-Luciferase Reporter Assay System (Promega) and corrected for the luciferase activity of the internal control plasmid, i.e., pRL-CMV.

2.7 Real-time PCR

Poly(A)$^+$ mRNA was extracted using Dynabeads mRNA DIRECT kit (Invitrogen) and cDNA synthesis was performed using the High-Capacity cDNA Reverse Transcription Kit (Applied Biosystems). Real-time PCR was performed on the CFX96 Real Time System (Bio-Rad) as described (31) and the housekeeping gene β-actin was used to correct expression values. Of note, β-actin expression was not altered by the experimental conditions used herein. All primers used here are listed in Supplementary Table 1.

2.8 Immunoblotting and immunofluorescence analyses

Western blotting analysis was performed as described (32). Briefly, cells were washed with cold PBS and lysed in Laemmli buffer. Immunoblotting was performed using antibodies against phospho-STAT1 (P-STAT1), phospho-STAT2 (P-STAT2), STAT1, STAT2 (all at 1:1000 dilution), and α-tubulin (1:5000). Peroxidase-conjugated antibodies (1:5000) were used as secondary antibodies. SuperSignal West Femto chemiluminescent substrate (Thermo Scientific, Rockford, IL, USA) and ChemiDoc XRS+ (Bio-Rad Laboratories, Hercules, CA, USA) were used to detect bands.

Immunofluorescence was carried out as described (21, 33). First, cells were washed with cold PBS and fixed with 4% paraformaldehyde. Afterwards, cells were permeabilised and incubated with the mouse anti-MHC Class I (W6/32) antibody (1:1000). The Alexa Fluor 568 polyclonal goat anti-mouse IgG was used as secondary antibody and Hoechst 33342 for counterstaining. Coverslips were mounted with fluorescent mounting medium (Dako, Carpintera, CA, USA) and images were taken on a Zeiss LSM900 microscope with Airyscan 2 (Zeiss-Vision, Munich, Germany) and a x40 objective. Quantification was performed using ZEN (version 3.3; Zeiss-Vision) and open-source FIJI (version 2.0; https://fiji.sc) softwares.

All antibodies used here are listed in Supplementary Table 2.

All the original, uncropped images representing immunoblots and microscopic photos are provided in the Supplementary Material.

2.9 Glucose-stimulated insulin secretion

After preincubation in modified Krebs-Ringer for 1 h, cells were sequentially stimulated with low (0 mmol/L) and high glucose (20 mmol/L) for 1 h (each stimulation) as previously described (34). Insulin secreted and insulin content from lysed cells were measured using a human insulin ELISA kit (Mercodia, Uppsala, Sweden) following the manufacturer's instructions. The amount of secreted insulin as *% of total insulin* was calculated as previously described (35) and data were normalized to insulin secretion at 20 mmol/L glucose in vehicle-treated cells without IFNα (considered as 100%). See Supplementary Material for further details.

2.10 Statistical analyses

The GraphPad Prism 7.0 software (GraphPad Software, La Jolla, CA, USA) was used for statistical analyses. Data are shown as mean ± SEM of independent experiments (*i.e.* considering EndoC-βH1 cells from different passages as $n = 1$). The statistical significance of differences between groups was evaluated using one-way ANOVA followed by Dunnett's test or two-way ANOVA followed by Sidak's test or Dunnett's test, as appropriate. Differences were considered statistically significant when $p \leq 0.05$.

3 Results

3.1 Deucravacitinib prevented IFNα effects without affecting β-cell survival and function

IFNα-mediated TYK2 activation leads to STAT1 and STAT2 phosphorylation, which will eventually upregulate several ISGs, including *HLA-ABC*, *CXCL10*, and *MX1* (Supplementary Figure 1A). Pre-treatment with deucravacitinib inhibited IFNα-

induced STAT1 and STAT2 phosphorylation in a dose-dependent manner, where deucravacitinib showed greater potency against IFNα-stimulated STAT1 phosphorylation (Figures 1A, B). We then selected two doses, 10 and 1000 nmol/L, for the follow-up experiments. Next, we examined how deucravacitinib affects the kinetics of IFNα-induced STAT activation. IFNα increased P-STAT1 and P-STAT2 levels, with a maximum effect at 1-4 h post-treatment and a return to baseline by 24 h (Figures 1C, D; Supplementary Figure 1B). Although STAT1 and STAT2 protein levels were already upregulated by 8 h, STAT2 expression reached peak level at 16 h, while STAT1 expression was still increasing by 24 h (Supplementary Figures 1C, D). Exposure to 1000 nmol/L deucravacitinib abrogated the IFNα-stimulated STAT1 and STAT2 phosphorylation and protein expression, whereas 10 nmol/L deucravacitinib had only a minor effect (Figures 1C, D and Supplementary Figures 1B–D). Furthermore, IFNα-induced MHC class I protein overexpression was blocked by 1000 nmol/L deucravacitinib (Figures 1E, F). Finally, deucravacitinib did not affect β-cell viability nor changed glucose-stimulated insulin secretion and insulin content in the absence or presence of IFNα (Supplementary Figures 1E–G).

3.2 IFNα, but not IFNγ signaling pathway was blocked by deucravacitinib

We compared deucravacitinib with ruxolitinib and baricitinib, two JAK1/JAK2 inhibitors previously tested in β-cells (13, 14). First, we measured the levels of P-STAT1 and P-STAT2 upon stimulation with IFNα or IFNγ (Figures 2A–C; Supplementary Figure 2).

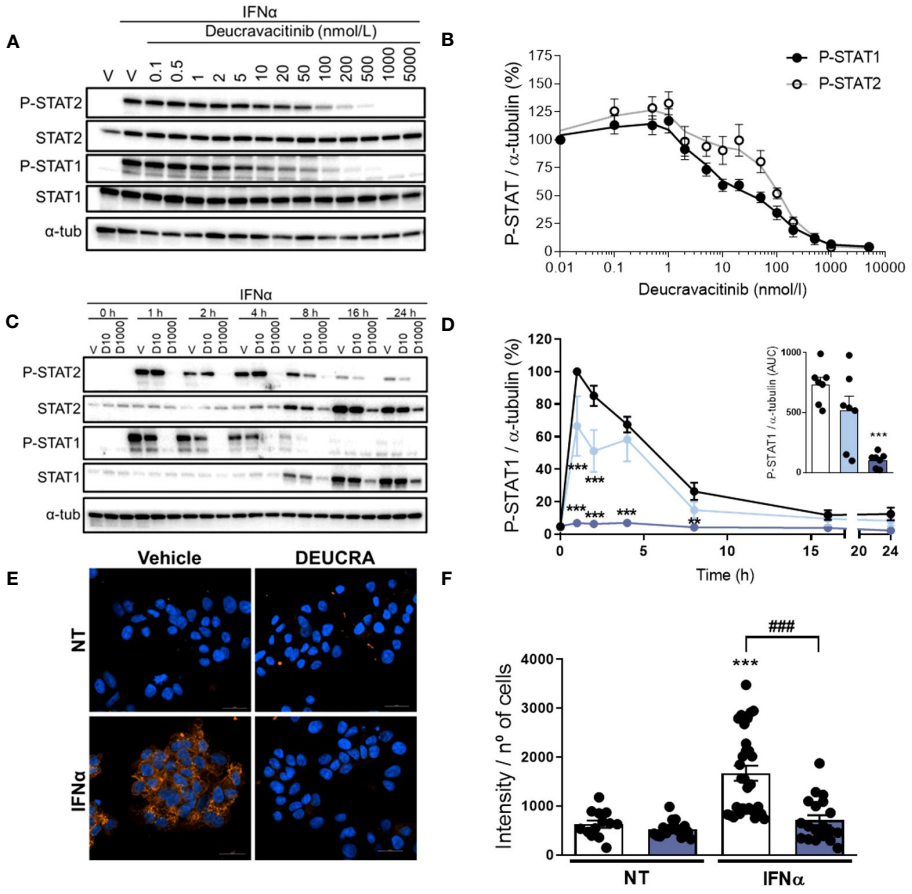

FIGURE 1
Deucravacitinib inhibits IFNα-mediated STAT phosphorylation and MHC class I overexpression. **(A, B)**: EndoC-βH1 cells were treated with vehicle (V) or pre-treated with the indicated deucravacitinib concentrations for 1 h. Afterwards, cells were left non-treated or treated with IFNα (1000 U/mL) in the absence or presence of deucravacitinib for 1 h. Representative immunoblots of P-STAT2, STAT2, P-STAT1, STAT1, and α-tubulin **(A)**, and quantification of P-STAT1 (black circles) and P-STAT2 (white circles) **(B)**. Values were normalized to α-tubulin, and then to the value of IFNα alone of each experiment (considered as 100%) (*n* = 4-6 independent experiments). **(C–F)**: EndoC-βH1 cells were treated with vehicle (V or Veh, black circles) or pre-treated with deucravacitinib (10 [D10, soft blue circles] and 1000 nmol/L [D1000, dark blue circles]) for 1 h. Afterwards, cells were left non-treated or treated with IFNα (1000 U/mL) in the absence or presence of deucravacitinib for 1–24 h **(C, D)** or 24 h **(E, F)**. **(C, D)**: Representative immunoblots of P-STAT2, STAT2, P-STAT1, STAT1, and α-tubulin **(C)**, and quantification of P-STAT1 **(D)**. The inset in **(D)** is the area under curve (AUC) of P-STAT1. Values were normalized to α-tubulin, and then to the highest value of each experiment (considered as 1) (*n* = 3-7 independent experiments). **(E, F)**: Immunocytochemistry analysis of MHC class I (red) and Hoechst 33342 (blue) upon exposure to IFNα in the absence (white bars) or presence of 1000 nmol/L deucravacitinib (dark blue bars) for 24 h. Representative images **(E)** and quantification **(F)** of MHC class I are shown (*n* = 13-30 images/coverslip from 3 different independent experiments). Data are mean ± SEM. *D*: $^{**}p \leq 0.01$, $^{***}p \leq 0.001$ vs. Vehicle + IFNα (two-way ANOVA plus Dunnett's test). F: vs. the respective non-treated (NT) (two-way ANOVA plus Sidak's test); $^{###}p \leq 0.001$, as indicated by bars (two-way ANOVA plus Dunnett's test).

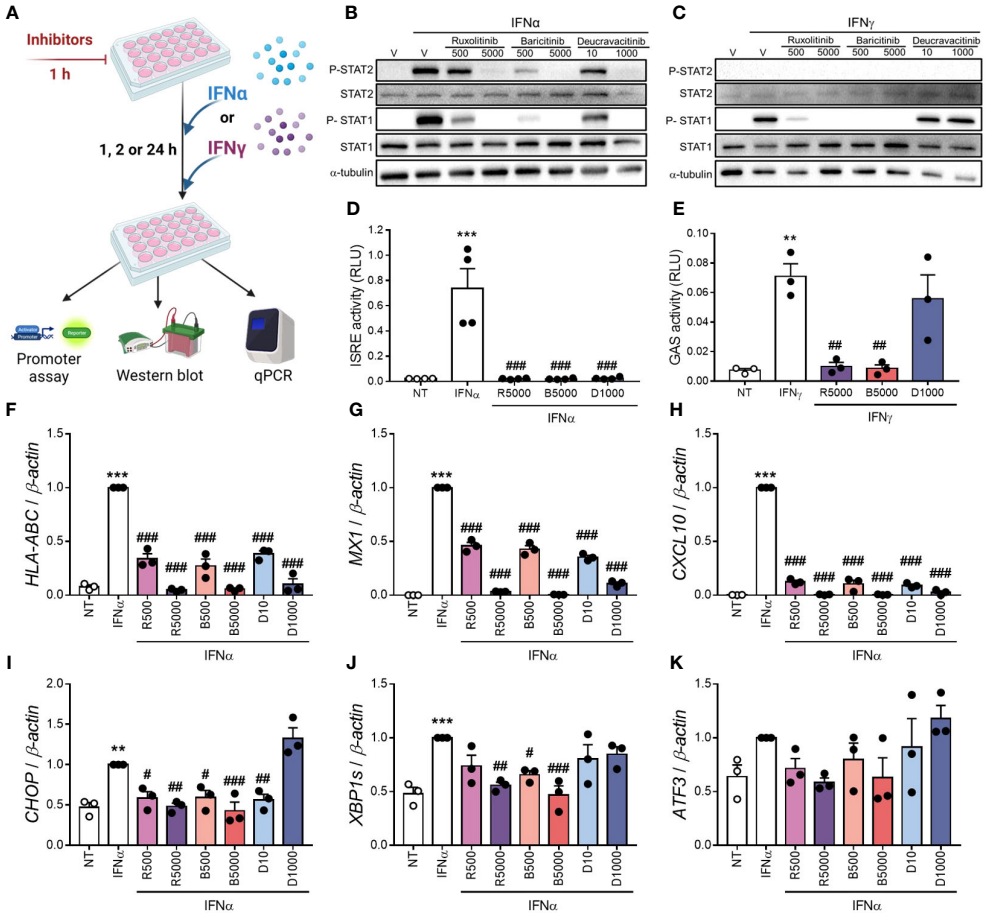

FIGURE 2
Deucravacitinib blocks IFNα- but not IFNγ-induced pathway. **(A)**: Experimental design of the pre-treatment with deucravacitinib and subsequent exposure to IFNα or IFNγ for 1, 2 or 24 h. EndoC-βH1 cells were treated with vehicle (V, white bars) or pre-treated with ruxolitinib (500 and 5000 nmol/L; R500 and R5000), baricitinib (500 and 5000 nmol/L; B500 and B5000), or deucravacitinib (10 and 1000 nmol/L; D10 and D1000) for 1 h. **(B, C)**: After the pre-treatment, cells were left non-treated (NT, white circles) or treated with either IFNα (1000 U/mL) **(B)** or IFNγ (1000 U/mL) **(C)** in the absence or presence of each inhibitor for 1 h. Representative immunoblots of P-STAT2, STAT2, P-STAT1, STAT1, and α-tubulin (n = 4-6 independent experiments). **(D, E)**: EndoC-βH1 cells were transfected with a pRL-CMV plasmid (used as internal control) plus either ISRE **(D)** or GAS **(E)** promoter reporter constructs. After 48 h of recovery, cells were pre-treated as described in **(A)** After the pre-treatment, cells were left non-treated (NT, white circles) or treated with either IFNα (1000 U/mL) for 2 h **(D)** or IFNγ (1000 U/mL) for 24 h **(E)** in the absence or presence of each inhibitor. Relative luciferase units (RLU) were measured by a luminescent assay (n = 3-4 independent experiments). **(F–K)**: EndoC-βH1 cells were pre-treated as described in **(A)** After the pre-treatment, cells were left non-treated (NT) or treated with IFNα (1000 U/mL) in the absence or presence of each inhibitor for 24 h. mRNA expression of *HLA-ABC* **(F)**, *MX1* **(G)**, *CXCL10* **(H)**, *CHOP* **(I)**, *XBP1s* **(J)**, and *ATF3* **(K)** was analyzed by real-time PCR, normalized to β-actin and then to the value of IFNα alone of each experiment (considered as 1) (n = 3 independent experiments). Data are mean ± SEM. $^{**}p \leq 0.01$, $^{***}p \leq 0.01$ vs. the respective non-treated (NT) (one-way ANOVA plus Dunnett's test). $^{\#}p \leq 0.05$, $^{\#\#}p \leq 0.01$, $^{\#\#\#}p \leq 0.001$ vs. IFNα **(D, F–K)** or IFNγ **(E)** (one-way ANOVA plus Dunnett's test).

Ruxolitinib, baricitinib, and deucravacitinib prevented IFNα-stimulated increase in P-STAT1 and P-STAT2 levels (Figure 2B; Supplementary Figures 2A, B). Nevertheless, deucravacitinib did not change IFNγ-induced STAT1 phosphorylation, whereas ruxolitinib and baricitinib blocked it (Figure 2C; Supplementary Figure 2C). We next assessed ISRE and GAS reporter activities upon stimulation with IFNα or IFNγ (Figures 2D, E). While all three inhibitors abrogated IFNα-stimulated ISRE reporter activity (Figure 2D), IFNγ-induced GAS activation was barely affected by deucravacitinib (Figure 2E). As TYK2 is not involved in the IFNγ-triggered signaling pathway, the lack of deucravacitinib effect in IFNγ-treated cells is expected.

3.3 Deucravacitinib blocked IFNα-induced upregulation of ISGs, but not ER stress markers

Assessement of the expression of some ISGs and ER stress markers showed that all three inhibitors prevented IFNα-induced upregulation of *HLA-ABC*, *CXCL10*, and *MX1* in a dose-dependent manner (Figures 2F–K). Although ruxolitinib and baricitinib inhibited the mRNA expression of the ER stress markers C/EBP homologous protein (*CHOP*) and spliced isoform of XBP1 X-box binding protein 1 (*XBP1s*), only 10 nmol/L deucravacitinib reduced *CHOP* expression (Figures 2I, J). None of these inhibitors

changed the expression of activating transcription factor 3 (*ATF3*) (Figure 2K).

3.4 Deucravacitinib prevented cytokine-induced effects in β-cells

Previous studies showed that a combination of IFNα + IL-1β, two cytokines that might be present in the islet milieu at early stages of insulitis, induces β-cell apoptosis, inflammation, and ER stress (11, 14, 23). Thus, we investigated whether deucravacitinib protects β-cells after IFNα + IL-1β exposure (Figure 3A). We observed that deucravacitinib completely prevented IFNα + IL-1β-induced apoptosis (Figures 3B, C). Moreover, deucravacitinib-treated cells showed reduced levels of P-STAT1 and STAT1 (Figure 3D; Supplementary Figures 3A, B) as well as *HLA-ABC*, *MX1*, *CHOP*, and *CXCL10* mRNA expression (Figures 3E–G, J). MHC class I protein expression and CXCL10 secretion were also decreased by TYK2 inhibition (Figures 3H, I, K).

We next evaluated whether deucravacitinib protects against cytokines that, as compared with IFNα, probably appear later in

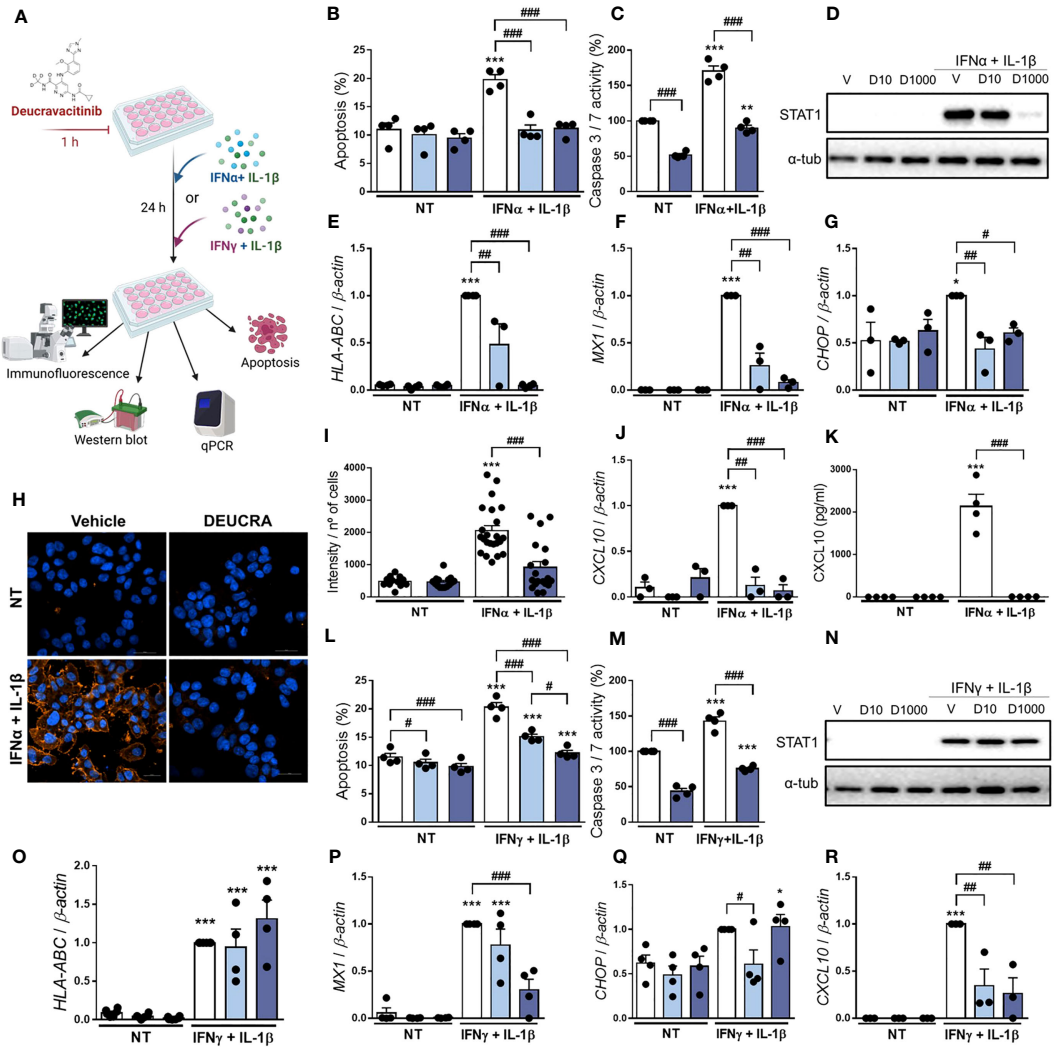

FIGURE 3
Pre-treatment with deucravacitinib prevents IFNα + IL-1β or IFNγ + IL-1β effects. **(A)**: Experimental design of the pre-treatment with deucravacitinib and subsequent exposure to cytokines for 24 h. EndoC-βH1 cells were treated with vehicle (V, white bars) or pre-treated with deucravacitinib (10 [D10, soft blue bars] and 1000 nmol/L [D1000, dark blue bars]) for 1 h. Afterwards, cells were left non-treated (NT) or treated with IFNα + IL-1β (1000 U/mL + 50 U/mL, respectively) **(B–K)** or IFNγ + IL-1β (1000 U/mL + 50 U/mL, respectively) **(L–R)** in the absence or presence of deucravacitinib for 24 h. **(B, L)**: Apoptosis was evaluated using Hoechst 33342/propidium iodide staining (n = 4 independent experiments). **(C, M)**: Caspase 3/7 activity was measured by a luminescent assay. Results are expressed as % vehicle-treated cells in the absence of cytokines (NT) (n = 4 independent experiments). **(D, N)**: Representative immunoblots of P-STAT1, STAT1, and α-tubulin (n = 4 independent experiments). **(E–G, J, O-R)**: mRNA expression of *HLA-ABC* **(E, O)**, *MX1* **(F, P)**, *CHOP* **(G, Q)**, and *CXCL10* **(J, R)** was analyzed by real-time PCR, normalized to β-actin and then to the value of Vehicle treated with IFNα + IL-1β **(E–G, J)** or IFNγ + IL-1β **(O-R)** (considered as 1) (n = 3-4 independent experiments). **(H, I)**: Immunocytochemistry analysis of MHC class I (red) and Hoechst 33342 (blue) upon exposure to IFNα + IL-1β in the absence (white bars) or presence of deucravacitinib (dark blue bars) for 24 h. Representative images **(H)** and quantification **(I)** of MHC class I are shown (12–23 images/coverslip from 3 different independent experiments). **(K)**: CXCL10 secreted to the medium was determined by ELISA (n = 4 independent experiments). Data are mean ± SEM. *$p \leq 0.05$, **$p \leq 0.01$, ***$p \leq 0.001$ vs. the respective non-treated (NT) (two-way ANOVA plus Sidak's test). $^{\#}p \leq 0.05$, $^{\#\#}p \leq 0.01$, $^{\#\#\#}p \leq 0.001$, as indicated by bars (two-way ANOVA plus Dunnett's test).

the progression of islet inflammation: IFNγ and IL-1β (36). After treatment for 24 h (Figure 3A), deucravacitinib inhibited IFNγ + IL-1β-induced apoptosis in a dose-dependent manner (60% and 92% protection at 10 and 1000 nmol/L, respectively) (Figure 3L). These results were confirmed by the caspase 3/7 activity (Figure 3M). Deucravacitinib did not affect IFNγ + IL-1β-induced STAT1 phosphorylation and protein expression (Figure 3N; Supplementary Figures 3C, D) or *HLA-ABC* mRNA expression (Figure 3O); in fact, 1000 nmol/L deucravacitinib increased P-STAT1 levels (Supplementary Figure 3C). Conversely, deucravacitinib diminished *MX1* and *CXCL10* mRNA expression, whereas *CHOP* was reduced only at 10 nmol/L deucravacitinib (Figures 3P–R).

3.5 The harmful effects of cytokines were partially inhibited by deucravacitinib

So far, we investigated whether pre-treatment with deucravacitinib prevents the effects of different cytokines in β-cells. Here, we assessed if deucravacitinib could abrogate these damaging effects. EndoC-βH1 cells were pre-treated with either IFNα + IL-1β or IFNγ + IL-1β for 24 h. Afterwards, 1000 nmol/L deucravacitinib was added for an additional 24 h still in the presence of cytokines (Figure 4A). Deucravacitinib partially decreased IFNα + IL-1β-induced apoptosis (60% decrease) (Figure 4B). IFNα + IL-1β-stimulated *HLA-ABC* mRNA expression remained unchanged in deucravacitinib-treated cells (Figure 4D), which agrees with previous data showing an IFNα-triggered long-lasting expression of *HLA-ABC* (13). STAT1 protein levels, CXCL10 secretion, and *CHOP* mRNA expression were reduced by 26-42% (Figures 4C, F, H; Supplementary Figure 3E), while the expression of *MX1* and *CXCL10* was completely inhibited by deucravacitinib (Figures 4E, G).

Similarly to IFNα + IL-1β, deucravacitinib diminished IFNγ + IL-1β-induced apoptosis (64% decrease) but did not modify *HLA-ABC* mRNA expression (Figures 4I, K). Protein levels of STAT1 and CXCL10, however, were not altered by TYK2 inhibition, whereas a slight, non-significant 30% reduction was seen in *CHOP* expression

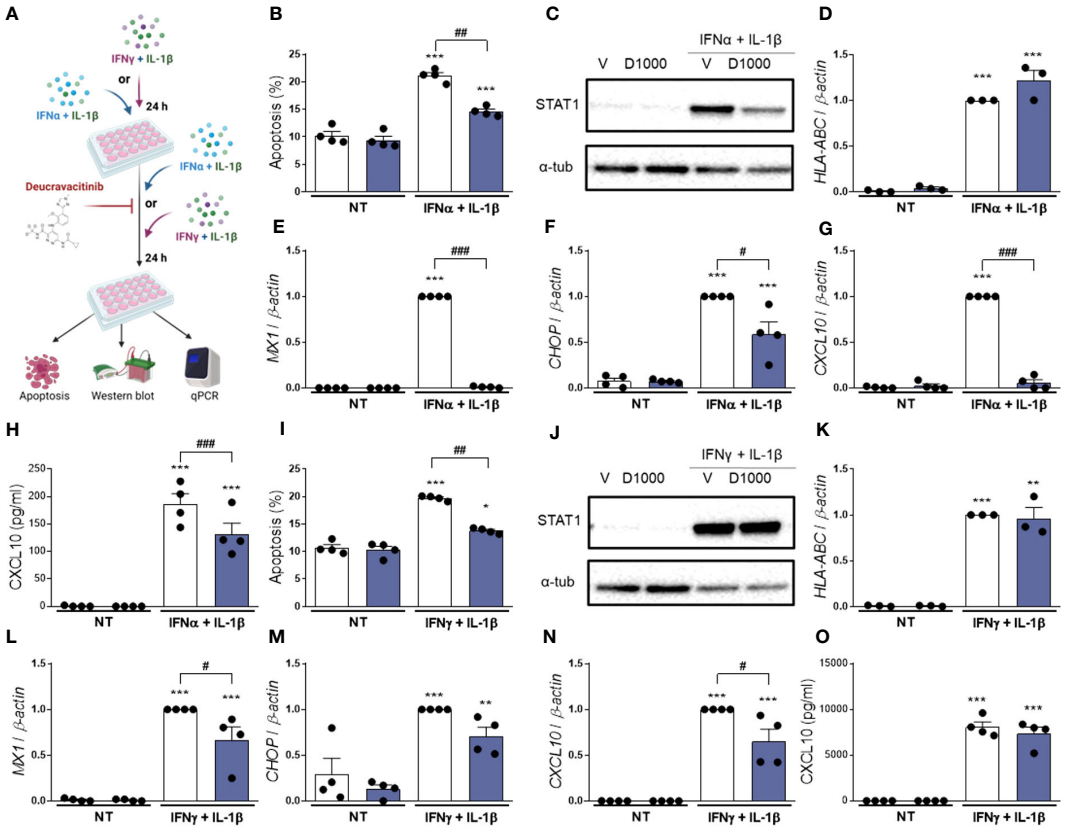

FIGURE 4
Treatment with deucravacitinib partially blocks IFNα + IL-1β- or IFNγ + IL-1β-induced changes. **(A)**: Experimental design of the pre-treatment with cytokines and subsequent exposure to IFNα + IL-1β or IFNγ + IL-1β in the presence of deucravacitinib for 24 h. EndoC-βH1 cells were left non-treated (NT) or pre-treated with IFNα + IL-1β (1000 U/mL + 50 U/mL, respectively) **(B–H)** or IFNγ + IL-1β (1000 U/mL + 50 U/mL, respectively) **(I–O)** for 24 h. Afterwards, cells were treated with vehicle (V, white bars) or 1000 nmol/L deucravacitinib (D1000, dark blue bars) in the absence (NT) or presence of IFNα + IL-1β or IFNγ + IL-1β for 24 h. **(B, I)**: Apoptosis was evaluated using Hoechst 33342/propidium iodide staining (*n* = 4 independent experiments). **(C, J)**: Representative immunoblots of STAT1 and α-tubulin (*n* = 4 independent experiments) **(D–G, K–N)**: mRNA expression of *HLA-ABC* **(D K)**, *MX1* **(E, L)**, *CHOP* **(F M)**, and *CXCL10* **(G, N)** was analyzed by real-time PCR, normalized to β-actin and then to the value of Vehicle treated with IFNα + IL-1β **(D–G)** or IFNγ + IL-1β **(K–N)** (considered as 1) (*n* = 3-4 independent experiments). **(H, O)**: CXCL10 secreted to the medium was determined by ELISA (*n* = 4 independent experiments). Data are mean ± SEM. *p ≤ 0.05, **p ≤ 0.01, ***p ≤ 0.001 vs. the respective non-treated (NT) (two-way ANOVA plus Sidak's test). #p ≤ 0.05, ##p ≤ 0.01, ###p ≤ 0.001, as indicated by bars (two-way ANOVA plus Dunnett's test).

(Figures 4J, M, O; Supplementary Figure 3F). Expression of *MX1* and *CXCL10* was only partially affected by deucravacitinib under IFNγ + IL-1β conditions (Figures 4L, N).

4 Discussion

Targeting the JAK-STAT pathway has emerged as a promising therapeutic approach for type 1 diabetes prevention/early treatment (3, 15). Although this strategy has been approved for treatment of some autoimmune diseases, including rheumatoid arthritis and psoriatic arthritis (37), there are no JAK inhibitors approved for type 1 diabetes. Nonetheless, recent preclinical data suggest that these inhibitors could be repurposed for this disease (13, 14, 16, 17, 22, 23, 38) and a clinical trial investigating whether baricitinib prevents the progressive, immune-mediated destruction of β-cells in type 1 diabetes patients is ongoing (39).

In the current study, we tested whether the TYK2 inhibitor deucravacitinib could protect human β-cells against the deleterious effects of IFNα and other cytokines. We focused on this TYK2 inhibitor for two reasons: first, due to TYK2 importance for type 1 diabetes pathogenesis. For instance, TYK2 regulates IFNα-mediated pro-apoptotic and proinflammatory pathways in β-cells (21, 22). Second, exploring a drug recently approved by the U.S. Food and Drug Administration to treat another autoimmune disease, namely plaque psoriasis (26), increases its repositioning potential for type 1 diabetes and facilitates the bench-to-bedside transition.

Deucravacitinib is a small-molecule ligand that binds to and stabilizes the TYK2 pseudokinase domain, leading to highly potent and selective allosteric TYK2 inhibition (24, 40). Inhibition of IFNα-induced STAT phosphorylation by deucravacitinib has been shown in several cell types, such as $CD3^+$ T cells, $CD19^+$ B cells, and $CD14^+$ monocytes (24). Here we showed that deucravacitinib also prevents IFNα-stimulated STAT1 and STAT2 phosphorylation in human EndoC-βH1 cell line. Furthermore, in agreement with previous findings (24), deucravacitinib also showed higher potency against TYK2-mediated phosphorylation of STAT1 compared with STAT2 phosphorylation in our experimental model. Notably, at the concentrations used in our study, deucravacitinib did not affect β-cell function and viability, which is a desired feature for a drug with therapeutic potential.

Compared with ruxolitinib and baricitinib, two clinically available JAK1/JAK2 inhibitors, deucravacitinib was more potent against IFNα-stimulated STAT phosphorylation, ISRE activity, and mRNA expression of *HLA-ABC*, *MX1*, and *CXCL10*. However, unlike ruxolitinib and baricitinib, deucravacitinib did not affect the IFNα-mediated upregulation of the ER stress markers *CHOP* and *XBP1s*. Our results partially agree with a previous publication reporting that two TYK2 inhibitors failed to prevent IFNα-induced *CHOP* expression in EndoC-βH1 cells (23). Prior studies have shown that other JAK/TYK2 inhibitors could prevent the detrimental effects of IFNα + IL-1β, such as apoptosis and inflammation (14, 23). Therefore, we investigated whether deucravacitinib could protect β-cells against the harmful effects of two different combinations of cytokines: IFNα + IL-1β (early insulitis) and IFNγ + IL-1β (late insulitis). In both scenarios, pre-treatment with deucravacitinib protected against cytokine-induced apoptosis and *CXCL10* mRNA expression. Additionally, in cells treated with IFNα + IL-1β, pre-treatment with deucravacitinib blocked the overexpression of MHC class I at the cell surface and CXCL10 secretion to the medium. Interestingly, while the IFNα + IL-1β-induced upregulation of *HLA-ABC*, *MX1*, and *CHOP* was inhibited by the pre-treatment with deucravacitinib, this inhibitor did not change the expression of *HLA-ABC* stimulated by IFNγ + IL-1β. Moreover, *MX1* and *CHOP* mRNA expression was only partially reduced by the pre-treatment with deucravacitinib in IFNγ + IL-1β-treated cells. Importantly, the addition of deucravacitinib when cytokine exposure was already ongoing could reduce the deleterious effects of these cytokines. Although it seems clear that deucravacitinib confers protection against IFNα + IL-1β by directly inhibiting the TYK2-mediated pathway, it remains to be answered how deucravacitinib protects against IFNγ + IL-1β-induced effects. Indeed, our present data suggest that deucravacitinib does not interfere with the IFNγ-mediated signaling pathway. One possibility might be the following: in β-cells, either IFNγ alone or in combination with IL-1β induce the expression of members of the interferon regulatory factor (IRF) family, such as IRF3 and IRF7 (41, 42). As IRF3 and IRF7 are potent activators of IFNα and IFNβ gene expression (43, 44), it is conceivable that IFNγ + IL-1β-induced IRF3 and IRF7 could lead to type I IFN expression and secretion. Then, secreted IFNα and/or IFNβ could stimulate the type I IFN receptor-TYK2 pathway in an autocrine fashion. In this context, deucravacitinib could inhibit this positive-feedback loop stimulated by IFNγ + IL-1β-induced IRF3 and IRF7 expression.

Based on our findings, it will be interesting to test whether novel small molecule TYK2 pseudokinase ligands (45) could also protect β-cells from IFNα deleterious effects. Nevertheless, we must bear in mind that completely inhibiting TYK2 may be counterproductive, as it might lead to susceptibility to microorganisms (e.g., mycobacteria and virus) and immunodeficiency (46). Thus, regardless of the TYK2 inhibitor chosen, we should focus on doses that induce a partial inhibition, as seen in individuals with a protective single nucleotide polymorphism in the *TYK2* gene (18), as it could offer maximal efficacy with reduced risk of developing secondary infections. Moreover, our data suggest that partial TYK2 inhibition obtained with low doses of deucravacitinib was enough to prevent most IFNα-induced harmful effects in β-cells, such as upregulation of the pro-apoptotic *CHOP*, MHC class I overexpression, and apoptosis (in the presence of IL-1β). One potential limitation of our study is its purely *in vitro* nature, which may limit our conclusions regarding the use of deucravacitinib to treat a disease as complex as type 1 diabetes. Conversely, our findings, along with others (22, 23), provide further preclinical evidence that TYK2 inhibitors could be considered a strategy for an early therapy for type 1 diabetes. The next logical step would be to investigate whether our *in vitro* findings could be translated to animal models of type 1 diabetes (e.g., NOD and RIP-B7.1 mice).

In conclusion, we provided evidence that deucravacitinib protects β-cells against the deleterious effects of proinflammatory cytokines, such as IFNα, IFNγ and IL-1β, without affecting β-cell function and survival. Our present findings add to the existing evidence that TYK2 inhibition may be an efficient treatment

strategy for type 1 diabetes. Moreover, these preclinical findings suggest that deucravacitinib could be repurposed to treat pre-symptomatic type 1 diabetes subjects (i.e., positive for 2–3 autoantibodies but still normoglycemic) or be introduced in the early stages of type 1 diabetes onset.

Data availability statement

The raw data supporting the conclusions of this article will be made available by the authors, without undue reservation.

Ethics statement

Ethical approval was not required for the studies on humans in accordance with the local legislation and institutional requirements because only commercially available established cell lines were used.

Author contributions

RS: Conceptualization, Data curation, Formal Analysis, Investigation, Methodology, Supervision, Visualization, Writing – original draft, Writing – review & editing. DG-L: Formal Analysis, Investigation, Writing – review & editing. AP-S: Formal Analysis, Investigation, Writing – review & editing. AN: Resources, Writing – review & editing. LM: Conceptualization, Data curation, Formal Analysis, Funding acquisition, Investigation, Methodology, Project administration, Resources, Supervision, Visualization, Writing – original draft, Writing – review & editing.

Funding

The authors declare financial support was received for the research, authorship, and/or publication of this article. LM is funded by the grant PID2020-117569RA-I00 by MCIN/AEI/10.13039/501100011033 and by the grant SEJI/2018/023 by Generalitat Valenciana. AN is supported by European Union's Horizon 2020 research and innovation programme under grant agreement GOLIATH No. 825489, by the grant PID2020-117294RB-I00 by MCIN/AEI/10.13039/501100011033, and by the grant PROMETEO II/2020/006 by Generalitat Valenciana. This research was supported by CIBER-Consorcio Centro de Investigación Biomédica en Red (CB07/08/0002), Instituto de Salud Carlos III, Ministerio de Ciencia e Innovación.

Acknowledgments

The authors are grateful to Beatriz Bonmati Botella, Maria Luisa Navarro, and Salomé Ramon from the Universidad Miguel Hernández de Elche, Spain, for their excellent technical support. Once again, we thank Dr. Izortze Santin, University of the Basque Country, Spain, for providing the luciferase reporter construct for ISRE. Figures 2A, 3A, 4A and Supplementary Figure 1A were created with BioRender.com.

Conflict of interest

The authors declare that the research was conducted in the absence of any commercial or financial relationships that could be construed as a potential conflict of interest.

The author(s) declared that they were an editorial board member of Frontiers, at the time of submission. This had no impact on the peer review process and the final decision.

Publisher's note

Supplementary material

The Supplementary Material for this article can be found online at: https://www.frontiersin.org/articles/10.3389/fimmu.2023.1263926/full#supplementary-material

References

1. Eizirik DL, Pasquali L, Cnop M. Pancreatic β-cells in type 1 and type 2 diabetes mellitus: different pathways to failure. *Nat Rev Endocrinol* (2020) 26:349–62. doi: 10.1038/s41574-020-0355-7

2. Mallone R, Eizirik DL. Presumption of innocence for beta cells: why are they vulnerable autoimmune targets in type 1 diabetes? *Diabetologia* (2020) 63:1999–2006. doi: 10.1007/s00125-020-05176-7

3. Marroqui L, Perez-Serna AA, Babiloni-Chust I, Dos Santos RS. Type I interferons as key players in pancreatic β-cell dysfunction in type 1 diabetes. *Int Rev Cell Mol Biol* (2021) 359:1–80. doi: 10.1016/bs.ircmb.2021.02.011

4. Foulis A, Farquharson M, Meager A. Immunoreactive alpha-interferon in insulin-secreting beta cells in type 1 diabetes mellitus. *Lancet* (1987) 2:1423–7. doi: 10.1016/S0140-6736(87)91128-7

5. Somoza N, Vargas F, Roura-Mir C, Vives-Pi M, Martí M, Jaraquemada D, et al. Pancreas in recent onset insulin-dependent diabetes mellitus: Changes in HLA, adhesion molecules and autoantigens, restricted T cell receptor Vβ usage, and cytokine profile. *J Immunol* (1994) 153:1360–77.

6. Huang X, Yuan J, Goddard A, Foulis A, James RFL, Lernmark Å, et al. Interferon expression in the pancreases of patients with type I diabetes. *Diabetes* (1995) 44:658–64. doi: 10.2337/diab.44.6.658

7. Lundberg M, Krogvold L, Kuric E, Dahl-Jørgensen K, Skog O. Expression of interferon-stimulated genes in insulitic pancreatic islets of patients recently diagnosed with type 1 diabetes. *Diabetes* (2016) 65:3104–10. doi: 10.2337/db16-0616

8. Ferreira RC, Guo H, Coulson RMR, Smyth DJ, Pekalski ML, Burren OS, et al. A type I Interferon transcriptional signature precedes autoimmunity in children

genetically at risk for type 1 diabetes. *Diabetes* (2014) 63:2538–50. doi: 10.2337/db13-1777

9. Kallionpaa H, Elo LL, Laajala E, Mykkanen J, Ricano-Ponce I, Vaarma M, et al. Innate immune activity is detected prior to seroconversion in children with HLA-conferred type 1 diabetes susceptibility. *Diabetes* (2014) 63:2402–14. doi: 10.2337/db13-1775

10. Apaolaza PS, Balcacean D, Zapardiel-Gonzalo J, Nelson G, Lenchik N, Akhbari P, et al. Islet expression of type I interferon response sensors is associated with immune infiltration and viral infection in type 1 diabetes. *Sci Adv* (2021) 7:eabd6527. doi: 10.1126/sciadv.abd6527

11. Marroqui L, Dos Santos RS, Op de beeck A, Coomans de Brachène A, Marselli L, Marchetti P, et al. Interferon-α mediates human beta cell HLA class I overexpression, endoplasmic reticulum stress and apoptosis, three hallmarks of early human type 1 diabetes. *Diabetologia* (2017) 60:656–67. doi: 10.1007/s00125-016-4201-3

12. Lombardi A, Tomer Y. Interferon alpha impairs insulin production in human beta cells via endoplasmic reticulum stress. *J Autoimmun* (2017) 80:48–55. doi: 10.1016/j.jaut.2017.02.002

13. Coomans de Brachène A, Dos Santos RS, Marroqui L, Colli ML, Marselli L, Mirmira RG, et al. IFN-α induces a preferential long-lasting expression of MHC class I in human pancreatic beta cells. *Diabetologia* (2018) 61:636–40. doi: 10.1007/s00125-017-4536-4

14. Colli ML, Ramos-Rodríguez M, Nakayasu ES, Alvelos MI, Lopes M, Hill JLE, et al. An integrated multi-omics approach identifies the landscape of interferon-α-mediated responses of human pancreatic beta cells. *Nat Commun* (2020) 11:2584. doi: 10.1038/s41467-020-16327-0

15. Eizirik DL, Szymczak F, Alvelos MI, Martin F. From pancreatic β-cell gene networks to novel therapies for type 1 diabetes. *Diabetes* (2021) 70:1915–25. doi: 10.2337/dbi20-0046

16. Trivedi PM, Graham KL, Scott NA, Jenkins MR, Majaw S, Sutherland RM, et al. Repurposed JAK1/JAK2 inhibitor reverses established autoimmune insulitis in NOD mice. *Diabetes* (2017) 66:1650–60. doi: 10.2337/db16-1250

17. Ge T, Jhala G, Fynch S, Akazawa S, Litwak S, Pappas EG, et al. The JAK1 selective inhibitor ABT 317 blocks signaling through interferon-γ and common γ Chain cytokine receptors to reverse autoimmune diabetes in NOD mice. *Front Immunol* (2020) 11:588543. doi: 10.3389/fimmu.2020.588543

18. Dendrou CA, Cortes A, Shipman L, Evans HG, Attfield KE, Jostins L, et al. Resolving TYK2 locus genotype-To-phenotype differences in autoimmunity. *Sci Transl Med* (2016) 8:363ra149. doi: 10.1126/scitranslmed.aag1974

19. Tao JH, Zou YF, Feng XL, Li J, Wang F, Pan FM, et al. Meta-analysis of TYK2 gene polymorphisms association with susceptibility to autoimmune and inflammatory diseases. *Mol Biol Rep* (2011) 38:4663–72. doi: 10.1007/s11033-010-0601-5

20. Wallace C, Smyth DJ, Maisuria-Armer M, Walker NM, Todd JA, Clayton DG. The imprinted DLK1-MEG3 gene region on chromosome 14q32.2 alters susceptibility to type 1 diabetes. *Nat Genet* (2010) 42:68–71. doi: 10.1038/ng.493

21. Marroqui L, Dos Santos RS, Fløyel T, Grieco FA, Santin I, Op De Beeck A, et al. TYK2, a candidate gene for type 1 diabetes, modulates apoptosis and the innate immune response in human pancreatic β-cells. *Diabetes* (2015) 64:3808–17. doi: 10.2337/db15-0362

22. Chandra V, Ibrahim H, Halliez C, Prasad RB, Vecchio F, Dwivedi OP, et al. The type 1 diabetes gene TYK2 regulates β-cell development and its responses to interferon-α. *Nat Commun* (2022) 13:6363. doi: 10.1038/s41467-022-34069-z

23. Coomans de Brachène A, Castela A, Op de Beeck A, Mirmira RG, Marselli L, Marchetti P, et al. Pre-clinical evaluation of TYK2 inhibitors for human beta cell protection in type 1 diabetes. *Diabetes Obes Metab* (2020) 22:1827–36. doi: 10.1111/dom.14104

24. Burke JR, Cheng L, Gillooly KM, Strnad J, Zupa-Fernandez A, Catlett IM, et al. Autoimmune pathways in mice and humans are blocked by pharmacological stabilization of the TYK2 pseudokinase domain. *Sci Transl Med* (2019) 11:eaaw1736. doi: 10.1126/scitranslmed.aaw1736

25. Morand E, Pike M, Merrill JT, van Vollenhoven R, Werth VP, Hobar C, et al. Deucravacitinib, a tyrosine kinase 2 inhibitor, in systemic lupus erythematosus: A phase II, randomized, double-blind, placebo-controlled trial. *Arthritis Rheumatol* (2022) 75:242–252. doi: 10.1002/art.42391

26. Hoy SM. Deucravacitinib: first approval. *Drugs* (2022) 82:1671–9. doi: 10.1007/s40265-022-01796-y

27. Ravassard P, Hazhouz Y, Pechberty S, Bricout-Neveu E, Armanet M, Czernichow P, et al. A genetically engineered human pancreatic β cell line exhibiting glucose-inducible insulin secretion. *J Clin Invest* (2011) 121:3589–97. doi: 10.1172/JCI58447

28. Brozzi F, Nardelli TR, Lopes M, Millard I, Barthson J, Igoillo-Esteve M, et al. Cytokines induce endoplasmic reticulum stress in human, rat and mouse beta cells via different mechanisms. *Diabetologia* (2015) 58:2307–16. doi: 10.1007/s00125-015-3669-6

29. Santin I, Dos Santos RS, Eizirik DL. Pancreatic beta cell survival and signaling pathways: Effects of type 1 diabetes-associated genetic variants. In: *Methods in Molecular Biology*. New York, NY, USA: Humana Press (2016). p. 21–54. doi: 10.1007/7651_2015_291

30. Dhayal S, Leslie KA, Baity M, Akhbari P, Richardson SJ, Russell MA, et al. Temporal regulation of interferon signalling in human EndoC-βH1 cells. *J Mol Endocrinol* (2022) 69:299–313. doi: 10.1530/JME-21-0224

31. Villar-Pazos S, Martinez-Pinna J, Castellano-Muñoz M, Alonso-Magdalena P, Marroqui L, Quesada I, et al. Molecular mechanisms involved in the non-monotonic effect of bisphenol-A on Ca2+ entry in mouse pancreatic β-cells. *Sci Rep* (2017) 7:11770. doi: 10.1038/s41598-017-11995-3

32. Babiloni-Chust I, dos Santos RS, Medina-Gali RM, Perez-Serna AA, Encinar J-A, Martinez-Pinna J, et al. G protein-coupled estrogen receptor activation by bisphenol-A disrupts the protection from apoptosis conferred by the estrogen receptors ERα and ERβ in pancreatic beta cells. *Environ Int* (2022) 164:107250. doi: 10.1016/j.envint.2022.107250

33. Perez-Serna AA, Dos Santos RS, Ripoll C, Nadal A, Eizirik DL, Marroqui L. BCL-XL overexpression protects pancreatic β-cells against cytokine- and palmitate-induced apoptosis. *Int J Mol Sci* (2023) 24:5657. doi: 10.3390/ijms24065657

34. Dos Santos RS, Medina-Gali RM, Babiloni-Chust I, Marroqui L, Nadal A. *In vitro* assays to identify metabolism-disrupting chemicals with diabetogenic activity in a human pancreatic β-cell model. *Int J Mol Sci* (2022) 23:5040. doi: 10.3390/ijms23095040

35. Tsonkova VG, Sand FW, Wolf XA, Grunnet LG, Ringgaard AK, Ingvorsen C, et al. The EndoC-βH1 cell line is a valid model of human beta cells and applicable for screenings to identify novel drug target candidates. *Mol Metab* (2018) 8:144–57. doi: 10.1016/j.molmet.2017.12.007

36. Colli ML, Szymczak F, Eizirik DL. Molecular footprints of the immune assault on pancreatic beta cells in type 1 diabetes. *Front Endocrinol* (2020) 11:568446. doi: 10.3389/fendo.2020.568446

37. Virtanen AT, Haikarainen T, Raivola J, Silvennoinen O. Selective JAKinibs: prospects in inflammatory and autoimmune diseases. *BioDrugs* (2019) 33:15–32. doi: 10.1007/s40259-019-00333-w

38. Colli ML, Hill JLE, Marroquí L, Chaffey J, Dos Santos RS, Leete P, et al. PDL1 is expressed in the islets of people with type 1 diabetes and is up-regulated by interferons-α and-γ via IRF1 induction. *EBioMedicine* (2018) 36:367–75. doi: 10.1016/j.ebiom.2018.09.040

39. Waibel M, Thomas HE, Wentworth JM, Couper JJ, MacIsaac RJ, Cameron FJ, et al. Investigating the efficacy of baricitinib in new onset type 1 diabetes mellitus (BANDIT)—study protocol for a phase 2, randomized, placebo controlled trial. *Trials* (2022) 23:433. doi: 10.1186/s13063-022-06356-z

40. Wrobleski ST, Moslin R, Lin S, Zhang Y, Spergel S, Kempson J, et al. Highly selective inhibition of tyrosine kinase 2 (TYK2) for the treatment of autoimmune diseases: discovery of the allosteric inhibitor BMS-986165. *J Med Chem* (2019) 62:8973–95. doi: 10.1021/acs.jmedchem.9b00444

41. Rasschaert J, Liu D, Kutlu B, Cardozo AK, Kruhøffer M, Ørntoft TF, et al. Global profiling of double stranded RNA- and IFN-γ-induced genes in rat pancreatic beta cells. *Diabetologia* (2003) 46:1641–57. doi: 10.1007/s00125-003-1245-y

42. Ylipaasto P, Kutlu B, Rasilainen S, Rasschaert J, Salmela K, Teerijoki H, et al. Global profiling of coxsackievirus- and cytokine-induced gene expression in human pancreatic islets. *Diabetologia* (2005) 48:1510–22. doi: 10.1007/s00125-005-1839-7

43. Honda K, Takaoka A, Taniguchi T. Type I inteferon gene induction by the interferon regulatory factor family of transcription factors. *Immunity* (2006) 25:349–60. doi: 10.1016/j.immuni.2006.08.009

44. Jefferies CA. Regulating IRFs in IFN driven disease. *Front Immunol* (2019) 10:325. doi: 10.3389/fimmu.2019.00325

45. Zhou Y, Li X, Shen R, Wang X, Zhang F, Liu S, et al. Novel small molecule tyrosine kinase 2 pseudokinase ligands block cytokine-induced TYK2-mediated signaling pathways. *Front Immunol* (2022) 13:884399. doi: 10.3389/fimmu.2022.884399

46. Minegishi Y, Saito M, Morio T, Watanabe K, Agematsu K, Tsuchiya S, et al. Human tyrosine kinase 2 deficiency reveals its requisite roles in multiple cytokine signals involved in innate and acquired immunity. *Immunity* (2006) 25:745–55. doi: 10.1016/j.immuni.2006.09.009

frontiers | Frontiers in Immunology

TYPE Original Research
PUBLISHED 27 October 2023
DOI 10.3389/fimmu.2023.1279603

OPEN ACCESS

EDITED BY
Chao Yang,
Zhejiang Ocean University, China

REVIEWED BY
Zhuang Shaoyong,
Shanghai Jiao Tong University, China
Guangchuan Wang,
Jinzhou Medical University, China

*CORRESPONDENCE
Xiaopeng Hu
xiaopeng_hu@sina.com

†These authors have contributed equally to this work and share the first authorship

RECEIVED 18 August 2023
ACCEPTED 16 October 2023
PUBLISHED 27 October 2023

CITATION
Li S, Zhang W and Hu X (2023) Comprehensive analysis of necroptosis-related genes in renal ischemia-reperfusion injury. *Front. Immunol.* 14:1279603. doi: 10.3389/fimmu.2023.1279603

Comprehensive analysis of necroptosis-related genes in renal ischemia-reperfusion injury

Shuai Li[1,2†], Weixun Zhang[1,2†] and Xiaopeng Hu[1,2*]

[1]Department of Urology, Beijing Chao-Yang Hospital, Capital Medical University, Beijing, China, [2]Institute of Urology, Capital Medical University, Beijing, China

Background: Oxidative stress is the primary cause of ischemia-reperfusion injury (IRI) in kidney transplantation, leading to delayed graft function (DGF) and implications on patient health. Necroptosis is believed to play a role in renal IRI. This research presents a comprehensive analysis of necroptosis-related genes and their functional implications in the context of IRI in renal transplantation.

Methods: The necroptosis-related differentially expressed genes (NR-DEGs) were identified using gene expression data from pre- and post-reperfusion renal biopsies, and consensus clustering analysis was performed to distinguish necroptosis-related clusters. A predictive model for DGF was developed based on the NR-DEGs and patients were divided into high- and low-risk groups. We investigated the differences in functional enrichment and immune infiltration between different clusters and risk groups and further validated them in single-cell RNA-sequencing (scRNA-seq) data. Finally, we verified the expression changes of NR-DEGs in an IRI mouse model.

Results: Five NR-DEGs were identified and were involved in various biological processes. The renal samples were further stratified into two necroptosis-related clusters (C1 and C2) showing different occurrences of DGF. The predictive model had a reliable performance in identifying patients at higher risk of DGF with the area under the curve as 0.798. Additionally, immune infiltration analysis indicated more abundant proinflammatory cells in the high-risk group, which was also found in C2 cluster with more DGF patients. Validation of NR-DEG in scRNA-seq data further supported their involvement in immune cells. Lastly, the mouse model validated the up-regulation of NR-DEGs after IR and indicated the correlations with kidney function markers.

Conclusions: Our research provides valuable insights into the identification and functional characterization of NR-DEGs in the context of renal transplantation and sheds light on their involvement in immune responses and the progression of IRI and DGF.

KEYWORDS

kidney transplantation, necroptosis, inflammatory cells, oxidative stress, ischemia-reperfusion injury, delayed graft function, predictive model

1 Introduction

Kidney transplantation (KT) is the optimal renal replacement treatment for end-stage renal disease, associated with lower mortality and enhanced quality of life in comparison to chronic dialysis treatment (1). Recently, the survival rates for patients and grafts have exceeded 96% and 91% correspondingly in their first year (2). However, the incidence of renal insufficiency and comorbidities after KT remains high, leading to potential loss of transplanted kidney function. Delayed graft function (DGF) is among the most frequent postoperative complications, with prevalence varying between 2% to 50% in different types of kidney grafts, which may be related to the use of expanded criteria donors and deceased cardiac dead (DCD) donors (3). At present, the standardized definition of DGF is controversial and cannot provide early warning signs (4, 5). Therefore, there is still a clinical demand for a non-invasive, robust, and more reliable diagnostics method to detect DGF.

Ischemia-reperfusion injury (IRI) induced by oxidative stress, is the primary cause of DGF, acute rejection, and chronic rejection (6), and is inevitable during KT (7). The imbalance between oxygen supply and demand could cause oxidative metabolic disorders, resulting in the death of tubular epithelial cells (TECs) and impairment of kidney function (8). During both the ischemic phase and subsequent reperfusion, cellular damage takes place and causes the loss of cellular polarity, impaired brush border, decreased intercellular adhesion, and cell death (3, 8). Necrosis, traditionally considered as a non-programmed cell death, is the main form of tubular cell death of renal IRI and acute kidney injury (AKI) (8–10). However, emerging evidence suggests the existence of highly regulated forms of non-apoptotic cell death with necrotic characteristics, known as regulated necrosis (RN) (6). RN can take various forms, including necroptosis, ferroptosis, necrosis driven by mitochondrial permeability transition (MPT), pyroptosis, and parthanatos. Among these, necroptosis and ferroptosis are the most extensively studied forms in the context of renal IRI. Necroptosis is characterized by its dependency on the kinase domain of receptor-interacting protein kinase (RIPK)-3 and the phosphorylation of mixed lineage kinase domain-like protein (MLKL) (9). It has been reported to contribute to several models of renal injury, including IRI (6), cisplatin-induced AKI (11), and contrast-induced nephropathy (12). Although numerous studies have explored potential protective therapies for renal IRI (13), their practical value remains controversial, and none of them has been translated to clinical application. Given the development of massive sequencing and genetic diagnosis techniques, it is essential to investigate the role of necroptosis in gene-based diagnostic and therapeutic strategies for DGF. It has been reported that necroptosis-related genes (NRGs) are upregulated early in the renal allograft and serve as risk factors for subsequent DGF (14). However, the association between NRGs and specific cell types or their role in the induction of specific immune responses during the process of renal IRI remains ambiguous.

In this study, we aimed to identify potential target genes by intersecting necroptosis-related genes and differentially expressed genes (DEGs) obtained from two gene expression omnibus (GEO) databases of KT. Based on the expression levels of necroptosis-related DEGs (NR-DEGs), we stratified the samples into two clusters with distinct molecular and clinical features. Subsequently, we developed a diagnostic model for predicting the occurrence of DGF based on the targeted NR-DEGs and categorized the samples into high- and low-risk groups. Furthermore, we conducted functional enrichment and immune-infiltration analyses to explore the potential mechanisms involved. Single-cell RNA-sequencing (scRNA-seq) data and cell-cell communication analyses were further utilized to investigate the relationship between necroptosis, NR-DEGs, and immune cells. Finally, we validated our findings using a mice kidney IRI model. In brief, our study provides novel necroptosis-related biomarkers for the early diagnosis of DGF after KT and enables the discrimination of patients at different risk levels.

2 Materials and methods

2.1 The gathering and analysis of bulk RNA-Seq data

The RNA-seq datasets utilized in this study were acquired from the GEO database (https://www.ncbi.nlm.nih.gov/geo/). Specifically, we accessed the GSE43974 dataset, comprising 188 renal biopsies before retrieval and 203 biopsies after reperfusion obtained from brain-dead (BD) kidney donors, DCD donors, and living donors. This dataset was used for the identification of hub genes and the development of the predictive model. Additionally, we utilized the GSE126805 dataset, which included protocol biopsies collected at different time points from 42 kidney transplant recipients, for validation purposes. The microarray datasets based on Illumina platforms were subjected to log2 transformation and normalized by R package "limma". The demographic characteristics are detailed in Table S1.

2.2 Identification of the necroptosis-related genes

From the GeneCards database (https://auth.lifemapsc.com/), a collection of 114 genes associated with necroptosis was acquired with a relevance score > 1 (Table S2). IRI-related DEGs between pre- and post-reperfusion from three different types of donor types (BD, DCD, and living donors) in the GSE43974 dataset were screened by "limma" R package with adj. $p < 0.05$ and $|logFC| \geq 0.5$, respectively. To screen out the NR-DEGs, a Venn analysis was

undertaken to identify the intersected genes of the above three different analyses and necroptosis-related genes.

2.3 Analysis of functional enrichment and immune infiltration

The Gene Ontology (GO) and Kyoto Encyclopedia of Genes and Genomes (KEGG) enrichment analyses of the common IRI-related DEGs among three donor types were performed by "clusterProfiler" R package (15–17). The evaluation of the abundance of 22 different immune cells was conducted using CIBERSORT (http://cibersort.stanford.edu/) (18).

2.4 Necroptosis-based consensus clustering analysis

To determine the molecular patterns associated with necroptosis in samples of IRI, consensus clustering analysis was performed based on the above NR-DEGs using the "ConsensusClusterPlus" R package (19). To ensure classification stability, 80% item resampling and a maximum evaluated k of 9 were used. The principal component analysis (PCA) was performed to validate cluster results.

2.5 Establishment of the predictive model

The machine learning algorithm was performed in the GSE43974 dataset to screen out necroptosis-related hub genes and construct a predictive model. The least absolute shrinkage and selection operator (LASSO) regression analysis, a variable selection method for regression models, was utilized to eliminate less informative features (20). The regression coefficients of each gene were estimated by the least squares method based on parameters obtained from the cross-validation. We conducted the LASSO regression analysis with 10-fold cross-validation (utilizing "glmnet" R package). The area under the receiver operator characteristic curve (AUROC) of the predictive model was evaluated through the "ROCR" R package.

Based on the necroptosis-related score derived from the risk prediction model, the samples of IRI were stratified into high- and low-risk groups, respectively.

2.6 Obtaining and analyzing scRNA-seq data

The scRNA-seq dataset GSE171639 consisting of two mice kidney samples following ischemic reperfusion or sham surgery was obtained from the GEO database (21). The kidneys were subjected to bilateral clamping of the renal pedicle for a duration of 30 minutes, after which reperfusion was allowed for 6-7 hours. For further verification, additional scRNA-seq data of samples from mice kidneys after 27min ischemia or without any surgery were used (GSE193649) (22). The additional details of these datasets can be found in Table S1.

To preprocess the data, we utilized the "Seurat" R package. Several quality control measures were applied, including calculating the percentage of gene numbers, cell counts, and mitochondria sequencing counts. Cells exceeding a mitochondrial content of 50%, having fewer than 200 genes, and falling within the lower 10% and top 5% percentiles of unique gene distribution were removed for GSE171639 dataset (Figures S1A, B). Afterward, the cells were normalized for sequencing depth by utilizing the "NormalizeData" function with the default method of "LogNormalize". Using the "FindVariableFeatures" function, we detected the top 2,000 highly variable genes and then scaled them through the "ScaleData" function. Next, PCA was performed to identify significant principal components, and "harmony" R package was employed to integrate the data from each biological individual. Subsequently, the cells were clustered using the "FindNeighbors" and "FindClusters" functions (with a resolution of 0.65 for GSE171639 dataset) and visualized with uniform manifold approximation and projection (UMAP). To identify marker genes for each main cell cluster, the "FindAllMarker" function ($|logFC| > 0.3$, Minpct = 0.25) was employed. Subsequently, the prominent cell categories were identified according to the markers acquired from the CellMarker2.0 database (23) and previous studies (24–26). The top 3 markers for each cell type were selected and plotted on a heatmap.

2.7 Cell-cell communication analysis

The cell-cell communication networks were quantitatively inferred and visualized based on the CellChatDB of ligand-receptor pairs in humans and mice using the scRNA-seq data (GSE171639) and the "CellChat" R package (27). We compared the intercellular communication before and after ischemia-reperfusion (IR), and the minimum threshold of cells required in different cells was set to 10.

2.8 Analysis of gene set variation and enrichment

The gene set enrichment analysis for scRNA-seq was performed through GSVA implemented in the "GSVA" package (28). Gene sets were exported using the "GSEABase" R package. The enrichment score of each pathway in the significant cell types was calculated using t-values, and the differences between the sham and IRI groups were compared using the "limma" package. In addition, we visualized the distribution of necroptosis-related pathways with the UMAP function.

2.9 Mice and renal IRI model

C57BL/6N mice (8-10 weeks old, male) were obtained from Weitonglihua (Beijing, China) and were kept in a controlled

environment free from pathogens. The animal experiment was reviewed and approved by the Ethics Committee of Beijing Chao-Yang Hospital (2021-54). Before the operation, a minimum of one week was given for the mice to adapt to these conditions. Mice underwent IRI (n = 8) as described previously (29). For the procedure, the mice were anesthetized with pentobarbital (60 mg/kg) through an intraperitoneal injection and placed on a thermoregulated heating pad to maintain body temperature at 34 to 36 °C. The right kidney was removed and used as self-control, while the left renal pedicle was clamped for 30 minutes to induce renal ischemia. Subsequently, the clamp was released, allowing tissue reperfusion. Mice were euthanized 24 hours after renal IRI, and both serum and kidney tissues were collected.

2.10 Evaluation of kidney damage and renal function

The assessment of kidney injury was conducted based on the levels of blood urea nitrogen (BUN) and serum creatinine (SCr). Serum samples were isolated from the clotted whole blood samples through centrifugation at a speed of 3,000 revolutions per minute for 10 minutes and further subjected to BUN and SCr testing by an automated chemistry analyzer (Chemray 800).

2.11 Quantitative real-time PCR

As per the manufacturer's instructions, total RNA was extracted from the kidney samples using the FastPure Cell/Tissue Total RNA Isolation Kit V2 (Vazyme, RC112-01). The extracted RNA was then reverse transcribed to cDNA by HiScript III RT SuperMix for qPCR kit (Vazyme, R323-01). Subsequently, quantitative PCR (qPCR) was performed on an Applied Biosystems 7500 Fast Real-Time PCR System using the HiScript Q RT SuperMix for qPCR (Vazyme, R122-01). Gapdh was used as an internal reference gene for normalization during qPCR analysis. The primer sequences of the hub genes in this study can be found in Table S3.

2.12 Statistical analysis

The statistical analysis for this study was conducted using R software (version 4.1.3). To compare the variations in immune cell infiltration and gene expression levels among different groups, either a Student's t-test or Mann-Whitney U test was employed. A two-sided p value less than 0.05 was considered statistically significant.

3 Results

3.1 Identification of NR-DEGs and functional enrichment analysis

Differential expression analyses were performed in GSE43974 dataset. As a result, we identified 119, 173, and 90 DEGs from the BD, DCD, and living donor samples, respectively (Figures 1A–C). Among these, 78 DEGs were significantly differentially expressed in all three types of donors (Figure 1D). To gain insights into the biological function of these common IRI-related DEGs, we conducted functional enrichment analysis based on the GO and KEGG databases. GO analysis encompassed biological process (BP), cellular component (CC), and molecular function (MF). The top five enriched terms of each category are depicted in Figure 1I, Notably, the representative enriched terms including regulation of transcription from RNA polymerase II promoter in response to stress (GO: 0043618), RNA polymerase II transcription regulator complex (GO: 0090575), and DNA-binding transcription activator activity (GO: 0001216). Additionally, the KEGG pathway analysis (Figure 1H) revealed significant involvement of the IRI-related DEGs in MAPK signaling pathway (hsa: 04010), TNF signaling pathway (hsa: 04668), and IL-17 signaling pathway (hsa: 04657).

Next, we investigated the intersection of the 78 IRI-related DEGs from three types with the 114 NRGs and revealed 5 NR-DEGs (*NFKBIA, TNFAIP3, MYC, JUN, SERTAD1*, Figure 1E). We further visualized the expression of the NR-DEGs through a heatmap (Figure 1F) and validated these findings in an independent transplantation cohort (GSE126805) as well (Figure 1G), indicating that all the identified hub genes were significantly upregulated after IR.

3.2 Stratification of IRI samples based on NR-DEGs

We performed unsupervised consistent clustering and stratify the renal samples after IR based on the expression levels of the five NR-DEGs. The cumulative distribution curve appeared most horizontal in the middle section at k = 2, and the heatmap of clustering suggested a clear distinction between cluster 1 (C1) and cluster 2 (C2, Figures 2A, B). PCA further demonstrated a significant separation of the expression levels of the NR-DEGs between the two clusters (Figure 2C). Specifically, the five hub genes expressed at higher levels in C1 group, as evident from the heatmap (Figure 2D) and boxplot (Figure 2E). As for clinical characteristics, the C1 group had a lower proportion of patients who experienced DGF (35.2% compared to 52.1% in C2, Figure 2F). Moreover, the C1 group comprised a significantly lower number of kidney transplant recipients from DCD donors (16.4% compared to 42.7% in C2, Figure 2G).

3.3 Analysis of immune infiltration of necroptosis-related clusters

To explore the functional differences among the two necroptosis-related clusters, we conducted the GSVA utilizing hallmarks gene set (c2.cp.kegg.v2022.1.Hs.symbols.gmt) and visualized the results using a heatmap (Figure 2H). C1 group was positively associated with several pathways, including P53 signaling, MAPK signaling, T cell receptor signaling, chemokine signaling pathways, and apoptosis pathway. In contrast, C2 group showed enrichment in metabolic-

10.3389/fimmu.2023.1279603

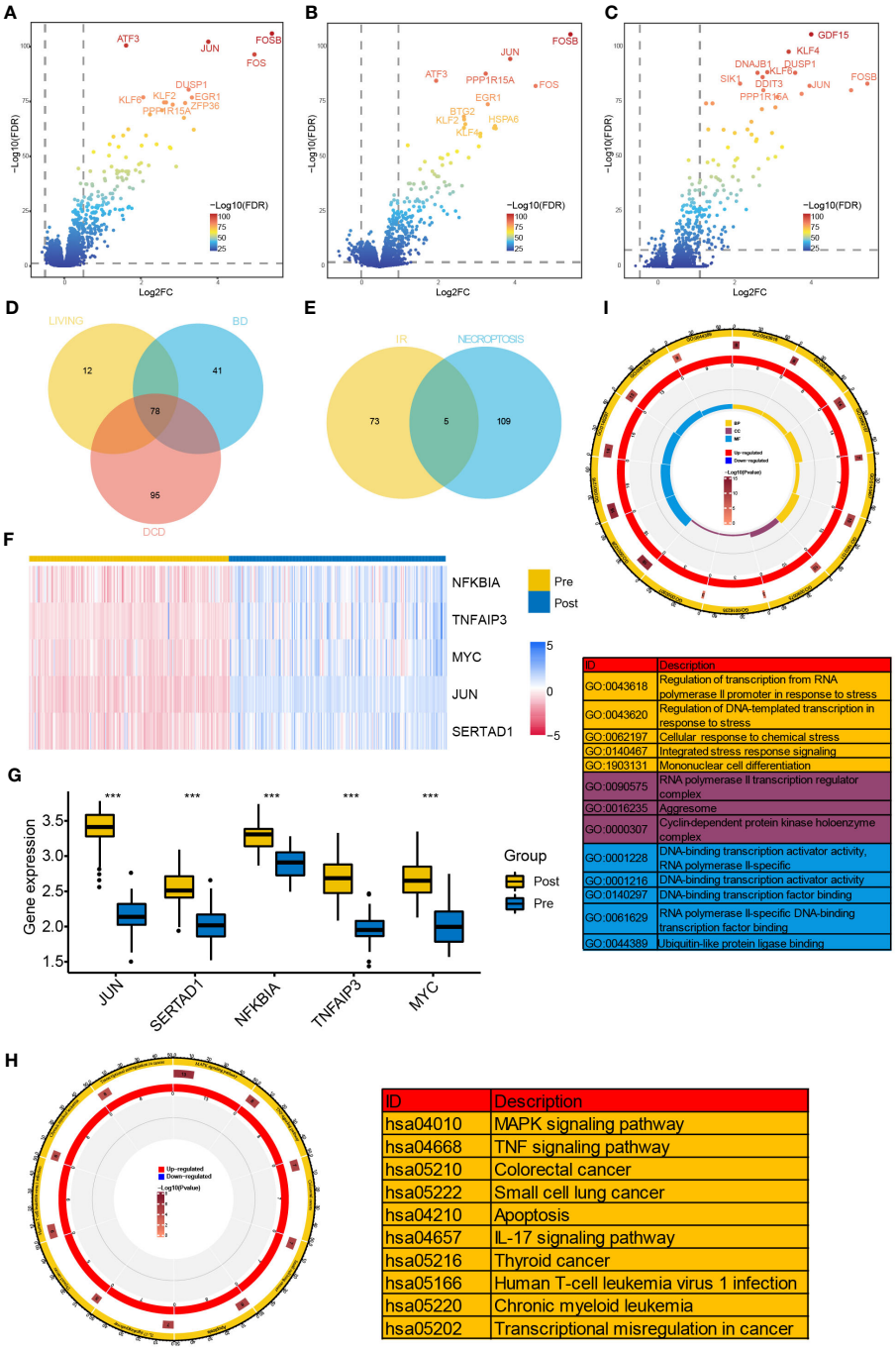

FIGURE 1
Identification of NR-DEGs and functional enrichment analysis of IRI-related DEGs. **(A–C)** Volcano plots of DEGs between samples before and after reperfusion in brain death **(A)**, cardiac death **(B)**, and healthy living donors **(C)**, respectively. **(D)** The Venn diagram showing the intersection of IRI-related DEGs among three kinds of donors. **(E)** The Veen diagram showing the intersection of DEGs from IR samples and necroptosis-related genes. **(F)** Heatmap of the expression of the 5 NR-DEGs in pre- and post-reperfusion samples in GSE43974. **(G)** Box plots showing the expression levels of the 5 NR-DEGs among pre- and post-reperfusion samples in GSE126805. **(H, I)** Chord plots presenting the distribution of the common IRI-related DEGs in KEGG and GO pathway analysis. NR-DEGs, necroptosis-related differentially expression genes; IRI, ischemia-reperfusion injury; BD, brain death; DCD, deceased cardiac dead; BP, biological process; CC, cellular component; MF, molecular function. *** P value < 0.001.

related pathways, including steroid hormone biosynthesis, cytochrome P450-mediated drug metabolism, and the pathway of retinol and linoleic acid metabolism.

Furthermore, we investigated the differential relative proportion of immune infiltrating cells between the two clusters. The results revealed that the C1 group exhibited higher abundance of naïve B cells, M1 macrophages, and memory resting CD4 T cells. In contrast, the C2 group had higher infiltration of memory B cells, gamma delta T cells, and naïve CD4 T cells (Figure 2I).

10.3389/fimmu.2023.1279603

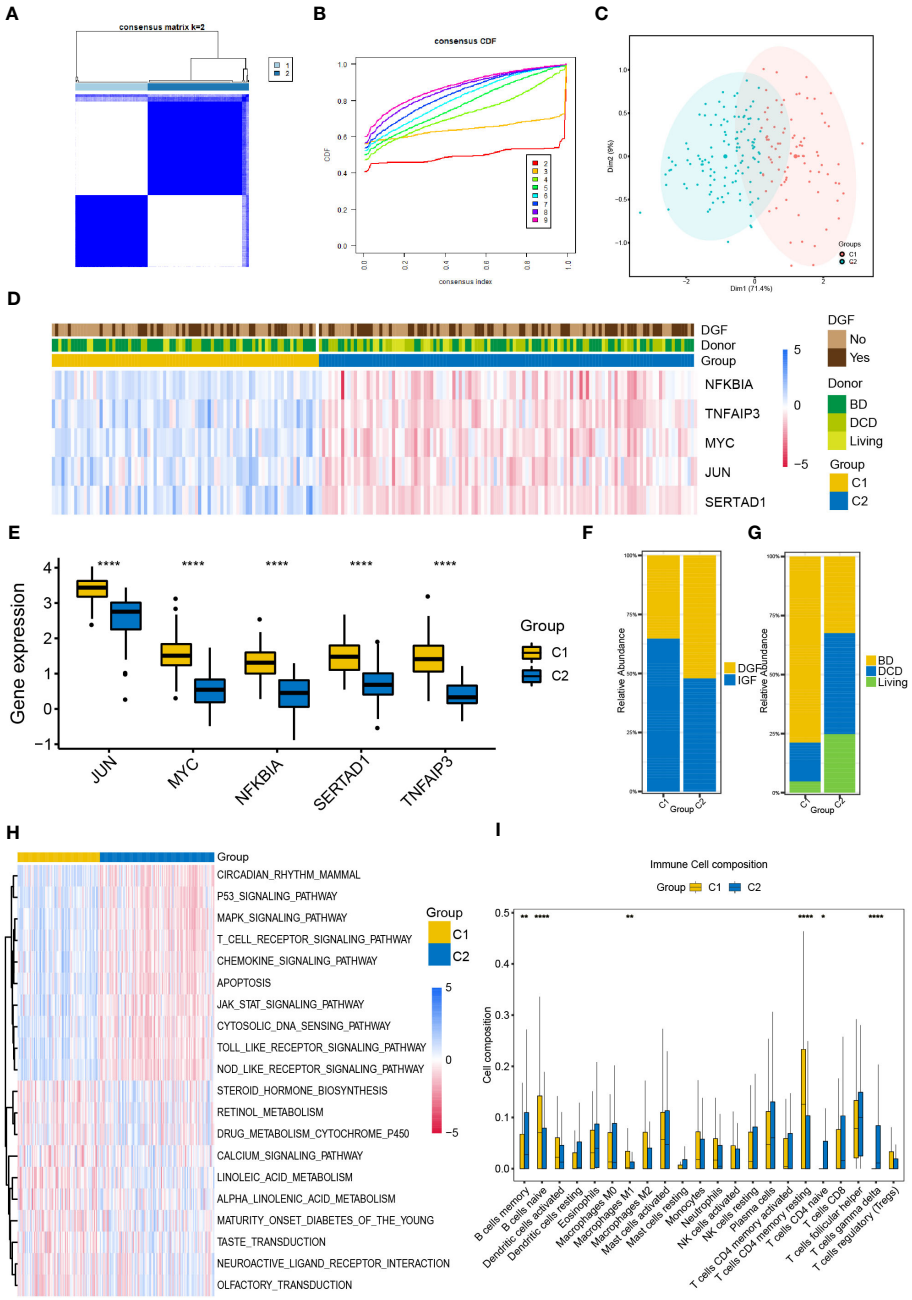

FIGURE 2
Classification of IR samples into two clusters by consensus clustering analysis. **(A)** Heatmap of consensus clustering analysis based on NR-DEGs. **(B)** Cumulative distribution function curves with k = 2-9. **(C)** PCA analysis of NR-DEGs between two clusters. **(D)** Heatmap showing the association between the expression levels of NR-DEGs and the clinical characteristics of two clusters. **(E)** Box plots showing the expression levels of the 5 NR-DEGs among two clusters in GSE43974. **(F, G)** Histograms comparing the occurrence of DGF and donor types between two clusters. **(H, I)** The GSVA enrichment analysis **(H)** and immune cell infiltration analysis **(I)** among the two clusters. IR, ischemia-reperfusion; NR-DEGs, necroptosis-related differentially expression genes; PCA, principal component analysis; DGF, delayed graft function; GSVA, gene set variation analysis; BD, brain death; DCD, deceased cardiac dead. *P value < 0.05; **P value < 0.01; ****P value < 0.0001.

3.4 Construction and validation of the DGF predictive model

DGF is a common manifestation seen after renal transplantation and always occurs after severe IRI (30). Therefore, we aimed to develop a predictive model for DGF based on the NR-DEGs from the GSE43974 dataset. We randomly divided these IRI samples into a discovery cohort and an internal validation cohort with a ratio of 7: 3. In the discovery cohort, we used 10-fold cross-validation for LASSO regression to minimize the prediction error and determine the contribution of each gene in the optimal model. The optimal value of log lambda (λ) was indicated by the left dashed vertical line in Figure 3A. In this case, all five NR-DEGs (*TNFAIP3, JUN, MYC, SERTAD1*, and *NFKBIA*) were included in the final

10.3389/fimmu.2023.1279603

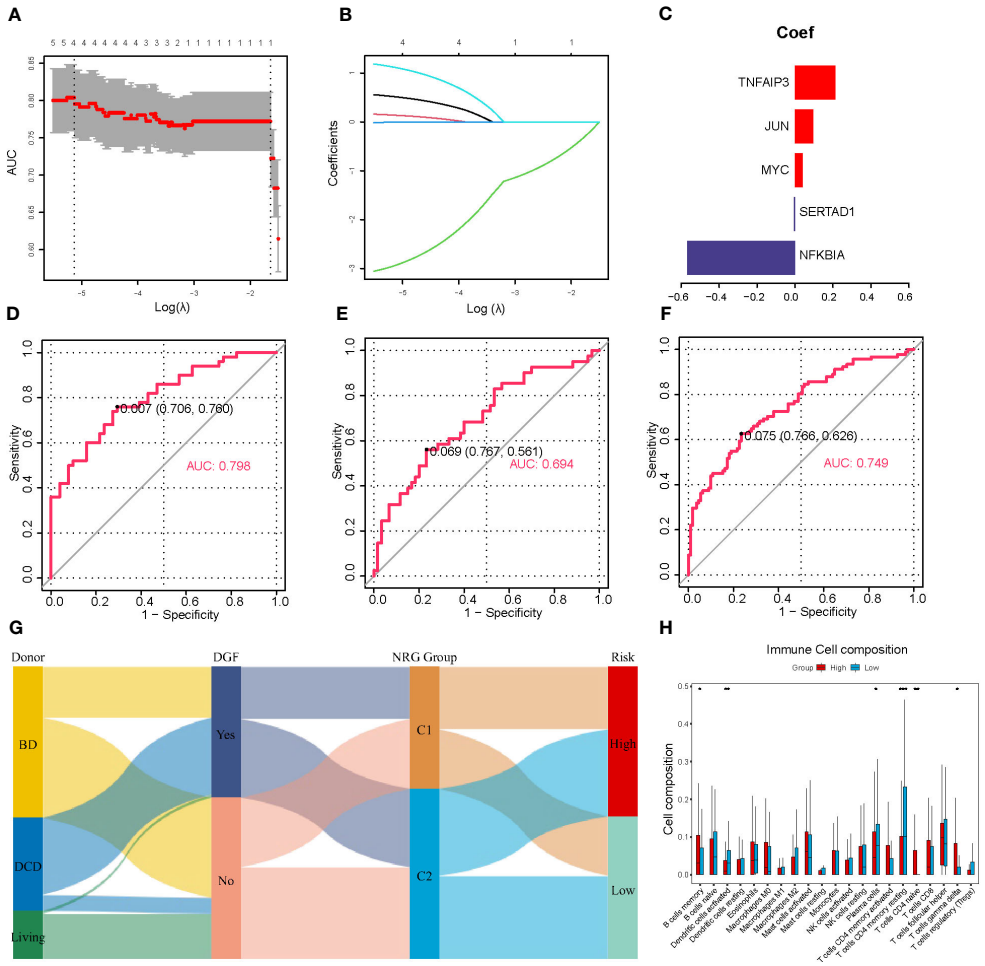

FIGURE 3
Establishment and validation of the prediction model for DGF. **(A)** Cross-validation plot according to the log of lambda in LASSO regression. **(B)** The coefficients of each NR-DEG over different values of the penalty parameter. **(C)** The final coefficients in the optimal predictive model. **(D-F)** The AUC of the prediction model based on LASSO regression in the discovery **(D)**, validation **(E)**, and whole cohorts **(F)**, respectively. **(G)** Alluvial diagram of donor types, the occurrence of DGF, NRG clusters, and risk groups. **(H)** The immune cell infiltration analysis between two risk groups divided with the risk scores. DGF, delayed graft function; NR-DEGs, necroptosis-related differentially expression genes; AUC, area under the receiver operator characteristic curve; NRG, necroptosis-related gene. *P value < 0.05; **P value < 0.01; ***P value < 0.001.

predictive model (Figures 3B, C). The area under the curve (AUC) of the prediction model in the discovery, internal validation, and whole cohorts were 0.798, 0.694, and 0.749 respectively, suggesting that the model was reliable in assessing the risk of DGF after renal transplantation (Figures 3D–F).

To further validate the performance of the prediction model, we categorized IRI samples into high- and low-risk groups based on the median risk score derived from the model. Figure 3H illustrates the results of immune infiltration analysis. The high-risk group exhibited a higher abundance of immune-related cells, including memory B cells, naïve CD4 T cells, and gamma delta T cells. Conversely, the low-risk group samples tended to have more activated dendritic cells, plasma cells, and memory resting CD4 T cells. These findings were consistent with the comparison between the necroptosis-related clusters, suggesting that the high-risk group samples had a greater accumulation of proinflammatory cell phenotypes. In addition, we utilized a Sankey diagram (Figure 3G) to visualize the relationships among various characteristics, including the type of donors, the occurrence of DGF, the necroptosis-related cluster, and the DGF risk.

3.5 Validation of the expression of NR-DEGs in scRNA-seq data

As for scRNA-seq data analysis, a total of 19,274 genes and 12,965 cells were included from the GSE171639 dataset after quality filtering and batch effects removal. Among these, 6,697 cells (51.7%) originated from IRI group and 6,268 cells (48.3%) were derived from sham surgery group. By applying PCA and UMAP algorithms, we divided the 12,965 cells into 23 clusters.

To identify cell types, we combined the CellMarker database and previous studies for mice kidneys (Figure 4A). The clusters were annotated as follows: cluster 0, 1, 2, 4, 6, 10, 11, and 13 were annotated as proximal tubule (7,732 cells); cluster 3 as neutrophil cell (1,328 cells); cluster 5 as loop of Henle (874 cells); cluster 7 and

10.3389/fimmu.2023.1279603

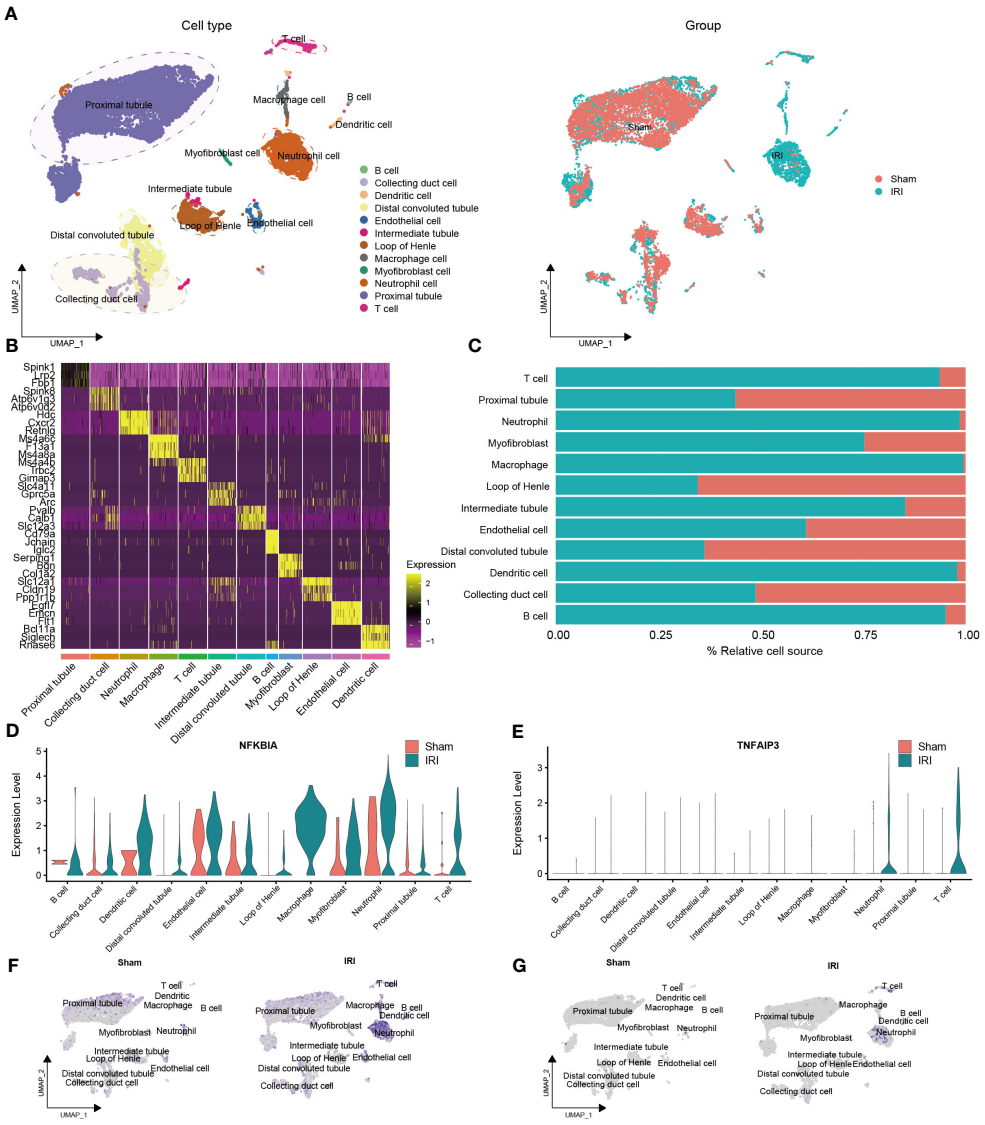

FIGURE 4
Validation of the NR-DEGs based on scRNA-seq analysis (GSE171639). **(A)** scRNA-seq identified clusters of cells in the sham and IRI kidneys. **(B)** Heatmap showing the top 3 differentially expressed markers in each cluster. **(C)** The proportion of each cell in different groups. **(D-G)** The expression levels of *NFKBIA* **(D, F)** and *TNFAIP3* **(E, G)** in different cells among pre- and post-IRI groups. NR-DEGs, necroptosis-related differentially expression genes; IRI, ischemia-reperfusion injury.

8 as distal convoluted tubule (1,133 cells); cluster 9, 12, 17, and 21 as collecting duct cell (910 cells); cluster 14 as T cell (254 cells); cluster 15 as endothelial cell (239 cells); cluster 16 as macrophage cell (173 cells); cluster 18 as intermediate tubule (102 cells); cluster 19 as myofibroblast cell (81 cells); cluster 20 and 23 as dendritic cell (98 cells); and cluster 22 as B cell (41 cells).

The top three marker genes in each cell subpopulation are presented in Figure 4B, and the proportion of different groups in each cell type is shown in Figure 4C. It is worth mentioning that T cells, neutrophils, macrophages, dendritic cells, and B cells were predominantly derived from the IRI group, which aligns with the immune infiltration analysis mentioned earlier. We then examined the expression of the five NR-DEGs in each cell type and observed that *NFKBIA*, *TNFAIP3*, *MYC*, and *SERTAD1* were mainly expressed in the IRI group (Figures 4D–G, Figures S2C–F). Specifically, *NFKBIA* exhibited high expression in macrophages, dendritic cells, T cells, and neutrophils; *TNFAIP3* was highly expressed in T cells and neutrophils; *MYC* was predominantly expressed in myofibroblast cells and intermediate tubules; *SERTAD1* was identified as being primarily expressed in myofibroblast cells, macrophages, neutrophils, and endothelial cells. Conversely, *JUN* was predominantly expressed in proximal tubules, intermediate tubules, and endothelial cells (Figures S2A, B).

Additionally, the identified cell types of single-cell samples from the GSE193649 dataset were presented in Figure S3A. Notably, the expression levels of the five NR-DEGs in GSE193649 dataset were also higher in immune cells of IRI group, such as neutrophils, macrophages, NK cells, and T cells (Figures S3C–F, Figures S4A–F). These findings suggested that the NR-DEGs are mainly highly expressed in immune cells, which are essential players in the process of IRI.

10.3389/fimmu.2023.1279603

3.6 GSVA and cell-cell communication networks

Following IRI, there was a notable increase in immune cell infiltration and higher relative expression of the NR-DEGs in kidneys. To understand the biological behaviors of these immune subtypes between IRI and sham groups, we performed gene set variation analysis in GSE171639 dataset. The histograms revealed significant enrichment of pathways associated with immune and inflammatory responses, including IL2-STAT5 signaling, TNFA signaling via NF-κB, TGF-β signaling, IL6-JAK-STAT3 signaling, IFN-α/γ response, and PI3K-AKT-mTOR signaling in the IRI group (Figures 5A–D, Figure S2G). Moreover, the processes of allograft rejection and apoptosis were also more active in the IRI group. Additionally, we compared the enrichment of necroptosis-related pathways using the Molecular Signatures Database (MSigDB, C2, CP: Reactome) with UMAP visualization (Figures 5G, H). The regulated necrosis and RIRK1-mediated regulated necrosis pathways were more enriched in immune cells in IRI groups, including neutrophil cells, dendritic cells, macrophage cells, B cells, and T cells. Similar enrichment analysis results of the necroptosis-related pathways were obtained in GSE193649 dataset (Figures S3G, H).

To investigate the aggregated cell–cell communication network in the presence or absence of IRI based on the scRNA-seq data, we examined the number and strength of interactions between different cell types. Circle plots (Figures 5E, F, Figures S2H, I) demonstrated that ligand–receptor interactions were mainly sent from the neutrophil cells, distal convoluted tubules, and myofibroblast cells in the sham group. However, in the IRI group, the communications between the other immune cells, such as B cells, T cells, and dendritic cells, with

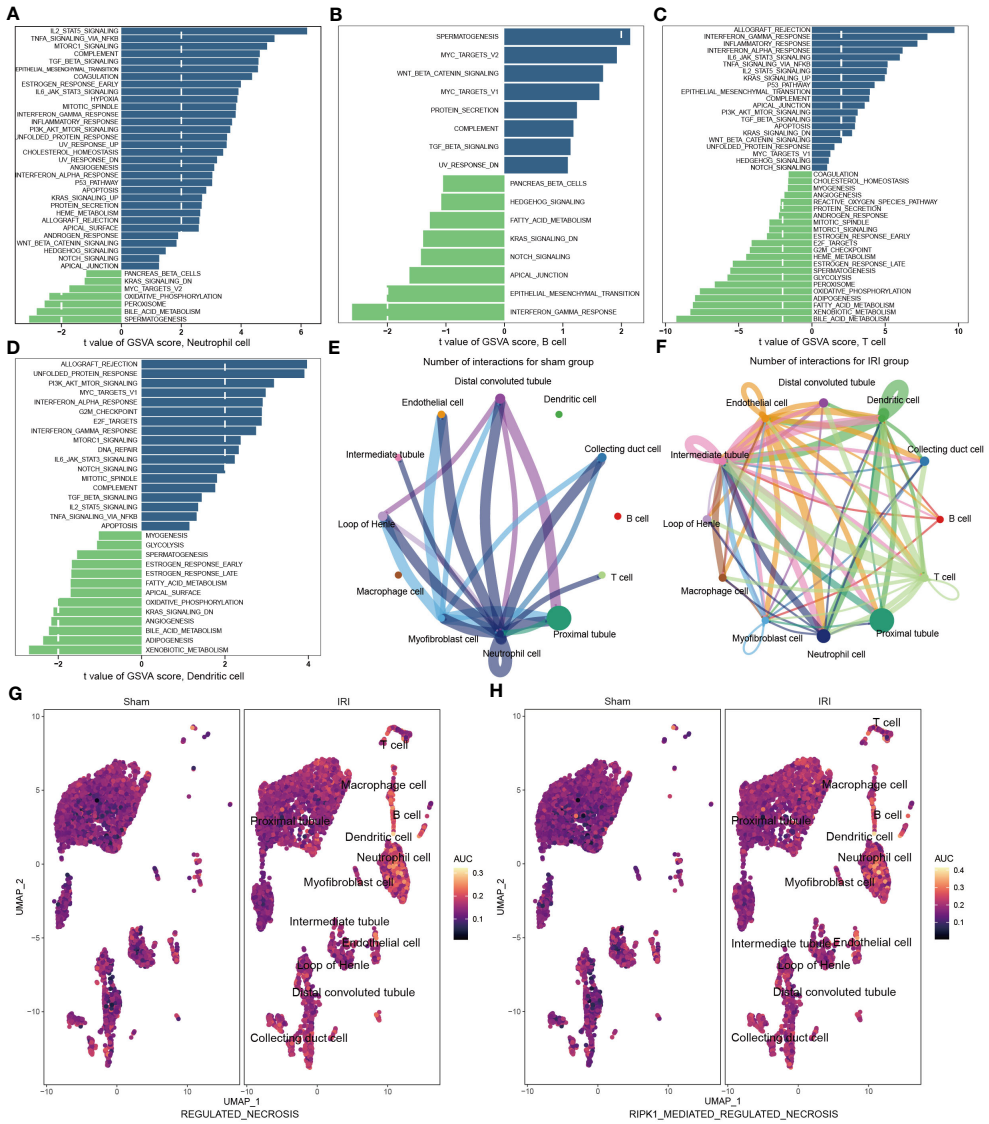

FIGURE 5
Functional enrichment and cell-cell communication analysis based on scRNA-seq data (GSE171639). **(A–D)** Differences in pathway activities scored in neutrophil cell **(A)**, B cell **(B)**, T cell **(C)**, and dendritic cell **(D)** by GSVA compared with sham and IRI groups. **(E, F)** The number of interactions among different cells in sham **(E)** and IRI groups **(F)**. **(G, H)** UMAP plots showing the necroptotic pathways enrichment scores in sham and IRI groups. GSVA, gene set variation analysis; IRI, ischemia-reperfusion injury.

epithelial and endothelial cells, were significantly increased. Together, these findings further support the notion of a more active necroptosis process and heightened immune responses after IRI, which may play critical roles in the pathogenesis of renal ischemia-reperfusion injury.

3.7 Validation of NR-DEGs in IRI model

To further investigate the important role of the 5 NR-DEGs in the context of kidney IRI, we conducted a model using male C57BL/6N mice. To accurately assess changes in gene expression before and after IR, we removed the right kidney and subjected the left kidney to ischemia-reperfusion treatment. The right kidney served as self-control, minimizing individual differences and potential errors. The PCR results of the same individual's kidneys, with and without IR, indicated that *MYC*, *NFKBIA*, *SERTAD1*, and *TNFAIP3* were upregulated after IR. However, in contrast to the findings from public databases, *JUN* was significantly downregulated after IR. This discrepancy might be attributed to the differential expression of *JUN* among various cell populations (Figures 6A–E). Additionally, we measured the levels of SCr and BUN in mice 24 hours after IR. The results showed consistent correlations with *TNFAIP3* and *NFKBIA*, which had significant contributions to the model established in this study, along with *MYC* (Figure 6F).

4 Discussion

Despite the improvement of patient and graft survival rates with scientific advances and increasing potency of immunosuppressants, DGF following renal IRI remains an intricate complication after kidney transplantation, resulting in increased morbidity and resource utilization, including longer hospital stays, post-acute care, and higher costs (4, 31). Existing biomarkers like neutrophil gelatinase-associated lipocalin (NGAL) and cystatin C are still not widely applied in clinical settings (32), and proposed models for DGF after deceased-donor transplantation may overestimate its incidence (33). Necroptosis, a caspase-independent form of RN, has been proven to be associated with various models of renal injury, including the oxidative stress-derived IRI (6). Our previous research has demonstrated the role of ferroptosis, another well-studied RN pathway, in acute cell-mediated rejection of KT (34). In the present study, we developed a novel predictive model for DGF occurrence based on necroptosis-related DEGs and revealed the interplay between necroptosis, the hub genes, and immune cells in the process of IRI induced by oxidative stress.

There is growing evidence indicating that necroptosis represents a pivotal component of cell death in renal IRI (35). Markers of necroptosis, including *RIPK1*, *RIPK3*, and *MLKL*, have been shown to be elevated *in vitro* during renal hypoxia/reoxygenation (H/R) injury and *in vivo* during renal IRI studies (36–38). An alleviated renal damage and preserved renal function were detected in the use of small molecule inhibitors like RIPK1 inhibitor Necrostatin-1 (Nec-1) or KO mice (38, 39). To identify potential genetic markers of DGF induced by renal IRI, we intersected DEGs between pre- and post-reperfusion samples with NEGs, resulting in five target NR-DEGs (*NFKBIA*, *TNFAIP3*, *MYC*, *JUN*, *SERTAD1*). All five NR-DEGs were significantly upregulated in post-reperfusion group. Among these, *NFKBIA* (NF-κB inhibitor-α) serves as a direct upstream transcription factor of NF-κB, binding to NF-κB in the cytoplasm and inhibiting its translocation into the nucleus (40, 41). Yatim et al. proposed that NF-κB plays an important role in the activation of RIPK3-induced necroptosis (42). Moreover, it has been demonstrated

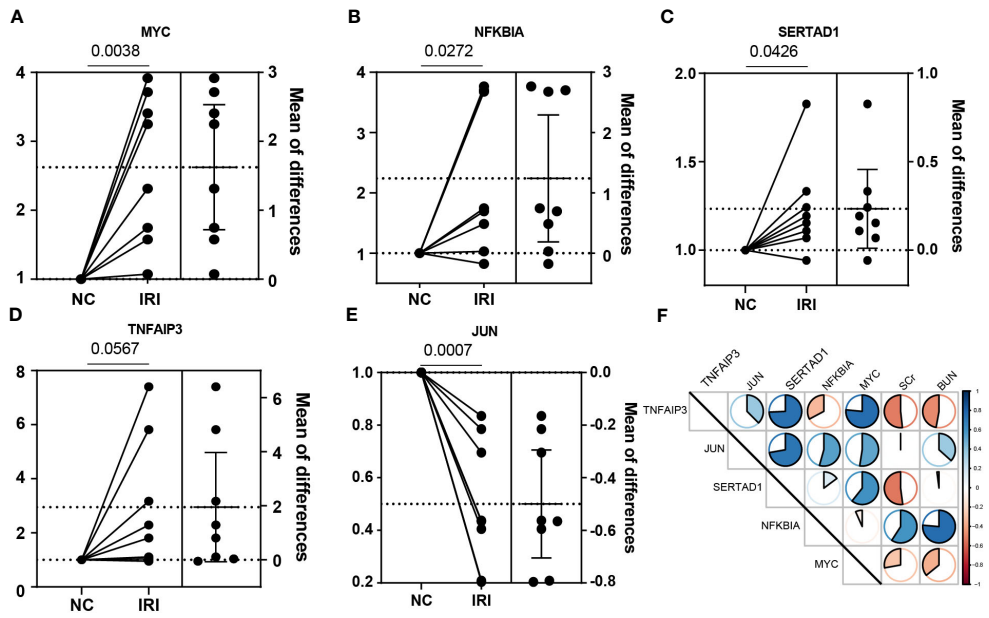

FIGURE 6
Experimental verification with the mice renal IRI model. **(A–E)** The relative mRNA expression of the NR-DEGs confirmed by qPCR (n = 8). **(F)** The correlation between the expression of NR-DEGs and indexes of renal function (BUN and SCr). IRI, ischemia-reperfusion injury; NR-DEGs, necroptosis-related differentially expression genes; SCr, serum creatinine; BUN, blood urea nitrogen.

that *NFKBIA* is upregulated in T- and B-cells during chronic antibody-mediated rejection in KT patients (43). *TNFAIP3* (tumor necrosis factor α-induced protein 3), an ubiquitin-editing enzyme, plays a role in inhibiting the activation of NF-κB and preventing the synthesis of other pro-inflammatory factors, thereby contributing to the regulation of necroptosis (44, 45). Polymorphisms of *TNFAIP3* in humans have been associated with autoimmune diseases and multiple cancers (46). *MYC*, a potent oncogene, is an oncoprotein that regulates various cellular processes (47). It functions as an antinecroptotic regulator by inhibiting the formation of RIPK3-RIPK1 complex (48). In addition, *JUN* is an important component of activating protein-1 (AP-1), which has been proven to regulate cell death and survival (49). C-Jun, the most intensively studied member of the JUN family, is associated with the necroptotic pathway, specifically the RIPK3-JNK-BNIP3 (c-Jun N-terminal kinase-BCL2 Interacting Protein 3) axis (50). *SERTAD1*, also known as SERTA domain-containing protein 1, belongs to the Sertad family (51) and functions as an oncoprotein that significantly contributes to oncogenesis and programmed cell death (PCD), including necroptosis (52). Additionally, *SERTAD1* has been implicated in promoting cell survival in response to the induction of reactive oxygen species by facilitating the ubiquitination of apoptosis signal-regulating kinase1 (ASK1) (53).

To elucidate distinct patterns of necroptosis modification, we conducted the unsupervised consistent clustering analysis based on the NR-DEGs. The renal samples were categorized into C1 and C2 clusters, where all five NR-DEGs exhibited higher expression in the C1 cluster. Notably, the C1 cluster showed a lower incidence of DGF and a higher proportion of recipients receiving kidneys from BD donors. These findings suggest that although the NR-DEGs are upregulated after IRI, they may confer a protective effect against renal damage and contribute to reduced complications, as we mentioned above.

The analysis of functional enrichment revealed that the IRI-related DEGs exhibited significant enrichment in the regulation of RNA polymerase II transcription and MAPK signaling, IL-17 signaling, and TNF signaling pathways. Similarly, the GSVA analysis between the two necroptosis-related clusters suggested a strong association of the C1 group with multiple immune-related pathways, including MAPK signaling, T cell receptor signaling, Toll-like receptor (TLR) signaling pathways, and apoptosis pathway. TNFα is a well-studied trigger of necroptosis cell death (6). Upon TNF binding to its receptor, TNF receptor 1 (TNFR1), various downstream molecules are recruited to form complex I, providing a platform to determine cell survival, apoptosis, or necroptosis (54). *In vitro* studies have demonstrated that a combination of TNFα, interferon (IFN)-γ, and the weak inducer of TNF signaling (TWEAK) can induce necroptosis in TECs (55). TLRs are constitutively expressed in various renal cells. Activation of TLRs induces the interaction between downstream molecules and complex IIb (composed of RIPK1 and RIPK3), leading to MLKL-dependent necroptosis (56). These findings suggest that the proinflammatory pathways associated with necroptosis may be significantly inhibited in C1 cluster.

Since IRI is inevitable in surgical procedures of KT and is the primary cause of DGF, it is of utmost clinical importance to identify patients at higher risk of DGF early and accurately. In the present study, we developed an early predictive model based on the five NR-DEGs through LASSO regression analysis. The performance of this predictive model was robust and satisfactory in both the discovery cohort (AUROC = 0.798) and the whole cohort (AUROC = 0.749). To explore the underlying mechanism, we stratified the renal samples into low- and high-risk groups and examined the immune cell infiltration. High-risk samples exhibited higher infiltration of memory B cells, naïve CD4 T cells, and gamma delta T cells, which were also prevalent in samples of C2 cluster characterized by a higher incidence of DGF. This suggests that specific immune cells potentially served as a bridging link function between necroptosis and the progression of DGF. Therefore, we conducted single-cell data analysis to further corroborate the validity of our model genes.

To substantiate our findings, we utilized two published single-cell datasets of mouse renal samples obtained with or without IR. In the IRI group, immune cells such as T cells, B cells, dendritic cells, and neutrophils were more abundant, concomitant with higher expression levels of the NR-DEGs, particularly in neutrophils and macrophages. During renal IRI, damaged cells release damage-associated molecular patterns and proinflammatory cytokines such as TNFα and IL-1α, which can bind to cell surface receptors like TLRs, resulting in dendritic cell migration and activation of T cells and macrophages as observed in our intercellular communication (6, 57). Previous research has proved that B-cell and T-cell deficient mice are protected from renal IRI (58). While, necroptosis, as an immunity-related programmed cell death, regulates the proliferation of lymphocytes and is crucial for their survival (59). RIP1 is essential for B cell development and is more highly expressed in immature B cells and peripheral mature B cells (60). Zhang et al. indicated that the proliferation response of $RIP^{-/-}$ B cells induced by TLR and lipopolysaccharide (LPS) was reduced compared to $RIP^{+/+}$ B cells (61). Besides, caspase-8 is the key molecule of T cell homeostasis, and the impaired T cell proliferation in caspase 8-deficient mice can be rescued by blocking RIP1 with Nec-1 or through gene knockout, indicating that the necroptotic signaling in T cells is regulated by caspase-8 (59, 62, 63). Recent studies demonstrated that the RIRK1-dependent necroptosis is reduced during macrophage cell differentiation (64), while TNFα derived from macrophages induces necroptosis (65). Additionally, it has been suggested that IR-induced AKI depends on the migration of neutrophils into kidneys (66). Necroptosis in neutrophils can be induced by activating TLRs, IFN-α receptors, TNF receptors, and other factors (67, 68). Early research reported that inhibiting XIAP (X-linked inhibitor of apoptosis family of protein) resulted in increased ubiquitylation of neutrophil RIPK1 (69), restricted RIPK3-dependent cell death in dendritic cells (70), and limited macrophages necroptosis (71).

We further analyzed the functional differences between immune cells before and after IR. It is worth noting that the necroptosis-related pathways, including TNFα signaling and IFN response, were enriched in these immune cells after IR (6, 54), supporting the biological plausibility of our findings. *MYC*, one of the NR-DEGs, known as a negative regulator of necroptosis (47), showed increased activity in the IRI group in our study, possibly due to the proteasomal degradation of *MYC* stimulated by RIPK3. In addition, previous studies have also linked necroptosis to an immune response in various diseases, encompassing IL6-JAK-STAT3 and IL2-STAT5 signaling pathways (72, 73). Activation of TAK1 (TGF-β activated kinase 1) can induce RIPK3-dependent

necroptosis (74). RIPK1 facilitates the reciprocal stimulations between TAK1 and RIPK3, in turn mediates TAK1-RIPK1-RIPK3 binding, which decides whether the necroptosis occurs or not (75). Meanwhile, the enrichment of "regulated necrosis" and "RIPK1 mediated regulated necrosis" was observed in the IRI group, especially in proinflammatory cells. Together, these findings are consistent with prior studies and highlight the important contributions of immune cells in the regulation of necroptosis after renal IR. The results not only support the validity of the prediction models but also provide potential targets for addressing necroptosis-related renal oxidative stress damage.

Our findings were experimentally validated using the mouse renal IRI model. We observed that all the identified NR-DEGs were upregulated after IR, except for *JUN*. This confirmed the role of necroptotic progress. Furthermore, the negative correlations between *TNFAIP3* and *MYC* with kidney function markers also indicated a potential protective action of these genes in necroptosis (45, 48). While, the *NFKBIA* was associated with higher BUN and SCr, likely due to its role in suppressing cell survival induced by NF-kB (76).

The primary strengths of this study lie in the construction of a predictive model for DGF based on the concept of necroptosis. The study successfully demonstrated the correlation between NR-DEGs, oxidative stress, and immune cells, providing valuable insights into the role of necroptotic cell death in renal IRI. Nevertheless, a portion of dead cells were filtered out to improve the accuracy of cell identification among scRNA-seq analysis, which may lead to the loss of information related to necroptosis. Additionally, to ensure the reliability and applicability of the prediction model, further validation using data from multicenter and KT patients is necessary. Furthermore, considering the potential of NR-DEGs as targets for preventing DGF, it is imperative to conduct an experimental investigation to understand the cellular and molecular mechanism through which these genes influence renal IRI. Such investigations could pave the way for potential therapeutic interventions to improve outcomes in kidney transplantation.

5 Conclusions

To summarize, our study has identified five NR-DEGs and confirmed their expression levels by utilizing scRNA-seq data and a mouse IRI model. We developed a novel diagnostic model based on the five genes, enabling us to predict the occurrence of DGF more accurately. Furthermore, we observed distinct differences in necroptotic immune cell profiles and proinflammatory responses between the low- and high-risk groups, highlighting the clinical relevance of our findings. By offering insights into the underlying mechanisms and potential predictive markers, our study may aid clinicians in decision-making and provide potential therapeutic strategies for the prevention of IRI and DGF in kidney transplantation.

Data availability statement

Publicly available datasets were analyzed in this study. This data can be found here: GSE43974, GSE171639, GSE126805, and GSE193649 (https://www.ncbi.nlm.nih.gov/geo/).

Ethics statement

The animal study was approved by The Ethics Committee of Beijing Chaoyang Hospital Affiliated to Capital Medical University. The study was conducted in accordance with the local legislation and institutional requirements.

Author contributions

SL: Conceptualization, Data curation, Methodology, Visualization, Writing – original draft. WZ: Conceptualization, Data curation, Methodology, Visualization, Writing – review & editing. XH: Conceptualization, Supervision, Writing – review & editing.

Funding

The author(s) declare that no financial support was received for the research, authorship, and/or publication of this article.

Acknowledgments

The authors would like to extend their gratitude to GEO for supplying the open-access databases utilized in this study.

Conflict of interest

The authors declare that the research was conducted in the absence of any commercial or financial relationships that could be construed as a potential conflict of interest.

Publisher's note

Supplementary material

The Supplementary Material for this article can be found online at: https://www.frontiersin.org/articles/10.3389/fimmu.2023.1279603/full#supplementary-material

References

1. Tonelli M, Wiebe N, Knoll G, Bello A, Browne S, Jadhav D, et al. Systematic review: kidney transplantation compared with dialysis in clinically relevant outcomes. *Am J Transplant* (2011) 11:2093–109. doi: 10.1111/j.1600-6143.2011.03686.x

2. Liu H, Ren L, Fan B, Wang W, Hu X, Zhang X. Artificial intelligence algorithm-based MRI in the diagnosis of complications after renal transplantation. *Contrast Media Mol Imaging* (2022) 2022:8930584. doi: 10.1155/2022/8930584

3. Perico N, Cattaneo D, Sayegh MH, Remuzzi G. Delayed graft function in kidney transplantation. *Lancet* (2004) 364:1814–27. doi: 10.1016/S0140-6736(04)17406-0

4. Siedlecki A, Irish W, Brennan DC. Delayed graft function in the kidney transplant. *Am J Transplant* (2011) 11:2279–96. doi: 10.1111/j.1600-6143.2011.03754.x

5. Malhotra R, Katz R, Jotwani V, Ambrosius WT, Raphael KL, Haley W, et al. Urine markers of kidney tubule cell injury and kidney function decline in SPRINT trial participants with CKD. *Clin J Am Soc Nephrol* (2020) 15:349–58. doi: 10.2215/CJN.02780319

6. Pefanis A, Ierino FL, Murphy JM, Cowan PJ. Regulated necrosis in kidney ischemia-reperfusion injury. *Kidney Int* (2019) 96:291–301. doi: 10.1016/j.kint.2019.02.009

7. Nieuwenhuijs-Moeke GJ, Pischke SE, Berger SP, Sanders JSF, Pol RA, Struys MMRF, et al. Ischemia and reperfusion injury in kidney transplantation: relevant mechanisms in injury and repair. *J Clin Med* (2020) 9(1):253. doi: 10.3390/jcm9010253

8. Bonventre JV, Yang L. Cellular pathophysiology of ischemic acute kidney injury. *J Clin Invest* (2011) 121:4210–21. doi: 10.1172/JCI45161

9. Kers J, Leemans JC, Linkermann A. An overview of pathways of regulated necrosis in acute kidney injury. *Semin Nephrol* (2016) 36:139–52. doi: 10.1016/j.semnephrol.2016.03.002

10. Fuchs Y, Steller H. Live to die another way: modes of programmed cell death and the signals emanating from dying cells. *Nat Rev Mol Cell Biol* (2015) 16:329–44. doi: 10.1038/nrm3999

11. Linkermann A, Bräsen JH, Darding M, Jin MK, Sanz AB, Heller J-O, et al. Two independent pathways of regulated necrosis mediate ischemia-reperfusion injury. *Proc Natl Acad Sci U.S.A.* (2013) 110:12024–9. doi: 10.1073/pnas.1305538110

12. Linkermann A, Heller J-O, Prókai A, Weinberg JM, De Zen F, Himmerkus N, et al. The RIP1-kinase inhibitor necrostatin-1 prevents osmotic nephrosis and contrast-induced AKI in mice. *J Am Soc Nephrol* (2013) 24:1545–57. doi: 10.1681/ASN.2012121169

13. Saat TC, Akker EKvd, Ijzermans JNM, Dor FJMF, de Bruin RWF. Improving the outcome of kidney transplantation by ameliorating renal ischemia reperfusion injury: lost in translation? *J Transl Med* (2016) 14:20. doi: 10.1186/s12967-016-0767-2

14. Bi Q, Wu J-Y, Qiu X-M, Li Y-Q, Yan Y-Y, Sun Z-J, et al. Identification of potential necroinflammation-associated necroptosis-related biomarkers for delayed graft function and renal allograft failure: a machine learning-based exploration in the framework of predictive, preventive, and personalized medicine. *EPMA J* (2023) 14:307–28. doi: 10.1007/s13167-023-00320-w

15. Kanehisa M. Toward understanding the origin and evolution of cellular organisms. *Protein Sci* (2019) 28:1947–51. doi: 10.1002/pro.3715

16. Kanehisa M, Furumichi M, Sato Y, Kawashima M, Ishiguro-Watanabe M. KEGG for taxonomy-based analysis of pathways and genomes. *Nucleic Acids Res* (2023) 51:D587–92. doi: 10.1093/nar/gkac963

17. Kanehisa M, Goto S. KEGG: kyoto encyclopedia of genes and genomes. *Nucleic Acids Res* (2000) 28:27–30. doi: 10.1093/nar/28.1.27

18. Newman AM, Liu CL, Green MR, Gentles AJ, Feng W, Xu Y, et al. Robust enumeration of cell subsets from tissue expression profiles. *Nat Methods* (2015) 12:453–7. doi: 10.1038/nmeth.3337

19. Wilkerson MD, Hayes DN. ConsensusClusterPlus: a class discovery tool with confidence assessments and item tracking. *Bioinformatics* (2010) 26:1572–3. doi: 10.1093/bioinformatics/btq170

20. Wei H, Sun J, Shan W, Xiao W, Wang B, Ma X, et al. Environmental chemical exposure dynamics and machine learning-based prediction of diabetes mellitus. *Sci Total Environ* (2022) 806:150674. doi: 10.1016/j.scitotenv.2021.150674

21. Melo Ferreira R, Sabo AR, Winfree S, Collins KS, Janosevic D, Gulbronson CJ, et al. Integration of spatial and single-cell transcriptomics localizes epithelial cell-immune cross-talk in kidney injury. *JCI Insight* (2021) 6(12):e147703. doi: 10.1172/jci.insight.147703

22. Gaedcke S, Sinning J, Dittrich-Breiholz O, Haller H, Soerensen-Zender I, Liao CM, et al. Single cell versus single nucleus: transcriptome differences in the murine kidney after ischemia-reperfusion injury. *Am J Physiol Renal Physiol* (2022) 323:F171–81. doi: 10.1152/ajprenal.00453.2021

23. Hu C, Li T, Xu Y, Zhang X, Li F, Bai J, et al. CellMarker 2.0: an updated database of manually curated cell markers in human/mouse and web tools based on scRNA-seq data. *Nucleic Acids Res* (2023) 51:D870–6. doi: 10.1093/nar/gkac947

24. De Chiara L, Conte C, Semeraro R, Diaz-Bulnes P, Angelotti ML, Mazzinghi B, et al. Tubular cell polyploidy protects from lethal acute kidney injury but promotes consequent chronic kidney disease. *Nat Commun* (2022) 13:5805. doi: 10.1038/s41467-022-33110-5

25. Rudman-Melnick V, Adam M, Potter A, Chokshi SM, Ma Q, Drake KA, et al. Single-cell profiling of AKI in a murine model reveals novel transcriptional signatures, profibrotic phenotype, and epithelial-to-stromal crosstalk. *J Am Soc Nephrol* (2020) 31:2793–814. doi: 10.1681/ASN.2020010052

26. Zhao Z, Wu J, Xu H, Zhou C, Han B, Zhu H, et al. XJB-5-131 inhibited ferroptosis in tubular epithelial cells after ischemia-reperfusion injury. *Cell Death Dis* (2020) 11:629. doi: 10.1038/s41419-020-02871-6

27. Jin S, Guerrero-Juarez CF, Zhang L, Chang I, Ramos R, Kuan C-H, et al. Inference and analysis of cell-cell communication using CellChat. *Nat Commun* (2021) 12:1088. doi: 10.1038/s41467-021-21246-9

28. Hänzelmann S, Castelo R, Guinney J. GSVA: gene set variation analysis for microarray and RNA-seq data. *BMC Bioinf* (2013) 14:7. doi: 10.1186/1471-2105-14-7

29. Hesketh EE, Czopek A, Clay M, Borthwick G, Ferenbach D, Kluth D, et al. Renal ischaemia reperfusion injury: a mouse model of injury and regeneration. *J Vis Exp* (2014) 88:51816. doi: 10.3791/51816-v

30. Jiang B, Wang S, Song G, Jiang Q, Fan M, Fang C, et al. Hedgehog-induced ZFYVE21 promotes chronic vascular inflammation by activating NLRP3 inflammasomes in T cells. *Sci Signal* (2023) 16:eabo3406. doi: 10.1126/scisignal.abo3406

31. Yarlagadda SG, Coca SG, Formica RN, Poggio ED, Parikh CR. Association between delayed graft function and allograft and patient survival: a systematic review and meta-analysis. *Nephrol Dial Transplant* (2009) 24:1039–47. doi: 10.1093/ndt/gfn667

32. Lai C, Yee SY, Ying T, Chadban S. Biomarkers as diagnostic tests for delayed graft function in kidney transplantation. *Transpl Int* (2021) 34:2431–41. doi: 10.1111/tri.14132

33. Nashan B, Abbud-Filho M, Citterio F. Prediction, prevention, and management of delayed graft function: where are we now? *Clin Transplant* (2016) 30:1198–208. doi: 10.1111/ctr.12832

34. Zhang W, Gong L, Zhang D, Hu X. Ferroptosis related gene signature in T cell-mediated rejection after kidney transplantation. *BMC Med Genomics* (2023) 16:11. doi: 10.1186/s12920-023-01440-y

35. Choi ME, Price DR, Ryter SW, Choi AMK. Necroptosis: a crucial pathogenic mediator of human disease. *JCI Insight* (2019) 4(15):e128834. doi: 10.1172/jci.insight.128834

36. Liu S-S, Chen Y-Y, Wang S-X, Yu Q. Protective effect of dabrafenib on renal ischemia-reperfusion injury in *vivo* and in *vitro*. *Biochem Biophys Res Commun* (2020) 522:395–401. doi: 10.1016/j.bbrc.2019.11.105

37. Shen B, Mei M, Pu Y, Zhang H, Liu H, Tang M, et al. Necrostatin-1 attenuates renal ischemia and reperfusion injury via meditation of HIF-1α/mir-26a/TRPC6/PARP1 signaling. *Mol Ther Nucleic Acids* (2019) 17:701–13. doi: 10.1016/j.omtn.2019.06.025

38. Linkermann A, Bräsen JH, Himmerkus N, Liu S, Huber TB, Kunzendorf U, et al. Rip1 (receptor-interacting protein kinase 1) mediates necroptosis and contributes to renal ischemia/reperfusion injury. *Kidney Int* (2012) 81:751–61. doi: 10.1038/ki.2011.450

39. Newton K, Dugger DL, Maltzman A, Greve JM, Hedehus M, Martin-McNulty B, et al. RIPK3 deficiency or catalytically inactive RIPK1 provides greater benefit than MLKL deficiency in mouse models of inflammation and tissue injury. *Cell Death Differ* (2016) 23:1565–76. doi: 10.1038/cdd.2016.46

40. Karin M. NF-kappaB as a critical link between inflammation and cancer. *Cold Spring Harb Perspect Biol* (2009) 1:a000141. doi: 10.1101/cshperspect.a000141

41. Bredel M, Scholtens DM, Yadav AK, Alvarez AA, Renfrow JJ, Chandler JP, et al. NFKBIA deletion in glioblastomas. *N Engl J Med* (2011) 364:627–37. doi: 10.1056/NEJMoa1006312

42. Yatim N, Jusforgues-Saklani H, Orozco S, Schulz O, Barreira da Silva R, Reis e Sousa C, et al. RIPK1 and NF-κB signaling in dying cells determines cross-priming of $CD8^+$ T cells. *Science* (2015) 350:328–34. doi: 10.1126/science.aad0395

43. Kong F, Ye S, Zhong Z, Zhou X, Zhou W, Liu Z, et al. Single-cell transcriptome analysis of chronic antibody-mediated rejection after renal transplantation. *Front Immunol* (2021) 12:767618. doi: 10.3389/fimmu.2021.767618

44. Wertz IE, O'Rourke KM, Zhou H, Eby M, Aravind L, Seshagiri S, et al. De-ubiquitination and ubiquitin ligase domains of A20 downregulate NF-kappaB signalling. *Nature* (2004) 430:694–9. doi: 10.1038/nature02794

45. Garcia-Carbonell R, Wong J, Kim JY, Close LA, Boland BS, Wong TL, et al. Elevated A20 promotes TNF-induced and RIPK1-dependent intestinal epithelial cell death. *Proc Natl Acad Sci U.S.A.* (2018) 115:E9192–200. doi: 10.1073/pnas.1810584115

46. Catrysse L, Vereecke L, Beyaert R, van Loo G. A20 in inflammation and autoimmunity. *Trends Immunol* (2014) 35:22–31. doi: 10.1016/j.it.2013.10.005

47. Seong D, Jeong M, Seo J, Lee J-Y, Hwang CH, Shin H-C, et al. Identification of MYC as an antinecroptotic protein that stifles RIPK1-RIPK3 complex formation. *Proc Natl Acad Sci U.S.A.* (2020) 117:19982–93. doi: 10.1073/pnas.2000979117

48. Lee E-W, Seong D, Song J. Cytoplasmic MYC is an anti-necroptotic protein. *Mol Cell Oncol* (2020) 7:1817697. doi: 10.1080/23723556.2020.1817697

49. Raivich G, Behrens A. Role of the AP-1 transcription factor c-Jun in developing, adult and injured brain. *Prog Neurobiol* (2006) 78:347–63. doi: 10.1016/j.pneurobio.2006.03.006

50. Horvath C, Jarabicova I, Kura B, Kalocayova B, Faurobert E, Davidson SM, et al. Novel, non-conventional pathways of necroptosis in the heart and other organs: Molecular mechanisms, regulation and inter-organelle interplay. *Biochim Biophys Acta Mol Cell Res* (2023) 1870:119534. doi: 10.1016/j.bbamcr.2023.119534

51. Lai IL, Wang S-Y, Yao Y-L, Yang W-M. Transcriptional and subcellular regulation of the TRIP-Br family. *Gene* (2007) 388:102–9. doi: 10.1016/j.gene.2006.10.008

52. Jung S, Li C, Duan J, Lee S, Kim K, Park Y, et al. TRIP-Br1 oncoprotein inhibits autophagy, apoptosis, and necroptosis under nutrient/serum-deprived condition. *Oncotarget* (2015) 6:29060–75. doi: 10.18632/oncotarget.5072

53. Hong S-W, Shin J-S, Lee Y-M, Kim D-G, Lee S-Y, Yoon DH, et al. p34 (SEI-1) inhibits ROS-induced cell death through suppression of ASK1. *Cancer Biol Ther* (2011) 12:421–6. doi: 10.4161/cbt.12.5.15972

54. Jun W, Benjanuwattra J, Chattipakorn SC, Chattipakorn N. Necroptosis in renal ischemia/reperfusion injury: A major mode of cell death? *Arch Biochem Biophys* (2020) 689:108433. doi: 10.1016/j.abb.2020.108433

55. Zhang D-W, Shao J, Lin J, Zhang N, Lu B-J, Lin S-C, et al. RIP3, an energy metabolism regulator that switches TNF-induced cell death from apoptosis to necrosis. *Science* (2009) 325:332–6. doi: 10.1126/science.1172308

56. Yu Z, Jiang N, Su W, Zhuo Y. Necroptosis: A novel pathway in neuroinflammation. *Front Pharmacol* (2021) 12:701564. doi: 10.3389/fphar.2021.701564

57. Chadha R, Heidt S, Jones ND, Wood KJ. Th17: contributors to allograft rejection and a barrier to the induction of transplantation tolerance? *Transplantation* (2011) 91:939–45. doi: 10.1097/TP.0b013e3182126eeb

58. Burne-Taney MJ, Yokota-Ikeda N, Rabb H. Effects of combined T- and B-cell deficiency on murine ischemia reperfusion injury. *Am J Transplant* (2005) 5:1186–93. doi: 10.1111/j.1600-6143.2005.00815.x

59. Lu JV, Chen HC, Walsh CM. Necroptotic signaling in adaptive and innate immunity. *Semin Cell Dev Biol* (2014) 35:33–9. doi: 10.1016/j.semcdb.2014.07.003

60. Cusson N, Oikemus S, Kilpatrick ED, Cunningham L, Kelliher M. The death domain kinase RIP protects thymocytes from tumor necrosis factor receptor type 2-induced cell death. *J Exp Med* (2002) 196:15–26. doi: 10.1084/jem.20011470

61. Zhang J, Zhang H, Li J, Rosenberg S, Zhang EC, Zhou X, et al. RIP1-mediated regulation of lymphocyte survival and death responses. *Immunol Res* (2011) 51:227–36. doi: 10.1007/s12026-011-8249-3

62. Ch'en IL, Beisner DR, Degterev A, Lynch C, Yuan J, Hoffmann A, et al. Antigen-mediated T cell expansion regulated by parallel pathways of death. *Proc Natl Acad Sci U.S.A.* (2008) 105:17463–8. doi: 10.1073/pnas.0808043105

63. Degterev A, Maki JL, Yuan J. Activity and specificity of necrostatin-1, small-molecule inhibitor of RIP1 kinase. *Cell Death Differ* (2013) 20:366. doi: 10.1038/cdd.2012.133

64. Robinson N, Ganesan R, Hegedűs C, Kovács K, Kufer TA, Virág L. Programmed necrotic cell death of macrophages: Focus on pyroptosis, necroptosis, and parthanatos. *Redox Biol* (2019) 26:101239. doi: 10.1016/j.redox.2019.101239

65. Hsu S-K, Chang W-T, Lin IL, Chen Y-F, Padalwar NB, Cheng K-C, et al. The role of necroptosis in ROS-mediated cancer therapies and its promising applications. *Cancers (Basel)* (2020) 12(8):2185. doi: 10.3390/cancers12082185

66. Li Z, Ludwig N, Thomas K, Mersmann S, Lehmann M, Vestweber D, et al. The pathogenesis of ischemia-reperfusion induced acute kidney injury depends on renal neutrophil recruitment whereas sepsis-induced AKI does not. *Front Immunol* (2022) 13:843782. doi: 10.3389/fimmu.2022.843782

67. Zhu C-L, Wang Y, Liu Q, Li H-R, Yu C-M, Li P, et al. Dysregulation of neutrophil death in sepsis. *Front Immunol* (2022) 13:963955. doi: 10.3389/fimmu.2022.963955

68. Wang X, Yousefi S, Simon H-U. Necroptosis and neutrophil-associated disorders. *Cell Death Dis* (2018) 9:111. doi: 10.1038/s41419-017-0058-8

69. Wicki S, Gurzeler U, Wei-Lynn Wong W, Jost PJ, Bachmann D, Kaufmann T. Loss of XIAP facilitates switch to TNFα-induced necroptosis in mouse neutrophils. *Cell Death Dis* (2016) 7:e2422. doi: 10.1038/cddis.2016.311

70. Yabal M, Müller N, Adler H, Knies N, Groß CJ, Damgaard RB, et al. XIAP restricts TNF- and RIP3-dependent cell death and inflammasome activation. *Cell Rep* (2014) 7:1796–808. doi: 10.1016/j.celrep.2014.05.008

71. Lawlor KE, Khan N, Mildenhall A, Gerlic M, Croker BA, D'Cruz AA, et al. RIPK3 promotes cell death and NLRP3 inflammasome activation in the absence of MLKL. *Nat Commun* (2015) 6:6282. doi: 10.1038/ncomms7282

72. Miao Y, Liu J, Liu X, Yuan Q, Li H, Zhang Y, et al. Machine learning identification of cuproptosis and necroptosis-associated molecular subtypes to aid in prognosis assessment and immunotherapy response prediction in low-grade glioma. *Front Genet* (2022) 13:951239. doi: 10.3389/fgene.2022.951239

73. Zhou Z, Wu J, Ma W, Dong F, Wang J. Pan-Cancer analyses of Necroptosis-Related genes as a potential target to predict immunotherapeutic outcome. *J Cell Mol Med* (2023) 27:204–21. doi: 10.1111/jcmm.17634

74. Mihaly SR, Ninomiya-Tsuji J, Morioka S. TAK1 control of cell death. *Cell Death Differ* (2014) 21:1667–76. doi: 10.1038/cdd.2014.123

75. O'Donnell MA, Perez-Jimenez E, Oberst A, Ng A, Massoumi R, Xavier R, et al. Caspase 8 inhibits programmed necrosis by processing CYLD. *Nat Cell Biol* (2011) 13:1437–42. doi: 10.1038/ncb2362

76. Grivennikov S, Karin E, Terzic J, Mucida D, Yu G-Y, Vallabhapurapu S, et al. IL-6 and Stat3 are required for survival of intestinal epithelial cells and development of colitis-associated cancer. *Cancer Cell* (2009) 15:103–13. doi: 10.1016/j.ccr.2009.01.001

frontiers | Frontiers in Immunology

TYPE Review
PUBLISHED 08 November 2023
DOI 10.3389/fimmu.2023.1273570

OPEN ACCESS

EDITED BY
Chung Nga Ko,
C-MER International Eye Research Center, China

REVIEWED BY
Adriana Sumoza-Toledo,
Universidad Veracruzana, Mexico
Andras Perl,
Upstate Medical University, United States
Kuo-Hui Su,
The University of Toledo, United States

*CORRESPONDENCE
Kenneth Maiese
wntin75@yahoo.com

RECEIVED 06 August 2023
ACCEPTED 23 October 2023
PUBLISHED 08 November 2023

CITATION
Maiese K (2023) The impact of aging and oxidative stress in metabolic and nervous system disorders: programmed cell death and molecular signal transduction crosstalk.
Front. Immunol. 14:1273570.
doi: 10.3389/fimmu.2023.1273570

The impact of aging and oxidative stress in metabolic and nervous system disorders: programmed cell death and molecular signal transduction crosstalk

Kenneth Maiese*

Innovation and Commercialization, National Institutes of Health, Bethesda, MD, United States

Life expectancy is increasing throughout the world and coincides with a rise in non-communicable diseases (NCDs), especially for metabolic disease that includes diabetes mellitus (DM) and neurodegenerative disorders. The debilitating effects of metabolic disorders influence the entire body and significantly affect the nervous system impacting greater than one billion people with disability in the peripheral nervous system as well as with cognitive loss, now the seventh leading cause of death worldwide. Metabolic disorders, such as DM, and neurologic disease remain a significant challenge for the treatment and care of individuals since present therapies may limit symptoms but do not halt overall disease progression. These clinical challenges to address the interplay between metabolic and neurodegenerative disorders warrant innovative strategies that can focus upon the underlying mechanisms of aging-related disorders, oxidative stress, cell senescence, and cell death. Programmed cell death pathways that involve autophagy, apoptosis, ferroptosis, and pyroptosis can play a critical role in metabolic and neurodegenerative disorders and oversee processes that include insulin resistance, β-cell function, mitochondrial integrity, reactive oxygen species release, and inflammatory cell activation. The silent mating type information regulation 2 homolog 1 (*Saccharomyces cerevisiae*) (SIRT1), AMP activated protein kinase (AMPK), and Wnt1 inducible signaling pathway protein 1 (WISP1) are novel targets that can oversee programmed cell death pathways tied to β-nicotinamide adenine dinucleotide (NAD^+), nicotinamide, apolipoprotein E (APOE), severe acute respiratory syndrome (SARS-CoV-2) exposure with coronavirus disease 2019 (COVID-19), and trophic factors, such as erythropoietin (EPO). The pathways of programmed cell death, SIRT1, AMPK, and WISP1 offer exciting prospects for maintaining metabolic homeostasis and nervous system function that can be compromised during aging-related disorders and lead to cognitive impairment, but these pathways have dual roles in determining the ultimate fate of cells and organ systems that warrant thoughtful insight into complex autofeedback mechanisms.

KEYWORDS

AMPK, APOE-ε4, autophagy, diabetes mellitus, ferroptosis, pyroptosis, SIRT1, WISP1

1 Introduction

Disorders such as diabetes mellitus (DM) and cellular metabolic disease are increasing in prevalence throughout the world. Over a thirty-five year course from the year 1980, the number of individuals with DM increased from one hundred eight million to over four hundred twenty-two million individuals (1, 2). By the year 2045, seven hundred million individuals may have DM (3, 4). From the years 2013 to 2016, the prevalence of DM has risen from over nine percent (5). DM is a chronic disorder that affects all organs of the body leading to cardiac disease, retinal disease, hepatic injury, cerebral ischemia, limb amputation, and renal failure (5–18). Almost one half billion individuals have DM and at least half of the four million deaths that occur per year with DM impact individuals less than seventy years of age (1, 7, 19–22). Ten percent of the population in the United States (US) are currently reported to suffer from DM (23, 24). However, it is believed that many additional individuals have disorders of metabolism or have elevated risk to develop DM, but remain undiagnosed at present (3, 16, 21, 25–37). It is estimated that in individuals greater than eighteen years old, seven million may not be correctly diagnosed as having DM and more than thirty-five percent of US adults may have prediabetes due to elevations in their fasting glucose and hemoglobin A1c (HbA_{1c}) parameters (7, 38). Globally, four hundred million individuals are estimated to have metabolic disease or be at risk for developing DM (3, 39–41).

Metabolic disease affects low and middle income countries more than high income developed countries with approximately eighty percent of people residing in low-income nations (3, 42). This may be a result of the prevalence of DM being affected by a number of parameters that include socioeconomic status, comorbidities such as infection with the severe acute respiratory syndrome coronavirus (SARS-CoV-2), and level of education (43–54). In regard to education level, those individuals with less than a high school education represent thirteen percent of DM patients, individuals with a high school education equal ten percent of DM patients, and those individuals with more than a high school education represent approximately seven percent of DM patients (2). Other factors that can contribute to the development and progression of DM include limited exercise, tobacco consumption, high serum cholesterol, hypertension, and obesity (8, 13, 48, 55–57). Obesity alters a number of pathways in the body and can impact oxidative stress cell injury, stem cell survival, inflammation, aging processes, and the maintenance of mitochondrial function (21, 33, 40, 51, 56, 58–73). As a result, the additional body weight fosters insulin insensitivity and glucose intolerance that progresses to DM (19, 24, 28, 36, 74–80) (Table 1).

Additional challenges for the care of individuals with DM involve financial expenditures. At least twenty thousand United States Dollars (USD) on an annual basis is necessary for the basic care of people with DM that can involve the maintenance of glucose homeostasis, wound care, and nutritional education (6, 9, 19, 20, 28, 41, 74, 81–87). Yet, the required resources for DM care is growing and is greater than seven hundred sixty billion USD with an additional seventy billion USD necessary for those with severe disability and loss of function (3). Greater than seventeen percent of the Gross Domestic Product in the US is consumed for the care of people with DM (88).

The debilitating nature of DM affects the entire body and leads to the degeneration of all organ systems (6, 7, 12, 16, 19, 21, 24, 27, 31, 34, 36, 46, 60, 85, 89–94). In particular, the metabolic disorders affect the nervous system and can lead to cognitive impairment, peripheral neuropathies, demyelinating disorders, and risk for developing infection as well as memory loss (Figure 1). An additional risk that includes metabolic disease for the development of neurodegenerative disorders is the observed rise in lifespan (95–100). Life expectancy is increasing especially in developed nations (101) and over the past fifty years the number of people greater than the age of sixty-five has increased greater than one hundred percent (4, 68, 96, 97, 102–113). Neurodegenerative disorders comprise a portion of non-communicable diseases (NCDs) and over seventy to seventy-five percent of the deaths that occur each year are due to NCDs (8, 22, 56, 60, 114–116). The increase in lifespan coincides with the rise of NCDs (91, 111, 117–129). As a result, the increase in lifespan for the world's population has resulted in an increased prevalence for diseases of the nervous system (117, 130–133). Nervous system disorders comprise greater than six hundred disease entities, lead to the death of over seven million people annually, and can impact greater than one billion people (111, 117, 134–146). In relation to financial exposure, more than eight hundred billion USD in the US is required annually to

TABLE 1 Highlights The Impact of Aging and Oxidative Stress in Metabolic and Nervous System Disorders: Programmed Cell Death and Molecular Signal Transduction Crosstalk.

•With the increase in global lifespan and non-communicable diseases, metabolic disease affects low and middle income countries more than high income developed countries and by the year 2045, it is estimated that over seven hundred million individuals will have diabetes mellitus (DM).
•Metabolic disorders are intimately tied to the development and progression of neurodegenerative disorders that comprise over six hundred disease entities, impact greater than one billion people, and can lead to dementia as the 7th leading cause of death.
•Aging processes, oxidative stress, dysfunction in telomere processing, and cell senescence are underlying mechanisms for the progression of metabolic disorders and neurodegenerative disease.
•Programmed cell death pathways of autophagy, apoptosis, ferroptosis, and pyroptosis can oversee a number of critical cellular functions that include reactive oxygen species (ROS) generation, the proliferation and size of pancreatic β-cells, insulin resistance, mitochondrial integrity, β-amyloid (Aβ) and tau brain deposition, and inflammatory cell activation.
•The silent mating type information regulation 2 homolog 1 *(Saccharomyces cerevisiae)* (SIRT1), AMP activated protein kinase (AMPK), and Wnt1 inducible signaling pathway protein 1 (WISP1) are novel targets that can oversee programmed cell death pathways tied to β-nicotinamide adenine dinucleotide (NAD^+), nicotinamide, apolipoprotein E (APOE), severe acute respiratory syndrome (SARS-CoV-2) exposure with coronavirus disease 2019 (COVID-19), and trophic factors, such as erythropoietin (EPO) that can oversee these pathways such as with SIRT1 and AMPK.
•The pathways of programmed cell death, SIRT1, AMPK, and WISP1 offer exciting insights for maintaining metabolic homeostasis and neurovascular cell integrity that can be compromised during aging-related processes that can lead to cognitive loss, but these pathways have dual roles in determining the ultimate fate of cells and organ function that can have complex autofeedback mechanisms.

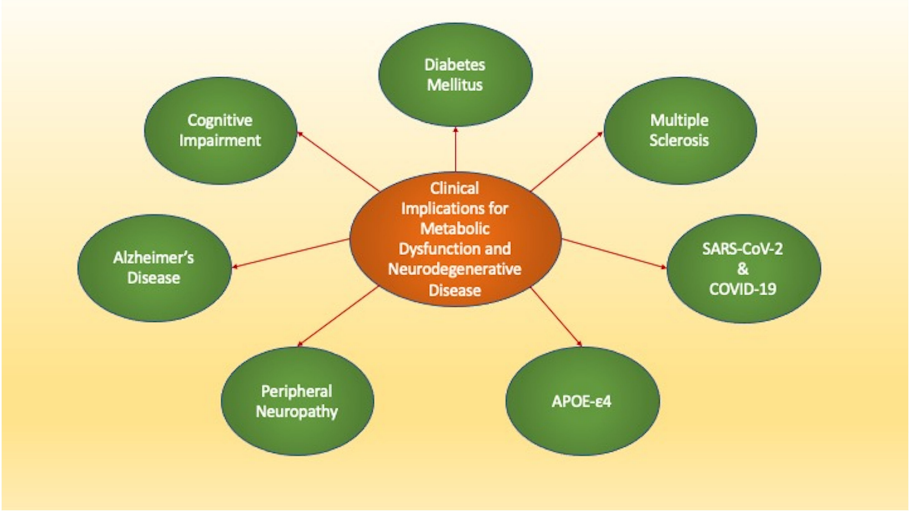

FIGURE 1
The Clinical Implications of Metabolic Dysfunction and Neurodegenerative Disease. Loss of metabolic homeostasis can lead to multiple disorders. Metabolic disorders affect both the peripheral and central nervous systems and can be affected by several risk factors. These disorders include diabetes mellitus that affects all systems of the body, cognitive impairment, Alzheimer's disease, Multiple Sclerosis, and peripheral neuropathies. Additional entities such as the apolipoprotein E (APOE-ε4) gene, severe acute respiratory syndrome coronavirus (SARS-CoV-2), and coronavirus disease 2019 (COVID-19) can lead to memory loss, cognitive failure, and cortical vascular disease.

care for multiple neurological disorders that include stroke, trauma, epilepsy, back pain, Parkinson's disease (PD), Huntington's disease (HD), amyotrophic lateral sclerosis (ALS), and dementia (116). Cognitive loss can be the most significant burden to the financial system and these cost considerations do not include the expenses required for companion care, social health programs, and senior daily care with the additional greater than seventy million clinicians and social workers needed to fill these unmet needs (22, 116, 147). These additional services will reach 2 trillion USD annually in the US and more than four million people will need over four billion USD for treatment each year. The market for dementia could exceed eleven billion USD (34, 141, 148). Furthermore, additional significant costs involve other neurological disorders, such as PD with greater than fifty-five billion USD necessary for care in the US annually. In the year 2030, the number of those affected with PD is predicted to double. Present expenses are currently at a large annual cost per individual of approximately twenty-five thousand USD per year (5, 97, 137, 144, 146, 149–165).

2 The intimate relationship among metabolic disease, oxidative stress, aging, and neurodegenerative disorders

Metabolic disorders, such as DM, increase the risk for the onset and progression of neurodegenerative disorders through multiple pathways. DM is a primary mechanism for the onset of cardiovascular disease that can ultimately lead to disorders of the nervous system (8, 53, 166–170). When compared to people that do not have DM, individuals with DM can have two times the risk of developing cardiac disability or cerebral ischemia (40, 43, 91, 108, 111). DM results in insulin resistance (9, 19, 24, 60, 80, 90, 171–174), vascular injury (16, 19, 26, 27, 29, 30, 32, 33, 61, 74, 86, 87, 170, 175–182), alterations in cerebral blood flow (2, 7, 9, 53, 91, 176, 183), endothelial dysfunction (19, 27, 40, 83, 94, 184), mitochondrial injury (13, 28, 53, 60, 115, 172, 178, 185, 186), retinal disease (30, 66, 94, 187–189), stem cell loss (35, 38, 54, 66, 72, 77, 84, 111, 190), susceptibility to infections (34, 46, 48–51, 54, 92, 191, 192), and immune system dysfunction (30, 54, 64, 68, 84, 173, 178, 193–199).

DM and cellular metabolism also play a significant role in the processes of oxidative stress and aging (7, 16, 47, 64, 75, 89–91, 108, 178, 196, 200). DM can lead to changes in transcriptional networks, loss of mitochondrial homeostasis, inflammation, production of reactive oxygen species (ROS), and cell senescence (7, 16, 20, 21, 30, 32, 66, 78, 79, 90, 91, 108, 174, 178, 193, 194, 201–203). ROS that are generated during oxidative stress include hydrogen peroxide, superoxide free radicals, nitric oxide, singlet oxygen, and peroxynitrite (36, 37, 65, 90, 96, 113, 120, 137, 154, 180, 186, 204–218). During conditions that oversee the detrimental effects of ROS, antioxidant systems are in play that involve glutathione peroxidase, catalase, superoxide dismutase, and the nutrient vitamins B, K, E, D, and C (20, 34, 42, 47, 53, 100, 132, 186, 202, 217, 219–225). If these systems are overwhelmed or unable to limit excessive ROS production, mitochondrial injury, loss of DNA integrity, and shortened lifespan can occur (8, 34, 69, 78, 96, 104, 120, 122, 162, 207, 209, 218, 226–229). Oxidative stress can result in vascular endothelial cell injury (9, 40, 83, 230–234), neuronal cell compromise (24, 66, 122, 123, 152, 156, 162, 233, 235–245), alterations in neurotransmitters (69, 246, 247), myelin degradation (79, 224, 248–252), cell senescence (8, 33, 55, 112, 253–255), loss of stem cell proliferation (34, 66, 168, 228, 241, 251,

256–259), and cognitive impairment (7, 10, 120, 121, 200, 223, 243, 245, 260–266).

In regard to aging and cellular metabolism, the shortening of telomeres (TLs), complexes of deoxyribonucleic acid (DNA), can lead to the increased risk for the development of DM (8, 267) and greater cell senescence with the loss metabolic homeostasis (16, 33, 178, 190, 268). Changes in TL length can promote aging processes, cellular senescence, and neurodegeneration as well (70, 112, 113, 118, 154, 255, 269–275). TLs are positioned on chromosome ends and oversee replication of cells, preservation of the genomic DNA, and cell survival (8, 16, 274, 276–279). More than two thousand repetitions of double-stranded non-coding DNA with the "TTAGGG" sequence that is finalized with guanine rich single-stranded DNA compose TLs (8, 70, 139, 265, 279). Complexes of proteins that include CTC1-STN1-TEN1 (CST), shelterin, and telosome are part of the TL family (7, 139, 252). To oversee the division of cells, these proteins control function and stability of TLs that can lose twenty-five to over two hundred base pairs during the process of dividing cells. Telomerase protein can prevent the loss of base pairs in TLs by providing tandem repeat ribonucleic acid (RNA) templates (274, 276, 280). However, cell senescence ultimately ensues when TLs become very short with less than five hundred base pairs and telomerase function is impaired (33, 95, 102, 118, 134, 154, 221, 253, 255, 269, 272, 275, 281). At this point, tissues and organs cannot undergo repair, the immune system is less viable, and age-related disorders can progress (7, 73, 139, 164, 282–286). These events with the shortening of TLs and cellular senescence also promote oxidative stress and the release of ROS that impairs cell organelles, such as mitochondria and cellular energy homeostasis (7, 32, 104, 121, 122, 196, 282, 287, 288).

3 The clinical onset of metabolic mediated neurodegenerative disease

Given the ability of DM to lead to aging processes tied to oxidative stress, neuronal and vascular injury, mitochondrial dysfunction, stem cell loss, and immune system disorders, it becomes evident that loss of metabolic homeostasis with DM can result in multiple neurodegenerative disorders. Metabolic disorders can affect both the peripheral and central nervous systems (Figure 1). In the peripheral nervous system in the presence of DM, autonomic dysfunction (289–291) and neuropathies can be common and affect more than seventy-five percent of individuals (5, 38, 78, 79, 83, 290, 292).

In the central nervous system, cognitive loss with DM is a significant co-morbidity. DM results in memory impairment (7, 10, 55, 115, 200, 263, 293–296) and can lead to the onset and progression of Alzheimer's disease (AD) (2, 6, 28, 44, 89, 153, 201, 266, 297–302) (Figure 1). Dementia is present in all nations throughout the world and is now considered to be the seventh primary reason for death (109, 116, 131, 141, 144, 161, 164, 223, 252, 266, 303–308). At least five percent of the world's population has dementia and by the year 2050 it is believed that over one hundred fifty-five million people will have cognitive loss (2, 73, 97, 115, 126, 205, 226, 275, 309, 310). Of those individuals with dementia, approximately sixty percent of people have the sporadic form of AD and greater than ten percent are over the age of sixty-five (5, 110, 139, 148, 277, 311–313). Diagnosis for dementia can fall significantly behind the onset of the disorder and may not be recognized until twelve to twenty-four months after the initial clinical presentation (38, 252, 314). Currently, more than six million people in the US have the sporadic form of AD (5, 309, 315–318), but this is expected to increase to thirty million people during the next two decades (6, 7, 110, 205, 226, 245, 282, 319, 320). In contrast, familial AD (FAD) is present in about two hundred families in the world (6, 73, 110, 121, 134, 282, 311). FAD represents an autosomal dominant version of amyloid precursor protein (APP) gene that is mutated, occurs in variable single-gene mutations on chromosomes 1, 14, and 21, and is usually clinical present prior to fifty-five years of age (115, 321, 322).

Risk factors also exist for dementia that can have a metabolic basis as well. In experimental models, insulin signaling can be associated with AD pathology (71). Late-onset AD can result in the presence of the ϵ4 allele of the apolipoprotein E (APOE-ε4) gene (5, 7, 148, 161, 252, 323–325) (Figure 1). The risk for developing AD is more than twenty times greater in those individuals with two APOE-ϵ4 alleles. APOE is produced in liver cells and is vital for metabolic cellular function to oversee the homeostasis of lipids through the transport of triglycerides, phospholipids, and cholesterol (7, 127, 161, 325–328). In the brain, astrocytes produce APOE to modulate the transfer of cholesterol to neurons through APOE receptors (7, 127, 252, 326, 328, 329). Interestingly, β-amyloid (Aβ) can be removed and destroyed by APOE through apoptosis and the exposure of phosphatidylserine (PS) membranes that are a part of the apoptotic cell death process (330, 331). Other forms of APOE that do not involve APOE-ε4 may inhibit Aβ aggregation during PS membrane exposure (332). However, Aβ aggregation is not believed to be blocked by APOE-ϵ4 which can therefore allow amyloid deposition to proceed and potentially foster the development of AD (44, 161, 323, 332–334). APOE-ϵ4 also may assist with the infection of viral antigens and lead to cerebral microhemorrhages during severe acute respiratory syndrome (SARS-CoV-2) exposure with coronavirus disease 2019 (COVID-19) (326) (Figure 1). SARS-CoV-2, a β-coronavirus family virion, has resulted in a global pandemic (34, 46, 49, 50, 335, 336) and can attach to nasal epithelial cells (337) and neurovascular cells in the brain (54). These processes subsequently result in hyperactivation of the immune system (335, 336, 338–340). Following SARS-CoV-2 infection, memory loss and cognitive failure can develop and lead to long-COVID, also termed long-haul COVID, chronic COVID-19, or post-acute COVID (34, 49, 50, 325, 336, 341–345). The combination of APOE-ϵ4 and SARS-CoV-2 infection can lead to cognitive loss and cortical vascular disease (57, 97, 181, 226, 326, 346–350).

Multiple sclerosis (MS), an additional significant neurodegenerative disorder, also may develop as a result of metabolic disease, pathways of APOE-ϵ4, and Aβ deposition (125, 252, 350–359) (Figure 1). MS impacts large portions of the global population, affects greater than two and one-half million people, and is a primary disease of myelin and myelin producing cells that is immune system mediated (159, 351, 358, 360–364). MS appears to

lead to disease in more women than men (357) and can markedly impair cognitive function (252, 365, 366). The memory loss can be progressive in nature and affect both women and men (367). At least sixty-five percent of patients with MS have difficulty with memory recall and executive ability (252). Cognitive loss in MS patients may be tied to metabolic pathways and APOE-ϵ4 since individuals with MS can demonstrate lower cognitive function and delayed responses to stimuli (368). APOE serum levels are elevated in individuals with demyelinating optic neuritis and the genotype of *APOE* ϵ3/ϵ3 may lead to the male onset of optic neuritis (327). In the setting of APOE risk factors and metabolic dysfunction similar to AD that can increase susceptibility to viral infections, MS patients may experience higher rates of death during SARS-CoV-2 with COVID-19 (369). Treatment with metformin, commonly used during DM, can reduce the degree of functional impairment in obese individuals or those with DM during COVID-19 (52, 370). MS also may have common pathways with AD and Aβ (140, 252, 371). Tau seeding, also present in AD (7, 123, 311, 372–376), has been reported in the brains of MS patients (140) and this tau deposition may produce demyelination through injury to oligodendrocytes (128). Alterations in Aβ deposition similar to those observed in AD may also indicate early memory impairment in people with MS (371).

4 Addressing unmet clinical avenues for metabolic and neurodegenerative disorders

Multiple factors can impact the role of metabolic disorders that can lead to the onset and progression of neurodegenerative disease. If one focuses upon metabolic disease and DM, therapies that improve nutritional intake that can be complemented by pharmaceutical agents to assist with serum glucose homeostasis and insulin resistance may limit periods of hyperglycemia and the complications of hypoglycemia (6, 8, 16, 19–21, 25, 27–29, 49, 167, 175, 176, 370, 377–379). Yet, progression of DM even at a less marked pace will ensue and can be affected by off-target treatment effects that result in cellular injury, neuronal and vascular cell loss, and the atrophy of organs (33, 87, 172, 380). In the nervous system, a number of diverse pathways that involve inflammation, infection, circadian rhythm, excitotoxicity, metabotropic receptors, tau, Aβ, mitochondrial injury, acetylcholine loss, heavy metal toxicity, and oxidative stress can lead to cognitive loss (24, 33, 34, 42, 50, 63, 65, 66, 96, 106, 119, 121, 131, 165, 168, 175, 205, 223, 226, 261, 282, 286, 303, 330, 338, 346, 381–398). Current therapies for AD that employ cholinesterase inhibitors may limit memory loss but these treatments do not stop the progression of disease (115, 164, 299, 399, 400). Recent developments for AD to use immunotherapy to decrease Aβ load in the brain also may reduce memory loss, but these therapies are currently limited to a small group of patients that are not at risk for cerebral microhemorrhages and also such treatments do not prevent overall disease progression (119, 126, 401). In regard to MS, disease modifying therapies (DMTs) can reduce the frequency of relapses in relapsing–remitting MS, but disease progression can continue (252, 362, 371). For example, despite the reduction in brain volume loss with DMTs, cognitive impairment can continue unabated (402). These treatment considerations that rest on the side of metabolic disorders as well as neurodegenerative disease warrant new avenues of inquiry for the development of innovative therapeutic strategies that may address the onset and progression of these disorders. Novel pathways that may offer new insights into these disorders involve programmed cell death regulation, the silent mating type information regulation 2 homolog 1 (*Saccharomyces cerevisiae*) (SIRT1), AMP activated protein kinase (AMPK), and Wnt1 inducible signaling pathway protein 1 (WISP1) (Figure 2).

5 Programmed cell death in metabolic and nervous system diseases

Programmed cell death that involves autophagy, apoptosis, ferroptosis, and pyroptosis has a vital role in the determination of both metabolic and neurodegenerative disorders (Figure 2). Recent studies on exome sequence analysis indicate that metabolic cellular dysfunction directly affects neuronal cell death through DNA and apoptosis (403). In metabolic disorders, programmed cell death can affect neuronal survival (24, 122, 310, 404–411), vascular integrity (8, 40, 61, 87, 182, 188, 412–414), mitochondrial function (42, 61, 172, 186), and inflammation (36, 50, 87, 186, 415–418). In a similar manner, programmed cell death in the nervous system can lead to neuronal and non-neuronal cell injury (65, 121, 132–134, 143, 148, 155, 224, 240, 262, 376, 405, 419–428), cerebral ischemia (91, 122, 182, 405, 423, 427, 429–433), microglial cell loss (120, 125, 133, 152, 356, 421, 430, 434, 435), and dysfunction of pathways for cognitive function (100, 120, 121, 141, 143, 148, 260–262, 275, 301, 421, 436–440).

During autophagy, organelles in the cytoplasm as well as other subunits in the cell are recycled for future remodeling of tissues (5, 121, 376, 408, 409, 428, 441, 442). Of the different forms of autophagy, macroautophagy is the prominent type of autophagy that is usually described and consists of sequestering proteins and organelles in the cytoplasm of cells into autophagosomes that will be merged into lysosomes that can be degraded and recycled (117, 136, 141, 275, 443). During microautophagy, components of the cytoplasm are sequestered for eventual digestion through invagination of lysosomal membranes (97). In chaperone-mediated autophagy, protein "chaperones" are created in the cytoplasm to carry components of the cytoplasm over the membranes of lysosomes (134, 136, 444, 445).

Autophagy can foster beneficial outcomes during metabolic and neurodegenerative disorders. Activation of autophagy can be necessary for fatty acid metabolism during obesity (62) and for the oversight of muscle tissue generation (441). Autophagy can oversee the proliferation and size of pancreatic β-cells (446), may limit insulin resistance during inflammation with high serum lipids in obesity models of autophagy *Atg7* gene deletion (447), may prevent diabetic nephropathy with maintenance of Atg7, Atg5, and LC3 autophagy proteins (448), and can prevent DM progression

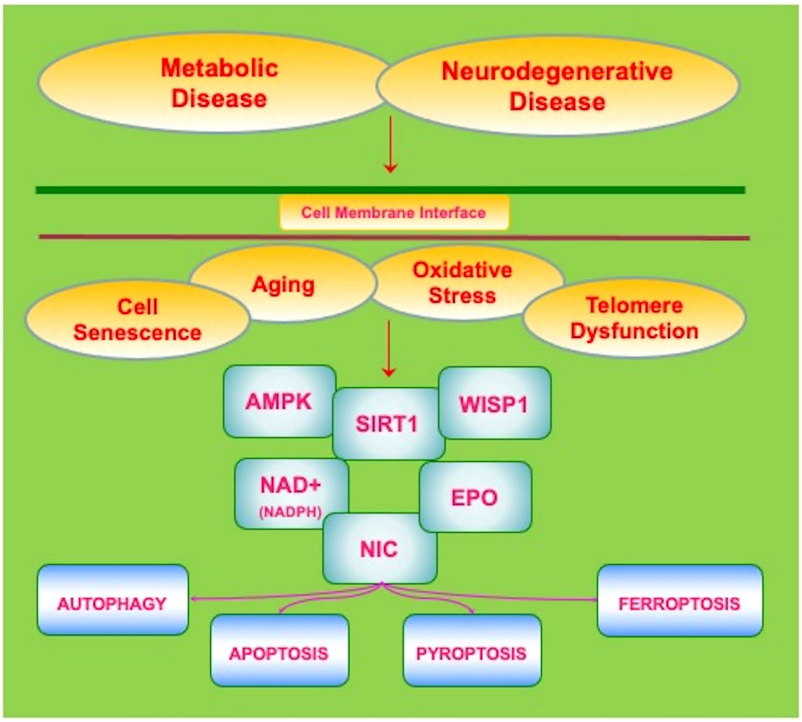

FIGURE 2
Innovative Avenues to Address Metabolic and Neurodegenerative Disease. Current therapies for metabolic and neurodegenerative disorders are unable to prevent the onset and progression of these disorders. The clinical course of these disorders is closely tied to intracellular process that are linked to aging-related disorders, telomere dysfunction, cellular senescence, and oxidative stress. Novel and innovative therapeutic strategies are needed to address metabolic and neurodegenerative diseases. Pathways that may offer new insights into these disorders involve the silent mating type information regulation 2 homolog 1 *(Saccharomyces cerevisiae)* (SIRT1), AMP activated protein kinase (AMPK), and Wnt1 inducible signaling pathway protein 1 (WISP1). These pathways are closely interconnected, can form complexes, and involve ß-nicotinamide adenine dinucleotide (NAD^+), nicotinamide (NIC), and trophic factors such as erythropoietin (EPO). Ultimately these pathways serve to provide oversight of programmed cell death mechanisms that involve autophagy, apoptosis, pyroptosis, and ferroptosis as well as mechanisms that can lead to mitochondrial stress such as with nicotinamide adenine dinucleotide phosphate (NADPH) depletion.

through promoting β-cell function and eliminating misfolded proteins and dysfunctional mitochondria (449). Increased physical activity in murine models helps control glucose serum regulation through autophagy pathways (450) that are tied to greater insulin efficacy (451) and improved function of microglial cells (416). In the brain, loss of autophagy activation can lead to memory impairment in AD with the progression of DM (44). The pathways that lead to the activation of autophagy may require inhibition of the mechanistic target of rapamycin (mTOR) with agents such as rapamycin or metformin (7, 49, 121, 284, 335, 359, 376, 393, 442, 452–457). In addition, activation of mTOR can inhibit autophagy induction through the phosphorylation of the autophagic related gene (*Atg*) protein Atg13 and UNC-51 like kinases (ULKs) such as UNC-51 like kinase 1 (ULK1) to prevent formation of the ULK-Atg13-FIP200 complex (97, 458). During mTOR inhibition and autophagy activation, reduction in ROS release occurs (459), dopamine cell survival is increased (460), neuronal demise is blocked through pathways of glutamine (461), and mitochondrial integrity is preserved (462). Autophagy activation can limit tau deposition (463) and reduce Aß accumulation with improved memory function and metabolic homeostasis (464). Control of blood mononuclear cells in MS during inflammation can be mediated by autophagy activation (465), induction of autophagy can improve the clinical outcome of relapsing-remitting and experimental autoimmune encephalomyelitis (466) and reduce retinal MS-induced degeneration (189), cytokine release and microglial activation is limited during autophagy activation in experimental autoimmune encephalomyelitis (358), and the risk for developing MS may be lessened during mTOR blockade and autophagy induction (359). Autophagy activity with metformin treatment also may lead to myelin repair with oligodendrocytes (356) and assist with the reduction of viral susceptibility during DM in over-weight individuals exposed to COVID-19 (52, 370).

However, there exists another side to autophagy that suggests careful modulation of activity is required for clinical disease. Cardiomyopathy (467), atherosclerosis (468), and endoplasmic reticulum stress (469) can ensue with advanced glycation end products (AGEs), elevated glucose exposure, and autophagy activation. Induction of autophagy can lead to the reduction in cardiac and liver tissue mass during treatments to improve glucose regulation (380), promote neuronal cell death under some conditions (470–472), prevent cerebral interneuron progenitor cell growth (473), result in mitochondrial injury (61, 145, 172,

216, 306, 379, 474–479), reduce numbers of progenitor endothelial cells (480), limit angiogenesis in the presence of elevated glucose (480), and lead to cognitive loss (141, 148, 275, 361, 393, 437). In addition, growth factor cell protection, such as with the trophic factor erythropoietin (EPO) (114, 304, 385, 481–484), requires decreases in autophagy activation in conjunction with modulation of mTOR, protein kinase B (Akt), the proline rich Akt substrate 40 kDa (PRAS40), and mammalian forkhead transcription factors to promote neuronal and vascular survival (145, 485–489).

Apoptotic cell injury can be initiated through pathways of oxidative stress (40, 68, 96, 120, 201, 216, 244, 245, 256, 260, 261, 303, 490–495) and inflammation (7, 36, 120, 143, 169, 212, 225, 256, 260, 275, 303, 310, 425, 430, 496–501) as part of metabolic and neurodegenerative disorders. Apoptotic cell death has early and late components that can occur in this process (97, 122, 408, 409, 426). The loss of PS membrane asymmetry is the early phase of apoptotic cell death (502–506). Once cells become injured, the PS residues become externalized on the cell membrane that attracts inflammatory microglia to recognize these injured cells and remove them from the central and peripheral nervous systems (502, 507–510). However, injured cells may recover if they are not engulfed by microglia. Treatments directed to restore PS membrane asymmetry for injured cells can then prevent microglial attraction and preserve the function of these necessary cells in the nervous system (66, 511–513). In contrast, the later phase of apoptotic cell death that consists of the destruction of nuclear deoxyribonucleic acid (DNA) (18, 96, 113, 229, 483, 514–518) and a cascade of caspase activation (65, 96, 130, 143, 347, 348, 405, 425, 483, 519) is not reversible.

Reductions in apoptosis activation can prevent cell injury during glial cell excessive activity and oxidative stress (120), limit dopaminergic cell demise during inflammatory cell activation (152), protect retinal cells during ischemia exposure (516), and increase neuronal cell survival during Aß toxicity (320, 520–522). Controlling apoptotic cell death also reduces inflammatory cell pathways (50, 186, 212, 225, 256, 260, 261, 418, 496, 497, 499, 500, 523–525) and can limit memory loss (7, 100, 143, 262, 421, 439). These pathways are significantly tied to microglial activity. Microglia account for about fifteen percent of the cells in the central nervous system and as noted can remove injured cells during apoptosis (97, 120, 133, 134, 152, 155, 425, 430, 502, 503). These inflammatory cells can release ROS to generate oxidative stress (7, 18, 62, 121, 282, 526–528) through pathways that involve Wnt signaling (2, 6, 97, 122, 181, 529–531), mammalian forkhead transcription factors (17, 67, 68, 117, 426, 519, 532), and growth factors with EPO (6, 145, 159, 482, 533–536). During cognitive dysfunction, microglial activity may lead to increased risk for the development of AD (141, 537) as well as endothelial dysfunction (119).

Ferroptosis is a process in the programmed cell death pathway that leads to the storage of iron in the cell that results in the inability to maintain glutathione homeostasis (225, 538, 539). Once oxidative defenses that require glutathione are lost, lipid peroxidation can ensue to result in the demise of cells (224, 229, 540). Ferroptosis can lead to cell death in multiple systems such as the musculoskeletal system (225), cardiovascular system (8, 540), and breast tissue (229). In the nervous system, ferroptosis may lead to cognitive impairment (7, 224, 274) and produce pathogenic T lymphocytes that lead to dysfunction in neuronal and glial cells (252, 538).

Given the associations of autophagy, apoptosis, and ferroptosis with inflammatory cell pathways, it is of interest to note that pyroptosis is part of the programmed cell death pathway that can specifically modulate inflammatory cell activity (5, 178, 410, 500, 541). The inflammasome, also known as the pyroptosome, is a supramolecular entity that initiates the pyroptotic cell death process. The inflammasome family of nucleotide-binding oligomerization domain and leucine-rich repeat-containing receptors (NLRs) has the members NLRP1, NLRP3, NLRP6, and NLRC4. Pattern recognition receptors responding to damage associated molecular pattern (DAMP) in host cells and pathogen-associated molecular pattern (PAMP) in families of microbes lead to the activation of inflammasomes and caspase 4, caspase 1, and caspase 5 (7, 303, 358, 515, 541–545). DAMP molecules with DNA and adenosine triphosphate (ATP) traverse through open cell membranes and lead to NLRP3 canonical inflammasome activation while caspase 5 and caspase 4 can result in noncanonical inflammasome activation with lipopolysaccharide proteins in infections with Gram-negative bacteria. For membranes to open, pores are formed through the degradation of N-terminal domain with the C-terminal domains as part of gasdermin proteins. Cytokines such as interleukin-1 family members are released to generate inflammatory reactions and require gasdermin since these cytokines cannot alone result in pore formation (2, 212, 515). Pyroptosis can result in cell injury as a result of cytokine release (410, 411) and lead to neuronal and vascular cell dysfunction that results in loss of memory and executive function (11, 60, 252, 263, 275, 298, 301, 344, 546). In addition, elevated cytokine release during pyroptosis can affect immune cell activity in the body (358) and lead to failed clinical outcomes, such as in MS patients, with elevated inflammasome levels (541).

6 SIRT1 regulation of cellular metabolism and neurodegeneration

The silent mating type information regulation 2 homolog 1 (*Saccharomyces cerevisiae*) (SIRT1) controls both cellular metabolism (11, 60, 111, 263, 275, 294, 298, 344, 400, 546–549) and neurodegeneration (98, 102, 117, 156, 210, 232, 240, 400, 438, 550–555). There exist mammalian homologues of Sir2 that are SIRT1, SIRT2, SIRT3, SIRT4, SIRT5, SIRT6, and SIRT7 (6, 12, 13, 97, 134, 255, 333, 556). SIRT1 exists in the brain, liver, heart, skeletal muscle, pancreas, adipose tissue, and spleen (16, 179, 210, 223, 440, 550, 557). SIRT1 is a histone deacetylase that controls transcription of DNA that involves acetyl group transfer from ϵ-N-acetyl lysine amino acids to DNA histones (6, 17, 70, 78, 106, 117, 223, 259, 309, 335, 558, 559) (Figure 2). Histone deacetylases oversee multiple cellular processes such as aging, wound healing, neuronal function, oxidative stress, transcription factor activity, cardiovascular function, and cancer (8, 78, 98, 175, 550, 560–563). One substrate

for SIRT1 is the coenzyme ß-nicotinamide adenine dinucleotide (NAD^+) (24, 42, 65, 70, 78, 96, 98, 111, 196, 330, 475, 550, 564).

SIRT1 regulation of cellular metabolic homeostasis can be critical to the onset and progression of disorders in the nervous system (13, 16, 17, 38, 98, 223, 259, 333, 544, 549, 565, 566). SIRT1 is dependent upon NAD^+ and nicotinamide (24, 98, 210, 255, 417, 475, 514, 550). As a precursor for NAD^+, nicotinamide is the amide form of vitamin B_3 (niacin) (8, 34, 42, 330, 378, 567–570). Nicotinamide can be produced through SIRT1 transferring of the acetyl residue of the histone acetyllysine residue to the ADP-ribose moiety of NAD^+. As part of a feedback pathway, nicotinamide can limit the activity of SIRT1 through the interception of an ADP-ribosyl-enzyme-acetyl peptide intermediate with the regeneration of NAD^+ (571). As a result, nicotinamide can bind to sirtuins through NAD^+ in the C pocket of sirtuins (572) and can noncompetitively inhibit SIRT1 (560) and prevent anti-inflammatory gene expression (573). In addition, SIRT1 activation through nicotinamide phosphoribosyltransferase (NAMPT) can occur with periods of glucose restriction. This leads to increases in NAD^+ and reduction in nicotinamide levels that become ineffective to block SIRT1 (574). Replenishment of NAD^+ can assist with cardiovascular health (53) with SIRT1 activation limiting inflammation, metabolic dysfunction, and cell injury (111, 113, 203). As an example during hyperglycemia, SIRT1 can increase vascular cell survival (575).

SIRT1 can oversee insulin sensitivity (8, 61, 78, 417, 576–578) and mitochondrial function (13, 34, 70, 240, 475, 558). SIRT1 expression is reduced in the liver and pancreas during high fat diets that can lead to insulin resistance (579). Elevated SIRT1 activity can modulate glucose and hepatic lipid processing to prevent metabolic syndrome dysfunction (580). SIRT1 controls insulin sensitivity via protein tyrosine phosphatase (PTP) (335, 581). SIRT1 also is a positive feedback system for insulin signaling through Akt and can lead to the activity of Akt through phosphotidylinositide 3-kinase (PI 3-K) (532, 581).

In the nervous system, SIRT1 activity can lead to neurite outgrowth and enhance neuronal survival in environments that limit nutrients (582). SIRT1 can foster survival for photoreceptor cells (583), prevent the senescence of endothelial cells (584), and enhance the function of mitochondria in embryonic stem cells during oxidative stress (585). The absence of SIRT1 activity may lead to dysregulation in the immune system such as during MS (406). SIRT1 activity may be required for limiting the toxicity of oxidative stress and preserving memory (262), fostering Aβ degradation (586), increase lifespan in higher level organisms (587), and protecting neuronal and vascular cells against oxidative stress (98, 134, 232, 240, 438, 502, 510, 550, 551, 554, 555, 588).

SIRT1 also functions through trophic factor regulation in metabolic and neurological disorders that is linked to NAD^+ activity (34, 145, 203, 499, 533–535, 589). The trophic factor EPO employs SIRT1 to block depolarization of mitochondrial, release of cytochrome c, induction of BCL2 associated agonist of cell death (Bad) activation, and caspase cleavage (510). EPO through SIRT1 can protect neurons (590) that may be responsible for SIRT1 synaptic memory improvement (223). As a result of SIRT1 activity, EPO prevents mitochondrial injury (483, 521, 536, 591–593), increases microglial survival (594), blocks caspase activity (520), protects human cardiomyocytes (592), and oversees cellular metabolism (304, 482, 595, 596).

7 Oversight of metabolic and nervous system disorders through AMPK

AMP-activated protein kinase (AMPK) is an important component of the mTOR pathway, is intimately associated with SIRT1, and is a significant target for metabolic and neurodegenerative disorders (2, 30, 38, 112, 113, 118, 218, 229, 452, 558, 559, 597–600) (Figure 2). AMPK can lead to the generation of adenosine triphosphate (ATP), improve insulin sensitivity, oversee the oxidation of fatty acids, and reduce levels of oxidative stress (30, 34, 229, 230, 234, 288, 309). Increased AMPK activity is present in diets high in fish oil that can prevent endothelial cell injury (601) and improve insulin sensitivity (451). In the nervous system, AMPK can limit stroke damage in animal models of DM (602), reduce tau deposition (463), regulate neuroinflammation (134, 226, 603), reduce Aß brain accumulation (604), block Aß toxicity (605), oversee mitophagy with ULK1 (606, 607) and improve cognition in experimental models with DM and AD (608). Pain sensation that can become problematic with peripheral neuropathies in DM can be attenuated in experimental models with AMPK (292).

A number of agents that are involved in metabolic homeostasis also rely upon AMPK. Nicotinamide can protect mitochondria with the activation of AMPK (288). In addition, metformin and biguanides control autophagy through AMPK. DM cardiac cell injury through the activation of autophagy with AMPK is reduced during treatment with metformin (609). As previously noted, activation of autophagy under some circumstances can reduce toxicity from oxidative stress (33, 121, 145, 189, 216, 226, 306, 309, 540) and may shift to beneficial oxidative metabolism (610). In addition, other pathways such as Wnt family members may require AMPK activity to reduce neuronal brain injury (611). AMPK signaling is necessary with inhibition of mTOR pathways for the maintenance of electrical activity of the brain for control of behavior (597), for the acceleration of myelin brain recovery during treatment with metformin (356), and for mitochondrial preservation during ferroptotic cell death (229). Without AMPK activity, cell death, cell senescence, and mitochondrial loss can result (16, 113).

Bidirectional pathways of modulation of activity also exist for SIRT1 and AMPK. SIRT1 expression leads to deacetylation of serine-threonine liver kinase B1 (LKB1) that may be through indirect or direct means and can result in AMPK activation (612). Although AMPK does not directly activate SIRT1, SIRT1 activity can increase with AMPK either by elevating the cellular NAD^+/NADH ratio that leads to deacetylation and downstream SIRT1 target activity changes to involve peroxisome proliferator-activated receptor-gamma coactivator-1α (PGC-1α) and forkhead transcription factors (613) or through increasing NAMPT to raise NAD^+ and lower SIRT1 inhibitors such as nicotinamide (574). Resveratrol, an activator of SIRT1, can elevate AMPK activity

through SIRT1 dependent or independent pathways (613, 614). Through combined pathways, AMPK and SIRT1 block mitochondrial loss (61) and limit endothelial cell death during elevated glucose exposure (575).

8 WISP1 in metabolic homeostasis and nervous system function

Closely coordinated with the pathways AMPK in metabolic and neurodegenerative disease is the Wnt1 inducible signaling pathway protein 1 (WISP1) (6, 75, 529, 615–618). WISP1 is a downstream target of the *wingless* pathway of Wnt proteins. Wnt proteins are cysteine-rich glycosylated proteins that can control cellular metabolism, stem cell proliferation, new vascular cell growth, musculoskeletal disease, nervous system sensation, and neuronal cell development (57, 83, 122, 181, 203, 346, 349, 350, 530, 531, 619, 620). Wnt signaling that includes Wnt1 can control autophagy (621–624), prevent endothelial cell death in experimental models of DM (412), limit dopaminergic neuron cell loss in PD (625), oversee repair of wounds during DM (626), assist with human β-cell proliferation (627), foster growth in the musculoskeletal system (57, 497, 628), and inhibit cognitive loss with DM and aging (629).

WISP1 is a CCN family member that consists of six secreted extracellular matrix associated proteins that are termed by the first three members of the family that include Cysteine-rich protein 61, Connective tissue growth factor, and Nephroblastoma over-expressed gene (130, 630) (Figure 2). WISP1 can be influenced by increased weight in humans, becomes elevated with insulin resistance in children and adolescents (616, 631), and is elevated during gestational DM (632). WISP1 may be vital for glucose homeostasis since it is over-expressed during regeneration of the pancreas (633), controls β-cell proliferation (75), and can control cellular senescence (634). WISP1 can stabilize atherosclerotic plaques (347) that can ultimately lead to cerebrovascular disease, can limit lipopolysaccharide-induced cell injury through pathways of Akt (348), can attenuate blood-brain barrier disruption (635), and decrease toxicity of oxidative stress and Aß exposure (97, 520, 522). However, it should be noted that WISP1, a trophic agent, also can promote tumorigenesis (281, 529, 636–642).

WISP1 is dependent upon the pathways of AMPK for glucose homeostasis and the ability to affect neuronal survival. WISP1 can oversee AMPK post-translational phosphorylation during cellular metabolism (6, 33, 455, 643–645). WISP1 controls the activation of AMPK activation by differentially decreasing phosphorylation of tuberous sclerosis 2 (TSC2) at serine^{1387}, an AMPK target, and increasing phosphorylation of TSC2 at threonine^{1462}, an Akt target (522). This process allows WISP1 to provide a minimal level of TSC2 and AMPK activity to offer a proper biological balance for optimum metabolic homeostasis and survival of cells. This balance in AMPK activation and levels is critical. Although AMPK activation can limit insulin resistance and oxidative stress (451) and assist with differentiation of adipocytes during lipid accumulation in obesity (646), under other conditions AMPK through autophagy may lead to cell injury. A fine balance of AMPK activity is necessary to increase basal autophagy activity and maintain neuronal and endothelial cell survival during periods of metabolic homeostasis loss (230, 234, 575, 584). AMPK can modulate apoptosis and autophagy during coronary artery disease (647) and ROS release (234, 648). This is also seen with the growth factor EPO. EPO controls AMPK during oxidative stress (522), inflammation (114, 385, 649), angiogenesis (650, 651), and modulation of endothelial nitric oxide synthase (652). The concentration of EPO and duration of treatment can influence a specific level of AMPK activity, as well as the activity of mTOR (114, 653–655). If this activity is not balanced, elevated EPO and AMK activity can lead to cell injury (656).

9 Discussion

With the increase in lifespan and NCDs, disorders of cellular metabolism that include DM and neurodegenerative disorders are increasing in prevalence throughout the world. These disorders may be significantly under diagnosed with estimates of at least thirty-five percent of individuals in developed countries not receiving appropriate care to slow the progression of metabolic and neurodegenerative disease. Metabolic and neurodegenerative disorders also impose a significant financial challenge for the treatment and care of individuals. It is expected that additional care costs for current unmet clinical and staffing needs will exceed over two trillion USD per year.

The clinical onset and progression of metabolic and neurodegenerative disorders is closely tied to aging, dysfunction in telomere processing, and the processes of cellular senescence and oxidative stress (Table 1). These underlying processes not only lead to neuronal and vascular death, mitochondrial loss, stem cell injury, and immune system dysfunction, but also result in significant co-morbidities in the nervous system leading autonomic dysfunction and peripheral neuropathies as well as cognitive loss. In fact, cognitive loss is now the seventh cause throughout the world for death and it is estimated that close to two hundred million individuals may have dementia by the year 2050. Although dementia may present in multiple neurological disorders, AD encompasses almost sixty percent of individuals with cognitive loss and it is estimated that more than sixty-five percent of people with MS have cognitive impairment. The cognitive loss in neurological disorders has an important metabolic basis and involves risk factors with APOE that can lead to the cognitive loss present in AD and MS as well as increase susceptibility to viral infections, such as during SARS-CoV-2 with COVID-19.

Metabolic disorders, such as DM, and neurologic disease remain a significant challenge for the treatment and care of individuals. Although strategies that address nutritional intake

and the use of pharmaceutical agents to control glucose homeostasis can slow disease progression of DM, clinical off-target effects can lead to progressive neuronal and vascular cell loss and the atrophy of organs in the body. To a similar degree, present therapies for AD assist with symptoms of memory loss, but do not halt disease progression. In addition, recently approved therapies and DMTs for AD and MS that involve immunotherapies may be suited for a small subset of people, such as with AD, and can achieve some decrease in disease progression but the overall course of cognitive loss in these disorders will continue unabated. These clinical challenges to address the interplay between metabolic and neurodegenerative disorders require innovative strategies that can focus upon the underlying mechanisms of aging, oxidative stress, cell senescence, and cell death.

Programmed cell death pathways that involve autophagy, apoptosis, ferroptosis, and pyroptosis can play an important role in DM and neurodegenerative disorders. Autophagy can regulate the proliferation and size of pancreatic β-cells, reduce insulin resistance, prevent diabetic nephropathy, and limit progression of DM through promoting β-cell function and eliminating misfolded proteins and dysfunctional mitochondria. Autophagy activation in conjunction with mTOR inhibition can reduce ROS release, protect dopamine cells, preserve mitochondrial integrity, reduce inflammatory processes that may lead to clinical relapses, limit Aß and tau brain deposition, reduce cytokine release and microglial activity, and repair myelin in the nervous system. In regard to apoptotic cell death, strategies that can limit apoptosis activation can prevent cell injury during excessive glial activity during oxidative stress, limit ischemic toxicity to retinal cells, preserve dopaminergic cells during inflammation, and block cell demise during Aß exposure. Similar to apoptotic cell injury but involving iron accumulation in the cell with the loss of glutathione homeostasis, ferroptosis leads to cognitive impairment, immune dysfunction in T lymphocytes that can injure neuronal and glial cells, and cell death in the musculoskeletal system, cardiovascular system, and breast tissue. Pyroptosis cell death involves inflammasome activation that yields cytokine release, cell injury, inflammatory cell dysfunction, and neurovascular injury with cognitive loss.

Given that pathways of programmed cell death play a dual role in determining the fate of cellular survival and organ systems, it is important to recognize that a balance among these pathways is essential to optimize clinical outcome. For example, activation of autophagy can lead to cardiac disease, atherosclerosis, block interneuron progenitor cell growth, foster neuronal death, lead to memory impairment, and prevent neurovascular protection with growth factors. As a result, the basal activity of autophagy should be considered since changes in the autophagic flux have been shown to limit the induction of cell senescence. With apoptosis, it can be equally as crucial to control early apoptotic pathways that involve PS membrane asymmetry in an effort to block the later phase progression of the apoptotic cascade and prevent nuclear DNA degradation that leads to cell death. In addition, apoptotic pathways are tightly linked to inflammatory cell activity. Although increased glial cell activity may contribute to oxidative stress and apoptosis, microglial cells can be beneficial at times with autophagy induction to maintain cholesterol homeostasis (133), provide protection during amyotrophic lateral sclerosis (657), and for the clearance of amyloid in the brain (598). Triggering receptor expressed on myeloid cells 2 (TREM2) that can foster microglial survival can prevent inflammation during AD through forkhead transcription factors (FoxOs), Wnt signaling, and microglial activation (323, 658).

Pathways with SIRT1, AMPK, and WISP1 also provide us with clues for maintaining a proper environmental homeostasis for cells especially during aging processes that can lead to cognitive loss. SIRT1 is dependent upon NAD^+ and nicotinamide and can control insulin sensitivity, prevent cell senescence, modulate immune system activity, promote Aβ degradation, and increase lifespan in higher organisms. In addition, mitochondrial oxidative stress can be dependent upon nicotinamide adenine dinucleotide phosphate (NADPH) depletion and increase of aldose reductase. These pathways are important in the pentose phosphate pathway that involves transaldolase, which is encoded by the *TALDO1* gene (659) and has been linked to Parkinson's disease (660). Such mitochondrial dysfunction can be mediated through mTOR pathways that lead to antiphospholipid antibodies (661). Yet, feedback pathways are required at times through nicotinamide and Akt for replenishment of NAD^+ and effective modulation of cellular pathways, such as those involving insulin signaling and inflammation. AMPK activation can improve insulin sensitivity, reduce oxidative stress toxicity, limit tau and Aß cell injury, and lead to cognitive improvement in conjunction with autophagy activation. Yet, during periods when autophagy activation can be detrimental, AMPK may require modulation to limit its activity. This loss of AMPK activity to alter autophagy pathways may negatively impact other pathways such as with SIRT1. There exist conditions when SIRT1 in conjunction with AMPK is required to prevent mitochondrial loss and vascular cell death. WISP1 also requires AMPK pathways to offer glucose homeostasis and protection of neuronal and vascular cells. The ability for WISP1 to effectively promote metabolic stability and cell survival is dependent upon WISP1 providing a proper biological balance of AMPK activity to foster cell survival, control inflammatory pathways, assist with growth factor protection, and prevent cell injury that can occur through autophagic and apoptotic mechanisms. The pathways of programmed cell death, SIRT1, AMPK, and WISP1 offer vital insights and are extremely attractive for identifying processes that can contribute to the onset and progression of metabolic and neurodegenerative diseases that can be linked to multiple entities such as APOE, SARS-CoV-2, NAD^+, nicotinamide, and trophic factors, such as EPO, but will require further insight into the elaborate relationship of these pathways for effective clinical translation.

Author contributions

KM: Conceptualization, Writing – original draft, Writing – review & editing.

Conflict of interest

The author declares that the research was conducted in the absence of any commercial or financial relationships that could be construed as a potential conflict of interest.

Funding

The author(s) declare financial support was received for the research, authorship, and/or publication of this article. This research was supported by the following grants to KM: American Diabetes Association, American Heart Association, NIH NIEHS, NIH NIA, NIH NINDS, NS053956, and NIH ARRA.

Publisher's note

References

1. Organization WH. *Global Report on Diabetes*. Geneva: World Health Organization (2016) p. 1–83.

2. Maiese K. Dysregulation of Metabolic flexibility: the impact of mtor on autophagy in neurodegenerative disease. *Int Rev Neurobiol* (2020) 155:1–35. doi: 10.1016/bs.irn.2020.01.009

3. International Diabetes Federation. *Diabetes. 9th Edition*. Brussels, Belgium: IDF Diabetes Atlas (2019).

4. Maiese K, Chong ZZ, Shang YC, Hou J. Novel avenues of drug discovery and biomarkers for diabetes mellitus. *J Clin Pharmacol* (2011) 51(2):128–52. doi: 10.1177/0091270010362904

5. Maiese K. The metabolic basis for nervous system dysfunction in alzheimer's disease, parkinson's disease, and huntington's disease. *Curr Neurovasc Res* (2023) 20 (3):314–33. doi: 10.2174/1567202620666230721122957

6. Maiese K. Cognitive impairment with diabetes mellitus and metabolic disease: innovative insights with the mechanistic target of rapamycin and circadian clock gene pathways. *Expert Rev Clin Pharmacol* (2020) 13(1):23–34. doi: 10.1080/17512433.2020.1698288

7. Maiese K. Cellular metabolism: A fundamental component of degeneration in the nervous system. *Biomolecules* (2023) 13(5):816. doi: 10.3390/biom13050816

8. Maiese K. Innovative therapeutic strategies for cardiovascular disease. *EXCLI J* (2023) 22:690–715. doi: 10.17179/excli2023-6306

9. Papachristoforou E, Lambadiari V, Maratou E, Makrilakis K. Association of glycemic indices (Hyperglycemia, glucose variability, and hypoglycemia) with oxidative stress and diabetic complications. *J Diabetes Res* (2020) 2020:7489795. doi: 10.1155/2020/7489795

10. Min AY, Yoo JM, Sok DE, Kim MR. Mulberry fruit prevents diabetes and diabetic dementia by regulation of blood glucose through upregulation of antioxidative activities and creb/bdnf pathway in alloxan-induced diabetic mice. *Oxid Med Cell Longev* (2020) 2020:1298691. doi: 10.1155/2020/1298691

11. Xu T, Liu J, Li XR, Yu Y, Luo X, Zheng X, et al. The mtor/nf-κb pathway mediates neuroinflammation and synaptic plasticity in diabetic encephalopathy. *Mol Neurobiol* (2021) 58(8):3848–62. doi: 10.1007/s12035-021-02390-1

12. Wang Z, Wu Q, Wang H, Gao Y, Nie K, Tang Y, et al. Diosgenin Protects against Podocyte Injury in Early Phase of Diabetic Nephropathy through Regulating Sirt6. *Phytomedicine: Int J phytotherapy phytopharmacology* (2022) 104:154276. doi: 10.1016/j.phymed.2022.154276

13. Wasserfurth P, Nebl J, Rühling MR, Shammas H, Bednarczyk J, Koehler K, et al. Impact of dietary modifications on plasma sirtuins 1, 3 and 5 in older overweight individuals undergoing 12-weeks of circuit training. *Nutrients* (2021) 13(11). doi: 10.3390/nu13113824

14. Miranda LMO, Agostini LDC, Lima WG, Camini FC, Costa DC. Silymarin attenuates hepatic and pancreatic redox imbalance independent of glycemic regulation in the alloxan-induced diabetic rat model. *BioMed Environ Sci* (2020) 33(9):690–700. doi: 10.3967/bes2020.090

15. Wang H, Zhang R, Wu X, Chen Y, Ji W, Wang J, et al. The wnt signaling pathway in diabetic nephropathy. *Front Cell Dev Biol* (2021) 9:701547. doi: 10.3389/fcell.2021.701547

16. Barcena ML, Tonini G, Haritonow N, Breiter P, Milting H, Baczko I, et al. Sex and age differences in ampk phosphorylation, mitochondrial homeostasis, and inflammation in hearts from inflammatory cardiomyopathy patients. *Aging Cell* (2023) 22(8):e13894. doi: 10.1111/acel.13894

17. Kostić M, Korićanac G, Tepavčević S, Stanišić J, Romić S, Ćulafić T, et al. Low-intensity exercise affects cardiac fatty acid oxidation by increasing the nuclear content of pparα, foxo1, and lipin1 in fructose-fed rats. *Metab Syndr Relat Disord* (2023) 21 (2):122–31. doi: 10.1089/met.2022.0078

18. Stojanovic D, Stojanovic M, Milenkovic J, Velickov A, Ignjatovic A, Milojkovic M. The multi-faceted nature of renalase for mitochondrial dysfunction improvement in cardiac disease. *Cells* (2023) 12(12):1607. doi: 10.3390/cells12121607

19. Jiang W, Ding K, Yue R, Lei M. Therapeutic effects of icariin and icariside ii on diabetes mellitus and its complications. *Crit Rev Food Sci Nutr* (2023) 1–26. doi: 10.1080/10408398.2022.2159317

20. Raghuvanshi DS, Chakole S, Kumar M. Relationship between vitamins and diabetes. *Cureus* (2023) 15(3):e36815. doi: 10.7759/cureus.36815

21. Raut SK, Khullar M. Oxidative stress in metabolic diseases: current scenario and therapeutic relevance. *Mol Cell Biochem* (2023) 478(1):185–96. doi: 10.1007/s11010-022-04496-z

22. World health organization. Description of the global burden of ncds, their risk factors and determinants. *Global Status Rep noncommunicable Dis 2010* (2011), 1–176.

23. *Centers for disease control and prevention* Vol. 314227-A. Atlanta, GA, USA: National Diabetes Statistics Report (2020) p. 1–30.

24. Maiese K. Nicotinamide as a foundation for treating neurodegenerative disease and metabolic disorders. *Curr Neurovasc Res* (2021) 18(1):134–49. doi: 10.2174/1567202617999210104220334

25. Ajiboye BO, Shonibare MT, Oyinloye BE. Antidiabetic activity of watermelon (Citrullus lanatus) juice in alloxan-induced diabetic rats. *J Diabetes Metab Disord* (2020) 19(1):343–52. doi: 10.1007/s40200-020-00515-2

26. Arildsen L, Andersen JV, Waagepetersen HS, Nissen JBD, Sheykhzade M. Hypermetabolism and impaired endothelium-dependent vasodilation in mesenteric arteries of type 2 diabetes mellitus db/db mice. *Diabetes Vasc Dis Res* (2019) 16 (6):1479164119865885. doi: 10.1177/1479164119865885

27. Bayaraa O, Inman CK, Thomas SA, Al Jallaf F, Alshaikh M, Idaghdour Y, et al. Hyperglycemic conditions induce rapid cell dysfunction-promoting transcriptional alterations in human aortic endothelial cells. *Sci Rep* (2022) 12(1):20912. doi: 10.1038/s41598-022-24999-5

28. Burillo J, Marqués P, Jiménez B, González-Blanco C, Benito M, Guillén C. Insulin resistance and diabetes mellitus in alzheimer's disease. *Cells* (2021) 10(5):1236. doi: 10.3390/cells10051236

29. Chen Y, Huang C, Zhu SY, Zou HC, Xu CY, Chen YX. Overexpression of hotair attenuates pi-induced vascular calcification by inhibiting wnt/β-catenin through regulating mir-126/klotho/sirt1 axis. *Mol Cell Biochem* (2021) 476(10):3551–61. doi: 10.1007/s11010-021-04164-8

30. Gong Q, Wang H, Yu P, Qian T, Xu X. Protective or harmful: the dual roles of autophagy in diabetic retinopathy. *Front Med (Lausanne)* (2021) 8:644121. doi: 10.3389/fmed.2021.644121

31. Karamzad N, Faraji E, Adeli S, Sullman MJM, Pourghassem Gargari B. The effect of menaquinone-7 supplementation on dp-ucmgp, pivkaii, inflammatory markers, and body composition in type 2 diabetes patients: A randomized clinical trial. *Nutr Diabetes* (2022) 12(1):15. doi: 10.1038/s41387-022-00192-5

32. Maiese K. New insights for oxidative stress and diabetes mellitus. *Oxid Med Cell Longev* (2015) 2015:875961. doi: 10.1155/2015/875961

33. Maiese K. Prospects and perspectives for wisp1 (Ccn4) in diabetes mellitus. *Curr Neurovasc Res* (2020) 17(3):327–31. doi: 10.2174/1567202617666200327125257

34. Maiese K. Nicotinamide: oversight of metabolic dysfunction through sirt1, mtor, and clock genes. *Curr Neurovasc Res* (2020) 17(5):765–83. doi: 10.2174/1567202617999201111195232

35. O'Donnell BT, Monjure TA, Al-Ghadban S, Ives CJ, L'Ecuyer MP, Rhee C, et al. Aberrant expression of cox-2 and foxg1 in infrapatellar fat pad-derived ascs from pre-diabetic donors. *Cells* (2022) 11(15):2367. doi: 10.3390/cells11152367

36. Ren L. Circular rna pip5k1a act as microrna-552-3p sponge to regulates inflammation, oxidative damage in glucolipotoxicity-induced pancreatic ins-1 β-cells via janus kinase 1. *Bioengineered* (2022) 13(3):5724–36. doi: 10.1080/21655979.2021.2022076

37. Zuo J, Zhang Z, Luo M, Zhou L, Nice EC, Zhang W, et al. Redox Signaling at the Crossroads of Human Health And disease. *MedComm (2020)* (2022) 3(2):e127. doi: 10.1002/mco2.127

38. Maiese K. Novel nervous and multi-system regenerative therapeutic strategies for diabetes mellitus with mtor. *Neural regeneration Res* (2016) 11(3):372–85. doi: 10.4103/1673-5374.179032

39. Harris MI, Eastman RC. Early detection of undiagnosed diabetes mellitus: A us perspective. *Diabetes Metab Res Rev* (2000) 16(4):230–6. doi: 10.1002/1520-7560(2000)9999:9999<::aid-dmrr122>3.0.co;2-w

40. Maiese K. Mtor: driving apoptosis and autophagy for neurocardiac complications of diabetes mellitus. *World J Diabetes* (2015) 6(2):217–24. doi: 10.4239/wjd.v6.i2.217

41. Maiese K, Chong ZZ, Shang YC. Mechanistic insights into diabetes mellitus and oxidative stress. *Curr Med Chem* (2007) 14(16):1729–38. doi: 10.2174/092986707781058968

42. Maiese K. New insights for nicotinamide: metabolic disease, autophagy, and mtor. *Front bioscience (Landmark edition)* (2020) 25:1925–73. doi: 10.2741/4886

43. Bahorik A, Bobrow K, Hoang T, Yaffe K. Increased risk of dementia in older female us veterans with alcohol use disorder. *Addiction* (2021) 116(8):2049–55. doi: 10.1111/add.15416

44. Caberlotto L, Nguyen TP, Lauria M, Priami C, Rimondini R, Maioli S, et al. Cross-disease analysis of alzheimer's disease and type-2 diabetes highlights the role of autophagy in the pathophysiology of two highly comorbid diseases. *Sci Rep* (2019) 9(1):3965. doi: 10.1038/s41598-019-39828-5

45. Karamzad N, Maleki V, Carson-Chahhoud K, Azizi S, Sahebkar A, Gargari BP. A systematic review on the mechanisms of vitamin K effects on the complications of diabetes and pre-diabetes. *BioFactors (Oxford England)* (2019) 46(1):21–37. doi: 10.1002/biof.1569

46. Pinchera B, Scotto R, Buonomo AR, Zappulo E, Stagnaro F, Gallicchio A, et al. Diabetes and covid-19: the potential role of mtor. *Diabetes Res Clin Pract* (2022) 186:109813. doi: 10.1016/j.diabres.2022.109813

47. Orkaby AR, Dushkes R, Ward R, Djousse L, Buring JE, Lee IM, et al. Effect of vitamin D3 and omega-3 fatty acid supplementation on risk of frailty: an ancillary study of a randomized clinical trial. *JAMA Network Open* (2022) 5(9):e2231206. doi: 10.1001/jamanetworkopen.2022.31206

48. Alves HR, Lomba GSB, Gonçalves-de-Albuquerque CF, Burth P. Irisin, exercise, and covid-19. *Front Endocrinol* (2022) 13:879066. doi: 10.3389/fendo.2022.879066

49. Bramante CT, Beckman KB, Mehta T, Karger AB, Odde DJ, Tignanelli CJ, et al. Metformin reduces sars-cov-2 in a phase 3 randomized placebo controlled clinical trial. *medRxiv* (2023). doi: 10.1101/2023.06.06.23290989

50. Maiese K. The mechanistic target of rapamycin (Mtor): novel considerations as an antiviral treatment. *Curr Neurovasc Res* (2020) 17(3):332–7. doi: 10.2174/1567202617666200425205122

51. Miller R, Wentzel AR, Richards GA. Covid-19: nad(+) deficiency may predispose the aged, obese and type2 diabetics to mortality through its effect on sirt1 activity. *Med Hypotheses* (2020) 144:110044. doi: 10.1016/j.mehy.2020.110044

52. Ong AN, Tan CC, Cañete MT, Lim BA, Robles J. Association between metformin use and mortality among patients with type 2 diabetes mellitus hospitalized for covid-19 infection. *J ASEAN Fed Endocr Soc* (2021) 36(2):133–41. doi: 10.15605/jafes.036.02.20

53. Rotllan N, Camacho M, Tondo M, Diarte-Añazco EMG, Canyelles M, Méndez-Lara KA, et al. Therapeutic potential of emerging nad+-increasing strategies for cardiovascular diseases. *Antioxidants (Basel Switzerland)* (2021) 10(12):1939. doi: 10.3390/antiox10121939

54. Swain O, Romano SK, Miryala R, Tsai J, Parikh V, Umanah GKE. Sars-cov-2 neuronal invasion and complications: potential mechanisms and therapeutic approaches. *J Neurosci* (2021) 41(25):5338–49. doi: 10.1523/jneurosci.3188-20.2021

55. Prattichizzo F, De Nigris V, Spiga R, Mancuso E, La Sala L, Antonicelli R, et al. Inflammageing and metaflammation: the yin and yang of type 2 diabetes. *Ageing Res Rev* (2018) 41:1–17. doi: 10.1016/j.arr.2017.10.003

56. Speer H, D'Cunha NM, Alexopoulos NI, McKune AJ, Naumovski N. Anthocyanins and human health-a focus on oxidative stress, inflammation and disease. *Antioxidants (Basel Switzerland)* (2020) 9(5):366. doi: 10.3390/antiox9050366

57. Maiese K. Picking a bone with wisp1 (Ccn4): new strategies against degenerative joint disease. *J Transl Sci* (2016) 1(3):83–5. doi: 10.15761/JTS.1000120

58. Liu Z, Gan L, Zhang T, Ren Q, Sun C. Melatonin alleviates adipose inflammation through elevating alpha-ketoglutarate and diverting adipose-derived exosomes to macrophages in mice. *J Pineal Res* (2018) 64(1):12455. doi: 10.1111/jpi.12455

59. Quesada I, de Paola M, Torres-Palazzolo C, Camargo A, Ferder L, Manucha W, et al. Effect of garlic's active constituents in inflammation, obesity and cardiovascular disease. *Curr Hypertens Rep* (2020) 22(1):6. doi: 10.1007/s11906-019-1009-9

60. Schell M, Wardelmann K, Kleinridders A. Untangling the effect of insulin action on brain mitochondria and metabolism. *J Neuroendocrinol* (2021) 33(4):e12932. doi: 10.1111/jne.12932

61. Yang J, Suo H, Song J. Protective role of mitoquinone against impaired mitochondrial homeostasis in metabolic syndrome. *Crit Rev Food Sci Nutr* (2021) 61(22):3857–387. doi: 10.1080/10408398.2020.1809344

62. Ciesielska K, Gajewska M. Fatty acids as potent modulators of autophagy activity in white adipose tissue. *Biomolecules* (2023) 13(2):255. doi: 10.3390/biom13020255

63. du Toit WL, Kruger R, Gafane-Matemane LF, Schutte AE, Louw R, Mels CMC. Markers of arterial stiffness and urinary metabolomics in young adults with early cardiovascular risk: the african-predict study. *Metabolomics* (2023) 19(4):28. doi: 10.1007/s11306-023-01987-y

64. Kahmini FR, Ghaleh HD, Shahgaldi S. Sirtuins: subtle regulators involved in convoluted mechanisms of pregnancy. *Cell Physiol Biochem* (2022) 56(6):644–62. doi: 10.33594/000000588

65. Chong ZZ, Li F, Maiese K. Oxidative stress in the brain: novel cellular targets that govern survival during neurodegenerative disease. *Prog Neurobiol* (2005) 75(3):207–46. doi: 10.1016/j.pneurobio.2005.02.004

66. Maiese K. Novel applications of trophic factors, wnt and wisp for neuronal repair and regeneration in metabolic disease. *Neural regeneration Res* (2015) 10(4):518–28. doi: 10.4103/1673-5374.155427

67. Maiese K, Chong ZZ, Hou J, Shang YC. Oxidative stress: biomarkers and novel therapeutic pathways. *Exp Gerontol* (2010) 45(3):217–34. doi: 10.1016/j.exger.2010.01.004

68. Maiese K, Chong ZZ, Shang YC. Outfoxing disease and disability: the therapeutic potential of targeting foxo proteins. *Trends Mol Med* (2008) 14(5):219–27. doi: 10.1016/j.molmed.2008.03.002

69. Fernandes J, Uppal K, Liu KH, Hu X, Orr M, Tran V, et al. Antagonistic interactions in mitochondria ros signaling responses to manganese. *Antioxidants (Basel Switzerland)* (2023) 12(4):804. doi: 10.3390/antiox12040804

70. Sun C, Bai S, Liang Y, Liu D, Liao J, Chen Y, et al. The role of sirtuin 1 and its activators in age-related lung disease. *BioMed Pharmacother* (2023) 162:114573. doi: 10.1016/j.biopha.2023.114573

71. Tramutola A, Lanzillotta S, Aceto G, Pagnotta S, Ruffolo G, Cifelli P, et al. Intranasal administration of kyccsrk peptide rescues brain insulin signaling activation and reduces alzheimer's disease-like neuropathology in a mouse model for down syndrome. *Antioxidants (Basel Switzerland)* (2023) 12(1):111. doi: 10.3390/antiox12010111

72. Muthu S, Jeyaraman M, Jeyaraman N, Rajendran RL, Gangadaran P. Where do we stand in stem cell therapy for the management of diabetes mellitus?-a scientometric research trend analysis from 1990 to 2020. *Bioengineering (Basel)* (2021) 8(11):159. doi: 10.3390/bioengineering8110159

73. Wang R, Zhu Y, Qin LF, Xu ZG, Gao XR, Liu CB, et al. Comprehensive bibliometric analysis of stem cell research in alzheimer's disease from 2004 to 2022. *Dement Geriatr Cognit Disord* (2023) 52(2):41–73. doi: 10.1159/000528886

74. Feng J, Wang H, Jing Z, Wang Y, Cheng Y, Wang W, et al. Role of magnesium in type 2 diabetes mellitus. *Biol Trace element Res* (2019) 196(1):74–85. doi: 10.1007/s12011-019-01922-0

75. Fernandez-Ruiz R, García-Alamán A, Esteban Y, Mir-Coll J, Serra-Navarro B, Fontcuberta-PiSunyer M, et al. Wisp1 is a circulating factor that stimulates proliferation of adult mouse and human beta cells. *Nat Commun* (2020) 11(1):5982. doi: 10.1038/s41467-020-19657-1

76. Guo T, Liu T, Sun Y, Liu X, Xiong R, Li H, et al. Sonodynamic therapy inhibits palmitate-induced beta cell dysfunction via pink1/parkin-dependent mitophagy. *Cell Death Dis* (2019) 10(6):457. doi: 10.1038/s41419-019-1695-x

77. Hu R, Zhu X, Yuan M, Ho KH, Kaverina I, Gu G. Microtubules and Gαo-signaling modulate the preferential secretion of young insulin secretory granules in islet β Cells via independent pathways. *PloS One* (2021) 16(7):e0241939. doi: 10.1371/journal.pone.0241939

78. Jalgaonkar MP, Parmar UM, Kulkarni YA, Oza MJ. Sirt1-foxos activity regulates diabetic complications. *Pharmacol Res* (2022) 175:106014. doi: 10.1016/j.phrs.2021.106014

79. Li R, Wang B, Wu C, Li D, Wu Y, Ye L, et al. Acidic fibroblast growth factor attenuates type 2 diabetes-induced demyelination via suppressing oxidative stress damage. *Cell Death Dis* (2021) 12(1):107. doi: 10.1038/s41419-021-03407-2

80. Quintana-Pérez JC, García-Dolores F, Valdez-Guerrero AS, Alemán-González-Duhart D, Arellano-Mendoza MG, Rojas Hernández S, et al. Modeling type 2 diabetes in rats by administering tacrolimus. *Islets* (2022) 14(1):114–27. doi: 10.1080/19382014.2022.2051991

81. Hill JH, Solt C, Foster MT. Obesity associated disease risk: the role of inherent differences and location of adipose depots. *Hormone Mol Biol Clin Invest* (2018) 33(2):20180012. doi: 10.1515/hmbci-2018-0012

82. Nie X, Wei X, Ma H, Fan L, Chen WD. The complex role of wnt ligands in type 2 diabetes mellitus and related complications. *J Cell Mol Med* (2021) 25(14):6479–95. doi: 10.1111/jcmm.16663

83. Sanabria-de la Torre R, García-Fontana C, González-Salvatierra S, Andújar-Vera F, Martínez-Heredia L, García-Fontana B, et al. The contribution of wnt signaling to vascular complications in type 2 diabetes mellitus. *Int J Mol Sci* (2022) 23(13):6995. doi: 10.3390/ijms23136995

84. Sun ZY, Yu TY, Jiang FX, Wang W. Functional maturation of immature β Cells: A roadblock for stem cell therapy for type 1 diabetes. *World J Stem Cells* (2021) 13 (3):193–207. doi: 10.4252/wjsc.v13.i3.193

85. Tan S, Zang G, Wang Y, Sun Z, Li Y, Lu C, et al. Differences of angiogenesis factors in tumor and diabetes mellitus. *Diabetes Metab Syndr Obes* (2021) 14:3375–88. doi: 10.2147/dmso.S315362

86. Zaiou M. Circrnas signature as potential diagnostic and prognostic biomarker for diabetes mellitus and related cardiovascular complications. *Cells* (2020) 9(3):659. doi: 10.3390/cells9030659

87. Zarneshan SN, Fakhri S, Farzaei MH, Khan H, Saso L. Astaxanthin targets pi3k/akt signaling pathway toward potential therapeutic applications. *Food Chem Toxicol* (2020) 145:111714. doi: 10.1016/j.fct.2020.111714

88. Centers for Medicare and Medicaid Services. *National health expenditure projections 2018-2027* (Baltimore, Maryland, USA). (2019).

89. Sonsalla MM, Lamming DW. Geroprotective interventions in the 3xtg mouse model of alzheimer's disease. *Geroscience* (2023) 45(3):1343–81. doi: 10.1007/s11357-023-00782-w

90. Singh A, Kukreti R, Saso L, Kukreti S. Mechanistic insight into oxidative stress-triggered signaling pathways and type 2 diabetes. *Molecules* (2022) 27(3):950. doi: 10.3390/molecules27030950

91. Liu L, Cao Q, Gao W, Li BY, Zeng C, Xia Z, et al. Melatonin ameliorates cerebral ischemia-reperfusion injury in diabetic mice by enhancing autophagy via the sirt1-bmal1 pathway. *FASEB J* (2021) 35(12):e22040. doi: 10.1096/fj.202002718RR

92. Heer CD, Sanderson DJ, Voth LS, Alhammad YMO, Schmidt MS, Trammell SAJ, et al. Coronavirus infection and parp expression dysregulate the nad metabolome: an actionable component of innate immunity. *J Biol Chem* (2020) 295(52):17986–96. doi: 10.1074/jbc.RA120.015138

93. Li J, Lin FH, Zhu XM, Lv ZM. Impact of diabetic hyperglycaemia and insulin therapy on autophagy and impairment in rat epididymis. *Andrologia* (2020) 52(11): e13889. doi: 10.1111/and.13889

94. Tomita Y, Lee D, Tsubota K, Kurihara T. Pparα Agonist oral therapy in diabetic retinopathy. *Biomedicines* (2020) 8(10):433. doi: 10.3390/biomedicines8100433

95. Maiese K. Driving neural regeneration through the mammalian target of rapamycin. *Neural regeneration Res* (2014) 9(15):1413–7. doi: 10.4103/1673-5374.139453

96. Maiese K. The bright side of reactive oxygen species: lifespan extension without cellular demise. *J Transl Sci* (2016) 2(3):185–7. doi: 10.15761/jts.1000138

97. Maiese K. The mechanistic target of rapamycin (Mtor) and the silent mating-type information regulation 2 homolog 1 (Sirt1): oversight for neurodegenerative disorders. *Biochem Soc Trans* (2018) 46(2):351–60. doi: 10.1042/bst20170121

98. Ministrini S, Puspitasari YM, Beer G, Liberale L, Montecucco F, Camici GG. Sirtuin 1 in endothelial dysfunction and cardiovascular aging. *Front Physiol* (2021) 12:733696. doi: 10.3389/fphys.2021.733696

99. Olejniczak I, Pilorz V, Oster H. Circle(S) of life: the circadian clock from birth to death. *Biol (Basel)* (2023) 12(3):383. doi: 10.3390/biology12030383

100. Yamamoto H, Shimomura N, Oura K, Hasegawa Y. Nacre extract from pearl oyster shell prevents D-galactose-induced brain and skin aging. *Mar Biotechnol (NY)* (2023) 25(4):503–18. doi: 10.1007/s10126-022-10192-2

101. National Center for Health Statistics. *National vital statisitcs system*. Hyattsville, Maryland, USA: National Center for Health Statistics Fact Sheet (2019) p. 1–2.

102. Begum MK, Konja D, Singh S, Chlopicki S, Wang Y. Endothelial sirt1 as a target for the prevention of arterial aging: promises and challenges. *J Cardiovasc Pharmacol* (2021) 78(Suppl 6):S63–s77. doi: 10.1097/fjc.0000000000001154

103. Braidy N, Liu Y. Nad+ Therapy in age-related degenerative disorders: A benefit/risk analysis. *Exp Gerontol* (2020) 132:110831. doi: 10.1016/j.exger.2020.110831

104. Castro-Portuguez R, Sutphin GL. Kynurenine pathway, nad(+) synthesis, and mitochondrial function: targeting tryptophan metabolism to promote longevity and healthspan. *Exp Gerontol* (2020) 132:110841. doi: 10.1016/j.exger.2020.110841

105. Chong ZZ, Maiese K. Mammalian target of rapamycin signaling in diabetic cardiovascular disease. *Cardiovasc Diabetol* (2012) 11(1):45. doi: 10.1186/1475-2840-11-45

106. Chong ZZ, Shang YC, Wang S, Maiese K. Sirt1: new avenues of discovery for disorders of oxidative stress. *Expert Opin Ther Targets* (2012) 16(2):167–78. doi: 10.1517/14728222.2012.648926

107. De Nobrega AK, Luz KV, Lyons LC. Resetting the aging clock: implications for managing age-related diseases. *Adv Exp Med Biol* (2020) 1260:193–265. doi: 10.1007/978-3-030-42667-5_9

108. Fischer F, Grigolon G, Benner C, Ristow M. Evolutionarily conserved transcription factors as regulators of longevity and targets for geroprotection. *Physiol Rev* (2022) 102(3):1449–94. doi: 10.1152/physrev.00017.2021

109. Ji JS, Liu L, Zeng Y, Yan LL. Effect of foxo3 and air pollution on cognitive function: A longitudinal cohort study of older adults in China from 2000 to 2014. *J Gerontol A Biol Sci Med Sci* (2022) 77(8):1534–41. doi: 10.1093/gerona/glac016

110. Lathe R, St Clair D. Programmed ageing: decline of stem cell renewal, immunosenescence, and alzheimer's disease. *Biol Rev Cambridge Philos Soc* (2023) 98(4):1424–58. doi: 10.1111/brv.12959

111. Maiese K. Sirt1 and stem cells: in the forefront with cardiovascular disease, neurodegeneration and cancer. *World J Stem Cells* (2015) 7(2):235–42. doi: 10.4252/wjsc.v7.i2.235

112. Tabibzadeh S. Signaling pathways and effectors of aging. *Front bioscience (Landmark edition)* (2021) 26:50–96. doi: 10.2741/4889

113. Watroba M, Szukiewicz D. Sirtuins at the service of healthy longevity. *Front Physiol* (2021) 12:724506. doi: 10.3389/fphys.2021.724506

114. Maiese K. Erythropoietin and mtor: A "One-two punch" for aging-related disorders accompanied by enhanced life expectancy. *Curr Neurovasc Res* (2016) 13 (4):329–40. doi: 10.2174/1567202613666160729164900

115. Maiese K. Sirtuins: developing innovative treatments for aged-related memory loss and alzheimer's disease. *Curr Neurovasc Res* (2018) 15(4):367–71. doi: 10.2174/1567202616666181128120003

116. World Health Organization. *Global action plan on the Public Health Response to Dementia 2017-2025* (Geneva, Switzerland). (2017). pp. 1–44.

117. Maiese K. Targeting the core of neurodegeneration: foxo, mtor, and sirt1. *Neural regeneration Res* (2021) 16(3):448–55. doi: 10.4103/1673-5374.291382

118. Yu M, Zhang H, Wang B, Zhang Y, Zheng X, Shao B, et al. Key signaling pathways in aging and potential interventions for healthy aging. *Cells* (2021) 10(3):660. doi: 10.3390/cells10030660

119. Adhikari UK, Khan R, Mikhael M, Balez R, David MA, Mahns D, et al. *Therapeutic Anti-Amyloid β Antibodies Cause Neuronal Disturbances*. Alzheimer's & dementia: the journal of the Alzheimer's Association (2022). doi: 10.1002/alz.12833

120. Ahmad R, Khan A, Rehman IU, Lee HJ, Khan I, Kim MO. Lupeol Treatment Attenuates activation of glial cells and oxidative-stress-mediated neuropathology in mouse model of traumatic brain injury. *Int J Mol Sci* (2022) 23(11):6086. doi: 10.3390/ijms23116086

121. Amini J, Sanchooli N, Milajerdi MH, Baeeri M, Haddadi M, Sanadgol N. The interplay between tauopathy and aging through interruption of upr/nrf2/autophagy crosstalk in the alzheimer's disease transgenic experimental models. *Int J Neurosci* (2023), 1–27. doi: 10.1080/00207454.2023.2210409

122. Guo T, Chen M, Liu J, Wei Z, Yuan J, Wu W, et al. Neuropilin-1 promotes mitochondrial structural repair and functional recovery in rats with cerebral ischemia. *J Trans Med* (2023) 21(1):297. doi: 10.1186/s12967-023-04125-3

123. Jarero-Basulto J, Rivera-Cervantes M, Gasca-Martínez D, García-Sierra F, Gasca-Martínez Y, Beas-Zárate C. Current evidence on the protective effects of recombinant human erythropoietin and its molecular variants against pathological hallmarks of alzheimer's disease. *Pharm (Basel Switzerland)* (2020) 13(424):1–22. doi: 10.3390/ph13120424

124. Liu B, Zhao G, Jin L, Shi J. Nicotinamide improves cognitive function in mice with chronic cerebral hypoperfusion. *Front Neurol* (2021) 12:596641. doi: 10.3389/fneur.2021.596641

125. Maiese K. The many facets of cell injury: angiogenesis to autophagy. *Curr Neurovasc Res* (2012) 9(2):1–2. doi: 10.2174/156720212800410911

126. Mavroidi B, Kaminari A, Matiadis D, Hadjipavlou-Litina D, Pelecanou M, Tzinia A, et al. The prophylactic and multimodal activity of two isatin thiosemicarbazones against alzheimer's disease in vitro. *Brain Sci* (2022) 12(6):806. doi: 10.3390/brainsci12060806

127. Pontifex MG, Martinsen A, Saleh RNM, Harden G, Tejera N, Müller M, et al. Apoe4 genotype exacerbates the impact of menopause on cognition and synaptic plasticity in apoe-tr mice. *FASEB J* (2021) 35(5):e21583. doi: 10.1096/fj.202002621RR

128. Torii T, Miyamoto Y, Nakata R, Higashi Y, Shinmyo Y, Kawasaki H, et al. Identification of tau protein as a novel marker for maturation and pathological changes of oligodendrocytes. *Glia* (2023) 71(4):1002–17. doi: 10.1002/glia.24322

129. Yalçin M, Mundorf A, Thiel F, Amatriain-Fernández S, Kalthoff IS, Beucke JC, et al. It's about time: the circadian network as time-keeper for cognitive functioning, locomotor activity and mental health. *Front Physiol* (2022) 13:873237. doi: 10.3389/fphys.2022.873237

130. Maiese K. Wisp1: clinical insights for a proliferative and restorative member of the ccn family. *Curr Neurovasc Res* (2014) 11(4):378–89. doi: 10.2174/1567202611666140912115107

131. Levine KS, Leonard HL, Blauwendraat C, Iwaki H, Johnson N, Bandres-Ciga S, et al. Virus exposure and neurodegenerative disease risk across national biobanks. *Neuron* (2023) 111(7):1086–93. doi: 10.1016/j.neuron.2022.12.029

132. Pradhan SS, Rao KR, Manjunath M, Saiswaroop R, Patnana DP, Phalguna KS, et al. Vitamin B(6), B(12) and folate modulate deregulated pathways and protein aggregation in yeast model of huntington disease. *3 Biotech* (2023) 13(3):96. doi: 10.1007/s13205-023-03525-y

133. Zhang WB, Huang Y, Guo XR, Zhang MQ, Yuan XS, Zu HB. Dhcr24 reverses alzheimer's disease-related pathology and cognitive impairment via increasing hippocampal cholesterol levels in 5xfad mice. *Acta neuropathologica Commun* (2023) 11(1):102. doi: 10.1186/s40478-023-01593-y

134. Maiese K. Targeting molecules to medicine with mtor, autophagy and neurodegenerative disorders. *Br J Clin Pharmacol* (2016) 82(5):1245–66. doi: 10.1111/bcp.12804

135. Borowicz-Reutt KK, Czuczwar SJ. Role of oxidative stress in epileptogenesis and potential implications for therapy. *Pharmacol Rep* (2020) 72(5):1218–26. doi: 10.1007/s43440-020-00143-w

136. Corti O, Blomgren K, Poletti A, Beart PM. Autophagy in neurodegeneration: new insights underpinning therapy for neurological diseases. *J Neurochem* (2020) 154 (4):e15002. doi: 10.1111/jnc.15002

137. Duitama M, Vargas-López V, Casas Z, Albarracin SL, Sutachan JJ, Torres YP. Trp channels role in pain associated with neurodegenerative diseases. *Front Neurosci* (2020) 14:782. doi: 10.3389/fnins.2020.00782

138. Kaur D, Behl T, Sehgal A, Singh S, Sharma N, Badavath VN, et al. Unravelling the potential neuroprotective facets of erythropoietin for the treatment of alzheimer's disease. *Metab Brain Dis* (2021) 37(1):1–16. doi: 10.1007/s11011-021-00820-6

139. Kuan XY, Fauzi NSA, Ng KY, Bakhtiar A. Exploring the causal relationship between telomere biology and alzheimer's disease. *Mol Neurobiol* (2023) 60(8):4169–83. doi: 10.1007/s12035-023-03337-4

140. LaCroix MS, Mirbaha H, Shang P, Zandee S, Foong C, Prat A, et al. Tau seeding in cases of multiple sclerosis. *Acta neuropathologica Commun* (2022) 10(1):146. doi: 10.1186/s40478-022-01444-2

141. Maiese K. Neurodegeneration, memory loss, and dementia: the impact of biological clocks and circadian rhythm. *Front bioscience (Landmark edition)* (2021) 26 (9):614–27. doi: 10.52586/4971

142. Mishra P, Davies DA, Albensi BC. The interaction between nf-κb and estrogen in alzheimer's disease. *Mol Neurobiol* (2022) 60(3):1515–26. doi: 10.1007/s12035-022-03152-3

143. Sabzali M, Eidi A, Khaksari M, Khastar H. Anti-inflammatory, antioxidant, and antiapoptotic action of metformin attenuates ethanol neurotoxicity in the animal model of fetal alcohol spectrum disorders. *Neurotox Res* (2022) 40(2):605–13. doi: 10.1007/s12640-022-00499-2

144. Salemi M, Mogavero MP, Lanza G, Mongioì LM, Calogero AE, Ferri R. Examples of inverse comorbidity between cancer and neurodegenerative diseases: A possible role for noncoding rna. *Cells* (2022) 11(12):1930. doi: 10.3390/cells11121930

145. Senousy MA, Hanafy ME, Shehata N, Rizk SM. Erythropoietin and bacillus calmette-guérin vaccination mitigate 3-nitropropionic acid-induced huntington-like disease in rats by modulating the pi3k/akt/mtor/P70s6k pathway and enhancing the autophagy. *ACS Chem Neurosci* (2022) 13(6):721–32. doi: 10.1021/acschemneuro.1c00523

146. Su LD, Wang N, Han J, Shen Y. Group 1 metabotropic glutamate receptors in neurological and psychiatric diseases: mechanisms and prospective. *Neuroscientist* (2021) 28(5):10738584211021018. doi: 10.1177/10738584211021018

147. World Health Organization. *Dementia: A public health priority*. Geneva: World Health Organization (2012) p. 1–4.

148. Maiese K. Taking Aim at Alzheimer's Disease through the Mammalian Target of Rapamycin. *Ann Med* (2014) 46(8):587–96. doi: 10.3109/07853890.2014.941921

149. Farmer K, Abd-Elrahman KS, Derksen A, Rowe EM, Thompson AM, Rudyk CA, et al. Mglur5 allosteric modulation promotes neurorecovery in a 6-ohda-toxicant model of parkinson's disease. *Mol Neurobiol* (2020) 57(3):1418–31. doi: 10.1007/s12035-019-01818-z

150. Galzigna L, De Iuliis A, Zanatta L. Enzymatic dopamine peroxidation in substantia nigra of human brain. *Clin Chim Acta* (2000) 300(1-2):131–8. doi: 10.1016/s0009-8981(00)00313-2

151. Gonzalo-Gobernado R, Perucho J, Vallejo-Muñoz M, Casarejos MJ, Reimers D, Jiménez-Escrig A, et al. Liver growth factor "Lgf" as a therapeutic agent for alzheimer's disease. *Int J Mol Sci* (2020) 21(3):9201. doi: 10.3390/ijms21239201

152. Jayaraj RL, Beiram R, Azimullah S, Mf NM, Ojha SK, Adem A, et al. Valeric acid protects dopaminergic neurons by suppressing oxidative stress, neuroinflammation and modulating autophagy pathways. *Int J Mol Sci* (2020) 21 (20):7670. doi: 10.3390/ijms21207670

153. Khan H, Tundis R, Ullah H, Aschner M, Belwal T, Mirzaei H, et al. Flavonoids targeting nrf2 in neurodegenerative disorders. *Food Chem Toxicol* (2020) 146:111817. doi: 10.1016/j.fct.2020.111817

154. Kowalska M, Piekut T, Prendecki M, Sodel A, Kozubski W, Dorszewska J. Mitochondrial and nuclear DNA oxidative damage in physiological and pathological aging. *DNA Cell Biol* (2020) 39(8):1410–20. doi: 10.1089/dna.2019.5347

155. Lei Q, Wu T, Wu J, Hu X, Guan Y, Wang Y, et al. Roles of α–Synuclein in gastrointestinal microbiome dysbiosis–Related parkinson's disease progression (Review). *Mol Med Rep* (2021) 24(4):734. doi: 10.3892/mmr.2021.12374

156. Li X, Feng Y, Wang XX, Truong D, Wu YC. The critical role of sirt1 in parkinson's disease: mechanism and therapeutic considerations. *Aging Dis* (2020) 11 (6):1608–22. doi: 10.14336/ad.2020.0216

157. Liu J, Liu H, Zhao Z, Wang J, Guo D, Liu Y. Regulation of actg1 and gsta2 is possible mechanism by which capsaicin alleviates apoptosis in cell model of 6-ohda-induced parkinson's disease. *Bioscience Rep* (2020) 40(6):BSR20191796. doi: 10.1042/bsr20191796

158. Maiese K. Biomarkers for parkinson's disease and neurodegenerative disorders: A role for non-coding rnas. *Curr Neurovasc Res* (2022) 19(2):127–30. doi: 10.2174/1567202619666220602125806

159. Maiese K, Chong ZZ, Shang YC, Wang S. Erythropoietin: new directions for the nervous system. *Int J Mol Sci* (2012) 13(9):11102–29. doi: 10.3390/ijms130911102

160. Marchetti B. Nrf2/wnt resilience orchestrates rejuvenation of glia-neuron dialogue in parkinson's disease. *Redox Biol* (2020) 36:101664. doi: 10.1016/j.redox.2020.101664

161. Margrett JA, Schofield T, Martin P, Poon LW, Masaki K, Donlon TA, et al. Novel functional, health, and genetic determinants of cognitive terminal decline: kuakini honolulu heart program/honolulu-asia aging study. *J Gerontol A Biol Sci Med Sci* (2021) 77(8):1525–33. doi: 10.1093/gerona/glab327

162. Odnokoz O, Nakatsuka K, Wright C, Castellanos J, Klichko VI, Kretzschmar D, et al. Mitochondrial redox signaling is critical to the normal functioning of the neuronal system. *Front Cell Dev Biol* (2021) 9:613036. doi: 10.3389/fcell.2021.613036

163. Querfurth H, Lee HK. Mammalian/mechanistic target of rapamycin (Mtor) complexes in neurodegeneration. *Mol neurodegeneration* (2021) 16(1):44. doi: 10.1186/s13024-021-00428-5

164. Ullah H, Hussain A, Asif M, Nawaz F, Rasool M. Natural products as bioactive agents in the prevention of dementia. *CNS Neurol Disord Drug Targets* (2023) 22 (4):466–76. doi: 10.2174/1871527321666220422085835

165. Wang Q, Zheng J, Pettersson S, Reynolds R, Tan EK. The link between neuroinflammation and the neurovascular unit in synucleinopathies. *Sci Adv* (2023) 9(7):eabq1141. doi: 10.1126/sciadv.abq1141

166. Liu JJ, Shentu LM, Ma N, Wang LY, Zhang GM, Sun Y, et al. Inhibition of nf-kappab and wnt/beta-catenin/gsk3beta signaling pathways ameliorates cardiomyocyte hypertrophy and fibrosis in streptozotocin (Stz)-induced type 1 diabetic rats. *Curr Med Sci* (2020) 40(1):35–47. doi: 10.1007/s11596-020-2144-x

167. Maiese K. Erythropoietin and diabetes mellitus. *World J Diabetes* (2015) 6 (14):1259–73. doi: 10.4239/wjd.v6.i14.1259

168. Maiese K, Chong ZZ, Shang YC, Hou J. Foxo proteins: cunning concepts and considerations for the cardiovascular system. *Clin Sci (Lond)* (2009) 116(3):191–203. doi: 10.1042/CS20080113

169. Maiese K, Hou J, Chong ZZ, Shang YC. A fork in the path: developing therapeutic inroads with foxo proteins. *Oxid Med Cell Longev* (2009) 2(3):119–29. doi: 10.4161/oxim.2.3.8916

170. Pabel S, Hamdani N, Luedde M, Sossalla S. Sglt2 inhibitors and their mode of action in heart failure-has the mystery been unravelled? *Curr Heart Fail Rep* (2021) 18 (5):315–28. doi: 10.1007/s11897-021-00529-8

171. Ciardullo S, Muraca E, Bianconi E, Cannistraci R, Perra S, Zerbini F, et al. Diabetes mellitus is associated with higher serum neurofilament light chain levels in the general us population. *J Clin Endocrinol Metab* (2023) 108(2):361–7. doi: 10.1210/clinem/dgac580

172. Maiese K. Programming apoptosis and autophagy with novel approaches for diabetes mellitus. *Curr Neurovasc Res* (2015) 12(2):173–88. doi: 10.2174/1567202612666150305110929

173. Maiese K. Foxo transcription factors and regenerative pathways in diabetes mellitus. *Curr Neurovasc Res* (2015) 12(4):404–13. doi: 10.2174/1567202612666150807112524

174. Pouresmaeil V, Al Abudi AH, Mahimid AH, Sarafraz Yazdi M, Es-Haghi A. Evaluation of serum selenium and copper levels with inflammatory cytokines and indices of oxidative stress in type 2 diabetes. *Biol Trace element Res* (2022) 201(2):617–26. doi: 10.1007/s12011-022-03191-w

175. Beegum F, Anunrajana PV, George KT, Divya KP, Begum F, Krishnadas N, et al. Sirtuins as therapeutic targets for improving delayed wound healing in diabetes. *J Drug Target* (2022) 30(9):911–926. doi: 10.1080/1061186x.2022.2085729

176. Chiareli RA, Carvalho GA, Marques BL, Mota LS, Oliveira-Lima OC, Gomes RM, et al. The role of astrocytes in the neurorepair process. *Front Cell Dev Biol* (2021) 9:665795. doi: 10.3389/fcell.2021.665795

177. Ding S, Zhu Y, Liang Y, Huang H, Xu Y, Zhong C. Circular rnas in vascular functions and diseases. *Adv Exp Med Biol* (2018) 1087:287–97. doi: 10.1007/978-981-13-1426-1_23

178. Geng K, Ma X, Jiang Z, Huang W, Gao C, Pu Y, et al. Innate immunity in diabetic wound healing: focus on the mastermind hidden in chronic inflammatory. *Front Pharmacol* (2021) 12:653940. doi: 10.3389/fphar.2021.653940

179. Hajibabaie F, Abedpoor N, Safavi K, Taghian F. Natural remedies medicine derived from flaxseed (Secoisolariciresinol diglucoside, lignans, and α-linolenic acid) improve network targeting efficiency of diabetic heart conditions based on computational chemistry techniques and pharmacophore modeling. *J Food Biochem* (2022) 46(12):e14480. doi: 10.1111/jfbc.14480

180. Liu P, Liu J, Wu Y, Xi W, Wei Y, Yuan Z, et al. Zinc supplementation protects against diabetic endothelial dysfunction via gtp cyclohydrolase 1 restoration. *Biochem Biophys Res Commun* (2020) 521(4):1049–54. doi: 10.1016/j.bbrc.2019.11.046

181. Maiese K, Li F, Chong ZZ, Shang YC. The wnt signaling pathway: aging gracefully as a protectionist? *Pharmacol Ther* (2008) 118(1):58–81. doi: 10.1016/j.pharmthera.2008.01.004

182. Zhou Q, Tang S, Zhang X, Chen L. Targeting pras40: A novel therapeutic strategy for human diseases. *J Drug Target* (2021) 29(7):703–715. doi: 10.1080/1061186x.2021.1882470

183. El-Marasy SA, Abdel-Rahman RF, Abd-Elsalam RM. Neuroprotective effect of vildagliptin against cerebral ischemia in rats. *Naunyn Schmiedebergs Arch Pharmacol* (2018) 391(10):1133–45. doi: 10.1007/s00210-018-1537-x

184. Januszewski AS, Watson CJ, O'Neill V, McDonald K, Ledwidge M, Robson T, et al. Fkbpl is associated with metabolic parameters and is a novel determinant of cardiovascular disease. *Sci Rep* (2020) 10(1):21655. doi: 10.1038/s41598-020-78676-6

185. Esterline RL, Vaag A, Oscarsson J, Vora J. Mechanisms in endocrinology: sglt2 inhibitors; clinical benefits by restoration of normal diurnal metabolism? *Eur J Endocrinol* (2018) 178(4):R113–25. doi: 10.1530/eje-17-0832

186. Mocayar Marón FJ, Ferder L, Reiter RJ, Manucha W. Daily and seasonal mitochondrial protection: unraveling common possible mechanisms involving vitamin D and melatonin. *J Steroid Biochem Mol Biol* (2020) 199:105595. doi: 10.1016/j.jsbmb.2020.105595

187. Mishra M, Duraisamy AJ, Kowluru RA. Sirt1- a guardian of the development of diabetic retinopathy. *Diabetes* (2018) 67(4):745–54. doi: 10.2337/db17-0996

188. Qi X, Mitter SK, Yan Y, Busik JV, Grant MB, Boulton ME. Diurnal rhythmicity of autophagy is impaired in the diabetic retina. *Cells* (2020) 9(4):905. doi: 10.3390/cells9040905

189. Casciano F, Zauli E, Rimondi E, Mura M, Previati M, Busin M, et al. The role of the mtor pathway in diabetic retinopathy. *Front Med (Lausanne)* (2022) 9:973856. doi: 10.3389/fmed.2022.973856

190. Kita A, Saito Y, Miura N, Miyajima M, Yamamoto S, Sato T, et al. Altered regulation of mesenchymal cell senescence in adipose tissue promotes pathological changes associated with diabetic wound healing. *Commun Biol* (2022) 5(1):310. doi: 10.1038/s42003-022-03266-3

191. Fadini GP, Morieri ML, Longato E, Avogaro A. Prevalence and impact of diabetes among people infected with sars-cov-2. *J endocrinological Invest* (2020) 43(6):867–9. doi: 10.1007/s40618-020-01236-2

192. Lally MA, Tsoukas P, Halladay CW, O'Neill E, Gravenstein S, Rudolph JL. Metformin is associated with decreased 30-day mortality among nursing home residents infected with sars-cov2. *J Am Med Dir Assoc* (2021) 22(1):193–8. doi: 10.1016/j.jamda.2020.10.031

193. Gutiérrez-Pliego LE, Martínez-Carrillo BE, Reséndiz-Albor AA, Valdés-Ramos R. Effect on adipose tissue of diabetic mice supplemented with N-3 fatty acids extracted from microalgae. *Endocr Metab Immune Disord Drug Targets* (2020) 20(5):728–35. doi: 10.2174/1871530320666200213111452

194. Li S, Vaziri ND, Swentek L, Takasu C, Vo K, Stamos MJ, et al. Prevention of autoimmune diabetes in nod mice by dimethyl fumarate. *Antioxidants (Basel Switzerland)* (2021) 10(2):193. doi: 10.3390/antiox10020193

195. Maiese K, Chong ZZ, Hou J, Shang YC. The "O" Class: crafting clinical care with foxo transcription factors. *Adv Exp Med Biol* (2009) 665:242–60. doi: 10.1007/978-1-4419-1599-3_18

196. Maiese K, Chong ZZ, Hou J, Shang YC. The vitamin nicotinamide: translating nutrition into clinical care. *Molecules* (2009) 14(9):3446–85. doi: 10.3390/molecules14093446

197. Rashidi S, Mansouri R, Ali-Hassanzadeh M, Mojtahedi Z, Shafiei R, Savardashtaki A, et al. The host mtor pathway and parasitic diseases pathogenesis. *Parasitol Res* (2021) 120(4):1151–66. doi: 10.1007/s00436-021-07070-6

198. Wen S, Jiang W, Zhou L. Islet autoantibodies in the patients with sjogren's syndrome and thyroid disease and risk of progression to latent autoimmune diabetes in adults: A case series. *Diabetes Metab Syndr Obes* (2021) 14:1025–33. doi: 10.2147/dmso.S295847

199. Zhuang X, Magri A, Hill M, Lai AG, Kumar A, Rambhatla SB, et al. The circadian clock components bmal1 and rev-erbα Regulate flavivirus replication. *Nat Commun* (2019) 10(1):377. doi: 10.1038/s41467-019-08299-7

200. Zhang Y, Yuan Y, Zhang J, Zhao Y, Zhang Y, Fu J. Astragaloside iv supplementation attenuates cognitive impairment by inhibiting neuroinflammation and oxidative stress in type 2 diabetic mice. *Front Aging Neurosci* (2022) 14:1004557. doi: 10.3389/fnagi.2022.1004557

201. Maiese K, Chong ZZ, Wang S, Shang YC. Oxidant stress and signal transduction in the nervous system with the pi 3-K, akt, and mtor cascade. *Int J Mol Sci* (2013) 13(11):13830–66. doi: 10.3390/ijms131113830

202. Liu C, Zhong C, Chen R, Zhou X, Wu J, Han J, et al. Higher dietary vitamin C intake is associated with a lower risk of gestational diabetes mellitus: A longitudinal cohort study. *Clin Nutr* (2020) 39(1):198–203. doi: 10.1016/j.clnu.2019.01.015

203. Maiese K. Triple play: promoting neurovascular longevity with nicotinamide, wnt, and erythropoietin in diabetes mellitus. *BioMed Pharmacother* (2008) 62(4):218–32. doi: 10.1016/j.biopha.2008.01.009

204. Akila Parvathy Dharshini S, Taguchi YH, Michael Gromiha M. Exploring the selective vulnerability in alzheimer disease using tissue specific variant analysis. *Genomics* (2019) 111(4):936–49. doi: 10.1016/j.ygeno.2018.05.024

205. Amanollahi M, Jameie M, Heidari A, Rezaei N. The dialogue between neuroinflammation and adult neurogenesis: mechanisms involved and alterations in neurological diseases. *Mol Neurobiol* (2022) 60(2):923–59. doi: 10.1007/s12035-022-03102-z

206. Barnett JA, Bandy ML, Gibson DL. Is the use of glyphosate in modern agriculture resulting in increased neuropsychiatric conditions through modulation of the gut-brain-microbiome axis? *Front Nutr* (2022) 9:827384. doi: 10.3389/fnut.2022.827384

207. Chen Z, He Y, Hu F, Li M, Yao Y. Genkwanin alleviates mitochondrial dysfunction and oxidative stress in a murine model of experimental colitis: the participation of sirt1. *Ann Clin Lab Sci* (2022) 52(2):301–13.

208. Lee SH, Lee JJ, Kim GH, Kim JA, Cho HS. Role of reactive oxygen species at reperfusion stage in isoflurane preconditioning-induced neuroprotection. *Brain Res* (2019) 1723:146405. doi: 10.1016/j.brainres.2019.146405

209. Ponzetti M, Rucci N, Falone S. Rna methylation and cellular response to oxidative stress-promoting anticancer agents. *Cell Cycle* (2023) 22(8):870–905. doi: 10.1080/15384101.2023.2165632

210. Teertam SK, Prakash Babu P. Differential role of sirt1/mapk pathway during cerebral ischemia in rats and humans. *Sci Rep* (2021) 11(1):6339. doi: 10.1038/s41598-021-85577-9

211. Wawi MJ, Mahler C, Inguimbert N, Marder TB, Ribou AC. A new mitochondrial probe combining pyrene and a triphenylphosphonium salt for cellular oxygen and free radical detection via fluorescence lifetime measurements. *Free Radic Res* (2022) 56(3-4):258–272. doi: 10.1080/10715762.2022.2077202

212. Wu L, Xiong X, Wu X, Ye Y, Jian Z, Zhi Z, et al. Targeting oxidative stress and inflammation to prevent ischemia-reperfusion injury. *Front Mol Neurosci* (2020) 13:28. doi: 10.3389/fnmol.2020.00028

213. Xiong J, Bonney S, Gonçalves RV, Esposito D. Brassinosteroids control the inflammation, oxidative stress and cell migration through the control of mitochondrial function on skin regeneration. *Life Sci* (2022) 307:120887. doi: 10.1016/j.lfs.2022.120887

214. Zadeh-Haghighi H, Simon C. Magnetic field effects in biology from the perspective of the radical pair mechanism. *J R Soc Interface* (2022) 19(193):20220325. doi: 10.1098/rsif.2022.0325

215. Zhang Y, Zhu X, Wang G, Chen L, Yang H, He F, et al. Melatonin rescues the ti particle-impaired osteogenic potential of bone marrow mesenchymal stem cells via the sirt1/sod2 signaling pathway. *Calcif Tissue Int* (2020) 107(5):474–88. doi: 10.1007/s00223-020-00741-z

216. Zhao HY, Li HY, Jin J, Jin JZ, Zhang LY, Xuan MY, et al. L-carnitine treatment attenuates renal tubulointerstitial fibrosis induced by unilateral ureteral obstruction. *Korean J Intern Med* (2020) 36(Suppl 1):S180–95. doi: 10.3904/kjim.2019.413

217. Zheng Z, Xie J, Ma L, Hao Z, Zhang W, Li L. Vitamin D receptor activation targets ros-mediated crosstalk between autophagy and apoptosis in hepatocytes in cholestasis mice. *Cell Mol Gastroenterol Hepatol* (2022) 15(4):887–901. doi: 10.1016/j.jcmgh.2022.10.011

218. Zhuang X, Ma J, Xu G, Sun Z. Shp-1 knockdown suppresses mitochondrial biogenesis and aggravates mitochondria-dependent apoptosis induced by all trans retinal through the sting/ampk pathways. *Mol Med* (2022) 28(1):125. doi: 10.1186/s10020-022-00554-w

219. Nikooyeh B, Zahedirad M, Kalayi A, Shariatzadeh N, Hollis BW, Neyestani TR. Improvement of vitamin D status through consumption of either fortified food products or supplement pills increased hemoglobin concentration in adult subjects: analysis of pooled data from two randomized clinical trials. *Nutr Health* (2023) 29(3):567–74. doi: 10.1177/02601060221085351

220. Zheng Y, Chen ZY, Ma WJ, Wang QZ, Liang H, Ma AG. B vitamins supplementation can improve cognitive functions and may relate to the enhancement of transketolase activity in a rat model of cognitive impairment associated with high-fat diets. *Curr Med Sci* (2021) 41(5):847–56. doi: 10.1007/s11596-021-2456-5

221. Zhou J, Chen H, Wang Q, Chen S, Wang R, Wang Z, et al. Sirt1 overexpression improves senescence-associated pulmonary fibrosis induced by vitamin D deficiency through downregulating il-11 transcription. *Aging Cell* (2022) 21(8):e13680. doi: 10.1111/acel.13680

222. Doroftei B, Ilie OD, Cojocariu RO, Ciobica A, Maftei R, Grab D, et al. Minireview exploring the biological cycle of vitamin B3 and its influence on oxidative stress: further molecular and clinical aspects. *Molecules* (2020) 25(15):3323. doi: 10.3390/molecules25153323

223. Jahan R, Yousaf M, Khan H, Shah SA, Khan AA, Bibi N, et al. Zinc ortho methyl carbonodithioate improved pre and post-synapse memory impairment via sirt1/P-jnk pathway against scopolamine in adult mice. *J neuroimmune Pharmacol* (2023) 18(1-2):183–94. doi: 10.1007/s11481-023-10067-w

224. Qin D, Li D, Wang C, Guo S. Ferroptosis and central nervous system demyelinating diseases. *J Neurochem* (2023) 165(6):759–71. doi: 10.1111/jnc.15831

225. Zhao C, Sun G, Li Y, Kong K, Li X, Kan T, et al. Forkhead box O3 attenuates osteoarthritis by suppressing ferroptosis through inactivation of nf-κb/mapk signaling. *J Orthop Translat* (2023) 39:147–62. doi: 10.1016/j.jot.2023.02.005

226. Maiese K. Moving to the rhythm with clock (Circadian) genes, autophagy, mtor, and sirt1 in degenerative disease and cancer. *Curr Neurovasc Res* (2017) 14(3):299–304. doi: 10.2174/1567202614666170718092010

227. Mladenovic Djordjevic A, Loncarevic-Vasiljkovic N, Gonos ES. Dietary restriction and oxidative stress: friends or enemies? *Antioxid Redox Signal* (2020) 34(5):421–38. doi: 10.1089/ars.2019.7959

228. Oyefeso FA, Muotri AR, Wilson CG, Pecaut MJ. Brain organoids: A promising model to assess oxidative stress-induced central nervous system damage. *Dev Neurobiol* (2021) 81(5):653–70. doi: 10.1002/dneu.22828

229. Zhong S, Chen W, Wang B, Gao C, Liu X, Song Y, et al. Energy stress modulation of ampk/foxo3 signaling inhibits mitochondria-associated ferroptosis. *Redox Biol* (2023) 63:102760. doi: 10.1016/j.redox.2023.102760

230. Maiese K. Warming up to new possibilities with the capsaicin receptor trpv1: mtor, ampk, and erythropoietin. *Curr Neurovasc Res* (2017) 14(2):184–9. doi: 10.2174/1567202614666170313105337

231. Meng J, Chen Y, Wang J, Qiu J, Chang C, Bi F, et al. Egcg protects vascular endothelial cells from oxidative stress-induced damage by targeting the autophagy-dependent pi3k-akt-mtor pathway. *Ann Transl Med* (2020) 8(5):200. doi: 10.21037/atm.2020.01.92

232. Piao S, Lee I, Jin SA, Kim S, Nagar H, Choi SJ, et al. Sirt1 activation attenuates the cardiac dysfunction induced by endothelial cell-specific deletion of crif1. *Biomedicines* (2021) 9(1):52. doi: 10.3390/biomedicines9010052

233. Wang F, Cao Y, Ma L, Pei H, Rausch WD, Li H. Dysfunction of cerebrovascular endothelial cells: prelude to vascular dementia. *Front Aging Neurosci* (2018) 10:376. doi: 10.3389/fnagi.2018.00376

234. Zhao D, Sun X, Lv S, Sun M, Guo H, Zhai Y, et al. Salidroside attenuates oxidized lowdensity lipoproteininduced endothelial cell injury via promotion of the ampk/sirt1 pathway. *Int J Mol Med* (2019) 43(6):2279–90. doi: 10.3892/ijmm.2019.4153

235. Aksenov MY, Aksenova MV, Butterfield DA, Geddes JW, Markesbery WR. Protein oxidation in the brain in alzheimer's disease. *Neuroscience* (2001) 103(2):373–83. doi: 10.1016/s0306-4522(00)00580-7

236. Chen GJ, Xu J, Lahousse SA, Caggiano NL, de la Monte SM. Transient hypoxia causes alzheimer-type molecular and biochemical abnormalities in cortical neurons: potential strategies for neuroprotection. *J Alzheimers Dis* (2003) 5(3):209–28. doi: 10.3233/jad-2003-5305

237. Dai C, Xiao X, Li J, Ciccotosto GD, Cappai R, Tang S, et al. Molecular mechanisms of neurotoxicity induced by polymyxins and chemo-prevention. *ACS Chem Neurosci* (2018) 10(1):120–31. doi: 10.1021/acschemneuro.8b00300

238. Fanoudi S, Hosseini M, Alavi MS, Boroushaki MT, Hosseini A, Sadeghnia HR. Everolimus, a mammalian target of rapamycin inhibitor, ameliorated streptozotocin-induced learning and memory deficits via neurochemical alterations in male rats. *Excli J* (2018) 17:999–1017. doi: 10.17179/excli2018-1626

239. Feng HX, Li CP, Shu SJ, Liu H, Zhang HY. A11, a novel diaryl acylhydrazone derivative, exerts neuroprotection against ischemic injury in vitro and in vivo. *Acta Pharmacol Sin* (2018) 40(2):160–9. doi: 10.1038/s41401-018-0028-4

240. Groen CM, Podratz JL, Pathoulas J, Staff N, Windebank AJ. Genetic reduction of mitochondria complex I subunits is protective against cisplatin-induced neurotoxicity in drosophila. *J Neurosci* (2021) 42(5):922–37. doi: 10.1523/jneurosci.1479-20.2021

241. Jaganjac M, Milkovic L, Zarkovic N, Zarkovic K. Oxidative stress and regeneration. *Free Radic Biol Med* (2022) 181:154–65. doi: 10.1016/j.freeradbiomed.2022.02.004

242. Li P, Liu H, Shi X, Prokosch V. Hydrogen sulfide: novel endogenous and exogenous modulator of oxidative stress in retinal degeneration diseases. *Molecules* (2021) 26(9):2411. doi: 10.3390/molecules26092411

243. Maiese K, Chong ZZ. Insights into oxidative stress and potential novel therapeutic targets for alzheimer disease. *Restor Neurol Neurosci* (2004) 22(2):87–104.

244. Samaiya PK, Krishnamurthy S, Kumar A. Mitochondrial dysfunction in perinatal asphyxia: role in pathogenesis and potential therapeutic interventions. *Mol Cell Biochem* (2021) 476(12):4421–34. doi: 10.1007/s11010-021-04253-8

245. Sharma VK, Singh TG, Singh S, Garg N, Dhiman S. Apoptotic pathways and alzheimer's disease: probing therapeutic potential. *Neurochem Res* (2021) 46(12):3103–22. doi: 10.1007/s11064-021-03418-7

246. El-Missiry MA, Othman AI, Amer MA, Sedki M, Ali SM, El-Sherbiny IM. Nanoformulated ellagic acid ameliorates pentylenetetrazol-induced experimental epileptic seizures by modulating oxidative stress, inflammatory cytokines and apoptosis in the brains of male mice. *Metab Brain Dis* (2019) 35(2):385–99. doi: 10.1007/s11011-019-00502-4

247. Motawi TK, Darwish HA, Hamed MA, El-Rigal NS, Naser AF. A therapeutic insight of niacin and coenzyme Q10 against diabetic encephalopathy in rats. *Mol Neurobiol* (2017) 54(5):3924. doi: 10.1007/s12035-016-9765-x

248. Dąbrowska-Bouta B, Strużyńska L, Sidoryk-Węgrzynowicz M, Sulkowski G. Memantine modulates oxidative stress in the rat brain following experimental autoimmune encephalomyelitis. *Int J Mol Sci* (2021) 22(21):11330. doi: 10.3390/ijms222111330

249. Dai C, Tang S, Biao X, Xiao X, Chen C, Li J. Colistin induced peripheral neurotoxicity involves mitochondrial dysfunction and oxidative stress in mice. *Mol Biol Rep* (2019) 46(2):1963–72. doi: 10.1007/s11033-019-04646-5

250. Govindappa PK, Talukder MAH, Gurjar AA, Hegarty JP, Elfar JC. An effective erythropoietin dose regimen protects against severe nerve injury-induced pathophysiological changes with improved neural gene expression and enhances functional recovery. *Int Immunopharmacol* (2020) 82:106330. doi: 10.1016/j.intimp.2020.106330

251. Oliveira ALL, Santos GGL, Espirito-Santo RF, Silva GSA, Evangelista AF, Silva DN, et al. Reestablishment of redox homeostasis in the nociceptive primary afferent as a mechanism of antinociception promoted by mesenchymal stem/stromal cells in oxaliplatin-induced chronic peripheral neuropathy. *Stem Cells Int* (2021) 2021:8815206. doi: 10.1155/2021/8815206

252. Maiese K. Cognitive impairment in multiple sclerosis. *Bioengineering (Basel)* (2023) 10(7):871. doi: 10.3390/bioengineering10070871

253. Liu W, Li Y, Luo B. Current perspective on the regulation of foxo4 and its role in disease progression. *Cell Mol Life Sci* (2020) 77(4):651–63. doi: 10.1007/s00018-019-03297-w

254. Puigoriol-Illamola D, Grinan-Ferre C, Vasilopoulou F, Leiva R, Vazquez S, Pallas M. 11beta-hsd1 inhibition by rl-118 promotes autophagy and correlates with reduced oxidative stress and inflammation, enhancing cognitive performance in samp8 mouse model. *Mol Neurobiol* (2018) 55(12):8904–15. doi: 10.1007/s12035-018-1026-8

255. Zhang GZ, Deng YJ, Xie QQ, Ren EH, Ma ZJ, He XG, et al. Sirtuins and intervertebral disc degeneration: roles in inflammation, oxidative stress, and mitochondrial function. *Clin Chim Acta* (2020) 508:33–42. doi: 10.1016/j.cca.2020.04.016

256. Bahrampour Juybari K, Pourhanifeh MH, Hosseinzadeh A, Hemati K, Mehrzadi S. Melatonin potentials against viral infections including covid-19: current evidence and new findings. *Virus Res* (2020) 287:198108. doi: 10.1016/j.virusres.2020.198108

257. Jarosz-Griffiths HH, Corbett NJ, Rowland HA, Fisher K, Jones AC, Baron J, et al. Proteolytic shedding of the prion protein via activation of metallopeptidase adam10 reduces cellular binding and toxicity of amyloid-beta oligomers. *J Biol Chem* (2019) 294(17):7085–97. doi: 10.1074/jbc.RA118.005364

258. Kuscu N, Gungor-Ordueri NE, Sozen B, Adiguzel D, Celik-Ozenci C. Foxo transcription factors regulate mouse preimplantation embryo development. *J Assist Reprod Genet* (2019) 36(12):2605. doi: 10.1007/s10815-019-01555-1

259. Maiese K. Harnessing the power of sirt1 and non-coding rnas in vascular disease. *Curr Neurovasc Res* (2017) 14(1):82–8. doi: 10.2174/1567202613666161129112822

260. Cheema PS, Nandi D, Nag A. Exploring the therapeutic potential of forkhead box O for outfoxing covid-19. *Open Biol* (2021) 11(6):210069. doi: 10.1098/rsob.210069

261. Fang Y, Lu L, Liang Y, Peng D, Aschner M, Jiang Y. Signal transduction associated with lead-induced neurological disorders: A review. *Food Chem Toxicol* (2021) 150:112063. doi: 10.1016/j.fct.2021.112063

262. Khan M, Ullah R, Rehman SU, Shah SA, Saeed K, Muhammad T, et al. 17beta-estradiol modulates sirt1 and halts oxidative stress-mediated cognitive impairment in a male aging mouse model. *Cells* (2019) 8(8):928. doi: 10.3390/cells8080928

263. Mahmoudi N, Kiasalari Z, Rahmani T, Sanaierad A, Afshin-Majd S, Naderi G, et al. Diosgenin attenuates cognitive impairment in streptozotocin-induced diabetic rats: underlying mechanisms. *Neuropsychobiology* (2021) 11:25–35. doi: 10.1159/000507398

264. Ruhal P, Dhingra D. Inosine improves cognitive function and decreases aging-induced oxidative stress and neuroinflammation in aged female rats. *Inflammopharmacology* (2018) 26(5):1317–29. doi: 10.1007/s10787-018-0476-y

265. Dhakal S, Kushairi N, Phan CW, Adhikari B, Sabaratnam V, Macreadie I. Dietary polyphenols: A multifactorial strategy to target alzheimer's disease. *Int J Mol Sci* (2019) 20(20):5090. doi: 10.3390/ijms20205090

266. Engin AB, Engin A. Alzheimer's disease and protein kinases. *Adv Exp Med Biol* (2021) 1275:285–321. doi: 10.1007/978-3-030-49844-3_11

267. Zhao J, Miao K, Wang H, Ding H, Wang DW. Association between telomere length and type 2 diabetes mellitus: A meta-analysis. *PloS One* (2013) 8(11):e79993. doi: 10.1371/journal.pone.0079993

268. Lamoke F, Shaw S, Yuan J, Ananth S, Duncan M, Martin P, et al. Increased oxidative and nitrative stress accelerates aging of the retinal vasculature in the diabetic retina. *PloS One* (2015) 10(10):e0139664. doi: 10.1371/journal.pone.0139664

269. Cai J, Qi H, Yao K, Yao Y, Jing D, Liao W, et al. Non-coding rnas steering the senescence-related progress, properties, and application of mesenchymal stem cells. *Front Cell Dev Biol* (2021) 9:650431. doi: 10.3389/fcell.2021.650431

270. Chung CL, Lawrence I, Hoffman M, Elgindi D, Nadhan K, Potnis M, et al. Topical rapamycin reduces markers of senescence and aging in human skin: an exploratory, prospective, randomized trial. *Geroscience* (2019) 41:6. doi: 10.1007/s11357-019-00113-y

271. Csicsar A, Tarantini S, Yabluchanskiy A, Balasubramanian P, Kiss T, Farkas E, et al. Role of endothelial nad+ Deficiency in age-related vascular dysfunction. *Am J Physiol Heart Circ Physiol* (2019) 316(6):H1253–H66. doi: 10.1152/ajpheart.00039.2019

272. Dorvash M, Farahmandnia M, Tavassoly I. A systems biology roadmap to decode mtor control system in cancer. *Interdiscip Sci* (2020) 12(1):1–11. doi: 10.1007/s12539-019-00347-6

273. Maiese K. Disease onset and aging in the world of circular rnas. *J Transl Sci* (2016) 2(6):327–9. doi: 10.15761/jts.1000158

274. Maiese K. The implications of telomere length: advanced aging, cell senescence, mri phenotypes, stem cells and alzheimer's disease. *Curr Neurovasc Res* (2023) 20(2):171–4. doi: 10.2174/1567202620666230510150337

275. Rapaka D, Bitra VR, Challa SR, Adiukwu PC. Mtor signaling as a molecular target for the alleviation of alzheimer's disease pathogenesis. *Neurochem Int* (2022) 155:105311. doi: 10.1016/j.neuint.2022.105311

276. Ferrara-Romeo I, Martinez P, Saraswati S, Whittemore K, Graña-Castro O, Thelma Poluha L, et al. The mtor pathway is necessary for survival of mice with short telomeres. *Nat Commun* (2020) 11(1):1168. doi: 10.1038/s41467-020-14962-1

277. Lai KY, Webster C, Kumari S, Gallacher JEJ, Sarkar C. The associations of socioeconomic status with incident dementia and alzheimer's disease are modified by leucocyte telomere length: A population-based cohort study. *Sci Rep* (2023) 13(1):6163. doi: 10.1038/s41598-023-32974-x

278. Okada M, Kim HW, Matsu-Ura K, Wang YG, Xu M, Ashraf M. Abrogation of age-induced microrna-195 rejuvenates the senescent mesenchymal stem cells by reactivating telomerase. *Stem Cells* (2015) 34(1):148–59. doi: 10.1002/stem.2211

279. Topiwala A, Nichols TE, Williams LZJ, Robinson EC, Alfaro-Almagro F, Taschler B, et al. Telomere length and brain imaging phenotypes in uk biobank. *PloS One* (2023) 18(3):e0282363. doi: 10.1371/journal.pone.0282363

280. Cardoso S, López IP, Piñeiro-Hermida S, Pichel JG, Moreira PI. Igf1r deficiency modulates brain signaling pathways and disturbs mitochondria and redox homeostasis. *Biomedicines* (2021) 9(2):158. doi: 10.3390/biomedicines9020158

281. Maiese K. Stem cell guidance through the mechanistic target of rapamycin. *World J Stem Cells* (2015) 7(7):999–1009. doi: 10.4252/wjsc.v7.i7.999

282. Amidfar M, Garcez ML, Kim YK. The shared molecular mechanisms underlying aging of the brain, major depressive disorder, and alzheimer's disease: the role of circadian rhythm disturbances. *Prog Neuropsychopharmacol Biol Psychiatry* (2023) 123:110721. doi: 10.1016/j.pnpbp.2023.110721

283. Chen YL, Hsieh CC, Chu PM, Chen JY, Huang YC, Chen CY. Roles of protein tyrosine phosphatases in hepatocellular carcinoma progression (Review). *Oncol Rep* (2023) 49(3):48. doi: 10.3892/or.2023.8485

284. Hafez N, Refaat L, ElGebaly OK, Elhariry HM, Ghareeb M, Fathalla LA. Prognostic value of rgs1 and mtor immunohistochemical expression in Egyptian multiple myeloma patients; a single center study. *PloS One* (2023) 18(7):e0288357. doi: 10.1371/journal.pone.0288357

285. Meng JJ, Shen JW, Li G, Ouyang CJ, Hu JX, Li ZS, et al. Light modulates glucose metabolism by a retina-hypothalamus-brown adipose tissue axis. *Cell* (2023) 186 (2):398–412.e17. doi: 10.1016/j.cell.2022.12.024

286. Xu Y, Wang Y, Jiang Y, Liu M, Zhong W, Ge Z, et al. Relationship between cognitive dysfunction and the promoter methylation of per1 and cry1 in patients with cerebral small vessel disease. *Front Aging Neurosci* (2023) 15:1174541. doi: 10.3389/fnagi.2023.1174541

287. Fakouri NB, Hou Y, Demarest TG, Christiansen LS, Okur MN, Mohanty JG, et al. Towards understanding genomic instability, mitochondrial dysfunction and aging. *FEBS J* (2018) 286(6):1058–73. doi: 10.1111/febs.14663

288. Lai YF, Wang L, Liu WY. Nicotinamide pretreatment alleviates mitochondrial stress and protects hypoxic myocardial cells via ampk pathway. *Eur Rev Med Pharmacol Sci* (2019) 23(4):1797–806. doi: 10.26355/eurrev_201902_17143

289. Albiero M, Poncina N, Tjwa M, Ciciliot S, Menegazzo L, Ceolotto G, et al. Diabetes causes bone marrow autonomic neuropathy and impairs stem cell mobilization via dysregulated P66shc and sirt1. *Diabetes* (2014) 63(4):1353–65. doi: 10.2337/db13-0894

290. Gomes MB, Negrato CA. Alpha-lipoic acid as a pleiotropic compound with potential therapeutic use in diabetes and other chronic diseases. *Diabetol Metab syndrome* (2014) 6(1):80. doi: 10.1186/1758-5996-6-80

291. Khoshdel A, Carney S, Gillies A, Mourad A, Jones B, Nanra R, et al. Potential roles of erythropoietin in the management of anaemia and other complications diabetes. *Diabetes Obes Metab* (2008) 10(1):1–9. doi: 10.1111/j.1463-1326.2007.00711.x

292. Atef MM, El-Sayed NM, Ahmed AAM, Mostafa YM. Donepezil improves neuropathy through activation of ampk signalling pathway in streptozotocin-induced diabetic mice. *Biochem Pharmacol* (2019) 159:1–10. doi: 10.1016/j.bcp.2018.11.006

293. Jenwitheesuk A, Nopparat C, Mukda S, Wongchitrat P, Govitrapong P. Melatonin regulates aging and neurodegeneration through energy metabolism, epigenetics, autophagy and circadian rhythm pathways. *Int J Mol Sci* (2014) 15 (9):16848–84. doi: 10.3390/ijms150916848

294. Lee HJ, Yang SJ. Supplementation with nicotinamide riboside reduces brain inflammation and improves cognitive function in diabetic mice. *Int J Mol Sci* (2019) 20 (17):4196. doi: 10.3390/ijms20174196

295. Ong WY, Wu YJ, Farooqui T, Farooqui AA. Qi fu yin-a ming dynasty prescription for the treatment of dementia. *Mol Neurobiol* (2018) 55(9):7389–400. doi: 10.1007/s12035-018-0908-0

296. Othman MAM, Rajab E, AlMubarak A, AlNaisar M, Bahzad N, Kamal A. Erythropoietin protects against cognitive impairment and hippocampal neurodegeneration in diabetic mice. *Behav Sci (Basel Switzerland)* (2018) 9(1):4. doi: 10.3390/bs9010004

297. Crespo MC, Tome-Carneiro J, Pintado C, Davalos A, Visioli F, Burgos-Ramos E. Hydroxytyrosol restores proper insulin signaling in an astrocytic model of alzheimer's disease. *BioFactors (Oxford England)* (2017) 43(4):540–8. doi: 10.1002/biof.1356

298. Fan X, Zhao Z, Wang D, Xiao J. Glycogen synthase kinase-3 as a key regulator of cognitive function. *Acta Biochim Biophys Sin* (2020) 52(3):219–30. doi: 10.1093/abbs/gmz156

299. Hu Z, Jiao R, Wang P, Zhu Y, Zhao J, De Jager P, et al. Shared causal paths underlying alzheimer's dementia and type 2 diabetes. *Sci Rep* (2020) 10(1):4107. doi: 10.1038/s41598-020-60682-3

300. Li F, Chong ZZ, Maiese K. Cell life versus cell longevity: the mysteries surrounding the nad(+) precursor nicotinamide. *Curr Med Chem* (2006) 13(8):883–95. doi: 10.2174/092986706776361058

301. Su M, Naderi K, Samson N, Youssef I, Fulop L, Bozso Z, et al. Mechanisms associated with type 2 diabetes as a risk factor for alzheimer-related pathology. *Mol Neurobiol* (2019) 56(8):5815–34. doi: 10.1007/s12035-019-1475-8

302. Yamashima T, Ota T, Mizukoshi E, Nakamura H, Yamamoto Y, Kikuchi M, et al. Intake of Ω-6 polyunsaturated fatty acid-rich vegetable oils and risk of lifestyle diseases. *Adv Nutr* (2020) 11(6):1489–509. doi: 10.1093/advances/nmaa072

303. Feng H, Xue M, Deng H, Cheng S, Hu Y, Zhou C. Ginsenoside and its therapeutic potential for cognitive impairment. *Biomolecules* (2022) 12(9):1310. doi: 10.3390/biom12091310

304. Fessel J. Cure of alzheimer's dementia requires addressing all of the affected brain cell types. *J Clin Med* (2023) 12(2049):1–14. doi: 10.3390/jcm12052049

305. Maiese K. Cognitive impairment and dementia: gaining insight through circadian clock gene pathways. *Biomolecules* (2021) 11(7):1–18. doi: 10.3390/biom11071002

306. Perluigi M, Di Domenico F, Barone E, Butterfield DA. Mtor in alzheimer disease and its earlier stages: links to oxidative damage in the progression of this dementing disorder. *Free Radic Biol Med* (2021) 169:382–96. doi: 10.1016/j.freeradbiomed.2021.04.025

307. Rehman IU, Khan A, Ahmad R, Choe K, Park HY, Lee HJ, et al. Neuroprotective effects of nicotinamide against mptp-induced parkinson's disease in mice: impact on oxidative stress, neuroinflammation, nrf2/ho-1 and tlr4 signaling pathways. *Biomedicines* (2022) 10(11):2929. doi: 10.3390/biomedicines10112929

308. Zhu G, Tong Q, Ye X, Li J, Zhou L, Sun P, et al. Phototherapy for cognitive function in patients with dementia: A systematic review and meta-analysis. *Front Aging Neurosci* (2022) 14:936489. doi: 10.3389/fnagi.2022.936489

309. Ding MR, Qu YJ, Hu B, An HM. Signal pathways in the treatment of alzheimer's disease with traditional chinese medicine. *BioMed Pharmacother* (2022) 152:113208. doi: 10.1016/j.biopha.2022.113208

310. Jayaraman A, Reynolds R. Diverse pathways to neuronal necroptosis in alzheimer's disease. *Eur J Neurosci* (2022) 56(9):5428–41. doi: 10.1111/ejn.15662

311. Rani S, Dhar SB, Khajuria A, Gupta D, Jaiswal PK, Singla N, et al. Advanced overview of biomarkers and techniques for early diagnosis of alzheimer's disease. *Cell Mol Neurobiol* (2023) 43(6):2491–523. doi: 10.1007/s10571-023-01330-y

312. Tong Z, Chu G, Wan C, Wang Q, Yang J, Meng Z, et al. Multiple metabolites derived from mushrooms and their beneficial effect on alzheimer's diseases. *Nutrients* (2023) 15(12):2758. doi: 10.3390/nu15122758

313. Wang MD, Zhang S, Liu XY, Wang PP, Zhu YF, Zhu JR, et al. Salvianolic acid B ameliorates retinal deficits in an early-stage alzheimer's disease mouse model through downregulating bace1 and Aβ Generation. *Acta Pharmacol Sin* (2023). doi: 10.1038/s41401-023-01125-3

314. Maiese K. Impacting dementia and cognitive loss with innovative strategies: mechanistic target of rapamycin, clock genes, circular non-coding ribonucleic acids, and rho/rock. *Neural regeneration Res* (2019) 14(5):773–4. doi: 10.4103/1673-5374.249224

315. Rantanen LM, Bitar M, Lampinen R, Stewart R, Quek H, Oikari LE, et al. An alzheimer's disease patient-derived olfactory stem cell model identifies gene expression changes associated with cognition. *Cells* (2022) 11(20):3258. doi: 10.3390/cells11203258

316. Schubert CR, Paulsen AJ, Pinto AA, Merten N, Cruickshanks KJ. Effect of long-term storage on the reliability of blood biomarkers for alzheimer's disease and neurodegeneration. *J Alzheimers Dis* (2022) 85(3):1021–9. doi: 10.3233/jad-215096

317. Shiravandi A, Yari F, Tofigh N, Kazemi Ashtiani M, Shahpasand K, Ghanian MH, et al. Earlier detection of alzheimer's disease based on a novel biomarker cis P-tau by a label-free electrochemical immunosensor. *Biosensors (Basel)* (2022) 12(10):879. doi: 10.3390/bios12100879

318. Tang B, Zeng W, Song LL, Wang HM, Qu LQ, Lo HH, et al. Extracellular vesicle delivery of neferine for the attenuation of neurodegenerative disease proteins and motor deficit in an alzheimer's disease mouse model. *Pharm (Basel Switzerland)* (2022) 15(1):83. doi: 10.3390/ph15010083

319. Agarwal D, Kumari R, Ilyas A, Tyagi S, Kumar R, Poddar NK. Crosstalk between epigenetics and mtor as a gateway to new insights in pathophysiology and treatment of alzheimer's disease. *Int J Biol macromolecules* (2021) 192:895–903. doi: 10.1016/j.ijbiomac.2021.10.026

320. Xu P, Wu Z, Peng Y, Gao J, Zheng F, Tan J, et al. Neuroprotection of triptolide against amyloid-beta1-42-induced toxicity via the akt/mtor/P70s6k-mediated autophagy pathway. *Acad Bras Cienc* (2022) 94(2):e20210938. doi: 10.1590/0001-3765202220210938

321. Filley CM, Rollins YD, Anderson CA, Arciniegas DB, Howard KL, Murrell JR, et al. The genetics of very early onset alzheimer disease. *Cogn Behav Neurol* (2007) 20 (3):149–56. doi: 10.1097/WNN.0b013e318145a8c8

322. Agis-Torres A, Solhuber M, Fernandez M, Sanchez-Montero JM. Multi-target-directed ligands and other therapeutic strategies in the search of a real solution for

alzheimer's disease. *Curr neuropharmacology* (2014) 12(1):2–36. doi: 10.2174/1570159x113116660047

323. Morris G, Berk M, Maes M, Puri BK. Could alzheimer's disease originate in the periphery and if so how so? *Mol Neurobiol* (2019) 56(1):406–34. doi: 10.1007/s12035-018-1092-y

324. Safdari Lord J, Soltani Rezaiezadeh J, Yekaninejad MS, Izadi P. The association of apoe genotype with covid-19 disease severity. *Sci Rep* (2022) 12(1):13483. doi: 10.1038/s41598-022-17262-4

325. Maiese K. Apolipoprotein-E4 allele (Apoe-E4) as a mediator of cognitive loss and dementia in long covid-19. *Curr Neurovasc Res* (2022) 19(5):435–9. doi: 10.2174/1567202619052212271146 24

326. Kurki SN, Kantonen J, Kaivola K, Hokkanen L, Mäyränpää MI, Puttonen H, et al. Apoe E4 associates with increased risk of severe covid-19, cerebral microhaemorrhages and post-covid mental fatigue: A finnish biobank, autopsy and clinical study. *Acta neuropathologica Commun* (2021) 9(1):199. doi: 10.1186/s40478-021-01302-7

327. Momkute L, Vilkeviciute A, Gedvilaite G, Dubinskaite G, Kriauciuniene L, Liutkeviciene R. Association of apoe serum levels and apoe E2, E3, and E4 alleles with optic neuritis. *Genes (Basel)* (2022) 13(7):1188. doi: 10.3390/genes13071188

328. Ojo JO, Reed JM, Crynen G, Vallabhaneni P, Evans J, Shackleton B, et al. Apoe genotype dependent molecular abnormalities in the cerebrovasculature of alzheimer's disease and age-matched non-demented brains. *Mol Brain* (2021) 14(1):110. doi: 10.1186/s13041-021-00803-9

329. Di Patre PL, Read SL, Cummings JL, Tomiyasu U, Vartavarian LM, Secor DL, et al. Progression of clinical deterioration and pathological changes in patients with alzheimer disease evaluated at biopsy and autopsy. *Arch Neurol* (1999) 56(10):1254–61. doi: 10.1001/archneur.56.10.1254

330. Maiese K, Chong ZZ. Nicotinamide: necessary nutrient emerges as a novel cytoprotectant for the brain. *Trends Pharmacol Sci* (2003) 24(5):228–32. doi: 10.1016/S0165-6147(03)00078-6

331. Maiese K, Vincent AM. Membrane asymmetry and DNA degradation: functionally distinct determinants of neuronal programmed cell death. *J Neurosci Res* (2000) 59(4):568–80. doi: 10.1002/(SICI)1097-4547(20000215)59:4<568::AID-JNR13>3.0.CO;2-R

332. Lee G, Pollard HB, Arispe N. Annexin 5 and Apolipoprotein E2 Protect against Alzheimer's Amyloid-Beta-Peptide Cytotoxicity by Competitive Inhibition at a Common Phosphatidylserine Interaction Site. *Peptides* (2002) 23(7):1249–63. doi: 10.1016/s0196-9781(02)00060-8

333. Cacabelos R, Carril JC, Cacabelos N, Kazantsev AG, Vostrov AV, Corzo L, et al. Sirtuins in alzheimer's disease: sirt2-related genophenotypes and implications for pharmacoepigenetics. *Int J Mol Sci* (2019) 20(5):1249. doi: 10.3390/ijms20051249

334. Zheng H, Jia L, Liu CC, Li Zhong ZR, Yang L, Chen XF, et al. Trem2 promotes microglial survival by activating wnt/beta-catenin pathway. *J Neurosci* (2017) 37 (7):1771–84. doi: 10.1523/jneurosci.2459-16.2017

335. Liu Z, Huang H, Yu Y, Jia Y, Li L, Shi X, et al. Exploring the potential mechanism of action of ursolic acid against gastric cancer and covid-19 using network pharmacology and bioinformatics analysis. *Curr Pharm Des* (2023) 29(16):1274–92. doi: 10.2174/1381612829666230510124716

336. Theoharides TC. Could sars-cov-2 spike protein be responsible for long-covid syndrome? *Mol Neurobiol* (2022) 59(3):1850–61. doi: 10.1007/s12035-021-02696-0

337. Sungnak W, Huang N, Becavin C, Berg M, Queen R, Litvinukova M, et al. Sars-cov-2 entry factors are highly expressed in nasal epithelial cells together with innate immune genes. *Nat Med* (2020) 26(5):681–7. doi: 10.1038/s41591-020-0868-6

338. Al-Qahtani AA, Pantazi I, Alhamlan FS, Alothaid H, Matou-Nasri S, Sourvinos G, et al. Sars-cov-2 modulates inflammatory responses of alveolar epithelial type ii cells via pi3k/akt pathway. *Front Immunol* (2022) 13:1020624. doi: 10.3389/fimmu.2022.1020624

339. Geier C, Perl A. Therapeutic mtor blockade in systemic autoimmunity: implications for antiviral immunity and extension of lifespan. *Autoimmun Rev* (2021) 20(12):102984. doi: 10.1016/j.autrev.2021.102984

340. Shirzad M, Nourigorji M, Sajedi A, Ranjbar M, Rasti F, Sourani Z, et al. Targeted therapy in coronavirus disease 2019 (Covid-19): implication from cell and gene therapy to immunotherapy and vaccine. *Int Immunopharmacol* (2022) 111:109161. doi: 10.1016/j.intimp.2022.109161

341. Jansen van Vuren E, Steyn SF, Brink CB, Möller M, Viljoen FP, Harvey BH. The neuropsychiatric manifestations of covid-19: interactions with psychiatric illness and pharmacological treatment. *BioMed Pharmacother* (2021) 135:111200. doi: 10.1016/j.biopha.2020.111200

342. Blagosklonny MV. From causes of aging to death from covid-19. *Aging (Albany NY)* (2020) 12(11):10004–21. doi: 10.18632/aging.103493

343. Borges do Nascimento IJ, Cacic N, Abdulazeem HM, von Groote TC, Jayarajah U, Weerasekara I, et al. Novel coronavirus infection (Covid-19) in humans: A scoping review and meta-analysis. *J Clin Med* (2020) 9(4):941. doi: 10.3390/jcm9040941

344. Gusev E, Sarapultsev A, Hu D, Chereshnev V. Problems of pathogenesis and pathogenetic therapy of covid-19 from the perspective of the general theory of pathological systems (General pathological processes). *Int J Mol Sci* (2021) 22 (14):7582. doi: 10.3390/ijms22147582

345. Cavalli E, Bramanti A, Ciurleo R, Tchorbanov AI, Giordano A, Fagone P, et al. Entangling covid-19 associated thrombosis into a secondary antiphospholipid antibody syndrome: diagnostic and therapeutic perspectives (Review). *Int J Mol Med* (2020) 46 (3):903–12. doi: 10.3892/ijmm.2020.4659

346. González-Fernández C, González P, González-Pérez F, Rodríguez F. Characterization of ex vivo and in vitro wnt transcriptome induced by spinal cord injury in rat microglial cells. *Brain Sci* (2022) 12(708):708. doi: 10.3390/brainsci12060708

347. Liu D, Zhang M, Tian J, Gao M, Liu M, Fu X, et al. Wnt1-inducible signalling pathway protein 1 stabilizes atherosclerotic plaques in apolipoprotein-E-deficient mice via the focal adhesion kinase/mitogen-activated extracellular signal-regulated kinase/extracellular signal-regulated kinase pathway. *J hypertension* (2022) 40(9):1666–81. doi: 10.1097/hjh.0000000000003195

348. Liu L, Xu S, Li P, Li L. A novel adipokine wisp1 attenuates lipopolysaccharide-induced cell injury in 3t3-L1 adipocytes by regulating the pi3k/akt pathway. *Obes Res Clin Pract* (2022) 16(2):122–9. doi: 10.1016/j.orcp.2022.03.001

349. Ren LL, Zhou JY, Liang SJ, Wang XQ. Impaired intestinal stem cell activity in etec infection: enterotoxins, cyclic nucleotides, and wnt signaling. *Arch Toxicol* (2022) 96(5):1213–25. doi: 10.1007/s00204-021-03213-x

350. Tang Y, Chen Y, Liu R, Li W, Hua B, Bao Y. Wnt signaling pathways: A role in pain processing. *Neuromolecular Med* (2022) 24(3):233–49. doi: 10.1007/s12017-021-08700-z

351. Marinelli C, Bertalot T, Zusso M, Skaper SD, Giusti P. Systematic review of pharmacological properties of the oligodendrocyte lineage. *Front Cell Neurosci* (2016) 10:27. doi: 10.1007/s13311-020-00923-5

352. Gökdoğan Edgünlü T, Ünal Y, Karakaş Çelik S, Genç Ö, Emre U, Kutlu G. The effect of foxo gene family variants and global DNA metylation on rrms disease. *Gene* (2020) 726:144172. doi: 10.1016/j.gene.2019.144172

353. Kell DB, Pretorius E. No effects without causes: the iron dysregulation and dormant microbes hypothesis for chronic, inflammatory diseases. *Biol Rev Cambridge Philos Soc* (2018) 93(3):1518–57. doi: 10.1111/brv.12407

354. Maiese K. Novel insights for multiple sclerosis and demyelinating disorders with apoptosis, autophagy, foxo, and mtor. *Curr Neurovasc Res* (2021) 18(2):1–4. doi: 10.2174/1567202618999210505124235

355. Oktelik FB, Yilmaz V, Turkoglu R, Akbayir E, Tuzun E, Deniz G, et al. Expression of akt1 and P-akt1 in peripheral T cell subsets of multiple sclerosis patients. *Acta Neurol Belg* (2020) 121(6):1777–82. doi: 10.1007/s13760-020-01518-9

356. Sanadgol N, Barati M, Houshmand F, Hassani S, Clarner T, Shahlaei M, et al. Metformin accelerates myelin recovery and ameliorates behavioral deficits in the animal model of multiple sclerosis via adjustment of ampk/nrf2/mtor signaling and maintenance of endogenous oligodendrogenesis during brain self-repairing period. *Pharmacol Rep* (2020) 72(3):641–58. doi: 10.1007/s43440-019-00019-8

357. Wallin MT, Culpepper WJ, Campbell JD, Nelson LM, Langer-Gould A, Marrie RA, et al. The prevalence of ms in the United States: A population-based estimate using health claims data. *Neurology* (2019) 92(10):e1029–e40. doi: 10.1212/wnl.0000000000007035

358. Xu L, Zhang C, Jiang N, He D, Bai Y, Xin Y. Rapamycin combined with mcc950 to treat multiple sclerosis in experimental autoimmune encephalomyelitis. *J Cell Biochem* (2019) 120(4):5160–8. doi: 10.1002/jcb.27792

359. Zhang YC, Fan KY, Wang Q, Hu JX, Wang Q, Zhang HY, et al. Genetically determined levels of mtor-dependent circulating proteins and risk of multiple sclerosis. *Neurol Ther* (2023) 12(3):751–62. doi: 10.1007/s40120-023-00455-y

360. Hemmer B, Cepok S, Zhou D, Sommer N. Multiple sclerosis - a coordinated immune attack across the blood brain barrier. *Curr Neurovasc Res* (2004) 1(2):141–50. doi: 10.2174/1567202043480152

361. Maiese K. The challenges for drug development: cytokines, genes, and stem cells. *Curr Neurovasc Res* (2012) 9(4):231–2. doi: 10.2174/156720212803530690

362. Martin A, Tegla CA, Cudrici CD, Kruszewski AM, Azimzadeh P, Boodhoo D, et al. Role of sirt1 in autoimmune demyelination and neurodegeneration. *Immunologic Res* (2015) 61(3):187–97. doi: 10.1007/s12026-014-8557-5

363. Mouzaki A, Rodi M, Dimisianos N, Emmanuil A, Kalavrizioti D, Lagoudaki R, et al. Immune parameters that distinguish multiple sclerosis patients from patients with other neurological disorders at presentation. *PloS One* (2015) 10(8):e0135434. doi: 10.1371/journal.pone.0135434

364. Rodi M, Dimisianos N, de Lastic AL, Sakellaraki P, Deraos G, Matsoukas J, et al. Regulatory cell populations in relapsing-remitting multiple sclerosis (Rrms) patients: effect of disease activity and treatment regimens. *Int J Mol Sci* (2016) 17(9):1398. doi: 10.3390/ijms17091398

365. Sun JJ, Ren QG, Xu L, Zhang ZJ. Lingo-1 antibody ameliorates myelin impairment and spatial memory deficits in experimental autoimmune encephalomyelitis mice. *Sci Rep* (2015) 5:14235. doi: 10.1038/srep14235

366. Yap SM, Davenport L, Cogley C, Craddock F, Kennedy A, Gaughan M, et al. Word finding, prosody and social cognition in multiple sclerosis. *J Neuropsychol* (2023) 17(1):32–62. doi: 10.1111/jnp.12285

367. Staff NP, Lucchinetti CF, Keegan BM. Multiple sclerosis with predominant, severe cognitive impairment. *Arch Neurol* (2009) 66(9):1139–43. doi: 10.1001/archneurol.2009.190

368. Naseri A, Baghernezhad K, Seyedi-Sahebari S, Alhoseini SA, Gholipour-Khalili E, Zafarani F, et al. (Apoe) genotype and cognitive outcomes in multiple sclerosis; a systematic review and meta-analysis. *Mult Scler Relat Disord* (2022) 65:104011. doi: 10.1016/j.msard.2022.104011

369. Fedeli U, Amidei CB, Avossa F, Schievano E, Kingwell E. Association of multiple sclerosis-related mortality with covid-19 and other common infections: A multiple causes of death analysis. *Eur J Neurol* (2023) 30(9):2870–3. doi: 10.1111/ene.15912

370. Bramante C, Ingraham N, Murray T, Marmor S, Hoversten S, Gronski J, et al. Observational study of metformin and risk of mortality in patients hospitalized with covid-19. *medRxiv* (2020). doi: 10.1101/2020.06.19.20135095

371. Tiu VE, Popescu BO, Enache II, Tiu C, Terecoasa E, Panea CA. Serum and csf biomarkers predict active early cognitive decline rather than established cognitive impairment at the moment of rrms diagnosis. *Diagnostics (Basel)* (2022) 12(11):2571. doi: 10.3390/diagnostics12112571

372. Diallo AB, Gay L, Coiffard B, Leone M, Mezouar S, Mege JL. Daytime variation in sars-cov-2 infection and cytokine production. *Microb Pathog* (2021) 158:105067. doi: 10.1016/j.micpath.2021.105067

373. Gu X, Zhu J. Roles of exosomes and exosomal micrornas in postoperative sleep disturbance. *Nat Sci Sleep* (2021) 13:1363–75. doi: 10.2147/nss.S310351

374. Lio CT, Kacprowski T, Klaedtke M, Jensen LR, Bouter Y, Bayer TA, et al. Small rna sequencing in the tg4-42 mouse model suggests the involvement of snornas in the etiology of alzheimer's disease. *J Alzheimers Dis* (2022) 87(4):1671–81. doi: 10.3233/jad-220110

375. Zhang W, Bai S, Yang J, Zhang Y, Liu Y, Nie J, et al. Foxo1 overexpression reduces Aβ Production and tau phosphorylation in vitro. *Neurosci Lett* (2020) 738:135322. doi: 10.1016/j.neulet.2020.135322

376. Zhao W, Xie C, Zhang X, Liu J, Liu J, Xia Z. Advances in the mtor signaling pathway and its inhibitor rapamycin in epilepsy. *Brain Behav* (2023) 13(6):e2995. doi: 10.1002/brb3.2995

377. El-Beltagy A, Saleh AMB, Attaallah A, Gahnem RA. Therapeutic role of azadirachta indica leaves ethanolic extract against diabetic nephropathy in rats neonatally induced by streptozotocin. *Ultrastruct Pathol* (2021) 46(6):391–406. doi: 10.1080/01913123.2021.1988015

378. Espinoza SE, Khosla S, Baur JA, de Cabo R, Musi N. Drugs targeting mechanisms of aging to delay age-related disease and promote healthspan: proceedings of a national institute on aging workshop. *J Gerontol A Biol Sci Med Sci* (2023) 78(Supplement_1):53–60. doi: 10.1093/gerona/glad034

379. McCoin CS, Franczak E, Deng F, Pei D, Ding WX, Thyfault JP. Acute exercise rapidly activates hepatic mitophagic flux. *J Appl Physiol* (2022) 132(3):862–73. doi: 10.1152/japplphysiol.00704.2021

380. Lee JH, Lee JH, Jin M, Han SD, Chon GR, Kim IH, et al. Diet control to achieve euglycemia induces significant loss of heart and liver weight via increased autophagy compared with ad libitum diet in diabetic rats. *Exp Mol Med* (2014) 46:e111. doi: 10.1038/emm.2014.52

381. Al-Kuraishy HM, Al-Buhadily AK, Al-Gareeb AI, Alorabi M, Hadi Al-Harcan NA, El-Bouseary MM, et al. Citicoline and covid-19: vis-À-vis conjectured. *Naunyn Schmiedebergs Arch Pharmacol* (2022) 395(12):1463–75. doi: 10.1007/s00210-022-02284-6

382. Al-Kuraishy HM, Al-Gareeb AI, Al-Maiahy TJ, Alexiou A, Mukerjee N, Batiha GE. Prostaglandins and non-steroidal anti-inflammatory drugs in covid-19. *Biotechnol Genet Eng Rev* (2022), 1–21. doi: 10.1080/02648725.2022.2122290

383. Assogna M, Di Lorenzo F, Martorana A, Koch G. Synaptic effects of palmitoylethanolamide in neurodegenerative disorders. *Biomolecules* (2022) 12 (8):1161. doi: 10.3390/biom12081161

384. Braun S, Zaucke F, Brenneis M, Rapp AE, Pollinger P, Sohn R, et al. The corpus adiposum infrapatellare (Hoffa's fat pad)-the role of the infrapatellar fat pad in osteoarthritis pathogenesis. *Biomedicines* (2022) 10(5):1071. doi: 10.3390/biomedicines10051071

385. Maiese K, Li F, Chong ZZ. New avenues of exploration for erythropoietin. *Jama* (2005) 293(1):90–5. doi: 10.1001/jama.293.1.90

386. Martins B, Vieira M, Delerue-Matos C, Grosso C, Soares C. Biological potential, gastrointestinal digestion, absorption, and bioavailability of algae-derived compounds with neuroprotective activity: A comprehensive review. *Mar Drugs* (2022) 20(6):362. doi: 10.3390/md20060362

387. Pan J, Zhou L, Zhang C, Xu Q, Sun Y. Targeting protein phosphatases for the treatment of inflammation-related diseases: from signaling to therapy. *Signal Transduct Target Ther* (2022) 7(1):177. doi: 10.1038/s41392-022-01038-3

388. Pantazi P, Clements T, Venø M, Abrahams VM, Holder B. Distinct non-coding rna cargo of extracellular vesicles from M1 and M2 human primary macrophages. *J Extracell Vesicles* (2022) 11(12):e12293. doi: 10.1002/jev2.12293

389. Liu M, Jiang L, Cao W, Wu J, Chen X. Identification of inhibitors and drug targets for human adenovirus infections. *Viruses* (2022) 14(5):959. doi: 10.3390/v14050959

390. Zhou Y, Xu J, Hou Y, Leverenz JB, Kallianpur A, Mehra R, et al. Network medicine links sars-cov-2/covid-19 infection to brain microvascular injury and neuroinflammation in dementia-like cognitive impairment. *Alzheimers Res Ther* (2021) 13(1):110. doi: 10.1186/s13195-021-00850-3

391. Zhuang X, Tsukuda S, Wrensch F, Wing PA, Schilling M, Harris JM, et al. The circadian clock component bmal1 regulates sars-cov-2 entry and replication in lung epithelial cells. *iScience* (2021) 24(10):103144. doi: 10.1101/2021.03.20.436163

392. Birnie MT, Claydon MDB, Troy O, Flynn BP, Yoshimura M, Kershaw YM, et al. Circadian regulation of hippocampal function is disrupted with corticosteroid treatment. *Proc Natl Acad Sci U.S.A.* (2023) 120(15):e2211996120. doi: 10.1073/pnas.2211996120

393. Li JB, Hu XY, Chen MW, Xiong CH, Zhao N, Ge YH, et al. P85s6k sustains synaptic glua1 to ameliorate cognitive deficits in alzheimer's disease. *Trans neurodegeneration* (2023) 12(1):1. doi: 10.1186/s40035-022-00334-w

394. Felten M, Dame C, Lachmann G, Spies C, Rubarth K, Balzer F, et al. Circadian rhythm disruption in critically ill patients. *Acta Physiol (Oxf)* (2023) 238(1):e13962. doi: 10.1111/apha.13962

395. Huang C, Zhang C, Cao Y, Li J, Bi F. Major roles of the circadian clock in cancer. *Cancer Biol Med* (2023) 20(1):1–24. doi: 10.20892/j.issn.2095-3941.2022.0474

396. Kalam F, James DL, Li YR, Coleman MF, Kiesel VA, Cespedes Feliciano EM, et al. Intermittent fasting interventions to leverage metabolic and circadian mechanisms for cancer treatment and supportive care outcomes. *J Natl Cancer Inst Monogr* (2023) 2023(61):84–103. doi: 10.1093/jncimonographs/lgad008

397. Chong ZZ, Kang JQ, Maiese K. Metabotropic glutamate receptors promote neuronal and vascular plasticity through novel intracellular pathways. *Histol Histopathol* (2003) 18(1):173–89. doi: 10.14670/HH-18.173

398. Lin SH, Maiese K. The metabotropic glutamate receptor system protects against ischemic free radical programmed cell death in rat brain endothelial cells. *J Cereb Blood Flow Metab* (2001) 21(3):262–75. doi: 10.1097/00004647-200103000-00010

399. Cheng X, Song C, Du Y, Gaur U, Yang M. Pharmacological treatment of alzheimer's disease: insights from drosophila melanogaster. *Int J Mol Sci* (2020) 21 (13):4621. doi: 10.3390/ijms21134621

400. Maiese K. Foxo proteins in the nervous system. *Anal Cell Pathol (Amst)* (2015) 2015:569392. doi: 10.1155/2015/569392

401. van Dyck CH, Swanson CJ, Aisen P, Bateman RJ, Chen C, Gee M, et al. Lecanemab in early alzheimer's disease. *N Engl J Med* (2023) 388(1):9–21. doi: 10.1056/NEJMoa2212948

402. Slezáková D, Kadlic P, Jezberová M, Boleková V, Valkovič P, Minar M. Brain volume loss in multiple sclerosis is independent of disease activity and might be prevented by early disease-modifying therapy. *Neurol Neurochir Pol* (2023) 57(3):282–8. doi: 10.5603/PJNNS.a2023.0031

403. Kaisinger LR, Kentistou KA, Stankovic S, Gardner EJ, Day FR, Zhao Y, et al. Large-scale exome sequence analysis identifies sex- and age-specific determinants of obesity. *Cell Genomics* (2023) 3(8):100362. doi: 10.1016/j.xgen.2023.100362

404. Dong J, Li H, Bai Y, Wu C. Muscone ameliorates diabetic peripheral neuropathy through activating akt/mtor signalling pathway. *J Pharm Pharmacol* (2019) 71(11):1706–13. doi: 10.1111/jphp.13157

405. Lan T, Xu Y, Li S, Li N, Zhang S, Zhu H. Cornin protects against cerebral ischemia/reperfusion injury by preventing autophagy via the pi3k/akt/mtor pathway. *BMC Pharmacol Toxicol* (2022) 23(1):82. doi: 10.1186/s40360-022-00620-3

406. Sharma N, Shandilya A, Kumar N, Mehan S. Dysregulation of sirt-1 signaling in multiple sclerosis and neuroimmune disorders: A systematic review of sirtuin activators as potential immunomodulators and their influences on other dysfunctions. *Endocr Metab Immune Disord Drug Targets* (2021) 21(10):1845–68. doi: 10.2174/1871530321666210309112234

407. Yang X, Huo F, Liu B, Liu J, Chen T, Li J, et al. Crocin inhibits oxidative stress and pro-inflammatory response of microglial cells associated with diabetic retinopathy through the activation of pi3k/akt signaling pathway. *J Mol Neurosci* (2017) 61(4):581–9. doi: 10.1007/s12031-017-0899-8

408. Klionsky DJ, Abdel-Aziz AK, Abdelfatah S, Abdellatif M, Abdoli A, Abel S, et al. Guidelines for the use and interpretation of assays for monitoring autophagy (4th edition). *Autophagy* (2021) 17(1):1–382. doi: 10.1080/15548627.2020.1797280

409. Maiese K, Chong ZZ, Shang YC, Wang S. Targeting disease through novel pathways of apoptosis and autophagy. *Expert Opin Ther Targets* (2012) 16(12):1203–14. doi: 10.1517/14728222.2012.719499

410. Farahani M, Niknam Z, Mohammadi Amirabad L, Amiri-Dashatan N, Koushki M, Nemati M, et al. Molecular pathways involved in covid-19 and potential pathway-based therapeutic targets. *BioMed Pharmacother* (2021) 145:112420. doi: 10.1016/j.biopha.2021.112420

411. Yan WT, Lu S, Yang YD, Ning WY, Cai Y, Hu XM, et al. Research trends, hot spots and prospects for necroptosis in the field of neuroscience. *Neural regeneration Res* (2021) 16(8):1628–37. doi: 10.4103/1673-5374.303032

412. Chong ZZ, Shang YC, Maiese K. Vascular injury during elevated glucose can be mitigated by erythropoietin and wnt signaling. *Curr Neurovasc Res* (2007) 4(3):194–204. doi: 10.2174/156720207781387150

413. Kandula V, Kosuru R, Li H, Yan D, Zhu Q, Lian Q, et al. Forkhead box transcription factor 1: role in the pathogenesis of diabetic cardiomyopathy. *Cardiovasc Diabetol* (2016) 15(1):44. doi: 10.1186/s12933-016-0361-1

414. Weikel KA, Cacicedo JM, Ruderman NB, Ido Y. Knockdown of gsk3beta increases basal autophagy and ampk signaling in nutrient-laden human aortic endothelial cells. *Bioscience Rep* (2016) 36(5):e00382. doi: 10.1042/bsr20160174

415. Barchetta I, Cimini FA, Ciccarelli G, Baroni MG, Cavallo MG. Sick fat: the good and the bad of old and new circulating markers of adipose tissue inflammation. *J endocrinological Invest* (2019) 42(11):1257–72. doi: 10.1007/s40618-019-01052-3

416. Hsieh CF, Liu CK, Lee CT, Yu LE, Wang JY. Acute glucose fluctuation impacts microglial activity, leading to inflammatory activation or self-degradation. *Sci Rep* (2019) 9(1):840. doi: 10.1038/s41598-018-37215-0

417. Maiese K, Chong ZZ, Shang YC, Wang S. Novel directions for diabetes mellitus drug discovery. *Expert Opin Drug Discovery* (2013) 8(1):35–48. doi: 10.1517/17460441.2013.736485

418. Ran D, Hong W, Yan W, Mengdie W. Properties and molecular mechanisms underlying geniposide-mediated therapeutic effects in chronic inflammatory diseases. *J Ethnopharmacol* (2021) 273:113958. doi: 10.1016/j.jep.2021.113958

419. Adle-Biassette H, Levy Y, Colombel M, Poron F, Natchev S, Keohane C, et al. Neuronal apoptosis in hiv infection in adults. *Neuropathol Appl Neurobiol* (1995) 21 (3):218–27. doi: 10.1111/j.1365-2990.1995.tb01053.x

420. Chong ZZ, Shang YC, Hou J, Maiese K. Wnt1 Neuroprotection Translates into Improved Neurological Function During Oxidant Stress and Cerebral Ischemia through Akt1 and Mitochondrial Apoptotic Pathways. *Oxid Med Cell Longev* (2010) 3(2):153–65. doi: 10.4161/oxim.3.2.11758

421. Fu L, Liu C, Chen L, Lv Y, Meng G, Hu M, et al. Protective effects of 1-methylnicotinamide on abeta1-42-induced cognitive deficits, neuroinflammation and apoptosis in mice. *J neuroimmune Pharmacol* (2019) 14(3):401–2. doi: 10.1007/s11481-018-09830-1

422. Groc L, Bezin L, Foster JA, Jiang H, Jackson TS, Weissmann D, et al. Lipid peroxidation-mediated oxidative stress and dopamine neuronal apoptosis in the substantia nigra during development. *Neurochem Int* (2001) 39(2):127–33. doi: 10.1016/s0197-0186(01)00013-4

423. He Z, Zhao Y, Zhu Y, Wang W, Liu X, Lu F. Interfering tug1 attenuates cerebrovascular endothelial apoptosis and inflammatory injury after cerebral ischemia/reperfusion via tug1/mir-410/foxo3 cerna axis. *Neurotox Res* (2021) 40(1):1–13. doi: 10.1007/s12640-021-00446-7

424. Ko HW, Han KS, Kim EY, Ryu BR, Yoon WJ, Jung YK, et al. Synergetic Activation of P38 Mitogen-Activated Protein Kinase and Caspase-3-Like Proteases for Execution of Calyculin a-Induced Apoptosis but Not N-Methyl-D-Aspartate-Induced Necrosis in Mouse Cortical Neurons. *J Neurochem* (2000) 74(6):2455–61. doi: 10.1046/j.1471-4159.2000.0742455.x

425. Mansour RM, El Sayed NS, Ahmed MAE, El-Sahar AE. Addressing peroxisome proliferator-activated receptor-gamma in 3-nitropropionic acid-induced striatal neurotoxicity in rats. *Mol Neurobiol* (2022) 59(7):4368–83. doi: 10.1007/s12035-022-02856-w

426. Zhao T, Miao H, Song Z, Li Y, Xia N, Zhang Z, et al. Metformin alleviates the cognitive impairment induced by benzo[a]Pyrene via glucolipid metabolism regulated by fto/foxo6 pathway in mice. *Environ Sci pollut Res Int* (2023) 30(26):69192–204. doi: 10.1007/s11356-023-27303-8

427. Zhao Y, Lützen U, Gohlke P, Jiang P, Herdegen T, Culman J. Neuroprotective and antioxidative effects of pioglitazone in brain tissue adjacent to the ischemic core are mediated by pi3k/akt and nrf2/are pathways. *J Mol Med (Berlin Germany)* (2021) 99 (8):1073–83. doi: 10.1007/s00109-021-02065-3

428. Mastrapasqua M, Rossi R, De Cosmo L, Resta A, Errede M, Bizzoca A, et al. Autophagy increase in merosin-deficient congenital muscular dystrophy type 1a. *Eur J Transl Myol* (2023) 33(3):11501. doi: 10.4081/ejtm.2023.11501

429. Chong ZZ, Li F, Maiese K. Cellular demise and inflammatory microglial activation during beta-amyloid toxicity are governed by wnt1 and canonical signaling pathways. *Cell Signal* (2007) 19(6):1150–62. doi: 10.1016/j.cellsig.2006.12.009

430. Dehghanian F, Soltani Z, Khaksari M. Can mesenchymal stem cells act multipotential in traumatic brain injury? *J Mol Neurosci* (2020) 70(5):677–88. doi: 10.1007/s12031-019-01475-w

431. Liu A, Wu J, Yang C, Wu Y, Zhang Y, Zhao F, et al. Trpm7 in chbp-induced renoprotection upon ischemia reperfusion-related injury. *Sci Rep* (2018) 8(1):5510. doi: 10.1038/s41598-018-22852-2

432. Simon F, Floros N, Ibing W, Schelzig H, Knapsis A. Neurotherapeutic potential of erythropoietin after ischemic injury of the central nervous system. *Neural regeneration Res* (2019) 14(8):1309–12. doi: 10.4103/1673-5374.253507

433. Zhang Z, Yang JL, Zhang LL, Chen ZZ, Chen JO, Cao YG, et al. 2-(2-Benzofuranyl)-2-Imidazoline Treatment within 5 Hours after Cerebral Ischemia/Reperfusion Protects the Brain. *Neural regeneration Res* (2018) 13(12):2111–8. doi: 10.4103/1673-5374.241461

434. Sun F, Li SG, Zhang HW, Hua FW, Sun GZ, Huang Z. Mirna-411 attenuates inflammatory damage and apoptosis following spinal cord injury. *Eur Rev Med Pharmacol Sci* (2020) 24(2):491–8. doi: 10.26355/eurrev_202001_20022

435. Yue J, Liang C, Wu K, Hou Z, Wang L, Zhang C, et al. Upregulated shp-2 expression in the epileptogenic zone of temporal lobe epilepsy and various effects of shp099 treatment on a pilocarpine model. *Brain Pathol* (2019) 30(2):373–85. doi: 10.1111/bpa.12777

436. Li Y, Liu L, Tian Y, Zhang J. Rapamycin improves sevoflurane–Induced cognitive dysfunction in aged rats by mediating autophagy through the tlr4/myd88/nf–κb signaling pathway. *Mol Med Rep* (2019) 20(4):3085–94. doi: 10.3892/mmr.2019.10541

437. Sun XL, Zhang JB, Guo YX, Xia TS, Xu LC, Rahmand K, et al. Xanthohumol ameliorates memory impairment and reduces the deposition of β-amyloid in app/ps1 mice via regulating the mtor/lc3ii and bax/bcl-2 signalling pathways. *J Pharm Pharmacol* (2021) 73(9):1230–9. doi: 10.1093/jpp/rgab052

438. Wang Y, Gao S, Zheng V, Chen L, Ma M, Shen S, et al. A novel pde4d inhibitor bpn14770 reverses scopolamine-induced cognitive deficits via camp/sirt1/akt/bcl-2 pathway. *Front Cell Dev Biol* (2020) 8:599389. doi: 10.3389/fcell.2020.599389

439. Zhang SH, Liu D, Hu Q, Zhu J, Wang S, Zhou S. Ferulic acid ameliorates pentylenetetrazol-induced seizures by reducing neuron cell death. *Epilepsy Res* (2019) 156:106183. doi: 10.1016/j.eplepsyres.2019.106183

440. Maiese K. Forkhead transcription factors: new considerations for alzheimer's disease and dementia. *J Transl Sci* (2016) 2(4):241–7. doi: 10.15761/JTS.1000146

441. Guo Y, Zeng Q, Brooks D, Geisbrecht ER. A conserved stripak complex is required for autophagy in muscle tissue. *Mol Biol Cell* (2023) 34(9):ar91. doi: 10.1091/mbc.E23-01-0006

442. Thomas SD, Jha NK, Ojha S, Sadek B. Mtor signaling disruption and its association with the development of autism spectrum disorder. *Molecules* (2023) 28 (4):1889. doi: 10.3390/molecules28041889

443. Eshraghi M, Ahmadi M, Afshar S, Lorzadeh S, Adlimoghaddam A, Rezvani Jalal N, et al. Enhancing autophagy in alzheimer's disease through drug repositioning. *Pharmacol Ther* (2022) 237:108171. doi: 10.1016/j.pharmthera.2022.108171

444. Moors TE, Hoozemans JJ, Ingrassia A, Beccari T, Parnetti L, Chartier-Harlin MC, et al. Therapeutic potential of autophagy-enhancing agents in parkinson's disease. *Mol neurodegeneration* (2017) 12(1):11. doi: 10.1186/s13024-017-0154-3

445. Zhou ZD, Selvaratnam T, Lee JCT, Chao YX, Tan EK. Molecular targets for modulating the protein translation vital to proteostasis and neuron degeneration in parkinson's disease. *Trans neurodegeneration* (2019) 8:6. doi: 10.1186/s40035-019-0145-0

446. Gu Y, Lindner J, Kumar A, Yuan W, Magnuson MA. Rictor/mtorc2 is essential for maintaining a balance between beta-cell proliferation and cell size. *Diabetes* (2011) 60(3):827–37. doi: 10.2337/db10-1194

447. Lim YM, Lim H, Hur KY, Quan W, Lee HY, Cheon H, et al. Systemic autophagy insufficiency compromises adaptation to metabolic stress and facilitates progression from obesity to diabetes. *Nat Commun* (2014) 5:4934. doi: 10.1038/ncomms5934

448. Ma L, Fu R, Duan Z, Lu J, Gao J, Tian L, et al. Sirt1 is essential for resveratrol enhancement of hypoxia-induced autophagy in the type 2 diabetic nephropathy rat. *Pathology Res Pract* (2016) 212(4):310–8. doi: 10.1016/j.prp.2016.02.001

449. Liu Z, Stanojevic V, Brindamour LJ, Habener JF. Glp1-derived nonapeptide glp1(28-36)Amide protects pancreatic beta-cells from glucolipotoxicity. *J Endocrinol* (2012) 213(2):143–54. doi: 10.1530/joe-11-0328

450. He C, Bassik MC, Moresi V, Sun K, Wei Y, Zou Z, et al. Exercise-induced bcl2-regulated autophagy is required for muscle glucose homeostasis. *Nature* (2012) 481 (7382):511–5. doi: 10.1038/nature10758

451. Liu Y, Palanivel R, Rai E, Park M, Gabor TV, Scheid MP, et al. Adiponectin stimulates autophagy and reduces oxidative stress to enhance insulin sensitivity during high fat diet feeding in mice. *Diabetes* (2014) 64(1):36–48. doi: 10.2337/db14-0267

452. Hua K, Li T, He Y, Guan A, Chen L, Gao Y, et al. Resistin secreted by porcine alveolar macrophages leads to endothelial cell dysfunction during haemophilus parasuis infection. *Virulence* (2023) 14(1):2171636. doi: 10.1080/21505594.2023.2171636

453. Tan C, Ai J, Zhu Y. Mtorc1-dependent protein and parkinson's disease: A mendelian randomization study. *Brain Sci* (2023) 13(4):536. doi: 10.3390/brainsci13040536

454. Chong ZZ, Shang YC, Maiese K. Cardiovascular disease and mtor signaling. *Trends Cardiovasc Med* (2011) 21(5):151–5. doi: 10.1016/j.tcm.2012.04.005

455. Maiese K, Chong ZZ, Shang YC, Wang S. Mtor: on target for novel therapeutic strategies in the nervous system. *Trends Mol Med* (2013) 19(1):51–60. doi: 10.1016/j.molmed.2012.11.001

456. Radulovic J, Gabbay V. Pfc mtor signaling as a biological signature for cognitive deficits in bipolar disorder without psychosis. *Cell Rep Med* (2021) 2(5):100282. doi: 10.1016/j.xcrm.2021.100282

457. Cappoli N, Mezzogori D, Tabolacci E, Coletta I, Navarra P, Pani G, et al. The mtor kinase inhibitor rapamycin enhances the expression and release of pro-inflammatory cytokine interleukin 6 modulating the activation of human microglial cells. *Excli J* (2019) 18:779–98. doi: 10.17179/excli2019-1715

458. Jung CH, Jun CB, Ro SH, Kim YM, Otto NM, Cao J, et al. Ulk-atg13-fip200 complexes mediate mtor signaling to the autophagy machinery. *Mol Biol Cell* (2009) 20 (7):1992–2003. doi: 10.1091/mbc.e08-12-1249

459. Javdan N, Ayatollahi SA, Choudhary MI, Al-Hasani S, Kobarfard F, Athar A, et al. Capsaicin Protects against Testicular Torsion Injury through Mtor-Dependent Mechanism. *Theriogenology* (2018) 113:247–52. doi: 10.1016/j.theriogenology.2018.03.012

460. Park A, Koh HC. Nf-kappab/mtor-mediated autophagy can regulate diquat-induced apoptosis. *Arch Toxicol* (2019) 93(5):1239–53. doi: 10.1007/s00204-019-02424-7

461. Zhao Y, Wang Q, Wang Y, Li J, Lu G, Liu Z. Glutamine Protects against Oxidative Stress Injury through Inhibiting the Activation of Pi3k/Akt Signaling Pathway in Parkinsonian Cell Model. *Environ Health Prev Med* (2019) 24(1):4. doi: 10.1186/s12199-018-0757-5

462. Dai C, Ciccotosto GD, Cappai R, Wang Y, Tang S, Hoyer D, et al. Rapamycin Confers Neuroprotection against Colistin-Induced Oxidative Stress, Mitochondria Dysfunction and Apoptosis through the Activation of Autophagy and Mtor/Akt/Creb Signaling Pathways. *ACS Chem Neurosci* (2017) 9(4):824–37. doi: 10.1021/acschemneuro.7b00323

463. Zhang ZH, Wu QY, Zheng R, Chen C, Chen Y, Liu Q, et al. Selenomethionine mitigates cognitive decline by targeting both tau hyperphosphorylation and autophagic clearance in an alzheimer's disease mouse model. *J Neurosci* (2017) 37(9):2449–62. doi: 10.1523/jneurosci.3229-16.2017

464. Han K, Jia N, Zhong Y, Shang X. S14g-humanin alleviates insulin resistance and increases autophagy in neurons of app/ps1 transgenic mouse. *J Cell Biochem* (2017) 19(4):3111–7. doi: 10.1002/jcb.26452

465. Damstra-Oddy JL, Warren EC, Perry CJ, Desfougères Y, Fitzpatrick JK, Schaf J, et al. Phytocannabinoid-dependent mtorc1 regulation is dependent upon inositol polyphosphate multikinase activity. *Br J Pharmacol* (2021) 178(5):1149–63. doi: 10.1111/bph.15351

466. Dello Russo C, Lisi L, Feinstein DL, Navarra P. Mtor kinase, a key player in the regulation of glial functions: relevance for the therapy of multiple sclerosis. *Glia* (2013) 61(3):301–11. doi: 10.1002/glia.22433

467. Lee Y, Hong Y, Lee SR, Chang KT. Autophagy contributes to retardation of cardiac growth in diabetic rats. *Lab Anim Res* (2012) 28(2):99–107. doi: 10.5625/lar.2012.28.2.99

468. Hu P, Lai D, Lu P, Gao J, He H. Erk and akt signaling pathways are involved in advanced glycation end product-induced autophagy in rat vascular smooth muscle cells. *Int J Mol Med* (2012) 29(4):613–8. doi: 10.3892/ijmm.2012.891

469. Martino L, Masini M, Novelli M, Beffy P, Bugliani M, Marselli L, et al. Palmitate activates autophagy in ins-1e beta-cells and in isolated rat and human pancreatic islets. *PloS One* (2012) 7(5):e36188. doi: 10.1371/journal.pone.0036188

470. Saleem S, Biswas SC. Tribbles pseudokinase 3 induces both apoptosis and autophagy in amyloid-beta-induced neuronal death. *J Biol Chem* (2017) 292(7):2571–85. doi: 10.1074/jbc.M116.744730

471. Li Q, Han Y, Du J, Jin H, Zhang J, Niu M, et al. Recombinant human erythropoietin protects against hippocampal damage in developing rats with seizures by modulating autophagy via the S6 protein in a time-dependent manner. *Neurochem Res* (2017) 43(2):465–76. doi: 10.1007/s11064-017-2443-1

472. Ding C, Zhang J, Li B, Ding Z, Cheng W, Gao F, et al. Cornin Protects Shsy5y Cells against Oxygen and Glucose Deprivationinduced Autophagy through the Pi3k/Akt/Mtor Pathway. *Mol Med Rep* (2017) 17(1):87–92. doi: 10.3892/mmr.2017.7864

473. Ka M, Smith AL, Kim WY. Mtor controls genesis and autophagy of gabaergic interneurons during brain development. *Autophagy* (2017) 13(8):1348–63. doi: 10.1080/15548627.2017.1327927

474. Fields CR, Bengoa-Vergniory N, Wade-Martins R. Targeting alpha-synuclein as a therapy for parkinson's disease. *Front Mol Neurosci* (2019) 12:299. doi: 10.3389/fnmol.2019.00299

475. Jobst M, Kiss E, Gerner C, Marko D, Del Favero G. Activation of autophagy triggers mitochondrial loss and changes acetylation profile relevant for mechanotransduction in bladder cancer cells. *Arch Toxicol* (2022) 97(1):217–33. doi: 10.1007/s00204-022-03375-2

476. Wang N, Luo Z, Jin M, Sheng W, Wang HT, Long X, et al. Exploration of age-related mitochondrial dysfunction and the anti-aging effects of resveratrol in zebrafish retina. *Aging (Albany NY)* (2019) 11(10):3117–37. doi: 10.18632/aging.101966

477. Xu G, Shen H, Nibona E, Wu K, Ke X, Al Hafiz MA, et al. Fundc1 is necessary for proper body axis formation during embryogenesis in zebrafish. *Sci Rep* (2019) 9(1):18910. doi: 10.1038/s41598-019-55415-0

478. Zeng Z, Liang J, Wu L, Zhang H, Lv J, Chen N. Exercise-induced autophagy suppresses sarcopenia through akt/mtor and akt/foxo3a signal pathways and ampk-mediated mitochondrial quality control. *Front Physiol* (2020) 11:583478. doi: 10.3389/fphys.2020.583478

479. Dechandt CRP, Ferrari GD, Dos Santos JR, de Oliveira JAC, da Silva-Jr RMP, Cunha AOS, et al. Energy metabolism and redox state in brains of wistar audiogenic rats, a genetic model of epilepsy. *Front Neurol* (2019) 10:1007. doi: 10.3389/fneur.2019.01007

480. Kim KA, Shin YJ, Akram M, Kim ES, Choi KW, Suh H, et al. High glucose condition induces autophagy in endothelial progenitor cells contributing to angiogenic impairment. *Biol Pharm Bull* (2014) 37(7):1248–52. doi: 10.1248/bpb.b14-00172

481. Fessel J. Supplementary pharmacotherapy for the behavioral abnormalities caused by stressors in humans, focused on post-traumatic stress disorder (Ptsd). *J Clin Med* (2023) 12(4):1680. doi: 10.3390/jcm12041680

482. Yang K, Zhang L, Chen W, Cheng J, Zhao X, Zhang Y, et al. Expression of epo and related factors in the liver and kidney of plain and tibetan sheep. *Histol Histopathol* (2023), 18592. doi: 10.14670/hh-18-592

483. Chong ZZ, Kang JQ, Maiese K. Erythropoietin is a novel vascular protectant through activation of akt1 and mitochondrial modulation of cysteine proteases. *Circulation* (2002) 106(23):2973–9. doi: 10.1161/01.cir.0000039103.58920.1f

484. García-Llano M, Pedroso-Ibáñez I, Morales-Chacón L, Rodríguez-Obaya T, Pérez-Ruiz L, Sosa-Testé I, et al. Short-term tolerance of nasally-administered neuroepo in patients with parkinson disease. *MEDICC Rev* (2021) 23(1):49–54. doi: 10.37757/mr2021.V23.N1.10

485. Chong ZZ, Maiese K. Erythropoietin involves the phosphatidylinositol 3-kinase pathway, 14-3-3 protein and foxo3a nuclear trafficking to preserve endothelial cell integrity. *Br J Pharmacol* (2007) 150(7):839–50. doi: 10.1038/sj.bjp.0707161

486. Maiese K, Hou J, Chong ZZ, Shang YC. Erythropoietin, forkhead proteins, and oxidative injury: biomarkers and biology. *ScientificWorldJournal* (2009) 9:1072–104. doi: 10.1100/tsw.2009.121

487. Chamorro ME, Wenker SD, Vota DM, Vittori DC, Nesse AB. Signaling pathways of cell proliferation are involved in the differential effect of erythropoietin and its carbamylated derivative. *Biochim Biophys Acta* (2013) 1833(8):1960–8. doi: 10.1016/j.bbamcr.2013.04.006

488. Chong ZZ, Shang YC, Wang S, Maiese K. Pras40 is an integral regulatory component of erythropoietin mtor signaling and cytoprotection. *PloS One* (2012) 7(9):e45456. doi: 10.1371/journal.pone.0045456

489. Wang GB, Ni YL, Zhou XP, Zhang WF. The akt/mtor pathway mediates neuronal protective effects of erythropoietin in sepsis. *Mol Cell Biochem* (2014) 385(1-2):125–32. doi: 10.1007/s11010-013-1821-5

490. BinMowyna MN, AlFaris NA. Kaempferol suppresses acetaminophen-induced liver damage by upregulation/activation of sirt1. *Pharm Biol* (2021) 59(1):146–56. doi: 10.1080/13880209.2021.1877734

491. Dai C, Xiao X, Zhang Y, Xiang B, Hoyer D, Shen J, et al. Curcumin attenuates colistin-induced peripheral neurotoxicity in mice. *ACS Infect Dis* (2020) 6(4):715–24. doi: 10.1021/acsinfecdis.9b00341

492. De Giorgi F, Lartigue L, Bauer MK, Schubert A, Grimm S, Hanson GT, et al. The permeability transition pore signals apoptosis by directing bax translocation and multimerization. *FASEB J* (2002) 16(6):607–9. doi: 10.1096/fj.01-0269fje

493. Deng D, Yan J, Wu Y, Wu K, Li W. Morroniside suppresses hydrogen peroxide-stimulated autophagy and apoptosis in rat ovarian granulosa cells through the pi3k/akt/mtor pathway. *Hum Exp Toxicol* (2020) 40(4):577–86. doi: 10.1177/0960327120960768

494. Hacioglu C, Kar F, Kanbak G. Reproductive effects of nicotinamide on testicular function and structure in old male rats: oxidative, apoptotic, hormonal, and morphological analyses. *Reprod Sci* (2021) 28(12):3352–60. doi: 10.1007/s43032-021-00647-7

495. Hajializadeh Z, Khaksari M. The protective effects of 17-β Estradiol and sirt1 against cardiac hypertrophy: A review. *Heart failure Rev* (2021) 27(2):725–38. doi: 10.1007/s10741-021-10171-0

496. Alloza I, Salegi A, Mena J, Navarro RT, Martin C, Aspichueta P, et al. Birc6 is associated with vulnerability of carotid atherosclerotic plaque. *Int J Mol Sci* (2020) 21(24):9387. doi: 10.3390/ijms21249387

497. Chen S, Li B. Mir-128-3p post-transcriptionally inhibits wisp1 to suppress apoptosis and inflammation in human articular chondrocytes via the pi3k/akt/nf-κb signaling pathway. *Cell Transplant* (2020) 29:963689720939131. doi: 10.1177/0963689720939131

498. Gallyas F Jr., Sumegi B, Szabo C. Role of akt activation in parp inhibitor resistance in cancer. *Cancers* (2020) 12(3):532. doi: 10.3390/cancers12030532

499. Govindappa PK, Elfar JC. Erythropoietin promotes M2 macrophage phagocytosis of schwann cells in peripheral nerve injury. *Cell Death Dis* (2022) 13(3):245. doi: 10.1038/s41419-022-04671-6

500. Ye M, Zhao Y, Wang Y, Xie R, Tong Y, Sauer JD, et al. Nad(H)-loaded nanoparticles for efficient sepsis therapy via modulating immune and vascular homeostasis. *Nat Nanotechnol* (2022) 17(8):880–90. doi: 10.1038/s41565-022-01137-w

501. Yang L, Cheng CF, Li ZF, Huang XJ, Cai SQ, Ye SY, et al. Berberine blocks inflammasome activation and alleviates diabetic cardiomyopathy via the miR-18a-3p/Gsdmd pathway. *Int J Mol Med* (2023) 51(6):49. doi: 10.1002/biof.1607

502. Hou J, Chong ZZ, Shang YC, Maiese K. Early apoptotic vascular signaling is determined by sirt1 through nuclear shuttling, forkhead trafficking, bad, and mitochondrial caspase activation. *Curr Neurovasc Res* (2010) 7(2):95–112. doi: 10.2174/156720210791184899

503. Shang YC, Chong ZZ, Hou J, Maiese K. Wnt1, foxo3a, and nf-kappab oversee microglial integrity and activation during oxidant stress. *Cell Signal* (2010) 22(9):1317–29. doi: 10.1016/j.cellsig.2010.04.009

504. Taveira GB, Mello EO, Souza SB, Monteiro RM, Ramos AC, Carvalho AO, et al. Programmed cell death in yeast by thionin-like peptide from capsicum annuum fruits involving activation of capases and extracelullar H(+) flux. *Bioscience Rep* (2018) 38(2):BSR20180119. doi: 10.1042/bsr20180119

505. Almasieh M, Catrinescu MM, Binan L, Costantino S, Levin LA. Axonal degeneration in retinal ganglion cells is associated with a membrane polarity-sensitive redox process. *J Neurosci* (2017) 37(14):3824–39. doi: 10.1523/jneurosci.3882-16.2017

506. Viola G, Bortolozzi R, Hamel E, Moro S, Brun P, Castagliuolo I, et al. Mg-2477, a new tubulin inhibitor, induces autophagy through inhibition of the akt/mtor pathway and delayed apoptosis in A549 cells. *Biochem Pharmacol* (2012) 83(1):16–26. doi: 10.1016/j.bcp.2011.09.017

507. Bailey TJ, Fossum SL, Fimbel SM, Montgomery JE, Hyde DR. The inhibitor of phagocytosis, O-phospho-L-serine, suppresses muller glia proliferation and cone cell regeneration in the light-damaged zebrafish retina. *Exp Eye Res* (2010) 91(5):601–12. doi: 10.1016/j.exer.2010.07.017

508. Shang YC, Chong ZZ, Hou J, Maiese K. Foxo3a governs early microglial proliferation and employs mitochondrial depolarization with caspase 3, 8, and 9

cleavage during oxidant induced apoptosis. *Curr Neurovasc Res* (2009) 6(4):223–38. doi: 10.2174/156720209789630302

509. Wei L, Sun C, Lei M, Li G, Yi L, Luo F, et al. Activation of wnt/beta-catenin pathway by exogenous wnt1 protects sh-sy5y cells against 6-hydroxydopamine toxicity. *J Mol Neurosci* (2013) 49(1):105–15. doi: 10.1007/s12031-012-9900-8

510. Hou J, Wang S, Shang YC, Chong ZZ, Maiese K. Erythropoietin employs cell longevity pathways of sirt1 to foster endothelial vascular integrity during oxidant stress. *Curr Neurovasc Res* (2011) 8(3):220–35. doi: 10.2174/156720211796558069

511. Kim S, Kang IH, Nam JB, Cho Y, Chung DY, Kim SH, et al. Ameliorating the effect of astragaloside iv on learning and memory deficit after chronic cerebral hypoperfusion in rats. *Molecules* (2015) 20(2):1904–21. doi: 10.3390/molecules20021904

512. Xin YJ, Yuan B, Yu B, Wang YQ, Wu JJ, Zhou WH, et al. Tet1-mediated DNA demethylation regulates neuronal cell death induced by oxidative stress. *Sci Rep* (2015) 5:7645. doi: 10.1038/srep07645

513. Yu T, Li L, Chen T, Liu Z, Liu H, Li Z. Erythropoietin attenuates advanced glycation endproducts-induced toxicity of schwann cells in vitro. *Neurochem Res* (2015) 40(4):698–712. doi: 10.1007/s11064-015-1516-2

514. Yousafzai NA, Jin H, Ullah M, Wang X. Recent advances of sirt1 and implications in chemotherapeutics resistance in cancer. *Am J Cancer Res* (2021) 11 (11):5233–48.

515. Maiese K. Pyroptosis, apoptosis, and autophagy: critical players of inflammation and cell demise in the nervous system. *Curr Neurovasc Res* (2022) 19:241–4. doi: 10.2174/1567202619666220729093449

516. Pang Y, Qin M, Hu P, Ji K, Xiao R, Sun N, et al. Resveratrol protects retinal ganglion cells against ischemia induced damage by increasing opa1 expression. *Int J Mol Med* (2020) 46(5):1707–20. doi: 10.3892/ijmm.2020.4711

517. Cui L, Weiyao J, Chenghong S, Limei L, Xinghua Z, Bo Y, et al. Rheumatoid arthritis and mitochondrial homeostasis: the crossroads of metabolism and immunity. *Front Med (Lausanne)* (2022) 9:1017650. doi: 10.3389/fmed.2022.1017650

518. Maiese K, Vincent AM. Critical temporal modulation of neuronal programmed cell injury. *Cell Mol Neurobiol* (2000) 20(3):383–400. doi: 10.1023/A:1007070311203

519. Razzaghi A, Choobineh S, Gaeini A, Soori R. Interaction of exercise training with taurine attenuates infarct size and cardiac dysfunction via akt-foxo3a-caspase-8 signaling pathway. *Amino Acids* (2023) 55(7):869–80. doi: 10.1007/s00726-023-03275-4

520. Shang YC, Chong ZZ, Wang S, Maiese K. Wnt1 inducible signaling pathway protein 1 (Wisp1) targets pras40 to govern beta-amyloid apoptotic injury of microglia. *Curr Neurovasc Res* (2012) 9(4):239–49. doi: 10.2174/156720212803530618

521. Shang YC, Chong ZZ, Wang S, Maiese K. Prevention of beta-amyloid degeneration of microglia by erythropoietin depends on wnt1, the pi 3-K/mtor pathway, bad, and bcl-xl. *Aging (Albany NY)* (2012) 4(3):187–201. doi: 10.18632/aging.100440

522. Shang YC, Chong ZZ, Wang S, Maiese K. Tuberous sclerosis protein 2 (Tsc2) modulates ccn4 cytoprotection during apoptotic amyloid toxicity in microglia. *Curr Neurovasc Res* (2013) 10(1):29–38. doi: 10.2174/156720213804806007

523. Bhowmick S, D'Mello V, Caruso D, Abdul-Muneer PM. Traumatic brain injury-induced downregulation of nrf2 activates inflammatory response and apoptotic cell death. *J Mol Med (Berlin Germany)* (2019) 97(12):1627–41. doi: 10.1007/s00109-019-01851-4

524. Chong ZZ, Li F, Maiese K. Stress in the brain: novel cellular mechanisms of injury linked to alzheimer's disease. *Brain Res Brain Res Rev* (2005) 49(1):1–21. doi: 10.1016/j.brainresrev.2004.11.005

525. Najjar RS, Turner CG, Wong BJ, Feresin RG. Berry-derived polyphenols in cardiovascular pathologies: mechanisms of disease and the role of diet and sex. *Nutrients* (2021) 13(2):387. doi: 10.3390/nu13020387

526. Liang H, Liu Q. The role of non-coding rna in lupus nephritis. *Hum Cell* (2023) 36(3):923–36. doi: 10.1007/s13577-023-00883-w

527. Scrimieri R, Locatelli L, Cazzaniga A, Cazzola R, Malucelli E, Sorrentino A, et al. Ultrastructural features mirror metabolic derangement in human endothelial cells exposed to high glucose. *Sci Rep* (2023) 13(1):15133. doi: 10.1038/s41598-023-42333-5

528. Wang J, Chen S, Zhao X, Guo Q, Yang R, Zhang C, et al. Effect of pparγ on oxidative stress in diabetes-related dry eye. *Exp Eye Res* (2023) 231:109498. doi: 10.1016/j.exer.2023.109498

529. Yeger H. Ccn proteins: opportunities for clinical studies-a personal perspective. *J Cell Commun Signal* (2023) 17(2):333–52. doi: 10.1007/s12079-023-00761-y

530. Sierra-Pagan JE, Dsouza N, Das S, Larson TA, Sorensen JR, Ma X, et al. Foxk1 regulates wnt signaling to promote cardiogenesis. *Cardiovasc Res* (2023) 119(8):1728–39. doi: 10.1093/cvr/cvad054

531. Zhang Y, Zhou H, Ding C. The ameliorative effect of cangfu daotan decoction on polycystic ovary syndrome of rodent model is associated with M6a methylation and wnt/β-catenin pathway. *Gynecol Endocrinol* (2023) 39(1):2181637. doi: 10.1080/09513590.2023.2181637

532. Farid HA, Sayed RH, El-Shamarka ME, Abdel-Salam OME, El Sayed NS. Pi3k/akt signaling activation by roflumilast ameliorates rotenone-induced parkinson's disease in rats. *Inflammopharmacology* (2023). doi: 10.1007/s10787-023-01305-x

533. Hu G, Wang T, Ma C. Epo activates pi3k-ikkα-cdk1 signaling pathway to promote the proliferation of glial cells under hypoxia environment. *Genet Mol Biol* (2022) 45(1):e20210249. doi: 10.1590/1678-4685-gmb-2021-0249

534. Liu H, Wang C, Sun X, Zhan C, Li Z, Qiu L, et al. Silk fibroin/collagen/hydroxyapatite scaffolds obtained by 3d printing technology and loaded with recombinant human erythropoietin in the reconstruction of alveolar bone defects. *ACS Biomater Sci Eng* (2022) 8(12):5245–56. doi: 10.1021/acsbiomaterials.2c00690

535. Sergio CM, Rolando CA. Erythropoietin regulates signaling pathways associated with neuroprotective events. *Exp Brain Res* (2022) 240(5):1303–15. doi: 10.1007/s00221-022-06331-9

536. Maiese K. Regeneration in the nervous system with erythropoietin. *Front bioscience (Landmark edition)* (2016) 21:561–96. doi: 10.2741/4408

537. Sun N, Victor MB, Park YP, Xiong X, Scannail AN, Leary N, et al. Human microglial state dynamics in alzheimer's disease progression. *Cell* (2023) 186(20):4386–403.e29. doi: 10.1016/j.cell.2023.08.037

538. Duarte-Silva E, Meuth SG, Peixoto CA. The role of iron metabolism in the pathogenesis and treatment of multiple sclerosis. *Front Immunol* (2023) 14:1137635. doi: 10.3389/fimmu.2023.1137635

539. Maiese K. Ferroptosis, iron metabolism, and forkhead transcription factors (Foxos). *Curr Neurovasc Res* (2023) 20(3):291–5. doi: 10.2174/1567202620666230706160056

540. He L, Yang Y, Chen J, Zou P, Li J. Transcriptional activation of enpp2 by foxo4 protects cardiomyocytes from doxorubicin–Induced toxicity. *Mol Med Rep* (2021) 24 (3):668. doi: 10.3892/mmr.2021.12307

541. Malhotra S, Hurtado-Navarro L, Pappolla A, Villar LMM, Río J, Montalban X, et al. Increased nlrp3 inflammasome activation and pyroptosis in patients with multiple sclerosis with fingolimod treatment failure. *Neurol Neuroimmunol Neuroinflamm* (2023) 10(3):e200100. doi: 10.1212/nxi.0000000000200100

542. Conti P, Ronconi G, Caraffa A, Gallenga CE, Ross R, Frydas I, et al. Induction of pro-inflammatory cytokines (Il-1 and il-6) and lung inflammation by coronavirus-19 (Covi-19 or sars-cov-2): anti-inflammatory strategies. *J Biol Regul Homeost Agents* (2020) 34(2):327–31. doi: 10.23812/conti-e

543. Crespo I, Fernández-Palanca P, San-Miguel B, Álvarez M, González-Gallego J, Tuñón MJ. Melatonin modulates mitophagy, innate immunity and circadian clocks in a model of viral-induced fulminant hepatic failure. *J Cell Mol Med* (2020) 24(13):7625–36. doi: 10.1111/jcmm.15398

544. Park MH, Gutierrez-Garcia AK, Choudhury M. Mono-(2-ethylhexyl) phthalate aggravates inflammatory response via sirtuin regulation and inflammasome activation in raw 264.7 cells. *Chem Res Toxicol* (2019) 32(5):935–42. doi: 10.1021/acs.chemrestox.9b00101

545. Vaamonde-Garcia C, Lopez-Armada MJ. Role of mitochondrial dysfunction on rheumatic diseases. *Biochem Pharmacol* (2019) 165:181–95. doi: 10.1016/j.bcp.2019.03.008

546. Qian D, Dai S, Sun Y, Yuan Y, Wang L. Mir-128-3p attenuates the neurotoxicity in rats induced by isoflurane anesthesia. *Neurotox Res* (2022) 40 (3):714–20. doi: 10.1007/s12640-022-00512-8

547. Toniolo S, Scarioni M, Di Lorenzo F, Hort J, Georges J, Tomic S, et al. Dementia and covid-19, a bidirectional liaison: risk factors, biomarkers, and optimal health care. *J Alzheimers Dis* (2021) 82(3):883–98. doi: 10.3233/jad-210335

548. Hassanein EHM, Saleh FM, Ali FEM, Rashwan EK, Atwa AM, Abd El-Ghafar OAM. Neuroprotective effect of canagliflozin against cisplatin-induced cerebral cortex injury is mediated by regulation of ho-1/ppar-Γ, sirt1/foxo-3, jnk/ap-1, tlr4/inos, and ang ii/ang 1-7 signals. *Immunopharmacol Immunotoxicol* (2023) 45(3):304–16. doi: 10.1080/08923973.2022.2143371

549. Maiese K. Sirtuins in metabolic disease: Innovative Therapeutic Strategies with Sirt1, Ampk, Mtor, and Nicotinamide. In: Maiese K, editor. *Sirtuin Biology in Cancer and Metabolic Disease: Cellular Pathways for Clinical Discovery*. Academic Press, Elsevier (2021), Cambridge, MA, USA; Elsevier, Amsterdam, The Netherlands: ISBN.

550. Fangma Y, Wan H, Shao C, Jin L, He Y. Research progress on the role of sirtuin 1 in cerebral ischemia. *Cell Mol Neurobiol* (2022) 43(5):1769–83. doi: 10.1007/s10571-022-01288-3

551. Kang X, Li C, Xie X, Zhan KB, Yang SQ, Tang YY, et al. Hydrogen sulfide inhibits homocysteine-induced neuronal senescence by up-regulation of sirt1. *Int J Med Sci* (2020) 17(3):310–9. doi: 10.7150/ijms.38602

552. Li H, Peng D, Zhang SJ, Zhang Y, Wang Q, Guan L. Buyang huanwu decoction promotes neurogenesis via sirtuin 1/autophagy pathway in a cerebral ischemia model. *Mol Med Rep* (2021) 24(5):791. doi: 10.3892/mmr.2021.12431

553. Maiese K. Novel treatment strategies for the nervous system: circadian clock genes, non-coding rnas, and forkhead transcription factors. *Curr Neurovasc Res* (2018) 15(1):81–91. doi: 10.2174/1567202615666180319151244

554. Yin Q, Wang JF, Xu XH, Xie H. Effect of lycopene on pain facilitation and the sirt1/mtor pathway in the dorsal horn of burn injury rats. *Eur J Pharmacol* (2020) 889:173365. doi: 10.1016/j.ejphar.2020.173365

555. Lee Y, Im E. Regulation of mirnas by natural antioxidants in cardiovascular diseases: focus on sirt1 and enos. *Antioxidants (Basel Switzerland)* (2021) 10(3):377. doi: 10.3390/antiox10030377

556. Mori M, Cazzaniga G, Meneghetti F, Villa S, Gelain A. Insights on the modulation of sirt5 activity: A challenging balance. *Molecules* (2022) 27(14):4449. doi: 10.3390/molecules27144449

557. Rong Y, Ren J, Song W, Xiang R, Ge Y, Lu W, et al. Resveratrol suppresses severe acute pancreatitis-induced microcirculation disturbance through targeting sirt1-foxo1 axis. *Oxid Med Cell Longev* (2021) 2021:8891544. doi: 10.1155/2021/8891544

558. Guimera AM, Clark P, Wordsworth J, Anugula S, Rasmussen LJ, Shanley DP. Systems modelling predicts chronic inflammation and genomic instability prevent effective mitochondrial regulation during biological ageing. *Exp Gerontol* (2022) 166:111889. doi: 10.1016/j.exger.2022.111889

559. Sadria M, Seo D, Layton AT. The mixed blessing of ampk signaling in cancer treatments. *BMC Cancer* (2022) 22(1):105. doi: 10.1186/s12885-022-09211-1

560. Bitterman KJ, Anderson RM, Cohen HY, Latorre-Esteves M, Sinclair DA. Inhibition of silencing and accelerated aging by nicotinamide, a putative negative regulator of yeast sir2 and human sirt1. *J Biol Chem* (2002) 277(47):45099–107. doi: 10.1074/jbc.M205670200

561. Guerra J, Devesa J. Usefulness of melatonin and other compounds as antioxidants and epidrugs in the treatment of head and neck cancer. *Antioxidants (Basel Switzerland)* (2021) 11(1):35. doi: 10.3390/antiox11010035

562. Maiese K, Chong ZZ, Shang YC, Wang S. Translating cell survival and cell longevity into treatment strategies with sirt1. *Rom J Morphol Embryol* (2011) 52 (4):1173–85.

563. Penteado AB, Hassanie H, Gomes RA, Silva Emery FD, Goulart Trossini GH. Human sirtuin 2 inhibitors, their mechanisms and binding modes. *Future Med Chem* (2023) 15(3):291–311. doi: 10.4155/fmc-2022-0253

564. Giacalone S, Spigariolo CB, Bortoluzzi P, Nazzaro G. Oral nicotinamide: the role in skin cancer chemoprevention. *Dermatol Ther* (2021) 34(3):e14892. doi: 10.1111/dth.14892

565. Chong MC, Silva A, James PF, Wu SSX, Howitt J. Exercise increases the release of nampt in extracellular vesicles and alters nad(+) activity in recipient cells. *Aging Cell* (2022) 21(7):e13647. doi: 10.1111/acel.13647

566. Potthast AB, Nebl J, Wasserfurth P, Haufe S, Eigendorf J, Hahn A, et al. Impact of nutrition on short-term exercise-induced sirtuin regulation: vegans differ from omnivores and lacto-ovo vegetarians. *Nutrients* (2020) 12(4):1004. doi: 10.3390/nu12041004

567. AlSaleh A, Shahid M, Farid E, Bindayna K. The effect of ascorbic acid and nicotinamide on panton-valentine leukocidin cytotoxicity: an ex vivo study. *Toxins (Basel)* (2023) 15(1):38. doi: 10.3390/toxins15010038

568. Kumar A, Ou Y. From bench to behaviour: the role of lifestyle factors on intraocular pressure, neuroprotection, and disease progression in glaucoma. *Clin Exp Ophthalmol* (2023) 51(4):380–94. doi: 10.1111/ceo.14218

569. Li M, Zhang L, Pan L, Zhou P, Yu R, Zhang Z, et al. Nicotinamide efficiently suppresses porcine epidemic diarrhea virus and porcine deltacoronavirus replication. *Viruses* (2023) 15(7):1591. doi: 10.3390/v15071591

570. Tai S-H, Chao L-C, Huang S-Y, Lin H-W, Lee A-H, Chen Y-Y, et al. Nicotinamide deteriorates post-stroke immunodepression following cerebral ischemia–reperfusion injury in mice. *Biomedicines* (2023) 11(8):2145. doi: 10.3390/biomedicines11082145

571. Jackson MD, Schmidt MT, Oppenheimer NJ, Denu JM. Mechanism of nicotinamide inhibition and transglycosidation by sir2 histone/protein deacetylases. *J Biol Chem* (2003) 278(51):50985–98. doi: 10.1074/jbc.M306552200

572. Avalos JL, Bever KM, Wolberger C. Mechanism of sirtuin inhibition by nicotinamide: altering the nad(+) cosubstrate specificity of a sir2 enzyme. *Mol Cell* (2005) 17(6):855–68. doi: 10.1016/j.molcel.2005.02.022

573. Zhang XM, Jing YP, Jia MY, Zhang L. Negative transcriptional regulation of inflammatory genes by group B3 vitamin nicotinamide. *Mol Biol Rep* (2012) 39 (12):10367–71. doi: 10.1007/s11033-012-1915-2

574. Fulco M, Cen Y, Zhao P, Hoffman EP, McBurney MW, Sauve AA, et al. Glucose restriction inhibits skeletal myoblast differentiation by activating sirt1 through ampk-mediated regulation of nampt. *Dev Cell* (2008) 14(5):661–73. doi: 10.1016/j.devcel.2008.02.004

575. Pal PB, Sonowal H, Shukla K, Srivastava SK, Ramana KV. Aldose reductase regulates hyperglycemia-induced huvec death via sirt1/ampk-alpha1/mtor pathway. *J Mol Endocrinol* (2019) 63(1):11–25. doi: 10.1530/jme-19-0080

576. Geng C, Xu H, Zhang Y, Gao Y, Li M, Liu X, et al. Retinoic acid ameliorates high-fat diet-induced liver steatosis through sirt1. *Sci China Life Sci* (2017) 60 (11):1234–41. doi: 10.1007/s11427-016-9027-6

577. Ghiasi R, Naderi R, Sheervalilou R, Alipour MR. Swimming training by affecting the pancreatic sirtuin1 (Sirt1) and oxidative stress, improves insulin sensitivity in diabetic male rats. *Hormone Mol Biol Clin Invest* (2019) 40(3). doi: 10.1515/hmbci-2019-0011

578. Xue P, Zhao J, Zheng A, Li L, Chen H, Tu W, et al. Chrysophanol alleviates myocardial injury in diabetic db/db mice by regulating the sirt1/hmgb1/nf-kappab signaling pathway. *Exp Ther Med* (2019) 18(6):4406–12. doi: 10.3892/etm.2019.8083

579. Chen YR, Fang SR, Fu YC, Zhou XH, Xu MY, Xu WC. Calorie restriction on insulin resistance and expression of sirt1 and sirt4 in rats. *Biochem Cell Biol* (2010) 88 (4):715–22. doi: 10.1139/O10-010

580. Caron AZ, He X, Mottawea W, Seifert EL, Jardine K, Dewar-Darch D, et al. The sirt1 deacetylase protects mice against the symptoms of metabolic syndrome. *FASEB J* (2014) 28(3):1306–16. doi: 10.1096/fj.13-243568

581. Frojdo S, Durand C, Molin L, Carey AL, El-Osta A, Kingwell BA, et al. Phosphoinositide 3-kinase as a novel functional target for the regulation of the insulin signaling pathway by sirt1. *Mol Cell Endocrinol* (2011) 335(2):166–76. doi: 10.1016/j.mce.2011.01.008

582. Guo W, Qian L, Zhang J, Zhang W, Morrison A, Hayes P, et al. Sirt1 overexpression in neurons promotes neurite outgrowth and cell survival through inhibition of the mtor signaling. *J Neurosci Res* (2011) 89(11):1723–36. doi: 10.1002/jnr.22725

583. Pan YR, Song JY, Fan B, Wang Y, Che L, Zhang SM, et al. Mtor may interact with parp-1 to regulate visible light-induced parthanatos in photoreceptors. *Cell Commun Signal* (2020) 18(1):27. doi: 10.1186/s12964-019-0498-0

584. Zhang H, Yang X, Pang X, Zhao Z, Yu H, Zhou H. Genistein Protects against Ox-Ldl-Induced Senescence through Enhancing Sirt1/Lkb1/Ampk-Mediated Autophagy Flux in Huvecs. *Mol Cell Biochem* (2019) 455((1-2):127–34. doi: 10.1007/s11010-018-3476-8

585. Ou X, Lee MR, Huang X, Messina-Graham S, Broxmeyer HE. Sirt1 positively regulates autophagy and mitochondria function in embryonic stem cells under oxidative stress. *Stem Cells* (2014) 32(5):1183–94. doi: 10.1002/stem.1641

586. Li MZ, Zheng LJ, Shen J, Li XY, Zhang Q, Bai X, et al. Sirt1 facilitates amyloid beta peptide degradation by upregulating lysosome number in primary astrocytes. *Neural regeneration Res* (2018) 13(11):2005–13. doi: 10.4103/1673-5374.239449

587. Balan V, Miller GS, Kaplun L, Balan K, Chong ZZ, Li F, et al. Life span extension and neuronal cell protection by drosophila nicotinamidase. *J Biol Chem* (2008) 283(41):27810–9. doi: 10.1074/jbc.M804681200

588. Wang S, Chong ZZ, Shang YC, Maiese K. Wisp1 neuroprotection requires foxo3a post-translational modulation with autoregulatory control of sirt1. *Curr Neurovasc Res* (2013) 10(1):54–60. doi: 10.2174/156720213804805945

589. Maiese K, Shang YC, Chong ZZ, Hou J. Diabetes mellitus: channeling care through cellular discovery. *Curr Neurovasc Res* (2010) 7(1):59–64. doi: 10.2174/156720210790820217

590. Wu H, Wang H, Zhang W, Wei X, Zhao J, Yan P, et al. Rhepo affects apoptosis in hippocampus of aging rats by upregulating sirt1. *Int J Clin Exp Pathol* (2015) 8 (6):6870–80.

591. Chong ZZ, Kang JQ, Maiese K. Erythropoietin fosters both intrinsic and extrinsic neuronal protection through modulation of microglia, akt1, bad, and caspase-mediated pathways. *Br J Pharmacol* (2003) 138(6):1107–18. doi: 10.1038/sj.bjp.0705161

592. Cui L, Guo J, Zhang Q, Yin J, Li J, Zhou W, et al. Erythropoietin activates sirt1 to protect human cardiomyocytes against doxorubicin-induced mitochondrial dysfunction and toxicity. *Toxicol Lett* (2017) 275:28–38. doi: 10.1016/j.toxlet.2017.04.018

593. Rey F, Ottolenghi S, Giallongo T, Balsari A, Martinelli C, Rey R, et al. Mitochondrial metabolism as target of the neuroprotective role of erythropoietin in parkinson's disease. *Antioxidants (Basel Switzerland)* (2021) 10(1):121. doi: 10.3390/antiox10010121

594. Shang YC, Chong ZZ, Wang S, Maiese K. Erythropoietin and wnt1 govern pathways of mtor, apaf-1, and xiap in inflammatory microglia. *Curr Neurovasc Res* (2011) 8(4):270–85. doi: 10.2174/156720211798120990

595. Entezari M, Flavarjani ZK, Ramezani A, Nikkhah H, Karimi S, Moghadam HF, et al. Combination of intravitreal bevacizumab and erythropoietin versus intravitreal bevacizumab alone for refractory diabetic macular edema: A randomized double-blind clinical trial. *Graefes Arch Clin Exp Ophthalmol* (2019) 257(11):2375–80. doi: 10.1007/s00417-019-04383-2

596. Montesano A, Bonfigli AR, De Luca M, Crocco P, Garagnani P, Marasco E, et al. Erythropoietin (Epo) haplotype associated with all-cause mortality in a cohort of italian patients with type-2 diabetes. *Sci Rep* (2019) 9(1):10395. doi: 10.1038/s41598-019-46894-2

597. Kim SH, Yu HS, Huh S, Kang UG, Kim YS. Electroconvulsive seizure inhibits the mtor signaling pathway via ampk in the rat frontal cortex. *Psychopharmacology* (2022) 239(2):443–54. doi: 10.1007/s00213-021-06015-2

598. Li X, Li K, Chu F, Huang J, Yang Z. Graphene oxide enhances β-amyloid clearance by inducing autophagy of microglia and neurons. *Chem Biol Interact* (2020) 325:109126. doi: 10.1016/j.cbi.2020.109126

599. Nejabati HR, Samadi N, Shahnazi V, Mihanfar A, Fattahi A, Latifi Z, et al. Nicotinamide and its metabolite N1-methylnicotinamide alleviate endocrine and metabolic abnormalities in adipose and ovarian tissues in rat model of polycystic ovary syndrome. *Chem Biol Interact* (2020) 324:109093. doi: 10.1016/j.cbi.2020.109093

600. Chong ZZ, Maiese K. The src homology 2 domain tyrosine phosphatases shp-1 and shp-2: diversified control of cell growth, inflammation, and injury. *Histol Histopathol* (2007) 22(11):1251–67. doi: 10.14670/HH-22.1251

601. Chiu SC, Chao CY, Chiang EI, Syu JN, Rodriguez RL, Tang FY. N-3 polyunsaturated fatty acids alleviate high glucose-mediated dysfunction of endothelial progenitor cells and prevent ischemic injuries both in vitro and in vivo. *J Nutr Biochem* (2017) 42:172–81. doi: 10.1016/j.jnutbio.2017.01.009

602. Liu P, Yang X, Hei C, Meli Y, Niu J, Sun T, et al. Rapamycin reduced ischemic brain damage in diabetic animals is associated with suppressions of mtor and erk1/2 signaling. *Int J Biol Sci* (2016) 12(8):1032–40. doi: 10.7150/ijbs.15624

603. Peixoto CA, de Oliveira WH, da Rocha Araujo SM, Nunes AKS. Ampk activation: role in the signaling pathways of neuroinflammation and neurodegeneration. *Exp Neurol* (2017) 298(PtA):31–41. doi: 10.1016/j.expneurol.2017.08.013

604. Zhao H, Wang ZC, Wang KF, Chen XY. Abeta peptide secretion is reduced by radix polygalaeinduced autophagy via activation of the ampk/mtor pathway. *Mol Med Rep* (2015) 12(2):2771–6. doi: 10.3892/mmr.2015.3781

605. Lin CL, Huang WN, Li HH, Huang CN, Hsieh S, Lai C, et al. Hydrogen-rich water attenuates amyloid beta-induced cytotoxicity through upregulation of sirt1-foxo3a by stimulation of amp-activated protein kinase in sk-N-mc cells. *Chem Biol Interact* (2015) 240:12–21. doi: 10.1016/j.cbi.2015.07.013

606. An T, Zhang X, Li H, Dou L, Huang X, Man Y, et al. Gpr120 facilitates cholesterol efflux in macrophages through activation of ampk signaling pathway. *FEBS J* (2020) 287(23):5080–95. doi: 10.1111/febs.15310

607. Hung CM, Lombardo PS, Malik N, Brun SN, Hellberg K, Van Nostrand JL, et al. Ampk/ulk1-mediated phosphorylation of parkin act domain mediates an early step in mitophagy. *Sci Adv* (2021) 7(15):eabg4544. doi: 10.1126/sciadv.abg4544

608. Du LL, Chai DM, Zhao LN, Li XH, Zhang FC, Zhang HB, et al. Ampk activation ameliorates alzheimer's disease-like pathology and spatial memory impairment in a streptozotocin-induced alzheimer's disease model in rats. *J Alzheimers Dis* (2015) 43 (3):775–84. doi: 10.3233/jad-140564

609. He C, Zhu H, Li H, Zou MH, Xie Z. Dissociation of bcl-2-beclin1 complex by activated ampk enhances cardiac autophagy and protects against cardiomyocyte apoptosis in diabetes. *Diabetes* (2013) 62(4):1270–81. doi: 10.2337/db12-0533

610. Moroz N, Carmona JJ, Anderson E, Hart AC, Sinclair DA, Blackwell TK. Dietary restriction involves nad -dependent mechanisms and a shift toward oxidative metabolism. *Aging Cell* (2014) 13(6):1075–85. doi: 10.1111/acel.12273

611. Gao J, Yao M, Chang D, Liu J. Mtor (Mammalian target of rapamycin): hitting the bull's eye for enhancing neurogenesis after cerebral ischemia? *Stroke* (2022) 54 (1):279–85. doi: 10.1161/strokeaha.122.040376

612. Lan F, Cacicedo JM, Ruderman N, Ido Y. Sirt1 modulation of the acetylation status, cytosolic localization, and activity of lkb1. Possible role in amp-activated protein kinase activation. *J Biol Chem* (2008) 283(41):27628–35. doi: 10.1074/jbc.M805711200

613. Canto C, Auwerx J. Caloric restriction, sirt1 and longevity. *Trends Endocrinol Metab* (2009) 20(7):325–31. doi: 10.1016/j.tem.2009.03.008

614. Herranz D, Serrano M. Sirt1: recent lessons from mouse models. *Nat Rev Cancer* (2010) 10(12):819–23. doi: 10.1038/nrc2962

615. Barchetta I, Cimini FA, Capoccia D, De Gioannis R, Porzia A, Mainiero F, et al. Wisp1 is a marker of systemic and adipose tissue inflammation in dysmetabolic subjects with or without type 2 diabetes. *J Endocr Soc* (2017) 1(6):660–70. doi: 10.1210/js.2017-00108

616. Liu L, Hu J, Yang L, Wang N, Liu Y, Wei X, et al. Association of wisp1/ccn4 with risk of overweight and gestational diabetes mellitus in chinese pregnant women. *Dis Markers* (2020) 2020:4934206. doi: 10.1155/2020/4934206

617. Murahovschi V, Pivovarova O, Ilkavets I, Dmitrieva RM, Docke S, Keyhani-Nejad F, et al. Wisp1 is a novel adipokine linked to inflammation in obesity. *Diabetes* (2015) 64(3):856–66. doi: 10.2337/db14-0444

618. Maiese K. Wnt1 inducible Signaling Pathway Protein 1 (Wisp1). In: *Encyclopedia of Signaling Molecules* (2017) (Cham, Switzerland). doi: 10.1007/978-1-4614-6438-9_101926-1

619. Gao J, Xu H, Rong Z, Chen L. Wnt family member 1 (Wnt1) overexpression-induced M2 polarization of microglia alleviates inflammation-sensitized neonatal brain injuries. *Bioengineered* (2022) 13(5):12409–20. doi: 10.1080/21655979.2022.2074767

620. Li P, Wu C, Guo X, Wen Y, Liu L, Liang X, et al. Integrative analysis of genome-wide association studies and DNA methylation profile identified genetic control genes of DNA methylation for kashin-beck disease. *Cartilage* (2021) 13(1_suppl):780s–8s. doi: 10.1177/1947603519858748

621. Fu Y, Chang H, Peng X, Bai Q, Yi L, Zhou Y, et al. Resveratrol inhibits breast cancer stem-like cells and induces autophagy via suppressing wnt/beta-catenin signaling pathway. *PloS One* (2014) 9(7):e102535. doi: 10.1371/journal.pone.0102535

622. Geng Y, Ju Y, Ren F, Qiu Y, Tomita Y, Tomoeda M, et al. Insulin receptor substrate 1/2 (Irs1/2) regulates wnt/beta-catenin signaling through blocking autophagic degradation of dishevelled2. *J Biol Chem* (2014) 289(16):11230–41. doi: 10.1074/jbc.M113.544999

623. Ortiz-Masia D, Cosin-Roger J, Calatayud S, Hernandez C, Alos R, Hinojosa J, et al. Hypoxic macrophages impair autophagy in epithelial cells through wnt1: relevance in ibd. *Mucosal Immunol* (2014) 7(4):929–38. doi: 10.1038/mi.2013.108

624. Wang S, Chong ZZ, Shang YC, Maiese K. Wisp1 (Ccn4) autoregulates its expression and nuclear trafficking of beta-catenin during oxidant stress with limited effects upon neuronal autophagy. *Curr Neurovasc Res* (2012) 9(2):91–101. doi: 10.2174/156720212800410858

625. L'Episcopo F, Tirolo C, Testa N, Caniglia S, Morale MC, Deleidi M, et al. Plasticity of subventricular zone neuroprogenitors in mptp (1-methyl-4-phenyl-1,2,3,6-tetrahydropyridine) mouse model of parkinson's disease involves cross talk between inflammatory and wnt/beta-catenin signaling pathways: functional consequences for neuroprotection and repair. *J Neurosci* (2012) 32(6):2062–85. doi: 10.1523/jneurosci.5259-11.2012

626. Sun TJ, Tao R, Han YQ, Xu G, Liu J, Han YF. Therapeutic potential of umbilical cord mesenchymal stem cells with wnt/beta-catenin signaling pathway pre-activated for the treatment of diabetic wounds. *Eur Rev Med Pharmacol Sci* (2014) 18(17):2460–4.

627. Aly H, Rohatgi N, Marshall CA, Grossenheider TC, Miyoshi H, Stappenbeck TS, et al. A novel strategy to increase the proliferative potential of adult human beta-cells while maintaining their differentiated phenotype. *PloS One* (2013) 8(6):e66131. doi: 10.1371/journal.pone.0066131

628. Cai D, Hong S, Yang J, San P. The effects of microrna-515-5p on the toll-like receptor 4 (Tlr4)/jnk signaling pathway and wnt1-inducible-signaling pathway protein 1 (Wisp-1) expression in rheumatoid arthritis fibroblast-like synovial (Rafls) cells following treatment with receptor activator of nuclear factor-kappa-B ligand (Rankl). *Med Sci Monit* (2020) 26:e920611. doi: 10.12659/msm.920611

629. Bayod S, Felice P, Andres P, Rosa P, Camins A, Pallas M, et al. Downregulation of canonical wnt signaling in hippocampus of samp8 mice. *Neurobiol Aging* (2015) 36 (2):720–39. doi: 10.1016/j.neurobiolaging.2014.09.017

630. Krupska I, Bruford EA, Chaqour B. Eyeing the cyr61/ctgf/nov (Ccn) group of genes in development and diseases: highlights of their structural likenesses and functional dissimilarities. *Hum Genomics* (2015) 9(1):24. doi: 10.1186/s40246-015-0046-y

631. Wang AR, Yan XQ, Zhang C, Du CQ, Long WJ, Zhan D, et al. Characterization of wnt1-inducible signaling pathway protein-1 in obese children and adolescents. *Curr Med Sci* (2018) 38(5):868–74. doi: 10.1007/s11596-018-1955-5

632. Sahin Ersoy G, Altun Ensari T, Subas S, Giray B, Simsek EE, Cevik O. Wisp1 is a novel adipokine linked to metabolic parameters in gestational diabetes mellitus. *J Matern Fetal Neonatal Med* (2016) 30(8):942–6. doi: 10.1080/14767058.2016.1192118

633. Lim HW, Lee JE, Shin SJ, Lee YE, Oh SH, Park JY, et al. Identification of differentially expressed mrna during pancreas regeneration of rat by mrna differential display. *Biochem Biophys Res Commun* (2002) 299(5):806–12. doi: 10.1016/s0006-291x(02)02741-9

634. Du J, Klein JD, Hassounah F, Zhang J, Zhang C, Wang XH. Aging increases ccn1 expression leading to muscle senescence. *Am J Physiol Cell Physiol* (2014) 306(1): C28–36. doi: 10.1152/ajpcell.00066.2013

635. He W, Lu Q, Sherchan P, Huang L, Hu X, Zhang JH, et al. Activation of Frizzled-7 Attenuates Blood-Brain Barrier Disruption through Dvl/β-Catenin/Wisp1 Signaling Pathway after Intracerebral Hemorrhage in Mice. *Fluids Barriers CNS* (2021) 18(1):44. doi: 10.1186/s12987-021-00278-9

636. Gaudreau PO, Clairefond S, Class CA, Boulay PL, Chrobak P, Allard B, et al. Wisp1 is associated to advanced disease, emt and an inflamed tumor microenvironment in multiple solid tumors. *Oncoimmunology* (2019) 8(5):e1581545. doi: 10.1080/2162402x.2019.1581545

637. Li Y, Wang F, Liu T, Lv N, Yuan X, Li P. Wisp1 induces ovarian cancer via the igf1/αvβ3/wnt axis. *J Ovarian Res* (2022) 15(1):94. doi: 10.1186/s13048-022-01016-x

638. Li Y, Zhu Z, Hou X, Sun Y. Lncrna afap1-as1 promotes the progression of colorectal cancer through mir-195-5p and wisp1. *J Oncol* (2021) 2021:6242798. doi: 10.1155/2021/6242798

639. Liu Y, Qin W, Zhang F, Wang J, Li X, Li S, et al. Association between wnt-1-inducible signaling pathway protein-1 (Wisp1) genetic polymorphisms and the risk of gastric cancer in guangxi chinese. *Cancer Cell Int* (2021) 21(1):405. doi: 10.1186/s12935-021-02116-2

640. Wang QY, Feng YJ, Ji R. High expression of wisp1 promotes metastasis and predicts poor prognosis in hepatocellular carcinoma. *Eur Rev Med Pharmacol Sci* (2020) 24(20):10445–51. doi: 10.26355/eurrev_202010_23396

641. Wang Y, Yang SH, Hsu PW, Chien SY, Wang CQ, Su CM, et al. Impact of wnt1-inducible signaling pathway protein-1 (Wisp-1) genetic polymorphisms and clinical aspects of breast cancer. *Medicine* (2019) 98(44):e17854. doi: 10.1097/md.0000000000017854

642. Zhu Y, Li W, Yang Y, Li Y, Zhao Y. Wisp1 indicates poor prognosis and regulates cell proliferation and apoptosis in gastric cancer via targeting akt/mtor signaling pathway. *Am J Transl Res* (2020) 12(11):7297–311.

643. Chong ZZ, Shang YC, Zhang L, Wang S, Maiese K. Mammalian target of rapamycin: hitting the bull's-eye for neurological disorders. *Oxid Med Cell Longev* (2010) 3(6):374–91. doi: 10.4161/oxim.3.6.14787

644. Kopp C, Hosseini A, Singh SP, Regenhard P, Khalilvandi-Behroozyar H, Sauerwein H, et al. Nicotinic acid increases adiponectin secretion from differentiated bovine preadipocytes through G-protein coupled receptor signaling. *Int J Mol Sci* (2014) 15(11):21401–18. doi: 10.3390/ijms151121401

645. Martinez de Morentin PB, Martinez-Sanchez N, Roa J, Ferno J, Nogueiras R, Tena-Sempere M, et al. Hypothalamic mtor: the rookie energy sensor. *Curr Mol Med* (2014) 14(1):3–21. doi: 10.2174/1566524013666131118103706

646. Lai CS, Tsai ML, Badmaev V, Jimenez M, Ho CT, Pan MH. Xanthigen suppresses preadipocyte differentiation and adipogenesis through down-regulation of ppargamma and C/ebps and modulation of sirt-1, ampk, and foxo pathways. *J Agric Food Chem* (2012) 60(4):1094–101. doi: 10.1021/jf204862d

647. Dong Y, Chen H, Gao J, Liu Y, Li J, Wang J. Molecular machinery and interplay of apoptosis and autophagy in coronary heart disease. *J Mol Cell Cardiol* (2019) 136:27–41. doi: 10.1016/j.yjmcc.2019.09.001

648. Shokri Afra H, Zangooei M, Meshkani R, Ghahremani MH, Ilbeigi D, Khedri A, et al. Hesperetin is a potent bioactivator that activates sirt1-ampk signaling pathway in hepg2 cells. *J Physiol Biochem* (2019) 75(2):125–33. doi: 10.1007/s13105-019-00678-4

649. Tsai CF, Kuo YH, Yeh WL, Wu CY, Lin HY, Lai SW, et al. Regulatory effects of caffeic acid phenethyl ester on neuroinflammation in microglial cells. *Int J Mol Sci* (2015) 16(3):5572–89. doi: 10.3390/ijms16035572

650. Chen GH, Li XL, Deng YQ, Zhou FM, Zou WQ, Jiang WX, et al. The Molecular Mechanism of Epo Regulates the Angiogenesis after Cerebral Ischemia through Ampk-Klf2 Signaling Pathway. *Crit Rev Eukaryot Gene Expr* (2019) 29(2):105–12. doi: 10.1615/CritRevEukaryotGeneExpr.2019029018

651. Wang D, Song Y, Zhang J, Pang W, Wang X, Zhu Y, et al. Ampk-klf2 signaling pathway mediates the proangiogenic effect of erythropoietin in endothelial colony-forming cells. *Am J Physiol Cell Physiol* (2017) 313(6):C674–c85. doi: 10.1152/ajpcell.00257.2016

652. Su KH, Yu YB, Hou HH, Zhao JF, Kou YR, Cheng LC, et al. Amp-activated protein kinase mediates erythropoietin-induced activation of endothelial nitric oxide synthase. *J Cell Physiol* (2012) 227(8):3053–62. doi: 10.1002/jcp.23052

653. Jang W, Kim HJ, Li H, Jo KD, Lee MK, Yang HO. The neuroprotective effect of erythropoietin on rotenone-induced neurotoxicity in sh-sy5y cells through the induction of autophagy. *Mol Neurobiol* (2015) 53(6):3812–21. doi: 10.1007/s12035-015-9316-x

654. Maiese K. Charting a course for erythropoietin in traumatic brain injury. *J Transl Sci* (2016) 2(2):140–4. doi: 10.15761/JTS.1000131

655. Wang L, Di L, Noguchi CT. Ampk is involved in mediation of erythropoietin influence on metabolic activity and reactive oxygen species production in white adipocytes. *Int J Biochem Cell Biol* (2014) 54:1–9. doi: 10.1016/j.biocel.2014.06.008

656. Andreucci M, Fuiano G, Presta P, Lucisano G, Leone F, Fuiano L, et al. Downregulation of cell survival signalling pathways and increased cell damage in hydrogen peroxide-treated human renal proximal tubular cells by alpha-erythropoietin. *Cell Prolif* (2009) 42(4):554–61. doi: 10.1111/j.1365-2184.2009.00617.x

657. Kubat Oktem E, Aydin B, Yazar M, Arga KY. Integrative analysis of motor neuron and microglial transcriptomes from sod1(G93a) mice models uncover potential drug treatments for als. *J Mol Neurosci* (2022) 72(11):2360–76. doi: 10.1007/s12031-022-02071-1

658. Wang Y, Lin Y, Wang L, Zhan H, Luo X, Zeng Y, et al. Trem2 ameliorates neuroinflammatory response and cognitive impairment via pi3k/akt/foxo3a signaling pathway in alzheimer's disease mice. *Aging (Albany NY)* (2020) 12:20862–79. doi: 10.18632/aging.104104

659. Oaks Z, Patel A, Huang N, Choudhary G, Winans T, Faludi T, et al. Cytosolic aldose metabolism contributes to progression from cirrhosis to hepatocarcinogenesis. *Nat Metab* (2023) 5(1):41–60. doi: 10.1038/s42255-022-00711-9

660. Monti C, Colugnat I, Lopiano L, Chiò A, Alberio T. Network analysis identifies disease-specific pathways for parkinson's disease. *Mol Neurobiol* (2018) 55(1):370–81. doi: 10.1007/s12035-016-0326-0

661. Oaks Z, Winans T, Caza T, Fernandez D, Liu Y, Landas SK, et al. Mitochondrial dysfunction in the liver and antiphospholipid antibody production precede disease onset and respond to rapamycin in lupus-prone mice. *Arthritis Rheumatol (Hoboken NJ)* (2016) 68(11):2728–39. doi: 10.1002/art.39791

frontiers | Frontiers in Immunology

TYPE Review
PUBLISHED 23 November 2023
DOI 10.3389/fimmu.2023.1281882

OPEN ACCESS

EDITED BY
Chao Yang,
Zhejiang Ocean University, China

REVIEWED BY
Huw Lewis,
GlaxoSmithKline, United Kingdom
Christopher Mark Norris,
University of Kentucky, United States

*CORRESPONDENCE
Tomasz Boczek
tomasz.boczek@umed.lodz.pl

RECEIVED 23 August 2023
ACCEPTED 06 November 2023
PUBLISHED 23 November 2023

CITATION
Mackiewicz J, Lisek M and Boczek T (2023) Targeting CaN/NFAT in Alzheimer's brain degeneration.
Front. Immunol. 14:1281882.
doi: 10.3389/fimmu.2023.1281882

Targeting CaN/NFAT in Alzheimer's brain degeneration

Joanna Mackiewicz, Malwina Lisek and Tomasz Boczek*

Department of Molecular Neurochemistry, Medical University of Lodz, Lodz, Poland

Alzheimer's disease (AD) is a neurodegenerative disorder characterized by a progressive loss of cognitive functions. While the exact causes of this debilitating disorder remain elusive, numerous investigations have characterized its two core pathologies: the presence of β-amyloid plaques and tau tangles. Additionally, multiple studies of postmortem brain tissue, as well as results from AD preclinical models, have consistently demonstrated the presence of a sustained inflammatory response. As the persistent immune response is associated with neurodegeneration, it became clear that it may also exacerbate other AD pathologies, providing a link between the initial deposition of β-amyloid plaques and the later development of neurofibrillary tangles. Initially discovered in T cells, the nuclear factor of activated T-cells (NFAT) is one of the main transcription factors driving the expression of inflammatory genes and thus regulating immune responses. NFAT-dependent production of inflammatory mediators is controlled by Ca^{2+}-dependent protein phosphatase calcineurin (CaN), which dephosphorylates NFAT and promotes its transcriptional activity. A substantial body of evidence has demonstrated that aberrant CaN/NFAT signaling is linked to several pathologies observed in AD, including neuronal apoptosis, synaptic deficits, and glia activation. In view of this, the role of NFAT isoforms in AD has been linked to disease progression at different stages, some of which are paralleled to diminished cognitive status. The use of classical inhibitors of CaN/NFAT signaling, such as tacrolimus or cyclosporine, or adeno-associated viruses to specifically inhibit astrocytic NFAT activation, has alleviated some symptoms of AD by diminishing β-amyloid neurotoxicity and neuroinflammation. In this article, we discuss the recent findings related to the contribution of CaN/NFAT signaling to the progression of AD and highlight the possible benefits of targeting this pathway in AD treatment.

KEYWORDS

calcineurin, NFAT, Alzheimer's disease, calcium, inflammation

Introduction

Alzheimer's disease (AD) is a chronic neurodegenerative disorder characterized by a progressive decline in cognitive and executive functions (1). Intensive research performed over the decades has revealed the complex mechanistic underpinnings of AD, involving a combination of age-dependent brain changes along with genetic predisposition, lifestyle,

and environmental factors (1). Despite relatively wide knowledge about its etiology, the cellular determinants of AD susceptibility or resilience and the key molecular changes driving disease progression are less understood.

Neuropathologically, AD-associated degeneration is linked to the deposition of amyloid-β (Aβ) fibrillary aggregates, occurring as neuritic plaques or vascular deposits, and hyperphosphorylated microtubule-associated protein tau. The latter is a major component of neurofibrillary tangles, neuropil threads, and neuritic plaque corona (2). However, the list of detected abnormalities is much longer and involves gliosis, neuroinflammation, oxidative stress, changes in neuronal plasticity, altered expression of glutamate and cholinergic receptors, Ca^{2+} homeostasis imbalance, and many others. The accumulation of these changes across the lifespan leads to impaired cognition and a higher risk of AD development. It is now well-accepted that many of these pathologies are a consequence of Ca^{2+} signaling deregulation, which is central to amyloid-evoked degeneration (3). Indeed, numerous independent biochemical, behavioral, electrophysiological, and molecular studies, which have been the subject of excellent reviews (1, 4, 5), have confirmed a link between Ca^{2+} deregulation and age-related memory deficits and worsening cognitive performance. Nonetheless, it is becoming apparent that Ca^{2+} imbalance is not restricted to neurons but also underlies the altered function of other non-neuronal cells, especially astrocytes. The relationship between astrocytic Ca^{2+} deregulation as a function of neurodegenerative diseases has been thoroughly discussed in comprehensive reviews (6–8). Several laboratories have provided strong evidence to imply that Ca^{2+}-dependent protein phosphatase calcineurin (CaN) links dysfunctional Ca^{2+} signaling to Aβ accumulation, neuroinflammation, and synaptotoxicity (3, 9–11). The activity of CaN is controlled by spatially and temporarily restricted intracellular Ca^{2+} elevations, which activate specific Ca^{2+} signal decoding proteins (12). CaN is required for both long-term potentiation and long-term depression, synaptic processes underlying learning and memory, and its activity positively correlated with cognitive loss in AD brains (13, 14). Perhaps, one of the most important downstream effectors linking Ca^{2+}/CaN signaling to the gene regulatory machinery is the nuclear factor of activated T-cells (NFAT). Mounting evidence, as will be discussed in the following sections, shows that CaN/NFAT drives or exacerbates the core symptoms of AD neuropathology. It is therefore critical to understand the upstream and downstream signals leading to the pathological activation of CaN/NFAT pathway to identify new therapeutic targets and develop new treatment strategies for AD. In this review, we summarize the emerging evidence that deficient CaN/NFAT could contribute to brain degeneration in AD.

Calcineurin

In healthy adults, CaN is widely expressed throughout the brain, with its highest concentration detected in neurons and low in glial cells (15–18). Structurally, the holoenzyme of CaN comprises two main subunits: a ~ 60 kDa catalytic subunit (CNA) and a ~19 kDa regulatory subunit (CNB) containing four Ca^{2+}-binding EF-hand motifs (12) (Figure 1).

Binding of calmodulin (CaM) to the regulatory domain of the catalytic subunit increases CaN phosphatase activity, decoding the upstream Ca^{2+} signals and translating them into a dephosphorylation pattern of cellular proteins. CaM itself is a small, evolutionary conserved protein expressed in all mammalian cells. It serves as a versatile Ca^{2+} sensor capable of responding to a wide range of Ca^{2+} concentrations (10^{-12} M - 10^{-16} M) due to the presence of four canonical Ca^{2+} binding EF hands possessing different affinities for Ca^{2+} (19). Upon binding Ca^{2+}, CaM undergoes a conformational change exposing the hydrophobic surface region for Ca^{2+}-dependent interaction with CaM-binding proteins (20). The Ca^{2+}/CaM complex interacts with targets that mediate crucial cellular processes such as inflammation, metabolism, apoptosis, short-term and long-term memory and the immune response (21–25). Continued research indicates that CaM binds to and affects many proteins involved in the onset and progression of AD and other neurodegenerative diseases (26–28). This involvement in neurodegeneration underscores the significance of CaM in the understanding the molecular mechanisms behind these diseases.

Among many Ca^{2+}-dependent protein phosphatases, CaN is the only one directly activated by Ca^{2+}/CaM and is one of the most sensitive enzymes responding to Ca^{2+} elevations. The cooperative interaction between Ca^{2+}, CaNB, and Ca^{2+}/CaM allows CaN to uniquely respond to discrete Ca^{2+} fluctuations (29). These features make CaN particularly vulnerable to alterations in Ca^{2+} homeostasis observed in AD. A growing body of evidence suggests that upregulation of CaN activity is directly linked to multiple neurodegenerative insults observed in Parkinson's disease (30), Alzheimer's disease (31), and Huntington's disease (32), all marked by impaired synaptic function, neuroinflammation, and neuronal loss. Moreover, abnormal activation of CaN has been observed in numerous cellular events traditionally linked to AD, including astrocyte activation, Aβ generation, neuronal apoptosis, synaptic toxicity, and behavioral deficits (14). The involvement of CaN is also supported by several studies showing altered CaN signaling in the brains of animals used to model the pathogenesis of neurodegenerative disorders (33–36).

Strong evidence for the contribution of CaN to the pathophysiology of AD in humans comes from the Taglialatela group (37). The results of a retrospective analysis of kidney transplant patients demonstrated that the administration of CaN inhbitors to prevent transplant rejection decreased the incidence of dementia and AD in this group compared to national data from the general population. The initially encouraging results were potentially limited by the small sample size. These findings have been recently replicated in a large cohort by Silva and colleagues (38), demonstrating that FK506, CsA, and sirolimus can reduce the risk of dementia compared to general population-like control. However, among the three immunosuppressive drugs, those that are capable of crossing the blood-brain barrier, like FK506, have a greater probability of reducing dementia. Since inflammatory mediators are strongly correlated with the accumulation of Aβ and induction of neuronal apoptosis, the potential role of CaN inhibitors in reducing the prevalence of dementia is not surprising. However, the study performed by Silva and colleagues delineates a

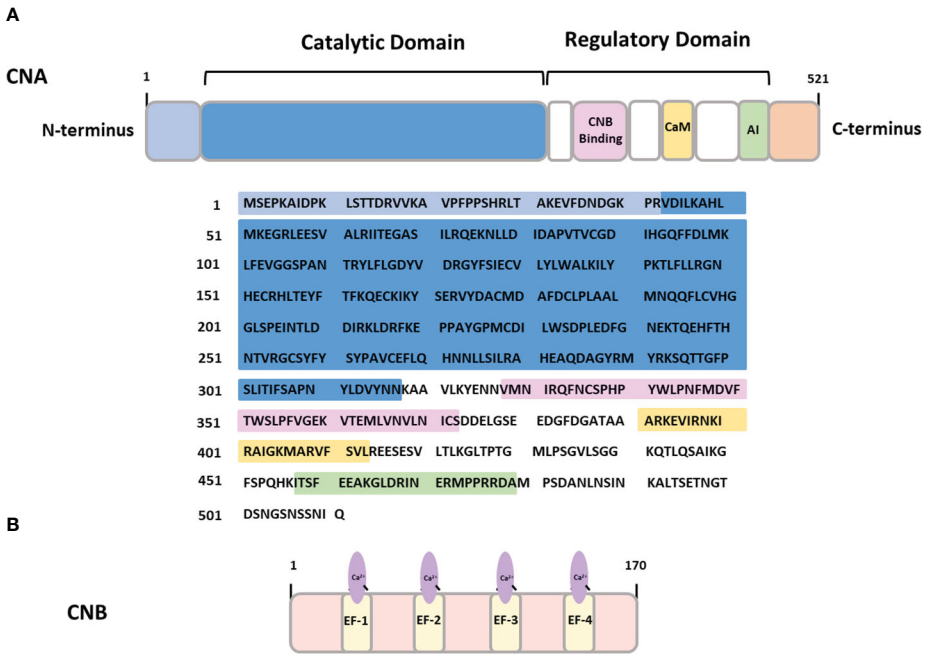

FIGURE 1
The structure of calcineurin **(A)** CNA- calcineurin subunit A containing binding sites for calcineurin subunit B (CNB binding), calmodulin binding domain (CaM) and autoinhibitory domain (AI). **(B)** CNB – calcineurin subunit B containing four Ca^{2+}-binding EF hand domains.

new therapeutic avenue based on brain-penetrant CaN inhibitors. In addition, it has been shown that CaN is heavily involved in the regulation of gene expression (39). For upstream and downstream regulatory mechanisms of CaN, we refer to the excellent reviews published recently (12, 40–42).

NFAT – structure, function and regulation

Proteins belonging to the NFAT family were originally described more than three decades ago as the transcriptional activators of interleukin-2 (IL-2) in T cells (43). It is now apparent that NFAT proteins play a key role not only during T-cell activation and differentiation but also in regulating the function of several types of immune cells, including B cells, mast cells, basophils, and natural killer cells (44). NFAT family members are involved in the induction and/or coordination of the immune response by modulating the expression of a large number of immunologically important genes. These genes include cytokines such as IL-2, IL-3, IL-4, IL-5, IL-8, IL-13, granulocyte-macrophage colony-stimulating factor (GM-CSF), and tumor necrosis factor-alpha (TNF-α), as well as cell-surface receptors CD40L and CTLA-4, and the apoptotic factor FasL (45).

NFAT family members are widely distributed throughout tissues, including the brain, and can regulate distinct developmental processes (46–49). The strong correlation between NFAT expression and vertebrate development was derived from mouse genetic experiments. For instance, deletion of NFATc1 caused dramatic defects in cardiac morphogenesis (50), NFATc2 null mice displayed abnormalities in chondrogenesis (51), disruption of NFATc3 resulted in dysregulation of myogenesis (52), whereas NFATc4 deficient mice were healthy and developmentally normal. Suchting et al. (53) have discussed the developmental relationship between nerve cells and vessels, pointing out several anatomical and functional parallels. In support of this, concurrent deletion of NFATc3 and NFATc4 produced significant impairments in vascular development but also massive defects in sensory axon projection (49). NFAT signaling is recognized as an essential pathway both in the adult and developing nervous system. In the brain, NFAT-dependent gene regulation has been shown to play a critical role in neuronal survival, proliferation, and differentiation (54–56), as well as synaptogenesis, corticogenesis, and neurotransmission (57–59).

In human, the NFAT family encompasses five different members: NFAT1 [also called NFATc2 or NFATp), NFAT2 (also called NFATc1 or NFATc), NFAT3 (also called NFATc4), NFAT4 (also called NFATc3 or NFATx) and NFAT5 (also called tonicity enhancer binding protein (TonEBP) or osmotic response element-binding protein (OREBP)] that are encoded by separate genes. Moreover, the alternative splicing of each of these family members results in a different number of variants. There are eight possible variants of NFATc2 and NFATc1 in mammalian cells. The splicing of NFATc3 generates six isoforms, and up to twenty-four in the case of NFATc4 (60). On the other hand, sixteen various transcripts of NFAT5 have been identified so far (61) (Table 1). Specific NFAT isoforms appear to exhibit preferential associations with different types of neuronal cells (3, 10, 62, 63). For instance, NFATc3 is prominently expressed in astrocytes and pericytes, with comparatively lower expression in neurons. This isoform is also

10.3389/fimmu.2023.1281882

TABLE 1 General features of NFAT family members and their distribution in the brain.

NFAT member	Alternative name(s)	Number of variants	Regulated by	CNS distribution
NFAT1	NFATc2 and NFATp	8	Ca^{2+}/Calcineurin	oflactory bulb, neuronal cell line
NFAT2	NFATc1 and NFATc	8	Ca^{2+}/Calcineurin	hypothalamus, hippocampus, cerebellum, olfactory bulb, and frontal cortex
NFAT3	NFATc4	24	Ca^{2+}/Calcineurin	olfactory bulb, cerebellum, and certain regions of the cortex
NFAT4	NFATc3 and NFATx	6	Ca^{2+}/Calcineurin	hippocampus, retinal ganglion cells
NFAT5	TonEBP and OREBP	16	Osmotic stress	cerebral cortex, hippocampus, hypothalamus, substantia nigra, cerebellum, medulla oblongata

significantly upregulated in activated astrocytes (3). In contrast, NFATc4 has a broader distribution within neurons compared to NFATc3. NFATc1 and NFATc2, in particular, display a stronger preference for glial cells.

Despite having different C- and N-terminal sequences, all family members contain a highly conserved DNA-binding domain (DBD), similar to the one in the NFκB/Rel family, and are activated, with the exception of NFAT5, by CaN (47). NFAT5 lacks an essential CaN binding site, and its activity is regulated by changes in tonicity (64). Structurally, NFAT1-4 exist as monomers and possess two tandem domains: a regulatory domain located in the N-terminus, which is known as the NFAT homology region (NHR), and a Rel homology domain (RHR), where the DBD is located (65). The NHR contains two CaN binding motifs: a Ca^{2+}-independent PXIXIT (where X denotes any amino acid) motif in the N-terminus, and a Ca^{2+}-dependent LXVP motif in the C-terminal portion of the NHR (65). Furthermore, the NHR possesses the nuclear localization signal (NLS) responsible for CaN-dependent nuclear translocation, extended serine-rich regions (SRR1, SRR2), and three serine-proline motifs (SP1, SP2, SP3) (65) (Figure 2). NFAT dephosphorylation is believed to expose the NLS sequence, 265-KRK-267, which is located upstream of the SP3 motif. A second potential NLS site, 682-KRK-684 is situated near the C-terminus of NFATc1 (66). It is well-documented that phosphorylation status of the regulatory domain governs DNA-binding affinity and NLS exposure. However, the mechanism of NLS activation has not been elucidated at a structural level. The most plausible hypothesis suggests that dephosphorylation initiates global changes in NFAT conformation, facilitating its transition from an inactive to an active state (67). This transition may involve alterations in interactions within NFAT itself or with binding protein partners (68–70).

The NHR domain is moderately conserved and shares 22-32% sequence homology among the distinct NFAT members, whereas the Rel-homology region, consisting of approximately 270 amino acids, shares 64-72% sequence identity between various NFAT members (65, 71). In contrast, NFAT5 exists as a homodimer and possesses only a Rel DNA-binding domain structurally homologous to the Ca^{2+}-dependent members, while the remaining 600 amino acids are entirely different (59).

Under resting conditions, the NHR domain is hyperphosphorylated within the SRR region and SP repeats, keeping the NFAT proteins in an inactive state and predominantly located in the cytoplasm (72). In response to elevated intracellular Ca^{2+}, CaN becomes activated and dephosphorylates NFAT, leading to its rapid import into the nucleus (72). Once in the nucleus, NFATs can couple intracellular changes in Ca^{2+} concentration to the activation/repression of gene transcription, either acting alone or more frequently in cooperation with other transcription factors (73). Many of the NFAT transcriptional partners have not been characterized yet, but biochemical reconstructions have

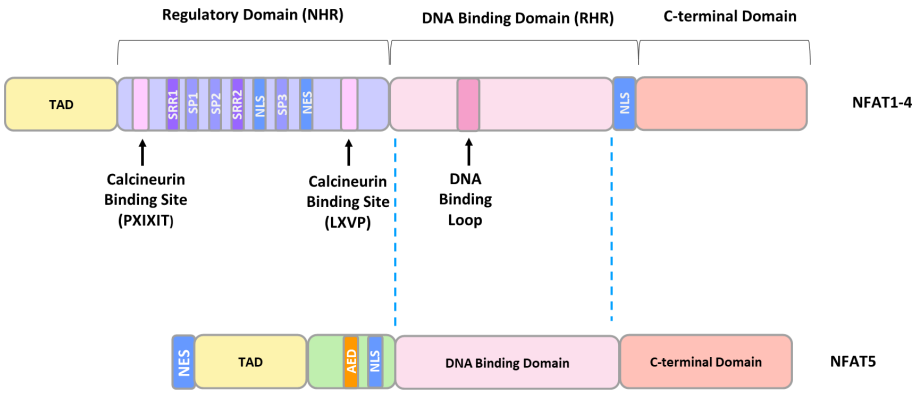

FIGURE 2
The general structure of NFAT proteins. TAD, transactivation domain; SRR, serine-rich region; SP, serine/proline motif; NLS, nuclear localization sequence; NES, nuclear exclusion sequence; AED, auxiliary export domain.

revealed several of them, including the cell life and death regulator activator protein 1 (AP1) and oncogenic regulators such as GATA binding protein 4 (GATA4) or myocyte enhancer factor 2 (MEF2) (46, 74). The nuclear accumulation of NFAT is counteracted by the synergistic actions of a set of protein kinases, including casein kinase 1 (CK1), glycogen synthase kinase 3 (GSK-3), and dual-specificity tyrosine-regulated kinases (DYRK) (55, 68, 75). These kinases can act in the cytosol to cause NFAT phosphorylation or in the nucleus to promote its rephosphorylation, facilitating nuclear export and transcription termination. CK1 functions as a maintenance and export kinase for NFATc2 (47). GSK-3 is classified as an export-type kinase, which phosphorylates the SP2 motif of NFATc2 and both, SP2 and SP3 motifs, of NFATc1 (47). In addition, phosphorylation of NFATc2 by GSK-3 requires previous phosphorylation by priming kinases including PKA or DYRK. Furthermore, DYRK1 functions as an export kinase which phosphorylates conserved SP3 motif in NFATc1 and NFATc2. In turn, DYRK2 can operate as a maintenance kinase, and phosphorylate the SP3 motif of NFATc1 and NFATc2 (47). Additionally, phosphorylation of SSR1 of NFATc1 by the c-Jun N-terminal kinase (JNK) or SSR1 of NFATc2 by the p38 mitogen-activated protein kinase (MAPK) has been shown to enhance cytosolic NFAT retention (69, 76, 77). However, it is not entirely clear whether kinases that phosphorylate NFAT under basal conditions also mediate its rephosphorylation in the nucleus and subsequent export back to the cytoplasm. Furthermore, NFAT transcriptional activity can be affected by different post-translational modifications, including acetylation or sumoylation, as well as phosphorylation events different from those regulating Ca^{2+}-dependent translocation (78–80). It has been demonstrated that sumoylation plays a privileged role in extensive cellular processes and appears to be an important mediator of neuronal and synaptic function (81). In rat primary hippocampal neurons, sumoylation effectively suppressed the transcriptional activity of NFATc1, NFATc2, and NFATc3 isoforms, while in cortical neurons, only the transcriptional activity of NFATc1 and NFATc2 was affected by sumoylation (82). These findings indicate that the regulation of particular NFAT isoforms may be cell type-specific.

Regulation of subcellular localization and activity of Ca^{2+}-dependent NFAT members is related to ligand binding to distinct cell-surface receptors (45, 46, 65, 83, 84). These receptors share a common feature: their ability to activate phosphatidylinositol-specific phospholipase C (PLC), thereby inducing Ca^{2+} entry through the plasma membrane. Activation of PLC triggers a cascade of events, including the hydrolysis of phosphatidylinositol 4,5-bisphosphate (PIP_2) and the release of inositol 1,4,5-triphosphate (IP_3), which in turn mobilizes intracellular Ca^{2+} through IP_3 receptors located in the membrane of the endoplasmic reticulum (ER) (85). The increase in Ca^{2+} concentration leads to CaN activation by binding to its CaN-B regulatory subunit or by coupling Ca^{2+}-dependent calmodulin to CaN. Efficient CaN-dependent dephosphorylation requires a docking interaction between NFAT and CaN. The PxIxIT sequence, located at the N-terminus of the NHR domain, serves as a primary docking site for CaN. Different NFAT members have unique PxIxIT sequences with a low affinity for calcineurin (Kd = 10–30 μM), which is essential to maintain sensitivity to environmental cues and restrict constitutive activation of NFAT (86). Aramburu and colleagues replaced the PxIxIT sequence of NFATc2 with VIVIT, a higher-affinity inhibitor identified through peptide selection. This peptide binds CaN with high affinity and efficiently competes with NFAT for CaN binding, thereby inhibiting NFAT nuclear accumulation (87). *In vivo* studies with transgenic mice carrying a mutation in the PxIxIT sequence of NFATc2 demonstrated enhanced cytokine production by differentiated T cells and exhibited deficiencies in embryonic and hematopoietic cell maturation (86). CaN dephosphorylates 13 out of 14 serines in NFATc2, which are conserved residues in all calcineurin-dependent NFAT members (67). It has been demonstrated that dephosphorylation of all 13 serine residues in NFATc2 is required to promote its nuclear localization (67). Furthermore, mutations of twelve serines to alanine, which imitate a nearly fully dephosphorylated state of NFATc2, lead to remarkable nuclear accumulation in both, resting and CsA-treated cells.

It is not fully understood whether site-specific dephosphorylation is an organized mechanism and what the consequences are for downstream signaling in specific cell types. However, the experiments using mass spectrometric analysis indicate that the SRR1 region, which is closely adjacent to the main CaN docking site, is preferentially dephosphorylated at low CaN activity (67). NFAT mutants with restricted deletions or S → A mutations in the SRR1 motif are more susceptible to dephosphorylation in the SP repeats by CaN compared to wild-type NFATs (87, 88). CaN-regulated NFAT activation is particularly important in resting conditions when the rise in Ca^{2+} due to its release from intracellular stores is not sufficient for direct NFAT activation (89).

The parameters for Ca^{2+}/CaN/NFAT activation can be regulated in various ways (Figure 3).

In neurons, NFAT activation occurs as a result of stimulation of tyrosine kinase receptors (Trk) coupled to PLCγ (90). Neurotrophins and netrins are upstream components of this signaling pathway. For example, it has been observed that overexpression of the TrkA receptor in cortical neurons supports NFAT transcriptional activation upon nerve growth factor (NGF) treatment (91). Additionally, Groth et al. (92) demonstrated that treatment of cultured spinal neurons with NGF enhanced NFAT-dependent transcription. Brain-derived neurotrophic factor (BDNF) has also been found to increase NFAT transcriptional activity in cultured cortical neurons, and this activation was abolished by co-treatment with CaN inhibitors such as CsA or FK506 (91). To illustrate the neurotrophic significance in the NFAT signaling pathway, Graef and colleagues (91) utilized an EGFP-NFATc4 hybrid to visualize NFATc4 subcellular localization in responsive cortical neurons. The data showed that NFATc4 was imported into the nucleus, and its transcriptional activity was enhanced in response to BDNF stimulation. Moreover, cultured hippocampal pyramidal neurons treated with BDNF also exhibited increased endogenous transcriptional activity of NFATc4 (92). It is worth mentioning that inhibition of PLC activity or depletion of intracellular Ca^{2+} stores attenuated the ability of BDNF to activate endogenous NFAT in hippocampal neurons (92, 93). These results collectively demonstrate that NFAT transcriptional complexes

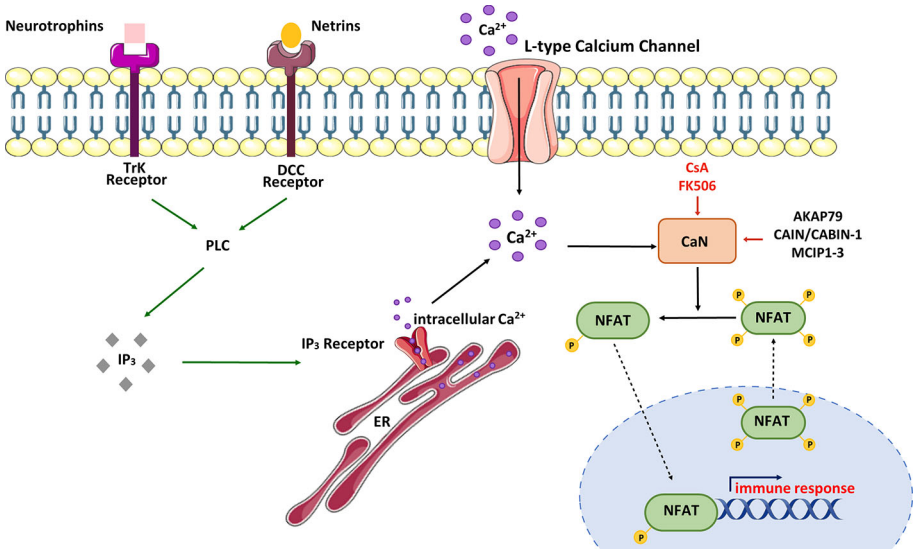

FIGURE 3
Schematic view of CaN/NFAT activation cycle. NFAT is activated in response to cell-surface receptors coupled to intracellular Ca^{2+} mobilization. Activated phospholipase C (PLC) generates inositol-1,4,5-triphosphate (IP_3), which binds IP_3 receptors located in the endoplasmic reticulum (ER). Stimulation of IP_3 receptors produces a brief spike in Ca^{2+} by depleting the ER stores. Ca^{2+} increases promote activation of calmodulin-dependent enzymes including calcineurin (CaN). CaN dephosphorylates multiple serines in NFAT protein leading to its nuclear import and activation of NFAT-dependent transcription of genes involved in immune response. NFAT rephosphorylation by multiple kinases triggers its nuclear export and cytosolic retention. CaN activity can be modulated by immunosuppressive drugs – cyclosporine A (CsA) and tacrolimus (FK506) or CaN-interacting proteins – AKAP79 (A-kinase anchoring protein 79), MCIPs (modulatory calcineurin-interacting proteins) or CAIN/CABIN-1 (endogenous inhibitor of CaN activity). In neurons, NFAT can be selectively activated by Ca^{2+} influx through L-type Ca^{2+} channels.

appear to be downstream of neurotrophin signaling, and their activity in neuronal development is regulated through PLC-dependent mechanisms.

A growing body of evidence indicates that NFAT transcription factors can also play a pivotal role in integrating signaling pathways involved in neuronal growth driven by guidance cues during synaptogenesis. In this process, molecules such as netrins are crucial for axon guidance and control during the development of neuronal circuits (94). Supporting this, failure in the elongation of commissural axons caused by triple deletion of NFAT (c2/c3/c4) was seen in mice bearing mutation in netrin-1 or netrin DCC receptor (95, 96). Additionally, it has been demonstrated that netrin-dependent axon extension in E13 rat dorsal spinal cord explants required CaN/NFAT signaling, and stimulation with netrin-1 promoted NFAT transcriptional activity via the DCC receptor (91).

The emptying of ER Ca^{2+} stores is a known trigger that initiates the process of capacitative Ca^{2+} influx across the plasma membrane, referred to as store-operated Ca^{2+} entry. In neurons, Ca^{2+} influx may also occur via voltage- or ligand-gated Ca^{2+} channels, each of which is regulated in a precisely coordinated manner. It is well recognized that neuronal L-type voltage-gated Ca^{2+} channels (LTCC) play a crucial role in various synaptic processes underlying learning and spatial memory formation in the hippocampus and other brain areas (97, 98). The activation of LTCC by high extracellular K^+ triggers the nuclear localization of NFAT in cultured hippocampal and DRG neurons (93, 99, 100). It has also been demonstrated that *N*-methyl-D-aspartate receptor stimulation leads to enhanced nuclear import of NFATc3 and NFATc4 in cortical neurons (101).NFAT activity can also be affected by intracellular inhibitors of CaN. Among the numerous endogenous proteins that have a pivotal role in regulating CaN activity is A-kinase anchoring protein 79 (AKAP79), which binds CaN and blocks its access to the substrates (102). It is worth mentioning that AKAP79 also binds protein kinase A (PKA), which is an NFAT kinase that prevents its nuclear import (103). Other regulators, such as CAIN/CABIN-1, can potentially inhibit CaN activity in a phosphorylation-dependent manner (104) and exert a similar effect on NFAT dephosphorylation and translocation, like the regulators of calcineurin (RCANs) or modulatory calcineurin-interacting proteins (MCIPs; MCIP1–3) (59). Studies have shown that RCANs may either positively or negatively affect the activation of CaN/NFAT signaling. Although the mechanistic explanation of how these proteins modulate CaN activity is still questionable, RCANs were found to participate in CaN biosynthesis or recycling, playing a role as chaperones (59).

Pharmacological inhibitors of CaN/NFAT with potential use in AD treatment

Relatively insensitive to classical inhibitors of phosphatases, CaN activity can be corroborated by two widely used immunosuppressive drugs: cyclosporine A (CsA) and FK506 (tacrolimus) (105, 106). CaN/NFAT signaling may also be inhibited by other molecules that differ in chemical properties and the mechanism of action (Table 2).

TABLE 2 Physicochemical characteristics of CaN/NFAT inhibitors.

Inhibitor	Characteristic profile				
	Composition	Mode of action	Binding partner	IC_{50}/K_d*	Side effects
CsA	A cyclic peptide of 11 amino acids	Complex blocks substrate access to the active centre of CaN	Cyclophilin	7 nM	Nephrotoxicity, hypertension, neurotoxicity
FK506	23-membered polyketide macrolide	Complex blocks substrate access to the active centre of CaN	FK506 binding protein (FKBP-12)	0.4 nM	Nephrotoxicity
VIVIT peptide	A 16 member linear L-peptide	Blocks CaN-NFATc interaction	No	0.5 μM* < 1 μM	Not observed
LxVP peptide	15 - mer peptide from NFATc1	Blocks CaN-NFATc interaction and regulates enzymatic activity of CaN	No	~ 0.3 μM	Not observed
Dipyridamole	Pyramidopyri-midine compound	Disrupts CaN-NFATc binding	No	~ 10 μM	Cytotoxicity, excitotoxicity under injurious conditions
INCA-6	Small organic molecule	Disrupts CaN-NFATc complex formation by covalent binding to CaN	No	~ 0.8 μM*	Cytotoxicity
A-28522	Small organic molecule	Inhibits NFAT activity	No	N/A	N/A
Q-134R	Hydroxyquinoline derivative	Partially inhbits NFAT activity	No	~ 400 nM	Not observed

N/A, not available.
*Kd.

Cyclosporine A

CsA has been employed in the treatment of organ transplant rejection since 1976 when Borel and colleagues demonstrated its immunosuppressive properties (107). The mechanism of action of CsA depends the formation of a complex with cytosolic proteins known as cyclophilins, particularly the 17 kDA cyclophilin A, which is highly abundant in T cells (108, 109). Cyclophilins, classified as immunophilins, possess peptidyl-proline-*cis-trans* isomerase (PPIase) activity that plays a role in ensuring proper protein folding (110). It has been established that CsA inhibits PPIase, although this effect is not associated with the mechanism of immunosuppression. The formation of a ternary complex involving CsA, cyclophilin A and CaNA inhibits calcineurin phosphatase activity and blocks the transcription of cytokine genes, including IL-2 and IL-4 (111). In addition to its impact on the CaN/NFAT pathway, CsA affects the activity of NF-κB and AP-1, transcription factors essential for the regulation of IL-2 gene expression (112, 113). CsA has been demonstrated to inhibit JNK and p38 MAPK signaling, as well as an antigen-specific Ca^{2+}-independent response (114, 115). Several early reports have indicated both pro-apoptotic and neuroprotective effects of CsA in neuronal and neuronal-glia mixed cultures (116–121). The pharmacological normalization of CaN activity can offer a certain degree of neuroprotection (122, 123), improve synaptic function (124), and reduce glial activation (125, 126) in experimental models of brain degeneration. However, despite the undeniable benefits of CsA, its use as an immunosuppressant is limited by potential side effects, including nephrotoxicity, neurotoxicity, and hepatotoxicity (127).

FK506 (tacrolimus)

Structurally, FK506 is a macrolide antibiotic with immunosuppressive properties. It forms a complex with immunophilin FK506 binding protein (FKBP12), and the FK506-FKB12 complex suppresses CaN-dependent NFAT signaling. Despite significant differences in structure and mechanism of action, CsA and FK506 surprisingly share similar biological effects (128, 129). However, FK506-induced immunosuppression is not solely due to the inhibition of the CaN/NFAT pathway but also involves other T-cell activation pathways (130). Unlike CsA, FK506 inhibits IL-2 induced IL-5 production by human $CD4^+$ T cells and T-cell proliferation stimulated by IL-2 and IL-7 (130). Moreover, FK506, but not CsA, decreases the expression of human-affinity IL-7 receptor and is more effective in controlling IL-2 production by T cells in patients receiving kidney transplantation. These data suggest that at least some of FK506's effects are mediated by CsA-insensitive signaling pathways (131). Regarding the immunosuppressive effects, it is evident that FK506 hinders processes further downstream in the T-cell activation cascade, beyond CaN activation. This is supported by the observed capacity of FK506 monotherapy to effectively manage steroid-resistant allograft rejection episodes, which is a critical distinction from CsA, as CsA lacks efficacy in the treatment of allograph rejection (132).

VIVIT and LxVP peptides

The VIVIT is a 16-mer oligopeptide (MAGPHPVIVITGPHEE) developed through an affinity- driven selection of peptides encoding

mutated versions of the wild NFAT protein sequence (SPRIEIT), which is characterized by a low affinity toward the PxIxIT consensus motif (87, 133). VIVIT exhibits a remarkable 25-fold higher potency in inhibiting NFATc dephosphorylation compared to the original SPRIEIT peptide. While 10 μM CsA/cyclophilin can completely inhibit CaN activity, it remained unaffected even at a concentration of up to 100 μM VIVIT. However, the presence of 100 μM VIVIT is sufficient to disrupt the interaction between CaN and NFAT, thus preventing NFAT dephosphorylation (87). Furthermore, VIVIT demonstrates superior selectivity in inhibiting NFAT compared to CsA and FK506. VIVIT has been demonstrated to inhibit the dephosphorylation of NFATc1, NFATc2 and NFATc3, as well as the nuclear import of NFATc2. Additionally, GFP-VIVIT suppresses NFAT-mediated expression of IL-2, IL-3, IL-13, TNF-α, macrophage inflammation protein 1 (MIP-1 α), and granulocyte-macrophage colony-stimulating factor (GM-CSF) in Jurkat T cells while not affecting CsA-regulated genes such as TNF-β and lymphotoxin-β (87). To date, there have been no reported toxic side effects associated with VIVIT. Its outstanding specificity in disrupting NFAT signaling without CaN activity in a general sense, makes VIVIT highly promising for reduced toxicity compared to CsA or FK506. Similarly, its cell-permeable analog, 11-R VIVIT, has demonstrated a lack of toxicity at doses up to 10 mg/kg (134). In this analog, VIVIT was fused to the C-terminal of a poly-arginine-based protein transduction domain (11R-VIVIT, RRRRRRRRRRR-GGG-MAGPHPVIVITGPHEE).

LxVP peptides are derived from CaN-docking NFATc sequence LxVP, and they compete for binding with activated CaN (135, 136). Notably, CaN exhibits a strong affinity for the LxVP motif of NFATc1, NFATc3 and NFATc4, while its binding affinity is considerably weaker for NFATc2, the predominant isoform in activated $CD4^+$ T cells (137). For instance, the GST-LxVPc1 peptide, consisting of 15 amino acids from human NFATc1, shows more efficient binding to CaN compared to any of the PxIxIT motifs found in NFATc1-c4. In contrast, the GST-LxVPc2 fusion peptide from NFATc2 does not bind to CaN under the same conditions. The LxVP effectively inhibits CaN activity when assessed with a phosphopeptide derived from the PKA regulatory subunit II, containing phosphoSer-95, and it increases phosphatase activity when evaluated using a nitrophenyl phosphate assay (135, 136). Therefore, similar to CsA and FK506, LxVPc1 can modify CaN's activity through an interaction with a site distinct from the active site. When GFP-LxVPc1 fusion protein is overexpressed in HeLa cells, it effectively inhibits NFATc2 dephosphorylation and nuclear translocation upon ionophore treatment. Similarly, in Jurkat T cells, it inhibits NFATc2 dephosphorylation and the expression of luciferase under the control of the IL-2 upon PMA/ionophore stimulation (135, 136).

Small molecular inhibitors acting on CaN molecule

Dipyridamole is a medication that serves as an inhibitor of nucleoside transport and a PDE3 (phosphodiesterase 3) inhibitor. When administered chronically, it effectively prevents the formation of blood clots, and when given in high doses over a short period, it induces the dilation of blood vessels. When combined with aspirin, it is an FDA-approved treatment for secondary prevention of stroke (138). In a screening of the Prestwick Chemical Library, which contains 880 biologically active molecules, Mulero and colleagues identified dipyridamole as a compound that competes with CaNA for binding to the RCAN1 peptide (139). Functional assessments of its inhibitory effect on CaN activity revealed that dipyridamole does not interferes with phosphatase activity. Its mechanism of action appears to involve a specific interaction with NFAT substrates. In line with this, dipyridamole inhibits NFAT nuclear translocation, NFAT activity and the expression of NFAT-dependent cytokine genes in human T cells (139). It has been suggested that, beyond its antiplatelet activity, this drug may also have an immunomodulatory effect *in vivo* (140, 141).

INCA

The **I**nhibitors of **N**FAT-**C**alcineurin **A**ssociation (INCAs) have been selected based on their ability to compete with the VIVIT peptide for binding to CaN. Among these, three compounds, namely INCA-1, INCA-2 and INCA-6 are capable of completely displacing VIVIT from CaN, and they achieve this at low micromolar concentrations by inducing an allosteric change in the NFAT-binding site (142). It is important to note, that the binding site of INCA1,2 and 6 is centered on Cys-266 of CaNA and does not involve PxIxIT core motif. Interestingly, particular INCAs differ in their mechanisms of action. For instance, INCA-6 is known to act on NFAT activity whereas the physiological effects of INCA2 are associated with a general inhibition of CaN activity (142). However, concentration-dependent cytotoxicity has been reported for all INCAs, suggesting potential limitation in their use in biological systems (142, 143).

Small molecular inhibitors not acting directly on CaN

A-285222, a member of bis-trifluoromethyl-pyrazole class, falls within the category of immunosuppressive agents known for their ability to inhibit NFAT activity in both human and non-human primate cells through a calcineurin-independent mechanism (144). When applied to intact T cells, A-285222 maintains NFAT in a phosphorylated state within the cytosol, preventing its nuclear accumulation, all while leaving AP-1 or NF-κB activation unaffected. Consequently, this drug effectively blocks NFAT-dependent cytokine gene transcription. It is important to note that while the drug shows potential as an immunosuppressive agent, it is associated with severe side effects, particularly neurotoxicity. Nevertheless, various cell-specific effects have been demonstrated (145–147).

Q134R is a hydroxyquinoline derivative known for its ability to penetrate the brain and inhibit both the induction of NFAT transcriptional activity and caspase-3 activity (148). Importantly, this drug does not have any impact on CaN itself, which means it

avoids the immunosuppressive adverse effects associated with other agents. Preclinical studies have showed its safety, good stability, and acceptable oral bioavailability. Phase I/A trials have been successfully completed, and the drug is currently progressing into phase II trials.

Contribution of NFAT isoforms to neuronal death in AD

Accumulating evidence suggests that NFAT activity is involved in several neuropathologies (59). In nervous tissue, abnormalities in CaN/NFAT signaling are increasingly related to a variety of pathological features associated with Alzheimer's disease (AD), including synaptic dysfunction, glial activation, and cell death (11) The prevalence of studies, as will be discussed in subsequent sections, indicates a causative relationship between NFAT and AD, and some of the first evidence has been provided by Abdul and colleagues who demonstrated a relationship between amyloid toxicity and NFAT signaling (10).

A postmortem study of human hippocampal tissue revealed increased nuclear translocation of individual NFAT members at different stages of AD, which correlated with the severity of cognitive decline (11). NFATc2 activation is especially critical in the early stages of AD, while selective NFATc4 activation occurs later when the control of neuronal Ca^{2+} homeostasis and reactive oxidative species production is lost, leading to further neurodegeneration, neuronal death, and ultimately, dementia (11). Moreover, levels of several cytokines increase as NFATc2 accumulates in the nucleus (11), which is consistent with its role in neuroinflammation occurring during the early stage of AD. Excessive activation of NFATc2/c4 at different stages of AD progression may contribute to synaptic dysfunction and cognitive decline.

In agreement with this hypothesis, inhibition of CaN/NFAT signaling pathway at each stage of AD progression should prevent degeneration of neuronal processes and slow down cognitive decline. Numerous studies on animal models of AD have demonstrated that CaN inhibitors, such as tacrolimus, showed neuroprotective and/or cognitive enhancing properties and extended lifespan (123, 149–151). In addition, Abdul et al. suggested that Aβ-induced neurodegeneration is associated with selective changes in NFAT signaling (10). In line with that, over-activation of CaN, enhancing nuclear localization of NFATc2 and NFATc4, correlated with increased dementia severity in the human hippocampus, while the subcellular localization of NFATc1 was cytoplasmic (10). Increased NFATc2 activation was revealed in AD patients with mild cognitive impairments, whereas NFATc4 showed a high nuclear accumulation in patients with severe dementia and AD (10).

While these results indicate the differential contribution of NFAT isoforms to AD pathology, other reports suggest that NFAT may be an essential component of signaling pathways pharmacologically targeted in AD treatment. Lithium has been proposed as a treatment for AD and other neurodegenerative disorders (152). However, its clinical use is limited due to a high rate of associated adverse side effects, and the mechanisms underlying those effects are not fully understood. It has been demonstrated that lithium can act as a repressor of GSK-3, with K_i values for GSK-3α (~3.5 mM) and GSK-3β (~2.0 mM) that exceed therapeutic lithium serum concentrations in humans (0.5–1.2 mM) (153–155). However, lithium, like other small molecule inhibitors, is unable to selectively suppress the activity of GSK-3 isoforms, and its impact on cognitive function is lost in aged AD transgenic mice (156). For these reasons, genetic approaches have been employed to assess whether there are isoform-specific effects of GSK-3. While the majority of these studies focuses on the contribution of GSK-3β, a growing body of evidence indicates a distinct role for both isoforms in Aβ pathology (157–160). For instance, *in vitro* and *in vivo* studies have revealed that hyperphosphorylation of tau promoted by GSK-3β leads to the formation of neurofibrillary tangles, which eventually trigger neurodegenerative conditions (161–167). It has also been reported that cleavage of the amyloid precursor protein (APP) into beta-amyloid peptide is meditated by GSK-3 β (166). In addition to APP, presenilin-1 (PS1) is involved in the aggregation of the pathogenic Aβ peptide and is regulated by GSK-3β (168, 169). This is supported by the study of Ly and colleagues, which showed that specific suppression of GSK-3β, but not GSK-3α, reduced Aβ formation via NF-αB-dependent transcriptional control of β-secretase 1 (170). In contrast, Hurtado et al. (171), using AAV-delivered shRNAs and GSK-3α conditional knockout mice, suggested that GSK-3α plays a predominant role in AD pathology. However, this study was limited by the use of newborn AD model mice and putative compensatory changes in the other GSK isoform. Given that overactivated GSK-3 is hypothesized to play a central role in the pathogenesis of AD (159), the beneficial effect of lithium would stem from the normalization of GSK-3 activity and the prevention of progressive Aβ production as well as local microglial-mediated inflammatory responses.

Transgenic mice with conditional expression of dominant-negative GSK-3β showed increased neuronal apoptosis and impaired motor coordination, a phenotype that can be reversed by the expression of a dominant-negative GSK-3β form (172). It has also been hypothesized that treatment with therapeutic levels of lithium can promote neuronal loss through GSK-3β inhibition (152). These observations strongly indicate that GSK-3 activity is critical for the viability of adult neurons, and any manipulations beyond physiological GSK-3 levels may pose a potential risk of neurological toxicity. A similar effect was observed in different cell types, including Jurkat cells, differentiated immortalized hippocampal neurons (173), HL-60 promyeoloblast cells (174), human lung carcinoma A549 cells (175), human choroidal melanoma cells (176), human leukemia NB4 cells (177), K562 human erythroleukemia cells (178), human cardiomyocytes (179) and multiple myeloma (180). On the other hand, an expanding body of literature has provided substantial evidence that lithium can confer neuroprotection against various insults [for a comprehensive review, refer to (181)].

Interestingly, lithium-induced apoptosis and motor deficits were associated with elevated nuclear accumulation of NFATc4 and NFATc3, leading to increased Fas ligand (FasL) expression and

its activation (152). The opposite effect was observed in mice lacking the Fas-receptor (*lpr* mice) or following CsA treatment. In addition, activation of the CaN/NFAT/FasL death signaling has been suggested in methamphetamine-induced neuronal apoptosis (182). The link between FasL regulation by NFAT is interesting as Fas and FasL are associated with neuronal degeneration in the AD brain and participate in Aβ-mediated cell death (183). *In vivo* treatment with CaN or NFAT inhibitors abolished NFAT-mediated FasL expression and attenuated neuronal apoptosis (184).

Experimental evidence suggests a possible role of NFATs in mediating the survival response. It has been demonstrated that in the presence of growth factors and neuronal activity mimicked by high extracellular KCl concentrations, both endogenous NFATc4 and exogenously expressed NFATc4 were localized to the nucleus of granule neurons (54). On the contrary, serum/K^+ deprivation led to NFATc4 nuclear export, which was strongly associated with the induction of neuronal apoptosis. Treatment with the GSK-3 inhibitor lithium chloride blocked the nuclear export of NFATc4 and cell death, suggesting a correlation between NFAT localization and neuronal survival. In line with that, NFATc4 knockdown resulted in enhanced apoptosis, observed even in a rich culture medium and high K^+. The expression of a constitutively active form of NFAT prevented neuronal cells from apoptosis induced by low K^+ or growth factor deprivation (54).

CaN/NFAT signaling and Aβ neuropathology

CaN/NFAT signaling has been recognized as a target for Aβ pathology in numerous studies [for review, see (3, 11)], highlighting the importance of Aβ-mediated Ca^{2+} homeostasis deregulation, which creates a favorable environment for CaN/NFAT activation. A report by Wu and colleagues showed that short exposure of primary cortical neurons to Aβ oligomers led to the dynamic progression of CaN activation and resulted in morphological changes in spines and postsynaptic proteins, while longer exposure led to NFAT accumulation in the nucleus and significant spine loss (35). Similarly, the loss of spines and dendritic branching simplification evoked by Aβ treatment in primary neurons were mimicked by constitutively active NFAT (185). Transfection with VIVIT-GFP before Aβ exposure greatly improved neuronal morphology despite the persistence of Aβ in the culture medium. Spine atrophy and neuronal abnormalities seen in the vicinity of amyloid plaques in APP/PS1 mice were prevented when AAV2-VIVIT was delivered by stereotactic intracortical injections (185). This suggests that selective disruption of CaN-NFAT interaction may be protective against Aβ synaptotoxicity. These findings also illuminate a possible mechanism underlying the lack of cognitive improvement by GSK-3 inhibitors in an AD clinical trial (186). Notably, Aβ-activated GSK-3 potentiates further Aβ production, creating a positive feedback loop. Activated GSK-3 phosphorylates NFAT, inhibiting CAN/NFAT apoptotic pathway, and consequently, GSK-3 inhibitors release this inhibitory brake, promoting NFAT-mediated neurodegeneration (186). Similarly, Aβ treatment of murine hippocampal neurons caused dysregulation in intracellular Ca^{2+} and impaired dendritic and axonal transport of BDNF (187). Exposure of mixed neuron/astrocyte culture to Aβ stimulated CaN/NFAT activity and triggered CaN proteolytic cleavage, resulting in an overall increase in intracellular CaN activity (188). The accumulation of both CaN and NFATc4 (but not NFATc2) in the nucleus of hippocampal tissue positively correlated with a higher level of soluble Aβ, which steadily increased as the severity of dementia progressed (10).

Mounting evidence indicates that activation of CaN/NFAT signaling may be linked to enhanced generation of Aβ peptides (3, 36). To support this, Hong and colleagues (189) showed that FK506 administered to 8-month-old APP/PS1 double transgenic mice reduced Aβ accumulation in the cortex and hippocampus while increasing matrix metalloproteinase-9 (MMP-9) expression, which is known to degrade Aβ (190). Moreover, increased MMP-9 colocalized with astrocytic marker GFAP (glial fibrillary acidic protein) in FK506-treated mice indicating that drug-dependent MMP-9 up-regulation originates from activated astrocytes. In line with that, no correlation between MMP-9 immunoreactivity and the neuronal marker NeuN was observed, though FK506 increased the level of PSD-95 and synaptophysin, proteins involved in postsynaptic density formation and vesicular neurotransmitter release, respectively. Similarly, intrahippocampal injections of AAV2-VIVIT under the astrocyte-specific promoter reduced Aβ pathology, normalized spontaneous synaptic activity, prevented dendritic degeneration, and improved cognition in the 5xFAD mouse model of AD (36). Furthermore, AAV2-mediated NFAT inhibition increased glutamate transporter-1 expression in hippocampal astrocytes and reduced the number of glutamate-evoked transients (36), suggesting CaN/NFAT-dependent loss of glutamate regulatory properties underlying hyperexcitability in AD. Another study pointed out astrocytic CaN/NFATc4 signaling activated in response to Ca^{2+} overload as one of the key pathological mechanisms driving Aβ generation by inducing β-secretase 1 (BACE1) transcription (191) (Figure 4).

BACE1 protein and activity were found to be elevated in the AD brain, suggesting that BCAE1 up-regulation may be a phenomenon occurring early in AD or accelerating AD progression (192). Importantly, $BACE1^{-/-}$ mice are devoid of Aβ amyloidosis, electrophysiological dysfunctions, and cognitive deficits (192), implying targeted BACE1 inhibition to improve Aβ-mediated loss of cognitive function in humans with AD. Although not verified in AD models, Mei and coworkers demonstrated that NFATc4 directly binds the BACE1 gene promoter and regulates its expression (191). It is worth noting that the development of potent BACE1 inhibitors presents numerous challenges. One of the major hurdles is the structural similarity of BACE1 to other aspartyl proteases, a family that includes several enzymes widely expressed through the human body, such as BACE2, pepsin, renin, cathepsin D, and cathepsin E (193). Thus, it is imperative to develop effective BACE1 inhibitors without affecting other proteases and to exclude off-target side effects (194, 195). Furthermore, another aspect of discovering successful BACE1 inhibitors is the relativity large size of the BACE1 active site (195). Moreover, another limiting factor is related to the ability of these molecules to pass through the blood-brain barrier (196). To date, despite tremendous efforts,

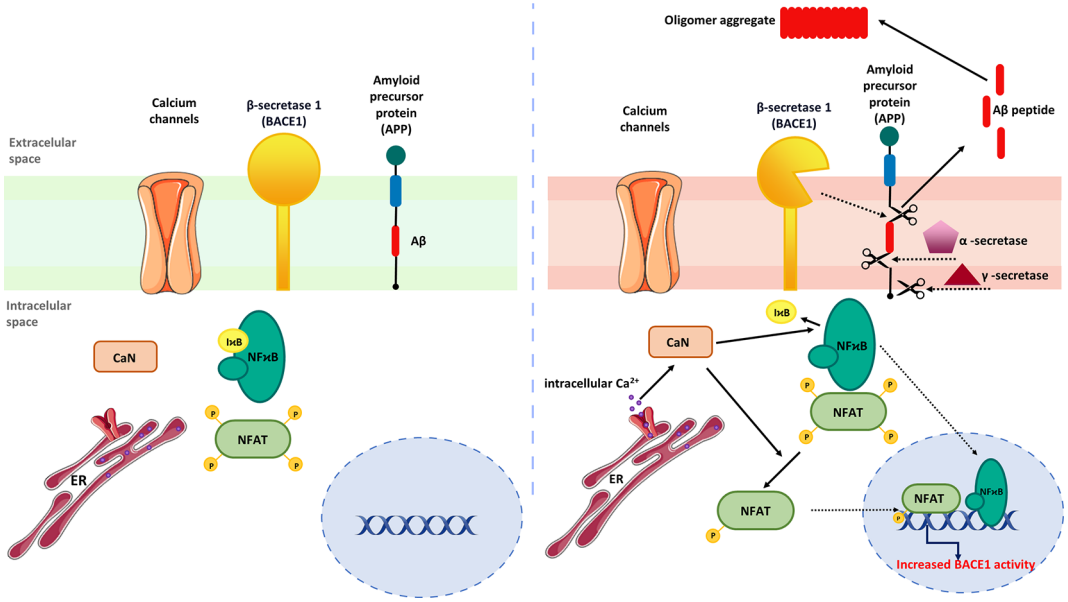

FIGURE 4
Regulation of astrocytic Aβ metabolism by CaN/NFAT signaling. (Left) In steady-state conditions, BACE expression is maintained at low level. (Right) Activation of astrocytes by upstream inflammatory mediators stimulates NFAT and NF-κB nuclear translocation and BACE1 upregulation. Increased BACE1 activity is associated with abnormal production of Aβ, which subsequently form amyloid plaques.

none of the BACE1 inhibitors has succeeded in demonstrating clinical value.

CaN/NFAT in AD-associated inflammatory signaling

Many studies now point to the contribution of neuroinflammation to the progression of neuropathological changes observed in AD. One of the signs that emerges early in the course of AD is astrocyte activation, which becomes more prominent during later stages when the amyloid and tau pathology is extensive (197). It is hypothesized that CaN/NFAT signaling serves as a critical mechanism triggering astrocyte phenotype switching and plays a pivotal role in astrogliosis and brain neuroinflammation. In astrocytes and microglia, CaN/NFAT is activated in response to a variety of neuroinflammatory mediators, including pro-inflammatory cytokines, glutamate, ATP, S100 protein, thrombin, vascular-injury factors, and Aβ. Once activated, CaN/NFAT may further potentiate the inflammatory response by driving the expression of numerous inflammatory factors, many of which are elevated in AD [reviewed in (198)]. It is well-accepted that Ca^{2+} homeostatic imbalance may aggravate AD through the pathological activation of neuronal networks but, in contrast to neurons, little is known about Ca^{2+} signaling specifically linked to glial CaN/NFAT activation. L-type voltage-dependent Ca^{2+} channels are likely to play a role, but the contribution of other plasma membrane transporters as well as those located in the ER cannot be ruled out (199).

Furthermore, CaN-dependent signaling may be a nodal point linking Ca^{2+} dyshomeostasis, Aβ accumulation, and neuroinflammation. In primary neurons, Aβ treatment stimulated a Ca^{2+}-dependent protease calpain, which cleaves C-terminal autoinhibitory domain, producing a constitutively active truncated version of CaN (ΔCaN, 48 kDa CN-Aα) insensitive to Ca^{2+}/CaM regulation (200) (Figure 5).

High levels of ΔCaN were detected in areas surrounding amyloid plaques in mouse and human brains (201, 202). Moreover, the levels of ΔCaN and active calpain correlated with one another in human hippocampal tissues of individuals with mild cognitive impairments when compared to age-matched controls (188). These changes were further linked to increased proteolysis of the NMDA receptor subunit 2B, which is necessary for long-term potentiation and memory formation (203, 204). This provides a mechanism by which oligomeric Aβ may contribute to brain degeneration through calpain-mediated CaN proteolysis and further overactivation of CaN/NFAT signaling. However, the molecular phenotype of ΔCaN-expressing astrocytes and their role in AD pathology have not been thoroughly studied. In primary neuronal cultures, heterologous expression of ΔCaN activated the transcription of several genes involved in immune response and morphogenesis (205). As many of these transcripts encode releasable cytokines and chemokines, CaN/NFAT signaling in activated astrocytes may contribute to cerebral vascular damage, reducing micronutrient delivery and compromising neuronal-glia interaction. The hypothesis of impaired microcirculation underlying AD development was postulated nearly 30 years ago (206) and has been widely discussed in multiple studies (207, 208). The plausible role of CaN/NFAT in AD-related vascular pathologies is further supported by recent work showing the upregulation of ΔCaN and NFAT signaling in astrocytes nearby regions of small vessel damage (209). Further evidence of aberrant astrocytic Ca^{2+}/CaN/NFAT signaling contributing to vascular

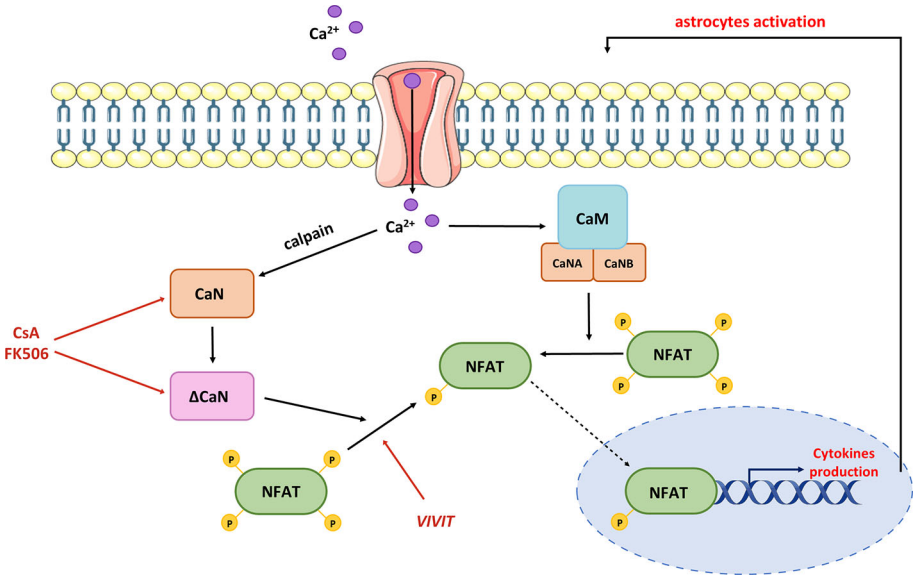

FIGURE 5
Contribution of hyperactive CaN/NFAT to pro-inflammatory cytokine production. Dysregulation of Ca^{2+} homeostasis leads to the production of truncated CaN fragment (ΔCaN), which is constitutively active. Hyperactivated CaN/NFAT sustains prolonged astrocytic activation and chronic neuroinflammation through a continuous stimulation of pro-inflammatory cytokine genes. Normalization of CaN/NFAT activity may be provided by commercial immunosuppressants such as cyclosporine A and tacrolimus (FK506), or the VIVIT peptide.

pathology associated with cognitive decline and dementia comes from the latest study of Sompol and colleagues (210). Using a diet-based model of hyperhomocysteinemia (HHcy), which recapitulates numerous features of AD, they demonstrated that VIVIT-mediated NFAT inhibition ameliorated astrocytic reactivity and improved blood flow in arterioles and capillaries. Moreover, the suppression of NFAT signaling preserved CA1 synaptic function and improved the cognitive performance of HHcy diet mice.

In addition to CaN overactivation studies, inhibition with either pharmacological drugs or targeted peptides revealed a similar relationship between CaN/NFAT and neuroinflammation. Targeting AAV2-VIVIT peptide to hippocampal astrocytes in APP/PS1 mice reduced glial activation, lowered Aβ levels, and improved cognitive and synaptic function (211). These findings align with previous reports showing high levels of CaN in activated astrocytes and its role in phenotype switching via NFAT signaling (46, 84, 205). Although the upstream signals leading to pathological activation of CaN in astrocytes are not well-characterized, heterologous expression of a constitutively active form of CaN upregulated genes linked to the activated phenotype, as well as numerous inflammatory-related genes (3). Astrocytic CaN/NFAT signaling has also been demonstrated to mediate the neurotoxic effects of several factors implicated in AD pathogenesis, including TNFα, CCL2, Cox2, GM-CSF, IL-6, IL-1β, and other cytokines (62, 202, 212–214). For instance, IL-1β promoted CaN/NFAT activation in primary astrocytes through IL-1 receptors and L-type Ca^{2+} channels without affecting CaN or NFAT expression levels (212). Interestingly, activated CaN/NFAT caused robust activation of CaN/NFAT in adjacent astrocytes via paracrine signaling. This observation places CaN/NFAT in the center of a positive feedback loop controlling local production of neuroinflammatory mediators.

An interesting approach based on reprogramming macrophages to become anti-inflammatory was proposed in a study conducted by Escolano and coworkers (215). By introducing the LxVP peptide that interferes with CaN-NFAT binding (for exact mechanism of action see *Pharmacological inhibitors of CaN/NFAT with potential use in AD treatment* section) they demonstrated that systemic or local peptide delivery via adenoviral gene transfer attenuated the inflammatory response *in vivo*. Mechanistically, LxVP-mediated CaN inhibition reduces the activity of MKP-1, a dual specificity protein phosphatase, releasing p38 MAPK kinase from MKP-1 repression. In murine mouse models, p38 MAPK kinase was associated with the activation of macrophage reprogramming (216). It has been reported that high dose of FK506, 500 times higher than necessary to suppress CaN, induces short-term p38 MAP kinase activation, reaching its peak at 30 min and subsequently decreasing (215). Furthermore, the application of pharmacological, non-toxic doses of CsA or FK506 effectively inhibits CaN activity, but does not trigger p38 MAPK kinase activation (215). These results strongly suggest that the anti-inflammatory phenotype of macrophages induced by LxVP requires the involvement of p38 MAP kinase. Additionally, the VIVIT peptide also failed to induce p38 activation (215). This unique feature of LxVP distinguishes its action from the properties of other CaN/NFAT inhibitors, such as CsA or FK506. However, before testing this therapy in patients, it would be particularly interesting to unravel the relationship between anti-inflammatory M2 macrophages and macrophages induced by LxVP peptide. Other strategies controlling immune cell function, such as NFAT's O-linked β-N-acetyl glucosamine modification (217), genetic deletion of soluble epoxide hydrolase (218), or oxygen-ozone therapy that activates immune function and suppresses inflammatory responses

through up-regulation of NF-κB, NFAT, and AP-1 signaling (219), should also be given special consideration.

Targeted inhibition of CaN/NFAT signaling, either by naturally occurring compounds or synthetic drugs, may effectively reduce neuroinflammation, thus offering a promising strategy in the treatment of AD (220, 221). However, the translational potential of many CaN inhibitors is markedly limited due to severe adverse effects, including neuro-muscular and renal dysfunction or progressive lymphopenia (222, 223). Despite many advantages over peptide/protein-based drugs, small chemical inhibitors of NFAT have not been widely described. Dipyridamoles can reduce inflammation and cytotoxicity and exert a neuroprotective effect under certain conditions (141, 224). However, their use is not without side effects (225). Another class of small organic molecules, known as INCAs, was initially promising due to their ability to displace VIVIT at low micromolar concentrations, but it turned out to be cytotoxic for certain cell lines when tested. Nonetheless, when administered at non-toxic low micromolar concentrations, INCA-2 and INCA-6 prevented the induction of mRNAs encoding TNFα, interferon-γ, and macrophage inflammatory proteins MIP-1α and MIP-1β (142), as well as some pro-inflammatory cytokines and chemokines (226). Other NFAT inhibitors, such as A-285222, have shown to reduce inflammation, but the experimental data on their use in neuronal or glial cells are very limited (227). Recently, a new hydroxyquinoline derivative, Q134R, has been demonstrated to reduce glial reactivity markers and improve synaptic function, without affecting Aβ load (148). Moreover, Q134R improved cognitive performance and showed no signs of lymphopenia, suggesting its efficacy comparable to CaN inhibitors but with fewer side effects.

AD-involved receptors signaling through CaN/NFAT

The role of NFAT signaling in AD pathogenesis has been demonstrated in numerous studies, but the upstream signaling leading to CaN/NFAT deregulation remains largely unresolved. Therefore, in this section we discuss how the function of receptors associated with AD affects CaN/NFAT signaling (Figure 6).

Transient receptor potential ankyrin 1

As previously discussed, Aβ-induced Ca^{2+} overload plays a pivotal role in cytokine secretion by activating CaN and its downstream targets, including NFAT and NF-κB (198). However, the intracellular proteins that regulate Aβ-mediated Ca^{2+} influx and drive the inflammatory response are still largely unresolved. One of the strong candidates is the transient receptor potential ankyrin 1 (TRPA1), which is a Ca^{2+}-permeable nonselective channel belonging to the TRP channel superfamily. It is widely expressed in the sensory neurons of the dorsal root ganglia, trigeminal ganglia, and nodose ganglia, as well as in hair cells and non-neuronal cells (228). TRPA1 responds to a variety of exogenous irritants and endogenous agonists to mediate inflammation and transmit pain (229–232). Due to these properties, TRPA1 is considered a promising target for novel analgesic and anti-inflammatory drugs. Furthermore, it is involved in temperature sensing and may play a role in the detection of infrared radiation and the avoidance of nociceptive heat (233–238).

Lee and colleagues demonstrated that TRPA1 is upregulated in the hippocampus of APP/PS1 mice (239). In this mouse model, Aβ

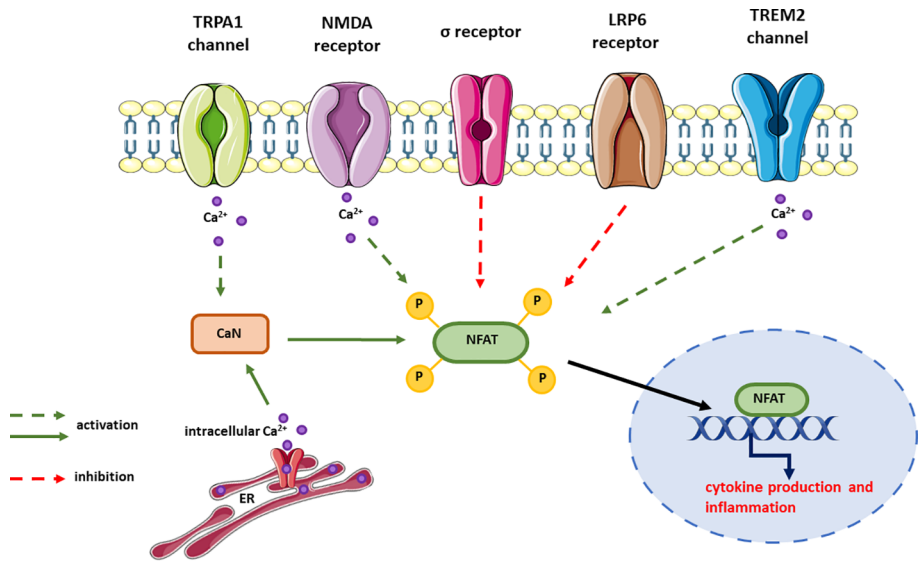

FIGURE 6
Receptors signaling through CaN/NFAT and their effect on NFAT activation. In most cases, the signaling pathways upstream NFAT but downstream the receptor is unknown and this is expressed as dotted line in the figure. The effect on NFAT activity has been measured either by changes in cytokine expression or release, or the activity of NFAT reporter.

triggers TRPA1-mediated Ca^{2+} accumulation and hyperexcitability of CA1 hippocampal neurons, suggesting that TRPA1 may function during the early onset of AD (240). Aβ-induced TRPA1-Ca^{2+} signaling has been shown to be a critical event in the activation of CaN/NFAT, leading to cytokine production and inflammation in astrocytes (239, 241). Consistent with this, genetic ablation of TRPA1 channel function in APP/PS1 mouse reduces Aβ-induced activation of CaN, decreases NFAT's DNA-binding activity in astrocytes, and lowers the levels of pro-inflammatory cytokines IL-1β, IL-6, and IL-4 in the brain. Furthermore, loss of TRPA1 function ameliorates AD progression and improves behavioral performance (239), highlighting the importance of astrocytic TRPA1-Ca^{2+}-CaN-NFAT signaling in the inflammatory process and AD progression.

Sigma receptor

Another channel implicated in AD pathology is the sigma receptor, a Ca^{2+}-sensitive chaperone located at the mitochondria-associated endoplasmic reticulum (242). Upon ligand binding, the sigma receptor translocates to the plasma membrane and interacts with various ion channels and G protein-coupled receptors (243). In terms of its mechanism, it operates as more of a signaling modulator than a conventional receptor, and its function encompass the regulation of lipid metabolism, control of both voltage- and non-voltage ion channels, maintenance of intracellular Ca^{2+} homeostasis, modulation of electrical activity, and potentially several other roles (244). Early studies have demonstrated the loss of sigma receptor in the CA1 area of the anterior hippocampus in AD patients, which correlates with damage to CA1 cells (245). The depletion of sigma receptor in the brain is thought to manifest early in the progression of AD, primarily impacting the frontal, temporal, and occipital brain regions (246). The development of preclinical models of AD has allowed researchers to determine the correlation between receptor level and the severity of AD, as well as uncover the neuroprotective properties of sigma receptor agonists (247, 248). For instance, BD-7373 and CB-184, agonists of the sigma-2 receptor subtype, exhibit a potent inhibitory effect on NFAT and NF-κB transcription, leading to decreased expression of TNFα, IL-2, and COX-2 genes, potentially reducing brain inflammation (249). Activation of the sigma-1 receptor, on the other hand, may inhibit γ-secretase activity and reduce Aβ production (250). However, Aβ accumulation and subsequent activation of CaN/NFAT have been shown to induce sigma receptor degradation through NFAT-dependent induction of BIP protein expression, promoting E3 ligase recruitment (251).

Triggering receptor expressed on myeloid cells 2

TREM2 was initially identified and characterized in human dendritic cells derived from blood monocytes and cultured *in vitro* with the granulocyte macrophage colony stimulating factor and IL-4 (252). It belongs to the immunoglobulin-lectin-like receptor superfamily and plays a role in the development of the AD phenotype (253). TREM2 is predominantly expressed in tissue macrophages, where it can be found both on cell surface and within intracellular compartments. Macrophages expressing TREM2 are located in various sites, including microglia in the central nervous system, specific macrophage subset in the liver, and osteoclast in bone (253). Research has shown that alterations in TREM2 expression affect multiple functions of microglia (254). Increasing TREM2 results in elevated level of chemokine receptors, enhanced cell migration, and improved phagocytosis. Conversely, decreased TREM2 expression inhibits the engulfing of apoptotic cells while increasing the expression of pro-inflammatory cytokines (254).

Characterization of the microglial transcriptome in TREM2-deficient mice has demonstrated the essential role of TREM2 in microglial response during Aβ accumulation (255). TREM2 can be directly modulated by Aβ and other components of Aβ plaques (253). Several studies have reported that TREM2 activation increases intracellular Ca^{2+} level and activates the NFAT reporter system, suggesting that NFAT may transmit signals downstream of TREM2 (252, 256, 257). The precise mechanism of TREM2-dependent NFAT activation in AD is not entirely clear, but a recent study by Zhao et al. revealed that Aβ42 oligomers promote TREM2-DAP12 interaction and SYK kinase phosphorylation, which plays an important role in NFAT signaling (258). Involvement of SYK kinase activating the PLCγ-CaN-NFAT pathway was also suggested by Lessard and colleagues (259). These authors demonstrated that the loss-of-function TREM2 mutation variant R47H, which has been associated with a higher incidence of AD (260), reduced Aβ internalization and NFAT signaling, establishing a direct link between Aβ aggregates, TREM2, and NFAT transcriptional activity. Modulation of NFAT transcriptional activity may also underlie TREM2's ability to sustain microglial response to Aβ accumulation and influence the production of inflammatory cytokines *in vivo*. This hypothesis is supported by the fact that apoptotic cells transduce the NFAT signal via TREM2, consistent with its function as a sensor of anionic and zwitterionic lipids presented on the surface of neurons exposed to Aβ (261, 262). The accumulation of phosphatidylserine (PS) and phosphatidylethanolamine (PE) on the neuronal cell membrane in the AD mouse brain (263) suggests that PC and PE may transduce signals via TREM2-NFAT (261, 264), potentially enhancing TREM2 activity and promoting a protective phenotype in microglia. Although it remains unclear which TREM2-regulated target genes may be responsible for the increased risk of AD, recent work with engineered TREM2 agonistic antibodies suggests that many of these genes may contain an NFAT response element (265). Activation of TREM2 by dedicated antibodies has been shown to enhance microglia-dependent clearance of Aβ plaques in 5XFAD mice, indicating their potential clinical use in AD treatment. The rationale for strategies aimed at normalizing TREM2 expression/activity in AD treatment is further supported by the latest finding of increased *Trem2* expression in 5XFAD mice (266).

Imidazoline 2 receptors

Imidazoline 2 receptors (I_2 receptors) represent a highly heterogenous group of non-adrenergic binding sites characterized by their high-affinity binding to [^{3}H]-idazoxan (267). Cellular distribution studies have indicated their presence on the outer mitochondrial membrane, and they have been suggested to potentially serve as novel allosteric binding sites for monoamine oxidase (MAO). Interestingly, another unrelated binding site is brain creatine kinase (268). Numerous biochemical and preclinical investigations, conducted using animal models of brain injury (269–272), suggest that ligands targeting I_2 receptors exhibit neuroprotective activity, in part by lowering body temperature – an effect known to be beneficial in cerebral ischemia (273). There is also evidence to suggest that I_2 receptors ligands may mitigate neurodegenerative processes, including cognitive decline, neuroinflammation, and oxidative stress (274).

Indeed, postmortem analysis of brain samples derived from AD patients revealed a higher density of imidazoline 2 receptors (I_2-IRs), and several pharmacological modulators of I_2-IRs activity have been successfully tested to reduce AD hallmarks (275–277). The mechanisms underlying the beneficial effects of I_2-IRs modulation are complex and, so far, largely unknown. Recent reports suggest that neuroprotective mechanisms may be ligand-specific. For instance, LSL6010 alone decreased Aβ plaque formation, tau hyperphosphorylation, and the expression of microglia markers in the 5XFAD mouse model. When administered in combination with donepezil, LSL6010 additionally reduced GFAP reactivity (276). In the same AD murine model, LSL60101 (garsevil) reduced the markers of oxidative stress and decreased the expression of the pro-apoptotic FADD protein in the hippocampus (275). Using the senescence-accelerated mouse prone 8 (SAMP8) model, which is considered a late-onset AD mouse model characterized by tau hyperphosphorylation and altered APP processing (278), Vassilopoulos and colleagues demonstrated that a newly synthesized I_2-IRs ligand, named B06, reduced the expression of pro-inflammatory cytokines by inhibiting CaN/NFATc1 signaling (274). Therefore, new-generation I_2-IRs ligands that affect NFAT-dependent transcription hold great neuroprotective potential in AD.

Low-density lipoprotein receptor-related protein 6

LRP6 belongs to the extended low-density lipoprotein receptor family and serves as a co-receptor in the canonical Wnt signaling. LRP6 is expressed in a widespread manner across human tissues, exhibiting both weak and strong expression patterns in different tissue types (279). Because of its function in Wnt/β-catenin pathway, it is required in the regulation of cell proliferation, specification, migration during development, and it is highly expressed in different types of cancer (280). Furthermore, clinical studies and genomic analysis have confirmed that LRP6 is associated with neurodegenerative diseases including AD (281). Conditional knockout of LRP6 in mice resulted in synaptic dysfunctions, accompanied by cognitive impairments and exacerbated memory deficits in the APP/PSEN1 AD model (282). Interestingly, downregulation of LRP6 expression and LRP6-mediated Wnt signaling were observed in the human brain affected by AD compared to age-matched controls (283). Several possible mechanisms have been proposed to explain how impaired LRP6 downstream signaling may worsen AD pathology. Firstly, LRP6 directly interacts with APP, and its deficiency may promote the amyloidogenic processing of APP, leading to increased endogenous Aβ levels (283). Secondly, LRP6 loss has been shown to increase the number of hippocampal astrocytes and microglia, promoting neuroinflammation through extensive production of pro-inflammatory cytokines (283). LRP6 may also contribute to AD pathology by regulating lipid metabolism, particularly ApoE-containing lipoproteins (284, 285). However, the role of glial and astrocytic LRP6 in the context of AD has not been widely studied. Recent research by Chow and colleagues revealed that LRP6 cell surface retention serves as a bimodal switch for astrocytic fuel metabolism (286). In the absence of LRP6, Wnt signaling activates the non-canonical Ca^{2+}-PKC-NFAT axis, favoring the utilization of glutamate-derived glutamine and branched chain amino acids over glucose. Increased levels of both NFATc2 and NFATc4 were observed in Wnt-exposed GFAP-Lrp6–/– astrocytes, but NFATc2 appears to be the isoform that regulates mitochondrial glutamine metabolism and the acquisition of a reactive phenotype. Depletion of these amino acids from the astrocyte microenvironment may impact synaptic functions and contribute to cognitive and memory deficits. Remodeling of the metabolic framework in astrocytes is an early change associated with late-onset AD (287). In the latest study, non-canonical Wnt5a/CaMKII/NFAT signaling has been shown to participate in the release of inflammatory factors and modulate the activation of microglia (288).

N-methyl-D-aspartate receptor

Physiologically, NMDARs are central to development of nervous system are involved in a numerous forms of synaptic transmission underlying learning and memory formation (289, 290). In AD, abnormal activation of NMDARs by a glutamate highly released from glial cells stimulates a massive Ca^{2+} influx and aberrant processing of Ca^{2+}/CaN signaling, promoting oxidative stress, neuroinflammation and cell death (291–293). Accumulating evidence indicates that function of NMDAR is dysregulated by Aβ and the disruption in Ca^{2+} homeostasis and glutamatergic synaptic transmission may be related to early cognitive deficits observed in AD (294–296). There are multiply potential way by which NMDAR contributes to Aβ pathology: first, Aβ are able to bind NMDAR extracellularly suggesting direct or indirect modulation of the receptor by amyloid β oligomers (297); second, Aβ facilitates NMDAR activation, which controls Aβ production and secretion (298, 299); third, NMDAR may be important mediator in Aβ-induced neurotoxicity (300) and fourth, due to the synaptic and extrasynaptic location, NMDAR may function as a downstream target in Aβ-induced synaptic depression (301). The interaction between Aβ and NMDAR rationalizes the clinical use of

memantine, a non-competitive NMDAR antagonist, in combination with acetylcholine inhibitor donepezil, to improve cognitive performance and life quality of patients with moderate to severe AD (302). The beneficial effects of memantine administration may involve reduction in neuroinflammation and overall improvement of brain function although the mechanisms of drug action are not completely understood. The participation of CaN/NFAT cannot be unequivocally excluded as other NMDAR antagonists such as MK-801 are known to abolish NMDAR-dependent NFAT activation (303, 304). Nonetheless, memantine/donepezil did not improve excessive agitation (305) and hippocampal atrophy (306) and the effectiveness of this therapy has been questioned in patients in advanced AD stages (307).

Recently, Turcu et al. developed an optimized, non-cytotoxic, memantine-like NMDAR antagonist, UB-ALT-EV, with high metabolic stability, low micromolar activity and excellent electrophysiological profile as NMDAR blocker (308). The drug rescued defective locomotion and reversed the disrupted chemotaxis behavior in *C. elegans*, which constitutively express human Aβ, suggesting the protection against Aβ toxicity in a manner similar to memantine. Importantly, UB-ALT-EV also enhanced short- and long-term working memory in 5XFAD mice (308). Strikingly, both UB-ALT-EV and memantine normalized CaN protein level, but only UB-ALT-EV, increased NFATc1 phosphorylation, thereby preventing its nuclear translocation (266). Further evaluation of UB-ALT-EV-exerted neuroprotection demonstrated a reduction in the production of several pro-inflammatory cytokines regulated by CaN/NFAT signaling, as well as a decrease in oxidative stress due to enhanced expression of anti-inflammatory mediators in the 5XFAD model (266). These results collectively indicate that UB-ALT-EV's capacity to reduce gliosis arises from its modulatory effect on NMDAR-dependent Ca^{2+} entry and CaN/NFATc1 downstream signaling.

In mature hippocampal neurons expressing both NMDAR2A and 2B subunits, Aβ-induced hippocampal dysfunctions and ER stress were largely reversed by ifenprodil, an antagonist of NMDAR2B subunits (297). Additionally, ifenprodil prevented the depletion of ER Ca^{2+} content, superoxide generation, and cell death, demonstrating the involvement of NMDAR2B in Aβ neurotoxicity. Considering that NMDAR-dependent NFAT activation and NFAT-mediated transcription are disrupted in primary neurons in the presence of ifenprodil (101), its anti-inflammatory action may involve the normalization of NFAT signaling.

Other Ca^{2+}-permeable receptors

In the *Drosophila* AD model, overexpression of human amyloid precursor protein (APP) induced synaptic hyperexcitability and concurrent upregulation of Ca^{2+}-related signaling genes, including Dmca1D (L-type Ca^{2+} channel), CaN, and the inositol 1,4,5-triphosphate receptor (IP3R) (309). Mechanistically, exaggerated Dmca1D expression promoted APP-dependent Ca^{2+} overload, leading to increased CaN activity. This, in turn, triggered NFAT-dependent transcription of IP3R. IP3R is a large-conductance cation channel located in the ER membrane, responsible for cytoplasmic Ca^{2+} increases that control cytoplasmic and mitochondrial processes, thereby regulating cell survival (310, 311). Aberrant Ca^{2+} signaling resulting from IP3R dysregulation has been implicated in several neurodegenerative diseases, including AD, and ER stress-related neuronal injury (312). For instance, IP3R has been previously shown to interact with presenilin mutants causing the familiar form of AD (FAD), leading to its gain-of-function enhancement in an Aβ-independent manner (313, 314). This gain-of-function has been suggested as a key factor behind altered IP3R-mediated Ca^{2+} release in sub-saturating IP3 concentrations, serving as a highly predictive diagnostic feature of AD (315). In light of this, the normalization of IP3R-dependent signaling has been found to restore normal cell function and improve memory in FAD-causing presenilin knock-in mice (316), as well as in triple-transgenic mouse models of FAD (317, 318). Furthermore, Shao et al. demonstrated that NFAT-mediated IP3R upregulation significantly contributes to synaptic downscaling machinery. The restoration of IP3R expression blocked synaptic excitability and miniature excitatory postsynaptic current (mEPSC) frequency (309). Therefore, substantial evidence supports the role of IP3R in contributing to the deregulation of Ca^{2+} homeostasis observed in AD. IP3R dysfunction may drive a series of pathological events leading to disease progression.

IP3R-mediated depletion of ER stores triggers the activation of SOCE (store-operated Ca^{2+} entry) from the extracellular milieu across the plasma membrane, resulting in a subsequent increase in cytosolic Ca^{2+}. Altered SOCE-mediated ER store refill is one of the hallmarks of AD, as reduced SOCE has been implicated in synaptic loss and cognitive decline in genetic mouse models as well as in human AD brain samples (319). However, the molecular mechanisms by which IP3R modulates SOCE in AD are not completely understood. A recent study by Sampieri et al. (320) demonstrated that ER depletion induced by G-protein coupled receptor and phospholipase C (PLC) activation stimulates the recruitment of IP3R to the STIM1 protein, which acts as the sensor for ER calcium load. The gradual decrease in STIM1 expression in the medial frontal gyrus of pathologically confirmed AD patients has been linked with disease progression and neurodegeneration mediated by the L-type voltage-dependent Ca^{2+} channel (321, 322). Interestingly, STIM1 expression is sensitive to inflammation (323, 324), suggesting that changes in Ca^{2+} influx through SOCE channels may occur during the early stages of AD development. Using a lipopolysaccharide (LPS)-induced model of AD neuroinflammation, Sun and coworkers (325) demonstrated that SOCE-mediated activation of the PLC/CaN/NFAT pathway up-regulated NADPH oxidase and NOD-like receptor family protein 1 (NLRP1) inflammasome, both playing a pivotal role in oxidative stress and neuronal inflammation. These studies collectively indicate that NFAT activation by pathological Ca^{2+} signals of different origins mediates neurotoxic Aβ effects and contributes to neuronal damage.

RCAN1 protein- an endogenous control for CaN/NFAT activity

An open question remains regarding the control mechanisms of endogenous CaN/NFAT activity. One of the candidates is the

regulator of calcineurin 1 (RCAN1), a small evolutionarily conserved protein that can directly bind to and inhibit CaN activity. RCAN1 has been implicated in various forms of brain degeneration, and its increased expression has been demonstrated in the cortex of patients with AD as well as during normal brain aging (326–329). A conclusive mechanistic explanation for the role of RCAN1 in neuronal death observed in AD has not yet been presented, although several hypotheses have been proposed. Overexpression of RCAN1 is known to induce the caspase-3 mediated apoptotic pathway, which can be blocked by the antioxidant lycopene, suggesting the involvement of oxidative stress (330). In line with this, Sun and coworkers proposed an isoform-specific regulation of RCAN1 by calcium overload, activating CaN/NFAT signaling and exacerbating caspase-3 mediated death (331). According to the study by Jing and colleagues, RCAN1 overexpression disrupts mitochondrial function and promotes apoptosis through the stabilization of adenine nucleotide translocator (ANT1) mRNA and Ca^{2+}-dependent induction of mitochondrial permeability transition pore opening (332). This is supported by the latest study, which shows the inhibition of NFAT and NF-κB transcriptional activity by the RCAN1 RNA aptamer R1SR13, resulting in the attenuation of apoptosis in neurons (333). RCAN1 may also contribute to AD pathology by enhancing N-glycosylation in the ER, thus significantly increasing Aβ production (334). The amyloid proteins and RCAN1 appear to be mutually regulated, as Aβ enhances RCAN1 expression, and RCAN1 reciprocally induces Aβ formation and potentiates its neurotoxicity (334–337). The transcription of RCAN1 can also be activated by NF-κB, a key mediator of brain inflammation in AD (338, 339), and repressed by its own protein in a negative loop. In this regulation, the activation of CaN/NFAT signaling attenuates NF- κB activity, whereas activated NF-κB potentiates NFAT-dependent transcription.

The function of RCAN has been demonstrated to be critical during development and in healthy synapses [reviewed in (340)]. Mice deficient in *rcan1/2* displayed neurological symptoms similar to CaNAβ-null mice, including enhanced locomotor activity and deficits in working memory (341). *Rcan1/2* loss-of-function impaired NFAT activation, suggesting that RCAN may also allow or facilitate CaN-NFAT coupling under certain conditions. This is further supported by a study of Liu and colleagues, which demonstrates that the phosphorylation of RCAN1 at Ser94 and Ser136 by TAK1 (Transforming growth factor beta-activated kinase 1) acts as a switch between inhibitory and permissive RCAN1 functions, thereby enhancing CaN signaling and facilitating NFATc1 nuclear translocation (342). This switch requires the formation of a multimolecular complex involving TAB2 (TGFβ activated kinase 1 binding protein 2) and RCAN1, followed by the recruitment of TAK1, TAB1 and CaN. This mechanism is not observed in *rcan1/2*-deficient mice. As TAK1 and its binding partner TAB1 can be activated by a variety of cytokines, including IL-1β or TNFα (343), RCAN1-dependent modulation of CaN activity may have profound consequences for glial response to pro-inflammatory stimuli. Other studies also confirmed that altering RCAN1 levels either by overexpression or knock-out approaches resulted in memory deficits and impaired synaptic plasticity, both of which are frequently observed in AD patients (344, 345).

Recently, RCAN1 knockdown or overexpression has been linked to age-related deficits in rest-activity and circadian rhythms, characteristic for AD and Down syndrome (346). In the latter, perturbed CaN/NFAT signaling was associated with a higher risk of developing amyloid pathology (347). RCAN1 has also been shown to interact with Dyrk1A, which is considered a candidate protein responsible for AD in the early stages of this disease (348). This interaction allows Dyrk1A-mediated RCAN1 phosphorylation and subsequent CaN inhibition, leading to reduced NFAT activity and enhanced Tau phosphorylation (349). Besides controlling RCAN1, Dyrk1 functions upstream of the GSK-3β kinase, inhibiting NFAT (349), and may directly phosphorylate the NFAT regulatory domain, counterbalancing the effects of CaN-mediated dephosphorylation (75). These observations suggest a direct link between Dyrk1 and RCAN1 in CaN/NFAT signaling, supporting the notion that altered RCAN1/Dyrk1 expression in AD may destabilize the NFAT circuit and contribute to neuropathogenic processes. In line with that, Dyrk1 inhibition by a novel drug, KVN93, reduced neuroinflammation, improved cognitive performance, and decreased Aβ plaque deposition in 5xFAD mice (350). A promising effect toward the amelioration of phenotypic defects observed in AD was also seen with CX-4945 (silmitasertib), which has already undergone clinical trials. Originally developed as a Dyrk1-targeting drug (351), CX-4945 turned out to be a dual Dyrk-1/GSK-3β inhibitor (352) with a strong modulatory effect on AD-related CaN/NFAT signaling and Tau phosphorylation in the mouse hippocampus.

Concluding remarks

The transcription factors of the NFAT family were originally characterized for their important role in the transcription of cytokine genes and other genes critical for the immune response. The role of NFAT in the neuroinflammatory response in AD is unquestionable. Yet, the reports emerging in recent years suggest that aberrant CaN/NFAT signaling may also play a central deleterious role in brain degeneration, linking amyloid pathology, Ca^{2+} dysregulation, and synapse deterioration. The molecular and phenotypic changes fueled by hyperactive CaN, and cell-specific maladaptive transcriptional programs, may arise early in AD and progress with cognitive decline. These deleterious changes in transcriptional control are observed both in neurons and astrocytes and likely involve the NFAT component. The numerous studies in transgenic animal AD models showing beneficial effects of CaN and/or NFAT inhibitors are consistent with this hypothesis. Further work is needed to better characterize the upstream signals leading to CaN/NFAT overactivation in AD and dissect the actions of this pathway on different transcriptional regulatory mechanisms. Moreover, it would be desirable to unravel how these changes drive synaptic malfunction and how targeted molecular interventions may help slow down cognitive decline.

Author contributions

JM: Conceptualization, Resources, Software, Visualization, Writing – original draft, Writing – review & editing. ML: Software, Supervision, Visualization, Writing – original draft, Writing – review & editing. TB: Conceptualization, Funding acquisition, Resources, Supervision, Writing – original draft, Writing – review & editing.

Funding

The author(s) declare financial support was received for the research, authorship, and/or publication of this article. This work was supported by the National Science Centre (Narodowe Centrum Nauki) grant no. UMO-2019/33/B/NZ4/00587.

Conflict of interest

The authors declare that the research was conducted in the absence of any commercial or financial relationships that could be construed as a potential conflict of interest.

Publisher's note

References

1. A. s. Association. 2016 Alzheimer's disease facts and figures. *Alzheimers Dement* (2016) 12(4):459–509. doi: 10.1016/j.jalz.2016.03.001

2. Arendt T, Stieler JT, Holzer M. Tau and tauopathies. *Brain Res Bull* (2016) 126(Pt 3):238–92. doi: 10.1016/j.brainresbull.2016.08.018

3. Sompol P, Norris CM. Ca. *Front Aging Neurosci* (2018) 10:199. doi: 10.3389/fnagi.2018.00199

4. A. s. A. C. H. Workgroup. Calcium Hypothesis of Alzheimer's disease and brain aging: A framework for integrating new evidence into a comprehensive theory of pathogenesis. *Alzheimers Dement* (2017) 13(2):178–182.e17. doi: 10.1016/j.jalz.2016.12.006

5. Pchitskaya E, Popugaeva E, Bezprozvanny I. Calcium signaling and molecular mechanisms underlying neurodegenerative diseases. *Cell Calcium* (2018) 70:87–94. doi: 10.1016/j.ceca.2017.06.008

6. Vardjan N, Verkhratsky A, Zorec R. Astrocytic pathological calcium homeostasis and impaired vesicle trafficking in neurodegeneration. *Int J Mol Sci* (2017) 18(2). doi: 10.3390/ijms18020358

7. Verkhratsky A, Nedergaard M. Physiology of astroglia. *Physiol Rev* (2018) 98 (1):239–389. doi: 10.1152/physrev.00042.2016

8. Sobolczyk M, Boczek T. Astrocytic calcium and cAMP in neurodegenerative diseases. *Front Cell Neurosci* (2022) 16:889939. doi: 10.3389/fncel.2022.889939

9. Rodríguez-Giraldo M, González-Reyes RE, Ramirez-Guerrero S, Bonilla-Trilleras CE, Guardo-Maya S, Nava-Mesa MO. Astrocytes as a therapeutic target in alzheimer's disease-comprehensive review and recent developments. *Int J Mol Sci* (2022) 23(21). doi: 10.3390/ijms232113630

10. Abdul HM, Sama MA, Furman JL, Mathis DM, Beckett TL, Weidner AM, et al. Cognitive decline in Alzheimer's disease is associated with selective changes in calcineurin/NFAT signaling. *J Neurosci* (2009) 29(41):12957–69. doi: 10.1523/JNEUROSCI.1064-09.2009

11. Abdul HM, Furman JL, Sama MA, Mathis DM, Norris CM. NFATs and alzheimer's disease. *Mol Cell Pharmacol* (2010) 2(1):7–14.

12. Creamer TP. Calcineurin. *Cell Commun Signal* (2020) 18(1):137. doi: 10.1186/s12964-020-00636-4

13. Lian Q, Ladner CJ, Magnuson D, Lee JM. Selective changes of calcineurin (protein phosphatase 2B) activity in Alzheimer's disease cerebral cortex. *Exp Neurol* (2001) 167(1):158–65. doi: 10.1006/exnr.2000.7534

14. Reese LC, Taglialatela G. A role for calcineurin in Alzheimer's disease. *Curr Neuropharmacol* (2011) 9(4):685–92. doi: 10.2174/157015911798376316

15. Goto S, Matsukado Y, Mihara Y, Inoue N, Miyamoto E. Calcineurin in human brain and its relation to extrapyramidal system. Immunohistochemical study on postmortem human brains. *Acta Neuropathol* (1986) 72(2):150–6. doi: 10.1007/BF00685977

16. Goto S, Matsukado Y, Mihara Y, Inoue N, Miyamoto E. The distribution of calcineurin in rat brain by light and electron microscopic immunohistochemistry and enzyme-immunoassay. *Brain Res* (1986) 397(1):161–72. doi: 10.1016/0006-8993(86)91381-8

17. Polli JW, Billingsley ML, Kincaid RL. Expression of the calmodulin-dependent protein phosphatase, calcineurin, in rat brain: developmental patterns and the role of nigrostriatal innervation. *Brain Res Dev Brain Res* (1991) 63(1-2):105–19. doi: 10.1016/0165-3806(91)90071-p

18. Kuno T, Mukai H, Ito A, Chang CD, Kishima K, Saito N, et al. Distinct cellular expression of calcineurin A alpha and A beta in rat brain. *J Neurochem* (1992) 58 (5):1643–51. doi: 10.1111/j.1471-4159.1992.tb10036.x

19. Chin D, Means AR. Calmodulin: a prototypical calcium sensor," (in eng). *Trends Cell Biol* (2000) 10(8):322–8. doi: 10.1016/s0962-8924(00)01800-6

20. Zhang M, Abrams C, Wang L, Gizzi A, He L, Lin R, et al. "Structural basis for calmodulin as a dynamic calcium sensor. *Structure* (2012) 20(5):911–23. doi: 10.1016/j.str.2012.03.019

21. Hogan PG, Lewis RS, Rao A. Molecular basis of calcium signaling in lymphocytes: STIM and ORAI. *Annu Rev Immunol* (2010) 28:491–533. doi: 10.1146/annurev.immunol.021908.132550

22. Oh-hora M, Rao A. Calcium signaling in lymphocytes. *Curr Opin Immunol* (2008) 20(3):250–8. doi: 10.1016/j.coi.2008.04.004

23. Colbran RJ, Brown AM. Calcium/calmodulin-dependent protein kinase II and synaptic plasticity. *Curr Opin Neurobiol* (2004) 14(3):318–27. doi: 10.1016/j.conb.2004.05.008

24. Mulkey RM, Endo S, Shenolikar S, Malenka RC. Involvement of a calcineurin/inhibitor-1 phosphatase cascade in hippocampal long-term depression. *Nature* (1994) 369(6480):486–8. doi: 10.1038/369486a0

25. Hussey JW, Limpitikul WB, Dick IE. Calmodulin mutations in human disease. *Channels (Austin)* (2023) 17(1):2165278. doi: 10.1080/19336950.2023.2165278

26. O'Day DH, Eshak K, Myre MA. Calmodulin binding proteins and alzheimer's disease. *J Alzheimers Dis* (2015) 46(3):553–69. doi: 10.3233/JAD-142772

27. Berrocal M, Sepulveda MR, Vazquez-Hernandez M, Mata AM. Calmodulin antagonizes amyloid-β peptides-mediated inhibition of brain plasma membrane Ca(2+)-ATPase. *Biochim Biophys Acta* (2012) 1822(6):961–9. doi: 10.1016/j.bbadis.2012.02.013

28. O'Day DH. Calmodulin binding domains in critical risk proteins involved in neurodegeneration. *Curr Issues Mol Biol* (2022) 44(11):5802–14. doi: 10.3390/cimb44110394

29. Rusnak F, Mertz P. Calcineurin: form and function. *Physiol Rev* (2000) 80 (4):1483–521. doi: 10.1152/physrev.2000.80.4.1483

30. Caraveo G, Auluck PK, Whitesell L, Chung CY, Baru V, Mosharov EV, et al. Calcineurin determines toxic versus beneficial responses to α-synuclein. *Proc Natl Acad Sci USA* (2014) 111(34):E3544–52. doi: 10.1073/pnas.1413201111

31. Qian W, Yin X, Hu W, Shi J, Gu J, Grundke-Iqbal I, et al. Activation of protein phosphatase 2B and hyperphosphorylation of Tau in Alzheimer's disease. *J Alzheimers Dis* (2011) 23(4):617–27. doi: 10.3233/JAD-2010-100987

32. Pineda JR, Pardo R, Zala D, Yu H, Humbert S, Saudou F. Genetic and pharmacological inhibition of calcineurin corrects the BDNF transport defect in Huntington's disease. *Mol Brain* (2009) 2(33). doi: 10.1186/1756-6606-2-33

33. Overk CR, Rockenstein E, Florio J, Cheng Q, Masliah E. Differential calcium alterations in animal models of neurodegenerative disease: Reversal by FK506. *Neuroscience* (2015) 310:549–60. doi: 10.1016/j.neuroscience.2015.08.068

34. Mukherjee A, Morales-Scheihing D, Gonzalez-Romero D, Green K, Taglialatela G, Soto C. Calcineurin inhibition at the clinical phase of prion disease reduces neurodegeneration, improves behavioral alterations and increases animal survival. *PloS Pathog* (2010) 6(10):e1001138. doi: 10.1371/journal.ppat.1001138

35. Wu HY, Hudry E, Hashimoto T, Uemura K, Fan ZY, Berezovska O, et al. Distinct dendritic spine and nuclear phases of calcineurin activation after exposure to amyloid-β revealed by a novel fluorescence resonance energy transfer assay. *J Neurosci* (2012) 32(15):5298–309. doi: 10.1523/JNEUROSCI.0227-12.2012

36. Sompol P, Furman JL, Pleiss MM, Kraner SD, Artiushin IA, Batten SR, et al. Calcineurin/NFAT signaling in activated astrocytes drives network hyperexcitability in Aβ-bearing mice. *J Neurosci* (2017) 37(25):6132–48. doi: 10.1523/JNEUROSCI.0877-17.2017

37. Taglialatela G, Rastellini C, Cicalese L. Reduced incidence of dementia in solid organ transplant patients treated with calcineurin inhibitors. *J Alzheimers Dis* (2015) 47 (2):329–33. doi: 10.3233/JAD-150065

38. Silva JD, Taglialatela G, Jupiter DC. Reduced prevalence of dementia in patients prescribed tacrolimus, sirolimus, or cyclosporine. *J Alzheimers Dis* (2023) 95(2):585–97. doi: 10.3233/JAD-230526

39. Im SH, Rao A. Activation and deactivation of gene expression by Ca2+/calcineurin-NFAT-mediated signaling. *Mol Cells* (2004) 18(1):1–9.

40. Alothaid H, Aldughaim MSK, Alamri SS, Alrahimi JSM, Al-Jadani SH. Role of calcineurin biosignaling in cell secretion and the possible regulatory mechanisms. *Saudi J Biol Sci* (2021) 28(1):116–24. doi: 10.1016/j.sjbs.2020.08.042

41. Ulengin-Talkish I, Cyert MS. A cellular atlas of calcineurin signaling. *Biochim Biophys Acta Mol Cell Res* (2023) 1870(1):119366. doi: 10.1016/j.bbamcr.2022.119366

42. Thiel G, Schmidt T, Rössler OG. Ca. *Cells* (2021) 10(4). doi: 10.3390/cells10040875

43. Shaw JP, Utz PJ, Durand DB, Toole JJ, Emmel EA, Crabtree GR. Identification of a putative regulator of early T cell activation genes. *Science* (1988) 241(4862):202–5. doi: 10.1126/science.3260404

44. Kuklina EM, Shirshev SV. Role of transcription factor NFAT in the immune response. *Biochem (Mosc)* (2001) 66(5):467–75. doi: 10.1023/a:1010238931555

45. Kiani A, Rao A, Aramburu J. Manipulating immune responses with immunosuppressive agents that target NFAT. *Immunity* (2000) 12(4):359–72. doi: 10.1016/s1074-7613(00)80188-0

46. Crabtree GR, Olson EN. NFAT signaling: choreographing the social lives of cells. *Cell* (2002) 109Suppl:S67–79. doi: 10.1016/s0092-8674(02)00699-2

47. Macian F. NFAT proteins: key regulators of T-cell development and function. *Nat Rev Immunol* (2005) 5(6):472–84. doi: 10.1038/nri1632

48. Schulz RA, Yutzey KE. Calcineurin signaling and NFAT activation in cardiovascular and skeletal muscle development. *Dev Biol* (2004) 266(1):1–16. doi: 10.1016/j.ydbio.2003.10.008

49. Graef IA, Chen F, Chen L, Kuo A, Crabtree GR. Signals transduced by Ca(2+)/calcineurin and NFATc3/c4 pattern the developing vasculature. *Cell* (2001) 105 (7):863–75. doi: 10.1016/s0092-8674(01)00396-8

50. Ranger AM, Grusby MJ, Hodge MR, Gravallese EM, de la Brousse FC, Hoey T, et al. The transcription factor NF-ATc is essential for cardiac valve formation. *Nature* (1998) 392(6672):186–90. doi: 10.1038/32426

51. Ranger AM, Gerstenfeld LC, Wang J, Kon T, Bae H, Gravallese EM, et al. The nuclear factor of activated T cells (NFAT) transcription factor NFATp (NFATc2) is a repressor of chondrogenesis. *J Exp Med* (2000) 191(1):9–22. doi: 10.1084/jem.191.1.9

52. Oukka M, Ho IC, de la Brousse FC, Hoey T, Grusby MJ, Glimcher LH. The transcription factor NFAT4 is involved in the generation and survival of T cells. *Immunity* (1998) 9(3):295–304. doi: 10.1016/s1074-7613(00)80612-3

53. Suchting S, Bicknell R, Eichmann A. Neuronal clues to vascular guidance. *Exp Cell Res* (2006) 312(5):668–75. doi: 10.1016/j.yexcr.2005.11.009

54. Benedito AB, Lehtinen M, Massol R, Lopes UG, Kirchhausen T, Rao A, et al. The transcription factor NFAT3 mediates neuronal survival. *J Biol Chem* (2005) 280 (4):2818–25. doi: 10.1074/jbc.M408741200

55. Arron JR, Winslow MM, Polleri A, Chang CP, Wu H, Gao X, et al. NFAT dysregulation by increased dosage of DSCR1 and DYRK1A on chromosome 21. *Nature* (2006) 441(7093):595–600. doi: 10.1038/nature04678

56. Schwartz N, Schohl A, Ruthazer ES. Neural activity regulates synaptic properties and dendritic structure in vivo through calcineurin/NFAT signaling. *Neuron* (2009) 62 (5):655–69. doi: 10.1016/j.neuron.2009.05.007

57. de la Fuente V, Freudenthal R, Romano A. Reconsolidation or extinction: transcription factor switch in the determination of memory course after retrieval. *J Neurosci* (2011) 31(15):5562–73. doi: 10.1523/JNEUROSCI.6066-10.2011

58. Quadrato G, Benevento M, Alber S, Jacob C, Floriddia EM, Nguyen T, et al. Nuclear factor of activated T cells (NFATc4) is required for BDNF-dependent survival of adult-born neurons and spatial memory formation in the hippocampus. *Proc Natl Acad Sci USA* (2012) 109(23):E1499–508. doi: 10.1073/pnas.1202068109

59. Kipanyula MJ, Kimaro WH, Seke Etet PF. The emerging roles of the calcineurin-nuclear factor of activated T-lymphocytes pathway in nervous system functions and diseases. *J Aging Res vol* (2016) 2016, 5081021. doi: 10.1155/2016/5081021

60. Vihma H, Pruunsild P, Timmusk T. Alternative splicing and expression of human and mouse NFAT genes. *Genomics* (2008) 92(5):279–91. doi: 10.1016/j.ygeno.2008.06.011

61. Lee N, Kim D, Kim WU. Role of NFAT5 in the immune system and pathogenesis of autoimmune diseases. *Front Immunol* (2019) 10, 270:270. doi: 10.3389/fimmu.2019.00270

62. Manocha GD, Ghatak A, Puig KL, Kraner SD, Norris CM, Combs CK. NFATc2 modulates microglial activation in the AβPP/PS1 mouse model of alzheimer's disease. *J Alzheimers Dis* (2017) 58(3):775–87. doi: 10.3233/JAD-151203

63. Furman JL, Sompol P, Kraner SD, Pleiss MM, Putman EJ, Dunkerson J, et al. Blockade of astrocytic calcineurin/NFAT signaling helps to normalize hippocampal synaptic function and plasticity in a rat model of traumatic brain injury. *J Neurosci* (2016) 36(5):1502–15. doi: 10.1523/JNEUROSCI.1930-15.2016

64. López-Rodríguez C, Aramburu J, Jin L, Rakeman AS, Michino M, Rao A. Bridging the NFAT and NF-kappaB families: NFAT5 dimerization regulates cytokine gene transcription in response to osmotic stress. *Immunity* (2001) 15(1):47–58. doi: 10.1016/s1074-7613(01)00165-0

65. Rao A, Luo C, Hogan PG. Transcription factors of the NFAT family: regulation and function. *Annu Rev Immunol* (1997) 15:707–47. doi: 10.1146/annurev.immunol.15.1.707

66. Takeuchi K, Roehrl MH, Sun ZY, Wagner G. Structure of the calcineurin-NFAT complex: defining a T cell activation switch using solution NMR and crystal coordinates. *Structure* (2007) 15(5):587–97. doi: 10.1016/j.str.2007.03.015

67. Okamura H, Aramburu J, García-Rodríguez C, Viola JP, Raghavan A, Tahiliani M, et al. Concerted dephosphorylation of the transcription factor NFAT1 induces a conformational switch that regulates transcriptional activity. *Mol Cell* (2000) 6(3):539–50. doi: 10.1016/s1097-2765(00)00053-8

68. Beals CR, Sheridan CM, Turck CW, Gardner P, Crabtree GR. Nuclear export of NF-ATc enhanced by glycogen synthase kinase-3. *Science* (1997) 275(5308):1930–4. doi: 10.1126/science.275.5308.1930

69. Porter CM, Havens MA, Clipstone NA. Identification of amino acid residues and protein kinases involved in the regulation of NFATc subcellular localization. *J Biol Chem* (2000) 275(5):3543–51. doi: 10.1074/jbc.275.5.3543

70. Neal JW, Clipstone NA. Glycogen synthase kinase-3 inhibits the DNA binding activity of NFATc. *J Biol Chem* (2001) 276(5):3666–73. doi: 10.1074/jbc.M004888200

71. Hogan PG, Chen L, Nardone J, Rao A. Transcriptional regulation by calcium, calcineurin, and NFAT. *Genes Dev* (2003) 17(18):2205–32. doi: 10.1101/gad.1102703

72. Vaeth M, Feske S. NFAT control of immune function: New Frontiers for an Abiding Trooper. *F1000Res* (2018) 7(260). doi: 10.12688/f1000research.13426.1

73. Flanagan WM, Corthésy B, Bram RJ, Crabtree GR. Nuclear association of a T-cell transcription factor blocked by FK-506 and cyclosporin A. *Nature* (1991) 352 (6338):803–7. doi: 10.1038/352803a0

74. Bettelli E, Dastrange M, Oukka M. Foxp3 interacts with nuclear factor of activated T cells and NF-kappa B to repress cytokine gene expression and effector functions of T helper cells. *Proc Natl Acad Sci USA* (2005) 102(14):5138–43. doi: 10.1073/pnas.0501675102

75. Gwack Y, Sharma S, Nardone J, Tanasa B, Iuga A, Srikanth S, et al. A genome-wide Drosophila RNAi screen identifies DYRK-family kinases as regulators of NFAT. *Nature* (2006) 441(7093):646–50. doi: 10.1038/nature04631

76. Chow CW, Rincón M, Cavanagh J, Dickens M, Davis RJ. Nuclear accumulation of NFAT4 opposed by the JNK signal transduction pathway. *Science* (1997) 278 (5343):1638–41. doi: 10.1126/science.278.5343.1638

77. Whitehurst CE, Geppert TD. MEK1 and the extracellular signal-regulated kinases are required for the stimulation of IL-2 gene transcription in T cells. *J Immunol* (1996) 156(3):1020–9. doi: 10.4049/jimmunol.156.3.1020

78. García-Rodríguez C, Rao A. Nuclear factor of activated T cells (NFAT)-dependent transactivation regulated by the coactivators p300/CREB-binding protein (CBP. *J Exp Med* (1998) 187(12):2031–6. doi: 10.1084/jem.187.12.2031

79. Yang T, Davis RJ, Chow CW. Requirement of two NFATc4 transactivation domains for CBP potentiation. *J Biol Chem* (2001) 276(43):39569–76. doi: 10.1074/jbc.M102961200

80. Terui Y, Saad N, Jia S, McKeon F, Yuan J. Dual role of sumoylation in the nuclear localization and transcriptional activation of NFAT1. *J Biol Chem* (2004) 279 (27):28257–65. doi: 10.1074/jbc.M403153200

81. Henley JM, Craig TJ, Wilkinson KA. Neuronal SUMOylation: mechanisms, physiology, and roles in neuronal dysfunction. *Physiol Rev* (2014) 94:1249–85. doi: 10.1152/physrev.00008.2014

82. Vihma H, Luhakooder M, Pruunsild P, Timmusk T. Regulation of different human NFAT isoforms by neuronal activity. *J Neurochem* (2016) 137(3):394–408. doi: 10.1111/jnc.13568

83. Crabtree GR. "Generic signals and specific outcomes: signaling through Ca2+, calcineurin, and NF-AT," (in eng). *Cell* (1999) 96(5):611–4. doi: 10.1016/s0092-8674(00)80571-1

84. Horsley V, Pavlath GK. NFAT: ubiquitous regulator of cell differentiation and adaptation. *J Cell Biol* (2002) 156(5):771–4. doi: 10.1083/jcb.200111073

85. Berridge MJ, Lipp P, Bootman MD. The versatility and universality of calcium signalling. *Nat Rev Mol Cell Biol* (2000) 1(1):11–21. doi: 10.1038/35036035

86. Müller MR, Sasaki Y, Stevanovic I, Lamperti ED, Ghosh S, Sharma S, et al. Requirement for balanced Ca/NFAT signaling in hematopoietic and embryonic development. *Proc Natl Acad Sci USA* (2009) 106(17):7034–9. doi: 10.1073/pnas.0813296106

87. Aramburu J, Yaffe MB, López-Rodríguez C, Cantley LC, Hogan PG, Rao A. Affinity-driven peptide selection of an NFAT inhibitor more selective than cyclosporin A. *Science* (1999) 285(5436):2129–33. doi: 10.1126/science.285.5436.2129

88. Zhu J, Shibasaki F, Price R, Guillemot JC, Yano T, Dötsch V, et al. Intramolecular masking of nuclear import signal on NF-AT4 by casein kinase I and MEKK1. *Cell* (1998) 93(5):851–61. doi: 10.1016/s0092-8674(00)81445-2

89. Lewis RS. Calcium oscillations in T-cells: mechanisms and consequences for gene expression. *Biochem Soc Trans* (2003) 31(Pt 5):925–9. doi: 10.1042/bst0310925

90. Lewis RS. Calcium signaling mechanisms in T lymphocytes. *Annu Rev Immunol* (2001) 19:497–521. doi: 10.1146/annurev.immunol.19.1.497

91. Graef IA, Wang F, Charron F, Chen L, Neilson J, Tessier-Lavigne M, et al. Neurotrophins and netrins require calcineurin/NFAT signaling to stimulate outgrowth of embryonic axons. *Cell* (2003) 113(5):657–70. doi: 10.1016/s0092-8674(03)00390-8

92. Groth RD, Mermelstein PG. Brain-derived neurotrophic factor activation of NFAT (nuclear factor of activated T-cells)-dependent transcription: a role for the transcription factor NFATc4 in neurotrophin-mediated gene expression. *J Neurosci* (2003) 23(22):8125–34. doi: 10.1523/JNEUROSCI.23-22-08125.2003

93. Graef IA, Mermelstein PG, Stankunas K, Neilson JR, Deisseroth K, Tsien RW, et al. L-type calcium channels and GSK-3 regulate the activity of NF-ATc4 in hippocampal neurons. *Nature* (1999) 401(6754):703–8. doi: 10.1038/44378

94. Nguyen T, Di Giovanni S. NFAT signaling in neural development and axon growth. *Int J Dev Neurosci* (2008) 26(2):141–5. doi: 10.1016/j.ijdevneu.2007.10.004

95. Serafini T, Colamarino SA, Leonardo ED, Wang H, Beddington R, Skarnes WC, et al. Netrin-1 is required for commissural axon guidance in the developing vertebrate nervous system. *Cell* (1996) 87(6):1001–14. doi: 10.1016/s0092-8674(00)81795-x

96. Fazeli A, Dickinson SL, Hermiston ML, Tighe RV, Steen RG, Small CG, et al. Phenotype of mice lacking functional Deleted in colorectal cancer (Dcc) gene. *Nature* (1997) 386(6627):796–804. doi: 10.1038/386796a0

97. Langwieser N, Christel CJ, Kleppisch T, Hofmann F, Wotjak CT, Moosmang S. Homeostatic switch in hebbian plasticity and fear learning after sustained loss of Cav1.2 calcium channels. *J Neurosci* (2010) 30(25):8367–75. doi: 10.1523/JNEUROSCI.4164-08.2010

98. Moosmang S, Haider N, Klugbauer N, Adelsberger H, Langwieser N, Müller J, et al. Role of hippocampal Cav1.2 Ca2+ channels in NMDA receptor-independent synaptic plasticity and spatial memory. *J Neurosci* (2005) 25(43):9883–92. doi: 10.1523/JNEUROSCI.1531-05.2005

99. Oliveria SF, Dell'Acqua ML, Sather WA. AKAP79/150 anchoring of calcineurin controls neuronal L-type Ca2+ channel activity and nuclear signaling. *Neuron* (2007) 55(2):261–75. doi: 10.1016/j.neuron.2007.06.032

100. Ulrich JD, Kim MS, Houlihan PR, Shutov LP, Mohapatra DP, Strack S, et al. Distinct activation properties of the nuclear factor of activated T-cells (NFAT) isoforms NFATc3 and NFATc4 in neurons. *J Biol Chem* (2012) 287(45):37594–609. doi: 10.1074/jbc.M112.365197

101. Vashishta A, Habas A, Pruunsild P, Zheng JJ, Timmusk T, Hetman M. Nuclear factor of activated T-cells isoform c4 (NFATc4/NFAT3) as a mediator of antiapoptotic transcription in NMDA receptor-stimulated cortical neurons. *J Neurosci* (2009) 29 (48):15331–40. doi: 10.1523/JNEUROSCI.4873-09.2009

102. Klauck TM, Faux MC, Labudda K, Langeberg LK, Jaken S, Scott JD. Coordination of three signaling enzymes by AKAP79, a mammalian scaffold protein. *Science* (1996) 271(5255):1589–92. doi: 10.1126/science.271.5255.1589

103. Kashishian A, Howard M, Loh C, Gallatin WM, Hoekstra MF, Lai Y. AKAP79 inhibits calcineurin through a site distinct from the immunophilin-binding region. *J Biol Chem* (1998) 273(42):27412–9. doi: 10.1074/jbc.273.42.27412

104. Kim MJ, Jo DG, Hong GS, Kim BJ, Lai M, Cho DH, et al. Calpain-dependent cleavage of cain/cabin1 activates calcineurin to mediate calcium-triggered cell death. *Proc Natl Acad Sci USA* (2002) 99(15):9870–5. doi: 10.1073/pnas.152336999

105. Tredger JM, Brown NW, Dhawan A. Calcineurin inhibitor sparing in paediatric solid organ transplantation : managing the efficacy/toxicity conundrum. *Drugs* (2008) 68:1385–414:no. doi: 10.2165/00003495-200868100-00004

106. Höcker B, Tönshoff B. "Calcineurin inhibitor-free immunosuppression in pediatric renal transplantation: a viable option? *Paediatr Drugs* (2011) 13(1):49–69. doi: 10.2165/11538530-000000000-00000

107. Borel JF, Feurer C, Gubler HU, Stähelin H. Biological effects of cyclosporin A: a new antilymphocytic agent. *Agents Actions* (1976) 6(4):468–75. doi: 10.1007/BF01973261

108. Handschumacher RE, Harding MW, Rice J, Drugge RJ, Speicher DW. Cyclophilin: a specific cytosolic binding protein for cyclosporin A," (in eng). *Science* (1984) 226(4674):544–7. doi: 10.1126/science.6238408

109. Schreiber SL. Chemistry and biology of the immunophilins and their immunosuppressive ligands. *Science* (1991) 251(4991):283–7. doi: 10.1126/science.1702904

110. Wang P, Heitman J. The cyclophilins. *Genome Biol* (2005) 6(7):226. doi: 10.1186/gb-2005-6-7-226

111. Matsuda S, Koyasu S. Mechanisms of action of cyclosporine. *Immunopharmacology* (2000) 47(2-3):119–25. doi: 10.1016/s0162-3109(00)00192-2

112. Rincón M, Flavell RA. AP-1 transcriptional activity requires both T-cell receptor-mediated and co-stimulatory signals in primary T lymphocytes. *EMBO J* (1994) 13(18):4370–81. doi: 10.1002/j.1460-2075.1994.tb06757.x

113. Mattila PS, Ullman KS, Fiering S, Emmel EA, McCutcheon M, Crabtree GR, et al. The actions of cyclosporin A and FK506 suggest a novel step in the activation of T lymphocytes. *EMBO J* (1990) 9(13):4425–33. doi: 10.1002/j.1460-2075.1990.tb07893.x

114. Metcalfe S, Alexander D, Turner J. FK506 and cyclosporin A each inhibit antigen-specific signaling in the T cell line 171 in the absence of a calcium signal. *Cell Immunol* (1994) 158(1):46–58. doi: 10.1006/cimm.1994.1255

115. Matsuda S, Moriguchi T, Koyasu S, Nishida E. T lymphocyte activation signals for interleukin-2 production involve activation of MKK6-p38 and MKK7-SAPK/JNK signaling pathways sensitive to cyclosporin A. *J Biol Chem* (1998) 273(20):12378–82. doi: 10.1074/jbc.273.20.12378

116. Kaminska B, Figiel I, Pyrzynska B, Czajkowski R, Mosieniak G. Treatment of hippocampal neurons with cyclosporin A results in calcium overload and apoptosis which are independent on NMDA receptor activation. *Br J Pharmacol* (2001) 133 (7):997–1004. doi: 10.1038/sj.bjp.0704177

117. Canudas AM, Jordà EG, Verdaguer E, Jiménez A, Sureda FX, Rimbau V, et al. Cyclosporin A enhances colchicine-induced apoptosis in rat cerebellar granule neurons. *Br J Pharmacol* (2004) 141(4):661–9. doi: 10.1038/sj.bjp.0705664

118. Schnichels S, Schultheiss M, Klemm P, Blak M, Herrmann T, Melchinger M, et al. Cyclosporine A protects retinal explants against hypoxia. *Int J Mol Sci* (2021) 22 (19). doi: 10.3390/ijms221910196

119. Chen ZR, Ma Y, Guo HH, Lu ZD, Jin QH. Therapeutic efficacy of cyclosporin A against spinal cord injury in rats with hyperglycemia. *Mol Med Rep* (2018) 17(3):4369–75. doi: 10.3892/mmr.2018.8422

120. Ye F, Li X, Li F, Li J, Chang W, Yuan J, et al. Cyclosporin A protects against Lead neurotoxicity through inhibiting mitochondrial permeability transition pore opening in nerve cells. *Neurotoxicology* (2016) 57:203–13. doi: 10.1016/j.neuro.2016.10.004

121. Schultheiss M, Schnichels S, Mlynczak T, Dipl-Ing JH, Bartz-Schmidt KU, Szurman P, et al. Cyclosporine a protects RGC-5 cells from excitotoxic cell death. *J Glaucoma* (2014) 23(4):219–24. doi: 10.1097/IJG.0000000000000040

122. Xiong TQ, Chen LM, Tan BH, Guo CY, Li YN, Zhang YF, et al. The effects of calcineurin inhibitor FK506 on actin cytoskeleton, neuronal survival and glial reactions after pilocarpine-induced status epilepticus in mice. *Epilepsy Res* (2018) 140:138–47. doi: 10.1016/j.eplepsyres.2018.01.007

123. Kuchibhotla KV, Goldman ST, Lattarulo CR, Wu HY, Hyman BT, Bacskai BJ. Abeta plaques lead to aberrant regulation of calcium homeostasis in vivo resulting in structural and functional disruption of neuronal networks. *Neuron* (2008) 59(2):214–25. doi: 10.1016/j.neuron.2008.06.008

124. Kim S, Violette CJ, Ziff EB. Reduction of increased calcineurin activity rescues impaired homeostatic synaptic plasticity in presenilin 1 M146V mutant, (in eng). *Neurobiol Aging* (2015) 36:3239–46. doi: 10.1016/j.neurobiolaging.2015.09.007

125. Shah SZA, Zhao D, Taglialatela G, Hussain T, Dong H, Sabir N, et al. Combinatory FK506 and minocycline treatment alleviates prion-induced neurodegenerative events via caspase-mediated MAPK-NRF2 pathway. *Int J Mol Sci* (2019) 20(5). doi: 10.3390/ijms20051144

126. Fields JA, Overk C, Adame A, Florio J, Mante M, Pineda A, et al. Neuroprotective effects of the immunomodulatory drug FK506 in a model of HIV1-gp120 neurotoxicity. *J Neuroinflamm* (2016) 13(1):120. doi: 10.1186/s12974-016-0585-8

127. Graham RM. Cyclosporine: mechanisms of action and toxicity. *Cleve Clin J Med* (1994) 61(4):308–13. doi: 10.3949/ccjm.61.4.308

128. Thomson AW, Bonham CA, Zeevi A. Mode of action of tacrolimus (FK506): molecular and cellular mechanisms. *Ther Drug Monit* (1995) 17(6):584–91. doi: 10.1097/00007691-199512000-00007

129. Powell JD, Zheng Y. Dissecting the mechanism of T-cell anergy with immunophilin ligands. *Curr Opin Investig Drugs* (2006) 7(11):1002–7.

130. Mori A, Suko M, Kaminuma O, Inoue S, Ohmura T, Hoshino A, et al. IL-2-induced IL-5 synthesis, but not proliferation, of human CD4+ T cells is suppressed by FK506. *J Immunol* (1997) 158(8):3659–65.

131. Rostaing L, Puyoo O, Tkaczuk J, Peres C, Rouzaud A, Cisterne JM, et al. Differences in Type 1 and Type 2 intracytoplasmic cytokines, detected by flow cytometry, according to immunosuppression (cyclosporine A vs. tacrolimus) in stable renal allograft recipients. *Clin Transplant* (1999) 13(5):400–9. doi: 10.1034/j.1399-0012.1999.130506.x

132. Almawi WY, Melemedjian OK. Clinical and mechanistic differences between FK506 (tacrolimus) and cyclosporin A. *Nephrol Dial Transplant* (2000) 15(12):1916–8. doi: 10.1093/ndt/15.12.1916

133. Aramburu J, Garcia-Cózar F, Raghavan A, Okamura H, Rao A, Hogan PG. Selective inhibition of NFAT activation by a peptide spanning the calcineurin targeting site of NFAT. *Mol Cell* (1998) 1(5):627–37. doi: 10.1016/s1097-2765(00)80063-5

134. Kuriyama M, Matsushita M, Tateishi A, Moriwaki A, Tomizawa K, Ishino K, et al. A cell-permeable NFAT inhibitor peptide prevents pressure-overload cardiac hypertrophy. *Chem Biol Drug Des* (2006) 67(3):238–43. doi: 10.1111/j.1747-0285.2006.00360.x

135. Martínez-Martínez S, Rodríguez A, López-Maderuelo MD, Ortega-Pérez I, Vázquez J, Redondo JM. Blockade of NFAT activation by the second calcineurin binding site. *J Biol Chem* (2006) 281(10):6227–35. doi: 10.1074/jbc.M513885200

136. Rodríguez A, Roy J, Martínez-Martínez S, López-Maderuelo MD, Niño-Moreno P, Ortí L, et al. A conserved docking surface on calcineurin mediates interaction with substrates and immunosuppressants. *Mol Cell* (2009) 33(5):616–26. doi: 10.1016/j.molcel.2009.01.030

137. Adachi S, Amasaki Y, Miyatake S, Arai N, Iwata M. Successive expression and activation of NFAT family members during thymocyte differentiation. *J Biol Chem* (2000) 275(19):14708–16. doi: 10.1074/jbc.275.19.14708

138. Brown DG, Wilkerson EC, Love WE. A review of traditional and novel oral anticoagulant and antiplatelet therapy for dermatologists and dermatologic surgeons. *J Am Acad Dermatol* (2015) 72(3):524–34. doi: 10.1016/j.jaad.2014.10.027

139. Mulero MC, Aubareda A, Orzáez M, Messeguer J, Serrano-Candelas E, Martínez-Hoyer S, et al. Inhibiting the calcineurin-NFAT (nuclear factor of activated T cells) signaling pathway with a regulator of calcineurin-derived peptide without affecting general calcineurin phosphatase activity. *J Biol Chem* (2009) 284(14):9394–401. doi: 10.1074/jbc.M805889200

140. Borisy AA, Elliott PJ, Hurst NW, Lee MS, Lehar J, Price ER, et al. Systematic discovery of multicomponent therapeutics. *Proc Natl Acad Sci USA* (2003) 100 (13):7977–82. doi: 10.1073/pnas.1337088100

141. Weyrich AS, Denis MM, Kuhlmann-Eyre JR, Spencer ED, Dixon DA, Marathe GK, et al. Dipyridamole selectively inhibits inflammatory gene expression in platelet-monocyte aggregates. *Circulation* (2005) 111(5):633–42. doi: 10.1161/01.CIR.0000154607.90506.45

142. Kang S, Li H, Rao A, Hogan PG. Inhibition of the calcineurin-NFAT interaction by small organic molecules reflects binding at an allosteric site. *J Biol Chem* (2005) 280(45):37698–706. doi: 10.1074/jbc.M502247200

143. Roehrl MH, Kang S, Aramburu J, Wagner G, Rao A, Hogan PG. Selective inhibition of calcineurin-NFAT signaling by blocking protein-protein interaction with small organic molecules. *Proc Natl Acad Sci USA* (2004) 101(20):7554–9. doi: 10.1073/pnas.0401835101

144. Trevillyan JM, Chiou XG, Chen YW, Ballaron SJ, Sheets MP, Smith ML, et al. Potent inhibition of NFAT activation and T cell cytokine production by novel low molecular weight pyrazole compounds. *J Biol Chem* (2001) 276(51):48118–26. doi: 10.1074/jbc.M107919200

145. Bîrsan T, Dambrin C, Marsh KC, Jacobsen W, Djuric SW, Mollison KW, et al. Preliminary in vivo pharmacokinetic and pharmacodynamic evaluation of a novel calcineurin-independent inhibitor of NFAT. *Transpl Int* (2004) 17(3):145–50. doi: 10.1007/s00147-003-0676-1

146. Nilsson LM, Sun ZW, Nilsson J, Nordström I, Chen YW, Molkentin JD, et al. Novel blocker of NFAT activation inhibits IL-6 production in human myometrial arteries and reduces vascular smooth muscle cell proliferation. *Am J Physiol Cell Physiol* (2007) 292(3):C1167–78. doi: 10.1152/ajpcell.00590.2005

147. Jabr RI, Wilson AJ, Riddervold MH, Jenkins AH, Perrino BA, Clapp LH. Nuclear translocation of calcineurin Abeta but not calcineurin Aalpha by platelet-derived growth factor in rat aortic smooth muscle. *Am J Physiol Cell Physiol* (2007) 292 (6):C2213–25. doi: 10.1152/ajpcell.00139.2005

148. Sompol P, Gollihue JL, Kraner SD, Artiushin IA, Cloyd RA, Chishti EA, et al. Q134R: Small chemical compound with NFAT inhibitory properties improves behavioral performance and synapse function in mouse models of amyloid pathology. *Aging Cell* (2021) 20(7):e13416. doi: 10.1111/acel.13416

149. Dineley KT, Hogan D, Zhang WR, Taglialatela G. Acute inhibition of calcineurin restores associative learning and memory in Tg2576 APP transgenic mice. *Neurobiol Learn Mem* (2007) 88(2):217–24. doi: 10.1016/j.nlm.2007.03.010

150. Taglialatela G, Hogan D, Zhang WR, Dineley KT. Intermediate- and long-term recognition memory deficits in Tg2576 mice are reversed with acute calcineurin inhibition. *Behav Brain Res* (2009) 200(1):95–9. doi: 10.1016/j.bbr.2008.12.034

151. Yoshiyama Y, Higuchi M, Zhang B, Huang SM, Iwata N, Saido TC, et al. Synapse loss and microglial activation precede tangles in a P301S tauopathy mouse model. *Neuron* (2007) 53(3):337–51. doi: 10.1016/j.neuron.2007.01.010

152. Gómez-Sintes R, Lucas JJ. NFAT/Fas signaling mediates the neuronal apoptosis and motor side effects of GSK-3 inhibition in a mouse model of lithium therapy. *J Clin Invest* (2010) 120(7):2432–45. doi: 10.1172/JCI37873

153. Gould TD, Chen G, Manji HK. *In vivo* evidence in the brain for lithium inhibition of glycogen synthase kinase-3. *Neuropsychopharmacology* (2004) 29(1):32–8. doi: 10.1038/sj.npp.1300283

154. Beaulieu JM, Caron MG. Looking at lithium: molecular moods and complex behaviour. *Mol Interv* (2008) 8(5):230–41. doi: 10.1124/mi.8.5.8

155. Beaulieu JM, Marion S, Rodriguiz RM, Medvedev IO, Sotnikova TD, Ghisi V, et al. A beta-arrestin 2 signaling complex mediates lithium action on behavior. *Cell* (2008) 132(1):125–36. doi: 10.1016/j.cell.2007.11.041

156. Fiorentini A, Rosi MC, Grossi C, Luccarini I, Casamenti F. Lithium improves hippocampal neurogenesis, neuropathology and cognitive functions in APP mutant mice. *PloS One* (2010) 5(12):e14382. doi: 10.1371/journal.pone.0014382

157. Ma T, Tzavaras N, Tsokas P, Landau EM, Blitzer RD. Synaptic stimulation of mTOR is mediated by Wnt signaling and regulation of glycogen synthetase kinase-3. *J Neurosci* (2011) 31(48):17537–46. doi: 10.1523/JNEUROSCI.4761-11.2011

158. Phiel CJ, Wilson CA, Lee VM, Klein PS. "GSK-3alpha regulates production of Alzheimer's disease amyloid-beta peptides," (in eng). *Nature* (2003) 423(6938):435–9. doi: 10.1038/nature01640

159. Hooper C, Killick R, Lovestone S. The GSK3 hypothesis of Alzheimer's disease. *J Neurochem* (2008) 104(6):1433–9. doi: 10.1111/j.1471-4159.2007.05194.x

160. Kremer A, Louis JV, Jaworski T, Van Leuven F. GSK3 and alzheimer's disease: facts and fiction. *Front Mol Neurosci* (2011) 4:17. doi: 10.3389/fnmol.2011.00017

161. Hong M, Chen DC, Klein PS, Lee VM. Lithium reduces tau phosphorylation by inhibition of glycogen synthase kinase-3. *J Biol Chem* (1997) 272(40):25326–32. doi: 10.1074/jbc.272.40.25326

162. Spittaels K, Van den Haute C, Van Dorpe J, Geerts H, Mercken M, Bruynseels K, et al. Glycogen synthase kinase-3beta phosphorylates protein tau and rescues the axonopathy in the central nervous system of human four-repeat tau transgenic mice. *J Biol Chem* (2000) 275(52):41340–9. doi: 10.1074/jbc.M006219200

163. Leroy K, Boutajangout A, Authelet M, Woodgett JR, Anderton BH, Brion JP. The active form of glycogen synthase kinase-3beta is associated with granulovacuolar degeneration in neurons in Alzheimer's disease. *Acta Neuropathol* (2002) 103(2):91–9. doi: 10.1007/s004010100435

164. Sun W, Qureshi HY, Cafferty PW, Sobue K, Agarwal-Mawal A, Neufield KD, et al. Glycogen synthase kinase-3beta is complexed with tau protein in brain microtubules. *J Biol Chem* (2002) 277(14):11933–40. doi: 10.1074/jbc.M107182200

165. Ferrer I, BarraChina M, Puig B. Glycogen synthase kinase-3 is associated with neuronal and glial hyperphosphorylated tau deposits in Alzheimer's disease, Pick's disease, progressive supranuclear palsy and corticobasal degeneration. *Acta Neuropathol* (2002) 104(6):583–91. doi: 10.1007/s00401-002-0587-8

166. Engel T, Lucas JJ, Gómez-Ramos P, Moran MA, Avila J, Hernández F. Cooexpression of FTDP-17 tau and GSK-3beta in transgenic mice induce tau polymerization and neurodegeneration. *Neurobiol Aging* (2006) 27(9):1258–68. doi: 10.1016/j.neurobiolaging.2005.06.010

167. Engel T, Hernández F, Avila J, Lucas JJ. Full reversal of Alzheimer's disease-like phenotype in a mouse model with conditional overexpression of glycogen synthase kinase-3. *J Neurosci* (2006) 26(19):5083–90. doi: 10.1523/JNEUROSCI.0604-06.2006

168. Uemura K, Kuzuya A, Shimozono Y, Aoyagi N, Ando K, Shimohama S, et al. GSK3beta activity modifies the localization and function of presenilin 1. *J Biol Chem* (2007) 282(21):15823–32. doi: 10.1074/jbc.M610708200

169. Twomey C, McCarthy JV. Presenilin-1 is an unprimed glycogen synthase kinase-3beta substrate. *FEBS Lett* (2006) 580(17):4015–20. doi: 10.1016/j.febslet.2006.06.035

170. Ly PT, Wu Y, Zou H, Wang R, Zhou W, Kinoshita A, et al. Inhibition of GSK3β-mediated BACE1 expression reduces Alzheimer-associated phenotypes. *J Clin Invest* (2013) 123(1):224–35. doi: 10.1172/JCI64516

171. Hurtado DE, Molina-Porcel L, Carroll JC, Macdonald C, Aboagye AK, Trojanowski JQ, et al. Selectively silencing GSK-3 isoforms reduces plaques and tangles in mouse models of Alzheimer's disease. *J Neurosci* (2012) 32(21):7392–402. doi: 10.1523/JNEUROSCI.0889-12.2012

172. Gómez-Sintes R, Hernández F, Bortolozzi A, Artigas F, Avila J, Zaratin P, et al. Neuronal apoptosis and reversible motor deficit in dominant-negative GSK-3 conditional transgenic mice. *EMBO J* (2007) 26(11):2743–54. doi: 10.1038/sj.emboj.7601725

173. Song L, Zhou T, Jope RS. Lithium facilitates apoptotic signaling induced by activation of the Fas death domain-containing receptor. *BMC Neurosci* (2004) 5, 20. doi: 10.1186/1471-2202-5-20

174. Madiehe AM, Mampuru LJ, Tyobeka EM. Induction of apoptosis in HL-60 cells by lithium. *Biochem Biophys Res Commun* (1995) 209(2):768–74. doi: 10.1006/bbrc.1995.1565

175. Lan Y, Liu X, Zhang R, Wang K, Wang Y, Hua ZC. Lithium enhances TRAIL-induced apoptosis in human lung carcinoma A549 cells. *Biometals* (2013) 26(2):241–54. doi: 10.1007/s10534-012-9607-x

176. Zhang Q, Li H, Zhao X, Zhang H. LiCl induces apoptosis via CHOP/NOXA/Mcl-1 axis in human choroidal melanoma cells. *Cancer Cell Int* (2021) 21(1):96. doi: 10.1186/s12935-021-01778-2

177. Li L, Song H, Zhong L, Yang R, Yang XQ, Jiang KL, et al. Lithium chloride promotes apoptosis in human leukemia NB4 cells by inhibiting glycogen synthase kinase-3 beta. *Int J Med Sci* (2015) 12(10):805–10. doi: 10.7150/ijms.12429

178. Tang HR, He Q, Wang FC. [Mechanism of lithium chloride-induced proliferation inhibition and apoptosis of K562 leukemic cells]. *Zhongguo Shi Yan Xue Ye Xue Za Zhi* (2005) 13(6):979–82.

179. Hantson P. Mechanisms of toxic cardiomyopathy. *Clin Toxicol (Phila)* (2019) 57(1):1–9. doi: 10.1080/15563650.2018.1497172

180. Yao R, Sun X, Xie Y, Liu L, Han D, Yao Y, et al. Lithium chloride inhibits cell survival, overcomes drug resistance, and triggers apoptosis in multiple myeloma via activation of the Wnt/β-catenin pathway. *Am J Transl Res* (2018) 10(8):2610–8.

181. Grimes CA, Jope RS. The multifaceted roles of glycogen synthase kinase 3beta in cellular signaling. *Prog Neurobiol* (2001) 65(4):391–426. doi: 10.1016/s0301-0082(01)00011-9

182. Jayanthi S, Deng X, Ladenheim B, McCoy MT, Cluster A, Cai NS, et al. Calcineurin/NFAT-induced up-regulation of the Fas ligand/Fas death pathway is involved in methamphetamine-induced neuronal apoptosis. *Proc Natl Acad Sci USA* (2005) 102(3):868–73. doi: 10.1073/pnas.0404990102

183. Su JH, Anderson AJ, Cribbs DH, Tu C, Tong L, Kesslack P, et al. Fas and Fas ligand are associated with neuritic degeneration in the AD brain and participate in beta-amyloid-induced neuronal death. *Neurobiol Dis* (2003) 12(3):182–93. doi: 10.1016/s0969-9961(02)00019-0

184. Luoma JI, Zirpel L. Deafferentation-induced activation of NFAT (nuclear factor of activated T-cells) in cochlear nucleus neurons during a developmental critical period: a role for NFATc4-dependent apoptosis in the CNS. *J Neurosci* (2008) 28(12):3159–69. doi: 10.1523/JNEUROSCI.5227-07.2008

185. Hudry E, Wu HY, Arbel-Ornath M, Hashimoto T, Matsouaka R, Fan Z, et al. Inhibition of the NFAT pathway alleviates amyloid β neurotoxicity in a mouse model of Alzheimer's disease. *J Neurosci* (2012) 32(9):3176–92. doi: 10.1523/JNEUROSCI.6439-11.2012

186. Ayton S, Lei P. The Aβ-induced NFAT apoptotic pathway is also activated by GSK-3 inhibition: implications for Alzheimer therapeutics. *J Neurosci* (2012) 32 (28):9454–6. doi: 10.1523/JNEUROSCI.2143-12.2012

187. Gan KJ, Silverman MA. Dendritic and axonal mechanisms of Ca2+ elevation impair BDNF transport in Aβ oligomer-treated hippocampal neurons. *Mol Biol Cell* (2015) 26(6):1058–71. doi: 10.1091/mbc.E14-12-1612

188. Mohmmad Abdul H, Baig I, Levine H, Guttmann RP, Norris CM. Proteolysis of calcineurin is increased in human hippocampus during mild cognitive impairment and is stimulated by oligomeric Abeta in primary cell culture. *Aging Cell* (2011) 10(1):103–13. doi: 10.1111/j.1474-9726.2010.00645.x

189. Hong HS, Hwang JY, Son SM, Kim YH, Moon M, Inhee MJ. FK506 reduces amyloid plaque burden and induces MMP-9 in AβPP/PS1 double transgenic mice. *J Alzheimers Dis* (2010) 22(1):97–105. doi: 10.3233/JAD-2010-100261

190. Yan P, Hu X, Song H, Yin K, Bateman RJ, Cirrito JR, et al. Matrix metalloproteinase-9 degrades amyloid-beta fibrils in vitro and compact plaques in situ. *J Biol Chem* (2006) 281(34):24566–74. doi: 10.1074/jbc.M602440200

191. Mei Z, Yan P, Tan X, Zheng S, Situ B. Transcriptional regulation of BACE1 by NFAT3 leads to enhanced amyloidogenic processing. *Neurochem Res* (2015) 40 (4):829–36. doi: 10.1007/s11064-015-1533-1

192. Vassar R, Kovacs DM, Yan R, Wong PC. The beta-secretase enzyme BACE in health and Alzheimer's disease: regulation, cell biology, function, and therapeutic potential. *J Neurosci* (2009) 29(41):12787–94. doi: 10.1523/JNEUROSCI.3657-09.2009

193. Al-Tel TH, Semreen MH, Al-Qawasmeh RA, Schmidt MF, El-Awadi R, Ardah M, et al. Design, synthesis, and qualitative structure-activity evaluations of novel β-secretase inhibitors as potential Alzheimer's drug leads. *J Med Chem* (2011) 54 (24):8373–85. doi: 10.1021/jm201181f

194. Coimbra JRM, Marques DFF, Baptista SJ, Pereira CMF, Moreira PI, Dinis TCP, et al. Highlights in BACE1 inhibitors for alzheimer's disease treatment. *Front Chem* (2018) 6:178. doi: 10.3389/fchem.2018.00178

195. Citron M. Emerging Alzheimer's disease therapies: inhibition of beta-secretase. *Neurobiol Aging* (2002) 23(6):1017–22. doi: 10.1016/s0197-4580(02)00122-7

196. Yuan J, Venkatraman S, Zheng Y, McKeever BM, Dillard LW, Singh SB. Structure-based design of β-site APP cleaving enzyme 1 (BACE1) inhibitors for the treatment of Alzheimer's disease. *J Med Chem* (2013) 56(11):4156–80. doi: 10.1021/jm301659n

197. Kinney JW, Bemiller SM, Murtishaw AS, Leisgang AM, Salazar AM, Lamb BT. Inflammation as a central mechanism in Alzheimer's disease. *Alzheimers Dement (N Y)* (2018) 4:575–90. doi: 10.1016/j.trci.2018.06.014

198. Furman JL, Norris CM. Calcineurin and glial signaling: neuroinflammation and beyond. *J Neuroinflamm* (2014) 11:158. doi: 10.1186/s12974-014-0158-7

199. Guan PP, Cao LL, Yang Y, Wang P. Calcium ions aggravate alzheimer's disease through the aberrant activation of neuronal networks, leading to synaptic and cognitive deficits. *Front Mol Neurosci* (2021) 14:757515. doi: 10.3389/fnmol.2021.757515

200. Wu HY, Tomizawa K, Oda Y, Wei FY, Lu YF, Matsushita M, et al. Critical role of calpain-mediated cleavage of calcineurin in excitotoxic neurodegeneration. *J Biol Chem* (2004) 279(6):4929–40. doi: 10.1074/jbc.M309767200

201. Pleiss MM, Sompol P, Kraner SD, Abdul HM, Furman JL, Guttmann RP, et al. Calcineurin proteolysis in astrocytes: Implications for impaired synaptic function. *Biochim Biophys Acta* (2016) 1862(9):1521–32. doi: 10.1016/j.bbadis.2016.05.007

202. Watanabe K, Uemura K, Asada M, Maesako M, Akiyama H, Shimohama S, et al. "The participation of insulin-like growth factor-binding protein 3 released by astrocytes in the pathology of Alzheimer's disease," (in eng). *Mol Brain* (2015) 8(1):82. doi: 10.1186/s13041-015-0174-2

203. Cui Y, Jin J, Zhang X, Xu H, Yang L, Du D, et al. "Forebrain NR2B overexpression facilitating the prefrontal cortex long-term potentiation and enhancing working memory function in mice," (in eng). *PloS One* (2011) 6(5): e20312. doi: 10.1371/journal.pone.0020312

204. Plattner F, Hernández A, Kistler TM, Pozo K, Zhong P, Yuen EY, et al. "Memory enhancement by targeting Cdk5 regulation of NR2B," (in eng). *Neuron* (2014) 81(5):1070–83. doi: 10.1016/j.neuron.2014.01.022

205. Norris CM, Kadish I, Blalock EM, Chen KC, Thibault V, Porter NM, et al. Calcineurin triggers reactive/inflammatory processes in astrocytes and is upregulated in aging and Alzheimer's models. *J Neurosci* (2005) 25(18):4649–58. doi: 10.1523/JNEUROSCI.0365-05.2005

206. de la Torre JC. Impaired brain microcirculation may trigger Alzheimer's disease. *Neurosci Biobehav Rev* (1994) 18(3):397–401. doi: 10.1016/0149-7634(94)90052-3

207. Kurz C, Walker L, Rauchmann BS, Perneczky R. Dysfunction of the blood-brain barrier in Alzheimer's disease: Evidence from human studies," (in eng). *Neuropathol Appl Neurobiol* (2022) 48:no. doi: 10.1111/nan.12782

208. Badimon A, Torrente D, Norris EH. "Vascular dysfunction in alzheimer's disease: alterations in the plasma contact and fibrinolytic systems," (in eng). *Int J Mol Sci* (2023) 24(8). doi: 10.3390/ijms24087046

209. Kraner SD, Norris CM. Astrocyte activation and the calcineurin/NFAT pathway in cerebrovascular disease. *Front Aging Neurosci* (2018) 10:287. doi: 10.3389/fnagi.2018.00287

210. Sompol P, Gollihue JL, Weiss BE, Lin RL, Case SL, Kraner SD, et al. Targeting astrocyte signaling alleviates cerebrovascular and synaptic function deficits in a diet-based mouse model of small cerebral vessel disease. *J Neurosci* (2023) 43(10):1797–813. doi: 10.1523/JNEUROSCI.1333-22.2023

211. Furman JL, Sama DM, Gant JC, Beckett TL, Murphy MP, Bachstetter AD, et al. Targeting astrocytes ameliorates neurologic changes in a mouse model of Alzheimer's disease. *J Neurosci* (2012) 32(46):16129–40. doi: 10.1523/JNEUROSCI.2323-12.2012

212. Sama MA, Mathis DM, Furman JL, Abdul HM, Artiushin IA, Kraner SD, et al. Interleukin-1beta-dependent signaling between astrocytes and neurons depends critically on astrocytic calcineurin/NFAT activity. *J Biol Chem* (2008) 283(32):21953–64. doi: 10.1074/jbc.M800148200

213. Canellada A, Ramirez BG, Minami T, Redondo JM, Cano E. Calcium/calcineurin signaling in primary cortical astrocyte cultures: Rcan1-4 and cyclooxygenase-2 as NFAT target genes. *Glia* (2008) 56(7):709–22. doi: 10.1002/glia.20647

214. Nagamoto-Combs K, Combs CK. Microglial phenotype is regulated by activity of the transcription factor, NFAT (nuclear factor of activated T cells). *J Neurosci* (2010) 30(28):9641–6. doi: 10.1523/JNEUROSCI.0828-10.2010

215. Escolano A, Martínez-Martínez S, Alfranca A, Urso K, Izquierdo HM, Delgado M, et al. Specific calcineurin targeting in macrophages confers resistance to inflammation via MKP-1 and p38. *EMBO J* (2014) 33(10):1117–33. doi: 10.1002/embj.201386369

216. Schultze JL. Precision attack on calcineurin in macrophages: a new anti-inflammatory weapon. *EMBO J* (2014) 33(10):1087–8. doi: 10.1002/embj.201488178

217. de Jesus T, Shukla S, Ramakrishnan P. Too sweet to resist: Control of immune cell function by O-GlcNAcylation. *Cell Immunol* (2018) 333:85–92. doi: 10.1016/j.cellimm.2018.05.010

218. Lee HT, Lee KI, Chen CH, Lee TS. Genetic deletion of soluble epoxide hydrolase delays the progression of Alzheimer's disease. *J Neuroinflamm* (2019) 16 (1):267. doi: 10.1186/s12974-019-1635-9

219. Scassellati C, Ciani M, Galoforo AC, Zanardini R, Bonvicini C, Geroldi C. Molecular mechanisms in cognitive frailty: potential therapeutic targets for oxygen-ozone treatment. *Mech Ageing Dev* (2020) 186:111210. doi: 10.1016/j.mad.2020.111210

220. Rojanathammanee L, Puig KL, Combs CK. Pomegranate polyphenols and extract inhibit nuclear factor of activated T-cell activity and microglial activation in vitro transgenic mouse model alzheimer disease. *J Nutr* (2013) 143(5):597–605. doi: 10.3945/jn.112.169516

221. Rojanathammanee L, Floden AM, Manocha GD, Combs CK. Attenuation of microglial activation in a mouse model of Alzheimer's disease via NFAT inhibition. *J Neuroinflamm* (2015) 12:42. doi: 10.1186/s12974-015-0255-2

222. Khalil MAM, Khalil MAU, Khan TFT, Tan J. Drug-induced hematological cytopenia in kidney transplantation and the challenges it poses for kidney transplant physicians. *J Transplant* (2018) 2018:9429265. doi: 10.1155/2018/9429265

223. Farouk SS, Rein JL. The many faces of calcineurin inhibitor toxicity-what the FK? *Adv Chronic Kidney Dis* (2020) 27(1):56–66. doi: 10.1053/j.ackd.2019.08.006

224. Farinelli SE, Greene LA, Friedman WJ. Neuroprotective actions of dipyridamole on cultured CNS neurons. *J Neurosci* (1998) 18(14):5112–23. doi: 10.1523/JNEUROSCI.18-14-05112.1998

225. Lobner D, Choi DW. Dipyridamole increases oxygen-glucose deprivation-induced injury in cortical cell culture. *Stroke* (1994) 25(10):2085–9;discussion 2089-90. doi: 10.1161/01.str.25.10.2085

226. Giblin MJ, Smith TE, Winkler G, Pendergrass HA, Kim MJ, Capozzi ME, et al. Nuclear factor of activated T-cells (NFAT) regulation of IL-1β-induced retinal vascular inflammation. *Biochim Biophys Acta Mol Basis Dis* (2021) 1867(12):166238. doi: 10.1016/j.bbadis.2021.166238

227. Kitamura N, Kaminuma O. Isoform-selective NFAT inhibitor: potential usefulness and development. *Int J Mol Sci* (2021) 22(5). doi: 10.3390/ijms22052725

228. Wang Z, Ye D, Ye J, Wang M, Liu J, Jiang H, et al. The TRPA1 channel in the cardiovascular system: promising features and challenges. *Front Pharmacol* (2019) 10:1253. doi: 10.3389/fphar.2019.01253

229. Takahashi N, Mori Y. TRP channels as sensors and signal integrators of redox status changes. *Front Pharmacol* (2011) 2:58. doi: 10.3389/fphar.2011.00058

230. Talavera K, Startek JB, Alvarez-Collazo J, Boonen B, Alpizar YA, Sanchez A, et al. Mammalian transient receptor potential TRPA1 channels: from structure to disease. *Physiol Rev* (2020) 100(2):725–803. doi: 10.1152/physrev.00005.2019

231. Nassini R, Materazzi S, Benemei S, Geppetti P. The TRPA1 channel in inflammatory and neuropathic pain and migraine. *Rev Physiol Biochem Pharmacol* (2014) 167:1–43. doi: 10.1007/112_2014_18

232. Wang X, Li Y, Wei H, Yang Z, Luo R, Gao Y, et al. Molecular architecture and gating mechanisms of the Drosophila TRPA1 channel. *Cell Discovery* (2023) 9(1):36. doi: 10.1038/s41421-023-00527-1

233. Story GM, Peier AM, Reeve AJ, Eid SR, Mosbacher J, Hricik TR, et al. ANKTM1, a TRP-like channel expressed in nociceptive neurons, is activated by cold temperatures. *Cell* (2003) 112(6):819–29. doi: 10.1016/s0092-8674(03)00158-2

234. Bandell M, Story GM, Hwang SW, Viswanath V, Eid SR, Petrus MJ, et al. Noxious cold ion channel TRPA1 is activated by pungent compounds and bradykinin. *Neuron* (2004) 41(6):849–57. doi: 10.1016/s0896-6273(04)00150-3

235. Hamada F, Rosenzweig M, Kang K, Pulver SR, Ghezzi A, Jegla TJ, et al. An internal thermal sensor controlling temperature preference in Drosophila. *Nature* (2008) 454(7201):217–20. doi: 10.1038/nature07001

236. Saito S, Banzawa N, Fukuta N, Saito CT, Takahashi K, Imagawa T, et al. Heat and noxious chemical sensor, chicken TRPA1, as a target of bird repellents and identification of its structural determinants by multispecies functional comparison. *Mol Biol Evol* (2014) 31(3):708–22. doi: 10.1093/molbev/msu001

237. Gracheva EO, Ingolia NT, Kelly YM, Cordero-Morales JF, Hollopeter G, Chesler AT, et al. Molecular basis of infrared detection by snakes. *Nature* (2010) 464 (7291):1006–11. doi: 10.1038/nature08943

238. Kang K, Panzano VC, Chang EC, Ni L, Dainis AM, Jenkins AM, et al. Modulation of TRPA1 thermal sensitivity enables sensory discrimination in Drosophila. *Nature* (2011) 481(7379):76–80. doi: 10.1038/nature10715

239. Lee KI, Lee HT, Lin HC, Tsay HJ, Tsai FC, Shyue SK, et al. Role of transient receptor potential ankyrin 1 channels in Alzheimer's disease. *J Neuroinflamm* (2016) 13 (1):92. doi: 10.1186/s12974-016-0557-z

240. Bosson A, Paumier A, Boisseau S, Jacquier-Sarlin M, Buisson A, Albrieux M. TRPA1 channels promote astrocytic Ca. *Mol Neurodegener* (2017) 12(1):53. doi: 10.1186/s13024-017-0194-8

241. Fernandez AM, Fernandez S, Carrero P, Garcia-Garcia M, Torres-Aleman I. Calcineurin in reactive astrocytes plays a key role in the interplay between proinflammatory and anti-inflammatory signals. *J Neurosci* (2007) 27(33):8745–56. doi: 10.1523/JNEUROSCI.1002-07.2007

242. Shi M, Chen F, Chen Z, Yang W, Yue S, Zhang J, et al. Sigma-1 receptor: A potential therapeutic target for traumatic brain injury. *Front Cell Neurosci* (2021) 15:685201. doi: 10.3389/fncel.2021.685201

243. Hayashi T, Su TP. Sigma-1 receptor chaperones at the ER-mitochondrion interface regulate Ca(2+) signaling and cell survival. *Cell* (2007) 131(3):596–610. doi: 10.1016/j.cell.2007.08.036

244. Pergolizzi J, Varrassi G, Coleman M, Breve F, Christo DK, Christo PJ, et al. The sigma enigma: A narrative review of sigma receptors. *Cureus* (2023) 15(3):e35756. doi: 10.7759/cureus.35756

245. Jansen KL, Faull RL, Storey P, Leslie RA. Loss of sigma binding sites in the CA1 area of the anterior hippocampus in Alzheimer's disease correlates with CA1 pyramidal cell loss. *Brain Res* (1993) 623(2):299–302. doi: 10.1016/0006-8993(93)91441-t

246. Mishina M, Ohyama M, Ishii K, Kitamura S, Kimura Y, Oda K, et al. Low density of sigma1 receptors in early Alzheimer's disease. *Ann Nucl Med* (2008) 22 (3):151–6. doi: 10.1007/s12149-007-0094-z

247. Sałaciak K, Pytka K. Revisiting the sigma-1 receptor as a biological target to treat affective and cognitive disorders. *Neurosci Biobehav Rev* (2022) 132:1114–36. doi: 10.1016/j.neubiorev.2021.10.037

248. Ma WH, Chen AF, Xie XY, Huang YS. Sigma ligands as potent inhibitors of Aβ and AβOs in neurons and promising therapeutic agents of Alzheimer's disease. *Neuropharmacology* (2021) 190:108342. doi: 10.1016/j.neuropharm.2020.108342

249. Iñiguez MA, Punzón C, Nieto R, Burgueño J, Vela JM, Fresno M. Inhibitory effects of sigma-2 receptor agonists on T lymphocyte activation. *Front Pharmacol* (2013) 4:23. doi: 10.3389/fphar.2013.00023

250. Kim WS, Fu Y, Dobson-Stone C, Hsiao JT, Shang K, Hallupp M, et al. Effect of fluvoxamine on amyloid-β Peptide generation and memory. *J Alzheimers Dis* (2018) 62 (4):1777–87. doi: 10.3233/JAD-171001

251. Fang M, Zhang P, Zhao Y, Jin A, Liu X. "Aβ mediates Sigma receptor degradation via CaN/NFAT pathway," (in eng). *Am J Transl Res* (2016) 8(8):3471–81.

252. Bouchon A, Hernández-Munain C, Cella M, Colonna M. A DAP12-mediated pathway regulates expression of CC chemokine receptor 7 and maturation of human dendritic cells. *J Exp Med* (2001) 194(8):1111–22. doi: 10.1084/jem.194.8.1111

253. Colonna M. The biology of TREM receptors. *Nat Rev Immunol* (2023) 23 (9):580–94. doi: 10.1038/s41577-023-00837-1

254. Takahashi K, Rochford CD, Neumann H. Clearance of apoptotic neurons without inflammation by microglial triggering receptor expressed on myeloid cells-2. *J Exp Med* (2005) 201(4):647–57. doi: 10.1084/jem.20041611

255. Zhou Y, Song WM, Andhey PS, Swain A, Levy T, Miller KR, et al. Human and mouse single-nucleus transcriptomics reveal TREM2-dependent and TREM2-independent cellular responses in Alzheimer's disease. *Nat Med* (2020) 26(1):131–42. doi: 10.1038/s41591-019-0695-9

256. Okuzono Y, Sakuma H, Miyakawa S, Ifuku M, Lee J, Das D, et al. Reduced TREM2 activation in microglia of patients with Alzheimer's disease. *FEBS Open Bio* (2021) 11(11):3063–80. doi: 10.1002/2211-5463.13300

257. Hamerman JA, Jarjoura JR, Humphrey MB, Nakamura MC, Seaman WE, Lanier LL. Cutting edge: inhibition of TLR and FcR responses in macrophages by triggering receptor expressed on myeloid cells (TREM)-2 and DAP12. *J Immunol* (2006) 177(4):2051–5. doi: 10.4049/jimmunol.177.4.2051

258. Zhao Y, Wu X, Li X, Jiang LL, Gui X, Liu Y, et al. TREM2 is a receptor for β-amyloid that mediates microglial function. *Neuron* (2018) 97(5):1023–1031.e7. doi: 10.1016/j.neuron.2018.01.031

259. Lessard CB, Malnik SL, Zhou Y, Ladd TB, Cruz PE, Ran Y, et al. High-affinity interactions and signal transduction between Aβ oligomers and TREM2. *EMBO Mol Med* (2018) 10(11). doi: 10.15252/emmm.201809027

260. Ulland TK, Colonna M. TREM2 - a key player in microglial biology and Alzheimer disease. *Nat Rev Neurol* (2018) 14(11):667–75. doi: 10.1038/s41582-018-0072-1

261. Wang Y, Cella M, Mallinson K, Ulrich JD, Young KL, Robinette ML, et al. TREM2 lipid sensing sustains the microglial response in an Alzheimer's disease model. *Cell* (2015) 160(6):1061–71. doi: 10.1016/j.cell.2015.01.049

262. Shirotani K, Hori Y, Yoshizaki R, Higuchi E, Colonna M, Saito T, et al. Aminophospholipids are signal-transducing TREM2 ligands on apoptotic cells. *Sci Rep* (2019) 9(1):7508. doi: 10.1038/s41598-019-43535-6

263. Bader Lange ML, St Clair D, Markesbery WR, Studzinski CM, Murphy MP, Butterfield DA. Age-related loss of phospholipid asymmetry in APP(NLh)/APP(NLh) x PS-1(P264L)/PS-1(P264L) human double mutant knock-in mice: relevance to Alzheimer disease. *Neurobiol Dis* (2010) 38(1):104–15. doi: 10.1016/j.nbd.2010.01.004

264. Poliani PL, Wang Y, Fontana E, Robinette ML, Yamanishi Y, Gilfillan S, et al. TREM2 sustains microglial expansion during aging and response to demyelination. *J Clin Invest* (2015) 125(5):2161–70. doi: 10.1172/JCI77983

265. Zhao P, Xu Y, Fan X, Li L, Li X, Arase H, et al. Discovery and engineering of an anti-TREM2 antibody to promote amyloid plaque clearance by microglia in 5XFAD mice. *MAbs* (2022) 14(1):2107971. doi: 10.1080/19420862.2022.2107971

266. Companys-Alemany J, Turcu AL, Vázquez S, Pallàs M, Griñán-Ferré C. Glial cell reactivity and oxidative stress prevention in Alzheimer's disease mice model by an optimized NMDA receptor antagonist. *Sci Rep* (2022) 12(1):17908. doi: 10.1038/s41598-022-22963-x

267. Regunathan S, Reis DJ. Imidazoline receptors and their endogenous ligands. *Annu Rev Pharmacol Toxicol* (1996) 36:511–44. doi: 10.1146/annurev.pa.36.040196.002455

268. Li JX. Imidazoline I. *Pharmacol Ther* (2017) 178:48–56. doi: 10.1016/j.pharmthera.2017.03.009

269. Han Z, Zhang HX, Tian JS, Zheng RY, Hou ST. "2-(-2-benzofuranyl)-2-imidazoline induces Bcl-2 expression and provides neuroprotection against transient cerebral ischemia in rats," (in eng). *Brain Res* (2010) 1361:pp. doi: 10.1016/j.brainres.2010.09.029

270. Han Z, Cheng ZH, Liu S, Yang JL, Xiao MJ, Zheng RY, et al. Neurovascular protection conferred by 2-BFI treatment during rat cerebral ischemia. *Biochem Biophys Res Commun* (2012) 424(3):544–8. doi: 10.1016/j.bbrc.2012.06.152

271. Han Z, Yang JL, Jiang SX, Hou ST, Zheng RY. Fast, non-competitive and reversible inhibition of NMDA-activated currents by 2-BFI confers neuroprotection," (in eng). *PloS One* (2013) 8:no. doi: 10.1371/journal.pone.0064894

272. Jiang SX, Zheng RY, Zeng JQ, Li XL, Han Z, Hou ST. "Reversible inhibition of intracellular calcium influx through NMDA receptors by imidazoline I(2) receptor antagonists. *Eur J Pharmacol* (2010) 629(1-3):12–9. doi: 10.1016/j.ejphar.2009.11.063

273. Craven JA, Conway EL. Effects of alpha 2-adrenoceptor antagonists and imidazoline2-receptor ligands on neuronal damage in global ischaemia in the rat. *Clin Exp Pharmacol Physiol* (1997) 24(2):204–7. doi: 10.1111/j.1440-1681.1997.tb01808.x

274. Vasilopoulou F, et al. I. *Geroscience* (2021) 43(2):965–83. doi: 10.1007/s11357-020-00281-2

275. Rodriguez-Arévalo S, Bagán A, Griñán-Ferré C, Vasilopoulou F, Pallàs M, Brocos-Mosquera I, et al. Benzofuranyl-2-imidazoles as imidazoline I. *Eur J Med Chem* (2021) 222:113540. doi: 10.1016/j.ejmech.2021.113540

276. Vasilopoulou F, Rodríguez-Arévalo S, Bagán A, Escolano C, Griñán-Ferré C, Pallàs M. Disease-modifying treatment with I. *Br J Pharmacol* (2021) 178(15):3017–33. doi: 10.1111/bph.15478

277. García-Sevilla JA, Escribá PV, Walzer C, Bouras C, Guimón J. Imidazoline receptor proteins in brains of patients with Alzheimer's disease. *Neurosci Lett* (1998) 247(2-3):95–8. doi: 10.1016/s0304-3940(98)00265-1

278. Morley JE, Farr SA, Kumar VB, Armbrecht HJ. The SAMP8 mouse: a model to develop therapeutic interventions for Alzheimer's disease. *Curr Pharm Des* (2012) 18 (8):1123–30. doi: 10.2174/138161212799315795

279. Brown SD, Twells RC, Hey PJ, Cox RD, Levy ER, Soderman AR, et al. Isolation and characterization of LRP6, a novel member of the low density lipoprotein receptor gene family. *Biochem Biophys Res Commun* (1998) 248(3):879–88. doi: 10.1006/bbrc.1998.9061

280. Alrefaei AF, Abu-Elmagd M. LRP6 receptor plays essential functions in development and human diseases. *Genes (Basel)* (2022) 13(1). doi: 10.3390/genes13010120

281. Jones ME, Büchler J, Dufor T, Palomer E, Teo S, Martin-Flores N, et al. A genetic variant of the Wnt receptor LRP6 accelerates synapse degeneration during aging and in Alzheimer's disease. *Sci Adv* (2023) 9(2):eabo7421. doi: 10.1126/sciadv.abo7421

282. Buechler J, Salinas PC. "Deficient wnt signaling and synaptic vulnerability in alzheimer's disease: emerging roles for the LRP6 receptor," (in eng). *Front Synaptic Neurosci* (2018) 10:38(38). doi: 10.3389/fnsyn.2018.00038

283. Liu CC, Tsai CW, Deak F, Rogers J, Penuliar M, Sung YM, et al. Deficiency in LRP6-mediated Wnt signaling contributes to synaptic abnormalities and amyloid pathology in Alzheimer's disease. *Neuron* (2014) 84(1):63–77. doi: 10.1016/j.neuron.2014.08.048

284. Jaeger S, Pietrzik CU. Functional role of lipoprotein receptors in Alzheimer's disease. *Curr Alzheimer Res* (2008) 5(1):15–25. doi: 10.2174/156720508783884675

285. Zhao N, Liu CC, Qiao W, Bu G. "Apolipoprotein E, receptors, and modulation of alzheimer's disease," (in eng). *Biol Psychiatry* (2018) 83(4):347–57. doi: 10.1016/j.biopsych.2017.03.003

286. Chow HM, Sun JK, Hart RP, Cheng KK, Hung CHL, Lau TM, et al. Low-density lipoprotein receptor-related protein 6 cell surface availability regulates fuel metabolism in astrocytes. *Adv Sci (Weinh)* (2021) 8(16):e2004993. doi: 10.1002/advs.202004993

287. Sonntag KC, Ryu WI, Amirault KM, Healy RA, Siegel AJ, McPhie DL, et al. Late-onset Alzheimer's disease is associated with inherent changes in bioenergetics profiles. *Sci Rep* (2017) 7(1):14038. doi: 10.1038/s41598-017-14420-x

288. Lu Y, Liu M, Guo X, Wang P, Zeng F, Wang H, et al. miR-26a-5p alleviates CFA-induced chronic inflammatory hyperalgesia through Wnt5a/CaMKII/NFAT signaling in mice. *CNS Neurosci Ther* (2023) 29(5):1254–71. doi: 10.1111/cns.14099

289. Kodis EJ, Choi S, Swanson E, Ferreira G, Bloom GS. N-methyl-D-aspartate receptor-mediated calcium influx connects amyloid-β oligomers to ectopic neuronal cell cycle reentry in Alzheimer's disease. *Alzheimers Dement* (2018) 14(10):1302–12. doi: 10.1016/j.jalz.2018.05.017

290. Liu J, Chang L, Song Y, Li H, Wu Y. The role of NMDA receptors in alzheimer's disease. *Front Neurosci* (2019) 13:43(43). doi: 10.3389/fnins.2019.00043

291. Uttara B, Singh AV, Zamboni P, Mahajan RT. Oxidative stress and neurodegenerative diseases: a review of upstream and downstream antioxidant therapeutic options. *Curr Neuropharmacol* (2009) 7(1):65–74. doi: 10.2174/157015909787602823

292. Sattler R, Tymianski M. Molecular mechanisms of glutamate receptor-mediated excitotoxic neuronal cell death. *Mol Neurobiol* (2001) 24(1-3):107–29. doi: 10.1385/MN:24:1-3:107

293. Vesce S, Rossi D, Brambilla L, Volterra A. "Glutamate release from astrocytes in physiological conditions and in neurodegenerative disorders characterized by neuroinflammation," (in eng). *Int Rev Neurobiol* (2007) 82(57-71). doi: 10.1016/S0074-7742(07)82003-4

294. Roselli F, Tirard M, Lu J, Hutzler P, Lamberti P, Livrea P, et al. Soluble beta-amyloid1-40 induces NMDA-dependent degradation of postsynaptic density-95 at glutamatergic synapses. *J Neurosci* (2005) 25(48):11061–70. doi: 10.1523/JNEUROSCI.3034-05.2005

295. Li Y, Chang L, Song Y, Gao X, Roselli F, Liu J, et al. Astrocytic gluN2A and gluN2B oppose the synaptotoxic effects of amyloid-β1-40 in hippocampal cells. *J Alzheimers Dis* (2016) 54(1):135–48. doi: 10.3233/JAD-160297

296. Parameshwaran K, Dhanasekaran M, Suppiramaniam V. Amyloid beta peptides and glutamatergic synaptic dysregulation. *Exp Neurol* (2008) 210(1):7–13. doi: 10.1016/j.expneurol.2007.10.008

297. Costa RO, Lacor PN, Ferreira IL, Resende R, Auberson YP, Klein WL, et al. Endoplasmic reticulum stress occurs downstream of GluN2B subunit of N-methyl-d-aspartate receptor in mature hippocampal cultures treated with amyloid-β oligomers. *Aging Cell* (2012) 11(5):823–33. doi: 10.1111/j.1474-9726.2012.00848.x

298. Verges DK, Restivo JL, Goebel WD, Holtzman DM, Cirrito JR. Opposing synaptic regulation of amyloid-β metabolism by NMDA receptors in vivo. *J Neurosci* (2011) 31(31):11328–37. doi: 10.1523/JNEUROSCI.0607-11.2011

299. Lesné S, et al. NMDA receptor activation inhibits alpha-secretase and promotes neuronal amyloid-beta production. *J Neurosci* (2005) 25(41):9367–77. doi: 10.1523/JNEUROSCI.0849-05.2005

300. Wang ZC, Zhao J, Li S. Dysregulation of synaptic and extrasynaptic N-methyl-D-aspartate receptors induced by amyloid-β. *Neurosci Bull* (2013) 29(6):752–60. doi: 10.1007/s12264-013-1383-2

301. Malinow R. New developments on the role of NMDA receptors in Alzheimer's disease. *Curr Opin Neurobiol* (2012) 22(3):559–63. doi: 10.1016/j.conb.2011.09.001

302. Owen RT. Memantine and donepezil: a fixed drug combination for the treatment of moderate to severe Alzheimer's dementia. *Drugs Today (Barc)* (2016) 52(4):239–48. doi: 10.1358/dot.2016.52.4.2479357

303. Ting SM, Zhao X, Zheng X, Aronowski J. Excitatory pathway engaging glutamate, calcineurin, and NFAT upregulates IL-4 in ischemic neurons to polarize microglia. *J Cereb Blood Flow Metab* (2020) 40(3):513–27. doi: 10.1177/0271678X19838189

304. Lisek M, Zylinska L, Boczek T. Ketamine and calcium signaling-A crosstalk for neuronal physiology and pathology. *Int J Mol Sci* (2020) 21(21). doi: 10.3390/ijms21218410

305. Fox C, Crugel M, Maidment I, Auestad BH, Coulton S, Treloar A, et al. Efficacy of memantine for agitation in Alzheimer's dementia: a randomised double-blind placebo controlled trial. *PloS One* (2012) 7(5):e35185. doi: 10.1371/journal.pone.0035185

306. Wilkinson D, Fox NC, Barkhof F, Phul R, Lemming O, Scheltens P. Memantine and brain atrophy in Alzheimer's disease: a 1-year randomized controlled trial. *J Alzheimers Dis* (2012) 29(2):459–69. doi: 10.3233/JAD-2011-111616

307. Reisberg B, Doody R, Stöffler A, Schmitt F, Ferris S, Möbius HJ. Memantine in moderate-to-severe Alzheimer's disease. *N Engl J Med* (2003) 348(14):1333–41. doi: 10.1056/NEJMoa013128

308. Turcu AL, Companys-Alemany J, Phillips MB, Patel DS, Griñán-Ferré C, Loza MI, et al. Design, synthesis, and in vitro and in *vivo* characterization of new memantine analogs for Alzheimer's disease. *Eur J Med Chem* (2022) 236:114354. doi: 10.1016/j.ejmech.2022.114354

309. Shao L, Zhang Y, Hao Y, Ping Y. Upregulation of IP. *Cell Rep* (2022) 38 (13):110594. doi: 10.1016/j.celrep.2022.110594

310. Bartok A, Weaver D, Golenár T, Nichtova Z, Katona M, Bánsághi S, et al. IP3 receptor isoforms differently regulate ER-mitochondrial contacts and local calcium transfer. *Nat Commun* (2019) 10(1):3726. doi: 10.1038/s41467-019-11646-3

311. Duchen MR. Mitochondria, calcium-dependent neuronal death and neurodegenerative disease. *Pflugers Arch* (2012) 464(1):111–21. doi: 10.1007/s00424-012-1112-0

312. Egorova PA, Bezprozvanny IB. Inositol 1,4,5-trisphosphate receptors and neurodegenerative disorders. *FEBS J* (2018) 285(19):3547–65. doi: 10.1111/febs.14366

313. Cheung KH, Shineman D, Müller M, Cárdenas C, Mei L, Yang J, et al. Mechanism of Ca2+ disruption in Alzheimer's disease by presenilin regulation of InsP3 receptor channel gating. *Neuron* (2008) 58(6):871–83. doi: 10.1016/j.neuron.2008.04.015

314. Cheung KH, Mei L, Mak DO, Hayashi I, Iwatsubo T, Kang DE, et al. Gain-of-function enhancement of IP3 receptor modal gating by familial Alzheimer's disease-linked presenilin mutants in human cells and mouse neurons. *Sci Signal* (2010) 3(114):ra22. doi: 10.1126/scisignal.2000818

315. Hirashima N, Etcheberrigaray R, Bergamaschi S, Racchi M, Battaini F, Binetti G, et al. Calcium responses in human fibroblasts: a diagnostic molecular profile for Alzheimer's disease. *Neurobiol Aging* (1996) 17(4):549–55. doi: 10.1016/0197-4580(96)00074-7

316. Guo Q, Fu W, Sopher BL, Miller MW, Ware CB, Martin GM, et al. Increased vulnerability of hippocampal neurons to excitotoxic necrosis in presenilin-1 mutant knock-in mice. *Nat Med* (1999) 5(1):101–6. doi: 10.1038/4789

317. Oddo S, Caccamo A, Shepherd JD, Murphy MP, Golde TE, Kayed R, et al. Triple-transgenic model of Alzheimer's disease with plaques and tangles: intracellular Abeta and synaptic dysfunction. *Neuron* (2003) 39(3):409–21. doi: 10.1016/s0896-6273(03)00434-3

318. Shilling D, Müller M, Takano H, Mak DO, Abel T, Coulter DA, et al. Suppression of InsP3 receptor-mediated Ca2+ signaling alleviates mutant presenilin-linked familial Alzheimer's disease pathogenesis. *J Neurosci* (2014) 34(20):6910–23. doi: 10.1523/JNEUROSCI.5441-13.2014

319. Secondo A, Bagetta G, Amantea D. On the role of store-operated calcium entry in acute and chronic neurodegenerative diseases. *Front Mol Neurosci* (2018) 11:87(87). doi: 10.3389/fnmol.2018.00087

320. Sampieri A, Santoyo K, Asanov A, Vaca L. Association of the IP3R to STIM1 provides a reduced intraluminal calcium microenvironment, resulting in enhanced store-operated calcium entry. *Sci Rep* (2018) 8(1):13252. doi: 10.1038/s41598-018-31621-0

321. Pascual-Caro C, Berrocal M, Lopez-Guerrero AM, Alvarez-Barrientos A, Pozo-Guisado E, Gutierrez-Merino C, et al. STIM1 deficiency is linked to Alzheimer's disease and triggers cell death in SH-SY5Y cells by upregulation of L-type voltage-operated Ca. *J Mol Med (Berl)* (2018) 96(10):1061–79. doi: 10.1007/s00109-018-1677-y

322. Pascual-Caro C, Espinosa-Bermejo N, Pozo-Guisado E, Martin-Romero FJ. Role of STIM1 in neurodegeneration. *World J Biol Chem* (2018) 9(2):16–24. doi: 10.4331/wjbc.v9.i2.16

323. Meng M, Huo R, Ma N, Chang G, Shen X. β-carotene alleviates LPS-induced inflammation through regulating STIM1/ORAI1 expression in bovine mammary epithelial cells. *Int Immunopharmacol* (2022) 113(Pt A):109377. doi: 10.1016/j.intimp.2022.109377

324. Xue Y, Zhou S, Xie W, Meng M, Ma N, Zhang H, et al. STIM1-orai1 interaction exacerbates LPS-induced inflammation and endoplasmic reticulum stress in bovine hepatocytes through store-operated calcium entry. *Genes (Basel)* (2022) 13(5). doi: 10.3390/genes13050874

325. Sun Z, Li X, Yang L, Dong X, Han Y, Li Y, et al. SOCE-mediated NFAT1-NOX2-NLRP1 inflammasome involves in lipopolysaccharide-induced neuronal damage and Aβ generation. *Mol Neurobiol* (2022) 59(5):3183–205. doi: 10.1007/s12035-021-02717-y

326. Cook CN, Hejna MJ, Magnuson DJ, Lee JM. Expression of calcipressin1, an inhibitor of the phosphatase calcineurin, is altered with aging and Alzheimer's disease. *J Alzheimers Dis* (2005) 8(1):63–73. doi: 10.3233/jad-2005-8108

327. Sun X, Wu Y, Chen B, Zhang Z, Zhou W, Tong Y, et al. Regulator of calcineurin 1 (RCAN1) facilitates neuronal apoptosis through caspase-3 activation. *J Biol Chem* (2011) 286(11):9049–62. doi: 10.1074/jbc.M110.177519

328. Wu Y, Song W. Regulation of RCAN1 translation and its role in oxidative stress-induced apoptosis. *FASEB J* (2013) 27(1):208–21. doi: 10.1096/fj.12-213124

329. Wong H, Levenga J, Cain P, Rothermel B, Klann E, Hoeffer C. RCAN1 overexpression promotes age-dependent mitochondrial dysregulation related to neurodegeneration in Alzheimer's disease. *Acta Neuropathol* (2015) 130(6):829–43. doi: 10.1007/s00401-015-1499-8

330. Lim S, Hwang S, Yu JH, Lim JW, Kim H. Lycopene inhibits regulator of calcineurin 1-mediated apoptosis by reducing oxidative stress and down-regulating Nucling in neuronal cells. *Mol Nutr Food Res* (2017) 61(5). doi: 10.1002/mnfr.201600530

331. Sun X, Wu Y, Herculano B, Song W. RCAN1 overexpression exacerbates calcium overloading-induced neuronal apoptosis. *PloS One* (2014) 9(4):e95471. doi: 10.1371/journal.pone.0095471

332. Jiang H, Zhang C, Tang Y, Zhao J, Wang T, Liu H, et al. The regulator of calcineurin 1 increases adenine nucleotide translocator 1 and leads to mitochondrial dysfunctions. *J Neurochem* (2017) 140(2):307–19. doi: 10.1111/jnc.13900

333. Yun Y, Zhang Y, Zhang C, Huang L, Tan S, Wang P, et al. Regulator of calcineurin 1 is a novel RNA-binding protein to regulate neuronal apoptosis. *Mol Psychiatry* (2021) 26(4):1361–75. doi: 10.1038/s41380-019-0487-0

334. Wang T, Liu H, Wang Y, Liu C, Sun X. RCAN1 increases Aβ generation by promoting N-glycosylation via oligosaccharyltransferase. *Curr Alzheimer Res* (2014) 11 (4):332–9. doi: 10.2174/1567205011666140331225855

335. Lloret A, Badia MC, Giraldo E, Ermak G, Alonso MD, Pallardó FV, et al. Amyloid-β toxicity and tau hyperphosphorylation are linked via RCAN1 in Alzheimer's disease. *J Alzheimers Dis* (2011) 27(4):701–9. doi: 10.3233/JAD-2011-110890

336. Wu Y, Deng Y, Zhang S, Luo Y, Cai F, Zhang Z, et al. Amyloid-β precursor protein facilitates the regulator of calcineurin 1-mediated apoptosis by downregulating proteasome subunit α type-5 and proteasome subunit β type-7. *Neurobiol Aging* (2015) 36(1):169–77. doi: 10.1016/j.neurobiolaging.2014.07.029

337. Lee S, Bang SM, Hong YK, Lee JH, Jeong H, Park SH, et al. The calcineurin inhibitor Sarah (Nebula) exacerbates Aβ42 phenotypes in a Drosophila model of Alzheimer's disease. *Dis Model Mech* (2016) 9(3):295–306. doi: 10.1242/dmm.018069

338. Ju Hwang C, Choi DY, Park MH, Hong JT. NF-κB as a key mediator of brain inflammation in alzheimer's disease. *CNS Neurol Disord Drug Targets* (2019) 18(1):3–10. doi: 10.2174/1871527316666170807130011

339. Zheng L, Liu H, Wang P, Song W, Sun X. Regulator of calcineurin 1 gene transcription is regulated by nuclear factor-kappaB. *Curr Alzheimer Res* (2014) 11 (2):156–64. doi: 10.2174/1567205010666131212114907

340. Peiris H, Keating DJ. The neuronal and endocrine roles of RCAN1 in health and disease. *Clin Exp Pharmacol Physiol* (2018) 45(4):377–83. doi: 10.1111/1440-1681.12884

341. Sanna B, Brandt EB, Kaiser RA, Pfluger P, Witt SA, Kimball TR, et al. Modulatory calcineurin-interacting proteins 1 and 2 function as calcineurin facilitators in vivo. *Proc Natl Acad Sci USA* (2006) 103(19):7327–32. doi: 10.1073/pnas.0509340103

342. Liu Q, Busby JC, Molkentin JD. Interaction between TAK1-TAB1-TAB2 and RCAN1-calcineurin defines a signalling nodal control point. *Nat Cell Biol* (2009) 11 (2):154–61. doi: 10.1038/ncb1823

343. Xu YR, Lei CQ. TAK1-TABs complex: A central signalosome in inflammatory responses. *Front Immunol* (2020) 11:608976. doi: 10.3389/fimmu.2020.608976

344. Dierssen M, Arqué G, McDonald J, Andreu N, Martínez-Cué C, Flórez J, et al. Behavioral characterization of a mouse model overexpressing DSCR1/ RCAN1. *PloS One* (2011) 6(2):e17010. doi: 10.1371/journal.pone.0017010

345. Hoeffer CA, Dey A, Sachan N, Wong H, Patterson RJ, Shelton JM, et al. The Down syndrome critical region protein RCAN1 regulates long-term potentiation and memory via inhibition of phosphatase signaling. *J Neurosci* (2007) 27(48):13161–72. doi: 10.1523/JNEUROSCI.3974-07.2007

346. Wong H, Buck JM, Borski C, Pafford JT, Keller BN, Milstead RA, et al. RCAN1 knockout and overexpression recapitulate an ensemble of rest-activity and circadian disruptions characteristic of Down syndrome, Alzheimer's disease, and normative aging. *J Neurodev Disord* (2022) 14(1):33. doi: 10.1186/s11689-022-09444-y

347. Asai M, Kinjo A, Kimura S, Mori R, Kawakubo T, Shirotani K, et al. Perturbed calcineurin-NFAT signaling is associated with the development of alzheimer's disease. *Biol Pharm Bull* (2016) 39(10):1646–52. doi: 10.1248/bpb.b16-00350

348. Janel N, Sarazin M, Corlier F, Corne H, de Souza LC, Hamelin L, et al. Plasma DYRK1A as a novel risk factor for Alzheimer's disease. *Transl Psychiatry* (2014) 4(8): e425. doi: 10.1038/tp.2014.61

349. Jung MS, Park JH, Ryu YS, Choi SH, Yoon SH, Kwen MY, et al. Regulation of RCAN1 protein activity by Dyrk1A protein-mediated phosphorylation. *J Biol Chem* (2011) 286(46):40401–12. doi: 10.1074/jbc.M111.253971

350. Lee HJ, Woo H, Lee HE, Jeon H, Ryu KY, Nam JH, et al. The novel DYRK1A inhibitor KVN93 regulates cognitive function, amyloid-beta pathology, and neuroinflammation. *Free Radic Biol Med* (2020) 160:575–95. doi: 10.1016/j.freeradbiomed.2020.08.030

351. Kim H, Lee KS, Kim AK, Choi M, Choi K, Kang M, et al. A chemical with proven clinical safety rescues Down-syndrome-related phenotypes in through DYRK1A inhibition. *Dis Model Mech* (2016) 9(8):839–48. doi: 10.1242/dmm.025668

352. Grygier P, Pustelny K, Nowak J, Golik P, Popowicz GM, Plettenburg O, et al. Silmitasertib (CX-4945), a clinically used CK2-kinase inhibitor with additional effects on GSK3β and DYRK1A kinases: A structural perspective. *J Med Chem* (2023) 66 (6):4009–24. doi: 10.1021/acs.jmedchem.2c01887

frontiers | Frontiers in Immunology

TYPE Review
PUBLISHED 07 December 2023
DOI 10.3389/fimmu.2023.1324021

OPEN ACCESS

EDITED BY
Shicheng Guo,
Arrowhead Pharmaceuticals, United States

REVIEWED BY
Yiyi Ji,
Duke University, United States
Minghan Yang,
New York University, United States
Tianyi Zhang,
Emory University, United States
Chongbo Yang,
Cornell University, United States

*CORRESPONDENCE
Ning Li
md.lining@whu.edu.cn
Bo Wang
rmh_wb@whu.edu.cn
Qing Geng
gengqingwhu@whu.edu.cn

†These authors have contributed equally to this work

RECEIVED 18 October 2023
ACCEPTED 27 November 2023
PUBLISHED 07 December 2023

CITATION
Liu Y, Wang R, Song C, Ding S, Zuo Y, Yi K, Li N, Wang B and Geng Q (2023) Crosstalk between neutrophil extracellular traps and immune regulation: insights into pathobiology and therapeutic implications of transfusion-related acute lung injury. *Front. Immunol.* 14:1324021. doi: 10.3389/fimmu.2023.1324021

Crosstalk between neutrophil extracellular traps and immune regulation: insights into pathobiology and therapeutic implications of transfusion-related acute lung injury

Yi Liu[1†], Rong Wang[2†], Congkuan Song[1†], Song Ding[1], Yifan Zuo[1], Ke Yi[1], Ning Li[1*], Bo Wang[1*] and Qing Geng[1*]

[1]Department of Thoracic Surgery, Renmin Hospital of Wuhan University, Wuhan, China, [2]Institute of Hematology, Union Hospital, Tongji Medical College, Huazhong University of Science and Technology, Wuhan, China

Transfusion-related acute lung injury (TRALI) is the leading cause of transfusion-associated death, occurring during or within 6 hours after transfusion. Reports indicate that TRALI can be categorized as having or lacking acute respiratory distress syndrome (ARDS) risk factors. There are two types of TRALI in terms of its pathogenesis: antibody-mediated and non-antibody-mediated. The key initiation steps involve the priming and activation of neutrophils, with neutrophil extracellular traps (NETs) being established as effector molecules formed by activated neutrophils in response to various stimuli. These NETs contribute to the production and release of reactive oxygen species (ROS) and participate in the destruction of pulmonary vascular endothelial cells. The significant role of NETs in TRALI is well recognized, offering a potential pathway for TRALI treatment. Moreover, platelets, macrophages, endothelial cells, and complements have been identified as promoters of NET formation. Concurrently, studies have demonstrated that the storage of platelets and concentrated red blood cells (RBC) can induce TRALI through bioactive lipids. In this article, recent clinical and pre-clinical studies on the pathophysiology and pathogenesis of TRALI are reviewed to further illuminate the mechanism through which NETs induce TRALI. This review aims to propose new therapeutic strategies for TRALI, with the hope of effectively improving its poor prognosis.

KEYWORDS

neutrophil extracellular traps, immune regulation, transfusion-related acute lung injury, neutrophil, therapy

1 Introduction

Transfusion-related acute lung injury (TRALI) is a severe condition characterized by acute non-cardiogenic pulmonary edema that occurs within 6 hours of transfusion. The latest definition has categorized TRAI into two types: type I (without ARDS risk factor) and type II (with ARDS risk factor or mild existing ARDS) (1). This complication remains a leading cause of transfusion-related fatalities, despite various preventive strategies. Histopathological features of TRALI include endothelial barrier disruption and neutrophil aggregation in the pulmonary vasculature. It is widely assumed that neutrophil respiratory burst releases reactive oxygen species (ROS), resulting in lung endothelial cell injury (2). However, the specific molecular events through which neutrophils are recruited and activated by lung endothelial cells, as well as how neutrophils activate and damage endothelial cells, remain poorly understood. Several models have been proposed to explain the pathophysiology of TRALI. The antibody-mediated hypothesis posits that leukocyte antibodies in transfused blood activate neutrophils, leading to lung endothelial cell damage and subsequent blood penetration into the alveoli, thus triggering TRALI (3). Generally, antibodies causing TRALI include human leukocyte antigen (HLA), human neutrophil antigen (HNA), and corresponding antibodies against the recipient antigen from the donor which, after infusion, initiate neutrophil activation. Controlled clinical studies have identified donor antibody infusion as a recognized cause of TRALI, with blood plasma leukocyte antibodies from female donors posing a particular risk (4). The incidence and mortality of TRALI have been observed to decrease in countries where male donors predominate, though massive transfusion remains an important factor in TRALI whether the blood is from a male or female donor (5). The "two-hit" model suggests that the patient's underlying clinical condition primes the lung endothelium by increasing the surface expression of adhesion molecules, thereby facilitating the attraction of neutrophils to the lung compartment. Subsequent blood transfusion then acts as the second hit, activating neutrophils via multiple components of the transfused blood products, either directly or indirectly (6). For instance, stored blood often contains higher levels of bioactive lipids, which have been implicated in the two-hit model based on animal models (7, 8). However, conflicting findings have emerged from randomized controlled trials and prospective human studies, indicating that transfusion of stored blood in the presence of endotoxemia does not consistently induce transfusion-related lung injury (9, 10). Furthermore, cases of TRALI have been reported in otherwise healthy individuals, prompting the proposal of a threshold model. This model attributes TRALI development to a combination of patient susceptibility and the number of risk factors present in the blood products. When the mass transfusion of blood products contains a high concentration of antibodies matching the recipient's antigen, the threshold for neutrophil activation may be surpassed, leading to severe TRALI. This model also highlights specific patient populations as being particularly susceptible to TRALI (11) (Figure 1). Despite being described separately, these hypotheses all share the common pathway of neutrophil activation in TRALI. Clarifying the mechanisms underlying neutrophil recruitment and activation, as well as the molecular events governing neutrophil-mediated endothelial cell damage, is critical for advancing our understanding and improving outcomes in TRALI.

Neutrophils are the largest subpopulation of leukocytes in the human body, serving as vital immune defenders through various mechanisms including respiratory burst, phagocytosis, secretion of antimicrobial substances, and the formation of neutrophil extracellular traps (NETs) in response to infectious conditions (12). However, under sterile conditions, extracellular activation of neutrophils may cause damage to normal tissues, such as in the case of TRALI. Although the role of massive ROS in endothelial damage has been described, the ability of neutrophils to form NETs in TRALI is a new piece of knowledge of TRALI pathophysiology. Initially, NETs were viewed as a programmed cell death process, involving the decondensation of nuclear chromatin DNA from activated neutrophils and its fusion with neutrophil granule contents to form a network released into the extracellular space. This network subsequently captures and eliminates microorganisms. However, in the last two decades, our understanding of the formation of NETs has evolved to encompass not only nuclear DNA but also mitochondrial DNA, as well as forms of NETs formation that do not involve cell death. Furthermore, it has been observed that NETs can also form in sterile inflammation, contributing to the progression of pathology (13). As a result, there has been extensive interest in investigating NETs, particularly in the context of sterile inflammation in TRALI. It is crucial to note that the processes governing the formation and function of NETs are subject to both intrinsic and extrinsic immune modulations of neutrophils in order to maintain tissue homeostasis. This delicate balance is essential in mediating between immune defense and tissue damage. Therefore, understanding the interplay between neutrophil extracellular traps and immune regulation may offer valuable insights for potential interventions in the treatment of TRALI resulting from neutrophil activation. Unfortunately, there are very few studies on NETs in TRALI. We therefore tried to summarize the inherent mechanisms of NETs related immune regulation from existing studies, and combined these with the existing evidence and characteristics of TRALI to illustrate the pathobiology and therapeutic implications of NETs in TRALI in order to provide a reference for future studies. In this review, we first provide an overview of the classical pathways and recent insights into NET formation and role of NETs in TRALI, emphasizing the importance of NETs in the development of TRALI. Moreover, we summarize NETs and their key pathways and important mediators of immune regulation, combined with the characteristics of TRALI to discuss the potential role of these immune regulations in the pathophysiological process of TRALI. Finally, we also discuss the translational significance of NET-related immune modulation in TRALI treatment.

Neutrophil activation is central to the development of TRALI. In the two-hit model (below), the first hit, such as the patient's clinical condition, activates endothelial cells and promotes the expression of intercellular adhesion molecule 1 (ICAM-1) and the secretion of chemokines and cytokines for the recruitment and

10.3389/fimmu.2023.1324021

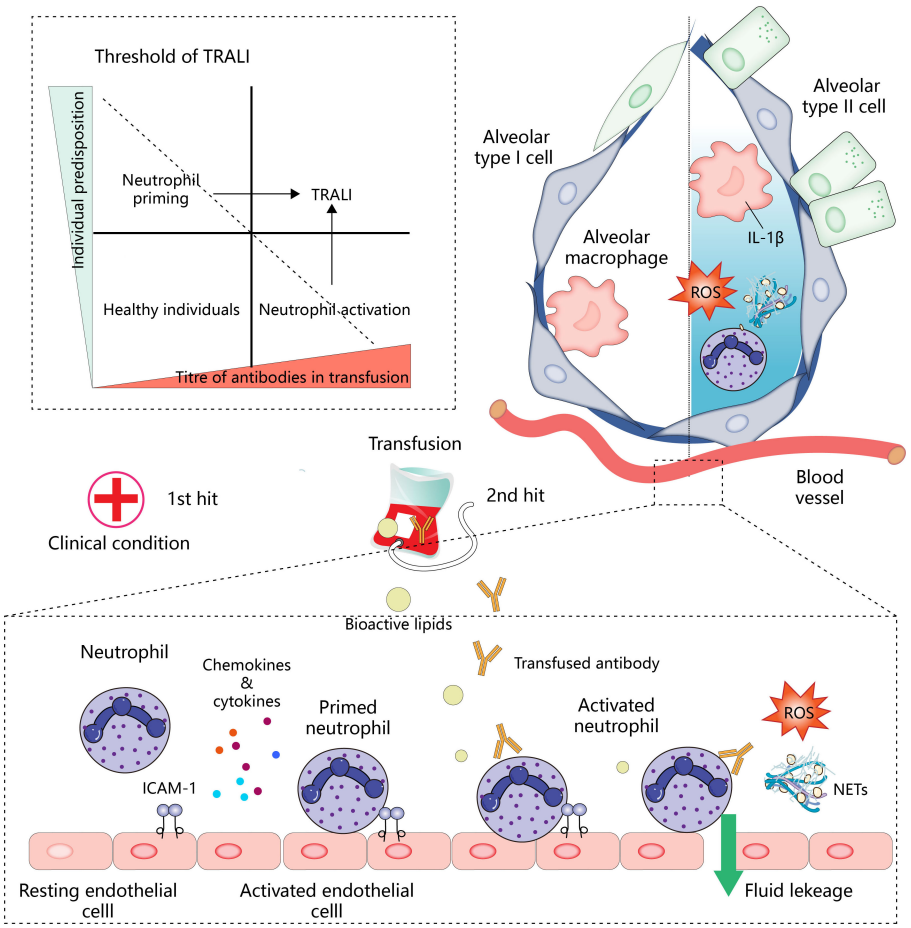

FIGURE 1
Overview of mechanisms of TRALI development.

initiation of neutrophils. Antibodies or other bioactive lipids in the transfusion components represent a second hit, which activates neutrophils, leading to lung endothelial injury and pulmonary edema. In addition, neutrophils infiltrating into the tissues will cooperate with other immune effector cells to amplify inflammation (upper right). Antibody-mediated neutrophil activation resembles the pattern of the second hit. The patient's predisposition and titer of antibody in transfusion work together to determine whether the threshold for developing TRALI is reached (upper left), and TRALI occurs when these interactions overcome specific thresholds.

2 Neutrophil extracellular trap formation

Accumulating evidence now challenges the traditional view of neutrophils as a homogeneous group of responders in the innate immune system. Rather, it suggests that neutrophils consist of more complex subpopulations with distinct functions during infection and inflammation. One subset of activated neutrophils, for instance, is involved in expelling their nuclear contents to clear pathogens, a process known as neutrophil extracellular trap formation. Initially documented by Brinkmann and colleagues, this phenomenon was observed when neutrophils were stimulated with phorbol myristate acetate (PMA), resulting in the release of a network composed of coated histones, neutrophil elastase(NE), myeloperoxidase (MPO), and cathepsin G. Although this process was initially labeled as NETosis, the concept of it being a form of cell death is being challenged by accumulating evidence. Vital NETs, for example, are formed by neutrophils under processes that do not involve cell death.

NETosis is a clearance mechanism employed by neutrophils in response to excessive or large pathogens and is dependent on the involvement of ROS, MPO, NE, and histone citrullination (Figure 2). The formation of NETs occurs through multiple pathways, with optimal ones including the production of ROS by NADPH oxidase, which stimulates MPO to release NE from granules to the cytoplasm, causing degradation of the actin cytoskeleton, impeding neutrophil movement and phagocytosis (14). Subsequently, NE enters the nucleus, where it cleaves histones, unwinds chromatin, and releases DNA. Furthermore, ROS is involved in the activation of protein arginine deaminase 4 (PAD 4), and the spike of cytoplasmic calcium participates in this process. Notably, extracellular ion concentration changes can exert significant effects on NETosis. For instance, elevated sodium ions in

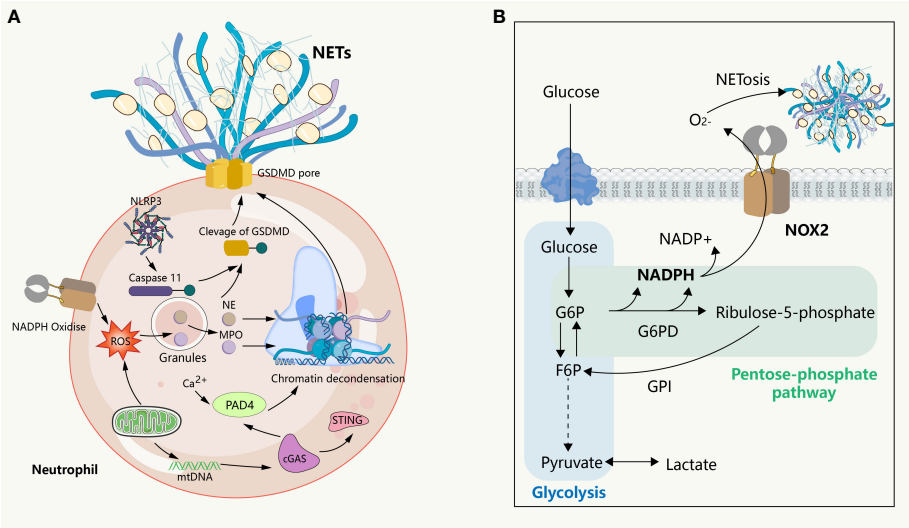

FIGURE 2
NETs formation and its intrinsic immune regulation of NETs formation. **(A)** NETs formation and the inflammatory pathway intrinsic to neutrophils. NADPH or mitochondrial ROS stimulates the sequential activation of neutrophil MPO and NE, followed by NE entering intranucleus to cleave histones, combined with histone citrullination of PAD 4 promoting chromatin decondensation. Subsequently, under the pore-forming action of GSDMD, the DNA network within the nucleus binds a variety of proteins to release into the extracellular cell. This process is usually affected by the cGAS, NLRP 3 signaling pathway. **(B)** The glucose metabolism in neutrophils. In the resting state, glycolysis is the primary way neutrophils acquire energy, where activated glycolysis is enhanced and a larger fraction of glucose enters the pentose phosphate pathway to support the ROS required to produce respiratory burst and NETs.

the extracellular environment can trigger calcium influx in neutrophils, thereby promoting the formation of NETs in the kidney medulla (15). It is thus imperative to comprehend the regulatory mechanisms associated with ion alterations in specific environments and their impact on neutrophil activation and NET release. The emergence of ion indicators has facilitated the characterization of ion dynamics, offering insights into the regulation of molecular biological processes in distinct physiological settings (16). PAD 4 triggers histone citrullination to promote chromatin decondensation in the neutrophil nuclei (17). The release of NETs into the extracellular space remains inconclusive; however, it has been suggested that cytoplasmic membrane rupture is the dominant view, with gasdermin D (GSDMD), a factor mediating cellular pyroptosis, possibly being involved in the release of the lytic form of NETs. However, subsequent observations question this involvement, as the initial experiment showed this process occurring 3-4 hours after the induction of NETs, whereas subsequent observations suggest that neutrophils can also release NETs within a very short period of time (5-60 minutes) without involving cell death, in a process known as vital NETosis where the plasma membrane is not disrupted and the release of NETs involves nuclear envelope blebbing and cell budding (18, 19). Additionally, in some experiments, NETs consisted of mitochondrial DNA, but not nuclear DNA (20, 21), suggesting that the underlying mechanism could be related to the mitochondria having an independent genome and being an important source of ROS outside of the NADPH oxidase. However, how this form of NETosis releases NETs to the extracellular environment remains unknown. These findings collectively suggest that NETs form through multiple overlapping mechanisms and that the components of DNA networks released into the extracellular space are heterogeneous in different scenarios.

NETs in the extracellular space contain several cytotoxic components, such as DNA, histones, proteases, and highly inflammatory compounds such as myeloperoxidase (MPO), lactotransferrin, LL-37, calprotectin, bactericidal/permeability increasing proteins, and pentraxin 3 (13, 22–26). When released, these components cause indiscriminate damage to both pathogens and bystander cells, thereby potentially contributing to host tissue damage, particularly in the vascular endothelium. Neutrophils release NETs during sterile inflammation, which occurs in response to inflammatory mediators shared with the immune system under sterile inflammatory conditions. This phenomenon is evident in highly vascularized organs such as the lung, where the microvascular endothelium serves as a platform for neutrophil activation and NET release. Furthermore, NETs attacking endothelial cells play a crucial role in the development of pulmonary edema in TRALI. Additionally, DAMPs released from dying neutrophils further activate the innate immune system and amplify the inflammatory response in TRALI. Numerous studies have shown that unregulated NETs play a role in the pathogenesis of various non-infectious diseases, including cancer (27), cardiovascular disease (28), systemic lupus erythematosus (29), rheumatoid arthritis (30), and digestive tract diseases (31), as well as TRALI. However, despite findings indicating the beneficial effects of removing NETs in various diseases, one study reported that NETs promote the resolution of neutrophil inflammation by aggregating and degrading cytokines and chemokines via serine proteases (32). This suggests that NETs may have a dual effect in sterile inflammation. Moreover, in sterile diseases involving

neutrophil activation, NETs are not the sole factor causing bystander cell damage, as the activation of ROS and other immune cells by neutrophil respiratory burst also contributes to the process. Consequently, simply targeting NETs may not be the optimal solution for disease treatment. Understanding the interaction between neutrophils and the body, particularly immune regulation, will deepen our understanding of the upstream and downstream effects of NETs and foster the development of improved disease treatments.

3 Role of NETs in TRALI

TRALI is characterized by lung endothelial damage and capillary endothelial penetration by activated neutrophils. Neutrophils are the primary component of the lung's innate immune system and, due to their size compared to lung capillaries, necessitate deformation to overcome the space constraints of the vascular bed. This results in a non-integrin-dependent close contact between neutrophils and vascular endothelium, permitting rapid recruitment and activation of neutrophils under pro-inflammatory conditions, thereby facilitating the rapid onset of TRALI. While it was previously believed that large amounts of ROS released by activated neutrophils were the major factor in endothelial damage, recent studies suggest that NETs also play a significant role in TRALI development. NET structures contain concentrated histones and granule proteins, and high concentrations of locally formed NETs in the pulmonary circulation may enhance the toxicity of neutrophil respiratory burst to endothelial cells (33, 34). The use of DNase1 to degrade NETs has been shown to reduce multiple vascular inflammations, including TRALI, but is not entirely effective in removing all NETs and their cytotoxic substances, such as histones. Circulation of these cytotoxic substances throughout the body post-degradation in the blood may not reach sufficient local concentrations to damage the endothelium. Additionally, extensive interaction between NETs and platelets, in combination with DNA scaffolds, may lead to the formation of thrombi and subsequently cause local ischemic injury in the lung (35, 36). Caudrillier and colleagues (33) first demonstrated NETs' involvement in endothelial damage in TRALI based on their human specimen-based study, showing that neutrophils in the lung's microvascular region were undergoing NETosis without forming NETs, despite detecting neutrophils in the alveoli. Another study in humans and mice revealed a substantial accumulation of NETs in the alveoli after anti H-2Kd mAb infusion, but only a small amount in the pulmonary microcirculation, significantly alleviating alveolar aggregation of NETs and decreasing blood oxygen saturation (37). A subsequent study also confirmed that NETs were formed in the alveoli (36). This difference may be attributed to the abundant presence of DNase1 in plasma, which can digest the DNA network of NETs, thereby affording maximum protection to the alveoli from NETs. Furthermore, under TRALI conditions, monocytes/macrophages in the alveoli produce significant amounts of inflammatory mediators, providing strong local stimulation to neutrophils for NET formation.

The induction of NETs can be attributed to various components present in the bloodstream. Studies have demonstrated that the infusion of red blood cells (RBC) can enhance neutrophil adhesion, thereby creating favorable conditions for neutrophil-mediated vascular endothelial injury (38). Furthermore, in long-stored blood, RBC hemolysis can result in hemin accumulation, which has been found to rapidly induce NET formation *in vitro* within 15 minutes, a notably shorter timeframe compared to the 3 hours required for the induction of NETs by PMA (39). Additionally, it has been reported that heme, featuring a porphyrin ring, activates neutrophils to release ROS, thereby potentially triggering subsequent NETosis (40). It can be speculated that the blood components that cause neutrophil activation may also lead to NETosis, but an elusive problem is that there are many factors of neutrophil activation in TRALI, and if NETs are only the product of neutrophil respiratory burst, then the elimination of NETs may not be enough to compensate for the impact of ROS on vascular endothelium and alveolar epithelium damage. Consequently, one may speculate that the blood components responsible for neutrophil activation may also lead to the formation of NETs. However, an unresolved issue pertains to the multitude of factors implicated in neutrophil activation in TRALI, underscoring the importance of resolving this issue for the advancement of therapeutic strategies.

4 Interactions of NETosis and immune regulation within neutrophils

4.1 Inflammasome signaling pathway

Macrophages and monocytes have widely characterized the lineage and signaling mechanism of the inflammasome. The inflammasome, which acts as a platform for caspase recruitment and activation, triggers the cleavage of the intracellular GSDMD precursor to produce N-terminal fragments (GSDMD-N). These mature N-terminal fragments then bind to the cell membrane in the form of polymers, forming large GSDMD pores that lead to plasma membrane permeabilization and pyroptosis. In contrast, there is a limited understanding of the inflammasome in neutrophils. Although neutrophils express components of the inflammasome and can undergo pyroptosis (41), they are generally resistant to pyroptosis triggered by multiple inducers (42–44). Interestingly, there is a significant interplay between the signaling pathways of inflammasome activation and NETosis, with GSDMD appearing to be the point of interaction between the two pathways. The widely accepted view is that the inflammasome activates GSDMD, leading to the formation of pores in the cell and nuclear membranes that facilitate the release of NETs into the extracellular space (45, 46). Additionally, PAD 4 increases posttranscriptional levels of NLRP3 and ASC, thereby promoting NLRP3 inflammasome/ASC puncta assembly and the production of downstream Caspase-1 and GSDMD-N (46). Furthermore, recent reports have shown that the

assembly of ASC puncta occurs at the early stage of NETosis and that the cleavage of the cytoskeleton and nuclear membrane by early formed Caspase-1 likely facilitates the release of NETs (47). However, subsequent studies have indicated that Caspase-11, rather than Caspase-1, is the primary executor of GSDMD cleavage in neutrophils, possibly due to the low expression levels of ASC and Caspase-1 in these cells (48). On the other hand, the PAD 4 enzyme is activated by spiking cytoplasmic calcium and triggers histone citrullination to promote chromatin decondensation, and PAD 4 is activated during caspase-11-driven NETosis, likely due to increased calcium influx through the GSDMD pore (48). However, it has also been proposed that GSDMD cleavage and activation in neutrophils is not independent of caspases but rather dependent on elastase released in granules in neutrophils (49), though neutrophil elastase cleaves several amino acids of GSDMD upstream of the canonical caspase cleavage site, this does not impair the ability of the GSDMD N-terminal inserted membrane to neutralize lysed cells (50). Another study showed that the NE released from the granule cleaves GSDMD, and the cleaved GSDMD forms pores on the granule, promoting further release of NE, which constitutes a feed-forward loop upstream of NETosis (51). Moreover, the pore-forming effect of GSDMD on mitochondria leads to endogenous mtDNA release and further activation of the cGAS-STING signaling pathway, thus promoting the release of NETs and aggravating lung ischemia-reperfusion injury (52). The cGAS also promotes the transcriptional activation of PAD 4 through STING signaling, thereby controlling the formation of NETs (53).

The controversial role of GSDMD in promoting neutrophil NETosis has been the subject of debate, particularly in light of reports indicating its dispensability in PMA-induced NETosis (54). Subsequent studies have reinforced this perspective by demonstrating that GSDMD knockdown in mouse neutrophils still resulted in the formation of NETs with the same kinetics and intensity as those formed by wild-type mouse neutrophils when triggered by classical NETosis inducers such as cytokines and complement factor (55). Therefore, it can be inferred that classical or non-classical stimuli of the inflammasome may not be essential for activating downstream processes of the inflammasome pathway, suggesting a potential disconnect between the requirement for GSDMD and inflammasome-mediated NET formation. Despite previous studies establishing the significance of GSDMD in NETosis, it is important to recognize the involvement of different types of cell-specific signals in NETosis. Consequently, investigating the signaling and regulatory role of GSDMD activation in NETosis will yield critical insights for disease interventions involving neutrophil activation, specifically in conditions such as TRALI. In addition, the release of NETs is also influenced by inflammatory factors from activated neutrophils or other immune cells, a topic we will delve into further. However, within the context of TRALI, the precise immune cell initiators of the immune cascade and the specific role of NETs within this cascade remain open questions.

4.2 Immunometabolism of neutrophils

Neutrophils are terminally differentiated leukocytes with the shortest lifespan in the body. They are released from the bone marrow into the blood, function in tissues, and are eventually cleared by other immune cells or returned to the bone marrow as senescent cells. This high degree of transcriptional activity in neutrophils is supported by continuous changes in energy metabolism. Mature neutrophils have minimal mitochondria, with respiratory chain complex inhibitors suggesting little contribution to ATP production (56). Instead, glycolysis is the main pathway by which neutrophils gain energy (57). Glucose enters neutrophils via glucose transporters and is catalyzed into glucose-6-phosphate (G6P) by hexokinase, subsequently entering the glycolytic pathway. When neutrophils were exposed to PMA in a glucose-free medium for 3 hours in previous studies, they lost their characteristic polymorphic nucleus, yet they did not release NETs. However, upon glucose addition, NETs were released within minutes, indicating that the chromatin decondensation phase of NET formation is independent of exogenous glucose, while its release is strictly dependent on glucose metabolism (58). Upregulation of regulatory enzymes in glycolysis, such as 6-phosphofructo-2-kinase/fructose-2,6-bisphosphatase (PFKFB3) and pyruvate kinase M2, is involved in regulating NET formation (59, 60), as neutrophils need to upregulate glycolysis to meet the increased bioenergy requirements for NET formation. In the physiological state, glucose-6-phosphate (G6P) can enter the pentose phosphate pathway (PPP) by the action of glucose-6-phosphate dehydrogenase (G6PD). In this pathway, G6P serves as a substrate for the production of NADPH, which functions as a cofactor and electron donor for NOX. Neutrophils, upon activation, shift their glucose metabolism from the glycolytic pathway to the pentose phosphate pathway, resulting in the subsequent production of NADPH. The NADPH produced acts as a precursor for the generation of superoxide and oxygen radicals under the mediation of NOX. These radicals, in turn, give rise to an abundance of ROS, thereby instigating the respiratory burst of neutrophils and triggering the formation of NETs (57, 61). This assertion finds support in a recent study wherein the inhibition of G6PD curbed the respiratory burst in neutrophils (62). Interestingly, to meet the elevated NADPH demand for neutrophil respiratory burst and the subsequent release of NETs, ribose-5-phosphate, produced through the pentose phosphate pathway, is further metabolized to fructose-6-phosphate (F6P), which is isomerized from G6P by glucose-6-phosphate isomerase (GPI). This process allows for the replenishment of G6P, which can then re-enter the pentose phosphate pathway and yield more NADPH. Flux analysis reveals that during intense oxidative events, neutrophils predominantly utilize the pentose cycle to generate NADPH (63). In contrast, activation of phosphofructokinase 1 to increase glycolytic flux inhibited NET release (64). These findings collectively imply that neutrophils possess a distinctive metabolic adaptability to produce NADPH as needed to facilitate their activation. In contrast, the

downregulation of respiratory bursts along with increased NET formation was observed in ARDS induced by COVID-19 (65, 66), suggesting that the pentose phosphate pathway-mediated respiratory burst may not be a conserved mechanism for NETosis. Given the limited glucose availability in lung tissue and local inflammatory regions, the ability of neutrophils to regulate glycogen storage further enhances tissue damage in TRALI, and activation of hypoxia pathways led to increased neutrophil glucose storage and glycolytic capacity, further aggravating the acute lung injury associated with neutrophil activation (67). Moreover, NETs can induce the release of neutrophil granules, producing ROS and subsequent NETosis via NOX2, further aggravating tissue damage (68). Although mitochondria do not appear to be important in neutrophil energy metabolism in neutrophils, their electron transport chain, especially complex III, also leads to mtROS production in a non-NADPH-dependent NETosis. mtROS has been shown to be required for spontaneous NETosis in patients with systemic lupus erythematosus (SLE) (21, 69). The mitochondria-related metabolic changes and mechanisms during neutrophil activation remain an open question, and an understanding of this process will deepen our understanding of NETosis and TRALI. In conclusion, the metabolic status of neutrophils has profound effects on NETosis, and in the context of TRALI, they will further mediate the initiation and progression of tissue damage.

Therefore, in their quiescent and activated states, neutrophils exhibit a high degree of metabolic flexibility that enables them to adapt to phenotypic changes. Although several classical examples of metabolic remodeling associated with respiratory burst and NETosis are recognized, they do not provide a comprehensive metabolic profile of neutrophils. When using inhibitors to target key enzymes in glucose metabolism, it is important to consider the off-target effects of inhibitors and the additional functions of these enzymes beyond classical metabolism. Failing to consider these issues may result in erroneous conclusions. For example, the inhibition of the neutral glycolytic enzyme glyceraldehyde phosphate dehydrogenase (GAPDH) results in the formation of NETs, which is not related to changes in the glycolytic pathway and PPP but is attributed to increased NE activity (Figure 2) (70).

5 Neutrophil exogenous immune regulator of NETosis

5.1 Macrophages

5.1.1 Inflammation boosting

Studies have demonstrated the involvement of lung macrophages in the pathological process of ALI/ARDS resulting from various causes. In inflammatory lesions, macrophage and NETs could provide inflammatory signals such as IL-1β that fuel each other. A study on atherosclerosis has supported this hypothesis, revealing that co-treatment of NETs with cholesterol induces macrophages to produce large amounts of IL-1 β, compared with only a small amount of IL-1 β release using cholesterol alone, implying an important role for NETs in initiating inflammasome activation within macrophages (71). Moreover, in TRALI, the extensive macrophage pyroptosis leads to increased release of IL-1 β, further promoting the release of NETs. Indeed, NETs interact with macrophages through various pathways, supporting positive feedback regulation. NETs can promote the transcription of NLRP 3 through the TLR 4/TLR 9/NFkB signaling pathway (72, 73), and also promote NLRP 3 activation through the ROS/thioredoxin-interacting protein (TXNIP) signaling pathway (72). Additionally, NETs promote the release of other inflammatory factors in macrophages. In renal fibrosis, it has been observed that neutrophil-specific knockdown of GSDMD or Cas-11 reversed the nuclear translocation of p65 in macrophages caused by NETs, and subsequent TGF-1 β release (74). Furthermore, NETs can mediate the activation of NLRP 3 through the TLR 7/TLR 9 signaling pathway (75). The components of NETs contain High-mobility group box 1 (HMGB1), a highly conserved nuclear protein. Studies have shown that NETs initiate the receptor for advanced glycation end products (RAGE) dynamin signaling in macrophages via HMGB1, leading to macrophage pyroptosis (76), suggesting NETs induce macrophage pyroptosis through mutually redundant pathways that amplify local inflammation. NETs also upregulate the activity of the macrophage epidermal growth factor receptor (EGFR), enhance the phosphorylation of Beclin-1 by EGFR, and inhibit autophagosome formation in macrophages, mediating further inflammasome activation (77). As a positive feedback for inflammatory amplification, released IL-1β from macrophages activates the inflammasome in neutrophils, thereby initiating a broader range of NETosis (78). This crosstalk amplifies the local inflammatory response, which, though contributing to a more intense antimicrobial effect in infectious diseases, exacerbates tissue injury in sterile inflammation. Furthermore, NETs cause a significant increase in ROS, promoting the deubiquitination of NLRP3 in alveolar macrophages and, in turn, mediating cell pyroptosis in septic lung injury (79).

The cGAS-STING signaling pathway in macrophages is also involved in recognizing NETs and promoting the NETosis-mediated inflammatory response by releasing type I IFN. Activation of STING by NETs has been observed to promote the pro-inflammatory phenotype transition in macrophages, contributing to stress-induced cardiac remodeling (80) and neuroinflammation (81). Interestingly, when taken up by macrophages via phagocytosis, NETs can escape from the lysosomes and activate the cytoplasmic cGAS, a process that requires the involvement of NE (82).

Based on the evidence described above, manipulating this inflammatory circuit becomes a potential treatment for NET-related diseases, particularly in TRALI, because as a sterile inflammation, sustained activation of neutrophils depends on the involvement of inflammatory factors. It should be noted that the extensive literature on NETs gives the impression that almost all pro-inflammatory molecules induce NETs. However, caution should be exercised in interpreting these results, as the recruitment and activation of neutrophils do not invariably lead to the release of NETs. Moreover, the presence of extracellular DNA

in neutrophil activation-associated inflammation cannot be solely attributed to NETs, since pro-inflammatory signaling-induced pyroptosis, necrosis, and apoptosis all result in the release of DNA outside the cell. Additionally, it is worth noting that under certain conditions, blocking inflammatory factors can improve disease progression and reduce NETosis; however, it is important to recognize that the observed positive effects on the disease may be a consequence of the overall reduction in inflammation.

5.1.2 NETs removal

Defects in the regulatory mechanisms responsible for the clearance of NETs may lead to persistent inflammation and deterioration of tissue damage. Physiological concentrations of DNase I in plasma are not sufficient to clear NETs, and, as adjuncts, phagocytes, especially macrophages, are important players in the clearance of NETs. It was previously suggested that NETs internalized by macrophages are degraded in the lysosomal region compartment (83). However, subsequent research revealed that NETs can also be degraded by DNase III outside lysosomes, indicating different nuclease subtypes involved in the degradation process. Notably, while macrophages can degrade NETs, the presence of NETs alone is not adequate to provoke inflammation in macrophages. Conversely, the combined stimulation of NETs may exacerbate LPS-induced inflammation in macrophages, suggesting that damage-associated molecular patterns (DAMPs) or other cytokines may be necessary in the local inflammatory cascade triggered by NETs (84). All types of polarized macrophages possess the capability to clear NETs through the endocytosis of NETs with secreted DNase 1 L3. The clearance of NETs by macrophages may be influenced by increased macrophage pinocytosis following proinflammatory stimulation and altered distribution of DNase by macrophage filopodia production (85). Although a large number of macrophages in the lung tissue are involved in the clearance of NETs during inflammation, proinflammatory macrophages exhibit enhanced NET clearance capacity (85). However, studies based on ARDS patients showed that alveolar macrophages from ARDS patients have a reduced ability to clear NETs, and this process can be reversed by metformin, an activator of AMPK (86), implying that the metabolic reprogramming of proinflammatory cells in a specific tissue context affects the clearance of NETs by macrophages. Additionally, both M1 and M2 polarized macrophages can directly reduce neutrophil NET formation through secreted factors, possibly involving the inhibition of neutrophil ROS (87). Exosomes derived from M2 macrophages can upregulate the endogenous inflammatory "stop signal" lipoprotein A4 (LXA 4) in neutrophils and downregulate the expression of CXCR 2 and ROS in neutrophils, thereby reducing neutrophil migration and NETosis (88). While the specific mechanisms through which macrophages regulate NETosis or NET removal remain unclear, it is evident that the interaction between macrophages and neutrophils is intricate. In some scenarios, they collaborate to establish inflammatory circuits for pathogen clearance or tissue damage, while in other instances, macrophages have an inherent capacity to clear NETs and inhibit neutrophil NETosis. Investigating the interplay between inflammatory progression and resolution involving macrophages and neutrophils is an intriguing area for further study, as it promises to deepen our comprehension of inflammatory diseases, including TRALI.

5.2 Dendritic cells and T cells

Plasmacytoid dendritic cells (pDC) express high levels of TLR 7 and TLR 9 that specifically recognize exogenous single-stranded nucleotides in the case of pathogen infection, producing large amounts of type I interferons (89). While pDCs typically do not react to their own DNA, modifications of extracellular DNA can alter this property. For instance, the antimicrobial peptide LL 37 has the capacity to convert inert endogenous DNA into a potent trigger for interferon production in pDCs by binding to DNA and forming aggregated and concentrated structures (90). Furthermore, DNA structures crosslinking multiple proteins within NETs have been demonstrated to carry multiple antimicrobial peptides, forming immunogenic complexes that activate innate pDCs via TLR 9, as evidenced in the autoimmune disease SLE (91). This activation leads to the generation of high levels of interferon-α through TLR 9 ligation, initiating the immune cascade (92–94). Subsequently, these cytokines enable neutrophils to undergo further NETosis, thereby fueling an inflammatory circuit and creating a positive feedback amplification of NETs. Additionally, dendritic cells (DCs) play a role in the clearance of NETs by releasing DNase1-like 3 (DNase1L3) to degrade NETs in the cell supernatants *in vitro* (84). The activation of pDC by NETs seems to bridge innate and adaptive immunity, with NETs initiating the release of inflammatory factors from macrophages, which will further activate helper T cells 17 (TH 17), and subsequently derived IL-17 will drive the chemokines CXCL 1 and CXCL 2 to promote neutrophil recruitment during inflammation (71). In a cigarette smoke-induced emphysema model, it was observed that NETs trigger pDC maturation, subsequently leading to the differentiation of naïve CD4+ T cells into TH17 (95, 96). Although these results imply the involvement of NETs in activating dendritic cells and T cells and promoting innate immunity, the interaction of NETs with adaptive immunity plays an important role in TRALI in the context of acute onset of TRALI.

The involvement of NETs in activating dendritic cells and T cells, as well as promoting innate immunity, has been well-documented in the context of chronic disease. However, it is essential to investigate whether this mechanism is conserved under acute and chronic inflammation, especially in the context of rapid-onset diseases. Therefore, it remains to be elucidated whether the interaction of NETs with adaptive immunity plays a significant role in the acute onset of TRALI.

5.3 Complement system

The complement system is a protein reaction system with a precise regulatory mechanism, comprising serine protein cascade

enzyme reactions involving continuous cleavage and activation of complement proteins, ultimately leading to target cell lysis through the formation of a membrane attack complex (MAC). In addition, the complement system is involved in the process of opsonization and acts as a danger signal to activate immune cells to initiate immune responses as well as to clear immune complexes (97). The complement system contributes to the induction of NETosis, the ability of S. aureus to induce neutrophil NETosis, and the blockade of complement receptor 1 (CR1) significantly reduces S. aureus-induced release of NETs (98). The process by which C5b-7 is deposited on endothelial cells that physically make contact with neutrophils forms an MAC that transfers to neutrophils and initiates NETosis (99). Pulmonary endothelial activation has been considered to be necessary for the TRALI secondary hit model. In fact, endothelial cell activation may play an important role in complement fixation and activation as recent studies show that antibodies to blood products targeting HLA/major histocompatibility complex (MHC) protein in TRALI are endothelial cells, which subsequently initiate endothelial cells to complement fixation, and depletion of complement reduces antibody-mediated lung injury and NETs (100). In TRALI, a deep exploration of the interactions between the endothelium, complement, and neutrophils will deepen our understanding of this disease. C5aR 1 signaling drives neutrophil NETosis in patients with COVID-19 and drives lung immunopathology in an NET-dependent manner (101). In the mouse TRALI model, C5a acts as a chemoattractant to recruit peripheral neutrophils to the lungs, triggering the formation of NETs in the lung tissue (102). Indeed, as an anaphylaxigin in the complement system, C5a not only recruits neutrophils and initiates upregulation of immune receptors such as TLRs and complement receptors, but also initiates strong NET responses through more profound mechanisms, such as triggering neutrophil NETosis by promoting mitochondrial ROS (103). Furthermore, NETs provide a scaffold for complement activation. Initially, NETs were shown to activate the classical complement pathway by binding complement C1q, and the presence of C1q prevents NETs from being degraded by DNase (104). Subsequent studies showed that NETs also structurally deposited components of the complement alternative activation pathway and that they could activate the complement cascade *in vitro* and in plasma (105, 106). Indeed, neutrophils contain multiple intrinsic components that have been shown to be involved in the activation of the complement system, such as MPO direct binding to acrolein and further induction of C3 activation and interaction of different components of neutrophil granules with properdin (107). When these intrinsic components bind to NETs at NETosis, it can be speculated that they play an important role in the activation of the complement system by NETs. These results imply that the interaction of NETs with the complement system warns the innate immune system to form a pro-inflammatory cycle, and although an attractive model, we still lack enough knowledge to construct this interaction model in TRALI (Figure 3).

Neutrophil recruitment and formation of NETs are promoted by activated complement. Concurrently, NETs serve as a platform for complement activation. Additionally, macrophages play a crucial role in providing inflammatory signals, such as IL-1β, to stimulate the formation of NETs. Subsequently, the formation of NETs further triggers macrophages to transition to a proinflammatory phenotype, effectively establishing an inflammatory feedback loop. Furthermore, macrophages are involved in the resolution of NETs through phagocytosis or the secretion of DNAase. In a similar inflammatory context, dendritic cells and neutrophils are capable of reciprocally providing inflammatory signals, such as IFN-α, resulting in the formation of inflammatory circuits. Moreover, dendritic cells activated by NETs can release IL-6, facilitating the maturation of TH17 cells, and thereby linking the innate and adaptive immune responses.

6 Therapeutic implications

Given the role of excessive generation or impaired clearance of NETs in tumors, digestive diseases, cardiovascular diseases, the nervous system, and respiratory diseases, several pharmacological pathways have emerged to inhibit NETosis/NETs, including targeted inhibition of NETosis-related PAD 4, NADPH oxidase and ROS generation, and the degradation of DNA in NETs by DNase, which has been well summarized in several excellent other recent reviews (108–110), However, these treatments have some inherent drawbacks, because NETs are only one of the players in inflammation in the complex process of disease progression, and simply targeting NETosis/NETs may not be sufficient to prevent other steps in the immune cascade and tissue damage, such as a strategy using DNase 1 that can only degrade the DNA skeleton of NETs and not alleviate histone-induced damage (111). Here, we will discuss possible therapeutic targets based on immune modulation of NETosis/NETs to attempt to expand the current therapeutic options for TRALI (Table 1; Figure 4).

Targeting the immunomodulation associated with NETs is a potential therapeutic tool for TRALI. Activation of the glycolytic pathway reduces the glucose into the PPP, further inhibiting the NETs associated with neutrophil respiratory burst. Therapeutic strategies targeting GSDMD may inhibit both macrophages and neutrophils, which would not only avoid their independent forms of death in the inflammatory state, respectively, but also avoid their mutual regulation after activation. Neutrophil activity is regulated by multiple cytokines/chemokines, and clearance of these cytokines is a potential therapeutic strategy for targeting NETs.

6.1 Targeting glycolytic pathway

Given that neutrophil activation and NET release depend on glycolysis as well as the pentose phosphate pathway, targeting upstream of glycolysis is a promising direction for intervention in TRALI. As mentioned above, the main pathological features of TRALI are neutrophil recruitment activation and endothelial barrier disruption, and inhibition of endothelial activation also prevents barrier system disruption and subsequent infiltration of neutrophil recruitment. It is worth noting that activation of the glycolytic pathway appears to be required for endothelial cell activation (122–124). In lung-related disease, endothelial-specific

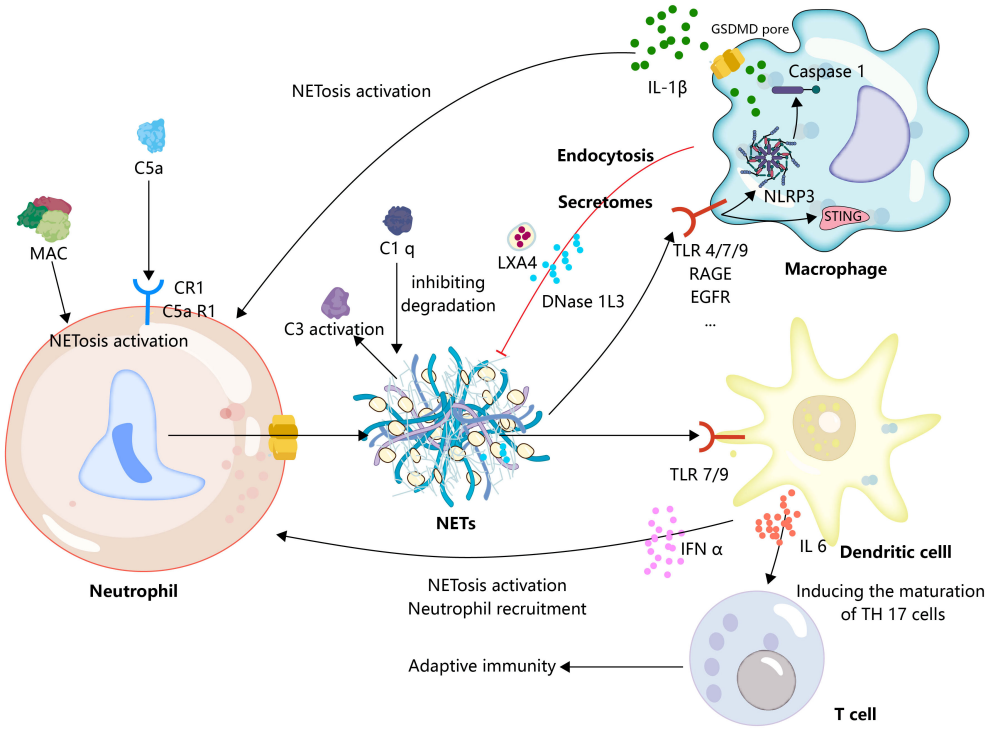

FIGURE 3
Extrinsic immunomodulation of neutrophils in NETs.

deletion of the glycolysis regulator PFKFB3 relieves sepsis-related acute lung injury and pulmonary hypertension (125, 126), and underlying mechanisms include inhibition of the glycolytic pathway, inhibiting NF- κB signaling and subsequent reduction of expression of surface adhesion molecules on endothelial cells, and thereby inhibiting neutrophil recruitment (126). Consistently, upregulation of PFKFB increased intracellular lactate levels, followed by activation of NF- κ B, resulting in increased endothelial permeability (127). Furthermore, inhibition of the glycolytic pathway also directly abolished histamine-induced vascular endothelial actin contraction, focal adhesion molecule junction formation, and endothelial barrier disruption (128). From this perspective, targeting glycolysis in TRALI seems to represent a dual benefit, as it not only inhibits endothelial activation-dependent neutrophil recruitment but also suppresses NET formation. It must be noted, however, that the energy biology of endothelial cells at the resting state depends on aerobic glycolysis, and another glycolytic PKM 2 in silent mouse lung endothelial cells depletes ATP required for the normal VE cadherin cycle of endothelial cells (129), leading to basal pulmonary microvascular permeability and pulmonary edema (130). One reason for these observed differences may be the different degrees of glycolysis inhibition. When ATP production is below the lowest amount required to maintain barrier homeostasis, the inhibition of neutrophil activation and NETosis may not be sufficient to counteract the additional lung damage from barrier homeostasis. Thus, the potential of inhibiting glycolysis as a treatment for TRALI needs to be balanced against the risk that it could also trigger TRALI. Furthermore, inhibiting glycolysis downstream may shift metabolic substrates to the pentose phosphate pathway, leading to increased NADPH production, which supports respiratory bursts and NET release. This paradox suggests that while glycolysis is involved in neutrophil activation, targeting the pentose phosphate pathway may be more effective in diseases induced by NETs, including TRALI. Recent studies have explored small molecule inhibitors that target key enzymes in the pentose phosphate pathway, such as G6PDi (62), to inhibit neutrophil respiratory bursts. Moreover, the small molecule NA-11 has been reported to reprogram metabolic flux from the pentose phosphate pathway back to the glycolytic pathway, thus inhibiting NOX2-dependent oxidative bursts in neutrophils (64). Therefore, targeting the pentose phosphate pathway represents a more suitable approach for addressing diseases induced by NETs, including TRALI.

In conclusion, the regulation of glucose metabolism has a profound impact on neutrophil respiratory burst and NETosis. However, the role of glycolysis inhibition in blocking NETosis is still under investigation. Currently, there is no research on TRALI, so a better understanding of the roles of glycolysis and the pentose phosphate pathway in experimental and clinical TRALI models could support the potential role of glucose metabolism as a therapeutic factor for TRALI.

6.2 Targeting inflammasome

Alveolar macrophages are key to initiating and resolving lung inflammation, and lung proinflammatory-activated macrophages normally recruit and activate a broader population of immune cells

TABLE 1 Representative drugs targeting immune regulation in neutrophils.

Principle	Classification	Intervention/ Drugs	Mechanisms	References
Targeting the glucose metabolism pathway.	Glycolytic agonist	NA-11	Activates the enzyme PFKL and redirects the metabolic flux from the pentose phosphate pathway back to the glycolytic pathway, consequently inhibiting the NOX 2-dependent oxidative burst in neutrophils.	(64)
	PPP inhibitor	G6PDi	Suppresses G6PD, thus blocking the PPP and respiratory burst	(62)
Targeting inflammasome	GSDMD inhibitor	Disulfiram	Inhibits GSDMD-mediated inflammasome activation	(112, 113)
		ivermectin	inhibits GSDMD oligomerization	(114)
	NE inhibitor	Necrostatin-1	Inhibition of NE activation and the subsequent activation of GSDMD by NE	(115, 116)
Targeting chemokines/cytokines and neutrophil receptors	Human monoclonal antibody against IL-8	HuMab 10F8	Blocks IL-8 to inhibit neutrophil migration	(117)
	Inhibitor of CXCR1 and CXCR2 receptors	Repertaxin	blocks CXCL 1/2 signaling in neutrophils	(118)
	IL-1 receptor inhibitor	IL-1 Ra	Blocks the signaling of IL-1 β in neutrophils	(119, 120)
	Human antibody against N-terminal domain of MK	anti-N-MK	Prevents neutrophil migration	(121)

to drive inflammatory diseases, including TRALI (131, 132). Activation of inflammasomes has been shown to be involved in most of the molecular biological processes of proinflammatory macrophage activation and drives multiple pathologic processes of acute lung injury (133–135), thus targeted regulation of the macrophage inflammasome seems a promising direction in the treatment of TRALI. As discussed earlier, inflammasome activation in macrophages promotes the recruitment of neutrophils as well as NET release, meanwhile, activated GSDMD downstream of the neutrophil inflammasome pathway on the nuclear and plasma membranes is critical for NET release, and targeted inhibition of the inflammasome or GSDMD may have unexpected effects in the treatment of TRALI. Sollberger et al. (51) have identified a small molecule LDC7559 that specifically suppresses GSDMD, which hinders membrane localization of GSDMD not only in NETosis in neutrophils but also IL-1 β release in monocytes/macrophages. Disulfiram, a drug approved by the FDA to treat alcohol addiction, has been shown to inhibit GSDMD-mediated inflammasome activation (136). A recent study suggests that pharmacological inhibition of GSDMD by disulfiram reduces the release of NETs from neutrophils and sepsis-mediated multiorgan damage (112). Disulfiram treatment also attenuated the formation of NETs as well as lung immunopathology in a mouse model of severe acute respiratory syndrome coronavirus type 2 infection (113), and also relieved the damage to the endothelium (137). Disulfiram also alleviated the diabetic foot injury mediated by NETs (45). Notably, recent data from animal models suggest that disulfiram can block NET formation and mitigate the pathological phenotype of TRALI (114). This finding highlights the potential for disulfiram as a therapeutic agent in treating TRALI and emphasizes the need for further investigation into the underlying mechanisms of its action in this context. The antiparasitic drug small molecule compound ivermectin was also shown to inhibit GSDMD oligomerization, alleviating the release of NETs and inhibiting *in situ* melanoma metastasis to the lung (138). The favorable effects of other GSDMD inhibitors such as necrosulfonamide (139) and exogenous dimethyl fumarate (115) have been evaluated in macrophages, and the following study seems to re-evaluate the contribution of these compounds in suppressing neutrophil NETs during inflammation. Moreover, targeted regulation upstream of GSDMD can also reduce NET-dependent organ damage. Necrostatin-1 has been shown to reduce inflammation in asthma by inhibiting NET formation (116), and subsequent studies showed that this inhibitory effect is achieved by inhibiting NE activation and subsequent expression of N-GSDMD (117). Thus, the necessity to reevaluate and adjust the use of these drugs is evident in the context of the simultaneous activation of both macrophages and neutrophils in TRALI.

In light of the established safety and efficacy of GSDMD inhibitors in clinical and animal models, it is imperative to reassess and modify the application of these drugs in the context of concurrent activation of macrophages and neutrophils in TRALI. The comprehensive understanding of neutrophil NETosis in TRALI is still incomplete, necessitating clarification on whether NETs in TRALI are released in a GSDMD-dependent manner. This clarification is pivotal before the consideration of GSDMD inhibitors for use.

6.3 Targeting chemokines/cytokines and neutrophil receptors

Dysregulation of chemokine/cytokine network has a significant effect on TRALI, characterized by the accumulation of activated

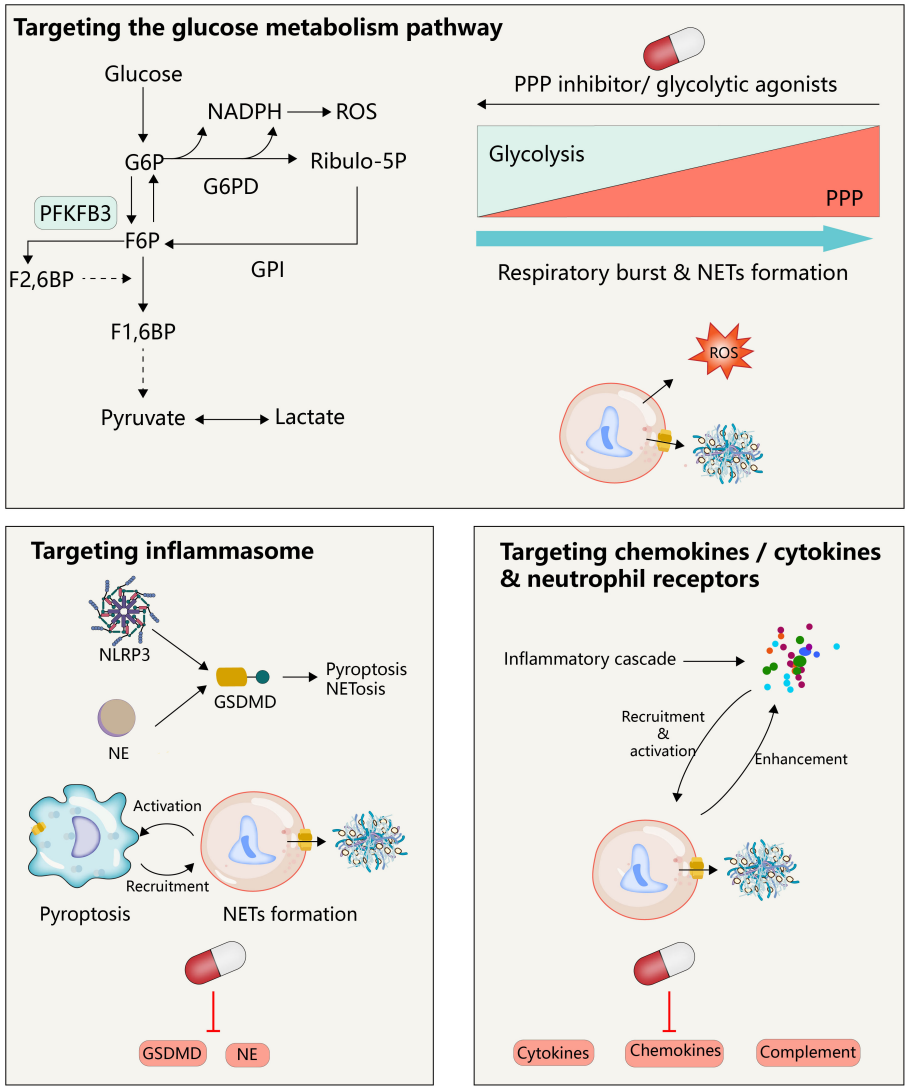

FIGURE 4
Therapeutic implications.

neutrophils in pulmonary microvascular regions, and re-regulation of this network contributes to the control of TRALI. In addition to controlling the massive release of the inflammatory cytokines resulting from the activation of inflammatory cells including macrophages and dendritic cells, blocking the ligand-receptor of inflammatory cells is a candidate strategy for targeting inhibiting neutrophil activation and release of NETs. HuMab 10F8 is a full human monoclonal antibody against IL-8, and it effectively neutralizes IL-8-dependent activation of human neutrophils and migration in mid-palmoplantar pustulosis phase (140). Subsequent studies showed that this antibody-based approach of blocking IL-8 to inhibit neutrophil migration similarly inhibited the formation of NETs (141). CXCR 1 and CXCR 2, the receptors blocking IL-8, exerted the same effect, and blocking CXCR 1/2 signaling in neutrophils using the small molecule inhibitor repertaxin protected from organ reperfusion injury (118), and subsequent studies supported that blockade of CXCR 1/2 signaling by repertaxin and pertussis toxin inhibited the release of neutrophil NETs (121). Furthermore, the neutrophil-expressed cytokine midkine mediates neutrophil trafficking and extravasation during acute inflammation, and the antibody anti-N-MK that specifically blocks the N-terminal domain of MK prevents neutrophil migration into the myocardium, thereby alleviating NETosis-driven myocardial inflammation (119). Consistent with this, IL-1 signaling triggered increased expression of leukocyte adhesion molecules on endothelial cells, with reduced neutrophils recruited on the endothelium following administration of the IL-1 α receptor inhibitor IL-1 Ra (120), while blockade of IL-1 β signaling reduced the formation of NETs in breast cancer (142). Blockade of complement signaling represents another strategy to target NETs, and currently, the monoclonal antibody eculizumab targeting the human complement component C5 and the inhibitor avacopan of the C5a receptor have been applied to atypical HUS and ANCA-Associated Vasculitis, respectively (143, 144). Although these drugs

have not been evaluated in the clearance of complement activation-associated NETs, based on the extensive interactions between the complement system and neutrophils and NETs, we speculate that these drugs may be potential candidates for TRALI therapy in the future.

It is important to recognize the need for a balanced evaluation of the application of HuMab 10F8, anti-N-MK, eculizumab, and avacopan in the context of TRALI, given the relevance of immunoglobulin-associated TRALI. A recent retrospective study in France highlighted seven cases of TRALI resulting from immunoglobulin infusion, indicating the potential for triggering TRALI through the exogenous infusion of therapeutic antibodies (145). Therefore, before targeting the therapeutic potential of chemokines/cytokines and neutrophil receptors, it is essential to rigorously define the risk of their potential triggering of antibody-mediated TRALI.

7 Concluding remarks

It is evident that NETosis does not act independently in inflammatory diseases such as TRALI; rather, it interacts closely with multiple immunomodulatory mechanisms in the human body. Therefore, a comprehensive understanding of these interactions is essential for unraveling the complex processes involved in TRALI initiation, progression, and recovery. Abnormally increased NETs in TRALI exacerbate damage to the endothelium and alveolar epithelium, and also influence other immune cells to produce proinflammatory mediators. This results in the coordination of various immune cells to sustain a detrimental inflammatory cycle. Several dysfunctions associated with TRALI pathophysiological processes create a favorable microenvironment for the formation and release of NETs, such as the feedforward activation of endothelial cells, and the oxygen-rich and glucose-deficient lung environment. Consequently, there is a clear need to explore the multifaceted biological processes of neutrophils and broader immune interactions, with a specific focus on NET formation and further regulation in the context of TRALI.

Author contributions

YL: Conceptualization, Methodology, Writing – original draft. RW: Conceptualization, Methodology, Writing – original draft. CS: Conceptualization, Methodology, Writing – original draft. SD: Methodology, Writing – original draft. YZ: Methodology, Writing – original draft. KY: Methodology, Writing – original draft. NL: Funding acquisition, Supervision, Writing – review & editing. BW: Funding acquisition, Supervision, Writing – review & editing. QG: Funding acquisition, Supervision, Writing – review & editing.

Funding

The author(s) declare financial support was received for the research, authorship, and/or publication of this article. This work was supported by grants from the National Natural Science Foundation of China (No. 8210082163, 81800343), the Fundamental Research Funds for the Central Universities (No. 2042021kf0081).

Conflict of interest

The authors declare that the research was conducted in the absence of any commercial or financial relationships that could be construed as a potential conflict of interest.

Publisher's note

All claims expressed in this article are solely those of the authors and do not necessarily represent those of their affiliated organizations, or those of the publisher, the editors and the reviewers. Any product that may be evaluated in this article, or claim that may be made by its manufacturer, is not guaranteed or endorsed by the publisher.

References

1. Vlaar APJ, Toy P, Fung M, Looney MR, Juffermans NP, Bux J, et al. A consensus redefinition of transfusion-related acute lung injury. *Transfusion* (2019) 59(7):2465–76. doi: 10.1111/trf.15311

2. Semple JW, Rebetz J, Kapur R. Transfusion-associated circulatory overload and transfusion-related acute lung injury. *Blood* (2019) 133(17):1840–53. doi: 10.1182/blood-2018-10-860809

3. Peters AL, Van Stein D, Vlaar AP. Antibody-mediated transfusion-related acute lung injury; from discovery to prevention. *Br J Haematol* (2015) 170(5):597–614. doi: 10.1111/bjh.13459

4. Toy P, Gajic O, Bacchetti P, Looney MR, Gropper MA, Hubmayr R, et al. Transfusion-related acute lung injury: incidence and risk factors. *Blood* (2012) 119 (7):1757–67. doi: 10.1182/blood-2011-08-370932

5. Schmickl CN, Mastrobuoni S, Filippidis FT, Shah S, Radic J, Murad MH, et al. Male-predominant plasma transfusion strategy for preventing transfusion-related acute lung injury: a systematic review. *Crit Care Med* (2015) 43(1):205–25. doi: 10.1097/CCM.0000000000000675

6. Silliman CC. The two-event model of transfusion-related acute lung injury. *Crit Care Med* (2006) 34(5 Suppl):S124–31. doi: 10.1097/01.CCM.0000214292.62276.8E

7. Silliman CC, Kelher MR, Khan SY, LaSarre M, West FB, Land KJ, et al. Experimental prestorage filtration removes antibodies and decreases lipids in RBC supernatants mitigating TRALI in *vivo*. *Blood* (2014) 123(22):3488–95. doi: 10.1182/blood-2013-10-532424

8. Xie R, Yang Y, Zhu Y, Gao L, Jiang X, Sun J, et al. Microparticles in red cell concentrates prime polymorphonuclear neutrophils and cause acute lung injury in a two-event mouse model. *Int Immunopharmacol* (2018) 55:98–104. doi: 10.1016/j.intimp.2017.11.029

9. Peters AL, van Hezel ME, Cortjens B, Tuip-de Boer AM, van Bruggen R, de Korte D, et al. Transfusion of 35-day stored RBCs in the presence of endotoxemia does not result in lung injury in humans. *Crit Care Med* (2016) 44(6):e412–9. doi: 10.1097/CCM.0000000000001614

10. Peters AL, Vervaart MA, van Bruggen R, de Korte D, Nieuwland R, Kulik W, et al. Non-polar lipids accumulate during storage of transfusion products and do not

contribute to the onset of transfusion-related acute lung injury. *Vox Sang* (2017) 112 (1):25–32. doi: 10.1111/vox.12453

11. Tung JP, Chiaretti S, Dean MM, Sultana AJ, Reade MC, Fung YL. Transfusion-related acute lung injury (TRALI): Potential pathways of development, strategies for prevention and treatment, and future research directions. *Blood Rev* (2022) 53:100926. doi: 10.1016/j.blre.2021.100926

12. Burn GL, Foti A, Marsman G, Patel DF, Zychlinsky A. The neutrophil. *Immunity* (2021) 54(7):1377–91. doi: 10.1016/j.immuni.2021.06.006

13. Papayannopoulos V. Neutrophil extracellular traps in immunity and disease. *Nat Rev Immunol* (2018) 18(2):134–47. doi: 10.1038/nri.2017.105

14. Metzler KD, Goosmann C, Lubojemska A, Zychlinsky A, Papayannopoulos V. A myeloperoxidase-containing complex regulates neutrophil elastase release and actin dynamics during NETosis. *Cell Rep* (2014) 8(3):883–96. doi: 10.1016/j.celrep.2014.06.044

15. Goldspink A, Schmitz J, Babyak O, Brauns N, Milleck J, Breloh AM, et al. Kidney medullary sodium chloride concentrations induce neutrophil and monocyte extracellular DNA traps that defend against pyelonephritis. *vivo Kidney Int* (2023) 104(2):279–92. doi: 10.1016/j.kint.2023.03.034

16. Torres Caban CC, Yang M, Lai C, Yang L, Subach FV, Smith BO, et al. Tuning the sensitivity of genetically encoded fluorescent potassium indicators through structure-guided and genome mining strategies. *ACS Sens* (2022) 7(5):1336–46. doi: 10.1021/acssensors.1c02201

17. Wang Y, Li M, Stadler S, Correll S, Li P, Wang D, et al. Histone hypercitrullination mediates chromatin decondensation and neutrophil extracellular trap formation. *J Cell Biol* (2009) 184(2):205–13. doi: 10.1083/jcb.200806072

18. Pilsczek FH, Salina D, Poon KK, Fahey C, Yipp BG, Sibley CD, et al. A novel mechanism of rapid nuclear neutrophil extracellular trap formation in response to Staphylococcus aureus. *J Immunol* (2010) 185(12):7413–25. doi: 10.4049/jimmunol.1000675

19. Yipp BG, Petri B, Salina D, Jenne CN, Scott BN, Zbytnuik LD, et al. Infection-induced NETosis is a dynamic process involving neutrophil multitasking in *vivo*. *Nat Med* (2012) 18(9):1386–93. doi: 10.1038/nm.2847

20. Yousefi S, Mihalache C, Kozlowski E, Schmid I, Simon HU. Viable neutrophils release mitochondrial DNA to form neutrophil extracellular traps. *Cell Death Differ* (2009) 16(11):1438–44. doi: 10.1038/cdd.2009.96

21. Lood C, Blanco LP, Purmalek MM, Carmona-Rivera C, De Ravin SS, Smith CK, et al. Neutrophil extracellular traps enriched in oxidized mitochondrial DNA are interferogenic and contribute to lupus-like disease. *Nat Med* (2016) 22(2):146–53. doi: 10.1038/nm.4027

22. Brinkmann V, Reichard U, Goosmann C, Fauler B, Uhlemann Y, Weiss DS, et al. Neutrophil extracellular traps kill bacteria. *Science* (2004) 303(5663):1532–5. doi: 10.1126/science.1092385

23. Jaillon S, Peri G, Delneste Y, Fremaux I, Doni A, Moalli F, et al. The humoral pattern recognition receptor PTX3 is stored in neutrophil granules and localizes in extracellular traps. *J Exp Med* (2007) 204(4):793–804. doi: 10.1084/jem.20061301

24. Lauth X, von Kockritz-Blickwede M, McNamara CW, Myskowski S, Zinkernagel AS, Beall B, et al. M1 protein allows Group A streptococcal survival in phagocyte extracellular traps through cathelicidin inhibition. *J Innate Immun* (2009) 1(3):202–14. doi: 10.1159/000203645

25. Urban CF, Ermert D, Schmid M, Abu-Abed U, Goosmann C, Nacken W, et al. Neutrophil extracellular traps contain calprotectin, a cytosolic protein complex involved in host defense against Candida albicans. *PLoS Pathog* (2009) 5(10): e1000639. doi: 10.1371/journal.ppat.1000639

26. Wigerblad G, Kaplan MJ. Neutrophil extracellular traps in systemic autoimmune and autoinflammatory diseases. *Nat Rev Immunol* (2023) 23(5):274–88. doi: 10.1038/s41577-022-00787-0

27. Herre M, Cedervall J, Mackman N, Olsson AK. Neutrophil extracellular traps in the pathology of cancer and other inflammatory diseases. *Physiol Rev* (2023) 103 (1):277–312. doi: 10.1152/physrev.00062.2021

28. Doring Y, Libby P, Soehnlein O. Neutrophil extracellular traps participate in cardiovascular diseases: recent experimental and clinical insights. *Circ Res* (2020) 126 (9):1228–41. doi: 10.1161/CIRCRESAHA.120.315931

29. Mistry P, Nakabo S, O'Neil L, Goel RR, Jiang K, Carmona-Rivera C, et al. Transcriptomic, epigenetic, and functional analyses implicate neutrophil diversity in the pathogenesis of systemic lupus erythematosus. *Proc Natl Acad Sci USA* (2019) 116 (50):25222–8. doi: 10.1073/pnas.1908576116

30. Chapman EA, Lyon M, Simpson D, Mason D, Beynon RJ, Moots RJ, et al. Caught in a trap? Proteomic analysis of neutrophil extracellular traps in rheumatoid arthritis and systemic lupus erythematosus. *Front Immunol* (2019) 10:423. doi: 10.3389/fimmu.2019.00423

31. Li T, Wang C, Liu Y, Li B, Zhang W, Wang L, et al. Neutrophil extracellular traps induce intestinal damage and thrombotic tendency in inflammatory bowel disease. *J Crohns Colitis* (2020) 14(2):240–53. doi: 10.1093/ecco-jcc/jjz132

32. Schauer C, Janko C, Munoz LE, Zhao Y, Kienhofer D, Frey B, et al. Aggregated neutrophil extracellular traps limit inflammation by degrading cytokines and chemokines. *Nat Med* (2014) 20(5):511–7. doi: 10.1038/nm.3547

33. Caudrillier A, Kessenbrock K, Gilliss BM, Nguyen JX, Marques MB, Monestier M, et al. Platelets induce neutrophil extracellular traps in transfusion-related acute lung injury. *J Clin Invest* (2012) 122(7):2661–71. doi: 10.1172/JCI61303

34. Xu J, Zhang X, Pelayo R, Monestier M, Ammollo CT, Semeraro F, et al. Extracellular histones are major mediators of death in sepsis. *Nat Med* (2009) 15 (11):1318–21. doi: 10.1038/nm.2053

35. McDonald B, Davis RP, Kim SJ, Tse M, Esmon CT, Kolaczkowska E, et al. Platelets and neutrophil extracellular traps collaborate to promote intravascular coagulation during sepsis in mice. *Blood* (2017) 129(10):1357–67. doi: 10.1182/blood-2016-09-741298

36. Le A, Wu Y, Liu W, Wu C, Hu P, Zou J, et al. MiR-144-induced KLF2 inhibition and NF-kappaB/CXCR1 activation promote neutrophil extracellular trap-induced transfusion-related acute lung injury. *J Cell Mol Med* (2021) 25(14):6511–23. doi: 10.1111/jcmm.16650

37. Thomas GM, Carbo C, Curtis BR, Martinod K, Mazo IB, Schatzberg D, et al. Extracellular DNA traps are associated with the pathogenesis of TRALI in humans and mice. *Blood* (2012) 119(26):6335–43. doi: 10.1182/blood-2012-01-405183

38. van Hezel ME, Boshuizen M, Peters AL, Straat M, Vlaar AP, Spoelstra-de Man AME, et al. Red blood cell transfusion results in adhesion of neutrophils in human endotoxemia and in critically ill patients with sepsis. *Transfusion* (2020) 60(2):294–302. doi: 10.1111/trf.15613

39. Kono M, Saigo K, Takagi Y, Takahashi T, Kawauchi S, Wada A, et al. Heme-related molecules induce rapid production of neutrophil extracellular traps. *Transfusion* (2014) 54(11):2811–9. doi: 10.1111/trf.12700

40. Kono M, Saigo K, Takagi Y, Kawauchi S, Wada A, Hashimoto M, et al. Morphological and flow-cytometric analysis of haemin-induced human neutrophil activation: implications for transfusion-related acute lung injury. *Blood Transfus* (2013) 11(1):53–60. doi: 10.2450/2012.0141-11

41. Santoni K, Pericat D, Gorse L, Buyck J, Pinilla M, Prouvensier L, et al. Caspase-1-driven neutrophil pyroptosis and its role in host susceptibility to Pseudomonas aeruginosa. *PloS Pathog* (2022) 18(7):e1010305. doi: 10.1371/journal.ppat.1010305

42. Chen KW, Gross CJ, Sotomayor FV, Stacey KJ, Tschopp J, Sweet MJ, et al. The neutrophil NLRC4 inflammasome selectively promotes IL-1beta maturation without pyroptosis during acute Salmonella challenge. *Cell Rep* (2014) 8(2):570–82. doi: 10.1016/j.celrep.2014.06.028

43. Karmakar M, Minns M, Greenberg EN, Diaz-Aponte J, Pestonjamasp K, Johnson JL, et al. N-GSDMD trafficking to neutrophil organelles facilitates IL-1beta release independently of plasma membrane pores and pyroptosis. *Nat Commun* (2020) 11(1):2212. doi: 10.1038/s41467-020-16043-9

44. Kovacs SB, Oh C, Maltez VI, McGlaughon BD, Verma A, Miao EA, et al. Neutrophil caspase-11 is essential to defend against a cytosol-invasive bacterium. *Cell Rep* (2020) 32(4):107967. doi: 10.1016/j.celrep.2020.107967

45. Yang S, Feng Y, Chen L, Wang Z, Chen J, Ni Q, et al. Disulfiram accelerates diabetic foot ulcer healing by blocking NET formation via suppressing the NLRP3/Caspase-1/GSDMD pathway. *Transl Res* (2023) 254:115–27. doi: 10.1016/j.trsl.2022.10.008

46. Munzer P, Negro R, Fukui S, di Meglio L, Aymonnier K, Chu L, et al. NLRP3 inflammasome assembly in neutrophils is supported by PAD4 and promotes NETosis under sterile conditions. *Front Immunol* (2021) 12:683803. doi: 10.3389/fimmu.2021.683803

47. Aymonnier K, Ng J, Fredenburgh LE, Zambrano-Vera K, Munzer P, Gutch S, et al. Inflammasome activation in neutrophils of patients with severe COVID-19. *Blood Adv* (2022) 6(7):2001–13. doi: 10.1182/bloodadvances.2021005949

48. Chen KW, Monteleone M, Boucher D, Sollberger G, Ramnath D, Condon ND, et al. Noncanonical inflammasome signaling elicits gasdermin D-dependent neutrophil extracellular traps. *Sci Immunol* (2018) 3(26). doi: 10.1126/sciimmunol.aar6676

49. Kambara H, Liu F, Zhang X, Liu P, Bajrami B, Teng Y, et al. Gasdermin D exerts anti-inflammatory effects by promoting neutrophil death. *Cell Rep* (2018) 22(11):2924–36. doi: 10.1016/j.celrep.2018.02.067

50. Shi J, Zhao Y, Wang K, Shi X, Wang Y, Huang H, et al. Cleavage of GSDMD by inflammatory caspases determines pyroptotic cell death. *Nature* (2015) 526(7575):660–5. doi: 10.1038/nature15514

51. Sollberger G, Choidas A, Burn GL, Habenberger P, Di Lucrezia R, Kordes S, et al. Gasdermin D plays a vital role in the generation of neutrophil extracellular traps. *Sci Immunol* (2018) 3(26). doi: 10.1126/sciimmunol.aar6689

52. Zhao C, Liang F, Ye M, Wu S, Qin Y, Zhao L, et al. GSDMD promotes neutrophil extracellular traps via mtDNA-cGAS-STING pathway during lung ischemia/reperfusion. *Cell Death Discov* (2023) 9(1):368. doi: 10.1038/s41420-023-01663-z

53. Suksawad N, Udompornpitak K, Thawinpipat N, Korwattanamongkol P, Visitchanakun P, Phuengmaung P, et al. Cyclic GMP-AMP synthase (cGAS) deletion reduces severity in bilateral nephrectomy mice through changes in neutrophil extracellular traps and mitochondrial respiration. *Biomedicines* (2023) 11 (4). doi: 10.3390/biomedicines11041208

54. Chauhan D, Demon D, Vande Walle L, Paerewijck O, Zecchin A, Bosseler L, et al. GSDMD drives canonical inflammasome-induced neutrophil pyroptosis and is dispensable for NETosis. *EMBO Rep* (2022) 23(10):e54277. doi: 10.15252/embr.202154277

55. Stojkov D, Claus MJ, Kozlowski E, Oberson K, Scharen OP, Benarafa C, et al. NET formation is independent of gasdermin D and pyroptotic cell death. *Sci Signal* (2023) 16(769):eabm0517. doi: 10.1126/scisignal.abm0517

56. van Raam BJ, Sluiter W, de Wit E, Roos D, Verhoeven AJ, Kuijpers TW. Mitochondrial membrane potential in human neutrophils is maintained by complex III activity in the absence of supercomplex organisation. *PLoS One* (2008) 3(4):e2013. doi: 10.1371/journal.pone.0002013

57. Lambeth JD, Neish AS. Nox enzymes and new thinking on reactive oxygen: a double-edged sword revisited. *Annu Rev Pathol* (2014) 9:119–45. doi: 10.1146/annurev-pathol-012513-104651

58. Rodriguez-Espinosa O, Rojas-Espinosa O, Moreno-Altamirano MM, Lopez-Villegas EO, Sanchez-Garcia FJ. Metabolic requirements for neutrophil extracellular traps formation. *Immunology* (2015) 145(2):213–24. doi: 10.1111/imm.12437

59. Awasthi D, Nagarkoti S, Sadaf S, Chandra T, Kumar S, Dikshit M. Glycolysis dependent lactate formation in neutrophils: A metabolic link between NOX-dependent and independent NETosis. *Biochim Biophys Acta Mol Basis Dis* (2019) 1865 (12):165542. doi: 10.1016/j.bbadis.2019.165542

60. Liu D, Xiao M, Zhou J, Wang P, Peng J, Mao W, et al. PFKFB3 promotes sepsis-induced acute lung injury by enhancing NET formation by CXCR4(hi) neutrophils. *Int Immunopharmacol* (2023) 123:110737. doi: 10.1016/j.intimp.2023.110737

61. Azevedo EP, Rochael NC, Guimaraes-Costa AB, de Souza-Vieira TS, Ganilho J, Saraiva EM, et al. A metabolic shift toward pentose phosphate pathway is necessary for amyloid fibril- and phorbol 12-myristate 13-acetate-induced neutrophil extracellular trap (NET) formation. *J Biol Chem* (2015) 290(36):22174–83. doi: 10.1074/jbc.M115.640094

62. Ghergurovich JM, Garcia-Canaveras JC, Wang J, Schmidt E, Zhang Z, TeSlaa T, et al. A small molecule G6PD inhibitor reveals immune dependence on pentose phosphate pathway. *Nat Chem Biol* (2020) 16(7):731–9. doi: 10.1038/s41589-020-0533-x

63. Britt EC, Lika J, Giese MA, Schoen TJ, Seim GL, Huang Z, et al. Switching to the cyclic pentose phosphate pathway powers the oxidative burst in activated neutrophils. *Nat Metab* (2022) 4(3):389–403. doi: 10.1038/s42255-022-00550-8

64. Amara N, Cooper MP, Voronkova MA, Webb BA, Lynch EM, Kollman JM, et al. Selective activation of PFKL suppresses the phagocytic oxidative burst. *Cell* (2021) 184 (17):4480–94.e15. doi: 10.1016/j.cell.2021.07.004

65. Leppkes M, Knopf J, Naschberger E, Lindemann A, Singh J, Herrmann I, et al. Vascular occlusion by neutrophil extracellular traps in COVID-19. *EBioMedicine* (2020) 58:102925. doi: 10.1016/j.ebiom.2020.102925

66. Borella R, De Biasi S, Paolini A, Boraldi F, Lo Tartaro D, Mattioli M, et al. Metabolic reprograming shapes neutrophil functions in severe COVID-19. *Eur J Immunol* (2022) 52(3):484–502. doi: 10.1002/eji.202149481

67. Sadiku P, Willson JA, Dickinson RS, Murphy F, Harris AJ, Lewis A, et al. Prolyl hydroxylase 2 inactivation enhances glycogen storage and promotes excessive neutrophilic responses. *J Clin Invest* (2017) 127(9):3407–20. doi: 10.1172/JCI90848

68. Domer D, Walther T, Moller S, Behnen M, Laskay T. Neutrophil extracellular traps activate proinflammatory functions of human neutrophils. *Front Immunol* (2021) 12:636954. doi: 10.3389/fimmu.2021.636954

69. Douda DN, Khan MA, Grasemann H, Palaniyar N. SK3 channel and mitochondrial ROS mediate NADPH oxidase-independent NETosis induced by calcium influx. *Proc Natl Acad Sci USA* (2015) 112(9):2817–22. doi: 10.1073/pnas.1414055112

70. Li Y, Hook JS, Ding Q, Xiao X, Chung SS, Mettlen M, et al. Neutrophil metabolomics in severe COVID-19 reveal GAPDH as a suppressor of neutrophil extracellular trap formation. *Nat Commun* (2023) 14(1):2610. doi: 10.1038/s41467-023-37567-w

71. Warnatsch A, Ioannou M, Wang Q, Papayannopoulos V. Inflammation. Neutrophil extracellular traps license macrophages for cytokine production in atherosclerosis. *Science* (2015) 349(6245):316–20. doi: 10.1126/science.aaa8064

72. Liu D, Yang P, Gao M, Yu T, Shi Y, Zhang M, et al. NLRP3 activation induced by neutrophil extracellular traps sustains inflammatory response in the diabetic wound. *Clin Sci (Lond)* (2019) 133(4):565–82. doi: 10.1042/CS20180600

73. Schneider AH, MaChado CC, Veras FP, Maganin AGM, de Souza FFL, Barroso LC, et al. Neutrophil extracellular traps mediate joint hyperalgesia induced by immune inflammation. *Rheumatol (Oxford)* (2021) 60(7):3461–73. doi: 10.1093/rheumatology/keaa794

74. Wang Y, Li Y, Chen Z, Yuan Y, Su Q, Ye K, et al. GSDMD-dependent neutrophil extracellular traps promote macrophage-to-myofibroblast transition and renal fibrosis in obstructive nephropathy. *Cell Death Dis* (2022) 13(8):693. doi: 10.1038/s41419-022-05138-4

75. Lin T, Hu L, Hu F, Li K, Wang CY, Zong LJ, et al. NET-triggered NLRP3 activation and IL18 release drive oxaliplatin-induced peripheral neuropathy. *Cancer Immunol Res* (2022) 10(12):1542–58. doi: 10.1158/2326-6066.CIR-22-0197

76. Chen L, Zhao Y, Lai D, Zhang P, Yang Y, Li Y, et al. Neutrophil extracellular traps promote macrophage pyroptosis in sepsis. *Cell Death Dis* (2018) 9(6):597. doi: 10.1038/s41419-017-0090-8

77. Sano M, Maejima Y, Nakagama S, Shiheido-Watanabe Y, Tamura N, Hirao K, et al. Neutrophil extracellular traps-mediated Beclin-1 suppression aggravates atherosclerosis by inhibiting macrophage autophagy. *Front Cell Dev Biol* (2022) 10:876147. doi: 10.3389/fcell.2022.876147

78. Yalcinkaya M, Fotakis P, Liu W, Endo-Umeda K, Dou H, Abramowicz S, et al. Cholesterol accumulation in macrophages drives NETosis in atherosclerotic plaques via IL-1beta secretion. *Cardiovasc Res* (2023) 119(4):969–81. doi: 10.1093/cvr/cvac189

79. Cui Y, Yang Y, Tao W, Peng W, Luo D, Zhao N, et al. Neutrophil extracellular traps induce alveolar macrophage pyroptosis by regulating NLRP3 deubiquitination, aggravating the development of septic lung injury. *J Inflamm Res* (2023) 16:861–77. doi: 10.2147/JIR.S366436

80. Wei X, Zou S, Xie Z, Wang Z, Huang N, Cen Z, et al. EDIL3 deficiency ameliorates adverse cardiac remodelling by neutrophil extracellular traps (NET)-mediated macrophage polarization. *Cardiovasc Res* (2022) 118(9):2179–95. doi: 10.1093/cvr/cvab269

81. Shi G, Liu L, Cao Y, Ma G, Zhu Y, Xu J, et al. Inhibition of neutrophil extracellular trap formation ameliorates neuroinflammation and neuronal apoptosis via STING-dependent IRE1alpha/ASK1/JNK signaling pathway in mice with traumatic brain injury. *J Neuroinflamm* (2023) 20(1):222. doi: 10.1186/s12974-023-02903-w

82. Apel F, Andreeva L, Knackstedt LS, Streeck R, Frese CK, Goosmann C, et al. The cytosolic DNA sensor cGAS recognizes neutrophil extracellular traps. *Sci Signal* (2021) 14(673). doi: 10.1126/scisignal.aax7942

83. Farrera C, Fadeel B. Macrophage clearance of neutrophil extracellular traps is a silent process. *J Immunol* (2013) 191(5):2647–56. doi: 10.4049/jimmunol.1300436

84. Lazzaretto B, Fadeel B. Intra- and extracellular degradation of neutrophil extracellular traps by macrophages and dendritic cells. *J Immunol* (2019) 203 (8):2276–90. doi: 10.4049/jimmunol.1800159

85. Haider P, Kral-Pointner JB, Mayer J, Richter M, Kaun C, Brostjan C, et al. Neutrophil extracellular trap degradation by differently polarized macrophage subsets. *Arterioscler Thromb Vasc Biol* (2020) 40(9):2265–78. doi: 10.1161/ATVBAHA.120.314883

86. Gregoire M, Uhel F, LesouHaitier M, Gacouin A, Guirriec M, Mourcin F, et al. Impaired efferocytosis and neutrophil extracellular trap clearance by macrophages in ARDS. *Eur Respir J* (2018) 52(2). doi: 10.1183/13993003.02590-2017

87. Manda-Handzlik A, Cieloch A, Kuzmicka W, Mroczek A, Stelmaszczyk-Emmel A, Demkow U, et al. Secretomes of M1 and M2 macrophages decrease the release of neutrophil extracellular traps. *Sci Rep* (2023) 13(1):15633. doi: 10.1038/s41598-023-42167-1

88. Jiao Y, Zhang T, Liu M, Zhou L, Qi M, Xie X, et al. Exosomal PGE2 from M2 macrophages inhibits neutrophil recruitment and NET formation through lipid mediator class switching in sepsis. *J BioMed Sci* (2023) 30(1):62. doi: 10.1186/s12929-023-00957-9

89. Swiecki M, Colonna M. The multifaceted biology of plasmacytoid dendritic cells. *Nat Rev Immunol* (2015) 15(8):471–85. doi: 10.1038/nri3865

90. Lande R, Gregorio J, Facchinetti V, Chatterjee B, Wang YH, Homey B, et al. Plasmacytoid dendritic cells sense self-DNA coupled with antimicrobial peptide. *Nature* (2007) 449(7162):564–9. doi: 10.1038/nature06116

91. Lande R, Ganguly D, Facchinetti V, Frasca L, Conrad C, Gregorio J, et al. Neutrophils activate plasmacytoid dendritic cells by releasing self-DNA-peptide complexes in systemic lupus erythematosus. *Sci Transl Med* (2011) 3(73):73ra19. doi: 10.1126/scitranslmed.3001180

92. Knight JS, Luo W, O'Dell AA, Yalavarthi S, Zhao W, Subramanian V, et al. Peptidylarginine deiminase inhibition reduces vascular damage and modulates innate immune responses in murine models of atherosclerosis. *Circ Res* (2014) 114(6):947–56. doi: 10.1161/CIRCRESAHA.114.303312

93. Garcia-Romo GS, Caielli S, Vega B, Connolly J, Allantaz F, Xu Z, et al. Netting neutrophils are major inducers of type I IFN production in pediatric systemic lupus erythematosus. *Sci Transl Med* (2011) 3(73):73ra20. doi: 10.1126/scitranslmed.3001201

94. Doring Y, Manthey HD, Drechsler M, Lievens D, Megens RT, Soehnlein O, et al. Auto-antigenic protein-DNA complexes stimulate plasmacytoid dendritic cells to promote atherosclerosis. *Circulation* (2012) 125(13):1673–83. doi: 10.1161/CIRCULATIONAHA.111.046755

95. Qiu SL, Zhang H, Tang QY, Bai J, He ZY, Zhang JQ, et al. Neutrophil extracellular traps induced by cigarette smoke activate plasmacytoid dendritic cells. *Thorax* (2017) 72(12):1084–93. doi: 10.1136/thoraxjnl-2016-209887

96. Zhang H, Qiu SL, Tang QY, Zhou X, Zhang JQ, He ZY, et al. Erythromycin suppresses neutrophil extracellular traps in smoking-related chronic pulmonary inflammation. *Cell Death Dis* (2019) 10(9):678. doi: 10.1038/s41419-019-1909-2

97. de Bont CM, Boelens WC, Pruijn GJM. NETosis, complement, and coagulation: a triangular relationship. *Cell Mol Immunol* (2019) 16(1):19–27. doi: 10.1038/s41423-018-0024-0

98. Palmer LJ, Damgaard C, Holmstrup P, Nielsen CH. Influence of complement on neutrophil extracellular trap release induced by bacteria. *J Periodontal Res* (2016) 51 (1):70–6. doi: 10.1111/jre.12284

99. Liu X, Wang Y, Bauer AT, Kirschfink M, Ding P, Gebhardt C, et al. Neutrophils activated by membrane attack complexes increase the permeability of melanoma blood vessels. *Proc Natl Acad Sci USA* (2022) 119(33):e2122716119. doi: 10.1073/pnas.2122716119

100. Cleary SJ, Kwaan N, Tian JJ, Calabrese DR, Mallavia B, Magnen M, et al. Complement activation on endothelium initiates antibody-mediated acute lung injury. *J Clin Invest* (2020) 130(11):5909–23. doi: 10.1172/JCI138136

101. Silva BM, Gomes GF, Veras FP, Cambier S, Silva GV, Quadros AU, et al. C5aR1 signaling triggers lung immunopathology in COVID-19 through neutrophil extracellular traps. *J Clin Invest* (2023) 133(12). doi: 10.1172/JCI163105

102. van der Velden S, van Osch TLJ, Seghier A, Bentlage A, Mok JY, Geerdes DM, et al. Complement activation drives Transfusion-related acute lung injury via macrophage trafficking and formation of NETs. *Blood* (2023). doi: 10.1182/blood.2023020484

103. Chen Y, Li X, Lin X, Liang H, Liu X, Zhang X, et al. Complement C5a induces the generation of neutrophil extracellular traps by inhibiting mitochondrial STAT3 to promote the development of arterial thrombosis. *Thromb J* (2022) 20(1):24. doi: 10.1186/s12959-022-00384-0

104. Leffler J, Martin M, Gullstrand B, Tyden H, Lood C, Truedsson L, et al. Neutrophil extracellular traps that are not degraded in systemic lupus erythematosus activate complement exacerbating the disease. *J Immunol* (2012) 188(7):3522–31. doi: 10.4049/jimmunol.1102404

105. Wang H, Wang C, Zhao MH, Chen M. Neutrophil extracellular traps can activate alternative complement pathways. *Clin Exp Immunol* (2015) 181(3):518–27. doi: 10.1111/cei.12654

106. Yuen J, Pluthero FG, Douda DN, Riedl M, Cherry A, Ulanova M, et al. NETosing neutrophils activate complement both on their own NETs and bacteria via alternative and non-alternative pathways. *Front Immunol* (2016) 7:137. doi: 10.3389/fimmu.2016.00137

107. O'Flynn J, Dixon KO, Faber Krol MC, Daha MR, van Kooten C. Myeloperoxidase directs properdin-mediated complement activation. *J Innate Immun* (2014) 6(4):417–25. doi: 10.1159/000356980

108. Zhao Z, Pan Z, Zhang S, Ma G, Zhang W, Song J, et al. Neutrophil extracellular traps: A novel target for the treatment of stroke. *Pharmacol Ther* (2023) 241:108328. doi: 10.1016/j.pharmthera.2022.108328

109. Cristinziano L, Modestino L, Antonelli A, Marone G, Simon HU, Varricchi G, et al. Neutrophil extracellular traps in cancer. *Semin Cancer Biol* (2022) 79:91–104. doi: 10.1016/j.semcancer.2021.07.011

110. Dos Santos Ramos A, Viana GCS, de Macedo Brigido M, Almeida JF. Neutrophil extracellular traps in inflammatory bowel diseases: Implications in pathogenesis and therapeutic targets. *Pharmacol Res* (2021) 171:105779. doi: 10.1016/j.phrs.2021.105779

111. Kolaczkowska E, Jenne CN, Surewaard BG, Thanabalasuriar A, Lee WY, Sanz MJ, et al. Molecular mechanisms of NET formation and degradation revealed by intravital imaging in the liver vasculature. *Nat Commun* (2015) 6:6673. doi: 10.1038/ncomms7673

112. Silva CMS, Wanderley CWS, Veras FP, Sonego F, Nascimento DC, Goncalves AV, et al. Gasdermin D inhibition prevents multiple organ dysfunction during sepsis by blocking NET formation. *Blood* (2021) 138(25):2702–13. doi: 10.1182/blood.2021011525

113. Silva CMS, Wanderley CWS, Veras FP, Goncalves AV, Lima MHF, Toller-Kawahisa JE, et al. Gasdermin-D activation by SARS-CoV-2 triggers NET and mediate COVID-19 immunopathology. *Crit Care* (2022) 26(1):206. doi: 10.1186/s13054-022-04062-5

114. Adrover JM, Carrau L, Daßler-Plenker J, Bram Y, Chandar V, Houghton S, et al. Disulfiram inhibits neutrophil extracellular trap formation and protects rodents from acute lung injury and SARS-CoV-2 infection. *JCI Insight* (2022) 7(5). doi: 10.1172/jci.insight.157342

115. Humphries F, Shmuel-Galia L, Ketelut-Carneiro N, Li S, Wang B, Nemmara VV, et al. Succination inactivates gasdermin D and blocks pyroptosis. *Science* (2020) 369(6511):1633–7. doi: 10.1126/science.abb9818

116. Han XA, Jie HY, Wang JH, Zhang XM, Wang J, Yu CX, et al. Necrostatin-1 ameliorates neutrophilic inflammation in asthma by suppressing MLKL phosphorylation to inhibiting NETs release. *Front Immunol* (2020) 11:666. doi: 10.3389/fimmu.2020.00666

117. Han X, Zhang X, Song R, Li S, Zou S, Tan Q, et al. Necrostatin-1 alleviates diffuse pulmonary haemorrhage by preventing the release of NETs via inhibiting NE/GSDMD activation in murine lupus. *J Immunol Res* (2023) 2023:4743975. doi: 10.1155/2023/4743975

118. Bertini R, Allegretti M, Bizzarri C, Moriconi A, Locati M, Zampella G, et al. Noncompetitive allosteric inhibitors of the inflammatory chemokine receptors CXCR1 and CXCR2: prevention of reperfusion injury. *Proc Natl Acad Sci USA* (2004) 101(32):11791–6. doi: 10.1073/pnas.0402090101

119. Weckbach LT, Grabmaier U, Uhl A, Gess S, Boehm F, Zehrer A, et al. Midkine drives cardiac inflammation by promoting neutrophil trafficking and NETosis in myocarditis. *J Exp Med* (2019) 216(2):350–68. doi: 10.1084/jem.20181102

120. Folco EJ, Mawson TL, Vromman A, Bernardes-Souza B, Franck G, Persson O, et al. Neutrophil extracellular traps induce endothelial cell activation and tissue factor production through interleukin-1alpha and cathepsin G. *Arterioscler Thromb Vasc Biol* (2018) 38(8):1901–12. doi: 10.1161/ATVBAHA.118.311150

121. Teijeira A, Garasa S, Gato M, Alfaro C, Migueliz I, Cirella A, et al. CXCR1 and CXCR2 chemokine receptor agonists produced by tumors induce neutrophil extracellular traps that interfere with immune cytotoxicity. *Immunity* (2020) 52(5):856–71.e8. doi: 10.1016/j.immuni.2020.03.001

122. Eelen G, de Zeeuw P, Simons M, Carmeliet P. Endothelial cell metabolism in normal and diseased vasculature. *Circ Res* (2015) 116(7):1231–44. doi: 10.1161/CIRCRESAHA.116.302855

123. Wu D, Huang RT, Hamanaka RB, Krause M, Oh MJ, Kuo CH, et al. HIF-1alpha is required for disturbed flow-induced metabolic reprogramming in human and porcine vascular endothelium. *Elife* (2017) 6. doi: 10.7554/eLife.25217

124. Schnitzler JG, Hoogeveen RM, Ali L, Prange KHM, Waissi F, van Weeghel M, et al. Atherogenic lipoprotein(a) increases vascular glycolysis, thereby facilitating inflammation and leukocyte extravasation. *Circ Res* (2020) 126(10):1346–59. doi: 10.1161/CIRCRESAHA.119.316206

125. Wang L, Cao Y, Gorshkov B, Zhou Y, Yang Q, Xu J, et al. Ablation of endothelial Pfkfb3 protects mice from acute lung injury in LPS-induced endotoxemia. *Pharmacol Res* (2019) 146:104292. doi: 10.1016/j.phrs.2019.104292

126. Cao Y, Zhang X, Wang L, Yang Q, Ma Q, Xu J, et al. PFKFB3-mediated endothelial glycolysis promotes pulmonary hypertension. *Proc Natl Acad Sci USA* (2019) 116(27):13394–403. doi: 10.1073/pnas.1821401116

127. Cantelmo AR, Conradi LC, Brajic A, Goveia J, Kalucka J, Pircher A, et al. Inhibition of the glycolytic activator PFKFB3 in endothelium induces tumor vessel normalization, impairs metastasis, and improves chemotherapy. *Cancer Cell* (2016) 30(6):968–85. doi: 10.1016/j.ccell.2016.10.006

128. Ziogas A, Sajib MS, Lim JH, Alves TC, Das A, Witt A, et al. Glycolysis is integral to histamine-induced endothelial hyperpermeability. *FASEB J* (2021) 35(3):e21425. doi: 10.1096/fj.202001634R

129. Gomez-Escudero J, Clemente C, Garcia-Weber D, Acin-Perez R, Millan J, Enriquez JA, et al. PKM2 regulates endothelial cell junction dynamics and angiogenesis via ATP production. *Sci Rep* (2019) 9(1):15022. doi: 10.1038/s41598-019-50866-x

130. Kim B, Jang C, Dharaneeswaran H, Li J, Bhide M, Yang S, et al. Endothelial pyruvate kinase M2 maintains vascular integrity. *J Clin Invest* (2018) 128(10):4543–56. doi: 10.1172/JCI120912

131. Wang L, Wu T, Yan S, Wang Y, An J, Wu C, et al. M1-polarized alveolar macrophages are crucial in a mouse model of transfusion-related acute lung injury. *Transfusion* (2020) 60(2):303–16. doi: 10.1111/trf.15609

132. Kapur R, Kasetty G, Rebetz J, Egesten A, Semple JW. Osteopontin mediates murine transfusion-related acute lung injury via stimulation of pulmonary neutrophil accumulation. *Blood* (2019) 134(1):74–84. doi: 10.1182/blood.2019000972

133. Sefik E, Qu R, Junqueira C, Kaffe E, Mirza H, Zhao J, et al. Inflammasome activation in infected macrophages drives COVID-19 pathology. *Nature* (2022) 606(7914):585–93. doi: 10.1038/s41586-022-04802-1

134. Yang HH, Duan JX, Liu SK, Xiong JB, Guan XX, Zhong WJ, et al. A COX-2/sEH dual inhibitor PTUPB alleviates lipopolysaccharide-induced acute lung injury in mice by inhibiting NLRP3 inflammasome activation. *Theranostics* (2020) 10(11):4749–61. doi: 10.7150/thno.43108

135. Luo D, Dai W, Feng X, Ding C, Shao Q, Xiao R, et al. Suppression of lncRNA NLRP3 inhibits NLRP3-triggered inflammatory responses in early acute lung injury. *Cell Death Dis* (2021) 12(10):898. doi: 10.1038/s41419-021-04180-y

136. Hu JJ, Liu X, Xia S, Zhang Z, Zhang Y, Zhao J, et al. FDA-approved disulfiram inhibits pyroptosis by blocking gasdermin D pore formation. *Nat Immunol* (2020) 21(7):736–45. doi: 10.1038/s41590-020-0669-6

137. Xie J, Zhu CL, Wan XJ, Zhao ZZ, Meng Y, Li P, et al. GSDMD-mediated NETosis promotes the development of acute respiratory distress syndrome. *Eur J Immunol* (2023) 53(1):e2250011. doi: 10.1002/eji.202250011

138. Zhang H, Xu X, Xu R, Ye T. Drug repurposing of ivermectin abrogates neutrophil extracellular traps and prevents melanoma metastasis. *Front Oncol* (2022) 12:989167. doi: 10.3389/fonc.2022.989167

139. Rathkey JK, Zhao J, Liu Z, Chen Y, Yang J, Kondolf HC, et al. Chemical disruption of the pyroptotic pore-forming protein gasdermin D inhibits inflammatory cell death and sepsis. *Sci Immunol* (2018) 3(26). doi: 10.1126/sciimmunol.aat2738

140. Skov L, Beurskens FJ, Zachariae CO, Reitamo S, Teeling J, Satijn D, et al. IL-8 as antibody therapeutic target in inflammatory diseases: reduction of clinical activity in palmoplantar pustulosis. *J Immunol* (2008) 181(1):669–79. doi: 10.4049/jimmunol.181.1.669

141. Alfaro C, Teijeira A, Onate C, Perez G, Sanmamed MF, Andueza MP, et al. Tumor-produced interleukin-8 attracts human myeloid-derived suppressor cells and elicits extrusion of neutrophil extracellular traps (NETs). *Clin Cancer Res* (2016) 22(15):3924–36. doi: 10.1158/1078-0432.CCR-15-2463

142. Gomes T, Varady CBS, Lourenco AL, Mizurini DM, Rondon AMR, Leal AC, et al. IL-1beta blockade attenuates thrombosis in a neutrophil extracellular trap-dependent breast cancer model. *Front Immunol* (2019) 10:2088. doi: 10.3389/fimmu.2019.02088

143. Zuber J, Fakhouri F, Roumenina LT, Loirat C, Fremeaux-Bacchi VFrench Study Group for a HCG. Use of eculizumab for atypical haemolytic uraemic syndrome and C3 glomerulopathies. *Nat Rev Nephrol* (2012) 8(11):643–57. doi: 10.1038/nrneph.2012.214

144. Jayne DRW, Merkel PA, Schall TJ, Bekker P, Group AS. Avacopan for the treatment of ANCA-associated vasculitis. *N Engl J Med* (2021) 384(7):599–609. doi: 10.1056/NEJMoa2023386

145. Baudel JL, Vigneron C, Pras-Landre V, Joffre J, Marjot F, Ait-Oufella H, et al. Transfusion-related acute lung injury (TRALI) after intravenous immunoglobulins: French multicentre study and literature review. *Clin Rheumatol* (2020) 39(2):541–6. doi: 10.1007/s10067-019-04832-7

10.3389/fimmu.2023.1324021

Appendix

The proteins/genes described in this review.

Proteins/targets	Abbreviations	Gene symbols
Human leukocyte antigen	HLA	*HLA*
Major histocompatibility complex	MHC	
Intercellular adhesion molecule 1	ICAM-1	*ICAM1*
Cathepsin G	/	*CTSD*
Neutrophil elastase	NE	*ELANE*
Myeloperoxidase	MPO	*MPO*
Lactotransferrin	/	*LTF*
LL-37	/	*CAMP*
Calprotectin	/	*S100A8, S100A9*
Pentraxin 3	/	*PTX3*
NOD-like receptor thermal protein domain associated protein 3	NLRP3	*NLRP3*
Apoptosis-associated speck-like protein containing a CARD	ASC	*PYCARD*
Cysteinyl aspartate specific proteinase-1	Caspase- 1	*CASP1*
Cysteinyl aspartate specific proteinase-11	Caspase- 11	*CASP11*
Cyclic guanosine monophosphate-adenosine monophosphate synthase	cGAS	*CGAS*
Stimulator of interferon response cGAMP interactor 1	STING1	*STING1*
6-phosphofructo-2-kinase/fructose-2,6-bisphosphatase	PFKFB3	*PFKFB3*
Pyruvate kinase M2	PKM2	*PKM*
Glucose-6-phosphate dehydrogenase	G6PD	*G6PD*
Glucose-6-phosphate isomerase	GPI	*GPI*
Phosphofructokinase 1	PFK-1	*PFKM/ PFKL/PFKP*
glyceraldehyde phosphate dehydrogenase	GAPDH	*GAPDH*
Interleukin- 1β	IL- 1β	*IL1B*
Interleukin- 8	IL-8	*IL8*
Interferon	IFN	*IFN*
Transforming growth factor-β	TGF-β	*TGFB1*
Toll-like receptor 4	TLR 4	*TLR 4*
Toll-like receptor 7	TLR 7	*TLR 7*
Toll-like receptor 9	TLR 9	*TLR 9*
Nuclear factor kappa-B	NF-κB	*NFKB1*
Thioredoxin-interacting protein	TXNIP	*TXNIP*
Beclin-1	/	*BECN1*
High-mobility group box 1	HMGB1	*HMGB1*
Receptor for advanced glycation end products	RAGE	*AGER*
Epidermal growth factor receptor	EGFR	*EGFR*
Adenosine 5'-monophosphate (AMP)-activated protein kinase	AMPK	*PRKAA, PRKAB, PRKAG*
CXC chemokine receptor 1/2	CXCR1/2	*CXCR1/2*
Deoxyribonuclease 1 like 3	DNase1L3	*DNASE1L3*
complement C3b/C4b receptor 1	CR1	*CR1*
VE cadherin	/	*CDH5*

frontiers | Frontiers in Immunology

TYPE Review
PUBLISHED 15 February 2024
DOI 10.3389/fimmu.2024.1352479

OPEN ACCESS

EDITED BY
Chung Nga Ko,
C-MER International Eye Research Center, China

REVIEWED BY
Yusuke Murakami,
Musashino University, Japan
Sandhya Bansal,
St. Joseph's Hospital and Medical Center, United States
Daniel Prantner,
University of Maryland, United States

*CORRESPONDENCE
Sutian Wang
wstlyt@126.com
Jianfeng Zhang
zhang-jianfeng@139.com

†These authors have contributed equally to this work

RECEIVED 08 December 2023
ACCEPTED 29 January 2024
PUBLISHED 15 February 2024

CITATION
Zhang K, Huang Q, Li X, Zhao Z, Hong C, Sun Z, Deng B, Li C, Zhang J and Wang S (2024) The cGAS-STING pathway in viral infections: a promising link between inflammation, oxidative stress and autophagy. *Front. Immunol.* 15:1352479. doi: 10.3389/fimmu.2024.1352479

The cGAS-STING pathway in viral infections: a promising link between inflammation, oxidative stress and autophagy

Kunli Zhang[1†], Qiuyan Huang[2,3†], Xinming Li[2], Ziqiao Zhao[1], Chun Hong[2], Zeyi Sun[1], Bo Deng[4], Chunling Li[1], Jianfeng Zhang[1,5*] and Sutian Wang[2,5*]

[1]State Key Laboratory of Swine and Poultry Breeding Industry, Institute of Animal Health, Guangdong Academy of Agricultural Sciences, Key Laboratory of Livestock Disease Prevention of Guangdong Province, Scientific Observation and Experiment Station of Veterinary Drugs and Diagnostic Techniques of Guangdong Province, Ministry of Agriculture and Rural Affairs, Guangzhou, China, [2]State Key Laboratory of Swine and Poultry Breeding Industry, Guangdong Key Laboratory of Animal Breeding and Nutrition, Institute of Animal Science, Guangdong Academy of Agricultural Sciences, Guangzhou, China, [3]College of Animal Science and Technology, Guangxi University, Nanning, China, [4]Division of Nephrology, Shanghai Ninth People's Hospital, Shanghai Jiao Tong University School of Medicine, Shanghai, China, [5]Maoming Branch, Guangdong Laboratory for Lingnan Modern Agriculture, Maoming, China

The host defence responses play vital roles in viral infection and are regulated by complex interactive networks. The host immune system recognizes viral pathogens through the interaction of pattern-recognition receptors (PRRs) with pathogen-associated molecular patterns (PAMPs). As a PRR mainly in the cytoplasm, cyclic GMP-AMP synthase (cGAS) senses and binds virus DNA and subsequently activates stimulator of interferon genes (STING) to trigger a series of intracellular signalling cascades to defend against invading pathogenic microorganisms. Integrated omic and functional analyses identify the cGAS-STING pathway regulating various host cellular responses and controlling viral infections. Aside from its most common function in regulating inflammation and type I interferon, a growing body of evidence suggests that the cGAS-STING signalling axis is closely associated with a series of cellular responses, such as oxidative stress, autophagy, and endoplasmic reticulum stress, which have major impacts on physiological homeostasis. Interestingly, these host cellular responses play dual roles in the regulation of the cGAS-STING signalling axis and the clearance of viruses. Here, we outline recent insights into cGAS-STING in regulating type I interferon, inflammation, oxidative stress, autophagy and endoplasmic reticulum stress and discuss their interactions with viral infections. A detailed understanding of the cGAS-STING-mediated potential antiviral effects contributes to revealing the pathogenesis of certain viruses and sheds light on effective solutions for antiviral therapy.

KEYWORDS

cGAS-STING, viral infection, innate immune, autophagy, inflammation, oxidative stress, virus-host interaction

1 Introduction

The innate immune system is the first line of defence against viral infections. The initiation of this early immune response depends on the recognition of certain viral structures known as pathogen-associated molecular patterns (PAMPs). Hosts' pattern recognition receptors (PRRs) recognize viral PAMPs, activating intracellular signalling pathways and inducing the expression of pro-inflammatory cytokines and antiviral genes that play antiviral effects. Through decades of research, six major classes of PRRs have been identified, including toll-like receptors (TLRs), retinoic acid-inducible gene (RIG)-I-like receptors (RLRs), NOD-like receptors (NLRs), C-type lectin receptors (CLRs), nucleic acid recognition receptors, and other innate immune receptors (such as scavenger receptors, complement receptors) (1, 2). These PRRs are mainly distributed on the cell surface, cytoplasm or lysosomes and induce innate immune responses and inflammatory responses through specific signal transduction pathways to promote virus clearance. In addition, the biological functions of PRRs have also included the activation of cells and complement, induction of cytophagy and cell death. Although the study of PRRs has been a hot area in immunology research, the role of these receptors in host defence and viral infection still needs to be further explored.

Interferon (IFN)-induced signalling pathway is the most important antiviral approach for the host and is activated by downstream signals of many PRRs (3, 4). Generally, binding of IFN to its receptor activates the downstream JAK-STAT pathway, resulting in increased transcription of IFN-stimulated genes (ISGs) (5). The ISG transcription proteins, such as myxovirus resistance (Mx), cholesterol 25-hydroxylase (CH25H) and oligoadenylate synthetase (OAS), play key roles in antiviral defences (6–8). In the early stages of viral infection, however, PRRs-mediated inflammatory response is also of great importance during antiviral processes. Interleukin-1 (IL-1) and tumour necrosis factor (TNF) can activate nuclear factor-κB (NF-κB) and induce IFN production, which further helps to remove viruses (9, 10). In addition, viral infection always affects cellular physiological states and metabolic processes, including oxidative stress, autophagy, and endoplasmic reticulum (ER) stress (11–13). Many studies have found that viral infections generally lead to a redox imbalance in the cellular environment (11). Oxidative stress is initially recognized as a means of combating viruses and protecting the host, contributing to apoptosis (14). However, with the development of research, more and more researchers found that oxidative stress promoted viral replication, which was a common mechanism used by some specific viruses (15). It is important to investigate the key molecular mechanisms used by viruses to interact with mitochondria and induce oxidative stress. As viruses need to use host cells to synthesize viral proteins, ER stress is always activated during viral infections. Understanding the complex mechanism of ER stress in viral infection is an important step in developing effective antiviral strategies. As an intracellular basic metabolic process (also known as type II programmed cell death), autophagy protects cells from toxic protein accumulation, organelle dysfunction, and viral infection by decomposing and recycling superfluous or potentially dangerous cytosolic entities. However, autophagy is a double-edged sword during viral infection. Studies have shown that some viruses have acquired the ability to hijack and subvert autophagy for their benefit (13). To sum up, all these factors affect the antiviral ability of the host.

As a newly identified PRR, cyclic GMP-AMP synthase (cGAS) recognizes viral, endogenous mitochondrial and genomic DNA in the cytoplasm and plays an important role in innate antiviral immunity (16). The conformation of cGAS changes upon binding to DNA, producing cGAMP, which is detected by the stimulator of interferon genes (STING) at the endoplasmic reticulum (17). Ishikawa and Barber have identified STING as an endoplasmic reticulum protein that has IFN-induced function in response to viral and intracellular DNA stimulation (18). The activated STING translocates to the Golgi apparatus, where it recruits TANK-binding kinase 1 (TBK1) and interferon regulatory factor 3 (IRF3) to form a complex (19). TBK1 then induces phosphorylation and oligomerization of IRF3. As a result, the activated IRF3 translocates into the nucleus, where it triggers the transcription of type I IFNs and ISGs that perform antiviral functions. Moreover, the cGAS-STING pathway is also involved in regulating the NF-κB-driven inflammatory immune response in vertebrate cells (20, 21). In addition, it has also been suggested that the cGAS-STING signalling axis is closely associated with oxidative stress, autophagy, and ER stress which affect the antiviral capability of the host (22–24). The inactivated STING is located in the endoplasmic reticulum, and the migration of activated STING is always accompanied by ER stress (25). Furthermore, ER stress can induce reactive oxygen species (ROS), which in turn, initiates the apoptotic process via constant oxidative stress (26). Additionally, the latest evidence suggests that the induction of autophagy is a highly conserved function of the cGAS-STING signalling axis (24). These researches suggest that these host cellular responses play significant roles in cGAS-STING-mediated viral infection. In this review, to further understand the regulatory mechanism among the cGAS-STING pathway, inflammation, IFN, oxidative stress, ER stress, and autophagy during viral infection, we discuss their interactions, which would facilitate revealing the pathogenesis of certain viruses and shed light on effective solutions for antiviral therapy.

2 Integrated omic and functional analyses identify the cGAS-STING pathway controlling viral infections and regulating various host defence responses

More and more multi-omics studies have confirmed the important role of cGAS-STING in the course of viral infections. Transcriptome analysis revealed that the expressions of IFNs (IFNA2, IFNA4, IFNA1, IFNA13, IFNB1, IFNL2 and IFNL3), ISGs (IFIT2, BST2, IRF7, OASL, MX1, IFITM1, IFIT2, IFI35, IFIH1, ISG15, CXCL10 and CXCL9) and pro-inflammatory cytokines (TNF, IL6, IL1B and IL1A) in skin from COVID-19 patients are significantly different from those of healthy donors (27). Further study found the activation of the cGAS-STING signal

was the main cause of this large amount of type I IFNs and pro-inflammatory cytokines. In addition, cell death induced by severe acute respiratory syndrome coronavirus 2 (SARS-CoV-2) infection was also attributed to cGAS-STING activity. A proteomic study revealed that many vital PRRs, including TLR2, RIG-I, MDA5 (melanoma differentiation-associated gene 5) and cGAS, were upregulated in Japanese encephalitis virus (JEV)-infected fibroblasts (28). Similar results are also reported in SARS-COV-2, Zika virus (ZIKV), and dengue virus (DENV) infection (29–31). By analysing the mass spectrometry-based proteomic characterization of post-translational modifications, many novel sites of cGAS were identified, which affected cGAS activity and signal transduction (32–34). Recently, an interesting study showed that the gut microbiota can mediate peripheral cGAS-STING activation, which promotes host resistance to systemic viral infections (35). This evidence shows that cGAS-STING plays a key role in host resistance to viral infection. Further functional studies revealed that the activated cGAS phosphorylates its downstream effector protein STING at the Ser365 position upon viral infection and subsequently promotes type I IFN production and ISGs expression via TBK1-IRF3 and JAK-STAT pathways. These factors and signals are generally considered the most effective antiviral approaches (16, 36). Depletion of cGAS and STING enhanced virus replication and spread, which further confirmed their antiviral roles (28, 37). Although cGAS and STING play pivotal roles in the recognition of viral DNA, more and more evidence indicates they also play crucial functions in the host's innate immune response against specific RNA viruses lacking DNA intermediates (38). Mice with a cGAS deficiency displayed heightened susceptibility to West Nile virus (WNV), a positive sense single-stranded RNA virus (36). The absence of cGAS likely results in a reduction of basal transcript levels of specific antiviral genes, making cells more susceptible to WNV infection. Simultaneously, mice lacking STING exhibit heightened susceptibility to RNA viral infections, and STING-deficient cells manifest an impaired ability to mount innate immune responses against RNA viruses, including vesicular stomatitis virus (VSV) and Sendai virus (SeV) (39). During RNA viral infection, it was observed that the cGAS-STING pathway is activated via indirect mechanisms, including the induction of mitochondrial stress and chromatin/nuclear membrane damage. This ultimately culminates in the liberation of intracellular double-stranded DNA into the cytoplasm, subsequently recognized by cGAS or alternative DNA sensors. RNA virus-induced cell membrane fusion has emerged as a pivotal process linking viral entry to the activation of STING. The comprehension of RNA viruses-cGAS-STING signalling interactions has markedly advanced, yet the precise mechanisms of activation of this pathway after RNA virus infections remain uncertain.

3 cGAS-STING-mediated IFN response is the crucial step in antiviral infection

cGAS is a cytosolic DNA sensor identified by Chen's group in 2013 (16). It has been demonstrated that dsDNA activates cGAS in a length-dependent but sequence-independent manner (40). The dsDNA from various sources such as DNA viruses, retroviruses, bacteria, phagocytosed dead cells, and self-DNA leaked from damaged mitochondria could interact with cGAS. cGAS senses dsDNA and catalyses the production of cGAMP to bind the C-terminal domain (CTD) domain of STING and then changes the conformation of STING to oligomerize. The oligomerization of STING migrates away from the ER and activates TBK1 by phosphorylation at serine 365. The activated TBK1 then phosphorylates the CTT pLxIS motif (Ser366) of STING to recruit IRF3. TBK1 phosphorylates IRF3 and induces the IRF3 dimer to enter the nucleus, promoting type I IFN production. Activated IFN can lead to the up-regulation of several hundreds of ISGs, which in turn promotes the secretion of pro-inflammatory cytokines.

3.1 DNA/RNA viruses sensing by the cGAS-STING pathway

There have been sufficient reports on the recognition of DNA viruses by cGAS-STING signal. It has been demonstrated that cGAS-STING induces type I IFN production and further inhibits cytomegalovirus (CMV) replication in primary human endothelial cells (41). In the central nervous system, the activation of the cGAS-STING pathway suppresses herpes simplex virus 1 (HSV-1) replication in mice microglial cells (42). Moreover, the replication of hepatitis B virus (HBV) is inhibited due to activation of the cGAS-STING pathway in both human liver cell lines and *in vivo* mouse models (43). Another study also found that high-level expression of STING restricts susceptibility to HBV by mediating type III IFN induction (44). African swine fever virus (ASFV) is a complex, cytoplasmic double-stranded DNA (dsDNA) virus currently expanding worldwide. The cGAS-STING pathway is efficiently activated during NH/P68 attenuated strain infection, producing large amounts of IFN-β to inhibit ASFV replication. In contrast, the virulent Armenia/07 virus blocks the synthesis of IFN-β by impairing STING activation during infection (45). However, with further research, cGAS-STING has also been confirmed to play an important role in the response to RNA virus infection. In 2013, Schoggins et al. used an ectopic expression system to verify that cGAS also widely inhibits several RNA viral infections (36). During the human immunodeficiency virus (HIV) infection, cGAS senses its RNA-DNA hybrid and dsDNA, inducing IFN production to inhibit virus replication via the cGAS-STING pathway (46). During the SARS-CoV-2 infection, virus spike (S) protein induced cell fusion and then damaged nuclei to form micronuclei. The micronuclei are sensed by cGAS and lead to the activation of STING, which further induces type I IFN production (37).

3.2 Viruses inhibit cGAS-STING-mediated IFN production and antiviral function

As induction of type I IFN mediated by the cGAS-STING axis is crucial for host antiviral responses, viruses have evolved various strategies to antagonize this signalling pathway for immune evasion

(Table 1). Numerous evasion mechanisms and immunomodulators have been identified in DNA viruses that target cGAS-STING signalling. It has been found that herpesviruses employed multiple strategies to antagonize the cGAS-STING pathway for immune evasion. The herpesvirus family includes HSV, CMV, varicella zoster virus (VZV), human herpesvirus (HHV), and Epstein Barr Virus (EBV), which are all DNA viruses. Human CMV (HCMV) tegument protein UL82 was reported to impair the translocation of STING from the ER to perinuclear microsomes and inhibit the recruitment of TBK1 and IRF3 to STING (58). Moreover, HCMV US9 was confirmed to disrupt STING oligomerization and STING-TBK1 association and block IRF3 nuclear translocation (59). The HSV-1 protein ICP27 interacts with the STING-TBK1 complex to inhibit IRF3 phosphorylation (53). The tegument proteins UL41 and UL46 of HSV-1 directly degrade cGAS mRNA or inhibit TBK1 activation, respectively (54, 55). Similarly, the murine CMV (MCMV) protein m152 was able to prevent the trafficking of STING from the ER to the endoplasmic reticulum-Golgi intermediate compartment (ERGIC), therefore inhibiting the interaction between STING and TBK1 (56). Pseudorabies virus (PRV) belongs to the alphaherpesvirus subfamily, which is also known as suid herpesvirus 1 or Aujeszky's disease virus and infects a broad range of vertebrates. A recent study showed that PRV tegument protein UL13 functions as a suppressor of STING-mediated signalling to inhibit IFN production and antiviral response via recruitment of E3 ligase RING-finger protein 5 (RNF5) to induce K27-/K29-linked ubiquitination and degradation of STING (57). ASFV also uses different viral proteins to target the cGAS-STING pathway, inhibiting IFN production and escaping the innate immunity of the host. So far, it has been found that MGF360-15R (pA276R), pDP96R, pE120R, pI215L, pMGF505-7R and L83L protein encoded by ASFV target different adaptor proteins of the cGAS-STING pathway to inhibit type I IFN production (49, 60). In conclusion, maintaining high levels of IFN by ensuring the cGAS-STING activity is critical for host resistance to viral infection. Although cGAS-STING is considered the most potent signalling pathway to induce IFN, Kiran et al. found that JEV-induced type I IFN is cGAS-STING-independent (28). Most researchers believe that TLR and RLR are the main factors that induce IFN production. Interestingly, increased viral load was observed in a cGAS-depleted environment when IFN-β levels were still high. It suggested that the abundance of IFN-β transcripts was not sufficient alone to restrict viral replication. Therefore, there might be additional antiviral approaches regulated by the cGAS-STING signal. With the deepening of research, multiple functional roles and specific mechanisms of cGAS-STING during viral infections were identified, especially its effects on inflammation, oxidative stress and cell death.

TABLE 1 The interaction between virus and cGAS-STING pathway on type I IFN production.

Viruses	Target	Function	Reference
HIV	cGAS	Sensing RNA-DNA hybrid and dsDNA to induce IFN	(46)
SARS-CoV-2	cGAS	Sensing micronuclei to induce IFN	(37)
CMV	cGAS-STING-IRF3	The IFN-I response is dependent on cGAS-STING-IRF3 signalling	(41)
HBV	cGAS/STING	Activating the cGAS-STING axis to induce ISG56	(47, 48)
ASFV	cGAS/STING/TBK1/IRF3	Virulent factors target adaptor proteins of the cGAS-STING pathway to inhibit type I IFN.	(45, 49–52)
HSV-1	cGAS/STING/TBK1;	ICP27 interacts with STING-TBK1 complex to inhibit IRF3 phosphorylation; UL41 and UL46 degrade cGAS mRNA or inhibit TBK1 activity	(53–55)
MCMV	STING	M152 prevents the trafficking of STING from the ER to the ERGIC to inhibit the interaction between STING and TBK1	(56)
PRV	STING	UL13 recruits E3 ligase RNF5 to induce K27-/K29-linked ubiquitination, and STING degradation inhibit IFN	(57)

4 Function of cGAS-STING in regulating inflammation during viral infection

The host inflammatory response responds to harmful stimuli and is tightly regulated. After the PRRs recognize the invading virus, hosts initiate inflammatory signal transduction and trigger inflammatory responses, which play essential roles in early antiviral processes. The inflammatory response regulatory network plays a key role in the host antiviral process to maintain the body's balance.

4.1 NF-κB is the key signal for cGAS-STING-induced inflammatory responses in viral infections

Recognition of viruses by PRRs causes the interaction of many adaptor molecules, which in turn initiate inflammatory signalling, including the NF-κB pathway, the JAK-STAT pathway, and the inflammasome pathway. The NF-κB pathway is thought to be the regulatory centre of the inflammatory response process. The NF-κB signalling pathway is involved in a variety of stress responses during viral infection, which in turn mediates various transcriptional processes and ultimately induces pro-inflammatory cytokine production. The SARS-CoV-2 infection causes varying degrees of respiratory symptoms and results in lung damage or even death in a significant number of cases. These severe cases are associated with high levels of pro-inflammatory cytokines and low antiviral responses (61). A recent study reported that in SARS-CoV-2

infected cells, the TBK1 and IRF3 pathways are blocked by several viral proteins. The SARS-CoV-2 infection causes mitochondrial stress/damage, DNA damage, cell death and leakage of mitochondrial DNA. These DNA activate the cGAS-STING axis and induce NF-κB activation to drive inflammatory immune response (21). cGAS-STING is recognized as a potential target for the treatment of SARS-CoV-2. And several STING-targeting drugs can attenuate the inflammatory response. The HIV/SIV (Simian immunodeficiency virus) research study showed that its Vpx proteins efficiently inhibit cGAS–STING-induced NF-κB signalling but not IRF3 activation, which further induces the production of several pro-inflammatory cytokines (62). In addition. ASFV protein pD345L has been found to suppress cGAS/STING-induced NF-κB activation (63). It is well known that NF-κB is the predominant regulator of inflammation and cGAS-STING can drive NF-κB activity during viral infections (21). Therefore, the role of cGAS-STING signalling in mediating inflammatory responses deserves more attention.

4.2 The cGAS-STING pathway interacts with the inflammasome complex in viral infections

NLRs also have powerful effects on inflammation induction. It has been proved that several NLRs, including NLRP1b, NLRP3, NLRC4, NLRP6 and NLRP12, are involved in the formation of inflammasome and regulate innate antiviral immunity. When viruses invade cells, NLRs recognize viral nucleic acids or endogenous molecules released from damaged or dying cells. Then, NLRs oligomerize and recruit pro-caspase-1 with or without ASC to form inflammasomes. In the inflammasome complex, caspase-1 can activate self-cleavage, and the activated caspase-1 cleaves pro-IL-1 and pro-IL-18 for their maturation and release. These mature pro-inflammatory cytokines then exert their antiviral function. IFN and pro-inflammatory cytokines are produced and function simultaneously during the host antiviral responses. Importantly, balance type I IFN production and inflammasome activation pathways are essential for immune homeostasis. Upon infection with HSV-1 or cytosolic DNA stimulation, STING engages with NLRP3, facilitating inflammasome activation via dual mechanisms (64). On one hand, STING recruits NLRP3 and promotes the localization of NLRP3 in the endoplasmic reticulum, thus promoting the formation of an inflammasome. On the other hand, STING interacts with NLRP3 to attenuate NLRP3 polyubiquitination associated with K48 and k63, thereby promoting inflammasome activation. It is widely known that the assembly of the NLRP3 inflammasome leads to the activation of caspase-1, which further results in the production of several pro-inflammatory cytokines. Caspase is the important link between inflammasome and inflammatory cytokines. Wang et al. found that caspase-1 interacted with cGAS to inhibit IFN production in DNA virus infection (65). This study also demonstrated that deficiency in inflammasome signalling enhanced host resistance to DNA viruses *in vitro* and *in vivo*. Moreover, this regulatory role also extended to other inflammatory caspases, including Caspase-4, 5, and 11 (65). These Caspases cut cGAS in conditions of non-canonical inflammasome activation. ZIKV, an RNA virus, has been reported to promote NLRP3 inflammasome activation to benefit its infection by stabilizing caspase-1 to suppress cGAS-mediated type I IFN signalling (31). The detailed mechanism is that the non-structural protein NS1 of ZIKV recruits the host deubiquitinase USP8 to cleave K11-linked poly-ubiquitin chains from caspase-1 at Lys134 to inhibit the proteasomal degradation of caspase-1. The enhanced stabilization of caspase-1 by NS1 promotes the cleavage of cGAS to inhibit the recognition of releasing mitochondrial DNA and then suppress type I IFN signalling. In addition, the activation of human caspase-3, an apoptotic caspase, has been demonstrated to cleave cGAS at D319, IRF3 at D121/125 and MAVS at D429/490, thus making apoptotic cells immunologically silent and negatively regulating DNA or RNA virus-induced cytokine production (66). Currently, there are few studies on the interaction between cGAS-STING and inflammasome signalling in viral infection, but the available evidence already suggests that the interplay between the cGAS-STING pathway and inflammasome complex affects IFN, inflammation and cell death. Therefore, this aspect deserves more attention.

5 The crosstalk between cGAS-STING signal and oxidative stress in viral infections

5.1 Oxidative stress is a double-edged sword in viral infections

Oxidative stress is an important pathological factor causing tissue damage, aging, tumours, and cardiovascular diseases. Under normal circumstances, oxidation and antioxidation are maintained in a balanced state. The oxidative and antioxidant systems in the body are disordered when harmful substances stimulate the organism. Excessive production of highly reactive molecules such as ROS and reactive nitrogen species (RNS) leads to the inhibition of antioxidant capacity, which tilts the equilibrium toward oxidation, resulting in oxidative stress. Oxidative stress is always associated with viral infections. Viral infection-induced ROS generation triggers oxidative stress in the organism and mediates apoptosis, which in turn mediates ROS and causes extensive damage, aggravating the disease process (67). For example, oxidative stress is a major characteristic of asthma and chronic obstructive pulmonary disease (COPD), and rhinovirus infection can make their condition worse. Oxidative stress attenuated the antiviral capacity of bronchial epithelial cells in asthma and COPD patients. Furthermore, oxidative stressor H_2O_2 could down-regulate the expression of epithelial cellular PRR TLR3 and antioxidants (SOD1 and SOD2), which suggested that ROS might have reduced the host's antiviral capacity and promoted viral infection (68). But in some other studies, to a certain degree, oxidative stress activates the antioxidant defence system and autophagy in the tissues and organs, which help to scavenge some of the ROS and induce stress defence (69). Oxidative stress-induced ROS can also activate autophagy and apoptosis through various specific mechanisms,

which induce cell death and inhibit virus replication. Moreover, H_2O_2 has been confirmed to regulate autophagy by inhibiting the autophagy-related gene (ATG) 4, which affects the lipidation of light chain 3 (LC3) and the degradation of pathogens (70). In addition, Latent Membrane Protein 1, a major EBV protein, facilitates ROS production, causes DNA damage and induces autophagy initiation (71). These studies suggest oxidative stress affects viral infection by directly regulating viral survival or indirectly affecting virus infection via apoptosis and autophagy.

5.2 cGAS-STING is a potential target that links oxidative stress and viral infection

It is widely known that the invading DNA virus will activate the cGAS-STING pathway, inducing type I IFN production and causing a range of innate immune responses. In recent studies, it has been found that STING is an upstream regulator of cellular oxidative stress. It is possible to regulate the level of lipid peroxidation and ROS by activating the cGAS-STING downstream signal ISG15. ISG15 is a member of the ISG family that induces IFN expression, contributes to "protein ISGylation", and interferes with ubiquitin modifications. STING can negatively regulate the ubiquitin-proteasome system through ISG15, resulting in increased interferon-mediated ROS (72, 73). Indeed, IFN-mediated protein ISGylation regulates the ubiquitin-proteasome system to increase cellular ROS. Furthermore, glutathione peroxidase (GPX), an antioxidant molecule, attenuates oxidative stress by reducing H_2O_2 to water, which is also inhibited by ISG15. STING knockdown elevates glutathione peroxidase (GPX) activity via inhibition of ISG15. Recently, Hayman et al. also found the knockdown of STING down-regulated expression of ISG15 and ROS-related genes, including HECT domain and RCC1-Like Domain-Containing Protein 5 (HERC5), kruppel-like factor 4 (KLF4), and dual oxidase 2 (DUOX2) (73–76). These results suggest that STING is an upstream regulator of the intracellular oxidation processes. However, it is worth noting that some other studies believe that oxidative stress is an important inducement of cGAS-STING activation. During HSV-1 infection, GPX4 is indispensable for cGAS-STING activation. Actually, GPX4 inactivation leads to cellular lipid peroxidation, which decreases host innate antiviral immune responses and promotes virus replication via inhibition of the cGAS-STING signalling axis (22). Mechanistically, GPX4 inactivation did not affect the binding of viral DNA to cGAS but suppressed the trafficking of STING to the Golgi apparatus by facilitating STING carbonylation at C88. Another interesting study showed ROS promoted the replication of murine gammaherpesvirus-68 (MHV68), a close genetic relative of KSHV and EBV. ROS suppressed the production of IFN in a STING-dependent manner (77). ROS inhibits STING dimerization by oxidizing Cysteine 147 on murine STING during MHV68 infection. Redox modification of STING is an important regulatory mechanism of STING activity during viral infection. It is generally known that viral infection usually leads to oxidative stress in host cells, including SARS-COV-2, influenza virus and Hepatitis C virus (HCV) (15, 78–80). Oxidative stress is closely related to mitochondrial dysfunction, which triggers mitochondrial DNA (mtDNA) damage and DNA leakage, activating the cGAS-STING pathway (Figure 1) (81). It remains uncertain whether oxidative stress is the cause or the consequence of cGAS-STING signalling activation during viral infection. And whether oxidative stress induces STING activity or inhibits STING activation is also controversial. Meanwhile, there are few reports about the direct interaction between the cGAS-STING signal and oxidative intermediates. Therefore, more research is needed to explore their relationship. However, it must be admitted that the alteration of the levels of oxidative stress affects the cGAS-STING pathway and host antiviral immunity.

6 Function of cGAS-STING regulates autophagy during viral infection

6.1 Autophagy in antiviral host defences

To accommodate the diverse needs of metabolism, intracellular substances are constantly synthesized and degraded to maintain homeostasis. Autophagy is an evolutionarily conserved metabolic process of eukaryotic cells that degrades or recycles intracellular proteins and organelles and plays a key role in activating and regulating early immune responses during viral infection (82). PRR signals interact with autophagy adaptor proteins to regulate a series of immune responses, which effectively eliminates pathogenic microorganisms. For example, activation of the TLR-MYD88/TRIF pathway can disrupt the interaction between B cell lymphoma-2 (BCL-2) and Beclin-1, which induces autophagy (83). The recognition of VSV and SeV by TLR7 requires the transport of cytosolic viral replication intermediates into the lysosome. ATG5 deletion would reduce TLR7-mediated IFN production (84). Many studies have suggested that autophagy can degrade viral components, particles, and host factors, which functions as an effective innate antiviral mechanism. HCV non-structural 5A (NS5A) protein, which is crucial for HCV replication, can be degraded in autophagosomes. Autophagy helps to remove HCV in the presence of ER protein Scotin (85). Autophagy facilitates selectively degrading the HIV-1 transactivator Tat, inhibiting viral transcription and virion production in $CD4^+$ T cells (86). There are also many other viruses, such as hepatitis B virus, porcine epidemic diarrhoea virus, and ZIKV, that are restricted by autophagy (87–89). On balance, viral infection is detected by multiple signalling pathways, and further triggers the activation of immune defences via autophagy.

6.2 Autophagy induction is an evolutionarily conserved function of the cGAS-STING signal

Earlier studies have mainly focused on the mechanism of IFN induction by the cGAS-STING pathway. This signalling pathway plays antiviral effects by regulating antiviral gene transcription. Of

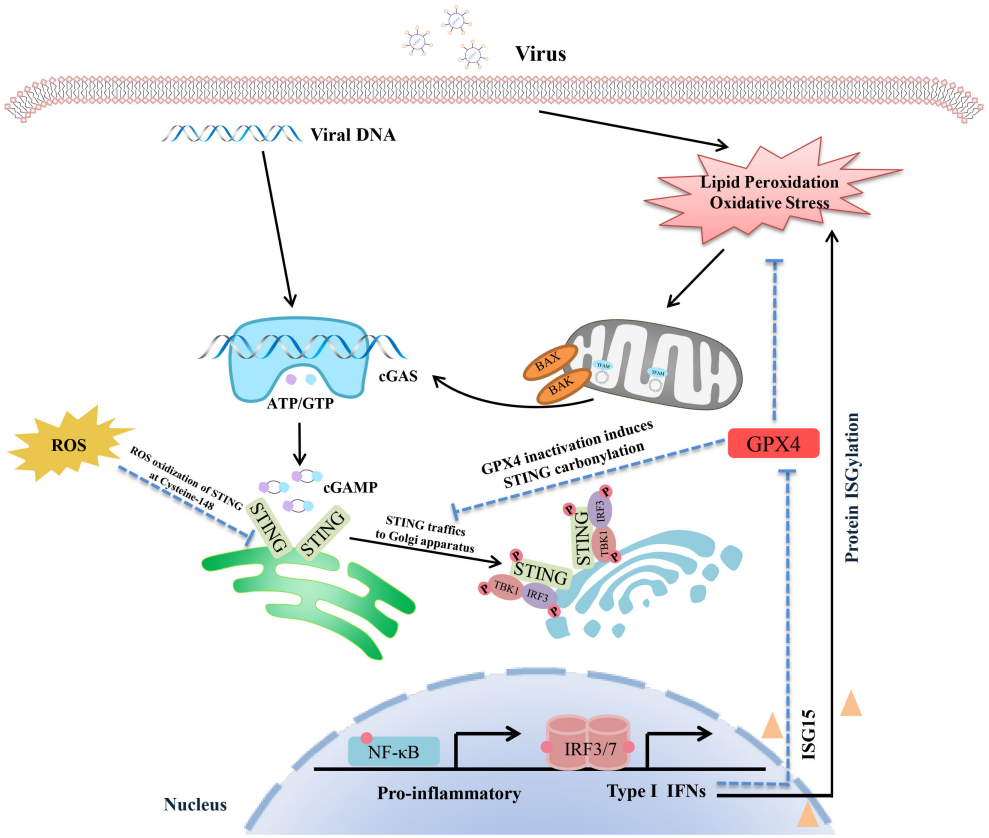

FIGURE 1
Schematic representation of the interaction between the cGAS-STING pathway and oxidative stress. The virus DNA and mtDNA can both be recognized by cGAS-STING signalling, inducing pro-inflammatory cytokines and IFN production via the TBK1-IRF3/NF-κB pathway. In addition, viral infection also triggers lipid peroxidation and oxidative stress, which lead to STING inactivation by facilitating STING carbonylation at C88. It is worth noting that GPX4 is a crucial nod connecting the cGAS-STING axis and oxidative stress. On the one hand, GPX4 activation inhibits oxidative stress, which ensures that the activated STING can be successfully transferred to the Golgi apparatus for further action. On the other hand, activation of the cGAS-STING-IFN axis promotes oxidative and inhibits GPX4 activity via ISG15 expression. In addition, ROS inhibits STING dimerization by oxidizing Cysteine 147 on STING. Redox modification of STING is an important regulatory mechanism of STING activity during viral infection.

interest, a growing number of researchers find cGAS-STING signalling axis regulates virus clearance more immediately through autophagy. Of which, the main function of STING in combatting HSV-1 infection seems to be attributed to autophagy activation rather than type I IFN production (90). A study found a mouse model harbouring a serine 365-to-alanine (S365A) mutation in STING remained resistant to HSV-1, despite the loss of STING-induced IFN activity. It seems that the activation of autophagy, triggered by STING, is contingent upon CTT and TBK1, yet remains uninfluenced by IRF3. Therefore, understanding the molecular mechanism of autophagy regulation by the cGAS-STING pathway is crucial. Saitoh et al. first found that the dsDNA of pathogenic microorganisms could induce co-localization of STING, ATG9a and LC3, which are important autophagy proteins (91). Subsequently, STING was identified as an essential factor that triggered autophagy under the stimulation of microbial DNA, which could degrade pathogens by delivering them to autophagosomes (92). Furthermore, a study showed that cGAS could directly bind to the coiled-coil domain of Beclin-1, which is a pivotal protein for autophagy initiation (93). As a result, this interaction inhibits the synthesis of cGAMP and IFN and promotes autophagy-mediated cytosolic DNA degradation by releasing Rubicon from the Beclin-1 complex. Notably, Gui et al. explained the mechanism of STING-mediated autophagy without TBK1 activation and IFN induction (24). When pathogenic microorganisms infect cells, cGAS recognizes cytosolic DNA and synthesizes cGAMP, which further binds to STING. As a result, STING translocates to the ERGIC by interaction with SEC24C. Then, ERGIC acts as a membrane source for LC3 lipidation, promoting autophagosome formation that degrades the DNA virus. In many invertebrates, such as drosophila and sea anemone *Nematostella vectensis*, their STING only participates in autophagy induction but not IFN response (24, 94). These research suggest that autophagy induction is an evolutionarily conserved function of the cGAS-STING signalling axis which predates the emergence of the IFN signalling. Additionally, the structural analysis showed that STING had a conserved LIR domain which was exposed to the cytoplasm by conformational changes upon activation (95). Consequently, the exposed LIR domain could directly interact with LC3 to activate autophagy, leading to the degradation of

STING itself and p-TBK1. This finding also showed STING could directly link immune activation to autophagy. So quite a few researchers believe that autophagy induction via STING trafficking is a primordial function of the cGAS pathway, which has long been thought that its primary function is to induce type I IFN production. Further studies show that STING orchestrates endoplasmic reticulum stress and the unfolded protein response via a novel UPR motif within the cyclic-dinucleotide-binding (CBD) domain. This motif exerts a negative regulatory effect on the Akt/tuberous sclerosis complex (TSC)/mammalian target of the rapamycin (mTOR) pathway, thereby amplifying canonical autophagy (25, 96). Several other studies also revealed the mechanisms of STING-mediated noncanonical autophagy (97, 98). Activated STING translocates from the endoplasmic reticulum to the ER-Golgi intermediate compartment and Golgi apparatus, contingent upon the coat protein II (COP II) complex and Arf GTPases. The ERGIC serves as a membrane reservoir for LC3 lipidation and the genesis of autophagosomes. Different from canonical autophagy, STING-elicited noncanonical autophagy operates independently of upstream autophagy modulators, including unc-51-like kinase 1 (ULK1), Beclin-1, and ATG9a, yet relies on downstream autophagy regulators such as ATG5 and ATG16L1 (24).

6.3 Viruses evade host immune defence by inducing autophagic degradation of cGAS/STING

Viruses have also evolved unique mechanisms to ensure their survival by influencing autophagy processes and cGAS-STING signalling. ASFV MGF505-7R, MGF505-11R and L83L proteins promote autophagy-lysosomal degradation of STING, thereby blocking the phosphorylation of the downstream signalling molecules TBK1 and IRF3 and impairing type I IFN production (51, 60, 99). PCV2 infection can induce cGAS degradation via the autophagy-lysosome pathway (100). Mechanically, PCV2 infection triggers the phosphorylation of cGAS at S278 through the PI3K/Akt pathway. This phosphorylation of cGAS promotes the K48-linked poly-ubiquitination of cGAS which interacts with autophagy receptor p62 for autophagic degradation in autolysosome. As a result, the autophagic degradation of cGAS inhibits cGAMP and IFN-β production, which further impair hosts' innate antiviral responses. Similarly, HBV X protein also can inhibit type I IFN production by boosting ubiquitination and autophagic degradation of cGAS (101). Except for cGAS, another autophagy receptor Coiled-coil domain containing 50 (CCDC50) associates with and targets STING for autophagic degradation (102). The MIU motifs of CCDC50 can recognize K63-polyubiquitinated STING and facilitate the conveyance TBof K63-polyubiquitinated STING to LC3B-marked autophagosomes, subsequently initiating autophagic degradation in a p62-independent way. During HSV-1 infection, the absence of CCDC50 promotes IFN and pro-inflammatory cytokines production and inhibits HSV-1 replication. These results suggest the autophagic degradation of cGAS-STING signalling during infections has a significant impact on type I IFN production and viral replication (Figure 2).

6.4 cGAS-STING-induced autophagy not only exerts direct antiviral effects but also influences host antiviral responses by affecting IFN signalling

Although many studies have been conducted on viral evasion of STING-induced IFN-mediated antiviral function, investigations about viral evasion of STING-induced autophagy-mediated antiviral function remain notably limited. Recently, an interesting study found that the bat STING can only induce autophagy and antiviral activity but not IFN induction (103). SARS-CoV-2 ORF3a constitutes a distinctive viral protein capable of interacting with STING, consequently disrupting the STING-LC3 association and impeding cGAS-STING-mediated autophagy, whilst preserving IRF3-Type I IFN induction. This novel functionality of ORF3a, different from targeting autophagosome-lysosome fusion, is a selective impediment of STING-mediated autophagy, thereby promoting viral proliferation. In addition, the interaction between the TBK1-IRF3-IFN pathway downstream of cGAS-STING and autophagy in viral infections is very complex. During infection, excessive accumulation of STING will trigger a strong inflammatory reaction, leading to deleterious effects on the host (93, 104). When the cGAS-STING pathway is activated, TBK1-IRF3 signalling downstream of STING will phosphorylate p62 at S403, which has a remarkably high affinity for ubiquitinated STING. As a result, the ubiquitinated STING is degraded in autophagosomes in an IRF3-dependent manner (105). Moreover, another research group also found that TBK1 could phosphorylate selective autophagy receptors optineurin (OPTN), NDP52, and TAX1BP1 linking ubiquitinated cargo to autophagic membranes (106). As is known to us all, type I IFN participates in activating JAK/STAT and PI3K/Akt pathways, which are always involved in autophagy induction (107). Type I IFN does not induce autophagy in STAT-deficient cells (108). PI3K/Akt signalling axis inhibits autophagy by activating mTORC1 and inhibiting the expression of forkhead box O (FOXO) and autophagy-related genes. At later time points, negative regulators of the PI3K/AKT/mTOR pathway are induced, inhibiting mTORC1 activity and inducing autophagy (107). Therefore, the TBK1-IRF3-IFN axis plays a crucial role in activating and regulating the host's immune and autophagy. At present, there are still some problems plaguing us. Some researchers believe cGAS-STING-mediated autophagy plays an antiviral role (90, 103, 109). But other research groups suggest that cGAS-STING-mediated autophagy contributes to inhibiting the antiviral function of the host by degrading cGAS/STING directly or by degrading key proteins downstream of the cGAS-STING pathway (Table 2) (51, 100, 117, 118). As a result, this process inhibits IFN production. The next question that needs to be solved is how to control the target of autophagic degradation in viral infection.

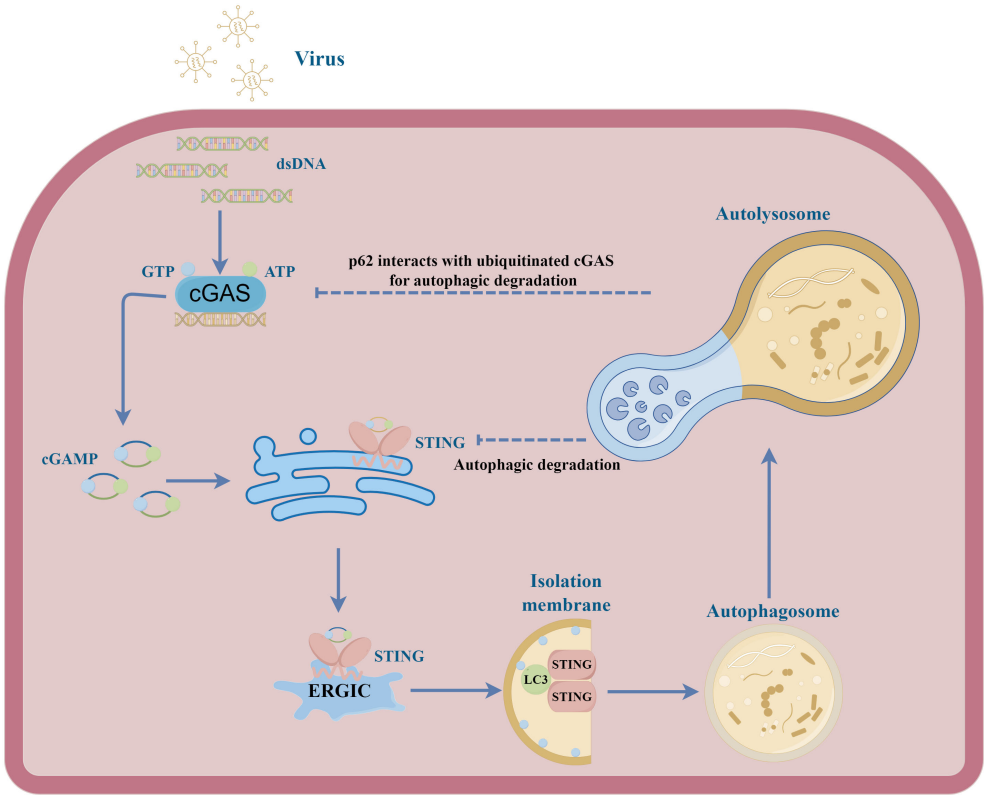

FIGURE 2
A schematic illustration depicting the interplay between cGAS-STING signal and autophagy in viral infection. Upon activation by cGAMP, STING undergoes translocation from the endoplasmic reticulum to the ERGIC. Within the ERGIC, STING has been implicated in the initiation of autophagy. The STING-containing ERGIC functions as a membrane source of LC3 lipidation, thereby triggering the formation of the autophagosome. Ultimately, the autophagosome fuses with the lysosome, effectuating the degradation of its contents. During different viral infections, the cGAS and STING can be degraded in autolysosome, inhibiting host antiviral responses.

7 Interactions between the cGAS-STING axis and ER stress during viral infection

7.1 The ER stress responses have important influences on viral survival

There is adequate evidence that the state of the endoplasmic reticulum also influences a variety of selective autophagy, including mitophagy and ER-phagy (119, 120). To further expand our understanding of the effects of cGAS-STING on autophagy and oxidative stress, we focus on the endoplasmic reticulum. The endoplasmic reticulum is a continuous membrane system widely distributed in the cytoplasm. It mainly performs the functions of intracellular material transport, glucose and lipid metabolism, and protein processing. In addition, ER also provides a membrane structure for the formation of autophagosomes and peroxisomes. Many viruses use the ER as a replication site, where they synthesize proteins, replicate genomes, and assemble virion (121). ER stress is usually triggered by calcium homeostasis disequilibrium, unfolded protein (UPR) accumulation and lipid dysregulation (122). ER stress is also considered to be a potential cause of mitophagy and ER-phagy (123, 124). Accumulation of viral proteins in ER can also induce ER stress (125). ER stress initiates UPR-mediated protein degradation pathways, apoptosis and autophagy in host cells, inhibiting or degrading the accumulation of viral proteins to maintain cellular homeostasis. Generally, different viruses selectively activate the PERK (proline-rich extensin-like receptor kinase)-eIF2α (eukaryotic translation initiation factor 2) pathway, IRE1α (inositol-requiring enzyme 1α)-XBP1 (X-box binding protein-1) pathway or ATF6 (activating transcription factor 6) pathway, leading to ER stress. Transmissible gastroenteritis virus (TGEV) can activate the PERK-eIF2α signalling pathway and subsequently diminish the synthesis of viral proteins by decreasing protein translation efficiency (126). The HCV negatively regulates ER stress via the IRE1α-XBP1 pathway, increasing the synthesis of viral proteins and facilitating viral infection (127). Influenza A virus promotes viral replication by inhibiting ER stress response factor XBP1 and limiting host protein production to alleviate ER stress (128). However, the UPR remains to be a double-edged sword during viral infection. Some viruses regulate UPR to promote survival by activating other cellular responses. For example, duck enteritis virus (DEV) can activate ER stress and autophagy in a PERK-eIF2α/IRE1α-XBP1 dependent manner. Inhibiting the expression of PERK and IRE1 helps to suppress autophagy and DEV replication (129).

TABLE 2 cGAS-STING-mediated autophagy plays a dual role during viral infection.

Viruses	Target	Function	References
HSV-1	STING	An S365A mutation in STING is resistant to HSV-1 by activating autophagy, despite lacking IFN responses	(90, 110)
HSV-1	cGAS-Beclin-1	The direct interaction between cGAS and Beclin-1 enhances autophagy-mediated pathogen DNA degradation	(93, 111)
HSV-1	GBP1-STING	GBP1 combines with STING and promotes autophagy, inhibiting HSV -1 infection in an IFN-independent manner	(112)
ZIKV	NF-κB-STING	In invertebrates, ZIKV-dependent NF-kB activation induces antiviral autophagy via activation of STING	(87, 113, 114)
HRV	STING	The STING-mediated antiviral activity required the induction of ATG5-dependent autophagy	(115)
PPRV	STING	STING regulates PPRV replication by activating the ATF6 pathway of UPRs to induce autophagy	(116)
ASFV	STING	ASFV MGF505-7R/11R interacted with STING and degrades STING expression by autophagy pathways, facilitating virus proliferation	(51, 99)
ASFV	cGAS-STING-TBK1	ASFV pA137R negatively regulates the cGAS-STING-mediated IFN via the autophagy-mediated TBK1 degradation	(117)
ASFV	TBK1-IRF7	ASFV MGF360-11L interacted with TBK1 and IRF7, degrading TBK1 and IRF7 via autophagy pathways.	(118)
PCV2	cGAS	PCV2 induces the cGAS ubiquitination degradation by autophagy, promoting virus infection	(100)

7.2 Endoplasmic reticulum localization of STING underlies its interaction with endoplasmic reticulum stress signalling

During viral infection, the viral DNA can be recognized by the cGAS and activates the cGAS-STING pathway, triggering a series of immune and cellular responses to protect the body, including ER stress (23). Notably, the inactivated STING is located on the outer membrane of the ER, and the migration of the activated STING and the activation of the STING-TBK1-IRF3 signal always occur simultaneously with ER stress. Several recent studies have shown a partial overlap between ER stress signals and the cGAS-STING signalling axis. During pathogenic microbial infection, phosphorylation of PERK was significantly impaired in STING-deficient macrophages. STING gain-of-function mutant N154S induces chronic ER stress by disrupting Ca2+ homeostasis. A newly identified STING CTD motif is involved in mediating ER stress in an IFN-independent manner (96). Similarly, deletion of the Ca^{2+} sensor STIM1 leads to spontaneous activation of the STING-TBK1-IRF3 pathway, which results in type I IFN-mediated ER stress (130). Moreover, higher levels of PERK phosphorylation were induced at times of the expression of STING (25). Furthermore, co-immunoprecipitation assay suggests that STING and PERK can interact directly and promote the removal of pathogenic microorganisms. Additionally, down-regulating the expression of PERK or IRE-1 inhibits STING activity (131). These research imply a link between ER stress and cGAS-STING signal. The interrelationship between downstream signalling molecules of cGAS-STING and ER stress was also illustrated in several reports. The activation of IRF3 by STING is initiated by ER stress (132). The signal that triggers the phosphorylation of IRF3 is derived from the ER. ER stress triggered the phosphorylation of IRF3 at S386 in an XBP1-independent manner, promoting IRF3 nuclear translocation (133). Moreover, ER stress can mobilize the ER-resident STING and facilitate the co-localization of STING and TBK1. Another research found that XBP1 splicing and IRF3 phosphorylation depend on the presence of STING (132). There is also evidence suggesting that several genes, including tyrosine kinase 2 (TYK2), STAT2 and IRF9, take part in IFN-induced ER stress, but the specific mechanism is still unclear (134). As yet, studies on the interaction between ER stress and the cGAS-STING pathway are mainly focused on metabolic and autoimmune diseases. More research is needed to further understand their role in viral infections.

8 Summary and perspectives

Viral infection and its serious consequences constantly threaten people's health and safety. Therefore, understanding the molecular basis of host antiviral immunity is beneficial for eliminating viruses and attenuating physiological impairments. Recent research on the cGAS-STING pathway has increased our understanding of the recognition and removal of viruses. Although we have outlined recent insights of cGAS-STING in regulating IFN, inflammation, oxidative stress, autophagy and endoplasmic reticulum stress upon virus infections, this signalling axis is also involved in some other early host antiviral processes, such as different types of cell death and metabolism (Figure 3). Stimulation with a high concentration of HSV-I triggers cGAS-STING-dependent apoptosis, which affects local immune responses (135). Mechanistically, the activated cGAS-STING promotes the accumulation of phosphorylation of IRF3, which relieves the inhibitory effect of Bcl-xL on mitochondrial outer membrane permeability and further induces apoptosis. In addition, MHV68 leads to STING-dependent necroptosis in primary macrophages (136). Type I IFN works in coordination with TNF to induce necroptosis through STING activation. Moreover, mtDNA stress can activate the cGAS-STING-mediated DNA sensing pathway, inducing autophagy-dependent ferroptosis via lipid peroxidation (137). Also, several studies have shown that the

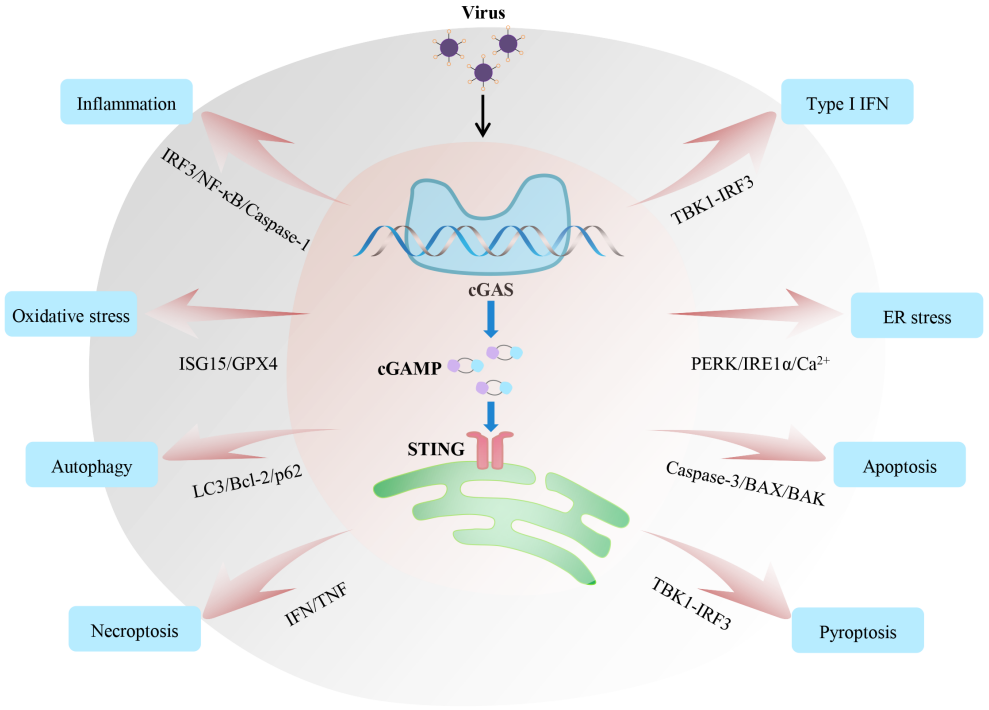

FIGURE 3
Regulatory mechanisms and functions of the cGAS-STING axis during viral infection. The cGAS-STING signalling axis widely participates in various immune and cellular responses, including inflammation, IFN, oxidative stress, endoplasmic reticulum stress, and different types of cell death during viral infection. All these responses affect the host's ability to fight off invading viruses. Based on relevant studies, we summarize the crucial signalling nodes or proteins involved in these processes.

activation of STING contributes to pyroptosis via the TBK1-IRF3 signal (138, 139). We speculate that inflammasomes and lysosomes may be the key links among different types of cell death downstream of cGAS-STING pathways during viral infection.

Notably, three different research groups have found that mtDNA released from mitochondria could activate the cGAS-STING signalling axis (81, 140, 141). That is, the cytoplasmic cGAS-STING can recognize both the invading pathogenic DNA and endogenous DNA. mtDNA is a double-stranded, circular molecule, which can be recognized by TLR9, AIM2 and cGAS, inducing immune responses (142–145). West et al. found mitochondrial transcription factor A (TFAM, a key regulatory factor in mtDNA transcription and replication) deficiency and mitochondrial stress would cause the leakage of mtDNA into the cytoplasm, activating the cGAS-STING axis and initiating type I IFN response (81). HSV-1 and VSV infection can induce TFAM depletion and mitochondrial stress, facilitating mtDNA release into the cytoplasm and triggering cGAS-STING-mediated antiviral immune responses (146). Mitochondrial dysfunction is not only the result of oxidative stress and inflammatory responses but also a trigger for selective autophagy (mitophagy). Moreover, mitochondrial dysfunction-mediated mtDNA cytosolic leakage can trigger antiviral innate immune response by activating the cGAS-STING pathway. Therefore, we believe that the mitochondrial dysfunction events in viral infections are key to linking cGAS-STING signalling, inflammation, oxidative stress, and autophagy.

Interestingly, RNA viruses, such as SARS-CoV-2, HIV and DENV, also activate the cGAS-STING axis, despite cGAS being a DNA PRR (36, 46, 147). Mechanistically, the activation of the cGAS-STING by retroviruses depends on their reverse transcription to produce DNA. cGAS-STING activity induced by other RNA viruses is partly due to mitochondrial damage caused by a viral infection, which in turn leads to the accumulation of mtDNA in the cytoplasm (30). Therefore, during virus invasion, we should not only consider the activation effect of the virus itself on the cGAS-STING signal but also pay attention to the influence of cellular physiological changes on it.

Although the advent of omic technologies greatly expands the objectives of our study, each omics analysis still has some limitations for different samples. Meanwhile, the occurrence and development of viral diseases is a complex network, and many factors, such as gene mutation, abnormal transcription and epigenetic changes, affect the host's physiological status. Combined multi-omics analysis can analyse multiple consecutive events of disease occurrence and identify the antiviral targets more precisely. Moreover, with the rapid development of gene-editing technology, using genome-wide CRISPR screening to identify host factors of the virus-infected cells is a current research hotspot. Integrating genome-wide CRISPR screening with multi-omic data seems to be a promising approach to understanding the virus-host interactive network. A research group have used this strategy to identify some novel and effective antiviral factors (148). This

method may help develop new strategies for improving host disease resistance and antiviral therapy.

Indeed, the cGAS-STING pathway plays a dual role in early antiviral immunity and cellular responses. On the one hand, intracellular DNA induces various cellular responses and the expression of type I IFN and pro-inflammatory cytokines to fight against invading viruses via the cGAS-STING-TBK1-IRF3/NF-κB axis. On the other hand, the invoked cell death and intracellular stress responses can regulate the upstream regulators and downstream effectors of cGAS-STING, affecting immune responses and pathogen clearance. For example, cGAS-STING-activated autophagy, in turn, degrades STING and suppresses the immune response (105). Some viruses have evolved various strategies to antagonize the cGAS-STING pathway for immune evasion. Under different infectious conditions, the activations of cGAS-STING signalling are not the same. The inactivation and overactivation of the cGAS-STING signal are both detrimental to pathogen clearance by the host. Inhibition of the cGAS-STING axis suppresses host antiviral responses. And overactivation of cGAS-STING would trigger a strong inflammatory reaction and drive immunopathology. Of great concern, cGAS/STING has become an effective drug target. Researchers are working on designing or screening small molecule drugs that can regulate cGAS/STING activity. Presently, great progress has been made in the research of cGAS inhibitors. Some drugs can directly interfere with DNA binding to cGAS or competitively bind cGAS, thereby inhibiting the initial activation of cGAS (149). However, the agonists targeting cGAS are relatively rare and need further study. Although research on cGAS-STING has become increasingly mature, how to accurately regulate the cGAS-STING activity and promote virus elimination by host cells still needs further exploration.

Author contributions

KZ: Conceptualization, Writing – original draft, Writing – review & editing. QH: Writing – original draft. XL: Writing – review & editing. ZZ: Writing – review & editing. CH: Writing – review & editing. ZS: Writing – review & editing. BD: Writing – review & editing. CL: Writing – review & editing. JZ: Conceptualization, Funding acquisition, Writing – review & editing. SW: Conceptualization, Writing – original draft, Writing – review & editing.

Funding

The author(s) declare financial support was received for the research, authorship, and/or publication of this article. The authors thank the following funding sources: the National Natural Science Foundation of China (32002298, 32002153, 82200747), Guangdong Basic and Applied Basic Research Foundation (2023A1515010528, 2023A1515012153), Fundamental Research Funds for State Key Laboratory of Swine and Poultry Breeding Industry (ZQQZ-38), the Special Fund for Scientific Innovation Strategy-Construction of High-Level Academy of Agriculture Science (R2021PY-QF006, R2023PY-QY013), the Project of Collaborative Innovation Center of GDAAS (XTXM202203-XT202217), and Guangdong modern breeding project (2022B0202090002).

Conflict of interest

The authors declare that the research was conducted in the absence of any commercial or financial relationships that could be construed as a potential conflict of interest.

Publisher's note

References

1. Takeuchi O, Akira S. Pattern recognition receptors and inflammation. *Cell* (2010) 140(6):805–20. doi: 10.1016/j.cell.2010.01.022

2. Li D, Wu M. Pattern recognition receptors in health and diseases. *Signal Transduct Target Ther* (2021) 6(1):291. doi: 10.1038/s41392-021-00687-0

3. Colonna M. TLR pathways and IFN-regulatory factors: to each its own. *Eur J Immunol* (2007) 37(2):306–9. doi: 10.1002/eji.200637009

4. Gokhale NS, Smith JR, Van Gelder RD, Savan R. RNA regulatory mechanisms that control antiviral innate immunity. *Immunol Rev* (2021) 304(1):77–96. doi: 10.1111/imr.13019

5. Mazewski C, Perez RE, Fish EN, Platanias LC. Type I interferon (IFN)-regulated activation of canonical and non-canonical signaling pathways. *Front Immunol* (2020) 11:606456. doi: 10.3389/fimmu.2020.606456

6. Spitaels J, Van Hoecke L, Roose K, Kochs G, Saelens X. Mx1 in hematopoietic cells protects against thogoto virus infection. *J Virol* (2019) 93(15):e00193-19. doi: 10.1128/JVI.00193-19

7. Zang R, Case JB, Yutuc E, Ma X, Shen S, Gomez Castro MF, et al. Cholesterol 25-hydroxylase suppresses SARS-CoV-2 replication by blocking membrane fusion. *Proc Natl Acad Sci U.S.A.* (2020) 117(50):32105–13. doi: 10.1073/pnas.2012197117

8. Chakrabarti A, Jha BK, Silverman RH. New insights into the role of RNase L in innate immunity. *J Interferon Cytokine Res* (2011) 31(1):49–57. doi: 10.1089/jir.2010.0120

9. Singh S, Singh TG. Role of nuclear factor kappa B (NF-κB) signalling in neurodegenerative diseases: an mechanistic approach. *Curr Neuropharmacol* (2020) 18(10):918–35. doi: 10.2174/1570159X18666200207120949

10. Oeckinghaus A, Hayden MS, Ghosh S. Crosstalk in NF-κB signaling pathways. *Nat Immunol* (2011) 12(8):695–708. doi: 10.1038/ni.2065

11. Camini FC, da Silva Caetano CC, Almeida LT, de Brito Magalhaes CL. Implications of oxidative stress on viral pathogenesis. *Arch Virol* (2017) 162(4):907–17. doi: 10.1007/s00705-016-3187-y

12. He B. Viruses, endoplasmic reticulum stress, and interferon responses. *Cell Death Differ* (2006) 13(3):393–403. doi: 10.1038/sj.cdd.4401833

13. Choi Y, Bowman JW, Jung JU. Autophagy during viral infection - a double-edged sword. *Nat Rev Microbiol* (2018) 16(6):341–54. doi: 10.1038/s41579-018-0003-6

14. Jacobson MD. Reactive oxygen species and programmed cell death. *Trends Biochem Sci* (1996) 21(3):83–6. doi: 10.1016/S0968-0004(96)20008-8

15. Foo J, Bellot G, Pervaiz S, Alonso S. Mitochondria-mediated oxidative stress during viral infection. *Trends Microbiol* (2022) 30(7):679–92. doi: 10.1016/j.tim.2021.12.011

16. Sun L, Wu J, Du F, Chen X, Chen ZJ. Cyclic GMP-AMP synthase is a cytosolic DNA sensor that activates the type I interferon pathway. *Science* (2013) 339(6121):786–91. doi: 10.1126/science.1232458

17. Ablasser A, Goldeck M, Cavlar T, Deimling T, Witte G, Rohl I, et al. cGAS produces a 2'-5'-linked cyclic dinucleotide second messenger that activates STING. *Nature* (2013) 498(7454):380–4. doi: 10.1038/nature12306

18. Ishikawa H, Barber GN. STING is an endoplasmic reticulum adaptor that facilitates innate immune signalling. *Nature* (2008) 455(7213):674–8. doi: 10.1038/nature07317

19. Tanaka Y, Chen ZJ. STING specifies IRF3 phosphorylation by TBK1 in the cytosolic DNA signaling pathway. *Sci Signal* (2012) 5(214):ra20. doi: 10.1126/scisignal.2002521

20. de Oliveira Mann CC, Orzalli MH, King DS, Kagan JC, Lee ASY, Kranzusch PJ. Modular architecture of the STING C-terminal tail allows interferon and NF-κB signaling adaptation. *Cell Rep* (2019) 27(4):1165–75.e5. doi: 10.1016/j.celrep.2019.03.098

21. Neufeldt CJ, Cerikan B, Cortese M, Frankish J, Lee JY, Plociennikowska A, et al. SARS-CoV-2 infection induces a pro-inflammatory cytokine response through cGAS-STING and NF-κB. *Commun Biol* (2022) 5(1):45. doi: 10.1038/s42003-021-02983-5

22. Jia M, Qin D, Zhao C, Chai L, Yu Z, Wang W, et al. Redox homeostasis maintained by GPX4 facilitates STING activation. *Nat Immunol* (2020) 21(7):727–35. doi: 10.1038/s41590-020-0699-0

23. Smith JA. STING, the endoplasmic reticulum, and mitochondria: is three a crowd or a conversation? *Front Immunol* (2020) 11:611347. doi: 10.3389/fimmu.2020.611347

24. Gui X, Yang H, Li T, Tan X, Shi P, Li M, et al. Autophagy induction *via* STING trafficking is a primordial function of the cGAS pathway. *Nature* (2019) 567(7747):262–6. doi: 10.1038/s41586-019-1006-9

25. Moretti J, Roy S, Bozec D, Martinez J, Chapman JR, Ueberheide B, et al. STING senses microbial viability to orchestrate stress-mediated autophagy of the endoplasmic reticulum. *Cell* (2017) 171(4):809–23 e13. doi: 10.1016/j.cell.2017.09.034

26. Zhang Y, Sun R, Geng S, Shan Y, Li X, Fang W. Porcine circovirus type 2 induces ORF3-independent mitochondrial apoptosis *via* PERK activation and elevation of cytosolic calcium. *J Virol* (2019) 93(7):e01784-18. doi: 10.1128/JVI.01784-18

27. Domizio JD, Gulen MF, Saidoune F, Thacker VV, Yatim A, Sharma K, et al. The cGAS-STING pathway drives type I IFN immunopathology in COVID-19. *Nature* (2022) 603(7899):145–51. doi: 10.1038/s41586-022-04421-w

28. Sharma KB, Chhabra S, Aggarwal S, Tripathi A, Banerjee A, Yadav AK, et al. Proteomic landscape of Japanese encephalitis virus-infected fibroblasts. *J Gen Virol* (2021) 102(9). doi: 10.1099/jgv.0.001657

29. Zhou Z, Zhang X, Lei X, Xiao X, Jiao T, Ma R, et al. Sensing of cytoplasmic chromatin by cGAS activates innate immune response in SARS-CoV-2 infection. *Signal Transduct Target Ther* (2021) 6(1):382. doi: 10.1038/s41392-021-00800-3

30. Sun B, Sundstrom KB, Chew JJ, Bist P, Gan ES, Tan HC, et al. Dengue virus activates cGAS through the release of mitochondrial DNA. *Sci Rep* (2017) 7(1):3594. doi: 10.1038/s41598-017-03932-1

31. Zheng Y, Liu Q, Wu Y, Ma L, Zhang Z, Liu T, et al. Zika virus elicits inflammation to evade antiviral response by cleaving cGAS *via* NS1-caspase-1 axis. *EMBO J* (2018) 37(18):e99347. doi: 10.15252/embj.201899347

32. Song B, Liu D, Greco TM, Cristea IM. Post-translational modification control of viral DNA sensors and innate immune signaling. *Adv Virus Res* (2021) 109:163–99. doi: 10.1016/bs.aivir.2021.03.001

33. Dai J, Huang YJ, He X, Zhao M, Wang X, Liu ZS, et al. Acetylation blocks cGAS activity and inhibits self-DNA-induced autoimmunity. *Cell* (2019) 176(6):1447–60.e14. doi: 10.1016/j.cell.2019.01.016

34. Song B, Greco TM, Lum KK, Taber CE, Cristea IM. The DNA sensor cGAS is decorated by acetylation and phosphorylation modifications in the context of immune signaling. *Mol Cell Proteomics* (2020) 19(7):1193–208. doi: 10.1074/mcp.RA120.001981

35. Erttmann SF, Swacha P, Aung KM, Brindefalk B, Jiang H, Hartlova A, et al. The gut microbiota prime systemic antiviral immunity *via* the cGAS-STING-IFN-I axis. *Immunity* (2022) 55(5):847–61.e10. doi: 10.1016/j.immuni.2022.04.006

36. Schoggins JW, MacDuff DA, Imanaka N, Gainey MD, Shrestha B, Eitson JL, et al. Pan-viral specificity of IFN-induced genes reveals new roles for cGAS in innate immunity. *Nature* (2014) 505(7485):691–5. doi: 10.1038/nature12862

37. Liu X, Wei L, Xu F, Zhao F, Huang Y, Fan Z, et al. SARS-CoV-2 spike protein-induced cell fusion activates the cGAS-STING pathway and the interferon response. *Sci Signal* (2022) 15(729):eabg8744. doi: 10.1126/scisignal.abg8744

38. Amurri L, Horvat B, Iampietro M. Interplay between RNA viruses and cGAS/STING axis in innate immunity. *Front Cell Infect Microbiol* (2023) 13:1172739. doi: 10.3389/fcimb.2023.1172739

39. Ishikawa H, Ma Z, Barber GN. STING regulates intracellular DNA-mediated, type I interferon-dependent innate immunity. *Nature* (2009) 461(7265):788–92. doi: 10.1038/nature08476

40. Civril F, Deimling T, de Oliveira Mann CC, Ablasser A, Moldt M, Witte G, et al. Structural mechanism of cytosolic DNA sensing by cGAS. *Nature* (2013) 498(7454):332–7. doi: 10.1038/nature12305

41. Lio CW, McDonald B, Takahashi M, Dhanwani R, Sharma N, Huang J, et al. cGAS-STING signaling regulates initial innate control of cytomegalovirus infection. *J Virol* (2016) 90(17):7789–97. doi: 10.1128/JVI.01040-16

42. Reinert LS, Lopusna K, Winther H, Sun C, Thomsen MK, Nandakumar R, et al. Sensing of HSV-1 by the cGAS-STING pathway in microglia orchestrates antiviral defence in the CNS. *Nat Commun* (2016) 7:13348. doi: 10.1038/ncomms13348

43. Zhao L, Yuan H, Wang Y, Geng Y, Yun H, Zheng W, et al. HBV confers innate immune evasion through triggering HAT1/acetylation of H4K5/H4K12/miR-181a-5p or KPNA2/cGAS-STING/IFN-I signaling. *J Med Virol* (2023) 95(7):e28966. doi: 10.1002/jmv.28966

44. Dansako H, Imai H, Ueda Y, Satoh S, Shimotohno K, Kato N. High-level expression of STING restricts susceptibility to HBV by mediating type III IFN induction. *FASEB bioAdv* (2019) 1(2):67–80. doi: 10.1096/fba.1022

45. Garcia-Belmonte R, Perez-Nunez D, Pittau M, Richt JA, Revilla Y. African Swine Fever Virus Armenia/07 Virulent Strain Controls Interferon Beta Production through the cGAS-STING Pathway. *J Virol* (2019) 93(12):e02298-18. doi: 10.1128/JVI.02298-18

46. Gao D, Wu J, Wu YT, Du F, Aroh C, Yan N, et al. Cyclic GMP-AMP synthase is an innate immune sensor of HIV and other retroviruses. *Science* (2013) 341(6148):903–6. doi: 10.1126/science.1240933

47. Dansako H, Ueda Y, Okumura N, Satoh S, Sugiyama M, Mizokami M, et al. The cyclic GMP-AMP synthetase-STING signaling pathway is required for both the innate immune response against HBV and the suppression of HBV assembly. *FEBS J* (2016) 283(1):144–56. doi: 10.1111/febs.13563

48. He J, Hao R, Liu D, Liu X, Wu S, Guo S, et al. Inhibition of hepatitis B virus replication by activation of the cGAS-STING pathway. *J Gen Virol* (2016) 97(12):3368–78. doi: 10.1099/jgv.0.000647

49. Zheng X, Nie S, Feng WH. Regulation of antiviral immune response by African swine fever virus (ASFV). *Virol Sin* (2022) 37(2):157–67. doi: 10.1016/j.virs.2022.03.006

50. Li J, Song J, Kang L, Huang L, Zhou S, Hu L, et al. pMGF505-7R determines pathogenicity of African swine fever virus infection by inhibiting IL-1β and type I IFN production. *PloS Pathog* (2021) 17(7):e1009733. doi: 10.1371/journal.ppat.1009733

51. Li D, Yang W, Li L, Li P, Ma Z, Zhang J, et al. African swine fever virus MGF-505-7R negatively regulates cGAS-STING-mediated signaling pathway. *J Immunol* (2021) 206(8):1844–57. doi: 10.4049/jimmunol.2001110

52. Huang L, Xu W, Liu H, Xue M, Liu X, Zhang K, et al. African Swine Fever Virus pI215L Negatively Regulates cGAS-STING Signaling Pathway through Recruiting RNF138 to Inhibit K63-Linked Ubiquitination of TBK1. *J Immunol* (2021) 207(11):2754–69. doi: 10.4049/jimmunol.2100320

53. Christensen MH, Jensen SB, Miettinen JJ, Luecke S, Prabakaran T, Reinert LS, et al. HSV-1 ICP27 targets the TBK1-activated STING signalsome to inhibit virus-induced type I IFN expression. *EMBO J* (2016) 35(13):1385–99. doi: 10.15252/embj.201593458

54. Su C, Zheng C. Herpes Simplex Virus 1 Abrogates the cGAS/STING-Mediated Cytosolic DNA-Sensing Pathway *via* Its Virion Host Shutoff Protein, UL41. *J Virol* (2017) 91(6):e02414-16. doi: 10.1128/JVI.02414-16

55. You H, Zheng S, Huang Z, Lin Y, Shen Q, Zheng C. Herpes simplex virus 1 tegument protein UL46 inhibits TANK-binding kinase 1-mediated signaling. *mBio* (2019) 10(3):e00910-19. doi: 10.1128/mBio.00919-19

56. Stempel M, Chan B, Juranic Lisnic V, Krmpotic A, Hartung J, Paludan SR, et al. The herpesviral antagonist m152 reveals differential activation of STING-dependent IRF and NF-κB signaling and STING's dual role during MCMV infection. *EMBO J* (2019) 38(5):e100983. doi: 10.15252/embj.2018100983

57. Kong Z, Yin H, Wang F, Liu Z, Luan X, Sun L, et al. Pseudorabies virus tegument protein UL13 recruits RNF5 to inhibit STING-mediated antiviral immunity. *PloS Pathog* (2022) 18(5):e1010544. doi: 10.1371/journal.ppat.1010544

58. Fu YZ, Su S, Gao YQ, Wang PP, Huang ZF, Hu MM, et al. Human cytomegalovirus tegument protein UL82 inhibits STING-mediated signaling to evade antiviral immunity. *Cell Host Microbe* (2017) 21(2):231–43. doi: 10.1016/j.chom.2017.01.001

59. Choi HJ, Park A, Kang S, Lee E, Lee TA, Ra EA, et al. Human cytomegalovirus-encoded US9 targets MAVS and STING signaling to evade type I interferon immune responses. *Nat Commun* (2018) 9(1):125. doi: 10.1038/s41467-017-02624-8

60. Cheng M, Kanyema MM, Sun Y, Zhao W, Lu Y, Wang J, et al. African swine fever virus L83L negatively regulates the cGAS-STING-mediated IFN-I pathway by recruiting tollip to promote STING autophagic degradation. *J Virol* (2023) 97(2):e0192322. doi: 10.1128/jvi.01923-22

61. Polak SB, Van Gool IC, Cohen D, von der Thusen JH, van Paassen J. A systematic review of pathological findings in COVID-19: a pathophysiological timeline and possible mechanisms of disease progression. *Modern Pathol: an Off J United States Can Acad Pathol Inc* (2020) 33(11):2128–38. doi: 10.1038/s41379-020-0603-3

62. Su J, Rui Y, Lou M, Yin L, Xiong H, Zhou Z, et al. HIV-2/SIV Vpx targets a novel functional domain of STING to selectively inhibit cGAS-STING-mediated NF-κB signalling. *Nat Microbiol* (2019) 4(12):2552–64. doi: 10.1038/s41564-019-0585-4

63. Chen H, Wang Z, Gao X, Lv J, Hu Y, Jung YS, et al. ASFV pD345L protein negatively regulates NF-κB signalling by inhibiting IKK kinase activity. *Vet Res* (2022) 53(1):32. doi: 10.1186/s13567-022-01050-z

64. Wang W, Hu D, Wu C, Feng Y, Li A, Liu W, et al. STING promotes NLRP3 localization in ER and facilitates NLRP3 deubiquitination to activate the inflammasome upon HSV-1 infection. *PloS Pathog* (2020) 16(3):e1008335. doi: 10.1371/journal.ppat.1008335

65. Wang Y, Ning X, Gao P, Wu S, Sha M, Lv M, et al. Inflammasome activation triggers caspase-1-mediated cleavage of cGAS to regulate responses to DNA virus infection. *Immunity* (2017) 46(3):393–404. doi: 10.1016/j.immuni.2017.02.011

66. Ning X, Wang Y, Jing M, Sha M, Lv M, Gao P, et al. Apoptotic Caspases Suppress Type I Interferon Production *via* the Cleavage of cGAS, MAVS, and IRF3. *Mol Cell* (2019) 74(1):19–31 e7. doi: 10.1016/j.molcel.2019.02.013

67. Li F, Li J, Wang PH, Yang N, Huang J, Ou J, et al. SARS-CoV-2 spike promotes inflammation and apoptosis through autophagy by ROS-suppressed PI3K/AKT/mTOR signaling. *Biochim Biophys Acta Mol Basis Dis* (2021) 1867(12):166260. doi: 10.1016/j.bbadis.2021.166260

68. Menzel M, Ramu S, Calven J, Olejnicka B, Sverrild A, Porsbjerg C, et al. Oxidative stress attenuates TLR3 responsiveness and impairs anti-viral mechanisms in bronchial epithelial cells from COPD and asthma patients. *Front Immunol* (2019) 10:2765. doi: 10.3389/fimmu.2019.02765

69. Ornatowski W, Lu Q, Yegambaram M, Garcia AE, Zemskov EA, Maltepe E, et al. Complex interplay between autophagy and oxidative stress in the development of pulmonary disease. *Redox Biol* (2020) 36:101679. doi: 10.1016/j.redox.2020.101679

70. Scherz-Shouval R, Shvets E, Fass E, Shorer H, Gil L, Elazar Z. Reactive oxygen species are essential for autophagy and specifically regulate the activity of Atg4. *EMBO J* (2007) 26(7):1749–60. doi: 10.1038/sj.emboj.7601623

71. Wang L, Ning S. New look of EBV LMP1 signaling landscape. *Cancers (Basel)* (2021) 13(21):5451. doi: 10.3390/cancers13215451

72. Seifert U, Bialy LP, Ebstein F, Bech-Otschir D, Voigt A, Schroter F, et al. Immunoproteasomes preserve protein homeostasis upon interferon-induced oxidative stress. *Cell* (2010) 142(4):613–24. doi: 10.1016/j.cell.2010.07.036

73. Fan JB, Miyauchi-Ishida S, Arimoto K, Liu D, Yan M, Liu CW, et al. Type I IFN induces protein ISGylation to enhance cytokine expression and augments colonic inflammation. *Proc Natl Acad Sci U.S.A.* (2015) 112(46):14313–8. doi: 10.1073/pnas.1505690112

74. Hayman TJ, Baro M, MacNeil T, Phoomak C, Aung TN, Cui W, et al. STING enhances cell death through regulation of reactive oxygen species and DNA damage. *Nat Commun* (2021) 12(1):2327. doi: 10.1038/s41467-021-22572-8

75. Sies H, Jones DP. Reactive oxygen species (ROS) as pleiotropic physiological signalling agents. *Nat Rev Mol Cell Biol* (2020) 21(7):363–83. doi: 10.1038/s41580-020-0230-3

76. Wang S, Shi X, Wei S, Ma D, Oyinlade O, Lv SQ, et al. Krüppel-like factor 4 (KLF4) induces mitochondrial fusion and increases spare respiratory capacity of human glioblastoma cells. *J Biol Chem* (2018) 293(17):6544–55. doi: 10.1074/jbc.RA117.001323

77. Tao L, Lemoff A, Wang G, Zarek C, Lowe A, Yan N, et al. Reactive oxygen species oxidize STING and suppress interferon production. *Elife* (2020) 9:e57837. doi: 10.7554/eLife.57837

78. Saheb Sharif-Askari N, Saheb Sharif-Askari F, Mdkhana B, Hussain Alsayed HA, Alsafar H, Alrais ZF, et al. Upregulation of oxidative stress gene markers during SARS-COV-2 viral infection. *Free Radic Biol Med* (2021) 172:688–98. doi: 10.1016/j.freeradbiomed.2021.06.018

79. De Angelis M, Amatore D, Checconi P, Zevini A, Fraternale A, Magnani M, et al. Influenza virus down-modulates G6PD expression and activity to induce oxidative stress and promote its replication. *Front Cell Infect Microbiol* (2021) 11:804976. doi: 10.3389/fcimb.2021.804976

80. Paracha UZ, Fatima K, Alqahtani M, Chaudhary A, Abuzenadah A, Damanhouri G, et al. Oxidative stress and hepatitis C virus. *Virol J* (2013) 10:251. doi: 10.1186/1743-422X-10-251

81. West AP, Khoury-Hanold W, Staron M, Tal MC, Pineda CM, Lang SM, et al. Mitochondrial DNA stress primes the antiviral innate immune response. *Nature* (2015) 520(7548):553–7. doi: 10.1038/nature14156

82. Xiao Y, Cai W. Autophagy and viral infection. *Adv Exp Med Biol* (2020) 1207:425–32. doi: 10.1007/978-981-15-4272-5_30

83. Shrivastava S, Bhanja Chowdhury J, Steele R, Ray R, Ray RB. Hepatitis C virus upregulates Beclin1 for induction of autophagy and activates mTOR signaling. *J Virol* (2012) 86(16):8705–12. doi: 10.1128/JVI.00616-12

84. Lee HK, Lund JM, Ramanathan B, Mizushima N, Iwasaki A. Autophagy-dependent viral recognition by plasmacytoid dendritic cells. *Science* (2007) 315 (5817):1398–401. doi: 10.1126/science.1136880

85. Kim N, Kim MJ, Sung PS, Bae YC, Shin EC, Yoo JY. Interferon-inducible protein SCOTIN interferes with HCV replication through the autolysosomal degradation of NS5A. *Nat Commun* (2016) 7:10631. doi: 10.1038/ncomms10631

86. Sagnier S, Daussy CF, Borel S, Robert-Hebmann V, Faure M, Blanchet FP, et al. Autophagy restricts HIV-1 infection by selectively degrading Tat in CD4+ T lymphocytes. *J Virol* (2015) 89(1):615–25. doi: 10.1128/JVI.02174-14

87. Liu Y, Gordesky-Gold B, Leney-Greene M, Weinbren NL, Tudor M, Cherry S. Inflammation-induced, STING-dependent autophagy restricts zika virus infection in the drosophila brain. *Cell Host Microbe* (2018) 24(1):57–68 e3. doi: 10.1016/j.chom.2018.05.022

88. Kong N, Shan T, Wang H, Jiao Y, Zuo Y, Li L, et al. BST2 suppresses porcine epidemic diarrhea virus replication by targeting and degrading virus nucleocapsid protein with selective autophagy. *Autophagy* (2020) 16(10):1737–52. doi: 10.1080/15548627.2019.1707487

89. Miyakawa K, Nishi M, Ogawa M, Matsunaga S, Sugiyama M, Nishitsuji H, et al. Galectin-9 restricts hepatitis B virus replication *via* p62/SQSTM1-mediated selective autophagy of viral core proteins. *Nat Commun* (2022) 13(1):531. doi: 10.1038/s41467-022-28171-5

90. Yamashiro LH, Wilson SC, Morrison HM, Karalis V, Chung JJ, Chen KJ, et al. Interferon-independent STING signaling promotes resistance to HSV-1 in vivo. *Nat Commun* (2020) 11(1):3382. doi: 10.1038/s41467-020-17156-x

91. Saitoh T, Fujita N, Hayashi T, Takahara K, Satoh T, Lee H, et al. Atg9a controls dsDNA-driven dynamic translocation of STING and the innate immune response. *Proc Natl Acad Sci U.S.A.* (2009) 106(49):20842–6. doi: 10.1073/pnas.0911267106

92. Watson RO, Manzanillo PS, Cox JS. Extracellular M. tuberculosis DNA targets bacteria for autophagy by activating the host DNA-sensing pathway. *Cell* (2012) 150 (4):803–15. doi: 10.1016/j.cell.2012.06.040

93. Liang Q, Seo GJ, Choi YJ, Kwak MJ, Ge J, Rodgers MA, et al. Crosstalk between the cGAS DNA sensor and Beclin-1 autophagy protein shapes innate antimicrobial immune responses. *Cell Host Microbe* (2014) 15(2):228–38. doi: 10.1016/j.chom.2014.01.009

94. Martin M, Hiroyasu A, Guzman RM, Roberts SA, Goodman AG. Analysis of drosophila STING reveals an evolutionarily conserved antimicrobial function. *Cell Rep* (2018) 23(12):3537–50 e6. doi: 10.1016/j.celrep.2018.05.029

95. Liu D, Wu H, Wang C, Li Y, Tian H, Siraj S, et al. STING directly activates autophagy to tune the innate immune response. *Cell Death Differ* (2019) 26(9):1735–49. doi: 10.1038/s41418-018-0251-z

96. Wu J, Chen YJ, Dobbs N, Sakai T, Liou J, Miner JJ, et al. STING-mediated disruption of calcium homeostasis chronically activates ER stress and primes T cell death. *J Exp Med* (2019) 216(4):867–83. doi: 10.1084/jem.20182192

97. Fischer TD, Wang C, Padman BS, Lazarou M, Youle RJ. STING induces LC3B lipidation onto single-membrane vesicles *via* the V-ATPase and ATG16L1-WD40 domain. *J Cell Biol* (2020) 219(12):e202009128. doi: 10.1083/jcb.202009128

98. Ge L, Melville D, Zhang M, Schekman R. The ER-Golgi intermediate compartment is a key membrane source for the LC3 lipidation step of autophagosome biogenesis. *Elife* (2013) 2:e00947. doi: 10.7554/eLife.00947

99. Yang K, Huang Q, Wang R, Zeng Y, Cheng M, Xue Y, et al. African swine fever virus MGF505-11R inhibits type I interferon production by negatively regulating the cGAS-STING-mediated signaling pathway. *Vet Microbiol* (2021) 263:109265. doi: 10.1016/j.vetmic.2021.109265

100. Wang Z, Chen J, Wu X, Ma D, Zhang X, Li R, et al. PCV2 targets cGAS to inhibit type I interferon induction to promote other DNA virus infection. *PloS Pathog* (2021) 17(9):e1009940. doi: 10.1371/journal.ppat.1009940

101. Chen H, Jiang L, Chen S, Hu Q, Huang Y, Wu Y, et al. HBx inhibits DNA sensing signaling pathway *via* ubiquitination and autophagy of cGAS. *Virol J* (2022) 19 (1):55. doi: 10.1186/s12985-022-01785-3

102. Hou P, Lin Y, Li Z, Lu R, Wang Y, Tian T, et al. Autophagy receptor CCDC50 tunes the STING-mediated interferon response in viral infections and autoimmune diseases. *Cell Mol Immunol* (2021) 18(10):2358–71. doi: 10.1038/s41423-021-00758-w

103. Su J, Shen S, Hu Y, Chen S, Cheng L, Cai Y, et al. SARS-CoV-2 ORF3a inhibits cGAS-STING-mediated autophagy flux and antiviral function. *J Med Virol* (2022) 95 (1):e28175. doi: 10.1002/jmv.28175

104. Gall A, Treuting P, Elkon KB, Loo YM, Gale M Jr., Barber GN, et al. Autoimmunity initiates in nonhematopoietic cells and progresses *via* lymphocytes in an interferon-dependent autoimmune disease. *Immunity* (2012) 36(1):120–31. doi: 10.1016/j.immuni.2011.11.018

105. Prabakaran T, Bodda C, Krapp C, Zhang BC, Christensen MH, Sun C, et al. Attenuation of cGAS-STING signaling is mediated by a p62/SQSTM1-dependent autophagy pathway activated by TBK1. *EMBO J* (2018) 37(8):e97858. doi: 10.15252/embj.201797858

106. Richter B, Sliter DA, Herhaus L, Stolz A, Wang C, Beli P, et al. Phosphorylation of OPTN by TBK1 enhances its binding to Ub chains and promotes selective autophagy of damaged mitochondria. *Proc Natl Acad Sci U.S.A.* (2016) 113(15):4039–44. doi: 10.1073/pnas.1523926113

107. Schmeisser H, Bekisz J, Zoon KC. New function of type I IFN: induction of autophagy. *J Interferon Cytokine Res* (2014) 34(2):71–8. doi: 10.1089/jir.2013.0128

108. Schmeisser H, Fey SB, Horowitz J, Fischer ER, Balinsky CA, Miyake K, et al. Type I interferons induce autophagy in certain human cancer cell lines. *Autophagy* (2013) 9(5):683–96. doi: 10.4161/auto.23921

109. Tan T, Xia L. TRIM21 aggravates herpes simplex virus epithelial keratitis by attenuating STING-IRF3-mediated type I interferon signaling. *Front Microbiol* (2020) 11:703. doi: 10.3389/fmicb.2020.00703

110. Yum S, Li M, Fang Y, Chen ZJ. TBK1 recruitment to STING activates both IRF3 and NF-κB that mediate immune defense against tumors and viral infections. *Proc Natl Acad Sci U.S.A.* (2021) 118(14):e2100225118. doi: 10.1073/pnas.2100225118

111. Zhu H, Zhang R, Yi L, Tang YD, Zheng C. UNC93B1 attenuates the cGAS-STING signaling pathway by targeting STING for autophagy-lysosome degradation. *J Med Virol* (2022) 94(9):4490–501. doi: 10.1002/jmv.27860

112. Gu T, Yu D, Xu L, Yao YL, Yao YG. Tupaia GBP1 interacts with STING to initiate autophagy and restrict herpes simplex virus type 1 infection. *J Immunol* (2021) 207(11):2673–80. doi: 10.4049/jimmunol.2100325

113. Delorme-Axford E, Klionsky DJ. Inflammatory-dependent Sting activation induces antiviral autophagy to limit zika virus in the Drosophila brain. *Autophagy* (2019) 15(1):1–3. doi: 10.1080/15548627.2018.1539585

114. Liu Y, Cherry S. Zika virus infection activates sting-dependent antiviral autophagy in the Drosophila brain. *Autophagy* (2019) 15(1):174–5. doi: 10.1080/15548627.2018.1528813

115. Zhu Q, Hu H, Liu H, Shen H, Yan Z, Gao L. A synthetic STING agonist inhibits the replication of human parainfluenza virus 3 and rhinovirus 16 through distinct mechanisms. *Antiviral Res* (2020) 183:104933. doi: 10.1016/j.antiviral.2020.104933

116. Zhang R, Lin H, You Q, Zhang Z, Bai L, Chen F, et al. Peste des petits ruminants virus upregulates STING to activate ATF6-mediated autophagy. *J Virol* (2022) 96(20): e0137522. doi: 10.1128/jvi.01375-22

117. Sun M, Yu S, Ge H, Wang T, Li Y, Zhou P, et al. The A137R protein of african swine fever virus inhibits type I interferon production *via* the autophagy-mediated lysosomal degradation of TBK1. *J Virol* (2022) 96(9):e0195721. doi: 10.1128/jvi.01957-21

118. Yang K, Xue Y, Niu H, Shi C, Cheng M, Wang J, et al. African swine fever virus MGF360-11L negatively regulates cGAS-STING-mediated inhibition of type I interferon production. *Vet Res* (2022) 53(1):7. doi: 10.1186/s13567-022-01025-0

119. Liang JR, Lingeman E, Luong T, Ahmed S, Muhar M, Nguyen T, et al. A genome-wide ER-phagy screen highlights key roles of mitochondrial metabolism and ER-resident UFMylation. *Cell* (2020) 180(6):1160–77.e20. doi: 10.1016/j.cell.2020.02.017

120. Rowland AA, Voeltz GK. Endoplasmic reticulum-mitochondria contacts: function of the junction. *Nat Rev Mol Cell Biol* (2012) 13(10):607–25. doi: 10.1038/nrm3440

121. Bagchi P. Endoplasmic reticulum in viral infection. *Int Rev Cell Mol Biol* (2020) 350:265–84. doi: 10.1016/bs.ircmb.2019.10.005

122. Hetz C, Zhang K, Kaufman RJ. Mechanisms, regulation and functions of the unfolded protein response. *Nat Rev Mol Cell Biol* (2020) 21(8):421–38. doi: 10.1038/s41580-020-0250-z

123. Zhang X, Yuan Y, Jiang L, Zhang J, Gao J, Shen Z, et al. Endoplasmic reticulum stress induced by tunicamycin and thapsigargin protects against transient ischemic brain injury: Involvement of PARK2-dependent mitophagy. *Autophagy* (2014) 10 (10):1801–13. doi: 10.4161/auto.32136

124. Mochida K, Nakatogawa H. ER-phagy: selective autophagy of the endoplasmic reticulum. *EMBO Rep* (2022) 23(8):e55192. doi: 10.15252/embr.202255192

125. Banerjee A, Czinn SJ, Reiter RJ, Blanchard TG. Crosstalk between endoplasmic reticulum stress and anti-viral activities: A novel therapeutic target for COVID-19. *Life Sci* (2020) 255:117842. doi: 10.1016/j.lfs.2020.117842

126. Xue M, Fu F, Ma Y, Zhang X, Li L, Feng L, et al. The PERK arm of the unfolded protein response negatively regulates transmissible gastroenteritis virus replication by suppressing protein translation and promoting type I interferon production. *J Virol* (2018) 92(15):e00431-18. doi: 10.1128/JVI.00431-18

127. Chan SW. Unfolded protein response in hepatitis C virus infection. *Front Microbiol* (2014) 5:233. doi: 10.3389/fmicb.2014.00233

128. Mazel-Sanchez B, Iwaszkiewicz J, Bonifacio JPP, Silva F, Niu C, Strohmeier S, et al. Influenza A viruses balance ER stress with host protein synthesis shutoff. *Proc Natl Acad Sci U.S.A.* (2021) 118(36):e2024681118. doi: 10.1073/pnas.2024681118

129. Yin H, Zhao L, Jiang X, Li S, Huo H, Chen H. DEV induce autophagy *via* the endoplasmic reticulum stress related unfolded protein response. *PloS One* (2017) 12 (12):e0189704. doi: 10.1371/journal.pone.0189704

130. Srikanth S, Woo JS, Wu B, El-Sherbiny YM, Leung J, Chupradit K, et al. The Ca2+ sensor STIM1 regulates the type I interferon response by retaining the signaling adaptor STING at the endoplasmic reticulum. *Nat Immunol* (2019) 20(2):152–62. doi: 10.1038/s41590-018-0287-8

131. Zhang Y, Chen W, Wang Y. STING is an essential regulator of heart inflammation and fibrosis in mice with pathological cardiac hypertrophy *via* endoplasmic reticulum (ER) stress. *BioMed Pharmacother* (2020) 125:110022. doi: 10.1016/j.biopha.2020.110022

132. Petrasek J, Iracheta-Vellve A, Csak T, Satishchandran A, Kodys K, Kurt-Jones EA, et al. STING-IRF3 pathway links endoplasmic reticulum stress with hepatocyte apoptosis in early alcoholic liver disease. *Proc Natl Acad Sci U.S.A.* (2013) 110 (41):16544–9. doi: 10.1073/pnas.1308331110

133. Liu YP, Zeng L, Tian A, Bomkamp A, Rivera D, Gutman D, et al. Endoplasmic reticulum stress regulates the innate immunity critical transcription factor IRF3. *J Immunol* (2012) 189(9):4630–9. doi: 10.4049/jimmunol.1102737

134. Marroqui L, Dos Santos RS, Op de Beeck A, Coomans de Brachene A, Marselli L, Marchetti P, et al. Interferon-α mediates human beta cell HLA class I overexpression, endoplasmic reticulum stress and apoptosis, three hallmarks of early human type 1 diabetes. *Diabetologia* (2017) 60(4):656–67. doi: 10.1007/s00125-016-4201-3

135. Reinert LS, Rashidi AS, Tran DN, Katzilieris-Petras G, Hvidt AK, Gohr M, et al. Brain immune cells undergo cGAS/STING-dependent apoptosis during herpes simplex virus type 1 infection to limit type I IFN production. *J Clin Invest* (2021) 131(1): e136824. doi: 10.1172/JCI136824

136. Brault M, Olsen TM, Martinez J, Stetson DB, Oberst A. Intracellular nucleic acid sensing triggers necroptosis through synergistic type I IFN and TNF signaling. *J Immunol* (2018) 200(8):2748–56. doi: 10.4049/jimmunol.1701492

137. Li C, Zhang Y, Liu J, Kang R, Klionsky DJ, Tang D. Mitochondrial DNA stress triggers autophagy-dependent ferroptotic death. *Autophagy* (2021) 17(4):948–60. doi: 10.1080/15548627.2020.1739447

138. Yan M, Li Y, Luo Q, Zeng W, Shao X, Li L, et al. Mitochondrial damage and activation of the cytosolic DNA sensor cGAS-STING pathway lead to cardiac pyroptosis and hypertrophy in diabetic cardiomyopathy mice. *Cell Death Discovery* (2022) 8(1):258. doi: 10.1038/s41420-022-01046-w

139. Fang Y, Peng K. Regulation of innate immune responses by cell death-associated caspases during virus infection. *FEBS J* (2022) 289(14):4098–111. doi: 10.1111/febs.16051

140. White MJ, McArthur K, Metcalf D, Lane RM, Cambier JC, Herold MJ, et al. Apoptotic caspases suppress mtDNA-induced STING-mediated type I IFN production. *Cell* (2014) 159(7):1549–62. doi: 10.1016/j.cell.2014.11.036

141. Rongvaux A, Jackson R, Harman CC, Li T, West AP, de Zoete MR, et al. Apoptotic caspases prevent the induction of type I interferons by mitochondrial DNA. *Cell* (2014) 159(7):1563–77. doi: 10.1016/j.cell.2014.11.037

142. Hong EE, Okitsu CY, Smith AD, Hsieh CL. Regionally specific and genome-wide analyses conclusively demonstrate the absence of CpG methylation in human mitochondrial DNA. *Mol Cell Biol* (2013) 33(14):2683–90. doi: 10.1128/MCB.00220-13

143. Mankan AK, Schmidt T, Chauhan D, Goldeck M, Honing K, Gaidt M, et al. Cytosolic RNA:DNA hybrids activate the cGAS-STING axis. *EMBO J* (2014) 33 (24):2937–46. doi: 10.15252/embj.201488726

144. Jiang W, Li R, Zhang Y, Wang P, Wu T, Lin J, et al. Mitochondrial DNA mutations associated with type 2 diabetes mellitus in chinese uyghur population. *Sci Rep* (2017) 7(1):16989. doi: 10.1038/s41598-017-17086-7

145. Collins LV, Hajizadeh S, Holme E, Jonsson IM, Tarkowski A. Endogenously oxidized mitochondrial DNA induces *in vivo* and *in vitro* inflammatory responses. . *J Leukoc Biol* (2004) 75(6):995–1000. doi: 10.1189/jlb.0703328

146. Saffran HA, Pare JM, Corcoran JA, Weller SK, Smiley JR. Herpes simplex virus eliminates host mitochondrial DNA. *EMBO Rep* (2007) 8(2):188–93. doi: 10.1038/sj.embor.7400878

147. Li H, Zhou F, Zhang L. STING, a critical contributor to SARS-CoV-2 immunopathology. *Signal Transduct Target Ther* (2022) 7(1):106. doi: 10.1038/s41392-022-00967-3

148. Hou J, Wei Y, Zou J, Jaffery R, Liang S, Zheng C, et al. Integrated multi-omics analyses identify anti-viral host factors and pathways controlling SARS-CoV-2 infection. *Res Sq* (2022):rs.3.rs-1910932. doi: 10.21203/rs.3.rs-1910932/v1

149. Decout A, Katz JD, Venkatraman S, Ablasser A. The cGAS–STING pathway as a therapeutic target in inflammatory diseases. *Nat Rev Immunol* (2021) 21(9):548–69. doi: 10.1038/s41577-021-00524-z

frontiers | Frontiers in Immunology

TYPE Original Research
PUBLISHED 01 March 2024
DOI 10.3389/fimmu.2024.1340997

OPEN ACCESS

EDITED BY
Allan R. Brasier,
University of Wisconsin-Madison,
United States

REVIEWED BY
Qiaoyu Shao,
Brigham and Women's Hospital and Harvard Medical School, United States
Minghan Yang,
New York University, United States
Yiyi Ji,
Duke University, United States
Zhirong Zhao,
North China Electric Power University, China
Xiangxiang Hu,
University of Minnesota Twin Cities, United States
Qinglong Wang,
Beth Israel Deaconess Medical Center and Harvard Medical School, United States

*CORRESPONDENCE
Yue Xu
doctor_xuyue@sina.com
Xiaopeng Hu
xiaopeng_hu@sina.com

†These authors have contributed equally to this work and share first authorship

RECEIVED 19 November 2023
ACCEPTED 19 February 2024
PUBLISHED 01 March 2024

CITATION
Zhang H, Zheng C, Xu Y and Hu X (2024) Comprehensive molecular and cellular characterization of endoplasmic reticulum stress-related key genes in renal ischemia/reperfusion injury. *Front. Immunol.* 15:1340997. doi: 10.3389/fimmu.2024.1340997

Comprehensive molecular and cellular characterization of endoplasmic reticulum stress-related key genes in renal ischemia/reperfusion injury

Hao Zhang[1,2†], Chaoyue Zheng[1,2†], Yue Xu[1,2*] and Xiaopeng Hu[1,2*]

[1]Department of Urology, Beijing Chao-Yang Hospital, Capital Medical University, Beijing, China, [2]Institute of Urology, Capital Medical University, Beijing, China

Background: Renal ischemia-reperfusion injury (RIRI) is an inevitable complication in the process of kidney transplantation and lacks specific therapy. The study aims to determine the underlying mechanisms of RIRI to uncover a promising target for efficient renoprotection.

Method: Four bulk RNA-seq datasets including 495 renal samples of pre- and post-reperfusion were collected from the GEO database. The machine learning algorithms were utilized to ascertain pivotal endoplasmic reticulum stress genes. Then, we incorporated correlation analysis and determined the interaction pathways of these key genes. Considering the heterogeneous nature of bulk-RNA analysis, the single-cell RNA-seq analysis was performed to investigate the mechanisms of key genes at the single-cell level. Besides, 4-PBA was applied to inhibit endoplasmic reticulum stress and hence validate the pathological role of these key genes in RIRI. Finally, three clinical datasets with transcriptomic profiles were used to assess the prognostic role of these key genes in renal allograft outcomes after RIRI.

Results: In the bulk-RNA analysis, endoplasmic reticulum stress was identified as the top enriched pathway and three endoplasmic reticulum stress-related genes (PPP1R15A, JUN, and ATF3) were ranked as top performers in both LASSO and Boruta analyses. The three genes were found to significantly interact with kidney injury-related pathways, including apoptosis, inflammatory response, oxidative stress, and pyroptosis. For oxidative stress, these genes were more strongly related to oxidative markers compared with antioxidant markers. In single-cell transcriptome, the three genes were primarily upregulated in endothelium, distal convoluted tubule cells, and collecting duct principal cells among 12 cell types of renal tissues in RIRI. Furthermore, distal convoluted tubule cells and collecting duct principal cells exhibited pro-inflammatory status and the highest pyroptosis levels, suggesting their potential as main effectors of three key genes for mediating RIRI-associated injuries. Importantly, inhibition of these key genes using 4-phenyl butyric acid alleviated functional and histological damage in a mouse RIRI model. Finally, the three genes demonstrated highly prognostic value in predicting graft survival outcomes.

Conclusion: The study identified three key endoplasmic reticulum stress-related genes and demonstrated their prognostic value for graft survival, providing references for individualized clinical prevention and treatment of postoperative complications after renal transplantation.

KEYWORDS

renal ischemia-reperfusion injury, endoplasmic reticulum stress, renal transplantation, single-cell gene expression analysis, bioinformatics

1 Introduction

Renal ischemia-reperfusion injury (RIRI) refers to the pathological changes in the process of tissue re-oxygenation following ischemia (1). In renal transplantation, allograft kidneys inevitably undergo RIRI, causing delayed recovery of allograft function, acute rejection and even loss of allograft (2, 3). Many potential mechanisms of RIRI have been determined, including inflammatory responses, oxidative damage and endothelial dysfunction (4, 5). In detail, the oxidative and inflammatory status induced by ischemia is further exacerbated by the explosive production and dramatic accumulation of reactive oxygen species (ROS) after reperfusion (2, 3). Several techniques and drugs were developed to prevent or alleviate RIRI, including reduction of renal ischemic time, elimination of ROS, inflammation, and ischemic preconditioning (3, 6–8). Although these methods have been applied in clinical practice, the treatment outcomes for RIRI remain limited. Thus, future studies that explored potential mechanisms underlying RIRI are in unmet need for the development of novel strategies to efficiently prevent or mitigate RIRI.

Endoplasmic reticulum (ER) is a vital organelle for maintaining cellular homeostasis and acting a crucial role in protein synthesis, folding and structural maturation (9). Many factors, including hypoxia, oxidative stress, metabolic abnormalities, iron imbalance, calcium ion leakage, and viral infection, impair the ER protein-folding ability, causing the accumulation of unfolded and misfolded proteins. This resulting disorder of ER homeostasis refers to ER stress (ERS) (10–12). ERS has been reported to be involved in various renal diseases, including genetic mutations, acute kidney injury, diabetic nephropathy, and proteinuria (13). However, the underlying mechanisms of ERS in RIRI remain ambiguous. Several studies have identified ER molecular chaperones (BiP/GRP78 and GRP94) and found that unfolded protein response inducers could induce BiP/GRP78 and alleviate RIRI, suggesting the protective role of ERS in RIRI (14–17). On the contrary, intermedin was reported to protect against RIRI by repressing ERS and ERS-related apoptosis, indicating the pathogenic role of ERS in RIRI (18). Although this apparent discrepancy remains undefined, these experimental results are in accordance with the "double-edged sword" hypothesis of ERS. Specifically, the mild-moderate and severe ERS-induced cytoprotective unfolded protein response and pathological apoptotic pathways, respectively. Owing to the contradictory findings of ERS in RIRI, it is crucial to describe in detail the role of ERS in RIRI and identify key ERS-related genes based on large human and mouse datasets, which might serve as therapeutic targets.

In this research, we integrated bulk transcriptomic and single-cell RNA-seq datasets to elucidate the detailed mechanisms underlying ERS in RIRI. In bulk transcriptomic levels, the inducers and downstream targets of ERS were top upregulated in the renal tissue after reperfusion. Then, we enrolled the ERS-related gene sets and identified three key ERS-related genes, which were consistently upregulated among human and mouse datasets during RIRI. The three key ERS-related genes were strongly correlated with pathological pathways participating in RIRI, including NF-kappa B, inflammatory pathways, apoptosis, oxidative stress and pyroptosis. At the single-cell level, altered expressions of three key ERS-related genes before and after reperfusion were primarily observed in endothelium, DCT and CD-PC. Among these three cell types, DCT and CD-PC exhibited the pro-inflammatory status and the highest pyroptosis levels. In addition, the three genes were demonstrated as risk factors for allograft survival, deteriorated graft function and allograft loss. Overall, our results highlighted the crucial role of the three key ERS-related genes in RIRI and provided evidence for potential RIRI treatments targeting these three genes.

2 Materials and methods

2.1 Bulk RNA data collection and processing

We enrolled three human bulk RNA-seq datasets (GSE43974, GSE90861 and GSE126805) (19–21) comprising a total of 495 renal samples of pre- and post-reperfusion. The mouse bulk RNA-seq dataset (GSE98622) (22) included various post-reperfusion time points and was used for cross-species validation. In addition, three datasets (GSE21374, GSE52694, and GSE58601) (23–25) containing transcriptomic data of renal allografts and graft outcomes were collected for clinical analysis. All datasets were downloaded from

the publicly available GEO database, and data acquisition and application were accorded to GEO publication guidelines and data access policies.

The DESeq2 R package and limma R package were utilized for normalization and differential expressed gene (DEG) analysis of bulk RNA-seq data and bulk RNA array data, respectively (26, 27). For enrichment analysis, the Kyoto Encyclopedia of Genes and Genomes (KEGG) and Gene Ontology (GO) pathway analysis were conducted using the DAVID online enrichment tool (https://david.ncifcrf.gov). The single-sample gene set enrichment analysis (ssGSEA) by the gsva R package was implemented with gene sets as the reference, including hallmarks obtained from the Molecular Signatures Database (MSigDB) and cell-death-related gene signatures (28). The protein-protein interaction (PPI) networks were acquired from the STING online database and visualized by the Cytoscape software. The glmnet R package was used to apply the least absolute shrinkage and selection operator (LASSO) regression analysis to select candidate genes for further study. The relevance scores obtained from GeneCards presented the correlations between key genes and oxidative stress markers. The interactions with a relevance score ≥ 5 were applied by the Cytoscape software to construct networks of key genes and oxidative stress markers. The CIBERSORT algorithm (29) was utilized to infer the 22 immune cell populations of renal allografts. For the construction of miRNA- and transcription factors (TFs)-gene regulatory networks, miRNet (https://www.mirnet.ca/) and NetworkAnalyst (https://www.networkanalyst.ca/) were accessed to obtain miRNA and upstream TFs of selected genes, respectively (30, 31). Additionally, the Kaplan–Meier survival curve was used for assessing the prognostic value of key genes using the survival (https://github.com/therneau/survival) and survminer (https://github.com/kassambara/survminer) R packages.

2.2 Collection and analysis of single-cell transcriptome data

The mouse single-cell dataset (GSE161201) (32) contained one normal renal sample and two RIRI samples (samples from 6 hours and 24 hours post-reperfusion). The single-cell transcriptome data was processed and integrated using the Seurat R (33) and Harmony R (34) packages, respectively. The single-cell data matrices were filtered by custom criterion (cells expressing 500~3000 and with proportions of mitochondrial genes < 50% and ribosomal genes < 10% were retained). Marker genes for clusters were selected by the Seurat FindAllMarkers function (genes at least detected in 25% of cells in target population cells, $\log_2$FC > 0.25). Odds ratios (OR) of each cell cluster were calculated and characterized the tissue or sample distribution of meta-clusters (35). Cell–cell interaction analysis was conducted by the CellChat R package (www.cellchat.org). For enrichment analysis of target cell types, the Seurat FindMarkers function was implemented to calculate the log fold change of genes among different groups, applying for the gene set enrichment analysis (GSEA) with hallmarks as reference. The irGSEA R package (https://github.com/chuiqin/irGSEA/) was utilized to calculate the singscore of specific gene sets for single cells.

Supplementary Table 1 summarizes detailed information on the above data sets used in this study.

2.3 Experimental mouse RIRI model and estimation of renal damage

In animal experiments, twenty-four C57BL/6 mice (8 weeks old, male) were purchased from Weitonglihua (Beijing, China) and housed under a 12-hour light dark cycle with free access to food and water. All mice were kept in a pathogen-free environment and given a week to adapt to the conditions. The 4-phenyl butyric acid (4-PBA) (100mg/kg, intraperitoneally injected 1 h prior renal ischemia, MCE), an ERS inhibitor, was dissolved in phosphate buffered saline (PBS) and sodium hydroxide was applied to adjust pH to 7.4. Mice were categorized into four groups, including the sham group with PBS (sham + PBS group, n=6), IRI group with PBS (IRI + PBS group, n=6), IRI group with 4-PBA (IRI + 4-PBA group, n=6) and sham group with 4-PBA (sham + 4-PBA group, n=6). RIRI models were conducted with the following procedures: after anesthetized with intraperitoneal injection of pentobarbital, the right kidney was cut, and the left renal pedicle was clamped for thirty minutes in a heating pad (34°C - 36°C), followed by blood reperfusion for 24h. Mice in sham + PBS and sham + 4-PBA groups experienced the same processes without clamping of the left renal pedicle. All mice were euthanized 24 hours after corresponding operation and blood samples and left kidneys were then collected. The renal samples isolated from mice were fixed in 4% paraformaldehyde, embedded in paraffin and stained with Hematoxylin and eosin (H&E), periodic acid-Schiff staining (PAS) and terminal deoxynucleotidyl transferase dUTP nick end labeling (TUNEL) to assess renal histological injury in general. The blood samples were centrifugated at a speed of 3000 revolutions per minute for 10 minutes to get serum samples for blood urea nitrogen (BUN) and creatinine (Cre) measurements by an automated chemistry analyzer (Chemray 800).

2.4 qRT-PCR analysis

Total RNA was isolated from the kidneys using TRIzol reagent and then reverse transcribed to cDNA by a cDNA synthesis kit. The mRNA expression levels were normalized to the Ct values of the internal control gene (GAPDH), and fold changes were calculated compared with the control samples. Each sample was performed in triplicate in independent experiments. The primer sequences of three key ERS-related genes were listed in Supplementary Table 5.

2.5 Statistical analysis

The normality of the variable distribution was assessed using the D'Agostino and Pearson omnibus normality tests. Parameters with normal distribution were conducted contrasts by a two-tailed unpaired t-test and the Pearson correlation analysis. For variables that did not follow a normal distribution, the Mann-Whitney U test and Spearman correlation were employed. A significance level of less than 0.05 was considered statistically significant. We performed R software (version

4.0.5; http://www.r-project.org/) for statistical analysis and graphical representations.

3 Results

3.1 Biological processes and pathways activated during RIRI

The DEG analysis for GSE43974 was performed and identified 219 DEGs (177 up-regulated genes and 42 down-regulated genes) (Supplementary Table 2) based on the criterion (|logFC| > 0.5 and *FDR* < 0.05) (Figure 1A). The significantly enriched GO terms based on DEGs referred to "response to unfolded protein", "response to heat", "unfolded protein binding" and "protein binding involved in protein folding" (Figure 1B; Supplementary Table 3). The functionally KEGG pathway analysis displayed that the significantly top pathways involved in RIRI were the MAPK signaling pathway, protein processing in ER and NF–kappa B signaling pathway (Figure 1C; Supplementary Table 3). Overall, biological GO and KEGG pathway analyses indicated a response of renal tissues to unfolded proteins in the ER during post-reperfusion. Co-activation of the ERS, MAPK pathway and apoptosis as evidenced by significantly upregulated c-Jun N-terminal kinase (JNK) and CHOP (36) during RIRI pointed to interactions between ERS, JNK/p38 MAPK signaling and apoptosis (Figure 1D). Additionally, nuclear factor-kB (NF-kappa B) was demonstrated to be the target of ERS (37). In brief, ERS inducers and downstream targets were activated in the renal tissue after reperfusion.

3.2 Identification and verification of key ERS-related genes during RIRI

ERS-related genes (n=258) from two ERS-related gene sets (including GO RESPONSE TO ENDOPLASMICRETICULUM STRESS and GO REGULATION OF RESPONSE TO ENDOPLASMIC RETICULUM STRESS) were obtained from Molecular Signature Database v7.0 (MSigDB). Then, eight genes (*ATF3, PPP1R15A, CEBPB, PMAIP1, HSPA1A, ERN1, DDIT3*, and *JUN*) were selected through an intersection analysis between ERS-related genes and DEGs (Figure 2A). The PPI network showed that these eight genes were all strongly linked (Figure 2B). Three key genes (*PPP1R15A*, *JUN* and *ATF3*) were identified from these eight genes using the LASSO algorithm (Figures 2C, D), which ranked the top three by Boruta analysis (Figure 2E). Then, we found that these three key genes were also significantly elevated in two additional datasets (GSE90861 and GSE126805) during RIRI (Figure 2F). The mouse dataset (GSE98622) included transcriptomic data of sham control kidneys and post-reperfusion renal tissues at various post-reperfusion time points (2h, 4h, 24h, 2d, 3d, 7d, 14d, 28d, 6m and 12m). The time course analysis of three key genes using the GSE98622 dataset revealed that gene expression levels were significantly elevated during early reperfusion (2h, 4h and 24h) (Figure 2G). In addition, we also found

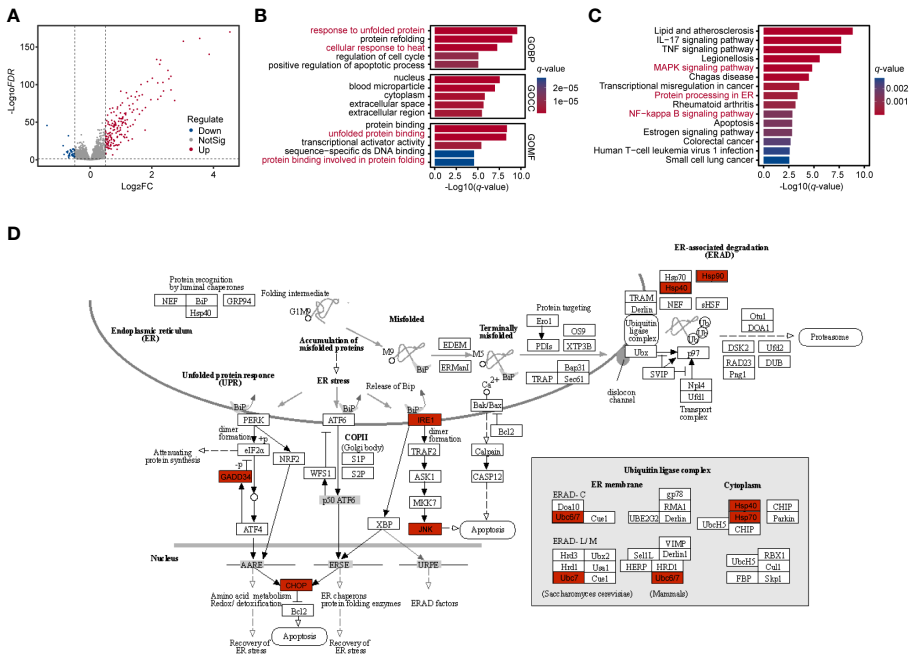

FIGURE 1
Enrichment analysis of renal tissues during RIRI. **(A)** Volcano plot shows DEGs between post-reperfusion and pre-reperfusion samples. Blue and red dots represent significantly downregulated genes and upregulated genes, respectively. **(B, C)** Bar plots showing top 5 Gene Ontology (GO) and Kyoto Encyclopedia of Genes and Genomes (KEGG) pathways for significantly differentially expressed genes during RIRI. Bar length and color represent log10-transformation with q-value of their corresponding pathways. **(D)** Top disturbed pathway during reperfusion of ischemically injured kidneys, namely Protein processing in ER (modified from KEGG pathway hsa04141). Significantly differentially expressed genes are indicated in red. RIRI, renal ischemia-reperfusion injury; DEG, differential expressed gene; ER, endoplasmic reticulum.

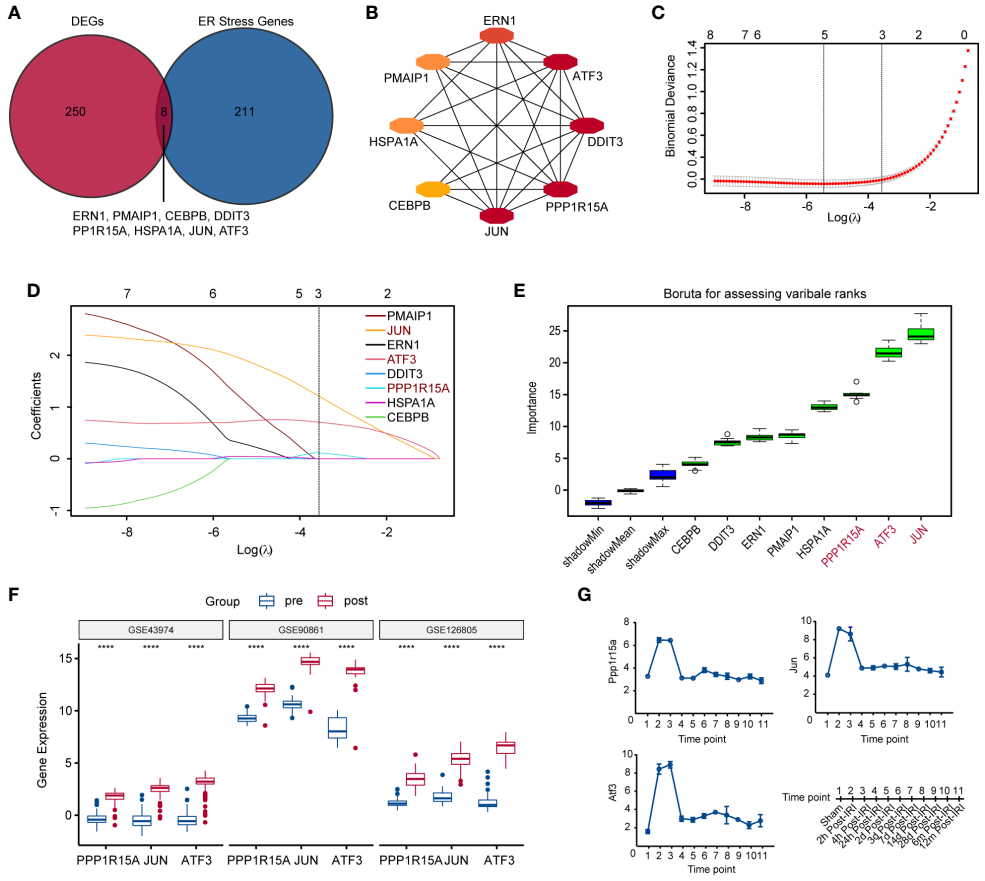

FIGURE 2
Identification and verification of key ERS-related genes during RIRI. **(A)** Veen plot shows the intersection of differentially significantly expressed genes (DEGs) and ERS-related genes. **(B)** The protein-protein interaction (PPI) network displaying eight tightly intersected genes. **(C)** The coefficient profiles of the LASSO regression model. **(D)** Cross-validation for tuning parameter screening in the LASSO regression model. **(E)** Boruta plot showing the importance (y-axis) of eight intersected genes. **(F)** Box plots showing the expression of three key ERS-gene after reperfusion in GSE43974, GSE90861 and GSE126805. **(G)** Line plots show changes in expression levels of three key ERS-related genes controls and RIRI samples at various post-reperfusion stages, including eleven different time points as illustrated on the bottom-right side. ERS, endoplasmic reticulum stress; LASSO, least absolute shrinkage and selection operator. ****p<0.0001.

that these three gene levels 6 months after RIRI were higher compared to pre-reperfusion samples (Figure 2G), suggesting that these three gene levels might serve as an indicator for the long-term prognosis of patients with renal transplantation.

3.3 Three key ERS-related genes exhibited closely related to inflammatory pathways, apoptosis, oxidative stress and pyroptosis during RIRI

In three independent RIRI datasets, the levels of apoptosis, hypoxia, inflammatory response and TNFα signaling via NF-kappa B were significantly higher than in pre-reperfusion samples (Supplementary Figures S1A–D). The correlation results showed that three key genes positively correlated with these kidney injury-related pathways across three human RIRI datasets (Figure 3A). Furthermore, inflammatory genes (*CCL2, CCL20, CCL8* and *CXCL2*) were demonstrated to positively correlate with all three genes. The chemokine genes (*CCL2, CCL20, CCL8* and *CXCL2*) displayed chemotactic activity for monocytes, basophils, lymphocytes and eosinophils (Figure 3B). However, analysis of immune cell abundances based on the bulk RNA dataset indicated that only eosinophils abundances showed significantly increased after reperfusion (Supplementary Figures S2A–D). Moreover, eosinophils infiltrating abundances were positively correlated with three key ERS-related gene expression levels (sure S2E). The GeneCard database was applied for correlation analysis between oxidative stress markers and the three genes, revealing that these genes were more strongly related to oxidative markers than antioxidant markers (Figure 3C). The networks of the three genes revealed that the oxidative markers, including total oxidant status (TOS), ROS and oxidized glutathione (GSSG) were strongly correlated with both *JUN* and *ATF3* (Figure 3D). In addition, among 11 PCD-related gene sets (28), pyroptosis was strongly and positively correlated with key ERS-gene expression levels across three human datasets (Figure 3E). The pyroptosis scores after RIRI exhibited significantly higher than those of pre-reperfusion in the three human datasets (Figure 3F).

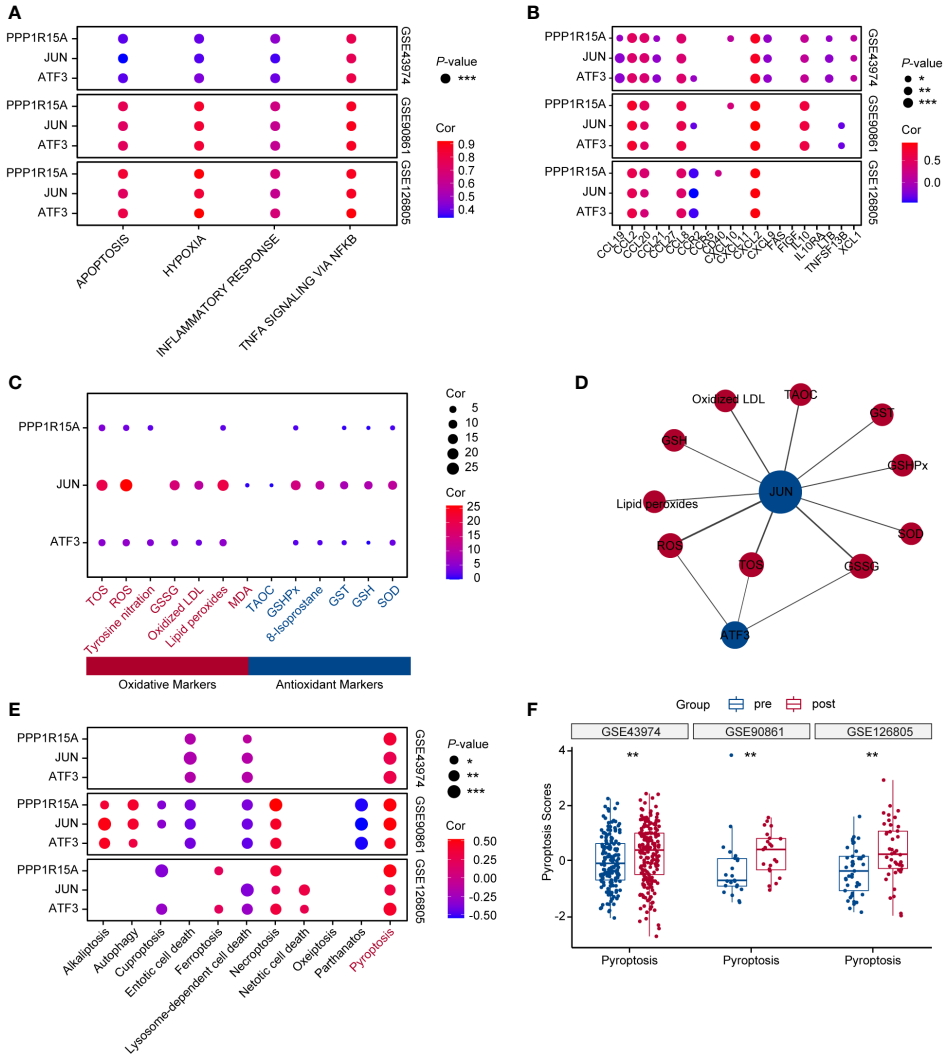

FIGURE 3
Key ERS-related genes show a crucial role for inflammatory pathways, apoptosis, oxidative stress and pyroptosis during RIRI. **(A)** Bubble chart displaying correlation analysis between key ERS-related gene expression levels and RIRI-related pathway scores. Bubble size and color are represented with p-values and coefficients of correlation analysis in GSE43974, GSE90861 and GSE126805. **(B)** Bubble plot showing correlation analysis between three key gene expression values and inflammatory gene expression levels. The p-values and coefficients of correlation analysis are indicated in bubble size and color. **(C)** Bubble plot of the relevance scores of key ERS-related gene expression levels and oxidative stress. Red text represents oxidative markers, and blue text represents antioxidant markers. **(D)** The networks of key ERS-genes with oxidative markers. Oxidative biomarkers and antioxidant biomarkers are indicated in red and blue. **(E)** Bubble plot of the relevance scores of key ERS-related gene expression levels and 11 programmed cell death levels. **(F)** Box plots showing pyroptosis scores between pre-and post-reperfusion in GSE43974, GSE90861 and GSE126805. *p < 0.05, **p<0.01, ***p<0.001.

3.4 Prediction of miRNA and TFs for three key ERS-related genes

The miRNA- and TF-mRNA interaction networks were comprised of 137 miRNAs and 174 TFs, respectively. For miRNA-mRNA regulatory interactions, 31 miRNAs, 113 miRNAs and 31 miRNAs target *PPP1R15A, JUN* and *ATF3*, respectively (Supplementary Figure S3A). Among them, ten miRNAs (hsa-mir-1-3p, hsa-mir-10b-5p, hsa-mir-16-5p, hsa-mir-17-5p, hsa-mir-21-3p, hsa-mir-24-3p, hsa-mir-30a-5p, hsa-mir-34a-5p, hsa-mir-124-3p and hsa-mir-191-5p) could regulate all three key ERS-related genes (Supplementary Figure S3A). For TF-mRNA regulatory interactions, *PPP1R15A, JUN* and *ATF3* could be regulated by 120 TFs, 73 TFs and 39 TFs, respectively (Supplementary Figure S3B). Eight TFs, including *ZFP37, SMAD5, REST, RAD21, KLF16, FOXJ2, ELF1*, and *BCL11B*, could regulate all three key ERS-related genes (Supplementary Figure S3B).

3.5 Altered expressions of key ERS-related genes during RIRI injury were primarily in the endothelium, DCT and CD-PC

The single-cell RNA-seq dataset (GSE161201) included 22,310 cells, comprising 5,246 cells from the sham control sample, 10,393

cells from the RIRI-6h sample and 6,671 cells from the RIRI-24h sample (Supplementary Figure S4A). After filtration, 16,658 cells were obtained, including 4,282 cells from the sham control sample, 6,515 cells from the RIRI-6h sample, and 5,861 cells from the RIRI-24h sample. Next, a total of 22 clusters within the integrated dataset were identified and visualized by the t-SNE algorithm (Supplementary Figure S4B). The anatomical mapping of various cell types to specific nephron segments were presented due to the complexity of kidney tissue (Figure 4A). The clusters were combined and assigned to 12 known cell types based on the marker genes from the previous studies (38–40) and CellMarker database (http://xteam.xbio.top/CellMarker/) (Figures 4B, C; Supplementary Table 4). The OR of each cell type was calculated and visualized by the heatmap to characterize the distribution of the 12 known cell lineages among the three groups. The ORs of cell types showed that renal tissues of 24h post-reperfusion exhibited higher levels offibroblasts, neutrophil cells and macrophages than renal tissues of the control and 6h post-reperfusion (Figure 4D). Cell-cell interaction analysis showed that the number of interactions and interaction strengths between neutrophils and other cell types were elevated after reperfusion (Supplementary Figures S4C, D). The gene expression density maps were analyzed to explore cell-specific changes in key ERS-related gene expression levels for each sample. The key ERS-related genes were mainly upregulated in endothelium, CD-PC and DCT of RIRI-6h or RIRI-24h samples compared with the sham control sample (Figures 5A–F). These results supported weak connections between the key ERS-gene levels and most immune cell abundances by bulk RNA-seq analysis, suggesting the vital role of ERS on non-immune cells (endothelium, CD-PC and DCT) during RIRI damage.

3.6 DCT and CD-PC presented with pro-inflammatory status and high pyroptosis scores

Functional enrichment analysis of the endothelium, CD-PC and DCT in RIRI-6h or RIRI-24h samples compared with the control sample showed a consistently significant enrichment of TNFα signaling via NF-kappa B (Figure 6A). Apart from the endothelium, DCT and CD-PC exhibited enrichment of pro-inflammatory pathways (complement, inflammatory response, IL-2/STAT5 signaling and IL-6/JAK/STAT3 signaling pathways) and apoptosis (Figure 6A). Based on these results, we speculated that DCT and CD-PC with pro-inflammatory and apoptotic status served as main senders or targets of ERS for mediating RIRI injury. In addition, density maps were applied to estimate the relevance scores of pyroptosis for each cell type and showed that DCT and CD-PC exhibited the highest pyroptosis scores among all cell types examined (Figure 6B). In both DCT and CD-PC, the relative levels of pyroptosis were significantly increased in the RIRI-6h or RIRI-24h samples compared with the sham control sample (Figure 6C). In brief, pyroptosis responses were mainly in DCT and CD-PC among other renal cells and were significantly elevated during RIRI.

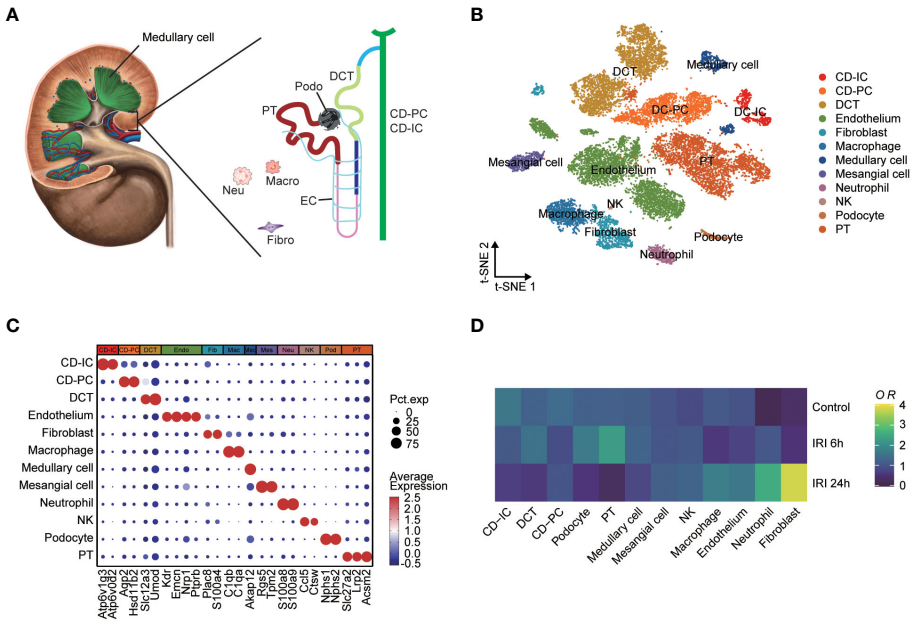

FIGURE 4
Single-cell characterization of mouse IRI kidneys. **(A)** Main cell types of mouse human kidney (CD-IC, collecting duct intercalated cells; CD-PC, collecting duct principal cells; DCT, distal convoluted tubule; EC, endothelium; Fibro, fibroblasts; Macro, macrophages; Neu, neutrophils; Podo, podocytes; PT, proximal tubule). **(B)** tSNE plot showing 16,658 cells from the sham control, IRI-6h and IRI-24h samples, colored by 12 major cell types. **(C)** Dotplot displaying the percent expressed cells and average expression levels of marker genes of 12 cell lineages. **(D)** Heatmap of relative abundances for each cell types among the sham control, IRI-6h and IRI-24h groups. The OR levels represent the cell abundances and range from 0 (blue) to 4 (yellow). tSNE, t-distributed stochastic neighbor embedding; OR, odds ratios.

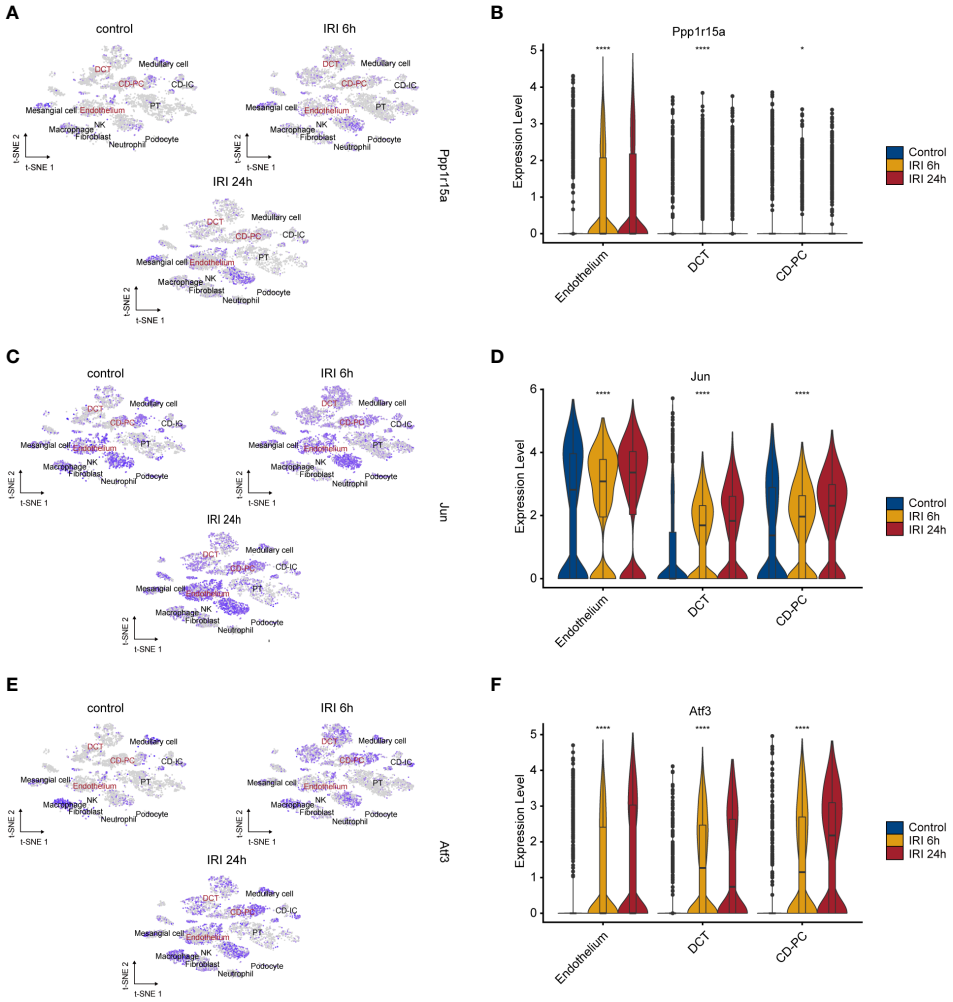

FIGURE 5
Characteristics of key ERS-gene expression levels during renal IRI. tSNE plots showing the expression of PPP1R15A **(A)**, JUN **(C)** and ATF3 **(E)** for 12 cell types. Intensities of color reveal normalized gene expression. Violine plots depicting significantly upregulation of PPP1R15A **(B)**, JUN **(D)** and ATF3 **(F)** in 6h and 24h post-reperfusion samples compared with sham control sample. *p<0.05, ****p<0.0001.

3.7 Inhibition of ERS alleviated RIRI and suppressed three key ERS-related genes in mice

A mouse RIRI model with or without 4-PBA was constructed to further unveil the role of ERS in RIRI (Figure 7A). The results showed that BUN and Cre were significantly elevated after reperfusion and renal impairment induced by RIRI was greatly ameliorated by 4-PBA application, manifested as the amelioration of functional damage (Figures 7B, C) and histological injuries (Figure 7D). Thus, we concluded that inhibition of ERS improved renal ischemia/reperfusion-associated injuries. The expression levels of three key ERS-related genes were further verified by qRT-PCR analysis. Compared with the sham group, the expression levels of these genes after RIRI were significantly higher than those in sham samples and greatly decreased in the group treated with 4-PBA (Figures 7E–G).

3.8 Prognostic value evaluation of key ERS-related genes

The 282 kidney recipients in the GSE21374 dataset were divided into high and low gene-expression groups dichotomized at the corresponding median of each key ERS-related gene level. Kaplan-Meier survival curves showed a trend toward worse prognosis for recipients with high expression of *PPP1R15A*, *JUN* and *ATF3* compared to those with low expression (Figures 8A, C, E). The area under the curve (AUC) of predictions for 1, 2, and 3 years was depicted in Figures 8B, D, F. The highest AUC values of *PPP1R15A*, *JUN* and *ATF3* were 0.668, 0.762, and 0.723, respectively. Besides, all three key ERS-related genes were significant risk factors for renal allograft survival (Figure 8G). The GSE52694 dataset included RNA profiles of 13 renal graft samples from patients with the diagnosis of borderline changes early (≤2 months). These samples were categorized into stable (STA, n=6) and deteriorated graft function

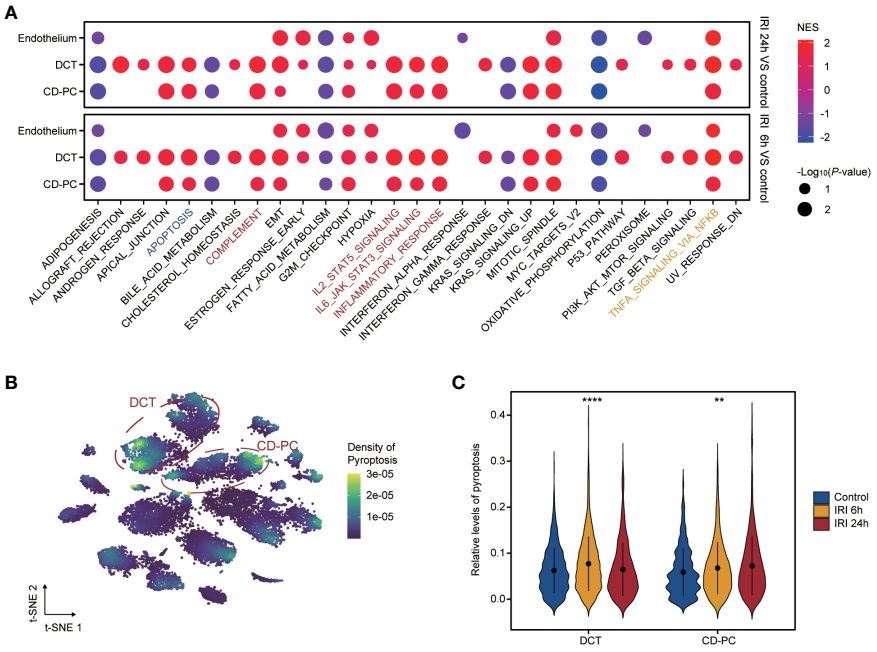

FIGURE 6
Functional profile of endothelium, CD-PC and DCT during renal IRI. **(A)** Dotplot showing the enriched hallmarks of endothelium, CD-PC and DCT between IRI 6h versus control versus e or IRI 24h versus control. Dot color and size present normalized enrichment scores (NES) and p-values obtained from GSEA analysis. The apoptosis, inflammatory pathways and TNFα signaling via NF-kappa B are labelled with blue, red and yellow colors. **(B)** tSNE plot revealing pyroptosis densities of 12 cell types. DCT and CD-PC cells circled in red exhibit the top density of pyroptosis. **(C)** Violine plot displaying significantly elevated pyroptosis levels in IRI 6h and IRI 24h samples compared with control sample in DCT and CD-PC. CD-PC, collecting duct principal cells; DCT, distal convoluted tubule; GSEA, gene set enrichment analysis. **p<0.01, ****p<0.0001.

(DGF, n=7) groups during 2 years after renal transplantation. All key ERS-related genes exhibited an increasing trend in the DGF group and JUN and ATF3 were significantly enhanced in the DGF group (Figure 8H). The receiver operating characteristic (ROC) curves indicated that all three key ERS-related genes with a high degree of reliability in accurately predicting allograft outcomes (PPP1R15A: AUC = 0.714; JUN: AUC = 0.952; ATF3: AUC = 0.881) (Figures 8I–K). In addition, a total of 28 renal biopsy samples (STA, n=20; graft loss, n=8) were applied for gene expression profiling and it was found that all three genes showed higher levels in the graft loss group than those in the STA group (Figure 8L). The AUCs of three key genes in predicting renal graft outcomes were greater than 0.7, which was considered as an acceptable predictive accuracy (Figures 8M–O). Overall, the three key ERS-related genes have prognostic values in predicting graft survival outcomes and assessing the risk of DGF and graft loss and the primary mechanisms by which the three genes affect RIRI are depicted schematically in Figure 9.

4 Discussion

RIRI, a common tissue after renal transplantation, causes delayed graft function, increases the risk of renal allograft rejection and even contributes to graft loss (2, 3). However, the underlying mechanisms of RIRI are complicated and there is no FDA-approved drugs for the treatment of RIRI in clinics (41). To fully determine the mechanisms of RIRI and identify potential new targets, we collected all available RIRI datasets with a large sample size and performed bulk RNA-seq analysis on these samples. Results showed that ERS was the top enriched pathway in RIRI. Among ERS-related genes, three key genes (*PPP1R15A*, *JUN* and *ATF3*) ranked top based on machine learning algorithms and were found to positively correlate with kidney injury-related pathways, including apoptosis, inflammatory response, oxidative stress, and pyroptosis. Our single-cell RNA-seq analysis suggested that DCT and CD-PC with pro-inflammatory status and the highest pyroptosis levels in RIRI were the main effectors of the three key genes. Furthermore, inhibition of the three key genes alleviated the functional and histological damage of RIRI. Importantly, renal allograft recipients with high levels of the three genes exhibited poor prognosis in long-term outcome and graft survival. The study is the first analysis to integrate multi-omics and clinical data for determining the crucial roles of three key ERS-related genes in RIRI, providing new ideas for clinical treatment.

Previous reports have shown that ERS is closely related to kidney diseases, including acute kidney injury, diabetic nephropathy and renal fibrosis (13). Hypoxia and ischemia as ER stressors caused the accumulation of misfolded proteins and eventually resulted in ERS (42). Several studies have found that RIRI can induce ERS in renal cells (43, 44). Some studies focusing on ER molecular chaperones identified the protective role of ERS in RIRI, while others on intermedin suggested the pathogenic role of ERS. However, the exact cause of the discrepancy and mechanisms

10.3389/fimmu.2024.1340997

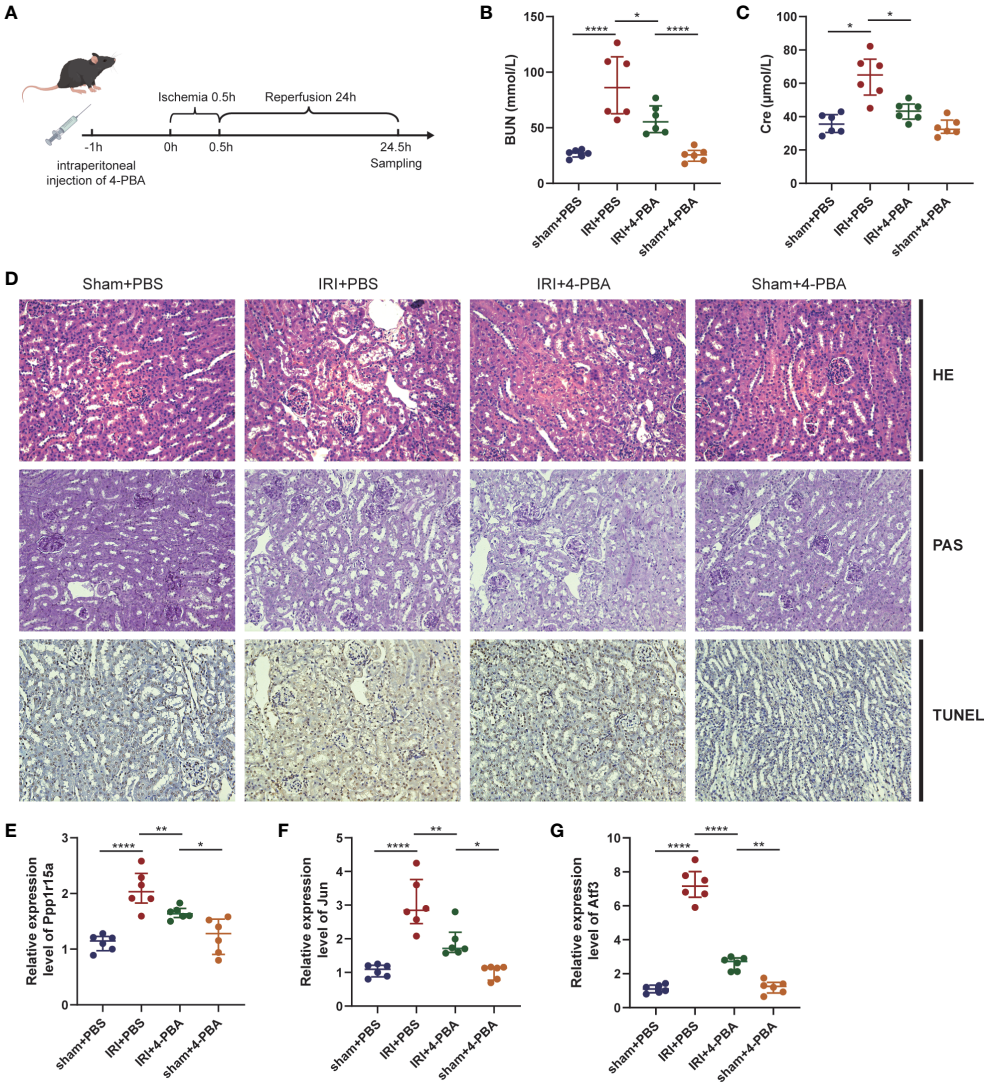

FIGURE 7
ERS in RIRI mouse model. **(A)** Pharmacotherapy of RIRI mouse model. The 4-phenyl butyric acid (4-PBA) is administered intraperitoneally to the mice 1 hour before ischemia. **(B, C)** Serum BUN and blood urea nitrogen (BUN) and creatinine (Cre) levels in mice. **(D)** Representative images of HE, PAS and TUNEL staining (×200 magnification) of renal tissues. mRNA levels of key ERS-related genes [PPP1R15A **(E)**, JUN **(F)** and ATF3 **(G)**] in RIRI mouse model. *P < 0.05, **P < 0.01, ****P < 0.0001, HE: hematoxylin and eosin staining, PAS, periodic acid-Schiff staining, TUNEL, terminal deoxynucleotidyl transferase dUTP nick end labeling staining.

underlying ERS in RIRI are still unclear. Currently, there is a lack of focus on measuring determinants of ERS or key ERS-related genes based on renal tissues of patients with RIRI. Our results showed that ERS was the top enriched pathway during RIRI across 336 samples, manifested as upregulation of ERS inducers and downstream targets, such as IRE1, CHOP, and JNK. For ERS-related genes, three key genes (PPP1R15A, JUN and ATF3) ranked top using machine learning algorithms and were significantly up-regulated in all three bulk-RNA datasets (including 495 samples). Importantly, these independent datasets were obtained from different centers and hence have high clinical heterogeneity. All the aforementioned results indicated the crucial role of ERS and identified three new ERS-related genes for further mechanistic studies of RIRI.

Previous studies have indicated that the three genes are involved in the process of ischemia-reperfusion injury or ischemia. The PERK and IRE pathways were activated in sustained ERS during neonatal hypoxia-ischemia, leading to a transient phosphorylation of eIF2α and an increased induction of PPP1R15A (45). JUN is a member of the AP-1 (Activator Protein-1) transcription factor family and is an important transcription factor downstream of ERK 1/2 and JNK in the signaling cascade, which were activated in response to ERS induced by coronary microembolization, ultimately leading to cardiomyocyte apoptosis (46–48). ATF3 is a gene that encodes a transcription factor, which is upregulated in ischemia-reperfusion injury including brain (49), liver (50), and cardiac microvascular (51). Studies have shown that the heterodimer of ATF3 can induce heat shock protein 27, which activates the Akt pathway and inhibits MEKK1-JNK, thereby inhibiting neuronal apoptosis (49). In addition to brain, liver and cardiac IRI, limited studies have been conducted on elucidating the

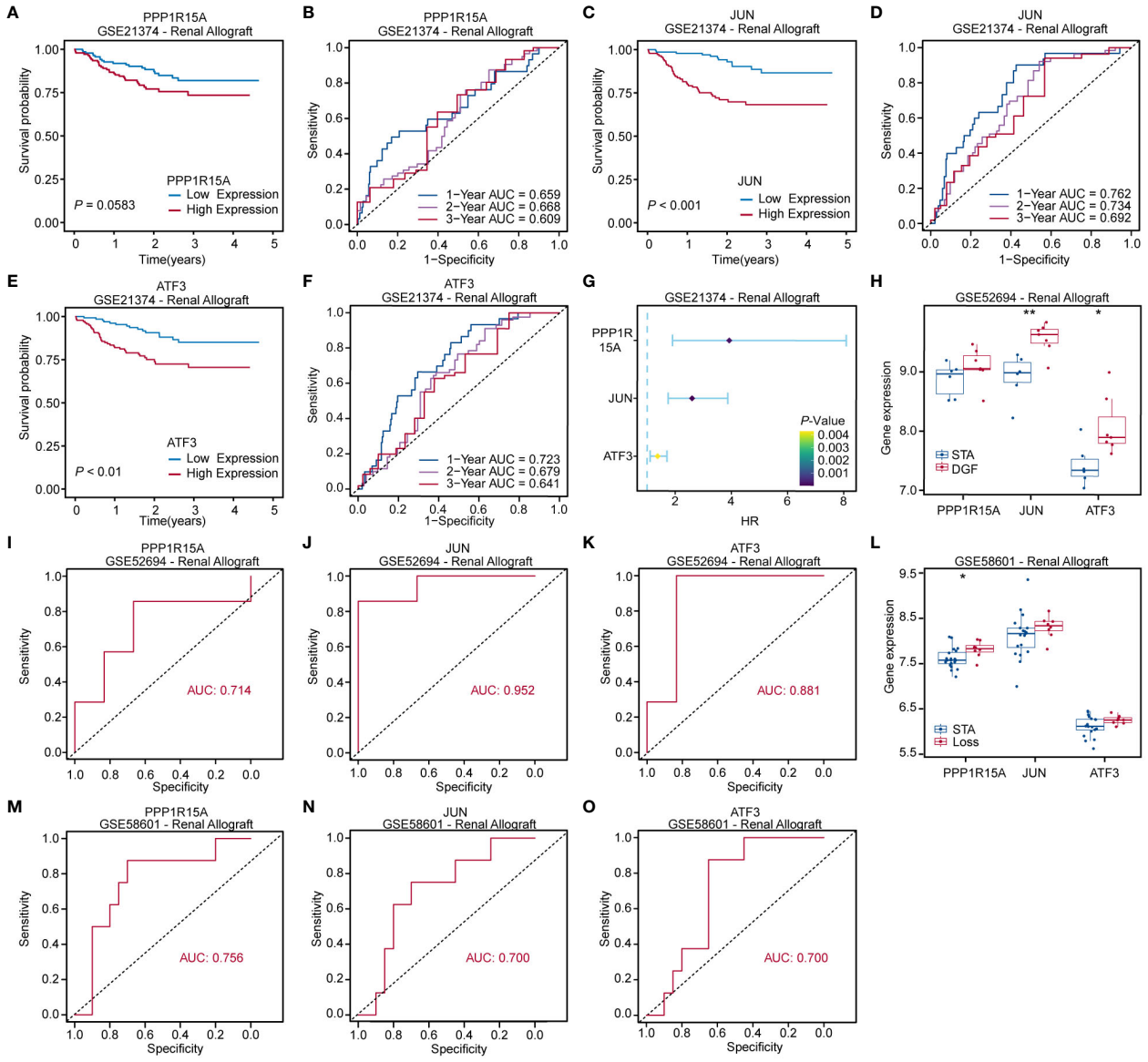

FIGURE 8
Prognostic value evaluation of key ERS-related genes. Kaplan-Meier and receiver operating characteristic (ROC) curves assessing prognostic values of PPP1R15A **(A, B)**, JUN **(C, D)** and ATF3 **(E, F)** expression levels for kidney recipients. **(G)** Forest plot based on univariable Cox regression analysis showing that key ERS-related genes are significantly risk factors for renal allograft survivals. **(H)** Boxplot comparing key ERS-related gene expression levels between kidney recipients with stable renal function (STA) and deteriorated graft function (DGF). **(I–K)** ROC curves showing that key ERS-related genes were able to accurately predict renal function after renal transplantation. **(L)** Boxplot comparing key ERS-related gene expression levels between kidney recipients with STA and allograft loss. **(M–O)** ROC curves revealing that three key genes exhibited acceptable predictive performance in renal allograft outcomes. *p<0.05, **p<0.01.

molecular roles of the three genes in RIRI. Thus, we incorporated correlation analysis to explore significantly enriched pathways associated with the three genes in RIRI. Results revealed that the three genes were correlated with inflammatory response, oxidative stress, NF-kappa B pathway, apoptosis and pyroptosis. ERS can directly initiate the inflammatory pathway, and the activation of the inflammatory pathway releases a large number of inflammatory factors, which in turn triggers ERS. This induces a pro-inflammatory positive feedback loop that further amplifies the inflammatory response (52, 53). In addition to inflammatory responses, ROS have been shown to act a crucial part in the pathology of IRI (54). Oxidative stress produced at the reperfusion stage might induce injury to the insulted tissues. This process is part of the term “oxygen paradox”, in which re-oxygenation of ischemic tissues generates injuries that largely exceed the injuries caused by ischemia alone (55). In recent years, studies showed that ROS destroyed ER functions and initiated unfold protein response and ERS *in vivo* and *in vitro* (56, 57). For NF-kappa B pathway, several studies have shown that ERS can activate the NF-kappa B pathway through facilitating TNF-α expressions and phosphorylation of p38 MAPK/NFκB signaling proteins (58–60). Apart from the NF-kappa B pathway, apoptotic

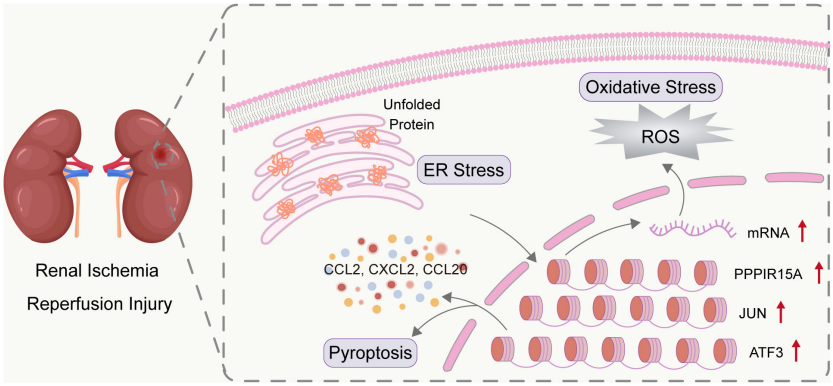

FIGURE 9
Overview of three key ERS-related genes in RIRI. RIRI induced the accumulation of unfold proteins and thus mediating the activation of ERS. The three genes (*PPP1R15A*, *JUN*, and *ATF3*) were determined as crucial ERS genes involved in RIRI. The three genes were biologically related to kidney-injury pathways (including inflammation, oxidative stress, and pyroptosis) and had clinical value in both acute injury and late graft outcomes.

pathways induced by ERS are an important type of apoptosis (61). The activation of the unfolded protein response initiated apoptotic cell death via up-regulation of CHOP, a pivotal marker of ERS (61). Besides, p38 can activate the transcription of CHOP through ATF6 and inhibition of p38 by SB203580 also restrained the expression of ERS markers, supporting the role of MAPK pathway in response to ERS-induced apoptosis. The first study on pyroptosis and RIRI can be traced back to 2014 and demonstrated that RIRI can induce pyroptosis in renal tubule epithelial cells by the CHOP-caspase-11 pathway (62). Furthermore, several subsequent studies indicated that GSDMD as the protein effector of pyroptosis acted as an executor and contributor to renal I/R injury (63–66). Overall, our results suggested that the three genes were involved in multiple pathological pathways of RIRI rather than a single process, emphasizing their importance. However, the specific mechanisms and the potential upstream and downstream relationships between the three genes and these interrelated pathways still need to be further studied.

Owing to the vulnerability of the renal proximal tubules, most studies have explored the potential mechanisms underlying RIRI using human renal proximal tubule epithelial cell line (HK2) rather than distal tubule cells. Surprisingly, the single-cell RNA-seq analysis indicated that endothelium, DCT and CD-PC exhibited significantly elevated expression levels of the three genes after renal reperfusion. Yoshio et al. also determined that oxygen-regulated protein (ORP150), a key chaperone for ERS in response to RIRI, was principally expressed in distal tubules (67). Besides, we leveraged scRNA-seq of RIRI to show that DCT and CD-PC exhibited pro-inflammatory status and the highest pyroptosis density among all cell types examined. While previous studies have provided a general understanding of the role of pyroptosis in the renal tubular epithelium, few studies have specifically addressed which segment of the tubular is affected (68, 69). We innovatively revealed that DCT and CD-PC may also be vital targets of pyroptosis in RIRI, providing new insights into the mechanism of RIRI. In addition to non-immune cells, innate and adaptive immune cells are also involved in IRI. IRI is a type of sterile inflammatory response but has similarities with the inflammation by pathogens (70). Infiltration of neutrophils occurs as early as 30 minutes after reperfusion, causing interstitial edema activation of the endothelium in peritubular capillaries (71). The neutrophils exacerbate kidney injury through secreting ROS (72) and inflammatory cytokines. Depleting neutrophils by anti ICAM-1 antibody can protect against RIRI (73, 74), demonstrating the determinants of neutrophils in acute kidney injury in mice. However, the pathological role of neutrophils is still not fully validated, and ICAM-1 blocking exhibits no beneficial effect on DGF after RIRI (75). Consistent with these human studies, our study found that the infiltrating neutrophils showed no significant differences between pre- and post-reperfusion in three cohorts. In contrast with bulk RNA-seq analysis, results of single-cell analysis revealed that the numbers of interactions and interaction strengths between neutrophils and other cell types were elevated after reperfusion, suggesting that cell-cell interaction between neutrophils and other cells may be more crucial than the levels of infiltrating neutrophils in RIRI.

The mice model of RIRI successfully validated the pathological role of three key ERS-related genes on acute kidney injury. In detail, compared with the RIRI group with PBS, the RIRI group treated with 4-PBA exhibited lower levels of the three genes and acute renal damage after reperfusion. In addition to acute kidney injury after RIRI, the patients recovered from RIRI may suffer from chronic kidney disease later (76–78). The maladaptive repair is determined to be a vital mechanism for renal fibrosis, inducing RIRI to chronic kidney disease (79). The ERS-induced apoptosis displayed a role in the progression of kidney fibrosis in the rat model (80). Thus, we collected three datasets with long-term follow-ups and found that the three genes exhibited highly prognostic values in renal allograft outcomes. Taken together, the three genes have clinical value for both acute injury and late graft outcomes. The 4-PBA has notable safety profiles *in vivo*, which is approved by the U.S. Food and Drug Administration for clinical use in urea-cycle disorders (81–83), suggesting its potential in RIRI treatment. However, the 4-PBA inhibited a panel of ERS-related genes beyond just the three genes,

and the impact of 4-PBA on the late development of renal fibrosis still needed to be evaluated. Although important roles for ERS were recognized by multi-omics analysis, only a small portion of ERS-relate genes were differentially expressed during RIRI. Compared with 4-PBA, new drugs targeting these three genes may result in better efficacy and minimal off-target effects.

The molecules identified in gene-miRNA and gene-TF regulatory networks may offer some clues to better understand the mechanisms of RIRI and can be potential drug targets. MiRNAs as small RNAs (18-24 nt in size) regulate the post-transcription of mRNAs and hence are involved in multiple biological processes, such as cell survival and stress response. Results showed that ten miRNAs (including hsa-mir-34a-5p, hsa-mir-30a-5p, hsa-mir-24-3p, hsa-mir-21-3p, hsa-mir-191-5p, hsa-mir-17-5p, hsa-mir-16-5p, hsa-mir-1-3p, hsa-mir-124-3p and hsa-mir-10b-5p) interacted with all three key ERS-related genes. Unsurprisingly, nine miRNAs of these ten miRNAs have been demonstrated to independently predict the occurrence of RIRI or prevent the development of RIRI in previous studies (84–91). The miRNAs, including miR-10b-5p, miR-16-5p, miR-24-3p, miR-34a-5p, and miR-191-5p, have been identified to aggravate RIRI through various mechanisms, such as downregulation of PIK3CA expression, regulation of autophagy and promotion of apoptosis. Conversely, miR-21-3p, miR-17-5p, miR-30a-5p, and miR-124-3p have been shown to alleviate IRI by targeting different pathways including caspase signaling pathway, death receptor 6, Beclin 1/ATG16 pathway, and TNFα/RIP1/RIP3 pathway. These findings provide important insights into the role of miRNAs in RIRI and could serve as potential therapeutic targets for future clinical interventions. In addition, eight upstream TFs (including ZFP37, SMAD5, REST, RAD21, KLF16, FOXJ2, ELF1 and BCL11B) could regulate all three key ERS-related genes in RIRI. Among these eight TFs, only REST has been confirmed to involve the process of RIRI. The previous study found that REST was a crucial inducer of ferroptosis in RIRI and inhibiting REST can alleviate the progression of chronic kidney disease from RIRI (92). The results of these studies suggest a great potential for these regulatory miRNAs and TFs as a class of therapeutic targets. The development of drugs may achieve better for controlling better through incorporating these regulatory molecules and ERS-related genes rather than focusing solely on ERS-related genes.

Our study still had some limitations. First, the living donor (LD) to deceased donor (DD) ratio of bulk-RNA datasets (GSE43974, GSE90861 and GSE126805) selected in the current research are different and the biological differences will inevitably produce an impact on our findings. Second, the RIRI mouse model has inherent limitations in recapitulating RIRI in human kidney transplantation (93, 94). Apart from their species heterogeneity, transplant process-related factors including organ retrieval, preservation, transport, and implantation can introduce additional variables and potential sources of injuries that are not present in the controlled laboratory environment of a mouse study (95, 96). Despite these limitations, the use of mouse models provides valuable mechanistic insights and serves as an initial screening platform for studying RIRI. Previous studies have demonstrated that there is a significant overlap between gene sets associated with IRI in both mouse models and published microarray data from deceased donor transplants of human kidneys (19, 22). Finally, additional clinical sample data needs to be established for further verifying the expression levels of the three genes and their correlations with clinical parameters.

5 Conclusion

In summary, we performed a multi-omics analysis to identify three key ERS-related genes in RIRI and identified their related biological processes involved in kidney injuries. The three genes have clinical value in both acute injury and late graft outcomes. The 4-PBA inhibiting the three genes alleviated acute kidney injury after RIRI, and its therapeutic impact on long-term outcomes is needed to be explored. In addition, there is an urgent need for new drugs specifically targeting the three genes, which may result in better efficacy and minimal off-target effects.

Data availability statement

The original contributions presented in the study are included in the article/Supplementary Material. Further inquiries can be directed to the corresponding authors.

Ethics statement

The animal study was reviewed and approved by the ethics committee of Beijing Chaoyang Hospital. The study was conducted in accordance with the local legislation and institutional requirements.

Author contributions

HZ: Conceptualization, Methodology, Visualization, Writing – original draft. CZ: Methodology, Visualization, Validation, Writing – original draft. YX: Conceptualization, Supervision, Methodology, Writing – review & editing. XH: Conceptualization, Funding acquisition, Supervision, Writing – review & editing.

Funding

The author(s) declare financial support was received for the research, authorship, and/or publication of this article. This work was supported by the General Program of the National Natural Science Foundation of China (NSFC) (81970645, 82170766).

Acknowledgments

We acknowledge GEO database for providing the platforms and contributors for uploading their meaningful datasets.

Conflict of interest

The authors declare that the research was conducted in the absence of any commercial or financial relationships that could be construed as a potential conflict of interest.

Publisher's note

All claims expressed in this article are solely those of the authors and do not necessarily represent those of their affiliated organizations, or those of the publisher, the editors and the reviewers. Any product that may be evaluated in this article, or claim that may be made by its manufacturer, is not guaranteed or endorsed by the publisher.

Supplementary material

The Supplementary Material for this article can be found online at: https://www.frontiersin.org/articles/10.3389/fimmu.2024.1340997/full#supplementary-material

References

1. Zhao H, Alam A, Soo AP, George AJT, Ma D. Ischemia-reperfusion injury reduces long term renal graft survival: mechanism and beyond. *EBioMedicine*. (2018) 28:31–42. doi: 10.1016/j.ebiom.2018.01.025

2. Zeng M, Wei X, Wu Z, Li W, Li B, Fei Y, et al. Reactive oxygen species contribute to simulated ischemia/reperfusion-induced autophagic cell death in human umbilical vein endothelial cells. *Med Sci Monit*. (2014) 20:1017–23. doi: 10.12659/MSM.890897

3. Lutz J, Thürmel K, Heemann U. Anti-inflammatory treatment strategies for ischemia/reperfusion injury in transplantation. *J Inflamm (Lond)*. (2010) 7:27. doi: 10.1186/1476-9255-7-27

4. Fang DYP, Lu B, Hayward S, de Kretser DM, Cowan PJ, Dwyer KM. The role of activin A and B and the benefit of Follistatin treatment in renal ischemia-reperfusion injury in mice. *Transplant Direct*. (2016) 2:e87. doi: 10.1097/TXD.0000000000000601

5. Chouchani ET, Pell VR, James AM, Work LM, Saeb-Parsy K, Frezza C, et al. A unifying mechanism for mitochondrial superoxide production during ischemia-reperfusion injury. *Cell Metab*. (2016) 23:254–63. doi: 10.1016/j.cmet.2015.12.009

6. Tennankore KK, Kim SJ, Alwayn IPJ, Kiberd BA. Prolonged warm ischemia time is associated with graft failure and mortality after kidney transplantation. *Kidney Int*. (2016) 89:648–58. doi: 10.1016/j.kint.2015.09.002

7. Nakagawa K, Koo DDH, Davies DR, Gray DWR, McLaren AJ, Welsh KI, et al. Lecithinized superoxide dismutase reduces cold ischemia-induced chronic allograft dysfunction. *Kidney Int*. (2002) 61:1160–9. doi: 10.1046/j.1523-1755.2002.00217.x

8. Hwang JK, Kim JM, Kim YK, Kim SD, Park SC, Kim JI, et al. The early protective effect of glutamine pretreatment and ischemia preconditioning in renal ischemia-reperfusion injury of rat. *Transplant Proc*. (2013) 45:3203–8. doi: 10.1016/j.transproceed.2013.08.028

9. Oakes SA, Papa FR. The role of endoplasmic reticulum stress in human pathology. *Annu Rev Pathol*. (2015) 10:173–94. doi: 10.1146/annurev-pathol-012513-104649

10. So J-S. Roles of endoplasmic reticulum stress in immune responses. *Mol Cells*. (2018) 41:705–16. doi: 10.14348/molcells.2018.0241

11. Martins AS, Alves I, Helguero L, Domingues MR, Neves BM. The unfolded protein response in homeostasis and modulation of mammalian immune cells. *Int Rev Immunol*. (2016) 35:457–76. doi: 10.3109/08830185.2015.1110151

12. Marciniak SJ, Ron D. Endoplasmic reticulum stress signaling in disease. *Physiol Rev*. (2006) 86:1133–49. doi: 10.1152/physrev.00015.2006

13. Taniguchi M, Yoshida H. Endoplasmic reticulum stress in kidney function and disease. *Curr Opin Nephrol Hypertens*. (2015) 24:345–50. doi: 10.1097/MNH.0000000000000141

14. Bush KT, George SK, Zhang PL, Nigam SK. Pretreatment with inducers of ER molecular chaperones protects epithelial cells subjected to ATP depletion. *Am J Physiol*. (1999) 277:F211–218. doi: 10.1152/ajprenal.1999.277.2.F211

15. Prachasilchai W, Sonoda H, Yokota-Ikeda N, Ito K, Kudo T, Imaizumi K, et al. The protective effect of a newly developed molecular chaperone-inducer against mouse ischemic acute kidney injury. *J Pharmacol Sci*. (2009) 109:311–4. doi: 10.1254/jphs.08272SC

16. Gao X, Fu L, Xiao M, Xu C, Sun L, Zhang T, et al. The nephroprotective effect of tauroursodeoxycholic acid on ischaemia/reperfusion-induced acute kidney injury by inhibiting endoplasmic reticulum stress. *Basic Clin Pharmacol Toxicol*. (2012) 111:14–23. doi: 10.1111/j.1742-7843.2011.00854.x

17. Gupta S, Li S, Abedin MJ, Noppakun K, Wang L, Kaur T, et al. Prevention of acute kidney injury by tauroursodeoxycholic acid in rat and cell culture models. *PLoS One*. (2012) 7:e48950. doi: 10.1371/journal.pone.0048950

18. Wang Y, Tian J, Qiao X, Su X, Mi Y, Zhang R, et al. Intermedin protects against renal ischemia-reperfusion injury by inhibiting endoplasmic reticulum stress. *BMC Nephrol*. (2015) 16:169. doi: 10.1186/s12882-015-0157-7

19. Damman J, Bloks VW, Daha MR, van der Most PJ, Sanjabi B, van der Vlies P, et al. Hypoxia and complement-and-coagulation pathways in the deceased organ donor as the major target for intervention to improve renal allograft outcome. *Transplantation*. (2015) 99:1293–300. doi: 10.1097/TP.0000000000000500

20. McGuinness D, Mohammed S, Monaghan L, Wilson PA, Kingsmore DB, Shapter O, et al. A molecular signature for delayed graft function. *Aging Cell*. (2018) 17:e12825. doi: 10.1111/acel.12825

21. Cippà PE, Sun B, Liu J, Chen L, Naesens M, McMahon AP. Transcriptional trajectories of human kidney injury progression. *JCI Insight*. (2018) 3:e123151. doi: 10.1172/jci.insight.123151

22. Liu J, Kumar S, Dolzhenko E, Alvarado GF, Guo J, Lu C, et al. Molecular characterization of the transition from acute to chronic kidney injury following ischemia/reperfusion. *JCI Insight*. (2017) 2:e94716. doi: 10.1172/jci.insight.94716

23. Einecke G, Reeve J, Sis B, Mengel M, Hidalgo L, Famulski KS, et al. A molecular classifier for predicting future graft loss in late kidney transplant biopsies. *J Clin Invest*. (2010) 120:1862–72. doi: 10.1172/JCI41789

24. Hrubá P, Brabcová I, Gueler F, Krejčík Z, Stránecký V, Svobodová E, et al. Molecular diagnostics identifies risks for graft dysfunction despite borderline histologic changes. *Kidney Int*. (2015) 88:785–95. doi: 10.1038/ki.2015.211

25. Kamal L, Broin PÓ, Bao Y, Ajaimy M, Lubetzky M, Gupta A, et al. Clinical, histological, and molecular markers associated with allograft loss in transplant glomerulopathy patients. *Transplantation*. (2015) 99:1912–8. doi: 10.1097/TP.0000000000000598

26. Love MI, Huber W, Anders S. Moderated estimation of fold change and dispersion for RNA-seq data with DESeq2. *Genome Biol*. (2014) 15:550. doi: 10.1186/s13059-014-0550-8

27. Ritchie ME, Phipson B, Wu D, Hu Y, Law CW, Shi W, et al. limma powers differential expression analyses for RNA-sequencing and microarray studies. *Nucleic Acids Res*. (2015) 43:e47. doi: 10.1093/nar/gkv007

28. Zou Y, Xie J, Zheng S, Liu W, Tang Y, Tian W, et al. Leveraging diverse cell-death patterns to predict the prognosis and drug sensitivity of triple-negative breast cancer patients after surgery. *Int J Surg*. (2022) 107:106936. doi: 10.1016/j.ijsu.2022.106936

29. Newman AM, Liu CL, Green MR, Gentles AJ, Feng W, Xu Y, et al. Robust enumeration of cell subsets from tissue expression profiles. *Nat Methods*. (2015) 12:453–7. doi: 10.1038/nmeth.3337

30. Peng S, Chen M, Yin M, Feng H. Identifying the potential therapeutic targets for atopic dermatitis through the immune infiltration analysis and construction of a ceRNA network. *Clin Cosmet Investig Dermatol*. (2021) 14:437–53. doi: 10.2147/CCID.S310426

31. Shen L, Zhou K, Liu H, Yang J, Huang S, Yu F, et al. Prediction of mechanosensitive genes in vascular endothelial cells under high wall shear stress. *Front Genet*. (2021) 12:796812. doi: 10.3389/fgene.2021.796812

32. Ide S, Kobayashi Y, Ide K, Strausser SA, Abe K, Herbek S, et al. Ferroptotic stress promotes the accumulation of pro-inflammatory proximal tubular cells in maladaptive renal repair. *Elife*. (2021) 10:e68603. doi: 10.7554/eLife.68603

33. Butler A, Hoffman P, Smibert P, Papalexi E, Satija R. Integrating single-cell transcriptomic data across different conditions, technologies, and species. *Nat Biotechnol*. (2018) 36:411–20. doi: 10.1038/nbt.4096

34. Korsunsky I, Millard N, Fan J, Slowikowski K, Zhang F, Wei K, et al. Fast, sensitive and accurate integration of single-cell data with Harmony. *Nat Methods*. (2019) 16:1289–96. doi: 10.1038/s41592-019-0619-0

35. Zheng L, Qin S, Si W, Wang A, Xing B, Gao R, et al. Pan-cancer single-cell landscape of tumor-infiltrating T cells. *Science*. (2021) 374:abe6474. doi: 10.1126/science.abe6474

36. Szegezdi E, Logue SE, Gorman AM, Samali A. Mediators of endoplasmic reticulum stress-induced apoptosis. *EMBO Rep*. (2006) 7:880–5. doi: 10.1038/sj.embor.7400779

37. Zhang K, Kaufman RJ. From endoplasmic-reticulum stress to the inflammatory response. *Nature*. (2008) 454:455–62. doi: 10.1038/nature07203

38. De Chiara L, Conte C, Semeraro R, Diaz-Bulnes P, Angelotti ML, Mazzinghi B, et al. Tubular cell polyploidy protects from lethal acute kidney injury but promotes consequent chronic kidney disease. *Nat Commun*. (2022) 13:5805. doi: 10.1038/s41467-022-33110-5

39. Wang Y, Li Y, Chen Z, Yuan Y, Su Q, Ye K, et al. GSDMD-dependent neutrophil extracellular traps promote macrophage-to-myofibroblast transition and renal fibrosis in obstructive nephropathy. *Cell Death Dis*. (2022) 13:693. doi: 10.1038/s41419-022-05138-4

40. Rudman-Melnick V, Adam M, Potter A, Chokshi SM, Ma Q, Drake KA, et al. Single-cell profiling of AKI in a murine model reveals novel transcriptional signatures, profibrotic phenotype, and epithelial-to-stromal crosstalk. *J Am Soc Nephrol*. (2020) 31:2793–814. doi: 10.1681/ASN.2020010052

41. Nieuwenhuijs-Moeke GJ, Pischke SE, Berger SP, Sanders JSF, Pol RA, Struys MMRF, et al. Ischemia and reperfusion injury in kidney transplantation: relevant mechanisms in injury and repair. *J Clin Med*. (2020) 9:253. doi: 10.3390/jcm9010253

42. Inagi R. Endoplasmic reticulum stress as a progression factor for kidney injury. *Curr Opin Pharmacol*. (2010) 10:156–65. doi: 10.1016/j.coph.2009.11.006

43. Fougeray S, Bouvier N, Beaune P, Legendre C, Anglicheau D, Thervet E, et al. Metabolic stress promotes renal tubular inflammation by triggering the unfolded protein response. *Cell Death Dis*. (2011) 2:e143. doi: 10.1038/cddis.2011.26

44. Tan X, Yu L, Yang R, Tao Q, Xiang L, Xiao J, et al. Fibroblast growth factor 10 attenuates renal damage by regulating endoplasmic reticulum stress after ischemia-reperfusion injury. *Front Pharmacol*. (2020) 11:39. doi: 10.3389/fphar.2020.00039

45. Badiola N, Penas C, Miñano-Molina A, Barneda-Zahonero B, Fadó R, Sánchez-Opazo G, et al. Induction of ER stress in response to oxygen-glucose deprivation of cortical cultures involves the activation of the PERK and IRE-1 pathways and of caspase-12. *Cell Death Dis*. (2011) 2:e149. doi: 10.1038/cddis.2011.31

46. Schonthaler HB, Guinea-Viniegra J, Wagner EF. Targeting inflammation by modulating the Jun/AP-1 pathway. *Ann Rheum Dis*. (2011) 70 Suppl 1:i109–112. doi: 10.1136/ard.2010.140533

47. Hess J, Angel P, Schorpp-Kistner M. AP-1 subunits: quarrel and harmony among siblings. *J Cell Sci*. (2004) 117:5965–73. doi: 10.1242/jcs.01589

48. Liu T, Zhou Y, Liu Y-C, Wang J-Y, Su Q, Tang Z-L, et al. Coronary microembolization induces cardiomyocyte apoptosis through the LOX-1-dependent endoplasmic reticulum stress pathway involving JNK/P38 MAPK. *Can J Cardiol*. (2015) 31:1272–81. doi: 10.1016/j.cjca.2015.01.013

49. Nakagomi S, Suzuki Y, Namikawa K, Kiryu-Seo S, Kiyama H. Expression of the activating transcription factor 3 prevents c-Jun N-terminal kinase-induced neuronal death by promoting heat shock protein 27 expression and Akt activation. *J Neurosci*. (2003) 23:5187–96. doi: 10.1523/JNEUROSCI.23-12-05187.2003

50. Haber BA, Mohn KL, Diamond RH, Taub R. Induction patterns of 70 genes during nine days after hepatectomy define the temporal course of liver regeneration. *J Clin Invest*. (1993) 91:1319–26. doi: 10.1172/JCI116332

51. Liu Y, Hu Y, Xiong J, Zeng X. Overexpression of activating transcription factor 3 alleviates cardiac microvascular ischemia/reperfusion injury in rats. *Front Pharmacol*. (2021) 12:598959. doi: 10.3389/fphar.2021.598959

52. Zhang K, Shen X, Wu J, Sakaki K, Saunders T, Rutkowski DT, et al. Endoplasmic reticulum stress activates cleavage of CREBH to induce a systemic inflammatory response. *Cell*. (2006) 124:587–99. doi: 10.1016/j.cell.2005.11.040

53. Grootjans J, Kaser A, Kaufman RJ, Blumberg RS. The unfolded protein response in immunity and inflammation. *Nat Rev Immunol*. (2016) 16:469–84. doi: 10.1038/nri.2016.62

54. McCord JM. Oxygen-derived free radicals in postischemic tissue injury. *N Engl J Med*. (1985) 312:159–63. doi: 10.1056/NEJM198501173120305

55. Yellon DM, Hausenloy DJ. Myocardial reperfusion injury. *N Engl J Med*. (2007) 357:1121–35. doi: 10.1056/NEJMra071667

56. Qu K, Shen N, Xu X, Su H, Wei J, Tai M, et al. Emodin induces human T cell apoptosis *in vitro* by ROS-mediated endoplasmic reticulum stress and mitochondrial dysfunction. *Acta Pharmacol Sin*. (2013) 34:1217–28. doi: 10.1038/aps.2013.58

57. Liu Z-W, Zhu H-T, Chen K-L, Dong X, Wei J, Qiu C, et al. Protein kinase RNA-like endoplasmic reticulum kinase (PERK) signaling pathway plays a major role in reactive oxygen species (ROS)-mediated endoplasmic reticulum stress-induced apoptosis in diabetic cardiomyopathy. *Cardiovasc Diabetol*. (2013) 12:158. doi: 10.1186/1475-2840-12-158

58. Akhter N, Wilson A, Arefanian H, Thomas R, Kochumon S, Al-Rashed F, et al. Endoplasmic reticulum stress promotes the expression of TNF-α in THP-1 cells by mechanisms involving ROS/CHOP/HIF-1α and MAPK/NF-κB pathways. *Int J Mol Sci*. (2023) 24:15186. doi: 10.3390/ijms242015186

59. Pahl HL, Baeuerle PA. The ER-overload response: activation of NF-kappa B. *Trends Biochem Sci*. (1997) 22:63–7. doi: 10.1016/s0968-0004(96)10073-6

60. Hu P, Han Z, Couvillon AD, Kaufman RJ, Exton JH. Autocrine tumor necrosis factor alpha links endoplasmic reticulum stress to the membrane death receptor pathway through IRE1alpha-mediated NF-kappaB activation and down-regulation of TRAF2 expression. *Mol Cell Biol*. (2006) 26:3071–84. doi: 10.1128/MCB.26.8.3071-3084.2006

61. Hu H, Tian M, Ding C, Yu S. The C/EBP homologous protein (CHOP) transcription factor functions in endoplasmic reticulum stress-induced apoptosis and microbial infection. *Front Immunol*. (2018) 9:3083. doi: 10.3389/fimmu.2018.03083

62. Yang J-R, Yao F-H, Zhang J-G, Ji Z-Y, Li K-L, Zhan J, et al. Ischemia-reperfusion induces renal tubule pyroptosis via the CHOP-caspase-11 pathway. *Am J Physiol Renal Physiol*. (2014) 306:F75–84. doi: 10.1152/ajprenal.00117.2013

63. Liu H, Chen Z, Weng X, Chen H, Du Y, Diao C, et al. Enhancer of zeste homolog 2 modulates oxidative stress-mediated pyroptosis *in vitro* and in a mouse kidney ischemia-reperfusion injury model. *FASEB J*. (2020) 34:835–52. doi: 10.1096/fj.201901816R

64. Tajima T, Yoshifuji A, Matsui A, Itoh T, Uchiyama K, Kanda T, et al. β-hydroxybutyrate attenuates renal ischemia-reperfusion injury through its anti-pyroptotic effects. *Kidney Int*. (2019) 95:1120–37. doi: 10.1016/j.kint.2018.11.034

65. Diao C, Chen Z, Qiu T, Liu H, Yang Y, Liu X, et al. Inhibition of PRMT5 attenuates oxidative stress-induced pyroptosis via activation of the Nrf2/HO-1 signal pathway in a mouse model of renal ischemia-reperfusion injury. *Oxid Med Cell Longev*. (2019) 2019:2345658. doi: 10.1155/2019/2345658

66. Pang Y, Zhang P-C, Lu R-R, Li H-L, Li J-C, Fu H-X, et al. Andrade-Oliveira Salvianolic acid B modulates caspase-1-mediated pyroptosis in renal ischemia-reperfusion injury via Nrf2 pathway. *Front Pharmacol*. (2020) 11:541426. doi: 10.3389/fphar.2020.541426

67. Bando Y, Tsukamoto Y, Katayama T, Ozawa K, Kitao Y, Hori O, et al. ORP150/HSP12A protects renal tubular epithelium from ischemia-induced cell death. *FASEB J*. (2004) 18:1401–3. doi: 10.1096/fj.03-1161fje

68. Fu Z-J, Wang Z-Y, Xu L, Chen X-H, Li X-X, Liao W-T, et al. HIF-1α-BNIP3-mediated mitophagy in tubular cells protects against renal ischemia/reperfusion injury. *Redox Biol*. (2020) 36:101671. doi: 10.1016/j.redox.2020.101671

69. Smith SF, Hosgood SA, Nicholson ML. Ischemia-reperfusion injury in renal transplantation: 3 key signaling pathways in tubular epithelial cells. *Kidney Int*. (2019) 95:50–6. doi: 10.1016/j.kint.2018.10.009

70. Chen GY, Nuñez G. Sterile inflammation: sensing and reacting to damage. *Nat Rev Immunol*. (2010) 10:826–37. doi: 10.1038/nri2873

71. Devarajan P. Update on mechanisms of ischemic acute kidney injury. *J Am Soc Nephrol*. (2006) 17:1503–20. doi: 10.1681/ASN.2006010017

72. Awad AS, Rouse M, Huang L, Vergis AL, Reutershan J, Cathro HP, et al. Compartmentalization of neutrophils in the kidney and lung following acute ischemic kidney injury. *Kidney Int*. (2009) 75:689–98. doi: 10.1038/ki.2008.648

73. Kelly KJ, Williams WW, Colvin RB, Meehan SM, Springer TA, Gutierrez-Ramos JC, et al. Intercellular adhesion molecule-1-deficient mice are protected against ischemic renal injury. *J Clin Invest*. (1996) 97:1056–63. doi: 10.1172/JCI118498

74. Kelly KJ, Williams WW, Colvin RB, Bonventre JV. Antibody to intercellular adhesion molecule 1 protects the kidney against ischemic injury. *Proc Natl Acad Sci USA*. (1994) 91:812–6. doi: 10.1073/pnas.91.2.812

75. Salmela K, Wramner L, Ekberg H, Hauser I, Bentdal O, Lins LE, et al. A randomized multicenter trial of the anti-ICAM-1 monoclonal antibody (enlimomab) for the prevention of acute rejection and delayed onset of graft function in cadaveric renal transplantation: a report of the European Anti-ICAM-1 Renal Transplant Study Group. *Transplantation*. (1999) 67:729–36. doi: 10.1097/00007890-199903150-00015

76. He L, Wei Q, Liu J, Yi M, Liu Y, Liu H, et al. AKI on CKD: heightened injury, suppressed repair, and the underlying mechanisms. *Kidney Int*. (2017) 92:1071–83. doi: 10.1016/j.kint.2017.06.030

77. Venkatachalam MA, Weinberg JM, Kriz W, Bidani AK. Failed tubule recovery, AKI-CKD transition, and kidney disease progression. *J Am Soc Nephrol*. (2015) 26:1765–76. doi: 10.1681/ASN.2015010006

78. Basile DP, Bonventre JV, Mehta R, Nangaku M, Unwin R, Rosner MH, et al. Progression after AKI: understanding maladaptive repair processes to predict and identify therapeutic treatments. *J Am Soc Nephrol*. (2016) 27:687–97. doi: 10.1681/ASN.2015030309

79. Yan M, Shu S, Guo C, Tang C, Dong Z. Endoplasmic reticulum stress in ischemic and nephrotoxic acute kidney injury. *Ann Med*. (2018) 50:381–90. doi: 10.1080/07853890.2018.1489142

80. Chiang C-K, Hsu S-P, Wu C-T, Huang J-W, Cheng H-T, Chang Y-W, et al. Endoplasmic reticulum stress implicated in the development of renal fibrosis. *Mol Med*. (2011) 17:1295–305. doi: 10.2119/molmed.2011.00131

81. Maestri NE, Brusilow SW, Clissold DB, Bassett SS. Long-term treatment of girls with ornithine transcarbamylase deficiency. *N Engl J Med*. (1996) 335:855–9. doi: 10.1056/NEJM199609193351204

82. Collins AF, Pearson HA, Giardina P, McDonagh KT, Brusilow SW, Dover GJ. Oral sodium phenylbutyrate therapy in homozygous beta thalassemia: a clinical trial. *Blood*. (1995) 85:43–9. doi: 10.1182/blood.V85.1.43.bloodjournal85143

83. Chen WY, Bailey EC, McCune SL, Dong JY, Townes TM. Reactivation of silenced, virally transduced genes by inhibitors of histone deacetylase. *Proc Natl Acad Sci USA*. (1997) 94:5798–803. doi: 10.1073/pnas.94.11.5798

84. Xu D, Li W, Zhang T, Wang G. miR-10a overexpression aggravates renal ischemia-reperfusion injury associated with decreased PIK3CA expression. *BMC Nephrol*. (2020) 21:248. doi: 10.1186/s12882-020-01898-3

85. Hao J, Wei Q, Mei S, Li L, Su Y, Mei C, et al. Induction of microRNA-17-5p by p53 protects against renal ischemia-reperfusion injury by targeting death receptor 6. *Kidney Int*. (2017) 91:106–18. doi: 10.1016/j.kint.2016.07.017

86. Hu H, Jiang W, Xi X, Zou C, Ye Z. MicroRNA-21 attenuates renal ischemia reperfusion injury via targeting caspase signaling in mice. *Am J Nephrol*. (2014) 40:215–23. doi: 10.1159/000368202

87. Liu X-J, Hong Q, Wang Z, Yu Y-Y, Zou X, Xu L-H. MicroRNA-34a suppresses autophagy in tubular epithelial cells in acute kidney injury. *Am J Nephrol*. (2015) 42:168–75. doi: 10.1159/000439185

88. Ke J, Zhao F, Luo Y, Deng F, Wu X. MiR-124 negatively regulated PARP1 to alleviate renal ischemia-reperfusion injury by inhibiting TNFα/RIP1/RIP3 pathway. *Int J Biol Sci*. (2021) 17:2099–111. doi: 10.7150/ijbs.58163

89. Chen H-H, Lan Y-F, Li H-F, Cheng C-F, Lai P-F, Li W-H, et al. Urinary miR-16 transactivated by C/EBPβ reduces kidney function after ischemia/reperfusion-induced injury. *Sci Rep*. (2016) 6:27945. doi: 10.1038/srep27945

90. Lorenzen JM, Kaucsar T, Schauerte C, Schmitt R, Rong S, Hübner A, et al. MicroRNA-24 antagonism prevents renal ischemia reperfusion injury. *J Am Soc Nephrol*. (2014) 25:2717–29. doi: 10.1681/ASN.2013121329

91. Wu X-Q, Tian X-Y, Wang Z-W, Wu X, Wang J-P, Yan T-Z. miR-191 secreted by platelet-derived microvesicles induced apoptosis of renal tubular epithelial cells and participated in renal ischemia-reperfusion injury via inhibiting CBS. *Cell Cycle*. (2019) 18:119–29. doi: 10.1080/15384101.2018.1542900

92. Gong S, Zhang A, Yao M, Xin W, Guan X, Qin S, et al. REST contributes to AKI-to-CKD transition through inducing ferroptosis in renal tubular epithelial cells. *JCI Insight*. (2023) 8:e166001. doi: 10.1172/jci.insight.166001

93. Doncheva NT, Palasca O, Yarani R, Litman T, Anthon C, Groenen MAM, et al. Human pathways in animal models: possibilities and limitations. *Nucleic Acids Res*. (2021) 49:1859–71. doi: 10.1093/nar/gkab012

94. Bagul A, Frost JH, Drage M. Stem cells and their role in renal ischaemia reperfusion injury. *Am J Nephrol*. (2013) 37:16–29. doi: 10.1159/000345731

95. Simona M-S, Alessandra V, Emanuela C, Elena T, Michela M, Fulvia G, et al. Evaluation of oxidative stress and metabolic profile in a preclinical kidney transplantation model according to different preservation modalities. *Int J Mol Sci*. (2023) 24:1029. doi: 10.3390/ijms24021029

96. Wei Q, Dong Z. Mouse model of ischemic acute kidney injury: technical notes and tricks. *Am J Physiol Renal Physiol*. (2012) 303:F1487–1494. doi: 10.1152/ajprenal.00352.2012

frontiers | Frontiers in Immunology

TYPE Original Research
PUBLISHED 18 April 2024
DOI 10.3389/fimmu.2024.1342977

OPEN ACCESS

EDITED BY
Chao Yang,
Zhejiang Ocean University, China

REVIEWED BY
Monisankar Ghosh,
Stony Brook University, United States
Björn Koos,
University Hospital Bochum GmbH, Germany

*CORRESPONDENCE
Patrizia Agostinis
patrizia.agostinis@kuleuven.be
Steven De Vleeschouwer
steven.devleeschouwer@uzleuven.be

†These authors have contributed equally to this work

RECEIVED 22 November 2023
ACCEPTED 03 April 2024
PUBLISHED 18 April 2024

CITATION
Yang Y, More S, De Smet F, De Vleeschouwer S and Agostinis P (2024) Antioxidant network-based signatures cluster glioblastoma into distinct redox-resistant phenotypes.
Front. Immunol. 15:1342977.
doi: 10.3389/fimmu.2024.1342977

Antioxidant network-based signatures cluster glioblastoma into distinct redox-resistant phenotypes

Yihan Yang[1,2,3†], Sanket More[2,3†], Frederik De Smet[4,5], Steven De Vleeschouwer[1,6,7*] and Patrizia Agostinis[2,3*]

[1]Research Group Experimental Neurosurgery and Neuroanatomy, Department of Neurosciences, KU Leuven, Leuven, Belgium, [2]Laboratory of Cell Death Research & Therapy, Department of Cellular and Molecular Medicine, KU Leuven, Leuven, Belgium, [3]Vlaams Instituut voor Biotechnologie (VIB) Center for Cancer Biology Research, Leuven, Belgium, [4]Department of Imaging and Pathology, KU Leuven, Leuven, Belgium, [5]Leuven Institute for Single-Cell Omics (LISCO), Leuven, Belgium, [6]Department of Neurosurgery, University Hospitals Leuven, Leuven, Belgium, [7]Leuven Brain Institute (LBI), KU Leuven, Leuven, Belgium

Introduction: Aberrant reactive oxygen species (ROS) production is one of the hallmarks of cancer. During their growth and dissemination, cancer cells control redox signaling to support protumorigenic pathways. As a consequence, cancer cells become reliant on major antioxidant systems to maintain a balanced redox tone, while avoiding excessive oxidative stress and cell death. This concept appears especially relevant in the context of glioblastoma multiforme (GBM), the most aggressive form of brain tumor characterized by significant heterogeneity, which contributes to treatment resistance and tumor recurrence. From this viewpoint, this study aims to investigate whether gene regulatory networks can effectively capture the diverse redox states associated with the primary phenotypes of GBM.

Methods: In this study, we utilized publicly available GBM datasets along with proprietary bulk sequencing data. Employing computational analysis and bioinformatics tools, we stratified GBM based on their antioxidant capacities and evaluated the distinctive functionalities and prognostic values of distinct transcriptional networks in silico.

Results: We established three distinct transcriptional co-expression networks and signatures (termed clusters C1, C2, and C3) with distinct antioxidant potential in GBM cancer cells. Functional analysis of each cluster revealed that C1 exhibits strong antioxidant properties, C2 is marked with a discrepant inflammatory trait and C3 was identified as the cluster with the weakest antioxidant capacity. Intriguingly, C2 exhibited a strong correlation with the highly aggressive mesenchymal subtype of GBM. Furthermore, this cluster holds substantial prognostic importance: patients with higher gene set variation analysis (GSVA)

scores of the C2 signature exhibited adverse outcomes in overall and progression-free survival.

Conclusion: In summary, we provide a set of transcriptional signatures that unveil the antioxidant potential of GBM, offering a promising prognostic application and a guide for therapeutic strategies in GBM therapy.

KEYWORDS

oxidative stress, GBM, bioinformatics, antioxidant phenotype, signatures, canonical GBM classification, transcription factors, prognosis

Introduction

Reactive oxygen species (ROS) are the by-products of multiple cellular and metabolic processes. It is widely acknowledged that low levels of ROS promote cell growth and differentiation (1), whereas higher levels of ROS can impart fatal damage to cellular components and trigger cell death (2). Cancer cells display basally high levels of ROS as compared to their normal counterparts. Several intrinsic genetic and metabolic alterations driving the malignant state, including oncogene expression and rewiring of major metabolic pathways, cause an imbalance in the cellular redox tone shifting the balance in favor of a pro-oxidant state, a condition known as "oxidative stress". To withstand oxidative stress and avoid irreparable damage to vital entities, malignant cells increase their capacity to detoxify the excessive production of ROS. As a consequence, failure to maintain a functional cellular antioxidant defense system causes inevitably ROS-driven cellular damage that results in cell demise which can occur through different regulated cell death (RCD) modalities (3–7). Efforts to maintain redox homeostasis in cancer cells can be challenged by the local tumor microenvironment, upon invasion of malignant cells in the bloodstream, which is notoriously more oxidizing, or colonization to a secondary site (8). Emerging data indicate that non-genetic mechanisms that contribute to tumor cell heterogeneity and drug resistance, involve transcriptional reprogramming of antioxidant response networks, which endorse cancer cells with an increased ability to cope with intrinsic and extrinsic oxidative stress (9–11). However, given the double-edged function of ROS, it remains unclear which changes in the intracellular redox tone are associated with various stages of malignancy, and when and how they contribute to the maintenance of cancer cell's plasticity.

This concept seems particularly applicable to glioblastoma multiforme (GBM), the most aggressive brain neoplasm hallmarked by high heterogeneity, which drives treatment resistance and tumor recurrence (12). The high metabolic rate of GBM leads to the generation of excessive amounts of ROS and metabolic adaptation in these cells plays an essential role in resistance to oxidative stress-induced cell death. Congruently, in response to chemo (temozolomide - TMZ) or radio-therapy GBM activates redox-sensitive transcription factors, including nuclear factor-κB (NF-κB), nuclear factor erythroid 2 p45-related factor 2 (NRF2), or HIF-1 that cooperate to support cancer cell survival and progression through cell-intrinsic and -extrinsic mechanisms (13, 14). Hence, how GBM strives to maintain redox pathways promoting tumorigenesis and resistance to anticancer therapies, while avoiding oxidative stress-induced killing remains an outstanding question.

In this perspective, it would be valuable to explore whether gene regulatory networks can capture different redox states are associated with the main GBM phenotypes. If so, this could help in understanding how glioma cell plasticity and redox signaling are co-regulated. Furthermore, given that several clinically available anticancer treatments kill cancer cells by directly or indirectly inducing lethal levels of ROS (14), an 'a priori' knowledge of the cancer cell's antioxidant capacity based on the co-expression of redox-regulating genes, may provide an indicator of the propensity of a ROS-inducing drug/treatment to be effective and be therefore clinically informative. Identifying such a gene signature redox-based classifier could provide an additional tool to predict GBM patient responses to therapies. Here we perform an in silico analysis to define a redox-gene expression signature that could provide useful insights into the propensity of a particular GBM state to undergo lethal oxidative stress.

Materials and methods

Software, signature of interest, datasets and workflow

Unless stated otherwise, R 4.2.2 and RStudio were used to perform our analysis based on the signature of redox controlling transcription factor network reported in a recent paper (15). Cancer cell line encyclopedia (CCLE) database, The Cancer Genome Atlas Program (TCGA) database and The Genotype-Tissue Expression (GTEx) portal were used. All the original data was transformed and parsed with the R package tidyverse. We used GBM cell lines (n = 59) from the CCLE database and downloaded raw data from weblink: https://sites.broadinstitute.org/ccle/. The background of each cell line was screened manually to confirm the pathological

diagnosis of GBM. Related information was extracted to build the clinical profile of the cohort. We utilized the in-house RNA-seq data of patient-derived GBM cell lines, which were isolated and maintained primarily from clinical GBM samples (n = 41; generated under study number S59804 and S61081), and the GBM TCGA database (n = 168) as the validation cohorts for our newly defined classifier and performed prognosis analysis with the TCGA cohort. Expression of normal tissue from GTEx was used to compensate for the lack of normal tissue data in the TCGA project. The workflow of the study can be found in Figure 1.

Consensus clustering and expression heatmap of the signature

We used CCLE GBM cohort for consensus clustering analysis. The expression of genes from the signature of redox controlling transcription factor network (15) was extracted as input matrix for clustering. With R package ConsensusClusterPlus, consensus matrix was built and stability assessment was performed to seek the optimal k value. We also confirmed the optimal k value with the function embedded in the package. In the end, k value of 3 was selected based on the stability of the clusters (Figure 2A; Supplementary Figures 1B–J). We, thereafter, found the three distinct groups of cell lines as the major clusters defined in our classification system. R package ComplexHeatmap was used to derive the heatmap for hierarchical clustering.

Functional annotation

Gene set variation analysis (GSVA) was first used to gain the score of antioxidant pathways described in our input signature. The score was calculated with the R package GSVA. Then, all the databases in the R package msigdbr were extracted for GSVA scoring to validate the consistency of the results. The results from the database included Hallmark, Gene Ontology (GO), Reactome, WikiPathways, BioCarta, the Pathway Interaction Database (PID), and Cancer Module (CM), which showed significant readout, were reported here. We built the heatmap with above mentioned R package to assign the function to each cluster. Next, we performed differential expression gene (DEG) analysis with R package DESeq2 on counts data to find the up-regulated and down-regulated genes in each cluster. Log2 fold-change of 0.5 and adjusted p value, derived from Benjamin-Hochberg correction, of 0.05 were set as the thresholds. R package EnhanceVolcano was used to generate the Volcano plot presenting differentially expressed genes. Gene set enrichment analysis (GSEA) was performed to assign the functions to the clusters. We used the function in R package clusterProfiler to obtain the result for this step.

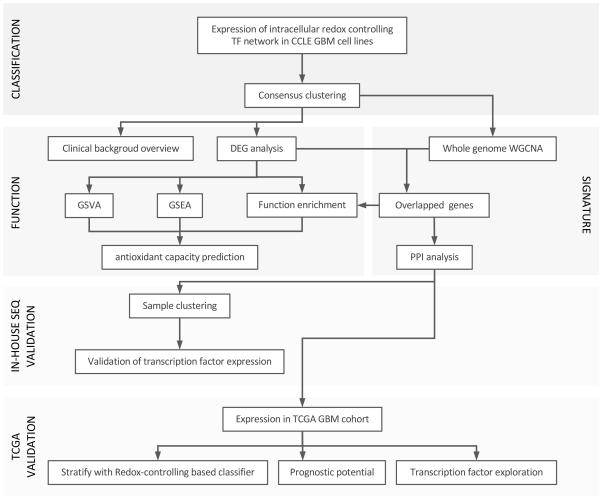

FIGURE 1
Workflow of the study. In general, we divided our analysis into three parts: 1) set up of the classification using redox homeostasis controlling transcription factor network; 2) function annotation and signature establishment; 3) validation by in-house RNA-seq and TCGA-GBM project, and prognosis analysis with TCGA GBM cohort.

Weighted gene co-expression network analysis and protein-protein interaction network construction

WGCNA was performed on the top 5000 expressed genes with R package WGCNA. This is to maintain the performance of the algorithm, in the meantime, to acquire the correlated modules with higher accuracy. Soft power was calculated, and we selected 5 as the optimal soft power to emphasize strong correlations and reduce the weaker (Supplementary Figure 3D). A signed network type was used to detect the co-expression gene modules. We took the three clusters as one set of traits, bringing along with clinical features and canonical GBM classification. A trait-module correlation was then produced. We gathered the genes from the, either positively or negatively, significantly correlated with each grouping as another bundle of gene lists to distinguish the three newly defined clusters. Next, we extracted the overlapped genes in the lists obtained from DEG analysis and the lists from WGCNA analysis to elucidate the signatures of the antioxidant GBM classification. STRING (https://string-db.org) was used as the tool for PPI analysis. To maximize the findings, we have utilized the default setting of active interaction sources from the webtool. These sources of interactions include textmining, experiments, databases, co-expression, neighborhood, gene fusion and co–occurrence. Results were imported into Cytoscape for network presentation. Plug-ins, cytoHubba and ClueGO of Cytoscape were used to search for the hub genes and annotate the functions.

Survival analysis

Overall survival (OS) and progression-free interval (PFI) data of GBM samples from the TCGA cohort was used as input for Kaplan-Meier survival analysis with R package survival and survminer. Categorically, we compared the samples with the different clusters C1-C3. Quantitatively, we calculated the GSVA scores of each signature in the whole cohort, and compared the prognostic values between the high and the low scores. For the single gene analysis, transcription factors in each signature were spotted by the

transcription factor database: http://humantfs.ccbr.utoronto.ca/index.php and http://bioinfo.life.hust.edu.cn/AnimalTFDB4/#/. Expression status was illustrated by violin plots derived from R package ggplot2. Again, related R packages were used to examine the prognostic values. Finally, the hazard ratio was evaluated with the function from the same R packages.

Results and discussion

Establishment of a GBM classification based on distinct antioxidant gene network phenotypes

The canonical GBM classification system based on transcriptomic differences fails to provide the fundamental biological characteristics that can guide the therapeutic propensity of the cellular states. Recently, in a study using an in silico pathway-based classifier, GBM was clustered into four main biological subtypes, characterized by divergent metabolic states (e.g. mitochondrial, glycolytic, lipid) and neurodevelopmental axis (16). Interestingly, the mitochondrial GBM phenotype, relying on oxidative phosphorylation and associated with higher levels of intracellular ROS, exhibited higher responses to radiation, a clinically relevant, ROS-inducing therapy in GBM. These studies further portrayed that GBM metabolic heterogeneity, possibly linked to a differential redox-tone, is linked to clinical outcomes.

To define a classification system for GBM, based on the intrinsic ability of cells to detoxify ROS and maintain redox homeostasis, we initially explored the RNAseq dataset from the CCLE database. We performed consensus clustering using the signature consisting of genes regulated by members of the antioxidant transcription factor network (15) (see Materials and Methods, and Supplementary Figure 1A). GBM cell lines could be segregated into three main clusters labeled C1, C2, and C3 (Figure 2A). Significant definers of each cluster included members of the activator protein-1 (AP-1) family of transcription factors, and genes involved in heme or iron metabolism and the detoxification of xenobiotics (15). Analysis of the expression of these genes across the GBM cell lines showed they were expressed prevalently in the C1 cluster, whereas their expression was low to very low in the C2 and C3 clusters, respectively (Figure 2A; Supplementary Figure 1A). This suggests that the C1 GBM cluster express a transcriptional network endowed with more robust antioxidant ability, compared with C2 and C3 (Figure 2B). Hierarchical clustering analysis resulted in a similar segregation of cell lines (Supplementary Figure 1). The clinical background of the individual sample can be visualized in Figure 2B.

To gain further insight into the molecular signature of each cluster, we performed GSVA utilizing different databases. We started the analysis using the Hallmark 50 database, and identified the term ROS pathway together with the terms Wnt/β-catenin signaling, and xenobiotic metabolism differentiating the three clusters, thus validating the signature (Figure 2C). Further GSVA analysis using literature-driven annotation of genes (genes used in the signature) revealed that all the terms related to antioxidant functions (e.g. scavenge ROS, provide reduced thioredoxin (TXN), synthesis of glutathione (GSH), generate NADPH, metabolize heme/iron and detoxify xenobiotics) and transcription factors (TF) regulating and antioxidant response were highly enriched in C1 followed by C2 while poorly coexpressed in C3 (Figure 2D). To gain further insights into the molecular pathways potentially contributing to the difference in redox signature across the three clusters, we performed GSVA using gene ontology (GO) and pathway analysis. The GO analysis identified terms, such as the regulation of PERK-mediated UPR, glutamate homeostasis, and response to fatty acids, enriched in C1 (Figure 2E; Supplementary Figures 2A, B). Pathway analysis using different databases (Reactome, WikiPathways, BioCarta, PID, and CM) identified PERK, NRF2, ferroptosis, iron homeostasis, and cytokine pathways driving inflammation, as dominant pathways differentiating the three clusters (Figure 2F; Supplementary Figures 2C–F).

The co-existence of the PERK branch of UPR and NRF2 in C1 is congruent with the relevant role of this ER stress sensor in the resistance to oxidative stress in cancer cells (17). In line, PERK mediates the phosphorylation of NRF2 on Thr-80, which unleashes NRF2 from its inhibitory association with KEAP1 thereby favoring NRF2 nuclear translocation and boosting the transcription of the anti-oxidant response genes (18). These genes include heme-oxygenase-1 (HO-1), which generates the antioxidant bilirubin and glutamate-cysteine ligase-catalytic subunit (GCLC), which is essential for the synthesis of the major intracellular anti-oxidant glutathione (GSH) (18). Furthermore, the PERK-eIF2α-ATF4 axis of the UPR also contributes to the mitigation of oxidative stress in cancer cells by the ATF4-mediated increase in amino acid transport and metabolism (19–21). Among other targets of this pathway, the expression of the glutamate transporter SLC7A11, which exchanges glutamate for the import of cystine, increases the intracellular concentration of GSH. In line with this, multiple studies have indicated that attenuation of glutamate homeostasis leads to the accumulation of ROS (22). In conjunction, the terms glutamate homeostasis, iron/heme homeostasis, and ferroptosis are also enriched in C1. In line with this, recent studies linked the PERK-NRF2-HO-1 axis of the ER stress pathway to the modulation of ferroptosis (23). Additionally, the increased presence of terms related to NADP activity within the molecular function (MF) ontology and the pentose phosphate pathway (PPP) in C1 may also be correlated with the increased activation of NRF2 (15). Several NADP-related terms were highly enriched in C1 followed by C2 at the level of MF in the GO analysis (Supplementary Figure 2A). Active NRF2 is associated with increased glucose uptake, which is preferentially metabolized through PPP resulting in increased reducing equivalent capacity, via the production of NADPH (24). NADPH is required for and consumed during fatty acid synthesis and the scavenging of ROS.

Of note, despite exhibiting a dominant antioxidant transcriptional network, the GBM C1 cluster also showed an enrichment of several terms related to the production of protumorigenic/angiogenic cytokines, such as IL-6, IL-7, IL-9 (25) and vascular endothelial growth factor (VEGF) (26) (Supplementary Figure 2D). This could be linked to a chronic activation of the UPR, coupling the upregulation of the PERK-NRF2 antioxidant response pathway, with the stimulation of NF-κB mediated proinflammatory cytokines (27, 28), an interesting conjecture to be explored in future functional studies. In GBM, β-catenin and components of the Wnt pathway are commonly found to be overexpressed, contributing to cancer initiation, proliferation and

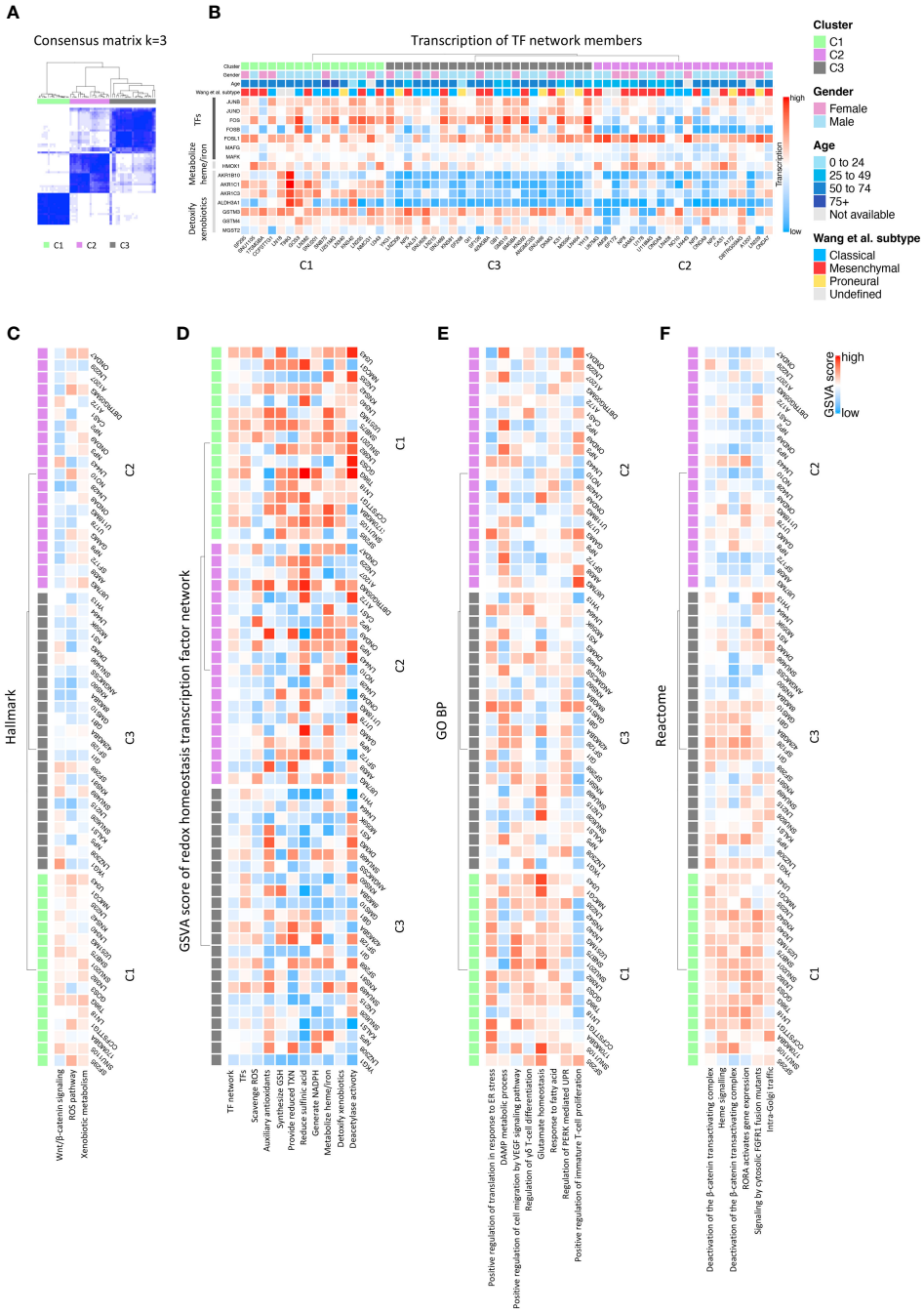

FIGURE 2
Consensus clustering of GBM CCLE cohort and function exploration. **(A)** Consensus matrix showing three distinct GBM clusters; **(B)** Major diversly expressed genes in the input signature; **(C)** Significant pathways evaluated by GSVA scoring in Hallmark database; **(D)** GSVA scores of each antioxidative pathways in the redox homeostasis transcription factor network; **(E)** Significant pathways evaluated by GSVA scoring in GO BP database; **(F)** Significant pathways evaluated by GSVA scoring in Reactome database.

invasion (29). It's worth noting that ROS, acting as signaling molecules, also exert control over the Wnt–β-catenin signaling pathway (30). Together, this suggests that the GBM C1 cluster deploys the ability to detoxify potentially harmful ROS while maintaining a redox-tone supporting protumorigenic cell intrinsic and extrinsic signaling pathways.

Taken together, this analysis portrays that compared with the other two clusters, the C1 identifies a GBM entity hallmarked by a heightened antioxidant and protumorigenic potential.

Identification of transcriptional networks governing differentiated antioxidant potentials

With the aim of identifying transcriptional networks with hub genes regulating the signature of each cluster, we integrated DEG analysis with the WGCNA method. DEG analysis identified 173, 356 and 220 genes upregulated, while 410, 684 and 174 genes

downregulated in C1, C2 and C3, respectively (Figures 3A–C; Supplementary Table 1). The results of GSEA on the upregulated gene set across each cluster were in line with GSVA, identifying genes involved in the NRF2 pathway, fatty acid metabolism and suppressors of ferroptosis (Supplementary Figure 3B) as highly expressed in C1 (Figure 3A; Supplementary Figure 3A). In contrast, C2 clustered genes of several inflammatory pathways such as response to LPS, cytokine active and IFN-α/γ response (Figure 3B; Supplementary 3C). Interestingly C3, which exhibits a limited ability to scavenge ROS, showed an enrichment for apoptosis pathway (Figure 3C).

Next, we used WGCNA to build gene modules of significantly correlating genes (Supplementary Figures 3E, F), and then evaluated how these modules relate to the clustering pattern by calculating Pearson correlations between each module and cluster (Supplementary Figure 3G, Supplementary Table 2). We integrated

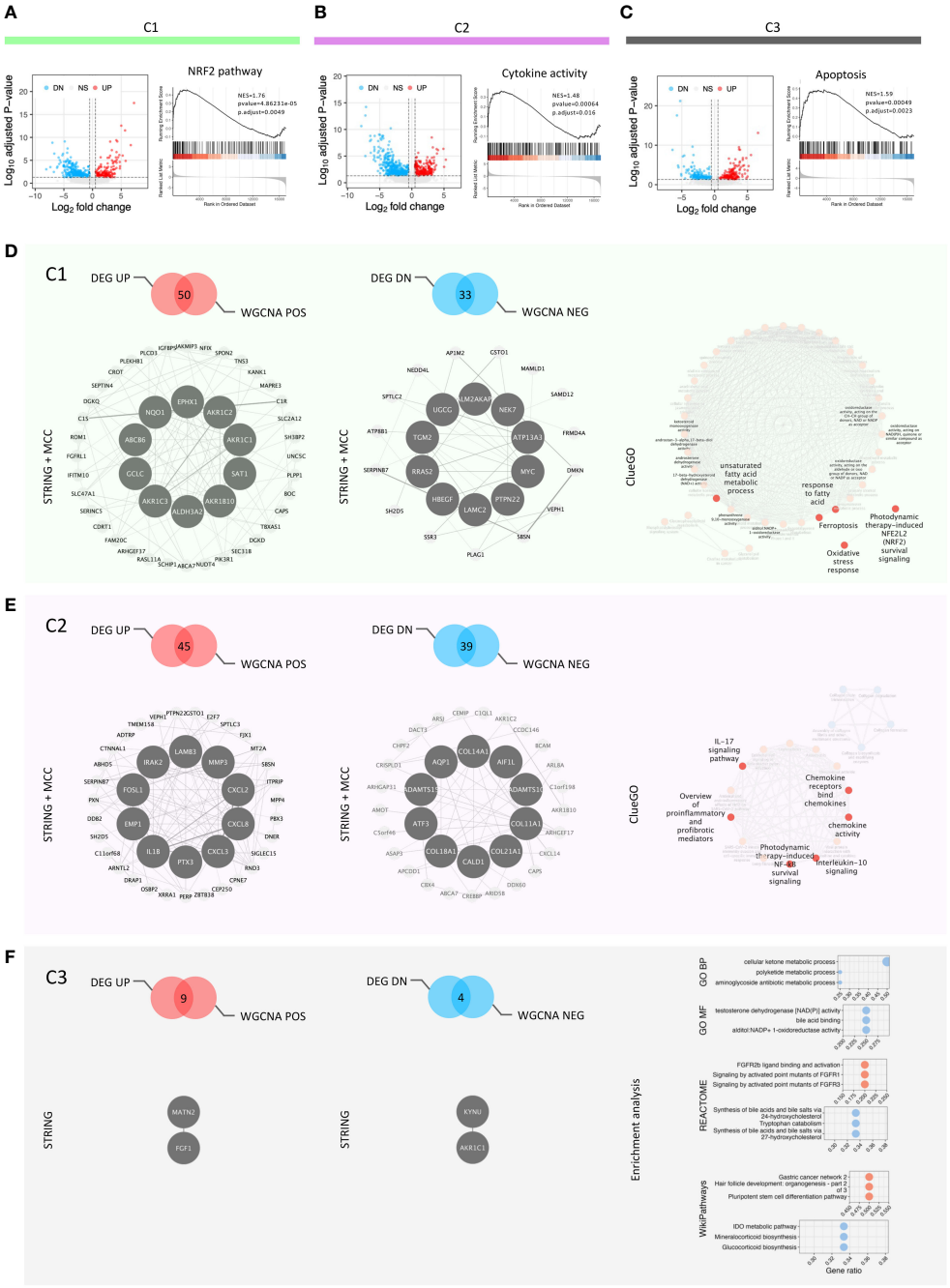

FIGURE 3
DEG analysis, GSEA and redox-based signatures. **(A–C)** Volcano plots showing DEG among the clusters and the key GSEA results in each cluster; **(D)** Feature panel of C1: positive and negative signatures, hub genes and function enriched; **(E)** Feature panel of C2: positive and negative signatures, hub genes and function enriched; **(F)** Feature panel of C3: positive and negative signatures, hub genes and function enriched.

the genes from modules correlating closely with each cluster and their DEGs (Figures 3D–F). The integrated gene lists were used as the input for STRING analysis to gain the protein-protein interaction network (PPI network) of each cluster. The PPI networks were incorporated into the Cytoscape software to characterize the hub genes regulating this network. The top ten hub genes were identified for each cluster, except C3, using the cytoHubba plug-in in Cytoscape (Figures 3D, E). The low number of input genes for C3 hindered this analysis (Figure 3F). We defined the coexisting genes in both positively correlated genes from WGCNA and up-regulated genes from DEG analysis as the signatures of the three clusters (Supplementary Table 3). Further, to identify the transcription factors in each signature, we utilized the database as described in the method section (Supplementary Figure 3H). We identified one [*NFIX* (31, 32)], six [*ZBTB38* (33), *ARNTL2* (34), *E2F7* (35), *PBX3* (36), *FOSL1* (37, 38), and *DRAP1*), and one (*LHX9* (39)] transcription factors in cluster C1, C2 and C3, respectively, potentially regulating the cluster (Supplementary Figure 3I). All these transcription factors are known to have a role in the development and progression of GBM. Moreover, they are either linked directly or indirectly in regulating ROS-mediated signaling pathways. To characterize the functionality of these integrated genesets, we used ClueGo which incorporates different databases to identify pathways these genes are enriched in (Figures 3D, E). The results of ClueGo were in line with GVSA and GSEA analysis, further validating our observation that C1 has the hallmark of an antioxidant phenotype, C2 is associated with an inflammatory phenotype, while C3 is characterized by a propensity to undergo ROS-mediated apoptosis.

We then tested whether the derived C1, C2 and C3 signatures correlated with the canonical classification of classical, mesenchymal and proneural GBM (40) (Supplementary Figure 4). Of note, the classical subtype was distributed mainly across C1, C2 and C3, suggesting that classical GBM are heterogenous in their redox homeostasis, likely depending on factors, such as the stage of the disease, mutational status, etc. Remarkably, the mesenchymal GBM subtype showed a major distribution in C2 (Supplementary Figure 4A). This observation was further validated statistically using a GSVA-based model of correlation (Supplementary Figure 4B). It has been previously shown that mesenchymal cells are associated with a high ROS index, which can lead to chronic inflammation eventually promoting cell growth (41). The proneural subtypes showed the highest distribution in C3 suggesting that proneural cell types have the weakest ROS-defending potential and could be targeted by ROS-inducing therapies. However the proneural phenotype is known to switch to the mesenchymal phenotype as an adaptive response in the presence of excess ROS (41, 42).

Next, we validated our signature with an in-house bulk RNAseq dataset derived from GBM patient-derived cell lines (PDCLs). Using the derived antioxidant network signatures, we could cluster these PDCLs into three distinct groups (Supplementary Figure 3J). Of note, analyzing the expression of the transcription factors associated with clusters C1, C2, and C3, we could demonstrate similar trends, with an expression of *ZBTB38*, *ARNTL2*, *E2F7*, *FOSL1*, and *DRAP1* high in C2 and *LHX9* high in C3 (Supplementary Figure 3K). Moreover, analyzing the correlation of C1, C2 and C3 signatures with the canonical subtype showed similar trend with PDCLs in mesenchymal subtypes showing major distribution in C2 (Supplementary Figures 4C, D).

Hence, the transcription factors identified for each gene network across different clusters may be predictive of GBM types that can benefit from particular ROS-induced therapeutic approaches. However, these observations require thorough functional investigations both *in vitro* and *in vivo* settings to confirm this assumption. The intriguing correlation between C2 with mesenchymal suggests that genomic-based classification of GBM can be associated with a differential redox homeostasis and antioxidant potential. This connection can be harnessed for targeted therapeutic approaches.

Prognostic significance of the redox-based classifier and the transcription factors associated

We utilized the TCGA-GBM dataset to examine whether our antioxidant transcription factor network-based classification system has any prognostic value. First, based on the signatures, GSVA scores of C1-C3 were calculated for each sample of TCGA-GBM study. Using these scores, we could divide the patients into three different sub-cohorts (Supplementary Figure 5A). Next, we characterized the prognostic value of each cluster both at the levels of overall survival (OS) (Figures 4A, C) and progression-free interval (PFI) (Figures 4B, D). Interestingly, C2 showed significantly worse prognosis both at the level of OS and PFI in both categorical and quantitative fashions (Figures 4A, B). According to the multivariate analysis, C2 showed a comparatively worse OS in GBM patients with a hazard ratio (HR) of 2.22 and a p-value of 0.010 (Figure 4C). Also, at the level of the PFI, C2 under-performed the other two phenotypes with an HR of 2.35 and a p-value of 0.013 based on multivariate survival analysis (Figure 4D).

We then focused on the transcription factors in the signature and wondered if they would provide more insights regarding GBM prognosis. We analyzed their expression in the TCGA-GBM cohort (Figures 4E–H; Supplementary Figure 5B–E). We found that all the transcription factors herein are differentially expressed compared with normal tissue. Except for ZBTB38 (Supplementary Figure 5B), all the other transcription factors are up-regulated in GBM, pointing to the re-design of redox-related mechanisms either due to the intrinsic ability of cancer cells or driven by the tumor microenvironment. We then checked the expression of each gene among the three clusters, and their prognostic value at the single gene level was underpinned (Figures 4I-N; Supplementary Figures 5B–E). We found that *FOSL1* is a potent predictor of both OS and PFI prognosis (Figure 4K). Lower expression of *FOSL1* indicates a better prognosis in GBM patients. Our finding shows that the patients stratifying in the C2 phenotype may have a preferable OS and PFI, and *FOLS1* can serve as a single gene biomarker predicting the survival of GBM patients.

In summary, we report the prognostic value of the classification of the redox homeostasis controlling network (Figure 5). Interestingly, C2 defined by the new classifier is adequate to

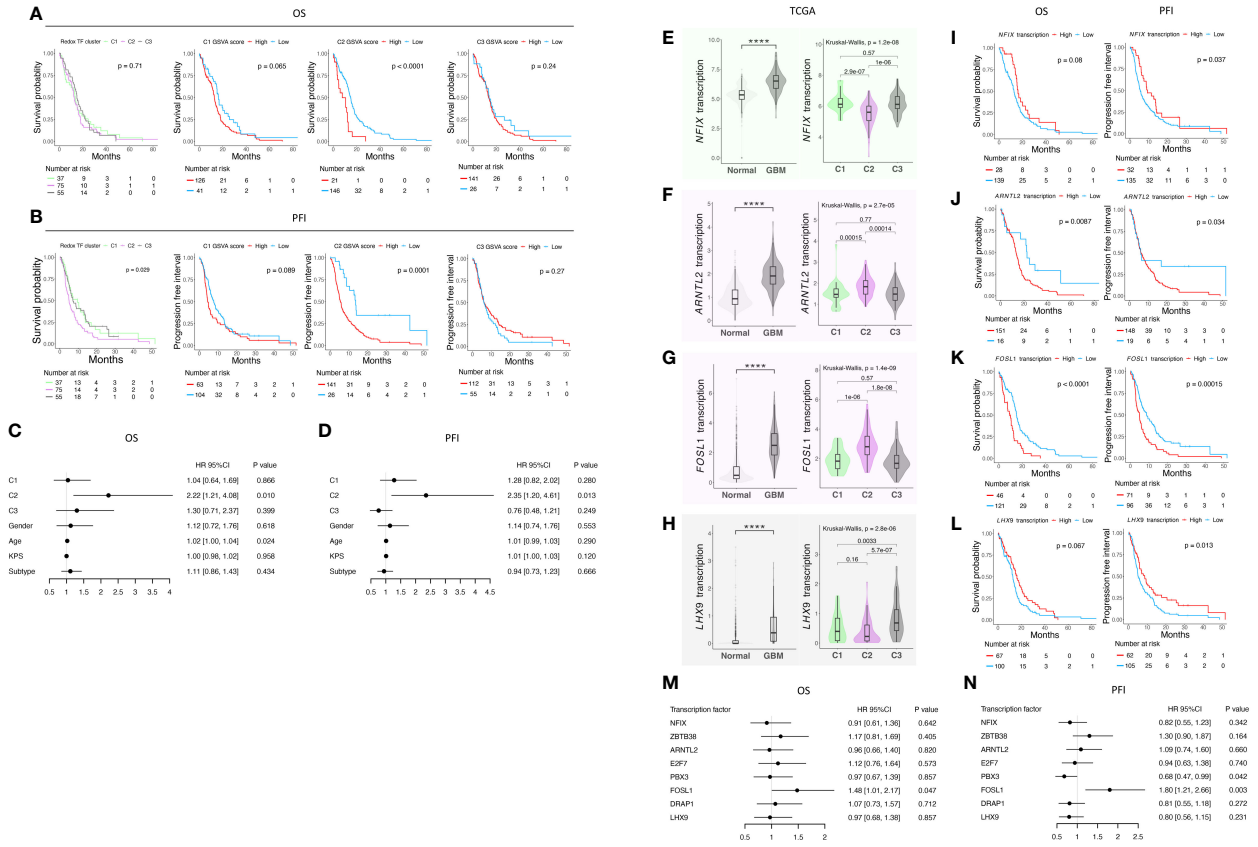

FIGURE 4
Survival analysis of the classification in TCGA GBM cohort and analysis of transcription factor in the signature of each cluster. **(A)** K-M curves of OS; **(B)** K-M curves of PFI; **(C)** Table of hazard ratio on OS; **(D)** Table of hazard ratio on PFI; **(E)** *NFIX* expression status and **(F)** its prognostic value; **(G)** *ARNTL2* expression status and **(H)** its prognostic value; **(I)** *FOSL1* expression status and **(J)** its prognostic value; **(K)** *LHX9* expression status and **(L)** its prognostic value; **(M)** Table of hazard ratio on OS; **(N)** Table of hazard ratio on PFI. **** indicates a p-value < 0.0001.

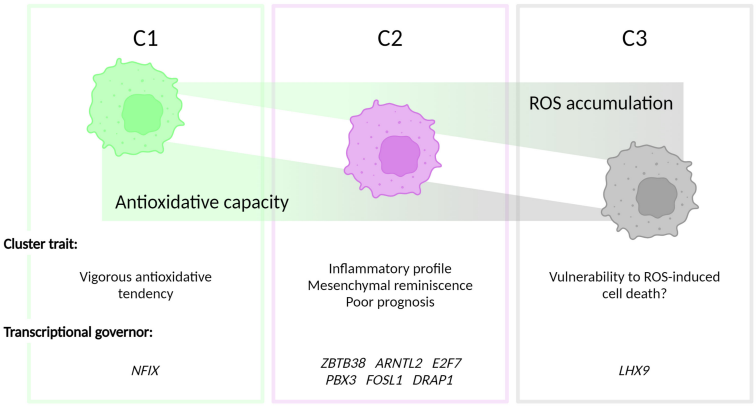

FIGURE 5
Figurative summary. GBM can be clustered into three groups, termed C1, C2 and C3, depending on the intrinsic antioxidative capacities. C1 is characterized by the strongest antioxidative potential. C2 has be discovered with the inflammatory phenotype and a correlation with mesenchymal GBM subtype. The antioxidation is dampened in C3, which, hypothetically, contributes to the vulnerability to ROS-triggered cell death in this cluster.

predict poor OS. Moreover, patients, who are classified as C2 phenotype, showed worsened PFI. Considering the function discovered in the enrichment analysis, C1 is marked as a cluster with a higher antioxidant potential compared with C2 and C3. In C2, a moderate level of ROS may function as a signaling molecule promoting GBM progression. The C3 phenotype has the weakest antioxidant potential and GBM clustered in this group may succumb to ROS-induced cell death. Among the transcription

factors in the C2 signature, *FOSL1* demonstrates a prognostic value in both OS and PFI. This suggests that *FOSL1* under-expression is an independent factor linked to longer OS and delayed tumor progression. Interestingly, *FOSL1* has been shown to boost the transition of proneural-to-mesenchymal via NF-κB signaling (37). In pancreatic cancer, metastasis can be overcome by the suppression of FOSL1 expression by SMAD4 (43). Of note, *FOSL1* expression has been functionally related to cancer angiogenesis and vascularization, suggesting that reprogramming of the redox tone in this GBM cluster may be associated with its heightened neovascularization potential.

In conclusion, our analysis shows that the C2 cluster is closely correlated with mesenchymal GBM. Due to the pervasive angiogenic phenotype of the mesenchymal subtype of GBM, *FOSL1* could be an interesting target for future studies assessing the biological and therapeutic function of this transcription factor in GBM.

Data availability statement

The original contributions presented in the study are included in the article/Supplementary Material. Further inquiries can be directed to the corresponding authors.

Author contributions

YY: Writing – review & editing, Writing – original draft, Visualization, Validation, Investigation, Formal analysis, Data curation. SM: Writing – review & editing, Writing – original draft, Validation, Formal analysis. FS: Writing – review & editing, Resources, Funding acquisition. SV: Writing – review & editing, Supervision, Funding acquisition. PA: Writing – review & editing, Writing – original draft, Supervision, Funding acquisition, Conceptualization.

Funding

The author(s) declare financial support was received for the research, authorship, and/or publication of this article. Research project funded by Kom op tegen Kanker (Stand up to Cancer). PA, SV, and FS are supported by the KotK grant. PA is supported by grants from the Flemish Research Foundation (FWO-Vlaanderen; G076617N, G049817N, G070115N), the EOS DECODE consortium N° 30837538, the EOS MetaNiche consortium N° 40007532, Stichting tegen Kanker (FAF-F/2018/1252) and the iBOF/21/053 ATLANTIS consortium.

Acknowledgments

We thank Dr. Basiel Cole, Dr. Swati Gupta and Marleen Derweduwe for expertise advice.

Conflict of interest

The authors declare that the research was conducted in the absence of any commercial or financial relationships that could be construed as a potential conflict of interest.

The author(s) declared that they were an editorial board member of Frontiers, at the time of submission. This had no impact on the peer review process and the final decision.

Publisher's note

Supplementary material

The Supplementary Material for this article can be found online at: https://www.frontiersin.org/articles/10.3389/fimmu.2024.1342977/full#supplementary-material

SUPPLEMENTARY FIGURE 1
(A) Multiple clustering algorithms underscore the robustness of antioxidative network-based classification. Expression heatmap and hierarchical clustering of antioxidative signature; **(B–J)** Consensus clustering with multiple k values.

SUPPLEMENTARY FIGURE 2
Heatmap of GSVA scoring biological function database. **(A)** GSVA score heatmap of GO MF database; **(B)** GSVA score heatmap of GO CC database; **(C)** GSVA score heatmap of WikiPathways database; **(D)** GSVA score heatmap of BioCarta database; **(E)** GSVA score heatmap of PID database; **(F)** GSVA score heatmap of CM database.

SUPPLEMENTARY FIGURE 3
(A) GSEA of C1; **(B)** Overlapping of ferroptosis signature with C1 signature; **(C)** GSEA of C2; **(D)** Soft power selection in WGCNA; **(E, F)** WGCNA modules presentation; **(G)** Module-trait correlations; **(H)** Transcription factors in each cluster signature and **(I)** their expression status in CCLE cohort; **(J)** redox clusters assignment of in-house GBM RNA-seq; **(K)** Expression of featured transcription factors in in-house cohort. SIG: signature.

SUPPLEMENTARY FIGURE 4
Bridging antioxidative clusters with GBM canonical classification. **(A)** Alluvial plot showing the cluster-subtype connection in CCLE cohort; **(B)** Correlation analysis of GSVA scores of signatures of antioxidative cluster and GBM canonical subtypes in CCLE cohort. **(C)** Alluvial plot showing the cluster-subtype connection in in-house cohort; **(D)** Correlation analysis of GSVA scores of signatures of redox cluster and GBM canonical subtypes in in-house cohort.

SUPPLEMENTARY FIGURE 4
(A) Subtype assignment in GBM samples from TCGA project; **(B)** *ZBTB38* expression status and its prognostic value; **(C)** *PBX3* expression status and its prognostic value; **(D)** *E2F7* expression status and its prognostic value; (E) *DRAP1* expression status and its prognostic value.

SUPPLEMENTARY FIGURE 5
(A) Subtype assignment in GBM samples from TCGA project; **(B)** *ZBTB38* expression status and its prognostic value; **(C)** *PBX3* expression status and its prognostic value; **(D)** *E2F7* expression status and its prognostic value; (E) *DRAP1* expression status and its prognostic value.

References

1. Ishikawa K, Takenaga K, Akimoto M, Koshikawa N, Yamaguchi A, Imanishi H, et al. ROS-generating mitochondrial DNA mutations can regulate tumor cell metastasis. *Science*. (2008) 320:661–4. doi: 10.1126/science.1156906

2. Noh J, Kwon B, Han E, Park M, Yang W, Cho W, et al. Amplification of oxidative stress by a dual stimuli-responsive hybrid drug enhances cancer cell death. *Nat Commun*. (2015) 6:6907. doi: 10.1038/ncomms7907

3. Verfaillie T, Rubio N, Garg AD, Bultynck G, Rizzuto R, Decuypere JP, et al. PERK is required at the ER-mitochondrial contact sites to convey apoptosis after ROS-based ER stress. *Cell Death Differ*. (2012) 19:1880–91. doi: 10.1038/cdd.2012.74

4. Evavold CL, Hafner-Bratkovič I, Devant P, D'Andrea JM, Ngwa EM, Boršić E, et al. Control of gasdermin D oligomerization and pyroptosis by the Ragulator-Rag-mTORC1 pathway. *Cell*. (2021) 184:4495–4511.e19. doi: 10.1016/j.cell.2021.06.028

5. Weindel CG, Martinez EL, Zhao X, Mabry CJ, Bell SL, Vail KJ, et al. Mitochondrial ROS promotes susceptibility to infection via gasdermin D-mediated necroptosis. *Cell*. (2022) 185:3214–3231.e23. doi: 10.1016/j.cell.2022.06.038

6. Dixon SJ, Lemberg KM, Lamprecht MR, Skouta R, Zaitsev EM, Gleason CE, et al. Ferroptosis: an iron-dependent form of nonapoptotic cell death. *Cell*. (2012) 149:1060–72. doi: 10.1016/j.cell.2012.03.042

7. Vaccaro A, Kaplan Dor Y, Nambara K, Pollina EA, Lin C, Greenberg ME, et al. Sleep loss can cause death through accumulation of reactive oxygen species in the gut. *Cell*. (2020) 181:1307–1328.e15. doi: 10.1016/j.cell.2020.04.049

8. Xing F, Hu Q, Qin Y, Xu J, Zhang B, Yu X, et al. The relationship of redox with hallmarks of cancer: the importance of homeostasis and context. *Front Oncol*. (2022) 12:862743. doi: 10.3389/fonc.2022.862743

9. Zhang Z, Qin S, Chen Y, Zhou L, Yang M, Tang Y, et al. Inhibition of NPC1L1 disrupts adaptive responses of drug-tolerant persister cells to chemotherapy. *EMBO Mol Med*. (2022) 14:e14903. doi: 10.15252/emmm.202114903

10. Piskounova E, Agathocleous M, Murphy MM, Hu Z, Huddlestun SE, Zhao Z, et al. Oxidative stress inhibits distant metastasis by human melanoma cells. *Nature*. (2015) 527:186–91. doi: 10.1038/nature15726

11. Diehn M, Cho RW, Lobo NA, Kalisky T, Dorie MJ, Kulp AN, et al. Association of reactive oxygen species levels and radioresistance in cancer stem cells. *Nature*. (2009) 458:780–3. doi: 10.1038/nature07733

12. Dejaegher J, Solie L, Hunin Z, Sciot R, Capper D, Siewert C, et al. DNA methylation based glioblastoma subclassification is related to tumoral T-cell infiltration and patient survival. *Neuro Oncol*. (2021) 23:240–50. doi: 10.1093/neuonc/noaa247

13. Olivier C, Oliver L, Lalier L, Vallette FM. Drug resistance in glioblastoma: the two faces of oxidative stress. *Front Mol Biosci*. (2020) 7:620677. doi: 10.3389/fmolb.2020.620677

14. Rubio N, Coupienne I, Di Valentin E, Heirman I, Grooten J, Piette J, et al. Spatiotemporal autophagic degradation of oxidatively damaged organelles after photodynamic stress is amplified by mitochondrial reactive oxygen species. *Autophagy*. (2012) 8:1312–24. doi: 10.4161/auto.20763

15. Hayes JD, Dinkova-Kostova AT, Tew KD. Oxidative stress in cancer. *Cancer Cell*. (2020) 38:167–97. doi: 10.1016/j.ccell.2020.06.001

16. Garofano L, Migliozzi S, Oh YT, D'Angelo F, Najac RD, Ko A, et al. Pathway-based classification of glioblastoma uncovers a mitochondrial subtype with therapeutic vulnerabilities. *Nat Cancer*. (2021) 2:141–56. doi: 10.1038/s43018-020-00159-4

17. Oakes SA. Endoplasmic reticulum stress signaling in cancer cells. *Am J Pathol*. (2020) 190:934–46. doi: 10.1016/j.ajpath.2020.01.010

18. He F, Ru X, Wen T. NRF2, a transcription factor for stress response and beyond. *Int J Mol Sci*. (2020) 21(13): 4777. doi: 10.3390/ijms21134777

19. He F, Zhang P, Liu J, Wang R, Kaufman RJ, Yaden BC, et al. ATF4 suppresses hepatocarcinogenesis by inducing SLC7A11 (xCT) to block stress-related ferroptosis. *J Hepatol*. (2023) 79:362–77. doi: 10.1016/j.jhep.2023.03.016

20. Kang L, Wang D, Shen T, Liu X, Dai B, Zhou D, et al. PDIA4 confers resistance to ferroptosis via induction of ATF4/SLC7A11 in renal cell carcinoma. *Cell Death Dis*. (2023) 14:193. doi: 10.1038/s41419-023-05719-x

21. Ye P, Mimura J, Okada T, Sato H, Liu T, Maruyama A, et al. Nrf2- and ATF4-dependent upregulation of xCT modulates the sensitivity of T24 bladder carcinoma cells to proteasome inhibition. *Mol Cell Biol*. (2014) 34:3421–34. doi: 10.1128/MCB.00221-14

22. Dixon SJ, Patel DN, Welsch M, Skouta R, Lee ED, Hayano M, et al. Pharmacological inhibition of cystine-glutamate exchange induces endoplasmic reticulum stress and ferroptosis. *eLife*. (2014) 3:e02523. doi: 10.7554/eLife.02523

23. Wei R, Zhao Y, Wang J, Yang X, Li S, Wang Y, et al. Tagitinin C induces ferroptosis through PERK-Nrf2-HO-1 signaling pathway in colorectal cancer cells. *Int J Biol Sci*. (2021) 17:2703–17. doi: 10.7150/ijbs.59404

24. Esteras N, Blacker TS, Zherebtsov EA, Stelmashuk OA, Zhang Y, Wigley WC, et al. Nrf2 regulates glucose uptake and metabolism in neurons and astrocytes. *Redox Biol*. (2023) 62:102672. doi: 10.1016/j.redox.2023.102672

25. Briukhovetska D, Dörr J, Endres S, Libby P, Dinarello CA, Kobold S. Interleukins in cancer: from biology to therapy. *Nat Rev Cancer*. (2021) 21:481–99. doi: 10.1038/s41568-021-00363-z

26. Kim Y-W, Byzova TV. Oxidative stress in angiogenesis and vascular disease. *Blood*. (2014) 123:625–31. doi: 10.1182/blood-2013-09-512749

27. Almanza A, Carlesso A, Chintha C, Creedican S, Doultsinos D, Leuzzi B, et al. Endoplasmic reticulum stress signalling - from basic mechanisms to clinical applications. *FEBS J*. (2019) 286:241–78. doi: 10.1111/febs.14608

28. Nakajima S, Kitamura M. Bidirectional regulation of NF-κB by reactive oxygen species: a role of unfolded protein response. *Free Radic Biol Med*. (2013) 65:162–74. doi: 10.1016/j.freeradbiomed.2013.06.020

29. Lee Y, Lee J-K, Ahn SH, Lee J, Nam D-H. WNT signaling in glioblastoma and therapeutic opportunities. *Lab Invest*. (2016) 96:137–50. doi: 10.1038/labinvest.2015.140

30. Funato Y, Michiue T, Asashima M, Miki H. The thioredoxin-related redox-regulating protein nucleoredoxin inhibits Wnt-beta-catenin signalling through dishevelled. *Nat Cell Biol*. (2006) 8:501–8. doi: 10.1038/ncb1405

31. Liu Z, Ge R, Zhou J, Yang X, Cheng KK-Y, Tao J, et al. Nuclear factor IX promotes glioblastoma development through transcriptional activation of Ezrin. *Oncogenesis*. (2020) 9:39. doi: 10.1038/s41389-020-0223-2

32. Ge R, Wang C, Liu J, Jiang H, Jiang X, Liu Z. A novel tumor-promoting role for nuclear factor IX in glioblastoma is mediated through transcriptional activation of GINS1. *Mol Cancer Res*. (2023) 21:189–98. doi: 10.1158/1541-7786.MCR-22-0504

33. Miotto B, Marchal C, Adelmant G, Guinot N, Xie P, Marto JA, et al. Stabilization of the methyl-CpG binding protein ZBTB38 by the deubiquitinase USP9X limits the occurrence and toxicity of oxidative stress in human cells. *Nucleic Acids Res*. (2018) 46:4392–404. doi: 10.1093/nar/gky149

34. Brady JJ, Chuang C-H, Greenside PG, Rogers ZN, Murray CW, Caswell DR, et al. An arntl2-driven secretome enables lung adenocarcinoma metastatic self-sufficiency. *Cancer Cell*. (2016) 29:697–710. doi: 10.1016/j.ccell.2016.03.003

35. Yang R, Wang M, Zhang G, Bao Y, Wu Y, Li X, et al. E2F7-EZH2 axis regulates PTEN/AKT/mTOR signalling and glioblastoma progression. *Br J Cancer*. (2020) 123:1445–55. doi: 10.1038/s41416-020-01032-y

36. Xu X, Bao Z, Liu Y, Jiang K, Zhi T, Wang D, et al. PBX3/MEK/ERK1/2/LIN28/let-7b positive feedback loop enhances mesenchymal phenotype to promote glioblastoma migration and invasion. *J Exp Clin Cancer Res*. (2018) 37:158. doi: 10.1186/s13046-018-0841-0

37. Chen Z, Wang S, Li H-L, Luo H, Wu X, Lu J, et al. FOSL1 promotes proneural-to-mesenchymal transition of glioblastoma stem cells via UBC9/CYLD/NF-κB axis. *Mol Ther*. (2022) 30:2568–83. doi: 10.1016/j.ymthe.2021.10.028

38. Marques C, Unterkircher T, Kroon P, Oldrini B, Izzo A, Dramaretska Y, et al. NF1 regulates mesenchymal glioblastoma plasticity and aggressiveness through the AP-1 transcription factor FOSL1. *eLife*. (2021) 10:e64846. doi: 10.7554/eLife.64846

39. Vladimirova V, Mikeska T, Waha A, Soerensen N, Xu J, Reynolds PC, et al. Aberrant methylation and reduced expression of LHX9 in Malignant gliomas of childhood. *Neoplasia*. (2009) 11:700–11. doi: 10.1593/neo.09406

40. Wang Q, Hu B, Hu X, Kim H, Squatrito M, Scarpace L, et al. Tumor evolution of glioma-intrinsic gene expression subtypes associates with immunological changes in the microenvironment. *Cancer Cell*. (2017) 32:42–56.e6. doi: 10.1016/j.ccell.2017.06.003

41. Koh LW-H, Koh GR-H, Ng FS-L, Toh TB, Sandanaraj E, Chong YK, et al. A distinct reactive oxygen species profile confers chemoresistance in glioma-propagating cells and associates with patient survival outcome. *Antioxid Redox Signal*. (2013) 19:2261–79. doi: 10.1089/ars.2012.4999

42. Wang Z, Zhang H, Xu S, Liu Z, Cheng Q. The adaptive transition of glioblastoma stem cells and its implications on treatments. *Signal Transduct Target Ther*. (2021) 6:124. doi: 10.1038/s41392-021-00491-w

43. Dai C, Rennhack JP, Arnoff TE, Thaker M, Younger ST, Doench JG, et al. SMAD4 represses FOSL1 expression and pancreatic cancer metastatic colonization. *Cell Rep*. (2021) 36:109443. doi: 10.1016/j.celrep.2021.109443

frontiers | Frontiers in Immunology

TYPE Original Research
PUBLISHED 06 September 2024
DOI 10.3389/fimmu.2024.1412382

OPEN ACCESS

EDITED BY
Chao Yang,
Zhejiang Ocean University, China

REVIEWED BY
Guangchuan Wang,
Jinzhou Medical University, China
Zhongyu Han,
Chengdu University of Traditional Chinese Medicine, China

*CORRESPONDENCE
Bingxue Bai
baibingxue@hrbmu.edu.cn

RECEIVED 04 April 2024
ACCEPTED 21 August 2024
PUBLISHED 06 September 2024

CITATION
Xu L, Guo W, Hao H, Yuan J and Bai B (2024) Computational recognition of regulator genes and signature for ferroptosis with implications on immunological properties and clinical management of atopic dermatitis. *Front. Immunol.* 15:1412382. doi: 10.3389/fimmu.2024.1412382

Computational recognition of regulator genes and signature for ferroptosis with implications on immunological properties and clinical management of atopic dermatitis

Lei Xu[1,2], Wenjuan Guo[1], Huirong Hao[1], Jinping Yuan[1] and Bingxue Bai[1]*

[1]Department of Dermatology, The Second Affiliated Hospital of Harbin Medical University, Harbin, China, [2]The Key Laboratory of Myocardial Ischemia, Chinese Ministry of Education, State Key Laboratory of Frigid Zone Cardiovascular Diseases (SKLFZCD), Harbin, China

Background: Atopic dermatitis (AD) is a common chronic dermatitis of autoimmune origin that considerably affects the quality of life of patients. Ferroptosis, a newly regulated form of cell death, is essential for inflammation-related damage-associated molecular patterns (DAMPs). In this study, we aimed to identify ferroptosis regulators relevant to AD pathogenesis and reveal the mechanisms by which ferroptosis regulates the pathogenesis of AD.

Methods: We analyzed the GEO AD cohorts (GSE16161, GSE32924, GSE107361, and GSE120721), identifying AD-related differentially expressed genes (DEGs) using edgeR. Co-expression and STRING database analyses were used to elucidate the interactions between DEGs and ferroptosis markers. Through functional enrichment analysis, we defined potential biological functions within the protein-protein interaction (PPI) network and developed FerrSig using LASSO regression. The utility of FerrSig in guiding the clinical management of AD was evaluated using the GSE32473 cohort. Subsequently, our in silico findings were confirmed, and mechanistic insights were expanded through both *in vitro* and *in vivo* studies, validating the relevance of FerrSig.

Results: In the GEO AD cohort, 278 DEGs were identified, including seven ferroptosis signature genes. Co-expression analysis and STRING database review revealed a 63-node PPI network linked to cell cycle and pro-inflammatory pathways. Four ferroptosis genes (*ALOXE3*, *FABP4*, *MAP3K14*, and *EGR1*) were selected to create FerrSig, which was significantly downregulated in samples collected from patients with AD. In addition, immune-related signaling pathways were significantly differentially enriched between the stratifications of samples collected from patients with AD with high and low ferritin levels, whereas in the GSE32473 cohort, FerrSig was significantly increased in cohorts effectively treated with pimecrolimus or betamethasone. Finally, *in vitro* and *in vivo* models showed a notable FerrSig decrease in patients with AD versus healthy control. Treatment with betamethasone and tacrolimus restored FerrSig, and the magnitude of the increase in FerrSig was higher in samples collected from

patients with AD with better efficacy assessments. In addition, FerrSig was significantly positively correlated with the ferroptosis inhibitors GPX4 and SLC7A11 and negatively correlated with reactive oxygen species (ROS) levels and p-STAT3/STAT3. This implies that the FerrSig signature genes may regulate ferroptosis through the JAK/STAT3 signaling pathway.

Conclusion: Our study further explored the pathogenesis of AD, and FerrSig could serve as a potential biomarker for identifying AD morbidity risks and determining treatment efficacy.

KEYWORDS

ferroptosis, atopic dermatitis, immunoregulation, drug therapy, tissue-specific genes

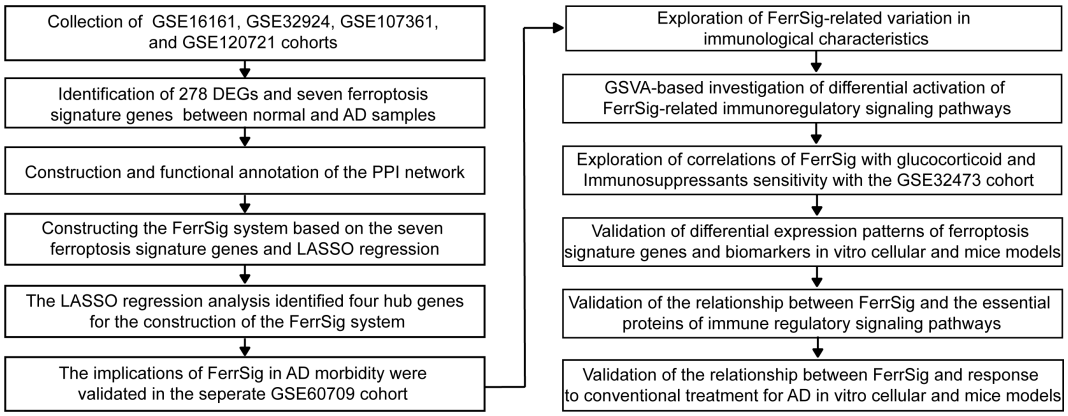

GRAPHICAL ABSTRACT
The overview of the study design

1 Introduction

Atopic dermatitis (AD) is the most common inflammatory skin disease. Its main clinical manifestations include lesions, rashes, and crusts on the extremities, head, and face, accompanied by intense itching and discomfort (1, 2). Some patients experience intractable itching, which seriously affects their quality of life (3). Epidemiological reports indicate that the combined prevalence of AD in the community is approximately 11%–13% (4, 5). Its prevalence is higher in children than in adults, with a combined prevalence of approximately 24% in children aged 0–5 (6). Therefore, the high prevalence of AD imposes a severe burden on public healthcare systems. In addition, several challenges remain in the clinical management of AD, including the absence of objective diagnostic tests, unavailability of publicly recognized specific biomarkers, and vulnerability to relapse (5, 7). Therefore, a more comprehensive understanding of its pathogenesis can help overcome these challenges and improve the early and accurate diagnosis and treatment of patients with AD.

Ferroptosis was first detected by Dixon et al. and is a form of cell death induced by ferrous ions and cell membrane lipid peroxidation (8). Recently, ferroptosis has been suggested to be involved in the pathophysiology of several immune-mediated diseases (9, 10). Evidence suggests that ferroptosis and the inflammatory response are mutually reinforcing. Ferroptosis triggers the intrinsic immune system by releasing inflammation-related damage-associated molecules, and immune cells stimulate an inflammatory response by recognizing the mechanisms of different patterns of cell death (11). For example, neutrophils can release extracellular traps through the ferroptosis pathway, activate toll-like receptors (TLR), and upregulate ROS levels (12). Excessive production of ROS promotes the release of pro-inflammatory cytokines and polarization of cytotoxic T cells, leading to AD morbidity and progression (13). Additionally, in psoriasis, which has a pathogenesis similar to that of AD, ROS-dependent ferroptosis is closely associated with the accumulation of inflammatory cytokines. Intervention strategies targeting ferroptosis can substantially reduce the intensity of inflammation and inhibit pathophysiological evolution (14, 15). Therefore, we speculate that ferroptosis may play an essential role in the pathophysiological development of AD. However, the mechanisms underlying ferroptosis regulation in AD have yet to

be explored, and a notable knowledge gap still exists in this field. Therefore, this study attempted to reveal the critical regulators of ferroptosis in AD and their potential regulatory mechanisms, and to construct AD morbidity models for guiding its clinical management.

In this study, we identified 278 differentially expressed genes (DEGs) and seven ferroptosis signature genes in multiple GEO cohorts. Furthermore, we constructed protein-protein interaction (PPI) networks and performed functional enrichment analysis. Ferroptosis signature genes and associated DEGs were highly enriched in signaling pathways involved in immune regulation, cell cycle checkpoints, and extracellular matrix reorganization. In addition, the constructed FerrSig model could accurately identify the risk of developing AD and was suggestive of a response to glucocorticoid and immunosuppressant therapies. Finally, in both *in vitro* cellular and mouse models, we observed elevated levels of ferroptosis in AD and validated the correlation between FerrSig expression and AD morbidity and treatment response. Overall, our study revealed that ferroptosis is involved in the pathophysiological evolution of AD. In addition, FerrSig may serve as a novel biomarker with clinical applicability, and its corresponding hub genes may be potential targets for clinical interventions in AD.

2 Materials and methods

2.1 Collection and pre-processing of data

Six AD-related cohorts were obtained from the GEO database (https://www.ncbi.nlm.nih.gov/geo/). Only samples of skin tissue origin were retained in all GEO cohorts. After excluding samples from the same patient source, samples from 64 patients with AD and 34 healthy controls were included in the GSE16161, GSE32924, GSE107361, and GSE120721 cohorts. They were used to identify the DEGs and construct an AD morbidity model. The GSE60709 cohort was used as an independent external dataset to validate the accuracy and stability of the AD morbidity model. The GSE32473 cohort contained information on patients with AD treated with pimecrolimus or betamethasone. This cohort was used for the analysis of therapeutic benefits. A list of ferroptosis regulators was obtained from the "FerrDb V2" database (http://www.zhounan.org/ferrdb/) (16). The "normalizeBetweenArrays" function in the "limma" package was used to normalize expression profiles from different GEO cohorts to avoid biased results due to variations in sequencing background.

2.2 Identification of DEGs

To ensure accuracy, we used the Robust Rank Aggregation method to identify DEGs in samples from healthy controls and patients with AD (17). First, based on the "edgeR" algorithm, we separately evaluated the differences in expression profiles between samples from healthy controls and AD samples in GSE16161, GSE32924, GSE107361, and GSE120721 cohorts. The list of candidate DEGs was determined according to the thresholds FDR<0.05 and |logFC|>1. Furthermore, based on the "RobustRankAggreg" package, we comprehensively analyzed the LogFC and FDR values distribution of the candidate DEGs and constructed a comprehensive ranking list. Only DEGs with consistent expression patterns in at least three cohorts were selected and considered differentially expressed between samples from healthy controls and patients with AD.

2.3 Co-expression analysis and construction of the PPI network

First, the co-expression relationships between ferroptosis signature genes and DEGs were identified using the Spearman correlation analysis. All co-expression relationships were retained at $p<0.05$. Furthermore, in the STRING database, we searched for all nodes in the co-expression network (https://cn.string-db.org/) (18). With Cor>0.4 as the threshold, 63 PPI were retained. Reconstruction of PPI networks was performed using the Cytoscape software (Version 3.9.2).

2.4 Functional enrichment analysis

The "clusterProfiler" package was served for Gene Ontology (GO) and the Kyoto Protocol Encyclopedia of Genes and Genomes (KEGG) functional enrichment analysis (19). Signaling pathways and biological functions that met the qvalue < 0.05 were considered significant. The "org.Hs.eg.db" package was used to translate gene symbols into ensemble IDs, which enabled the gene list to be read by the "enrichGO" or "enrichKEGG" algorithm.

In addition, the gene set enrichment analysis (GSEA) can identify variations in the enrichment levels of specific signaling pathways in different sample stratifications. This strategy was applied to identify the differences in the activity of immune regulatory signaling pathways between the high- and low-FerrSig subgroups. Gene sets for characterizing the immune regulatory signaling pathways were obtained from the GSEA database (https://www.gsea-msigdb.org/gsea/).

2.5 Identification of the AD morbidity model with LASSO regression

Least absolute shrinkage and selection operator (LASSO) regression were performed to identify the FerrSig AD morbidity model. Firstly, with the "createDataPartition" function in the "caret" package, we randomly and equally divided the integrated GEO cohort (including GSE16161, GSE32924, GSE107361, and GSE120721) into the train and test sets. The LASSO regression was implemented based on the "glmnet" package. After 1000 iterations and validated by the 10-fold cross-validation, the optimal penalty coefficient was $\log(\lambda) = -4.35$. Four ferroptosis signature genes (*ALOXE3*, *FABP4*, *MAP3K14*, and *EGR1*) had non-zero weight coefficient (Coef) values under these conditions. These are the principal components of ferroptosis signature genes in AD and are recognized as hub genes for ferroptosis in AD. FerrSig was

constructed using the following formula:

$$FerrSig = \sum_{i=1}^{n} Coef(Hub\ \ Genes_i) * Expression(Hub\ \ Genes_i)$$

2.6 Immune cell infiltration and ssGSEA

ssGSEA and its derivative algorithms were used to evaluate the enrichment levels of the immune signatures for each sample. Of these, 24 gene sets were obtained from the study by Bindea et al. (20), 17 from the ImmPort database (21), and 29 from the R&D system (RndSys, https://www.rndsystems.com/). The signatures of these gene sets were evaluated by the ssGSEA method based on the "GSEA" package. In addition, 22 immune cell signatures were calculated using the CIBERSORT algorithm, a derivative of ssGSEA, and used to evaluate immune cell infiltration patterns in AD (22).

2.7 Statistical methods and software

The Mann-Whitney U test was used to compare the differential distribution of relevant variables between the two subtypes or subgroups. Otherwise, we used the Kruskal–Wallis test for variance analysis. Correlations between the variables were verified using Spearman's correlation analysis. The accuracy of the morbidity model was determined with Receiver Operating Characteristic (ROC) curves and the areas under the curves (AUC).

This study was conducted using R version 4.1.1. The "pheatmap" package was used for plotting heatmaps. "ggplot2," "ggpubr," "ggExtra," "plyr," and "reshape2" packages could be used for plotting multiple figures, such as box plots and scatter diagrams. The Venn diagram was developed with the "Venn" package. The ROC curves were plotted by the "pROC" package. In addition, Perl scripts were used to preprocess the data (Strawberry-Perl-5.32.1.1).

2.8 Molecular biology experimental validation

2.8.1 *In vitro* cell assay

Human immortalized skin keratinocytes (HaCaT cells) were purchased from Kunming Cell Bank of Type Culture Collection, Chinese Academy of Science (Kunming, China) and cultured in Dulbecco's modified Eagle's medium (DMEM, Gibco) supplemented with 10% fetal bovine serum (FBS; Procell) and 1% penicillin-streptomycin (v/v, Gibco) at 37°C under a humidified atmosphere of 5% CO_2. The medium was changed every 2–3 d. HaCaT cells were cultured with 10 ng/mL of interferon-γ (IFN-γ; 10 ng/mL) and tumor necrosis factor-α (TNF-α; 10 ng/mL) for 24 h to induce the *in-vitro* AD model.

2.8.2 ROS detection

HaCaT cells were seeded at a density of 2×10^4 cells per well in 24-well plates. After 24 h of stimulation with 10 ng/mL of TNF-α/IFN-γ, intracellular ROS levels were assessed using a ROS detection kit (S0033S, Beyotime Biotechnology, China). Subsequently, the cells were incubated with 10 μM 2',7'-dichlorodihydrofluorescein diacetate (DCFH-DA) in the dark at 37°C for 20 min. Subsequently, the cells were washed thrice with serum-free medium. Fluorescence was captured using a fluorescence microscope (Leica, Wetzlar, Germany).

2.8.3 Animals

Female BALB/c mice (6 weeks of age, body weight: 18–22 g) provided by the Animal Laboratory Center of the Second Affiliated Hospital of Harbin Medical University were used to construct an *in vivo* AD model. They were maintained under standard conditions (temperature 21 ± 2°C; 12-h light/dark cycle) and an unlimited supply of a standard extruded pellet diet and water was provided. They were allowed a minimum of 1 week to acclimate to the colony room upon arrival. This study was conducted in accordance with the guidelines of the Declaration of Helsinki. All procedures complied with the National Institutes of Health Guide for the Care and Use of Laboratory Animals. All relevant experimental protocols were approved by the Institutional Animal Care and Use Committee of Harbin Medical University (ethical approval number: YJSDW2022-122).

Mice were divided into four groups: Control (ethanol), MC903 group (calcipotriol, Sigma-Aldrich, St. Louis, MO, USA), MC903+ tacrolimus group (0.1% TAC ointment, Protopic® from Astellas Pharma Inc. Tokyo, Japan), and the MC903+ glucocorticoid group (GLU ointment: 0.05% clobetasol propionate cream, Tianyao Ltd., Alocal Pharmacy Store, Tianjin, China). Two nmol MC903 was applied topically to each ear of the mice once daily for 7 d to induce AD-like skin lesions. After fully inducing dermatitis, 1 nmol MC903 was administered daily for 7 d to sustain skin inflammation. The treatment group received topical 0.1% TAC ointment and 0.05% GLU once daily for seven consecutive days. Ear thickness and scratching frequency were measured at the indicated time (Days 0,3.5.7,10, and 15). After the indicated time (Days 0,3.5.7,10, and 15) treatment, the mice were euthanized for the following experiments. The portion of the intervention area of the auricular skin of mice was fixed with 4% paraformaldehyde for histopathological Analysis, and other remaining tissues were stored at −80 °C for mRNA and protein extraction.

2.8.4 Histopathological analysis

After euthanizing and decapitating the mice, the whole ear tissues were fixed in 4% paraformaldehyde. The tissues were then dehydrated using increasing concentrations of alcohol and embedded in paraffin blocks. Finally, 5 μm sections were stained with hematoxylin and eosin (H&E) for evaluation of the epidermal thickness and inflammation. Images were taken using a light microscope (CX21; Olympus, Tokyo, Japan) to assess the histopathological changes in the mouse ears.

2.8.5 RT-PCR

Tissues with a diameter of 5 mm and HaCaT cells were lysed in 1 ml TRIzol reagent (Invitrogen) to extract total RNA. An all-in-one

First Strand cDNA Synthesis Kit (SM131; Sevenbio, Beijing, China) was used to reverse-transcribe RNA into cDNA. The thermal cycling apparatus was obtained from Thermo Fisher Scientific. RNA expression was determined using a real-time PCR detection system (CFX96, Bio-Rad) with SYBR Green Master Mix (SM143, Sevenbio, Beijing, China). The thermal cycling procedure was: 95°C (30s), 95°C (10s), 60°C (20s), and 72°C (25s). Results were standardized using GAPDH. And the mRNA expression levels were determined using the $2^{-\Delta\Delta CT}$ method. Primers were provided by RuiBiotech (Beijing, China), and the corresponding sequences are displayed in Table 1.

2.8.6 Western blot

Protein samples were extracted from the isolated mouse tissues with RIPA lysis buffer (P0013, Beyotime Biotechnology). Twenty-five micrograms of total protein of different molecular weights were separated on a 12.5% SDS-PAGE gel, which was maintained at 80 V for 30 min and 120 V for 90 min, and then transferred to PVDF membranes (3010040001; Roche Applied Science, Mannheim, Germany). The blocking of membranes were performed with TBST-5% BSA for 1 h at room temperature, and then incubated with primary antibodies GPX4 (ab125066, abcam, UK; 1:10000), XCT (ab175186, abcam, UK; 1:5000), Phospho-STAT3(Tyr705) (#9145, Cell Signaling Technology, USA; 1:2000), STAT3(10253-2-AP, Proteintech, Wuhan, Hubei, China; 1:2000), β-actin (TA-09, Zhongshanjinqiao, Inc., Beijing, China; 1:2000) overnight at 4°C. After incubation for 1 h at room temperature with secondary antibodies, ECL solution (Affinity, China) was used for image acquisition on a luminescent imaging workstation (Model 6600; Tanon, Shanghai, China). In addition, ImageJ (Version: 1.54 g, USA) was used to measure the epidermal thickness and calculate the gray values of the Western Blot strips.

2.8.7 Statistical and software

All data are presented as the mean ± standard deviation (SD) and were performed with the GraphPad Prism 5.0 software (GraphPad Software, CA, USA). One-way ANOVA followed by Turkey's multiple comparisons test and Student's *t*-test were used to measure the differences between multiple groups and two groups. Each dependent experiment was repeated at least three times, and a p-value < 0.05 was considered statistically significant.

3 Results

3.1 Identification of ferroptosis signature genes in AD

First, the expression profiles of the GSE16161, GSE32924, GSE107361, and GSE120721 cohorts were normalized to ensure that the background expression values corresponding to each sample were consistent (Supplementary Figure 1). Using the thresholds of |logFC|>1 and FDR<0.05, we separately identified 3470, 1100, 1758, and 2180 DEGs between normal and AD samples in the GSE16161, GSE32924, GSE107361, and GSE120721 cohorts, respectively (Figures 1A–D). Next, using the Robust Rank Aggregation method, we created a comprehensive ranking list of DEGs. Figure 1E presented the top 15 upregulated and down-regulated DEGs. A total of 278 DEGs with consistent expression patterns in at least three cohorts were considered differentially expressed between the samples from healthy controls and patients with AD. Finally, 7/483 ferroptosis regulators simultaneously belonged to these 278 DEGs (Figure 1F). These are considered to be ferroptosis signature genes in AD. ALOXE3, FABP4, and AQP5 were highly expressed in samples from healthy controls, whereas KIF20A, MAP3K14, EGR1, and HELLS were highly expressed in samples from patients with AD (Figure 1G). Evidence suggests that ALOXE3 can increase cellular resistance to ferroptosis and FABP4 can protect cells from oxidative stress (23, 24). Similarly, EGR1 is related to GPX4 axis activity and promotes ferroptosis (25). In addition, CHAC1 and PTGS2 were significantly highly expressed in samples collected from patients with AD, whereas the expression of GPX4 and SLC7A11 was relatively low (Figure 1H). PTGS2 regulates the biosynthesis of COX-2, which promotes inflammation and oxidative stress. CHAC1 catalyzes glutathione catabolism, and GPX4 and SLC7A11 are protective factors in cells

TABLE 1 Primer sequences for RT-PCR.

Genes	Forward	Revers
hMAP3K14	GAGGAAAGAGCCCATCCACC	TCAGACCTCCCACTTGCTGT
mMAP3K14	GGGGTCCTGCTTACTGAGAAAC	TTCATTCTGTGGACCTCGCC
hFABP4	AACCTTAGATGGGGGTGTCCT	ACGCATTCCACCACCAGTTT
mFABP4	CGACAGGAAGGTGAAGAGCAT	AACACATTCCACCACCAGCTT
hALOXE3	TGTTTGCCGGCGCTGTATT	TGTTTGCTTGCCTCTGACACA
mALOXE3	CTGGTTCCTACCTGAAGGCTG	AGCGCAACAGCAAGATCTCA
hEGR1	GTTACCCCAGCCAAACCACT	GTGGGTTGGTCATGCTCACT
mEGR1	AGCCTTCGCTCACTCCACTA	AGCTGGGATTGGTAGGTGGT
hGAPDH	CTGGGCTACACTGAGCACC	AAGTGGTCGTTGAGGGCAATG
mGAPDH	GGTTGTCTCCTGCGACTTCA	TGGTCCAGGGTTCTTACTCC

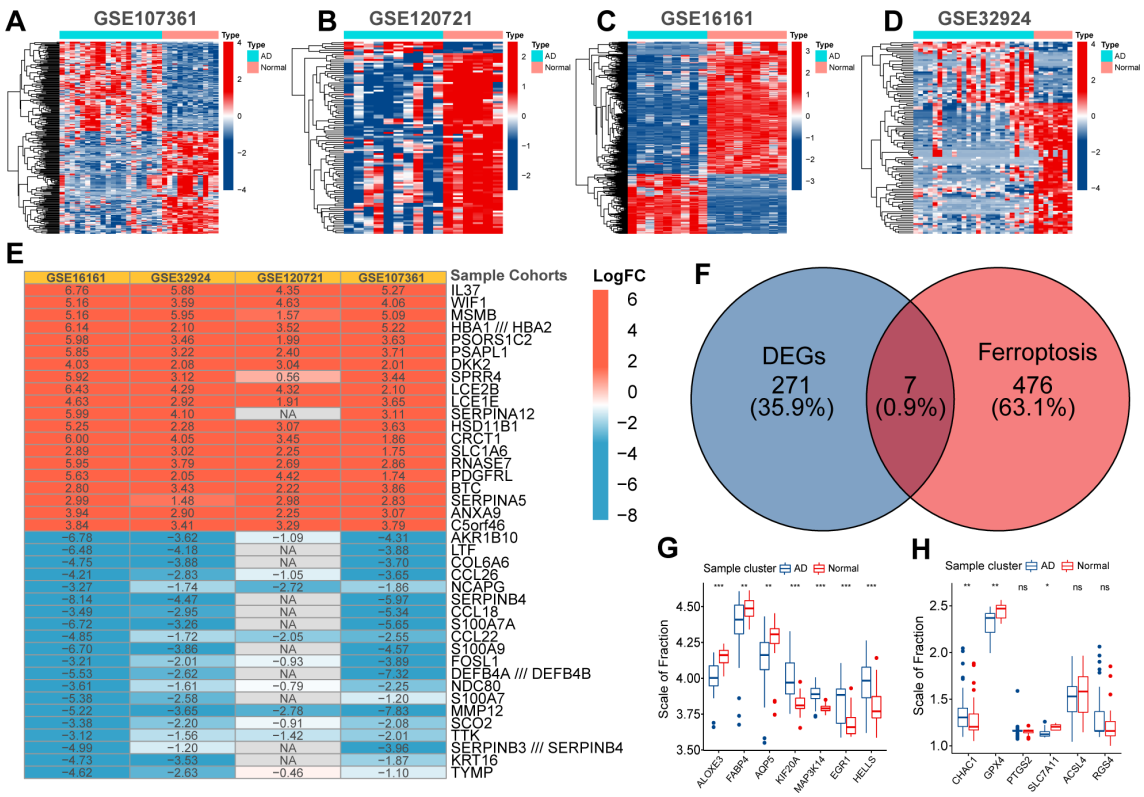

FIGURE 1
The Heatmap displayed the distribution of differentially expressed genes (DEGs) between normal and AD samples in GSE107361 **(A)**, GSE120721 **(B)**, GSE16161 **(C)**, and GSE32924 **(D)**. The robust rank aggregate heatmap presented the top 15 up-regulated and down-regulated DEGs in the ranking list **(E)**. Venn diagram presented the intersection between DEGs and ferroptosis regulators. These seven intersected genes were recognized as ferroptosis signature genes in AD **(F)**. Differential expression of ferroptosis signature genes **(G)** and ferroptosis biomarkers **(H)** between normal and AD samples. p<0.05 was indicated by "*", p<0.01 was indicated by "**", p<0.001 was indicated by "***".

under oxidative stress (11). Therefore, the ferroptosis process in AD might be activated. In summary, heterogeneity in the expression patterns of ferroptosis regulators exists between samples from patients with AD and healthy controls, and activation of ferroptosis is related to the pathogenesis of AD.

3.2 Construction of the PPI network and functional annotation

To further reveal the mechanisms by which these seven ferroptosis signature genes are involved in AD pathogenesis, we determined their co-expression relationships with the DEGs. After validation using the STRING database, 63 PPI relationships were retained (Figure 2A). Next, GO and KEGG functional enrichment analyses were performed on all nodes of the PPI network. These genes were highly enriched in multiple signaling pathways and molecular functions, including cell cycle regulation, immune cell chemotaxis and migration, cytokine activity, and extracellular matrix reorganization (Figures 2B, C). Alterations in cell-cycle regulation may be associated with ferroptosis activation (26). In addition, these ferroptosis signature genes can regulate multiple proinflammatory signaling pathways, and AD is known to be closely related to chronic inflammatory alterations. Therefore, these signature genes may regulate multiple biological pathways and have non-negligible value in AD pathogenesis.

3.3 Construction of the ferroptosis-related AD morbidity model

To quantify the risk of AD morbidity, we developed a genetic model with LASSO regression. After 10-fold cross-validation, the optimal penalty coefficient was log(λ) = −4.35 (Figure 3A). Under these conditions, four ferroptosis signature genes (*ALOXE3, FABP4, MAP3K14*, and *EGR1*) had nonzero weight coefficient (Coef) values (Figure 3B). Therefore, they were considered hub genes with the most significant effect on AD morbidity and were used in the construction of FerrSig. MAP3K14 and EGR1 were highly expressed in the AD subgroup, whereas *ALOXE3* and *FABP4* were highly expressed in samples from healthy controls (Figure 3C). As shown in Supplementary Table 1, The Coef values for *ALOXE3* and *FABP4* were positive, whereas those for *MAP3K14* and *EGR1* were negative. Therefore, FerrSig expression was downregulated in the AD subgroup (Figure 3D). For the ROC curves, the AUC values corresponding to FerrSig were 0.998 and 0.994 for the training and test sets, respectively (Figures 3E, F). Furthermore, a separate GEO cohort was used to verify the accuracy

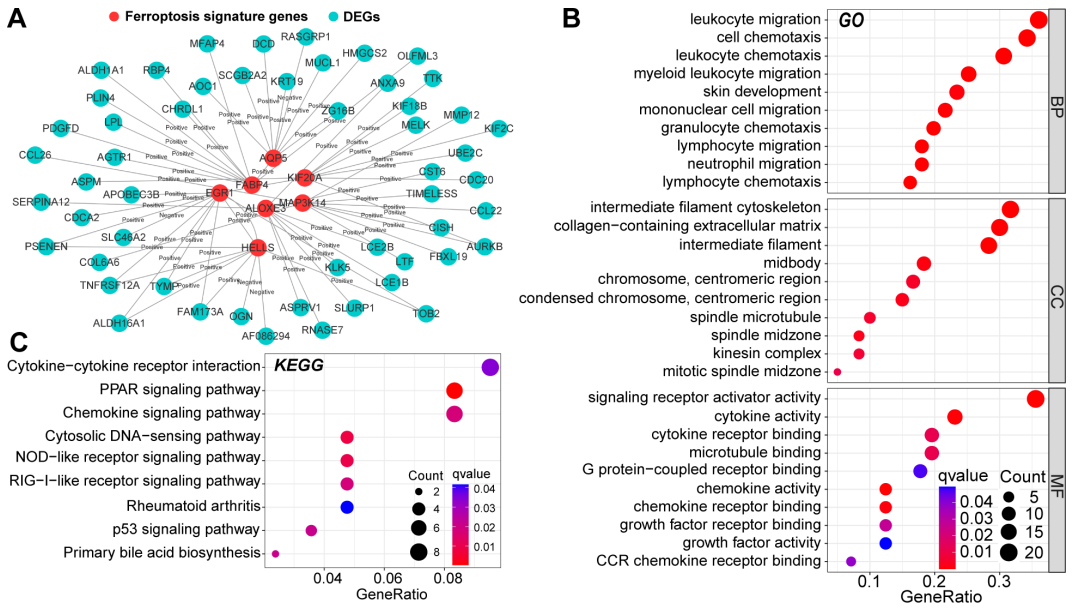

FIGURE 2
Protein-protein interaction (PPI) relationships between DEGs and ferroptosis signature genes **(A)**. Results of Gene Ontology (GO) **(B)** and the Kyoto Protocol Encyclopedia of Genes and Genomes (KEGG) **(C)** functional enrichment analysis of nodes in the PPI network. In this figure, the correlation analysis was performed with the "Spearman" correlation test. PPI with p<0.05 and Cor>0.4 in the String database could be included.

of FerrSig. In the GSE60709 cohort, FerrSig showed an AUC of 0.838 (Figure 3G). Therefore, the predictive capability of FerrSig was stable and its accuracy was relatively reliable across sample cohorts from different sources and origins. Furthermore, FerrSig was significantly negatively correlated with CHAC1 and PTGS2, further supporting a more activated ferroptotic process in AD (Figures 3H, I). In summary, FerrSig may serve as a potential quantitative marker of ferroptosis. In addition, FerrSig may be a reliable biomarker for the risk of AD morbidity.

3.4 The immune landscape analysis

Ferroptosis is an important mechanism in oxidative stress-related cell death. In addition, the inflammatory response was positively correlated with oxidative stress levels. In addition, the identified ferroptosis signature genes were highly enriched in multiple immune-related signaling pathways (Figures 2B, C). To clarify the mechanism by which ferroptosis participates in the pathogenesis of AD, we attempted to depict the immune landscape of AD and reveal the immunological significance of FerrSig.

First, we depicted the differences in immune cell infiltration patterns between normal and AD subgroups. As shown in Figures 4A–D, pro-inflammatory cells, including activated CD4/CD8 cells, Tfh cells, activated dendritic cells, natural killer cells, and B cells, were highly infiltrated in the AD subgroup. In contrast, the proportion of immunomodulatory cells, such as regulatory T cells (Tregs) and multiple resting immune cells, was significantly higher in the samples from healthy controls. In addition, the levels of various costimulatory factors, cytokines, chemokines, interleukins, and inflammation-promoting receptor signatures were significantly higher in the AD subgroup (Figure 4C). These results suggest that AD is characterized by a distinctive abnormal activation of inflammatory activities. Furthermore, we evaluated the correlation between FerrSig expression and the immune signatures. The enrichment levels of macrophages, DCs, activated CD4 + T cells, inflammatory activity, major histocompatibility complex class I cells, and Th2 cells were negatively correlated with FerrSig (Figure 4E). However, the activities of transforming growth factor-β, and Tregs were positively correlated with FerrSig (Figure 4E). Therefore, FerrSig may be negatively correlated with inflammatory activity. In addition, we noted that JAK/STAT, NF-κB, p53, NOD-receptor, and TLR signaling pathways were highly enriched in the low FerrSig subgroup (Figures 4F–H). However, in the high-ferritin subgroup, only signaling pathways related to normal cell metabolism and skin development were highly enriched. This indicated that low ferritin levels were closer to the pathological state of AD, further supporting the accuracy of our AD morbidity model. In summary, FerrSig could serve as a biomarker of the immune status in AD. This might be attributed to the possibility that ferroptosis and immune regulation share signaling pathways.

3.5 Therapeutic benefit of FerrSig

Finally, we evaluated the relationship between FerrSig and the therapeutic response in AD. Currently, the conventional therapeutic agents for AD are glucocorticoids and immunosuppressants. Therefore, we further explored this issue in the GSE32473 cohort, which received pimecrolimus or

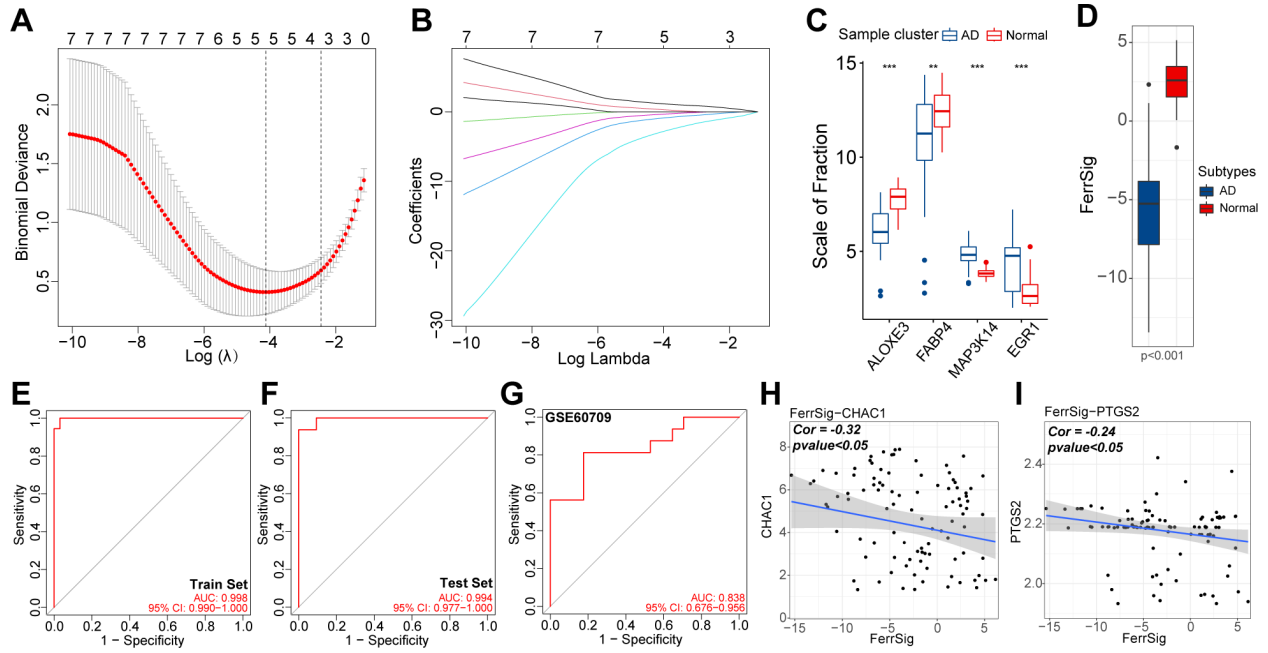

FIGURE 3
The relationship between lambda values and Binominal likelihood deviance **(A)** or variable coefficients **(B)** in the calculation of FerrSig by the least absolute shrinkage and selection operator (LASSO) regression. Differential expression of four LASSO hub genes between normal and AD samples **(C)**. Differential distribution in FerrSig between normal and AD samples **(D)**. ROC curves of FerrSig in the train set **(E)**, test set **(F)**, or the GSE60709 cohort **(G)**. Correlations between FerrSig and the expression of CHAC1 **(H)** and PTGS2 **(I)**. In this figure, the correlation analysis was performed with the "Spearman" correlation test. In the box plots, p<0.01 was indicated by "**", p<0.001 was indicated by "***", and the statistical analysis was performed by the Mann-Whitney U test.

betamethasone. After 22 d of treatment, the FerrSig levels were significantly elevated under improved conditions (Figure 5A). In addition, we noted that the expression of ALOXE3 and FABP4 sequentially increased in the baseline, pimecrolimus, and betamethasone subgroups, whereas the expression of MAP3K14 and EGR1 sequentially decreased (Figures 5B–E). Compared to Figure 3C, the expression profile of ferroptosis signature genes in the treated subgroups tended toward samples from healthy controls compared to samples at baseline. In addition, the expression of CHAC1 and PTGS2 significantly decreased in the treated subgroups, whereas GPX4 expression was upregulated (Figure 5F). These results indicate that conventional AD therapy may inhibit ferroptosis. In addition, FerrSig may serve as a biomarker of treatment response, and its elevation signified that these patients responded well to clinical management.

3.6 Validation by *in vivo* and *in vitro* experiments

The FerrSig model was validated using HaCaT cells. As shown in Figure 6A, after 24 h of stimulation with 10 ng/mL of TNF-α/IFN-γ, the ROS level was significantly increased. We noted that MAP3K14 and EGR1 expression levels were about 8- and 7-fold higher in the TNF-α/IFN-γ subgroup, whereas the expression of ALOXE3 and FABP4 was around 1/4 and 1/10 of that of the control (Figures 6B–E). These results are consistent with those shown in Figure 3C, further supporting the reliability of the FerrSig model in predicting AD morbidity.

Second, an *in vivo* AD morbidity model was constructed using Female BALB/c mice. First, we detected changes in the expression of ferroptosis signature genes at four time points: days 0, 3, 5, and 7. ALOXE3 and FABP4 were downregulated with increasing stimulation duration, and MAP3K14 and EGR1 expression was upregulated, which was consistent with the results in the cellular model (Figures 6F–I). Second, with the prolongation of stimulation, the ear thickness of the mice also gradually and significantly increased, as did the frequency of scratching (Figures 6J–M, Supplementary Figures S2, S3). In addition, compared to the control, the auricular skin of AD mice presented significant edema, dryness, and erythema in the auricular skin (Figure 6K, Supplementary Figure S3). These lesion characteristics became progressively more pronounced with increasing stimulation duration. These results further validate FerrSig as a reliable biomarker for predicting the pathogenesis and severity of AD.

Next, when the *in vivo* AD model was successfully constructed (day 7), two groups of AD mice were treated with tacrolimus or betamethasone. We similarly examined the differences in the expression of ferroptosis signature genes, auricular thickness, and number of scratches on days 10 and 15. The results showed that the symptoms of AD in the betamethasone- and tamoxifen-treated groups improved significantly by day 10, as evidenced by a reduction in skin lesions and frequency of scratching (Figures 7G, H). These changes were more pronounced as treatment progressed to day 15. Notably,

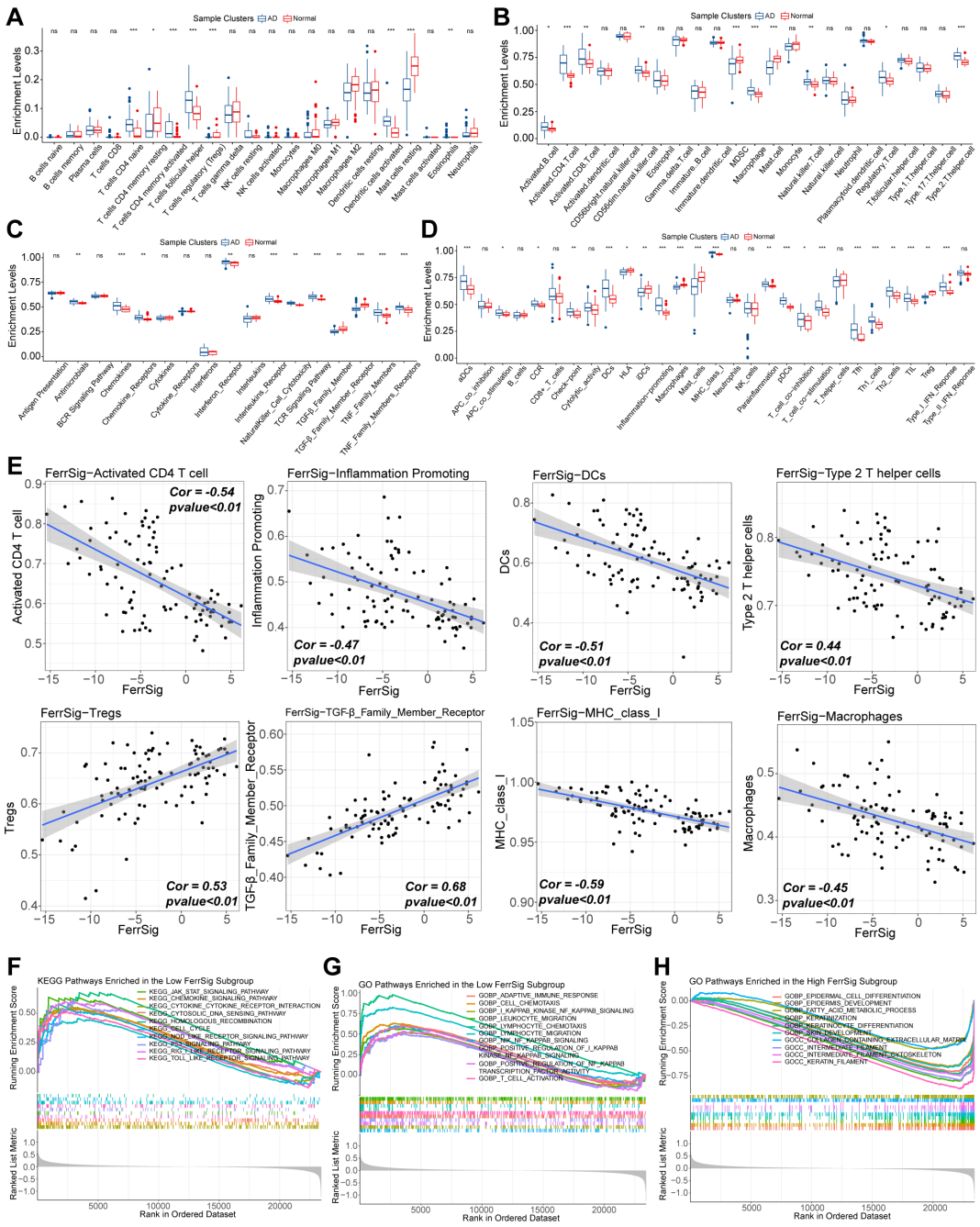

FIGURE 4
Differences in the enrichment levels of immune signatures of CIBERSORT **(A)**, works of Bindea et al. **(B)**, ImmPort database **(C)**, and the RndSys **(D)** between normal and AD samples. Correlations of FerrSig with immune signatures whose Cor was larger than 0.4 **(E)**. Top 10 highly enriched KEGG signaling pathways in the low FerrSig subgroups **(F)**. Top 10 highly enriched GO signaling pathways in the low FerrSig subgroups **(G)** and high FerrSig subgroups **(H)**. In this figure, the correlation analysis was performed with the "Spearman" correlation test. In the box plots, p<0.05 was indicated by "*", p<0.01 was indicated by "**", p<0.001 was indicated by "***", and the statistical analysis was performed by the Mann-Whitney U test.

the tacrolimus subgroup showed better improvement in appearance than the betamethasone subgroup (Figure 7I, Supplementary Figures S4A–C). Hematoxylin and eosin (H&E) staining revealed significant epidermal thickening, parakeratotic hyperkeratosis, epidermal hyperplasia, lymphocyte cytosis, and spongiogenesis in the skin of AD mice. Similarly, compared with betamethasone, tacrolimus-treated AD mice had epidermal thickness closer to that of healthy controls and showed a more pronounced improvement in epidermal thickening, parakeratotic hyperkeratosis, epidermal hyperplasia, lymphocyte cytosis, and spongiogenesis (Figure 7J, Supplementary Figures S4D–F). Therefore, we conclude that clinical regression was better in tacrolimus-treated AD mice than in mice treated with betamethasone. Furthermore, ALOXE3 and FABP4 were upregulated over time in both the betamethasone- and tacrolimus-treated subgroups, and the expression of MAP3K14 and EGR1 exhibited a progressive decrease (Figures 7A–D). Notably,

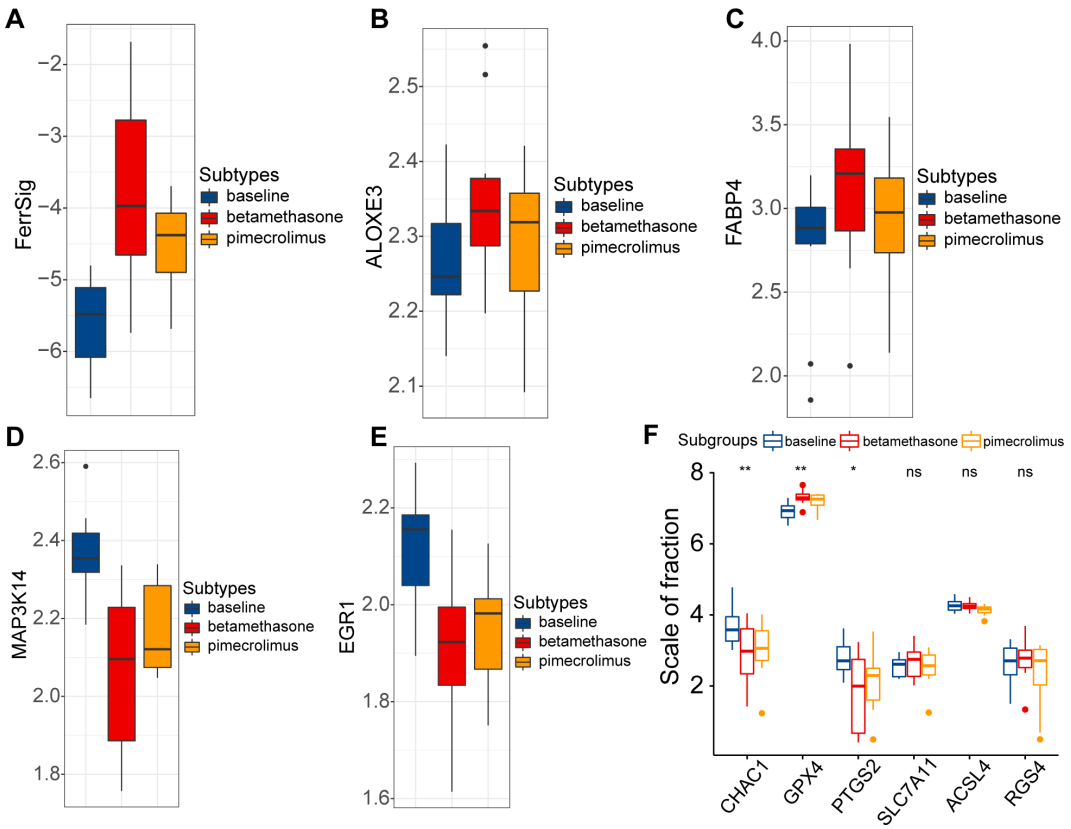

FIGURE 5
Differences in FerrSig **(A)** and expression of ALOXE3 **(B)**, FABP4 **(C)**, MAP3K14 **(D)**, EGR1 **(E)**, and ferroptosis biomarkers **(F)** between the baseline, pimecrolimus, and betamethasone subgroups. In the box plots, p<0.05 was indicated by "*", p<0.01 was indicated by "**", and the statistical analysis was performed by the Kruskal-Willis test.

tacrolimus-treated AD mice had significantly higher FerSig levels than untreated AD mice, second only to normal controls. Relatively poorly regressed betamethasone-treated mice showed a lower increase in FerrSig, but it was also significantly higher than that in AD mice (Figure 7F). In summary, FerrSig mice responded well to AD treatment.

Finally, we validated signaling pathways potentially relevant to FerrSig. Based on Figure 4F, we noted that the JAK/STAT3 signaling pathway changed most significantly in the low-ferritin subgroup. We noted that p-STAT3/STAT3 was significantly elevated in AD mice, implying that STAT3 phosphorylation was significantly activated, and the activity of the JAK/STAT3 signaling pathway was markedly upregulated (Figures 7K, M). SLC7A11 and GPX4 were significantly downregulated in AD mice, suggesting the activation of ferroptosis (Figures 7K, L, N). In addition, in both betamethasone- and tacrolimus-treated AD mice, we observed a rebound in GPX4 and SLC7A11 as well as a decrease in p-STAT3/STAT3 (Figures 7K–N). The magnitude of change in these metrics was greater in tacrolimus-treated AD mice with higher ferritin levels and better clinical regression (Figures 7E, F). Therefore, the FerrSig signature gene may regulate ferroptosis by participating in the JAK/STAT3 signaling pathway and regulating STAT3 phosphorylation, which makes FerrSig clinically significant for predicting AD pathogenesis and treatment regression.

4 Discussion

We thoroughly analyzed 278 DEGs in the samples collected from healthy controls and patients with AD. After extensive investigations, we identified seven signature genes directly linked to ferroptosis. Functional enrichment analysis revealed that these seven genes were significantly enriched in cell cycle checkpoints and immune regulation-related signaling pathways, which are crucial for ferroptosis and the development and progression of AD. To provide accurate results regarding the risk of AD, evolution of immunological characteristics, and response to traditional AD therapy, we developed a FerrSig model. The accuracy of this model was validated using a test set and independent GEO cohort. Finally, ferritin levels were significantly decreased in the AD subgroup in both *in vitro* cell and mouse models. In addition, in mice that responded better to betamethasone and tacrolimus therapy, we observed a significant increase in FerrSig and a corresponding significant decrease in ferroptosis. In summary, our study reveals the mechanism by which ferroptosis regulates the pathophysiological development of AD. Furthermore, FerrSig has the potential to be utilized as a new biomarker with clinical relevance, and the related hub genes may have important biological implications in the pathophysiological changes of AD and could be promising targets for clinical intervention.

10.3389/fimmu.2024.1412382

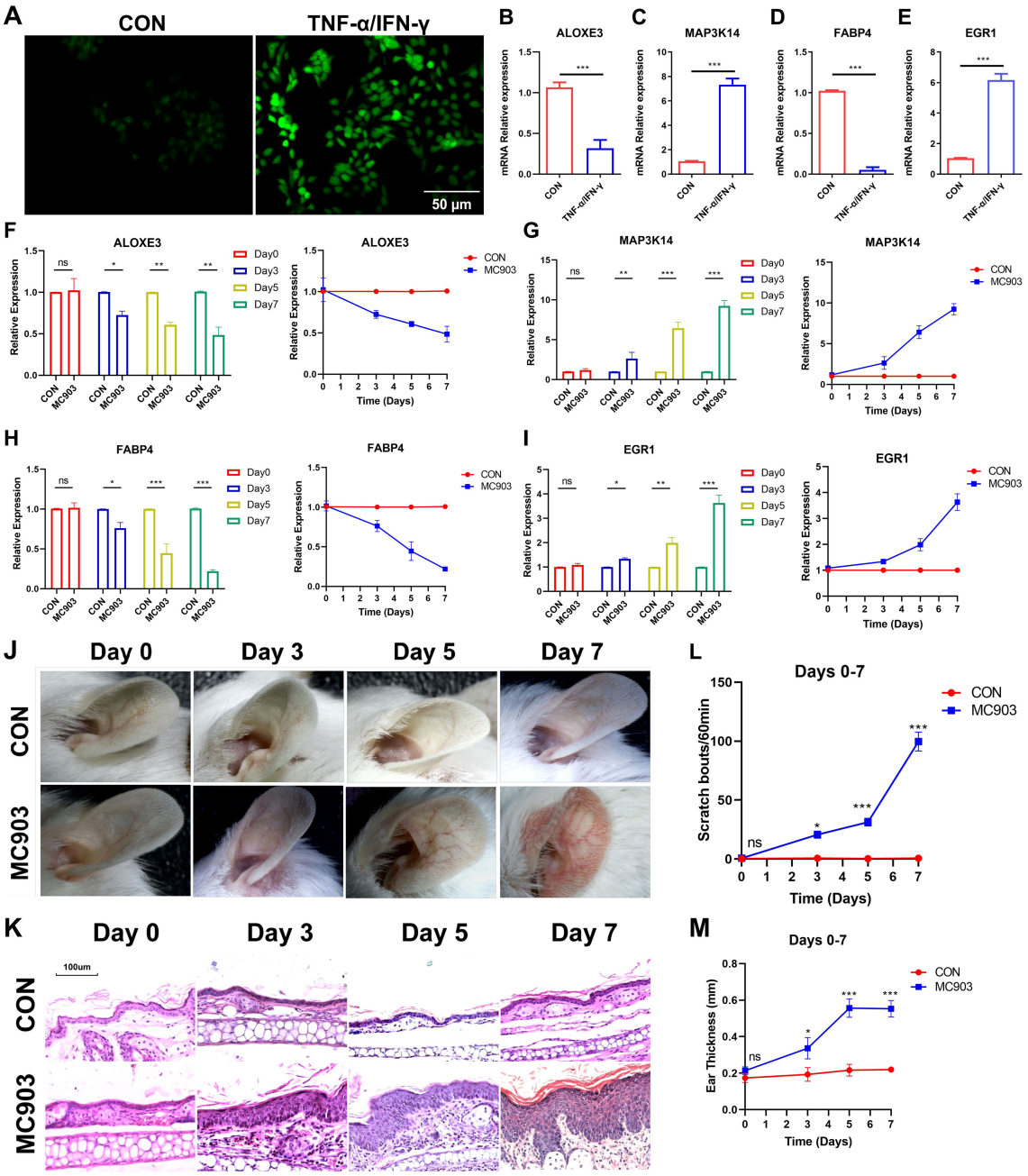

FIGURE 6
ROS fluorescent staining **(A)**. Differential expression of ALOXE3 **(B)**, MAP3K14 **(C)**, FABP4 **(D)**, and EGR1 **(E)** between CON and TNF-α/IFN-γ subgroups (MC903) in the cellular model. Differential expression of ALOXE3 **(F)**, MAP3K14 **(G)**, FABP4 **(H)**, and EGR1 **(I)** betweenthe CON and MC903 in the time points of 0 days, 3 days, 5 days, and 7 days of the mice model. Photograph of a large view of the intervention area of the mouse auricle in the time points of 0 days, 3 days, 5 days, and 7 days **(J)**. Photograph of H&E staining of mouse auricular intervention area tissue in the time points of 0 days, 3 days, 5 days, and 7 days **(K)**. Differences in scratching frequency **(L)** and auricular thickness **(M)** between CON and MC903 subgroups in the time points of 0 days, 3 days, 5 days, and 7 days. In this figure, p<0.05 was indicated by "*", p<0.01 was indicated by "**", p<0.001 was indicated by "***".

Ferroptosis is an emerging form of immunogenic cell death (ICD) that is characterized by iron-dependent lipid peroxidation (4, 27). Inflammation-related DAMPs should be closely associated with the activation and outbreak of inflammation in pathological states (28, 29). For example, the pattern recognition receptor (PRR) TLR4 can recognize or mediate ferroptosis-related cell death to induce myocardial tissue fibrosis and ischemia-reperfusion injury through biological signaling such as Trif or TRIM44 (30, 31). Also, ferroptosis is widespread in the pathogenesis of auto-immunogenic diseases (10, 32, 33). Of these, RA and psoriasis have similar pathogenic causative factors as AD and are essentially chronic sterile inflammatory diseases induced by abnormal oxidative stress states (2, 34–36). Notably, ROS in RA is closely associated with lipid peroxidation and abnormal mitochondrial

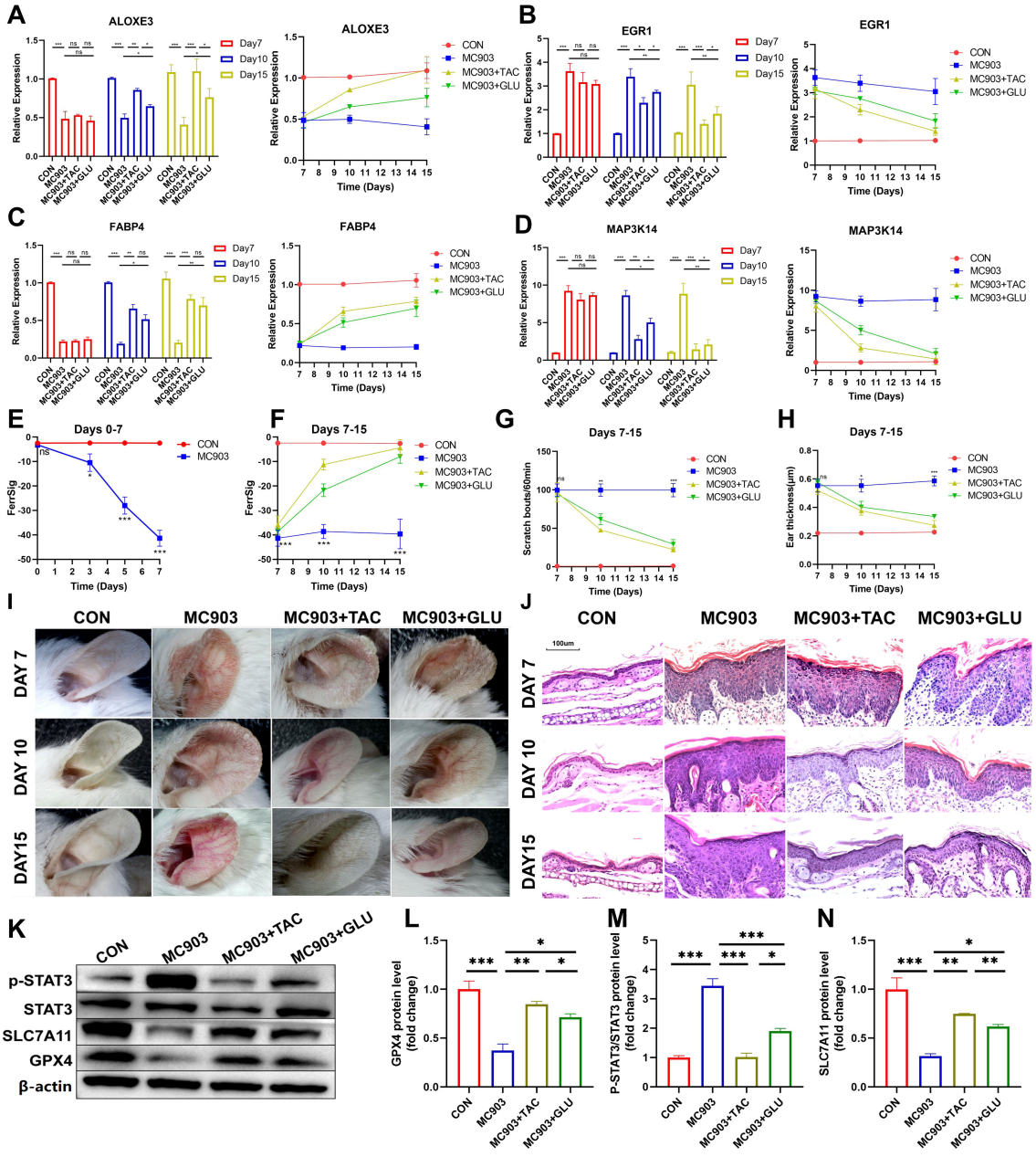

FIGURE 7
Differential expression of ALOXE3 **(A)**, EGR1 **(B)**, FABP4 **(C)**, and MAP3K14 **(D)** between the CON, MC903, MC903+TAC, and MC903+GLU subgroups between the CON, MC903, MC903+TAC, and MC903+GLU subgroups in the time points of 7 days, 10 days, and 15 days. Differences in FerrSig between the CON and MC903 subgroups in the time points of 0 days, 3 days, 5 days, and 7 days of the mice model **(E)**. Differences in FerrSig between the CON, MC903, MC903+TAC, and MC903+GLU subgroups in the time points of 7 days, 10 days, and 15 days of the mice model **(F)**. Differences in scratching frequency **(G)** and ear thickness **(H)** between the CON, MC903, MC903+TAC, and MC903+GLU subgroups in the time points of 7 days, 10 days, and 15 days. Photograph of a large view of the intervention area of the mouse auricle in the time points of 7 days, 10 days, and 15 days **(I)**. Photograph of H&E staining of mouse auricular intervention area tissue in the time points of 7 days, 10 days, and 15 days **(J)**. Differences in p-STAT3, STAT3, SLC7A11, GPX4, and β-actin protein expression between the CON, MC903, MC903+TAC, and MC903+GLU subgroups in the mice model **(K)**. Relative expression of GPX4 **(L)**, p-STAT3/STAT3 **(M)**, and SLC7A11 **(N)** between the CON, MC903, MC903+TAC, and MC903+GLU subgroups in the mice model.In this figure, $p<0.05$ was indicated by "*", $p<0.01$ was indicated by "**", $p<0.001$ was indicated by "***".

function and can increment inflammation by inducing the generation of TNF-α, interleukin-6 (IL-6), and IL-1β (37). Similarly, the upregulation of PTGS2 and TFRC expression and decreased FTL, GPX4, and FTH1 mRNA levels were observed in psoriasis samples (15). Blocking lipid peroxidation could remarkably inhibit ferroptosis and reduce cytokine production, including TNF-α, IL-6, IL-1α, IL-1β, IL-17, IL-22, IL-23, and IL25, as well as related products like MDA and 4-HNE (15, 38).. Similarly, PRR and cytokines play essential roles in the pathogenesis of AD. For example, TLR2 can induce p38 kinase phosphorylation, which drives monocytes to express high-affinity IgE receptors and exacerbates AD symptoms (39, 40). Cytokines such as IL-25 and IL-

33 can stimulate Langerhans cell activation and Th2 cell polarization, thereby mediating innate immune responses in AD pathogenesis (41, 42). Th2 cells and related pathways are important factors that induce ICD (43). Therefore, we speculated that ferroptosis might be activated in patients with AD with a background similar to that of autoimmune dysregulation. In our study, significant hyper-expression of CHAC1 and decreased expression of GPX4 and SLC7A11 were observed in samples from patients with AD. In addition, ROS levels were markedly increased in AD cells and tissues. These results support our hypotheses. In addition, the seven identified AD signature genes were highly enriched in cell cycle checkpoints and multiple immunoregulatory signaling pathways. The cell cycle checkpoint is related to the activity of the p53 signaling pathway and is one of the signals that induce ferroptosis (26). From the results of KEGG enrichment analysis, we noted that seven AD signature genes were also highly enriched in the p53 signaling pathway. In summary, ferroptosis may be closely associated with abnormal immune regulation in patients with AD. This may be involved in the pathophysiology of AD pathophysiology.

Based on the machine learning approach of LASSO regression, we identified four hub genes (*ALOXE3, FABP4, MAP3K14*, and *EGR1*) to construct the FerrSig model. ALOXE3 and FABP4 are key enzymes that transport the proteins associated with lipid metabolism. Previous studies have indicated that the pathogenesis of AD is accompanied by the inhibition of lipid metabolism (44, 45). In our study, FABP4 and ALOXE3 were also significantly hypoexpressed in samples from patients with AD. Subsequently, EGR1 and MAP3K14 are regulators of the NF-κB signaling pathway, and their high expression promotes the ferroptosis process (46). Additionally, EGR1, a critical transcription factor, has been repeatedly is highly expressed in AD tissues. EGR1 can regulate the inflammatory response in the pathogenesis of AD by modulating the IL4, MAPK, and TSLP signaling pathways (47–49). In our study, MAP3K14 and EGR1 were negatively correlated, whereas ALOXE3 and FABP4 were positively correlated with FerrSig. The overall manifestation was a significant decrease in the FerrSig levels in patients with AD. Thus, FerrSig reliably predicted the risk of AD Morbidity. Furthermore, we found that the JAK/STAT, NF-κB, NOD-receptor, and TLR signaling pathways were highly enriched in the low FerrSig subgroup. These inflammatory signaling pathways are closely associated with ferroptosis. For example, IFN-γ signaling can inhibit SLC7A11 expression via the JAK/STAT signaling pathway, which induces ferroptosis cell death (50). Our study also observed the activation of IFN-γ signaling and downregulation of SLC7A11 expression in AD. The activity of the NF-κB signaling pathway is closely related to the generation of cytokines such as IL-6 and IL-1β, as well as the infiltration levels of Th22 cells. It also influences the GPX4 axis and induce ferroptosis (51). In our study, essential proteins of these signaling pathways were highly expressed in AD tissues, suggesting that these pathways are highly activated during AD pathogenesis. Thus, these shared signaling pathways may be important mechanisms by which ferroptosis regulates the pathology of AD.

Finally, we investigated the correlation between FerrSig levels and sensitivity to conventional AD treatments. The results showed a significant increase in FerrSig levels in the treatment subgroup. These results were validated using a mouse model. In addition, the expression of CHAC1 and PTGS2 significantly decreased in the treated subgroups, whereas GPX4 expression was upregulated. Therefore, glucocorticoids and immunosuppressants may have inhibited the ferroptosis in AD. This may be related to the mechanisms underlying the effects of these two types of agents. Both cortisol and immunosuppressants can significantly suppress inflammatory responses and oxidative stress (52, 53). Furthermore, these agents have significant inhibitory effects on inflammatory signaling pathways, including JAK/STAT, NF-κB, and TLR (54–57). In the treatment subgroup, we also detected the downregulation of JAK/STAT signaling pathway activity. These molecular mechanisms may underlie the therapeutic predictive capabilities of FerrSig. In addition, upregulated FerrSig-related hub genes have the potential to serve as clinical intervention targets. MAP3K14 is the upstream kinase of NF-κB (58). EGR1 mainly acts on the GPX4 axis, and its overexpression can downregulate GPX4, thereby inducing ferroptosis (25). Strategies targeting EGR1 have been validated for selected diseases. Ai et al. postponed the progression of renal fibrosis by suppressing the expression of EGR1 (59). Whether these targets can be used as new clinical intervention paradigms for AD requires further investigation.

In this study, the FerrSig model identified ferroptosis-related genes combined with DEGs and PPI networks, reflecting genetic changes in onset of AD. FerrSig can serve as an early diagnostic biomarker by detecting gene expression to identify high-risk individuals, especially those with a family history or environmental risk factors, allowing early diagnosis or intervention to reduce incidence. The study showed that the FerrSig scores significantly increased after treatment with tacrolimus or betamethasone, indicating their potential for monitoring treatment efficacy and guiding personalized treatment plans. FerrSig scores can help evaluate patient responses to various treatments, optimize therapeutic strategies, and minimize adverse effects. Future integration with other clinical indicators, such as skin lesion scores and serum IgE levels, can provide a comprehensive assessment to predict prognosis and relapse risk, identify patients at high risk of chronicity or recurrence, and enable early intervention and management to reduce recurrence and disease burden.

This study has some limitations. First, our study was conducted on normal and AD sample cohorts and focused on the mechanisms related to ferroptosis in the pathogenesis of AD. However, due to the limited sample size available in the GEO database, we could not perform further stratification and subtype identification of the AD samples. Therefore, the biological functions of the ferroptosis marker genes identified during AD progression need to be further explored. In the future, we hope to further validate the prognostic predictive capability by collecting clinical samples, performing RNA-seq, and counting their prognostic and therapeutic information. Next, we aimed to individually interfere with the FerrSig Hub genes in both *in vitro* and *in vivo* models to further

refine their mechanisms of AD pathogenesis, prognosis, and therapy. In addition, heterogeneity and complexity between samples are non-negligible factors, and relevant studies have confirmed that heterogeneity could affect reactions to treatment (60). However, our study provides new insights into the pathophysiology and treatment of AD, with important implications.

5 Conclusion

Our study complements the exploration of the pathophysiological mechanisms underlying AD. We explored the potential interactions between ferroptosis and AD immunomodulation by revealing the changes in the activity of signaling pathways. These findings have led to a more comprehensive and precise understanding of the pathogenesis of AD. In addition, FerrSig may be a valid biomarker for recognizing the morbidity risk of AD and its response to conventional therapies. Further clarification and refinement of the biological function of ferroptosis in AD progression are needed. Through prospective studies, we can better understand pathophysiological changes and provide clinical benefits to patients with AD.

Data availability statement

The original contributions presented in the study are included in the article/Supplementary Material. Further inquiries can be directed to the corresponding author.

Ethics statement

The animal study was approved by Institutional Animal Care and Use Committee of Harbin Medical University. The study was conducted in accordance with the local legislation and institutional requirements.

Author contributions

LX: Writing – original draft, Validation, Software, Data curation. WG: Writing – review & editing, Data curation. HH: Writing – review & editing. JY: Writing – review & editing. BB: Writing – review & editing, Supervision, Project administration, Funding acquisition.

Funding

The author(s) declare financial support was received for the research, authorship, and/or publication of this article. The Project was supported by the National Natural Science Foundation of China (NSFC) 81872513.

Conflict of interest

The authors declare that the research was conducted in the absence of any commercial or financial relationships that could be construed as a potential conflict of interest.

Publisher's note

Supplementary material

The Supplementary Material for this article can be found online at: https://www.frontiersin.org/articles/10.3389/fimmu.2024.1412382/full#supplementary-material

References

1. Tsakok T, Woolf R, Smith CH, Weidinger S, Flohr C. Atopic dermatitis: the skin barrier and beyond. *Br J Dermatol*. (2019) 180:464–74. doi: 10.1111/bjd.16934

2. Ständer S. Atopic dermatitis. *N Engl J Med*. (2021) 384:1136–43. doi: 10.1056/NEJMra2023911

3. Jachiet M, Bieuvelet S, Argoud AL, Vallée M, Zinaï S, Lejeune FX, et al. Sleep disturbance in atopic dermatitis: a case-control study using actigraphy and smartphone-collected questionnaires. *Br J Dermatol*. (2020) 183:577–9. doi: 10.1111/bjd.19058

4. Nutten S. Atopic dermatitis: global epidemiology and risk factors. *Ann Nutr Metab*. (2015) 66 Suppl 1:8–16. doi: 10.1159/000370220

5. Silverberg JI. Public health burden and epidemiology of atopic dermatitis. *Dermatol Clin*. (2017) 35:283–9. doi: 10.1016/j.det.2017.02.002

6. Al-Naqeeb J, Danner S, Fagnan LJ, Ramsey K, Michaels L, Mitchell J, et al. The burden of childhood atopic dermatitis in the primary care setting: A report from the meta-LARC consortium. *J Am Board Fam Med*. (2019) 32:191–200. doi: 10.3122/jabfm.2019.02.180225

7. Abuabara K, Margolis DJ, Langan SM. The long-term course of atopic dermatitis. *Dermatol Clin*. (2017) 35:291–7. doi: 10.1016/j.det.2017.02.003

8. Dixon SJ, Lemberg KM, Lamprecht MR, Skouta R, Zaitsev EM, Gleason CE, et al. Ferroptosis: an iron-dependent form of nonapoptotic cell death. *Cell*. (2012) 149:1060–72. doi: 10.1016/j.cell.2012.03.042

9. Jiang X, Stockwell BR, Conrad M. Ferroptosis: mechanisms, biology and role in disease. *Nat Rev Mol Cell Biol*. (2021) 22:266–82. doi: 10.1038/s41580-020-00324-8

10. Lai B, Wu CH, Wu CY, Luo SF, Lai JH. Ferroptosis and autoimmune diseases. *Front Immunol*. (2022) 13:916664. doi: 10.3389/fimmu.2022.916664

11. Stockwell BR. Ferroptosis turns 10: Emerging mechanisms, physiological functions, and therapeutic applications. *Cell*. (2022) 185:2401–21. doi: 10.1016/j.cell.2022.06.003

12. Garcia-Romo GS, Caielli S, Vega B, Connolly J, Allantaz F, Xu Z, et al. Netting neutrophils are major inducers of type I IFN production in pediatric systemic lupus erythematosus. *Sci Transl Med*. (2011) 3:73ra20. doi: 10.1126/scitranslmed.3001201

13. Kim YE, Choi SW, Kim MK, Nguyen TL, Kim J. Therapeutic hydrogel patch to treat atopic dermatitis by regulating oxidative stress. *Nano Lett*. (2022) 22:2038–47. doi: 10.1021/acs.nanolett.1c04899

14. Liu L, Kang XX. ACSL4 is overexpressed in psoriasis and enhances inflammatory responses by activating ferroptosis. *Biochem Biophys Res Commun*. (2022) 623:1–8. doi: 10.1016/j.bbrc.2022.07.041

15. Shou Y, Yang L, Yang Y, Xu J. Inhibition of keratinocyte ferroptosis suppresses psoriatic inflammation. *Cell Death Dis*. (2021) 12:1009. doi: 10.1038/s41419-021-04284-5

16. Zhou N, Yuan X, Du Q, Zhang Z, Shi X, Bao J, et al. FerrDb V2: update of the manually curated database of ferroptosis regulators and ferroptosis-disease associations. *Nucleic Acids Res*. (2023) 51:D571–d82. doi: 10.1093/nar/gkac935

17. Kolde R, Laur S, Adler P, Vilo J. Robust rank aggregation for gene list integration and meta-analysis. *Bioinformatics*. (2012) 28:573–80. doi: 10.1093/bioinformatics/btr709

18. Szklarczyk D, Gable AL, Nastou KC, Lyon D, Kirsch R, Pyysalo S, et al. The STRING database in 2021: customizable protein-protein networks, and functional characterization of user-uploaded gene/measurement sets. *Nucleic Acids Res*. (2021) 49: D605–d12. doi: 10.1093/nar/gkaa1074

19. Yu G, Wang LG, Han Y, He QY. clusterProfiler: an R package for comparing biological themes among gene clusters. *Omics: J Integr Biol*. (2012) 16:284–7. doi: 10.1089/omi.2011.0118

20. Bindea G, Mlecnik B, Tosolini M, Kirilovsky A, Waldner M, Obenauf AC, et al. Spatiotemporal dynamics of intratumoral immune cells reveal the immune landscape in human cancer. *Immunity*. (2013) 39:782–95. doi: 10.1016/j.immuni.2013.10.003

21. Bhattacharya S, Andorf S, Gomes L, Dunn P, Schaefer H, Pontius J, et al. ImmPort: disseminating data to the public for the future of immunology. *Immunol Res*. (2014) 58:234–9. doi: 10.1007/s12026-014-8516-1

22. Newman AM, Liu CL, Green MR, Gentles AJ, Feng W, Xu Y, et al. Robust enumeration of cell subsets from tissue expression profiles. *Nat Methods*. (2015) 12:453–7. doi: 10.1038/nmeth.3337

23. Luis G, Godfroid A, Nishiumi S, Cimino J, Blacher S, Maquoi E, et al. Tumor resistance to ferroptosis driven by Stearoyl-CoA Desaturase-1 (SCD1) in cancer cells and Fatty Acid Biding Protein-4 (FABP4) in tumor microenvironment promote tumor recurrence. *Redox Biol*. (2021) 43:102006. doi: 10.1016/j.redox.2021.102006

24. Yang X, Liu J, Wang C, Cheng KK, Xu H, Li Q, et al. miR-18a promotes glioblastoma development by down-regulating ALOXE3-mediated ferroptotic and anti-migration activities. *Oncogenesis*. (2021) 10:15. doi: 10.1038/s41389-021-00304-3

25. Ding Y, Chen X, Liu C, Ge W, Wang Q, Hao X, et al. Identification of a small molecule as inducer of ferroptosis and apoptosis through ubiquitination of GPX4 in triple negative breast cancer cells. *J Hematol Oncol*. (2021) 14:19. doi: 10.1186/s13045-020-01016-8

26. Jiang L, Kon N, Li T, Wang SJ, Su T, Hibshoosh H, et al. Ferroptosis as a p53-mediated activity during tumour suppression. *Nature*. (2015) 520:57–62. doi: 10.1038/nature14344

27. Chen H, Han Z, Su J, Song X, Ma Q, Lin Y, et al. Ferroptosis and hepatocellular carcinoma: the emerging role of lncRNAs. *Front Immunol*. (2024) 15:1424954. doi: 10.3389/fimmu.2024.1424954

28. Murao A, Aziz M, Wang H, Brenner M, Wang P. Release mechanisms of major DAMPs. *Apoptosis*. (2021) 26:152–62. doi: 10.1007/s10495-021-01663-3

29. Proneth B, Conrad M. Ferroptosis and necroinflammation, a yet poorly explored link. *Cell Death Differ*. (2019) 26:14–24. doi: 10.1038/s41418-018-0173-9

30. Li W, Feng G, Gauthier JM, Lokshina I, Higashikubo R, Evans S, et al. Ferroptotic cell death and TLR4/Trif signaling initiate neutrophil recruitment after heart transplantation. *J Clin Invest*. (2019) 129:2293–304. doi: 10.1172/jci126428

31. Wu L, Jia M, Xiao L, Wang Z, Yao R, Zhang Y, et al. TRIM-containing 44 aggravates cardiac hypertrophy via TLR4/NOX4-induced ferroptosis. *J Mol Med (Berl)*. (2023) 101:685–97. doi: 10.1007/s00109-023-02318-3

32. Bock FJ, Tait SWG. Mitochondria as multifaceted regulators of cell death. *Nat Rev Mol Cell Biol*. (2020) 21:85–100. doi: 10.1038/s41580-019-0173-8

33. Han Z, Luo Y, Chen H, Zhang G, You L, Zhang M, et al. A deep insight into ferroptosis in renal disease: facts and perspectives. *Kidney Dis (Basel)*. (2024) 10:224–36. doi: 10.1159/000538106

34. Alivernini S, Firestein GS, McInnes IB. The pathogenesis of rheumatoid arthritis. *Immunity*. (2022) 55:2255–70. doi: 10.1016/j.immuni.2022.11.009

35. Griffiths CEM, Armstrong AW, Gudjonsson JE, Barker J. Psoriasis. *Lancet*. (2021) 397:1301–15. doi: 10.1016/s0140-6736(20)32549-6

36. Chen H, Han Z, Wang Y, Su J, Lin Y, Cheng X, et al. Targeting ferroptosis in bone-related diseases: facts and perspectives. *J Inflammation Res*. (2023) 16:4661–77. doi: 10.2147/JIR.S432111

37. Chang S, Tang M, Zhang B, Xiang D, Li F. Ferroptosis in inflammatory arthritis: A promising future. *Front Immunol*. (2022) 13:955069. doi: 10.3389/fimmu.2022.955069

38. Yang Y, Lin Y, Han Z, Wang B, Zheng W, Wei L. Ferroptosis: a novel mechanism of cell death in ophthalmic conditions. *Front Immunol*. (2024) 15:1440309. doi: 10.3389/fimmu.2024.1440309

39. Song Z, Deng X, Chen W, Xu J, Chen S, Zhong H, et al. Toll-like receptor 2 agonist Pam3CSK4 up-regulates FcεRI receptor expression on monocytes from patients with severe extrinsic atopic dermatitis. *J Eur Acad Dermatol Venereol*. (2015) 29:2169–76. doi: 10.1111/jdv.13172

40. Novak N, Bieber T. FcεRI-Toll-like receptor interaction in atopic dermatitis. *Curr Probl Dermatol*. (2011) 41:47–53. doi: 10.1159/000323295

41. Hvid M, Vestergaard C, Kemp K, Christensen GB, Deleuran B, Deleuran M. IL-25 in atopic dermatitis: a possible link between inflammation and skin barrier dysfunction? *J Invest Dermatol*. (2011) 131:150–7. doi: 10.1038/jid.2010.277

42. Savinko T, Matikainen S, Saarialho-Kere U, Lehto M, Wang G, Lehtimäki S, et al. IL-33 and ST2 in atopic dermatitis: expression profiles and modulation by triggering factors. *J Invest Dermatol*. (2012) 132:1392–400. doi: 10.1038/jid.2011.446

43. Devadas S, Das J, Liu C, Zhang L, Roberts AI, Pan Z, et al. Granzyme B is critical for T cell receptor-induced cell death of type 2 helper T cells. *Immunity*. (2006) 25:237–47. doi: 10.1016/j.immuni.2006.06.011

44. Brunner PM, He H, Pavel AB, Czarnowicki T, Lefferdink R, Erickson T, et al. The blood proteomic signature of early-onset pediatric atopic dermatitis shows systemic inflammation and is distinct from adult long-standing disease. *J Am Acad Dermatol*. (2019) 81:510–9. doi: 10.1016/j.jaad.2019.04.036

45. He H, Bissonnette R, Wu J, Diaz A, Saint-Cyr Proulx E, Maari C, et al. Tape strips detect distinct immune and barrier profiles in atopic dermatitis and psoriasis. *J Allergy Clin Immunol*. (2021) 147:199–212. doi: 10.1016/j.jaci.2020.05.048

46. Zhang J, He L, Li Q, Gao J, Zhang E, Feng H. EGR1 knockdown confers protection against ferroptosis and ameliorates intervertebral disc cartilage degeneration by inactivating the MAP3K14/NF-κB axis. *Genomics*. (2023) 115:110683. doi: 10.1016/j.ygeno.2023.110683

47. Wang HN, Ji K, Zhang LN, Xie CC, Li WY, Zhao ZF, et al. Inhibition of c-Fos expression attenuates IgE-mediated mast cell activation and allergic inflammation by counteracting an inhibitory AP1/Egr1/IL-4 axis. *J Transl Med*. (2021) 19:261. doi: 10.1186/s12967-021-02932-0

48. Yeo H, Ahn SS, Jung E, Lim Y, Lee YH, Shin SY. Transcription factor EGR1 regulates the expression of the clock gene PER2 under IL-4 stimulation in human keratinocytes. *J Invest Dermatol*. (2022) 142:2677–86.e9. doi: 10.1016/j.jid.2022.03.021

49. Yeo H, Ahn SS, Ou S, Yun SJ, Lim Y, Koh D, et al. The EGR1-artemin axis in keratinocytes enhances the innervation of epidermal sensory neurons during skin inflammation induced by house dust mite extract from dermatophagoidesfarinae. *J Invest Dermatol* 144(8):1817–28. (2024). doi: 10.1016/j.jid.2024.01.017

50. Yu X, Zhu D, Luo B, Kou W, Cheng Y, Zhu Y. IFNγ enhances ferroptosis by increasing JAK–STAT pathway activation to suppress SLCA711 expression in adrenocortical carcinoma. *Oncol Rep*. (2022) 47(5):97. doi: 10.3892/or.2022.8308

51. Wang C, Chen S, Guo H, Jiang H, Liu H, Fu H, et al. Forsythoside A mitigates alzheimer's-like pathology by inhibiting ferroptosis-mediated neuroinflammation via nrf2/GPX4 axis activation. *Int J Biol Sci*. (2022) 18:2075–90. doi: 10.7150/ijbs.69714

52. Vandewalle J, Luypaert A, De Bosscher K, Libert C. Therapeutic mechanisms of glucocorticoids. *Trends Endocrinol Metab*. (2018) 29:42–54. doi: 10.1016/j.tem.2017.10.010

53. Yang CH, Sheu JJ, Tsai TH, Chua S, Chang LT, Chang HW, et al. Effect of tacrolimus on myocardial infarction is associated with inflammation, ROS, MAP kinase and Akt pathways in mini-pigs. *J Atheroscler Thromb*. (2013) 20:9–22. doi: 10.5551/jat.14316

54. Bianchi M, Meng C, Ivashkiv LB. Inhibition of IL-2-induced Jak-STAT signaling by glucocorticoids. *Proc Natl Acad Sci U.S.A*. (2000) 97:9573–8. doi: 10.1073/pnas.160099797

55. Wang Z, Li X, Chen H, Han L, Ji X, Wang Q, et al. Resveratrol alleviates bleomycin-induced pulmonary fibrosis via suppressing HIF-1α and NF-κB expression. *Aging (Albany NY)*. (2021) 13:4605–16. doi: 10.18632/aging.202420

56. Srinivasan M, Walker C. Circadian clock, glucocorticoids and NF-κB signaling in neuroinflammation- implicating glucocorticoid induced leucine zipper as a molecular link. *ASN Neuro*. (2022) 14:17590914221120190. doi: 10.1177/17590914221120190

57. Broen JCA, van Laar JM. Mycophenolate mofetil, azathioprine and tacrolimus: mechanisms in rheumatology. *Nat Rev Rheumatol*. (2020) 16:167–78. doi: 10.1038/s41584-020-0374-8

58. Jimi E, Fei H, Nakatomi C. NF-κB signaling regulates physiological and pathological chondrogenesis. *Int J Mol Sci*. (2019) 20(24):6275. doi: 10.3390/ijms20246275

59. Ai K, Li X, Zhang P, Pan J, Li H, He Z, et al. Genetic or siRNA inhibition of MBD2 attenuates the UUO- and I/R-induced renal fibrosis via downregulation of EGR1. *Mol Ther Nucleic Acids*. (2022) 28:77–86. doi: 10.1016/j.omtn.2022.02.015

60. McGranahan N, Furness AJ, Rosenthal R, Ramskov S, Lyngaa R, Saini SK, et al. Clonal neoantigens elicit T cell immunoreactivity and sensitivity to immune checkpoint blockade. *Sci (New York NY)*. (2016) 351:1463–9. doi: 10.1126/science.aaf1490

Frontiers in Immunology

Explores novel approaches and diagnoses to treat immune disorders.

The official journal of the International Union of Immunological Societies (IUIS) and the most cited in its field, leading the way for research across basic, translational and clinical immunology.

Discover the latest Research Topics

See more →

Frontiers

Avenue du Tribunal-Fédéral 34
1005 Lausanne, Switzerland
frontiersin.org

Contact us

+41 (0)21 510 17 00
frontiersin.org/about/contact